PHOSPHOROUS HETEROATOM BOND FORMATION STRATEGIES

AND THE DEVELOPMENT OF GREEN SYNTHETIC METHODS

By

Jeffrey Ash II

Bachelor's of Science-Biochemistry
University of Nevada, Las Vegas
2019

A dissertation submitted in partial fulfillment
of the requirements for the

Doctor of Philosophy-Chemistry

Department of Chemistry and Biochemistry
College of Sciences
The Graduate College

University of Nevada, Las Vegas
May 2024

UNLV | GRADUATE COLLEGE

Dissertation Approval

The Graduate College
The University of Nevada, Las Vegas

May 1, 2024

This dissertation prepared by

Jeffrey Ash II

entitled

Phosphorous Heteroatom Bond Formation Strategies and the Development of Green Synthetic Methods

is approved in partial fulfillment of the requirements for the degree of

Doctor of Philosophy-Chemistry
Department of Chemistry and Biochemistry

Jun Kang, Ph.D.
Examination Committee Chair

Pradip Bhowmik, Ph.D.
Examination Committee Member

Dong-Chan Lee, Ph.D.
Examination Committee Member

Erica Marti, Ph.D.
Graduate College Faculty Representative

Alyssa Crittenden, Ph.D.
Vice Provost for Graduate Education & Dean of the Graduate College

Abstract

Strategies to forge phosphorous heteroatom bonds are in high demand as organophosphorus compounds have seen a variety of uses in medicinal chemistry, materials chemistry, and agricultural chemistry. Phosphorous monoacids are a challenging functional group to synthesize and current methods suffer from harsh conditions and limited substrate scope. Furthermore, fluorophosphine oxides have not yet been made in a sustainable way. An electrochemical synthetic is an attractive strategy as it would remove the need for conventional metal catalysts. However, a potential challenge to overcome is the low reactivity of fluoride. Synthetic methods to synthesize phosphorous monoacids and the electrochemical synthesis of fluorophosphine oxide are presented.

Thiophosphates are another functional group that interests organic chemists as they display important biological activity. The use and study of $P(O)OEt_2SH$ as a synthon for this functional group allow for unprecedented access to new synthetic methods to forge thiophosphates. The dual role of $P(O)OEt_2SH$ behaving as a Brønsted acid and thiolate nucleophile can be harnessed to synthesize thiophosphates under highly atom-economic, energy-neutral, catalyst-free, and additive-free conditions. This strategy has been used to develop green synthetic methodologies to access diaryl thiophosphate and phosphorous disulfides.

Another organosulfur functional group that has not been well studied is the hydrogen persulfide. Only three examples of hydrogen persulfides have been synthesized in the literature. Access to hydrogen persulfides is hampered by a difficult synthetic preparation method and

their inherent instability. New hydrogen persulfides have been synthesized and applied in the hydrothiolation of alkenes. Mechanism studies such as control experiments and isotope labeling experiments have been performed to elucidate the mechanism of this new transformation. The hydrothiolation of alkenes using hydrogen persulfides is a green strategy to access thioethers. This transformation is solvent-free, atom-economical, and an energy-neutral method.

Lastly, a Friedel-Crafts type reaction of beta naphthol has been explored to access allylation and benzylation products. The beta naphthol motif is important and has been used in medicinal chemistry and as an imaging reagent. The challenge of regioselectivity and allylic alcohol activation has been studied. Different reactions, such as phosphorylation and intramolecular annulation, also demonstrated the synthetic utility. This strategy is a catalytic, regioselective, and atom economical method, which can serve as a general strategy to functionalize arenols.

Acknowledgments

I want to thank my advisor, Dr. Kang. Dr. Kang was always supportive and had an open door for discussions about research. Having spent seven years in his lab, he has seen me and helped me grow from a novice to a full-fledged organic chemist. Additionally, Dr Kang has always pushed me to achieve and further develop ideas continually. I am happy and grateful to have been a part of his research group. And, I am proud of all the work I have done.

Next, I would like to thank Dr. Huang. I worked closely with Dr. Huang on a few projects when I first joined the Kang research group. He set an example of a good work ethic and taught me fundamental lab techniques. Working with Dr. Huang and learning from him was a pleasure when I began my journey as an organic chemist.

I would also like to thank Richard Cruse from Momentive for mentoring me during my summer synthetic chemist internship. It was refreshing to work with someone so experienced and passionate about chemistry. His love for distillation has rubbed off on me. Rick was also encouraging of my ideas and helped me with the design of my experiments.

I want to thank all Kang group members for their support and friendship and for dealing with me always in the lab.

Lastly, I would like to thank my parents and close friends for being my support network through this long journey.

Table of Contents

List of Tables

Table Page

List of Schemes

Scheme Page

Chapter I

Hydrolysis of P(V) Compounds to Form Organophosphorus Monoacids

1.1 Introduction and Background of P-O Bond Formation

Common P(V) phosphorus groups include phosphates, phosphonates, phosphinates, and phosphine oxides **(Scheme 1.1**).[1] A P(V) group serves to increase the lipophilicity of a molecule, which is important for drug design.[2] These functional groups contain a strong phosphoryl bond with a bond energy of 575 kJ/mol.[3] Likewise, due to its innate stability, the phosphoryl bond is difficult to activate in synthetic transformations.[4]

Scheme 1.1 Common P(V) Functional Groups

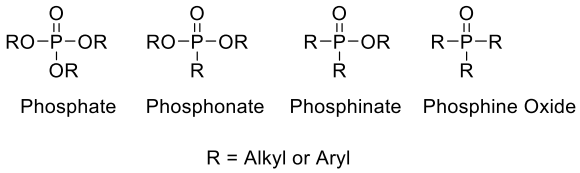

Synthetic organic chemists have been actively researching organophosphorus chemistry to forge P-O bonds. Their endearing interests stem from the fact that the P-O bond motif has found a multitude of uses across many disciplines (**Scheme 1.2**).[5-7] Selected examples include small molecules that treat cancer, glaucoma, and coronavirus (**Scheme 1.2**).[8-10] Additionally, phosphonates show interesting biological activity being utilized as a serine protease inhibitor and butyrophilin ligand prodrug (**Scheme 1.2**).[11]

Scheme 1.2 Selected Applications of P(V) Compounds

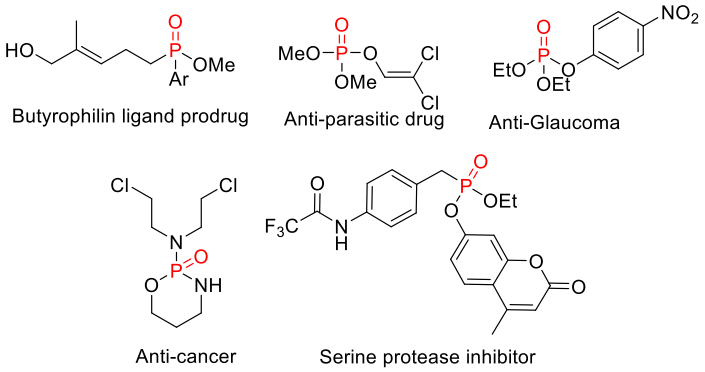

A conventional method of P-O bond formation begins with the reaction of chlorophosphines and chlorophosphine oxides with alkyl alcohols or arenols (**Scheme 1.3**).[12] In the presence of base, ethanol **2** will react with phosphine **1** to form phosphinite, which is then oxidized to afford phosphinate **3** in a yield of 75% (**Scheme 1.3**). The trivalent product can be

transformed into the more stable P(V) form by oxidation with hydrogen peroxide or elemental sulfur.[13] The innate disadvantage of this method lies with the chlorophosphine reagent, which is moisture-sensitive and is hydrolyzed to the secondary phosphine oxide in the presence of H_2O.[14] Schlenk line technique and careful handling of reagents should be applied to avoid low yield when working with chlorophosphines.

Scheme 1.3 P-O Bond Formation Using P(III) Chlorophosphine

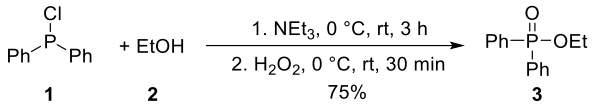

This drawback was addressed by British chemists Atherton and Todd in 1945, who pioneered the Atherton-Todd reaction (**Scheme 1.4**).[15] The reaction involves the removal of a proton from a P-H bond and transformation into a P-Cl bond, which is formed in situ and is reactive towards a nucleophilic substitution reaction. Atherton treated diisopropyl phosphite **4** with ammonia **5** in the presence of chlorinating agent CCl_4 to give phosphonamine **6** in a 65% yield (**Scheme 1.4**).

Scheme 1.4 Atherton-Todd Reaction

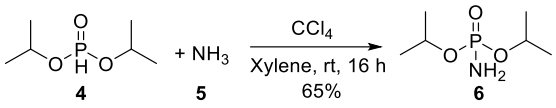

Secondary phosphine oxides exist in tautomeric equilibrium with its trivalent form (**Scheme 1.5**).[16] In the presence of base, the more reactive trivalent tautomer of diethyl phosphite is favored, which can be chlorinated by reacting with the formed quaternary ammonium chloride salt.[17] Subsequent nucleophilic attack installs the new phosphorous heteroatom bond. Since the seminal report in 1945, many synthetic methods using an Atherton-Todd disconnection have emerged (**Scheme 1.6**). The premise of the reaction is to transform the P-H bond into a P-X bond, which can then readily be substituted with an electron-rich heteroatom reaction partner. Further research in 2020 by Chen demonstrated a free radical-initiated Atherton Todd reaction (**Scheme 1.6**).[18] Diphenyl phosphine oxide **7** is chlorinated to generate a chlorophosphine oxide intermediate. The intermediate then was transformed to phosphinate **8** in 99% yield in the presence of methanol (**Scheme 1.6**) Their scope included aryl alcohols, aliphatic alcohols, and amines. Chloroform serves as the halide source in place of carcinogenic carbon tetrachloride.

Scheme 1.5 Tautomerism of Secondary Phosphine Oxide

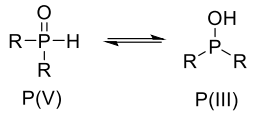

Han utilized this strategy to synthesize phosphinate **8** and reacted diphenylphosphine oxide **7** with SelectFluor to form a P-F bond in situ, which was displaced by methanol cosolvent to generate **8** in a yield of 93% (**Scheme 1.6**).[19]

Along with this, Prabhu also developed a strategy that involves the reaction between phosphite and heteroatom nucleophiles (alcohols, amines, sulfoximine) catalyzed by iodine and a peroxide additive (**Scheme 1.6**). Diethyl phosphite **9** reacts with iodine and hydrogen peroxide to form a P-I bond, which is then substituted by morpholine **10** to give phosphonamide **11** in a 78% yield (**Scheme 1.6**).[20] Benefits of this method include no metals, base, or prefunctionalization of reagents. However, the drawback of this method is the use of a harsh oxidant.

Therefore, to address this synthetic challenge, Han recently developed an electrochemical dehydrogenative phosphorylation of alcohols to synthesize phosphinates (**Scheme 1.6**).[21] Diphenyl phosphine oxide **7**, methanol, and TBAI (tetrabutylammonium iodide) are reacted under electrochemical conditions to give phosphinate **8** in a yield of 92% (**Scheme 1.6**). The benefit of electrochemistry is that the reaction is driven by electricity. Thus, no harsh

oxidizing or reducing agents are necessary because the redox reactions occur at the electrode surface. Anodic oxidation generates the reactive intermediate in situ, which is then trapped by methanol to afford the phosphinate product **8**.

Scheme 1.6 Recent Advances of The Atherton-Todd Reaction

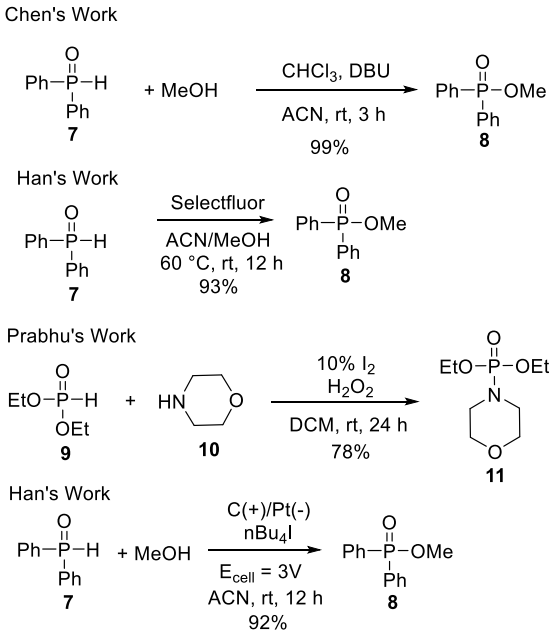

The Atherton-Todd reaction takes advantage of the low bond dissociation energy (BDE) of the P-H bond. This bond can be easily cleaved under basic or oxidative conditions. Diphenyl phosphine oxide has a P-H BDE of 317 kJ/mol.[22] Due to the oxygen's high electronegativity

(3.44), the P-O bond has a higher BDE of 80 kcal/mol.[23] This higher BDE can serve as an enthalpic energy barrier for reactions to be favorable.

One strategy to overcome this high BDE is to incorporate inductive effects. Replacement of alkane C-H bonds with C-F bonds will reduce the P-O BDE via inductive effect and allow for more facile nucleophilic substitution reactions. Okauchi utilized this strategy and demonstrated a transesterification reaction and displacement of the stable trifluoroethoxy group (**Scheme 1.7**).[24] Polyfluorinated phosphate **12** was reacted with alkyl alcohol **13** under basic conditions to generate **14** in a yield of 94% through substitution reaction (**Scheme 1.7**).[24] A disadvantage of this method is the requirement of prefunctionalized starting material **12**. The synthesis of **12** requires extra steps and limits the substrate scope of phosphonate.

Feringa has demonstrated a catalytic transesterification reaction using a copper (I) catalyst, ligand, aryliodonium salt **16**, and phosphonate **15q** to give mixed phosphonate **17** in a yield of 90% (**Scheme 1.7**).[25] The reaction proceeds through a copper (I) to copper (III) catalytic cycle. Oxidative insertion of the copper to the aryliodonium salt occurs, followed by an attack of the phosphoryl bond and reductive elimination to install the new P-O bond. This mild method offers a catalytic strategy to access mixed phosphonates. Although the Feringa group has reported the first catalytic mixed phosphonate synthesis, mixed phosphonate synthesis remains elusive.

The Kang research group has pioneered a triflic anhydride/pyridine activation strategy of pentavalent organophosphorus functional groups (phosphonate, phosphinate, phosphate, and thiophosphate) to synthesize mixed phosphorus compounds (**Scheme 1.7**).[26-28] Phosphonate

15a is reacted with triflic anhydride and pyridine, followed by the addition of phenol **18** to form mixed phosphonate **19** in a 92% yield (**Scheme 1.7**). This strategy offers direct functionalization of inert phosphonates in high yields and broad functional group tolerance. The key intermediate is a phosphoryl pyridin-1-ium, which is highly reactive towards nucleophilic substitution.

Scheme 1.7 Direct Aryloxylation Reaction from P-O Bond

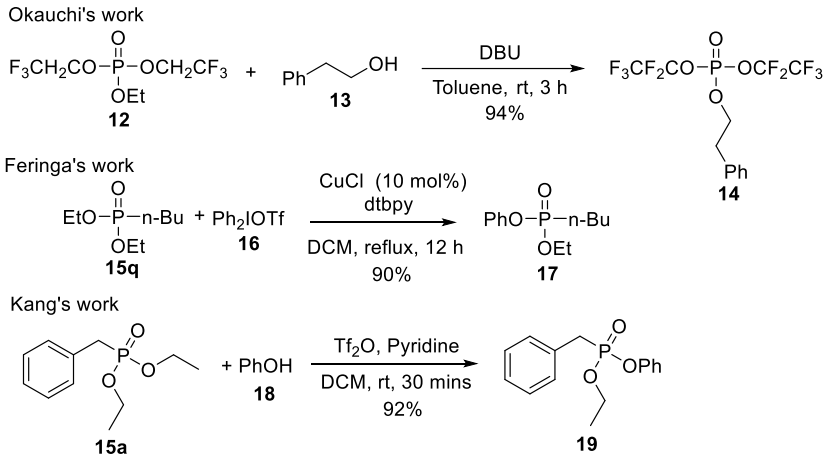

A unique P(V) functional group is the organophosphorus monoacid. Phosphonic monoacids have displayed unique biological properties as enzyme inhibitors, herbicides, and toxins (**Scheme 1.8**).[29-32] It is also commonly known that chiral BPA (binol phosphoric acid) is a popular catalyst for installing chiral centers on prochiral carbon atoms through reagent-

controlled enantioselective catalysis (**Scheme 1.8**).[33, 34] Radiochemists have also found a use for phosphorous mono acids as an extractant for metal complexes (**Scheme 1.8**).[35]

Scheme 1.8 Selected Applications of Phosphorous Monoacids

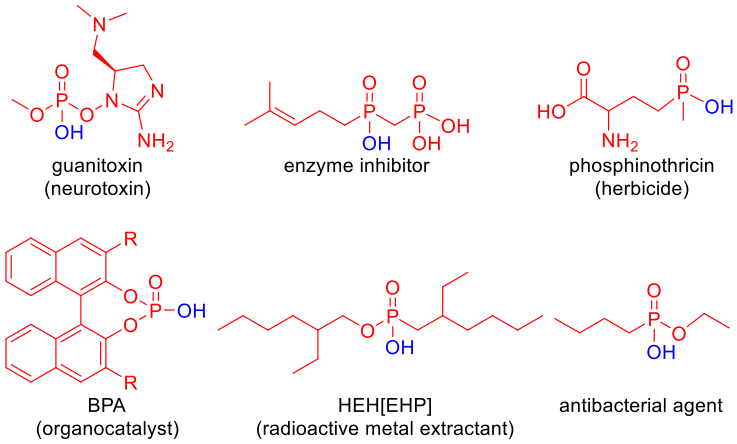

With many essential uses, the synthetic community has tried to synthesize this rare and elusive functional group. The common synthetic methods for synthesizing phosphorous monoacids are base hydrolysis, sodium azide-mediated deprotection reaction, triflic acid-catalyzed debenzylation, and Krapcho-type hydrolysis (**Scheme 1.9**).[36-39] Zhang employed base hydrolysis by heating phosphonate **15** in aqueous sodium hydroxide to form **20l** in a yield of 50% (**Scheme 1.9**).[36] This reaction, however, requires close monitoring to prevent the formation of the diacid. Gobec reported a sodium azide deprotection reaction by heating phosphonate **15**

with sodium azide in dimethylformamide (DMF) at elevated temperatures to form **20q** in a yield of 85% (**Scheme 1.9**).[37] These conditions are also harsh as prolonged heating is required, and sodium azide may be a safety concern for large and process-scale synthesis due to its high nitrogen content. Sodium azide, when heated to high temperatures, can rapidly decompose into sodium and three molecules of nitrogen gas.[40] In addition, the scope of the sodium azide deprotection reaction is limited to alkyl phosphonates.

The Han group released a debenzylation reaction of phosphonates using a triflic acid catalyst and heating conditions to form phosphoric acids.[39] Phosphonate **21** is heated with catalytic triflic acid to furnish **22** in a high yield of 93% (**Scheme 1.9**). A drawback to this synthetic method is that the method is only selective for a benzyl group. If multiple benzyl groups are present, they will be globally deprotected to the diacid. Flynn and coworkers have Krapcho hydrolysis to convert activated phosphonate **23** to **24** by refluxing sodium iodide in acetone (**Scheme 1.9**).[38] However, this method requires electron-withdrawing groups on the phosphonate to increase reactivity.

Although different synthetic approaches have been developed for mono phosphoric acid, there is a knowledge gap in developing a safe, chemoselective, substrate-tolerable transformation. This transformation should also avoid transition metal catalyst and sensitive chloride-containing reagents.

Scheme 1.9 Synthetic Methods of Phosphorus Monoacids

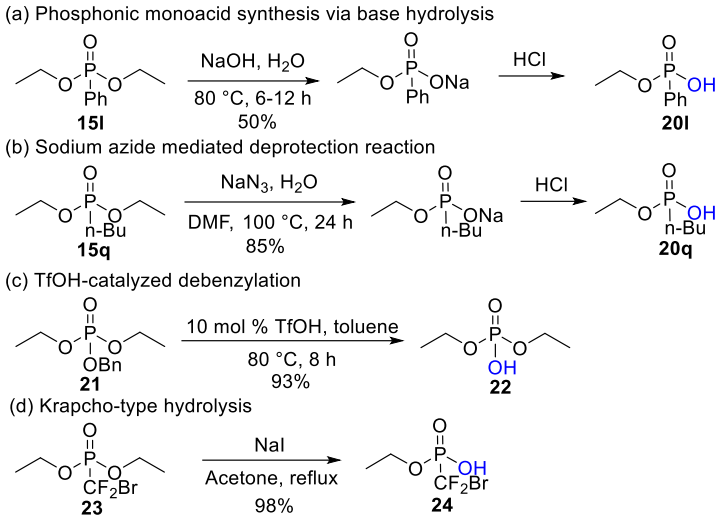

1.2 Specific Aim

This project aims to develop a synthetic method to access phosphorous monoacids that is mild, safe, chemoselective, and avoids using metal catalysts and sensitive chlorinating reagents.[41] The methodology should apply to alkyl and aryl phosphonates, have functional group tolerance, and be applied in synthesizing an active pharmaceutical ingredient (API).

1.3 Hydrolysis of P(V) Compounds to Form Organophosphorus Monoacids

Table 1.1 Optimization of Reaction Conditions for Phosphonic Acid Synthesis[a]

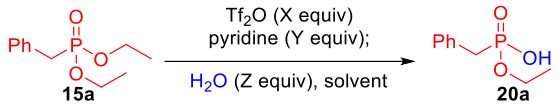

entry	X: Y: Z	solvent	Yield (%)[b]
1[c]	1.5: 2.0: 10	DCM	71
2[c]	1.5: 2.0: 10	ether	66
3[c]	1.5: 2.0: 10	CH_3CN	54
4[c]	1.5: 2.0: 10	DCE	76
5	1.5: 2.0: 10	DCM	79
6	1.5: 2.0: 12	DCM	83
7	1.5: 2.0: 20	DCM	94

[a]Reaction conditions: **15a** (0.2 mmol), Tf_2O (0.3 mmol), pyridine (0.4 mmol) in solvent (1.0 mL) for 10 min, then H_2O (4.0 mmol) for 1 h.

[b]Isolated yield. [c]30 minutes for the formation of the phosphoryl pyridinium.

We hypothesized that our triflic anhydride/pyridine activation strategy could be applied to P(V) functional groups to form a phosphoryl pyridin-1-ium intermediate, which can then be reacted with H_2O to give monosubstituted phosphonic acid. To test our hypothesis, benzyl phosphonate **15a** was employed as a model substrate (**Table 1.1**). Initially, the reaction was tested in DCM (dichloromethane) with an equivalence of 1.5:2.0:10 of triflic anhydride: pyridine: H_2O and gave **20a** with an isolated yield of 71% (**Table 1.1**, entry 1). Other solvents, such as ether, acetonitrile, and DCE (dichloroethane, did not dramatically increase the product yield (**Table 1.1**, entries 2-4). However, decreasing the time for the intermediate formation from 30 minutes to 10 minutes slightly improved the product yield to 79% (**Table 1.1**, entry 5). Presumably, this is due to the decomposition of the highly reactive intermediate during longer reaction times. Furthermore, the isolated yield was increased to 83% by adjusting the molar equivalent of H_2O to twelve (**Table 1.1**, entry 6). Since a positive effect on yield was observed by

increasing the equivalent of H_2O, the equivalence was further increased to twenty, and product **20a** was generated with a 94% yield (**Table 1.1**, entry 7). The excess of H_2O also serves to quench the unreacted triflic anhydride.

With the optimized reaction conditions, the reaction was tested with diverse phosphonates to probe the electronic and steric effects on the reaction outcome (**Table 1.2**). Benzylic and naphthyl phosphonates **15a** and **15b** gave the products **20a** and **20b** in a high yield of 94%. Alknyl phosphonate **15c** was well tolerated, providing **20c** with a high yield of 94% and no side reactions. Benzylic phosphonates **15d** and **15e** containing electron-donating groups (4-Me and 4-MeO) furnished the product **20d** and **20e** in 57% and 80% yields, respectively. Halogen-containing phosphonates **15f**-**15j** (4-Cl, 4-F, 4-Br, 2-F, and 2,4 dichloro) were also tolerated, giving the products **20f**-**20j** in synthetically useful to high yields of 34%-80%. A benzylic phosphonate **15k,** which contains a strong electron-withdrawing group (4-CF_3), formed product **20k** in a low yield of 32%. The low yield can be attributed to the reduced nucleophilicity of the phosphoryl bond, forming less reactive intermediate. Aryl phosphonates **15l** and **15m** gave the products **20l** and **20m** in synthetically useful yields of 64% and 49%, respectively. The steric effect was next investigated by employing sterically hindered phosphonate **15n**, which was still suitable to give product **20n** in a yield of 66%. Heterocyclic phosphonate **15o** was tolerated to give furyl phosphonic acid **20o** in a high yield of 70%. Aliphatic phosphonates **15p** and **15q** were suitable substrates to give **20p** and **20q** in yields of 66% and 79%, respectively.

Table 1.2 Phosphonate Electrophile Substrate Scope[a]

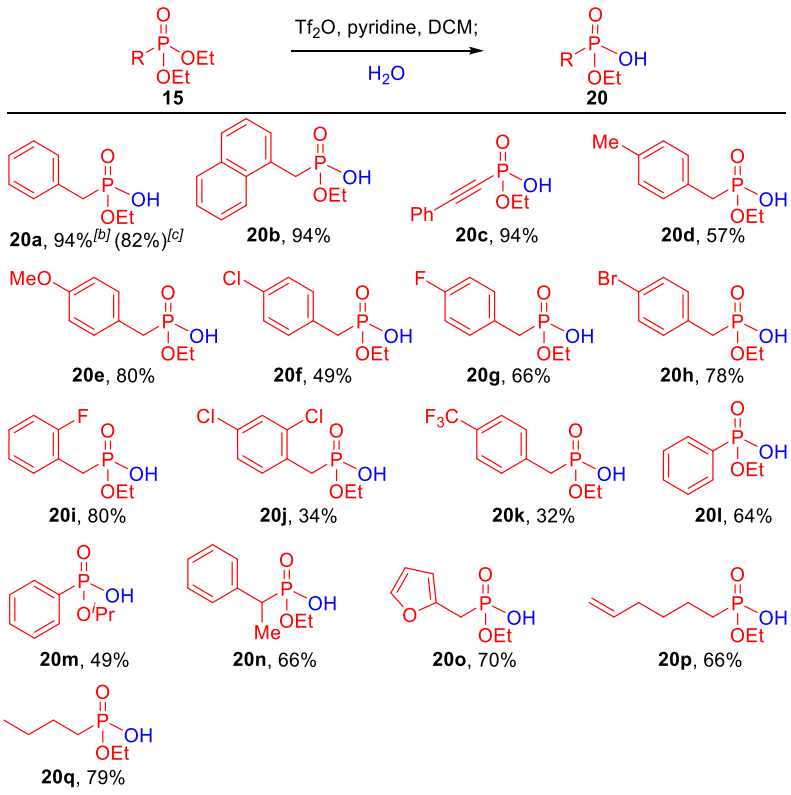

[a]Reaction conditions: **30** (0.2 mmol), Tf_2O (0.3 mmol), pyridine (0.4 mmol) in DCM (1.0 mL) for 10 min, then H_2O (4.0 mmol) for 1 h.

[b]Isolated yield.[c]Scale up experiment (5.0 mmol)

This transformation tolerates a wide range of substrate scope including aryl, alkyl, heteroarene, and alkynyl phosphonates. Aliphatic phosphonate **15q** is particularly interesting as it is an antigen 85c inhibitor of the mycobacterium cell wall and has application as a novel anti-tuberculosis API against drug-resistant forms of tuberculosis.[37] This methodology is applicable for synthesizing potential APIs. Next, a scale-up experiment (5.0 mmol) was successfully performed without sacrificing the product yield (**20a**, 82%).

Other P(V) functional groups (phosphinate and phosphoric acid) were explored to demonstrate the broad transformative applicability of the developed methodology (**Table 1.3**). By directly comparing the yields of **26a-26d** vs **26e-26h**, monosubstituted phosphinic acid yields are higher and more consistent than the yields of monosubstituted phosphoric acids (**Table 1.3**). This is presumably due to the increased nucleophilicity of the terminal oxygen of the phosphoryl bond being directly attached to electron-donating carbon atoms. The high electronegativity of the oxygen atom will result in a more electropositive and less reactive phosphoryl bond. Diphenyl phosphonate **25a** afforded the target product **26a** in a high yield of 81%. Benzylic phosphinates **25b** and **25c** provided the corresponding products **26b** and **26c** with 75% and 89% yield, respectively. Dibenzyl phosphinate **25d** also furnished the desired product **26d** in a yield of 75%.

Phosphates are the least reactive of P(V) functional groups towards nucleophilic substitution reactions.[42] The yields observed from monophosphoric acid synthesis were lower but tolerated (**Table 1.3**). Halogenated phosphate **25e** generated the product **26e** in a moderate yield of 67%. A phosphate containing an electron donating group (4-MeO) **25f** positively affected the yield of **26f**, giving 84%. Next, the steric effect was evaluated, and phosphates containing bulky aromatic groups (biphenyl and naphthyl) **25g** and **25h** were well tolerated, giving the target products **26g** and **26h** in moderate yields of 45% and 56%, respectively.

Table 1.3 Phosphinate/Phosphate Electrophile Substrate Scope[a]

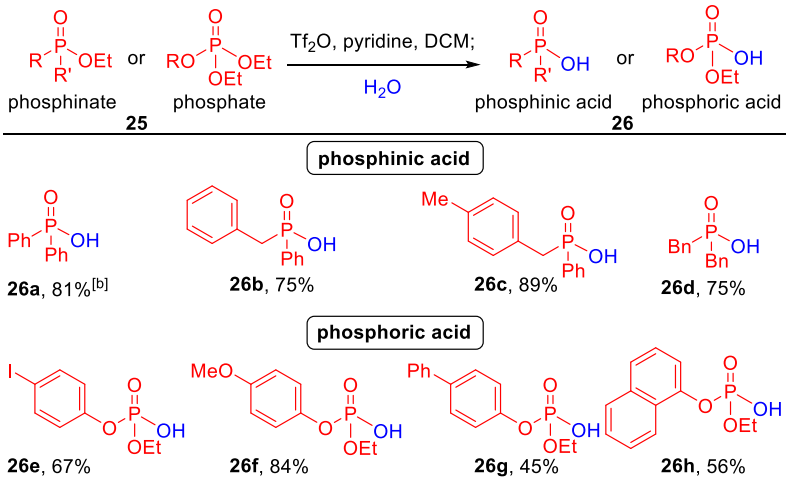

[a]Reaction conditions: **25** (0.2 mmol), Tf_2O (0.3 mmol), pyridine (0.4 mmol) in DCM (1.0 mL) for 10 min, then H_2O (4.0 mmol) for 1 h.

[b]Isolated yield.

A reasonable mechanism is proposed based on our group's previous work and outcomes from control experiments. (**Scheme 1.10**).[26] The terminal oxygen of phosphonate **15a** attacks triflic anhydride and forms phosphonium triflate **I**. Phosphonium triflate **I** then reacts with the generated triflate anion via an unimolecular substitution reaction (S_N1) type mechanism to create intermediate **II** and ethyl triflate byproduct. The triflate leaving group of **II** is then substituted by pyridine to form a highly reactive phosphorylpyrdin-1-ium intermediate **III**. Finally, adding H_2O to **III** forms product **20a** through a substitution reaction.

Scheme 1.10 Proposed Deprotection Mechanism

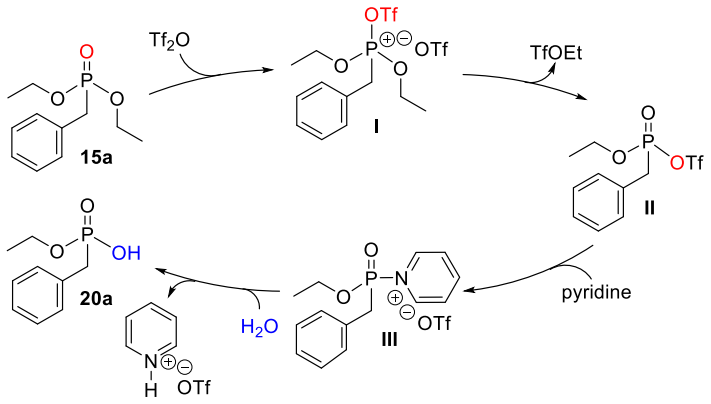

1.4 ^{18}O Isotope Labeling Study

Scheme 1.11 Oxygen Isotope Labeling Control Experiment

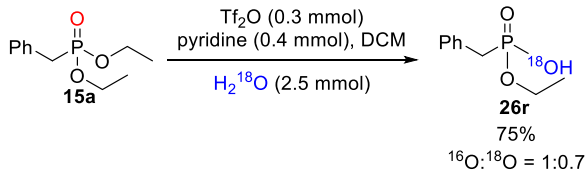

To gain further insight into the reaction mechanism, ^{18}O-labeled water ($H_2{}^{18}O$) was used as the nucleophile under the reaction conditions (**Scheme 1.11**). The experimental outcome

from the high resolution mass spectrometry spectrum (HRMS) reveals the ^{18}O was incorporated into the product at a ratio of 0.7:1.0 versus the ^{16}O product. A possible explanation for the ratio of unlabeled to radiolabeled oxygen is the hydrolysis of the product with non-labeled water during the acid/base workup procedure. The results tell us that the oxygen from the final product is from the ^{18}O-labeled water and not from the starting material, which provides evidence for the last step of the proposed mechanism.

Figure 1.1 HRMS Spectrum of ^{18}O-**25r**

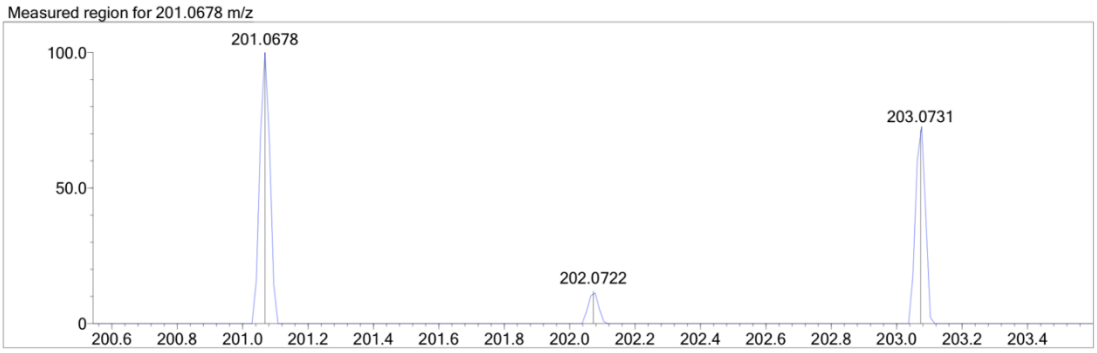

Base peak m/z 201.0678

Formula	Rel. Inten.	Ion	Meas. m/z	Pred. m/z
$C_9H_{13}O_3P$	100.00	[M+H]+	201.0678	201.0675
$C_9H_{13}O_2{}^{18}OP$	71.42	[M+H]+	203.0731	203.0718

1.5 Conclusion

We have developed a facile synthetic strategy to forge a P-O bond through a triflic anhydride/pyridine activation strategy that allows access to difficult to synthesize phosphorous monoacids. The method is chemoselective as only one alkoxy group is deprotected and is tolerant to a wide range of steric and electronic factors. Also, the method improves upon pre-existing methods that rely on challenging to handle chloride reagents, potentially explosive azide reagents, and harsh reaction conditions. The methodology has also been utilized to synthesize an active pharmaceutical ingredient with anti-tuberculosis properties. Phosphorous monoacids remain an elusive functional group in synthetic organic chemistry due to limited synthesis methods. These monoacids have great potential for use as active pharmaceutical ingredients, catalysts, and nucleophiles in intra/intermolecular reactions.

1.6 Experimental Procedure

1.6.1 General information

All reactions were carried out under air atmosphere in oven-dried glassware with magnetic stirring bar. Dry solvents (tetrahydrofuran, toluene, acetonitrile, diethyl ether, and dichloromethane) were obtained by solvent purification system under argon. All commercially available reagents were used as received without further purification. The tubes used for the reaction were showed in **Figure S1**. Purification of reaction products was carried out by flash column chromatography using silica gel 60 (230-400 mesh). Analytical thin layer chromatography was performed on 0.25 mm aluminum-backed silica gel 60-F plates. Visualization was accompanied with UV light and $KMnO_4$ solution. Concentration under reduced

pressure refers to the removal of volatiles using a rotary evaporator attached to a dry diaphragm pump (10-15 mm Hg) followed by pumping to a constant weight with an oil pump (<300 mTorr). Infrared (IR) spectra were recorded on an IR spectrometer with KBr wafers or a film on KBr plate. High-resolution mass spectra (HRMS) were recorded on liquid chromatography mass spectrometry ion trap time of flight (LCMS-IT-TOF) mass spectrometer using electrospray ionization (ESI) or atmospheric pressure chemical ionization (APCI). ^{1}H NMR spectra were recorded in $CDCl_3$ on 400 MHz NMR spectrometer. The ^{1}H chemical shifts are referenced to residual solvent signals at δ 7.26 ($CHCl_3$) or δ 0.00 (TMS). ^{1}H NMR coupling constants (*J*) are reported in Hertz (Hz) and multiplicities are indicated as follows: s (singlet), bs (broad singlet), d (doublet), t (triplet), q (quartet), m (multiplet), dd (doublet of doublets), dt (doublet of triplets), td (triplet of doublets), tt (triplet of triplets). ^{13}C NMR spectra were proton decoupled and recorded in $CDCl_3$ on 100.5 MHz NMR spectrometer. The ^{13}C chemical shifts are referenced to solvent signals at δ 77.16 ($CDCl_3$). ^{31}P NMR spectra were proton decoupled and recorded in $CDCl_3$ on 162 MHz NMR spectrometer. ^{31}P chemical shifts are reported relative to 85% H_3PO_4 (0.00 ppm) as an external standard.

Scheme S1. Pictorial description of reaction tubes for the reaction. A is 2 dram vial, B is 15 mL flask, and C is 30 mL flask.

1.6.2 General Procedure 1 Phosphonic Acid Synthesis

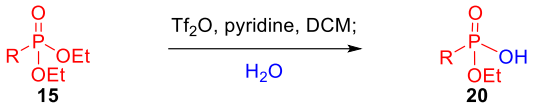

Phosphonate **15** (0.2 mmol, 1.0 equiv) was dissolved in DCM (1.0 mL) in a 2 dram vial. Tf_2O (0.3 mmol, 1.5 equiv) followed by pyridine (0.4 mmol, 2.0 equiv) was added to the solution and stirred for 10 mins. H_2O (4.0 mmol, 20.0 equiv) was added to the solution and stirred for 1 h. The mixture was concentrated to remove DCM and dissolved in Et_2O (2.0 mL). NaOH (0.35 M, 2.0 mL) was added to the solution and stirred for 30 mins. The solution was then transferred to a separatory funnel, and the aqueous layer was collected. The aqueous layer was acidified with 5% HCl (5.0 ml) and extracted with DCM (3x10.0 mL). The organic extract was dried over Na_2SO_4, filtered, and then concentrated to give **20**.

1.6.3 General Procedure 2 Phosphinic or Phosphoric acid Synthesis

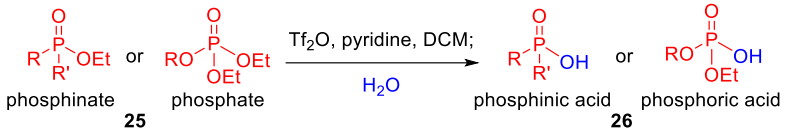

Phosphinate/Phosphate (0.2 mmol, 1.0 equiv) was dissolved in DCM (1.0 mL). Tf_2O (0.3 mmol, 1.5 equiv) followed by pyridine (0.4 mmol, 2.0 equiv) was added to the solution and stirred for 10 mins. H_2O (4.0 mmol, 20.0 equiv) was added to the solution and stirred for 1 h. The mixture was concentrated to remove DCM and dissolved in Et_2O (2.0 mL). NaOH (0.35 M, 2.0 mL) was added to the solution and stirred for 1 h. The solution was then transferred to a separatory funnel, and the aqueous layer was removed. The aqueous layer was acidified with 5% HCl (5.0 mL) and extracted with DCM (3x10.0 mL). The organic extract was dried over Na_2SO_4, filtered, and then concentrated to give **26**.

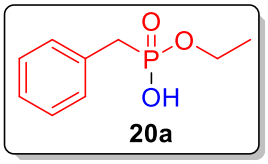

20a

ethyl hydrogen benzylphosphonate (20a). 37.5 mg, 94%; as an oil; **IR** ν (KBr, cm^{-1}) 3062, 2981, 2920, 2318, 1496, 1246, 1053, 786, 689, 586; ^{1}H NMR (400 MHz, $CDCl_3$) δ 11.38 (s, 1H), 7.30-7.20 (m, 5H), 3.90-3.83 (m, 2H), 3.02 (d, *J* = 22.0 Hz, 2H), 1.19 (t, *J* = 7.2 Hz); ^{13}C NMR (100.5 MHz, $CDCl_3$) δ 131.5 (d, *J* = 8.9 Hz), 128.4 (d, *J* = 3.0 Hz), 127.9 (d, *J* = 6.7 Hz), 126.8 (d, *J* = 3.7 Hz), 61.6 (d, *J* = 7.0 Hz), 33.7 (d, *J* = 140.1 Hz), 16.1 (d, *J* = 6.0 Hz); ^{31}P NMR (162 MHz, $CDCl_3$): δ 29.50; HRMS(ESI): m/z calcd. for $C_{10}H_{13}O_3P$ ([M+H]+): 201.0675; found 201.0675.

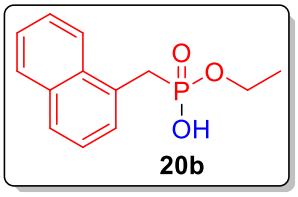

20b

ethyl hydrogen (naphthalen-1-ylmethyl)phosphonate (20b). 46.8 mg, 94%; as an oil; **IR** ν (KBr, cm^{-1}) 3047, 2981, 2283, 1647, 1597, 1396,1041, 779.2, 640, 555; ^{1}H NMR (400 MHz, $CDCl_3$) δ 11.58 (s, 1H), 7.99 (d, *J* = 8.4 Hz, 1H), 7.78-7.75 (m, 1H), 7.69 (d, *J* = 8.4 Hz, 1H), 7.49-7.41 (m, 2H), 7.38-7.32 (m, 2H), 3.72-3.65 (m, 2H), 3.41 (d, *J* = 22.4 Hz, 2H), 1.05 (t, *J* = 6.8 Hz, 3H); ^{13}C NMR (100.5 MHz, $CDCl_3$) δ 133.8 (d, *J* = 2.2 Hz), 132.0 (d, *J* = 5.3 Hz), 128.6 (d, *J* = 7.4 Hz), 128.4, 127.9 (d, *J* = 9.7 Hz), 127.6 (d, *J* = 4.5 Hz), 126.0, 125.7, 125.3 (d, *J* = 4.4 Hz), 124.5 (d, *J* = 1.5 Hz), 61.6 (d, *J* = 6.7 Hz), 30.7 (d, *J* = 141.3 Hz), 16.1 (d, *J* = 6.7 Hz), ^{31}P NMR (162 MHz, $CDCl_3$): δ 29.44; HRMS(ESI): m/z calcd. for $C_{13}H_{15}O_3P$ ([M+H]+): 251.0832; found 251.0813.

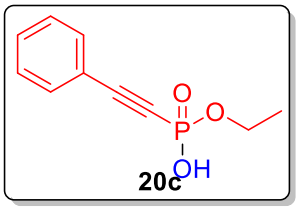

20c

ethyl hydrogen (phenylethynyl)phosphonate (20c). 39.0 mg, 94%; as an oil; **IR** ν (KBr, cm^{-1}) 3059, 2985, 2904, 2465, 1639, 1392, 1037, 856, 759, 690, 540; ^{1}H NMR (400 MHz, $CDCl_3$) δ 11.95 (s, 1H), 7.55-7.53 (m, 2H), 7.44-7.40 (m, 1H), 7.35-7.31 (m, 2H), 4.26-4.18 (m, 2H), 1.39 (t, *J* = 7.2 Hz); ^{13}C NMR (100.5 MHz, $CDCl_3$) δ 132.6 (d, *J* = 2.2 Hz), 130.6, 128.5, 119.6 (d, *J* = 6.0 Hz), 98.6 (d, *J* = 56.1 Hz), 80.6,

63.3 (d, *J* = 5.2 Hz), 16.0 (d, *J* = 7.4 Hz), ^{31}P NMR (162 MHz, $CDCl_3$): δ -3.47; HRMS(ESI): m/z calcd. for $C_{10}H_{11}O_3P$ ([M+H]+): 211.0519; found 211.0511.

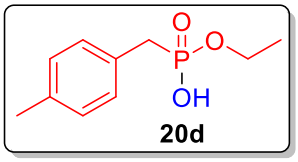

20d

ethyl hydrogen 4-methylbenzylphosphonate (20d). 24.4 mg, 57%; as a white solid; mp 64-65 °C; **IR** ν (KBr, cm^{-1}) 2989, 2920, 2310, 1643, 1516, 1246, 1199, 1035, 983; ^{1}H NMR (400 MHz, $CDCl_3$) δ 10.48 (s, 1h), 7.14 (d, *J* = 7.6 Hz, 2H), 7.08 (d, *J* = 8.0 Hz, 2H), 3.87 (t, *J* = 21.6 Hz, 2H), 2.98 (d, *J* = 20 Hz , 2H), 2.28 (s, 3H), 1.20 (t, *J* = 6.8 Hz, 3H); ^{13}C NMR (100.5 MHz, $CDCl_3$) δ 136.3, 129.7 (d, *J* = 3.8 Hz), 129.1, 128.3 (d, *J* = 8.2 Hz), 61.5 (d, *J* = 4.4 Hz), 33.4 (d, *J* = 140.2 Hz), 21.0, 16.2 (d, *J* = 3.7 Hz), ^{31}P NMR (162 MHz, $CDCl_3$): δ 30.13; HRMS(ESI): m/z calcd. for $C_{10}H_{15}O_3P$ ([M+H]+): 215.0832; found 215.0832.

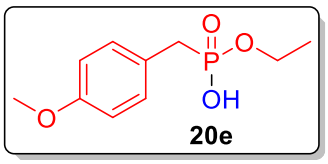

20e

ethyl hydrogen 4-methoxybenzylphosphonate (20e). 36.8 mg, 80%; as a white solid; mp 102-104 °C; **IR** ν (KBr, cm^{-1}) 3035, 2978, 2912, 2322, 1608, 1512, 1253, 987, 844, 567; ^{1}H NMR (400 MHz, $CDCl_3$) δ 11.71 (s, 1h), 7.17 (d, *J* = 8.0 Hz, 2H), 6.83 (d, *J* = 8.8 Hz, 2H), 3.87 (t, *J* = 6.8 Hz, 2H), 3.74 (s, 3H), 2.98 (d, *J* = 21.2 Hz, 2H) 1.20 (t, *J* = 7.2 Hz, 3H); ^{13}C NMR (100.5 MHz, $CDCl_3$) δ 158.5, 130.8 (d, *J* = 5.2 Hz), 123.3 (d, *J* = 8.2 Hz), 113.9, 61.5 (d, *J* = 6.7 Hz), 55.1, 32.8 (d, *J* = 143.6 Hz), 16.2 (d, *J* = 5.2 Hz), ^{31}P NMR (162 MHz, $CDCl_3$): δ 30.22; HRMS(ESI): m/z calcd. for $C_{10}H_{15}O_4P$ ([M+H]+): 231.0781; found 231.0781.

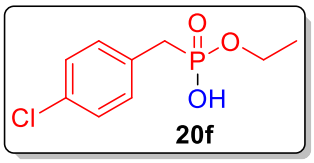

20f

ethyl hydrogen 4-chlorobenzylphosphonate (20f). 22.9 mg, 49%; as a white solid; mp 83-84 °C; **IR** ν (KBr, cm^{-1}) 2981, 2603, 2276, 1681, 1411, 1192, 840, 655; ^{1}H NMR (400 MHz, $CDCl_3$) δ 10.31 (s, 1H), 7.27-7.25 (m, 2H), 7.19 (dd, *J* = 8.4 Hz, *J* = 1.6 Hz, 2H), 3.91-3.84 (m, 2H) 3.01 (d, *J* = 22.0 Hz, 2H), 1.22 (t, *J* =

6.8 Hz, 3H); ^{13}C NMR (100.5 MHz, $CDCl_3$) δ 132.8 (d, *J* = 4.5 Hz), 131.7 (d, *J* = 6.7 Hz), 129.9 (d, *J* = 8.9 Hz), 128.6 (d, *J* = 3.0 Hz), 61.7 (d, *J* = 6.7 Hz), 33.1 (d, *J* = 141.3 Hz), 16.2 (d, *J* = 5.9 Hz), ^{31}P NMR (162 MHz, $CDCl_3$): δ 29.04; HRMS(ESI): m/z calcd. for $C_9H_{12}O_3PCl$ ([M+H]+): 235.0285; found 235.0264.

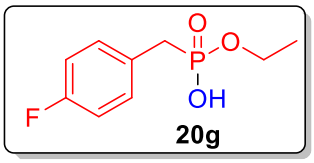

20g

ethyl hydrogen 4-fluorobenzylphosphonate (20g). 28.9 mg, 66%; as a white solid; mp 94-96 °C; **IR** ν (KBr, cm^{-1}) 3051, 2989, 2322, 1600, 1512, 1219, 987, 844, 794, 567; ^{1}H NMR (400 MHz, $CDCl_3$) δ 11.64 (s, 1H), 7.26-7.22 (m, 2H), 6.98-6.96 (m, 2H), 3.89-3.88 (m, 2H), 3.14-3.06 (m, 2H), 1.21 (t, *J* = 6.4 Hz, 3H); ^{13}C NMR (100.5 MHz, CH_3OD) δ 161.9 (dd, *J* = 243.5 Hz, 3.8 Hz), 131.2 (d, *J* = 7.4 Hz), 128.3 (dd, *J* = 9.7 Hz, 3.8 Hz) , 114.7 (dd, *J* = 21.7 Hz, 3.0 Hz), 61.4 (d, *J* = 6.7 Hz) , 32.3 (d, *J* = 137.6 Hz), 15.3 (d, *J* = 6.7 Hz); ^{31}P NMR (162 MHz, CH_3OD): δ 26.68; HRMS(ESI): m/z calcd. for $C_9H_{12}O_3FP$ ([M+H]+): 219.0581; found 219.0557.

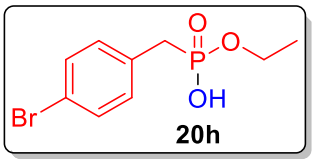

20h

ethyl hydrogen 4-bromobenzylphosphonate (20h). 42.8 mg, 78%; as a white solid; mp 83-85 °C; **IR** ν (KBr, cm^{-1}) 2981, 2276, 1693, 1489, 1404, 1192, 987, 837, 628; ^{1}H NMR (400 MHz, $CDCl_3$) δ 12.23 (s, 1H), 7.41 (d, *J* = 8.0 Hz, 2H), 7.13 (dd, *J* = 8.2 Hz, *J* = 2.4 Hz, 2H), 3.91-3.83 (m, 2H), 2.99 (d, *J* = 22.0 Hz, 2H), 1.22 (t, *J* = 7.2 Hz, 3H); ^{13}C NMR (100.5 MHz, $CDCl_3$) δ 131.6, 131.5, 130.5 (d, *J* = 8.0 Hz), 120.9 (d, *J* = 5.0 Hz), 61.7 (d, *J* = 7.4 Hz), 33.2 (d, *J* = 141.3 Hz), 16.2 (d, *J* = 6.7 Hz); ^{31}P NMR (162 MHz, $CDCl_3$): δ 28.76; HRMS(ESI): m/z calcd. for $C_9H_{12}O_3BrP$ ([M+H]+): 278.9780 ; found 278.9752.

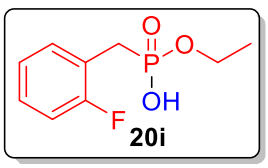

20i

ethyl hydrogen 2-fluorobenzylphosphonate (20i). 34.8 mg, 80%; as a white solid; mp 66-68 °C; **IR** ν (KBr, cm^{-1}) 3043, 2981, 2912, 2310, 1492,

1041, 860, 756, 555; ^{1}H NMR (400 MHz, $CDCl_3$) δ 11.27 (s, 1H), 7.35 (t, *J* = 7.2 Hz, 1H), 7.20 (q, *J* = 7.2 Hz, 2h), 7.09-7.01 (m, 2H), 3.95 (s, 2H), 3.13 (d, *J* = 19.6 Hz, 2H), 1.22 (t, *J* = 7.2 Hz, 3H); ^{13}C NMR (100.5 MHz, $CDCl_3$) δ 160.9 (d, *J* = 246.8 Hz), 131.8 (d, *J* = 2.2 Hz), 128.6 (d, *J* = 8.2 Hz), 124.0 (d, *J* = 3.7 Hz), 118.9 (d, *J* = 13.4 Hz), 115.3 (d, *J* = 22.4 Hz), 61.9 (d, *J* = 34 Hz), 26.9 (d, *J* = 134.5 Hz), 16.1; ^{31}P NMR (162 MHz, $CDCl_3$): δ 28.81; HRMS(ESI): m/z calcd. for $C_9H_{12}O_3FP$ ([M+H]+): 219.0581; found 219.0560.

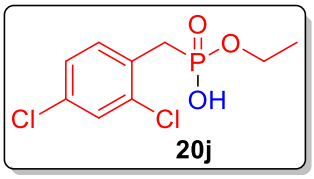

20j

ethyl hydrogen 2,4-dichlorobenzylphosphonate (20j). 20.1 mg, 34%; as an oil; **IR** ν(KBr, cm^{-1}) 2981, 2276, 1589, 1041, 852, 740, 686, 597; ^{1}H NMR (400 MHz, $CDCl_3$) δ 10.41 (s, 1H), 7.39 (d, *J* = 2.0 Hz, 1H), 7.32 (d, *J* = 8.4 Hz, 1H), 7.19 (dd, *J* = 8.4, *J* = 2.0 Hz, 1H), 3.97-3.93 (m, 2H), 3.26 (d, *J* = 22.0 Hz, 2H), 1.25 (t, *J* = 6.8 Hz, 3H); ^{13}C NMR (100.5 MHz, $CDCl_3$) δ 135.2, 133.4, 132.4, 129.4, 128.5, 127.0, 62.0, 30.4 (d, *J* = 151.1 Hz), 16.2 ; ^{31}P NMR (162 MHz, $CDCl_3$): δ 28.19; HRMS(ESI): m/z calcd. for $C_9H_{11}O_3PCl_2$ ([M+H]+): 268.9864; found 268.9864.

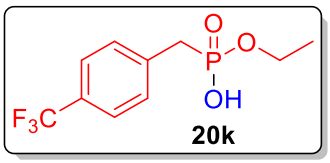

20k

ethyl hydrogen 4-(trifluoromethyl)benzylphosphonate (20k). 17.0 mg, 32%; as a white solid; mp 133-135 °C; **IR** ν(KBr, cm^{-1}) 3055, 2989, 2935, 2268, 1674, 1338, 1118, 983, 852, 628; ^{1}H NMR (400 MHz, $CDCl_3$) δ 10.0 (s, 1H), 7.55 (d, *J* = 2.0 Hz, 2H), 7.38 (d, *J* = 2.0 Hz, 2H), 3.87 (s, 2H), 3.11 (d, *J* = 19.2 Hz, 2H), 1.20 (t, *J* = 7.2 Hz, 3H); ^{13}C NMR (100.5 MHz, $CDCl_3$) δ 135.7, 130.2, 129.2 (q, *J* = 32.86 Hz), 125.4-125.2 (m) , 122.7, 61.8, 33.9, (d, *J* = 121.2 Hz), 16.1; ^{31}P NMR (162 MHz, $CDCl_3$): δ 28.65; HRMS(ESI): m/z calcd. for $C_{10}H_{12}O_3F_3P$ ([M+H]+): 269.0549; found 269.0531.

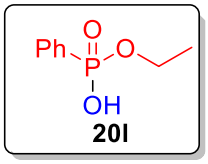

20l

ethyl hydrogen phenylphosphonate (20l). 23.7 mg, 64%; as an oil; **IR** ν (KBr, cm^{-1}) 3059, 2981, 2357, 1438, 1134, 748, 694; ^{1}H NMR (400 MHz, $CDCl_3$) δ 11.33 (s, 1H), 7.82-7.77 (m, 2H), 7.57-7.43 (m, 3H), 4.15-4.04 (m, 2H), 1.33-1.25 (m, 3H); ^{13}C NMR (100.5 MHz, $CDCl_3$) δ 132.2, 131.3 (d, *J* = 10.45 Hz), 128.5, 128.4, 62.0, 16.2; ^{31}P NMR (162 MHz, $CDCl_3$): δ 21.21; HRMS(ESI): m/z calcd. for $C_8H_{11}O_3P$ ([M+H]+): 187.0519; found 187.0516.

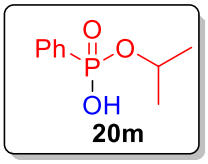

20m

isopropyl hydrogen phenylphosphonate (20m). 19.7 mg**,** 49%; as an oil; **IR** ν (KBr, cm^{-1}) 3059, 2978, 2927, 2272, 1215, 995, 748; ^{1}H NMR (400 MHz, $CDCl_3$) δ 9.54 (s, 1H), 7.82-7.77 (m, 2H), 7.53-7.49 (m, 1H), 7.42-7.41 (m, 2H), 4.70-4.64 (m, 1H), 1.29 (td, *J* = 29.6, 6.0 Hz, 6H); ^{13}C NMR (100.5 MHz, $CDCl_3$) δ 131.7 (d, *J* = 9.6 Hz), 131.2 (d, *J* = 10.4 Hz), 128.5 (d, *J* = 5.2 Hz), 128.2 (d, *J* = 3.0 Hz), 71.0 (d, *J* = 5.9 Hz), 23.9 (d, *J* = 4.0 Hz), 23.8 (d, *J* = 3.9 Hz) ; ^{31}P NMR (162 MHz, $CDCl_3$): δ 20.63; HRMS(ESI): m/z calcd. for $C_9H_{13}O_3P$ ([M+H]+): 201.0675; found 201.0671.

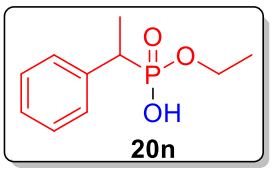

20n

ethyl hydrogen (1-phenylethyl)phosphonate (20n). 28.2 mg, 66%; as an oil; **IR** ν (KBr, cm^{-1}) 3059, 2981, 2935, 2310, 1492, 1199, 810, 771, 689, 597 ^{1}H NMR (400 MHz, $CDCl_3$) δ 11.94 (s, 1H), 7.32-7.26 (m, 4H), 7.25-7.19 (m, 1H), 3.89-3.78 (m, 2H), 3.10 (dq, *J* = 14.8 Hz, *J* = 7.2 Hz, 1H), 1.51 (dd, *J* = 18.4 Hz, *J* = 7.6 Hz, 3H), 1.18-1.15 (m, 3H); ^{13}C NMR (100.5 MHz, $CDCl_3$) δ 137.4 (d, *J* = 6.7 Hz), 128.7 (d, *J* = 5.9 Hz), 128.3 (d, *J* = 2.2 Hz) 126.9 (d, *J* = 3.0 Hz), 61.6 (d, *J* = 7.4 Hz), 38.0 (d, *J* = 39.39 Hz), 16.2 (d, *J* = 5.9 Hz), 15.1 (d, *J* = 5.2 Hz), ^{31}P NMR (162 MHz, $CDCl_3$): δ 32.89; HRMS(ESI): m/z calcd. for $C_{10}H_{15}O_3P$ ([M+H]+): 215.0832; found 215.0810.

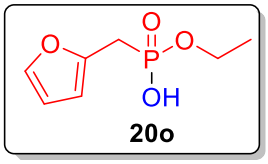

20o

ethyl hydrogen (furan-2-ylmethyl)phosphonate (20o). 26.7 mg, 70%; as a dark oil; 2981, 2920, 2357, 1716, 1161, 1041, 789, 740; ^{1}H NMR (400 MHz, $CDCl_3$) δ 8.74 (s, 1H), 7.34 (s, 1H), 6.32-6.31 (m, 1H), 6.25-6.24 (m, 1H), 4.07-3.99 (m, 2H), 3.22 (d, *J* = 21.2 Hz, 2H), 1.28 (t, *J* = 7.2 Hz, 3H); ^{13}C NMR (100.5 MHz, $CDCl_3$) δ 145.5 (d, *J* = 8.9 Hz), 141.9 (d, *J* = 3.7 Hz), 110.7 (d, *J* = 3.0 Hz), 108.2 (d, *J* = 7.4 Hz), 62.1 (d, *J* = 6.7 Hz), 26.8 (d, *J* = 146.62 Hz), 16.2 (d, *J* = 6.7 Hz); ^{31}P NMR (162 MHz, $CDCl_3$): δ 27.27; HRMS(ESI): m/z calcd. for $C_7H_{11}O_4P$ ([M+H]+): 191.0468; found 191.0468.

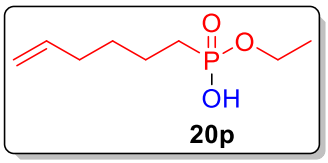

20p

ethyl hydrogen hex-5-en-1-ylphosphonate (20p). 24.8 mg, 66%; as an oil; **IR** ν (KBr, cm^{-1}) 3074, 2978, 2931, 2310, 1442, 1045, 817, 636; ^{1}H NMR (400 MHz, $CDCl_3$) δ 11.60 (s, 1H), 5.82-5.73 (m, 1H), 5.03-4.93 (m, 2H), 4.12-4.04 (m, 2H), 2.09-2.04 (m, 2H), 1.78-1.58 (m, 4H), 1.52-1.30 (m, 2H), 1.33 (t, *J* = 7.2 Hz, 3H); ^{13}C NMR (100.5 MHz, $CDCl_3$) δ 138.2, 114.76, 60.9 (d, *J* = 6.7 Hz), 33.2, 29.7 (d, *J* = 17.2 Hz), 25.7 (*J* = 142.9 Hz), 21.7 (d, *J* = 5.3 Hz), 16.3 (d, *J* = 6.7 Hz), ^{31}P NMR (162 MHz, $CDCl_3$): δ 35.95; HRMS(ESI): m/z calcd. for $C_8H_{17}O_3P$ ([M+H]+): 193.0988; found 193.0979.

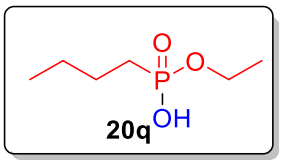

20q

ethyl hydrogen butylphosphonate (20q).[43] 26.6 mg, 79%; as an oil; ^{1}H NMR (400 MHz, $CDCl_3$) δ 12.23 (s, 1H), 4.12-4.05 (m, 2H), 1.78-1.69 (m, 2H), 1.65-1.54 (m, 2H), 1.46-1.38 (m, 2H), 1.36-1.34 (m, 3H), 0.91 (t, *J* = 8.0 Hz, 3H); ^{13}C NMR (100.5 MHz, $CDCl_3$) δ 60.8, 25.5 (d, *J* = 142.9 Hz), 24.2 (d, *J* = 5.2 Hz), 23.5 (d, *J* = 17.8 Hz), 16.2 (d, *J* = 6.7 Hz), 13.5; ^{31}P NMR (162 MHz, $CDCl_3$): δ 36.08.

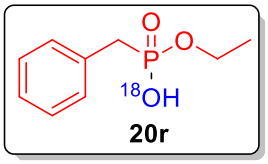

20r

ethyl hydrogen benzylphosphonate (20r). 30.1 mg, 75%; as an oil; ; **IR** ν (KBr, cm^{-1}) 2981, 2912, 1654, 1600, 1496, 1454, 1045, 987, 794, 698, 582;

^{1}H NMR (400 MHz, $CDCl_3$) δ 10.74 (s, 1H), 7.30-7.20 (m, 5H), 3.91-3.83 (m, 2H), 3.03 (d, *J* = 22.0 Hz, 2H), 1.19 (t, *J* = 7.2 Hz, 3H); ^{13}C NMR (100.5 MHz, $CDCl_3$) δ 131.5 (d, *J* = 9.6 Hz), 129.8 (d, *J* = 6.7 Hz), 128.3 (d, *J* = 3.0 Hz), 126.7 (d, *J* = 3.0 Hz), 61.5 (d, *J* = 6.7 Hz), 33.7 (d, *J* = 139.8 Hz), 16.1 (d, *J* = 6.0 Hz); ^{31}P NMR (162 MHz, $CDCl_3$): δ 29.40; HRMS(ESI): m/z calcd. for $C_{10}H_{13}O_2{}^{18}OP$ ([M+H]+): 203.0718; found 203.0731.

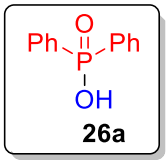

26a

diphenylphosphinic acid (26a). 35.5 mg, 81%; as a white crystal; mp 194-195 °C; **IR** ν(KBr, cm^{-1}) 3074, 2920, 2360, 1438, 1130, 960, 729, 694; ^{1}H NMR (400 MHz, $CDCl_3$) δ 11.09 (s, 1H), 7.73-7.68 (m, 4H), 7.45-7.41 (m, 2H), 7.334-7.32 (m, 4H); ^{13}C NMR (100.5 MHz, $CDCl_3$) δ 132.7 (d, *J* = 139.8 Hz), 131.8 (d, *J* = 3.0 Hz), 131.2 (d, *J* = 10.4 Hz), 128.3 (d, *J* = 13.4 Hz); ^{31}P NMR (162 MHz, $CDCl_3$): δ 31.87; HRMS(ESI): m/z calcd. for $C_{10}H_{15}O_3P$ ([M+H]+): 219.0569; found 219.0550.

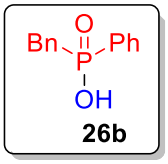

26b

benzyl(phenyl)phosphinic acid (26b). 33.8 mg, 75%; as a white crystal; mp 135-137 °C; **IR** ν(KBr, cm^{-1})3059, 2920, 2850, 2357, 1408, 1199, 960, 694; ^{1}H NMR (400 MHz, CD_3OD) 7.63-7.51 (m, 3H). 7.44-7.39 (m, 2H), 7.17-7.16 (m, 3H), 7.06-7.04 (m, 2H), 3.28 (d, *J* = 14.4 Hz, 2H); ^{13}C NMR (100.5 MHz, CD_3OD) δ 131.9 (d, *J* = 3.0 Hz), 131.8, 131.5 (d, *J* = 130.8 Hz), 131.2 (d, *J* = 9.7 Hz), 129.7 (d, *J* = 6.0 Hz) , 128.0 (d, *J* = 12.7 Hz), 127.8 (d, *J* = 3.7 Hz), 126.2 (d, *J* = 3.7 Hz), 37.8 (d, *J* = 94.26 Hz); ^{31}P NMR (162 MHz, CD_3OD): δ 37.39; HRMS(ESI): m/z calcd. for $C_{15}H_{17}O_2P$ ([M+H]+): 261.1039; found 261.1004.

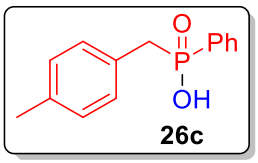

26c

(4-methylbenzyl)(phenyl)phosphinic acid (26c). 39.1 mg, 89%; as a white crystal; mp 166-168 °C; **IR** ν(KBr, cm^{-1}) 3051, 2920, 2314, 1512, 1126, 964, 833, 694, 547; ^{1}H NMR (400 MHz, CD_3OD) δ 7.63-7.51 (m, 3H) 7.44-7.40

(m, 2H), 6.99 (d, *J* = 7.6 Hz, 2H), 6.93 (dd, *J* = 8.4 Hz, 2.4 Hz, 2H), 3.23 (d, *J* = 18.0 Hz, 2H), 2.25 (s, 3H); ^{13}C NMR (100.5 MHz, CD_3OD) δ 135.9 (d, *J* = 3.7 Hz), 131.8 (d, *J* = 3.0 Hz), 131.5 (d, *J* = 130.14 Hz), 131.2 (d, *J* = 9.7 Hz), 129.5 (d, *J* = 5.2 Hz), 128.6 (d, *J* = 7.4 Hz), 128.4 (d, *J* = 2.9 Hz), 127.9 (d, *J* = 12.6 Hz), 37.32 (d, *J* = 94.2 Hz), 19.6; ^{31}P NMR (162 MHz, CD_3OD): δ 37.42; HRMS(ESI): m/z calcd. for $C_{16}H_{19}O_2P$ ([M+H]+): 275.1195; found 275.1171.

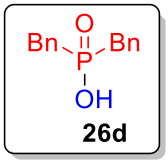

26d

dibenzylphosphinic acid (26d).[44] 35.1 mg. 75%; as a white solid; ^{1}H NMR (400 MHz, $CDCl_3$) δ 12.10 (s, 1H), 7.28-7.17 (m, 10H), 2.86 (d, *J* = 16.8 Hz, 4H); ^{13}C NMR (100.5 MHz, $CDCl_3$) δ 131.3 (d, *J* = 7.4 Hz), 130.0 (d, *J* = 6.0 Hz), 128.5 (d, *J* = 2.2 Hz), 126.8 (d, *J* = 3.0 Hz), 35.9 (d, *J* = 89.0 Hz); ^{31}P NMR (162 MHz, $CDCl_3$): δ 51.22.

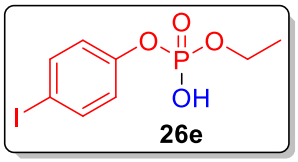

26e

ethyl (4-iodophenyl) hydrogen phosphate (4e). 44.0 mg, 67%; as an oil; **IR** ν (KBr, cm^{-1}) 3089, 2981, 2310, 1577, 1481, 929, 829, 744, 698, 601; ^{1}H NMR (400 MHz, $CDCl_3$) δ 11.66 (s, 1H), 7.64-7.53 (m, 2H), 6.99-6.92 (m, 2H), 4.17-4.10 (m, 2H), 1.31 (t, *J* = 6.8 Hz, 3H); ^{13}C NMR (100.5 MHz, $CDCl_3$) δ 150.5 (d, *J* = 6.7 Hz), 138.6, 122.4 (d, *J* = 4.5 Hz), 88.76, 64.8 (d, *J* = 5.2 Hz), 15.9 (d, *J* = 6.7 Hz), ^{31}P NMR (162 MHz, $CDCl_3$): δ -4.51; HRMS(ESI): m/z calcd. for $C_8H_{10}O_4PI$ ([M+H]+): 328.9434; found 324.9404.

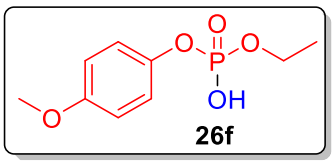

26f

ethyl (4-methoxyphenyl) hydrogen phosphate (26f). 38.6 mg, 84%; as an oil; **IR** ν (KBr, cm^{-1}) 2985, 2908, 2310, 1504, 833, 775, 690, 636; ^{1}H NMR (400 MHz, $CDCl_3$) δ 12.45 (s, 1H), 7.11 (dd, *J* = 23.6, 1.6 Hz, 2H), 6.85-6.78 (m, 2H), 4.17-4.10 (m, 2H), 1.31 (td, *J* = 6.8, 0.8 Hz, 3H); ^{13}C NMR (100.5 MHz, $CDCl_3$) δ 156.7, 144.1 (d, *J* = 6.7 Hz), 121.0 (d, *J* = 4.4 Hz), 114.5, 64.5 (d, *J* = 6.0 Hz), 55.5, 15.9 (d,

J = 6.7 Hz), ^{31}P NMR (162 MHz, $CDCl_3$): δ -3.39; HRMS(ESI): m/z calcd. for $C_9H_{13}O_5P$ ([M+H]+): 233.0573; found 233.0555.

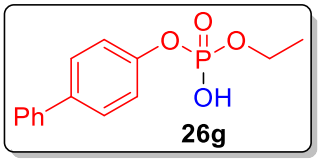

26g

[1,1'-biphenyl]-4-yl ethyl hydrogen phosphate (26g). 25.1 mg, 45%; as an orange solid; mp 96-97 °C; **IR** ν (KBr, cm^{-1}) 3059, 2985, 2908, 2357, 1485, 1033, 840, 759, 686; ^{1}H NMR (400 MHz, $CDCl_3$) δ 10.90 (s, 1H), 7.50-7.47 (m, 4H), 7.42-7.37 (m, 2H), 7.34-7.29 (m, 1H), 7.24 (d, *J* = 8.0 Hz, 2H), 4.22-4.15 (m, 2H), 1.35-1.31 (m, 3H); ^{13}C NMR (100.5 MHz, $CDCl_3$) δ 150.0 (d, *J* = 6.7 Hz), 140.1, 138.1, 128.8, 128.3, 127.3, 126.9, 120.4 (d, *J* = 5.2 Hz), 64.7 (d, *J* = 6.0 Hz), 16.0 (d, *J* = 7.4 Hz), ^{31}P NMR (162 MHz, $CDCl_3$): δ -4.08; HRMS(ESI): m/z calcd. for $C_{12}H_{13}O_4P$ ([M+H]+): 253.0624; found 253.0599.

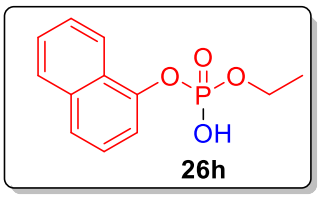

26h

ethyl naphthalen-1-yl hydrogen phosphate (4h). 28.0 mg, 56%; as an oil; **IR** ν (KBr, cm^{-1}) 3055, 2985, 2908, 2306, 1597, 1462, 1392, 1230, 1087, 972, 771, 698; ^{1}H NMR (400 MHz, $CDCl_3$) δ 12.20 (s, 1H), 8.16-8.14 (m, 1H), 7.81-7.79 (m, 1H), 7.61 (d, *J* = 8.0 Hz, 1H), 7.50-7.46 (m, 2H), 7.39 (d, *J* = 7.6 Hz, 1H), 7.31 (t, *J* = 8.0 Hz, 1H), 4.19-4.11 (m, 2H), 1.27 (t, *J* = 7.6 Hz); ^{13}C NMR (100.5 MHz, $CDCl_3$) δ 146.5 (d, *J* = 6.7 Hz), 134.7, 127.6, 126.6, 126.4 (d, *J* = 6.7 Hz), 126.3, 125.4, 124.9, 121.8, 115.0 (d, *J* = 2.9 Hz), 64.8 (d, *J* = 6.0 Hz), 15.9 (d, *J* = 6.7 Hz), ^{31}P NMR (162 MHz, $CDCl_3$): δ -3.91; HRMS(ESI): m/z calcd. for $C_{14}H_{15}O_4P$ ([M+H]+): 279.0781; found 279.0765.

Chapter II

Iodine Mediated Anodic Fluorination for P-F Bond Construction

2.1 Introduction and Background of P-F Bond Formation

Scheme 2.1 Selected Applications of P-F Containing Compounds

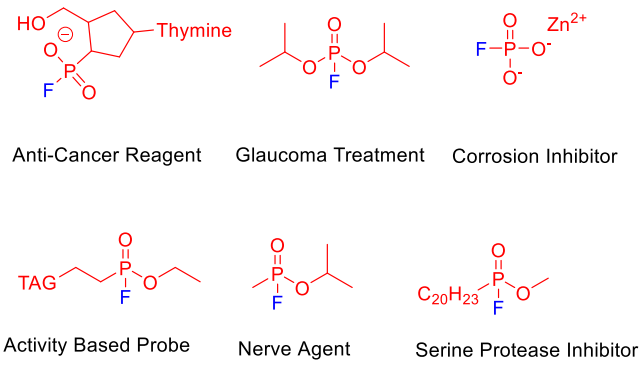

Organophosphorus compounds with a P-F bond have found many important uses.[45-50] They have been used in the area of medicinal chemistry by serving as an anti-cancer reagent and glaucoma medicine.[45, 46] Furthermore, zinc(II) phosphorofluoridate has been utilized as a corrosion inhibitor.[47] Fluorophosphonates have been used in activity-based proteomics as probes

for the study of enzymes.[48] A nefarious use for fluorophosphonates is as a deadly chemical weapon such as Sarin.[49] Lastly, fluorophosphonates serve as highly potent serine protease inhibitors that will inhibit the majority of serine hydrolase and serine protease enzymes (**Scheme 2.1**).[50]

P-F bond formation can be achieved by either nucleophilic or electrophilic fluorination (**Scheme 2.2** and **Scheme 2.3**). Nucleophilic fluorination involves the formation of a P-X bond followed by nucleophilic substitution by metal fluoride.

Dubey has demonstrated that phosphite **9a** is chlorinated in situ by trichloroacetonitrile and reacted with potassium fluoride to give fluorophosphonate **27** in a yield of 89% (**Scheme 2.2**).[51] Dubey also demonstrated a copper(II) chloride mediated fluorination to give fluorophosphonate **27** in a yield of 92% (**Scheme 2.2**).[52] Bornemann applied the same activation strategy by reacting diphenyl phosphine oxide **7a** with trichloroisocyanuric acid and potassium fluoride to produce fluorophosphine oxide **28a** in a yield of 65% (**Scheme 2.2**).[53] In addition, Kirby demonstrated that phosphoric acid **29** with a good leaving group such as imidazole can also be fluorinated by nucleophilic fluorination to give **30** in a yield of 95% (**Scheme 2.2**).[54] This approach by Kirby removes the need for a stoichiometric amount of chlorinating agent. However, it still requires a prefunctionalized starting material. To address these shortcomings, Yang reported a catalytic approach to fluorophosphine oxide using copper (II) bromide catalyst, 2,3- Dichloro-5,6-dicyano-1,4-benzoquinone (DDQ), and sodium fluoride as the fluorine source to afford **28a** in a yield of 90% (**Scheme 2.2**).[55]

Scheme 2.2 Nucleophilic Fluorination for P-F Bond Construction

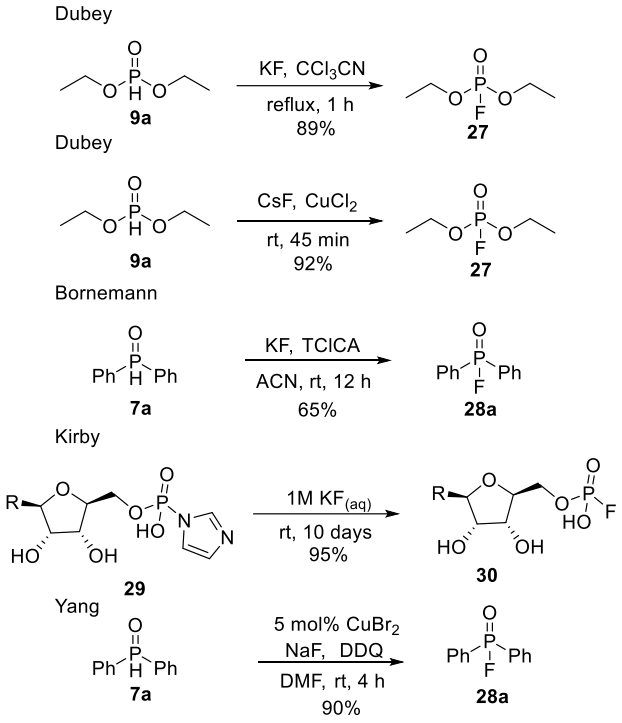

Electrophilic fluorinating reagents such as Selectfluor, SOF_2, XeF_2, DAST, SO_2FCl, and COF_2 have been used to construct the P-F bond (**Scheme 2.3**).[19, 56-60] These methods rely on the P(V) to P(III) tautomerization and reaction with a source of electrophilic fluorine. Zhang disclosed that secondary phosphine oxide **7a** could react with Selectfluor **31a** to give phosphoric fluoride **28a** in a high yield of 91% under mild conditions (**Scheme 2.3**).[19] Michalski used trivalent trimethyl silyl phosphite **32a** and sulfuryl chloride fluoride **31b** under cryogenic temperatures to give fluorophosphonate **27** in a high yield (**Scheme 2.3**). Michalski demonstrated sulfonyl fluoride **31c** served as an electrophilic fluorinating reagent for the fluorination of phosphine oxide **9a** to produce fluorophosphate **27** in high yield.[57] A major drawback of this work is the

use of sulfonyl fluoride, which is neurotoxic and a greenhouse gas. Kirsanov used diethylaminosulfur trifluoride (DAST) to fluorinate **32b** to **33** in a high yield of 93%.[58] Similarly, Stang revealed the reaction of diphenyl phosphine oxide **7** with xenon fluoride **31e** to give fluorophosphine oxide **28a** in a high yield of 99%.[59] All the described methodologies have one key disadvantage, the electrophilic fluorinating agents are moisture sensitive and difficult to handle. To address these disadvantages, Chen used fluorinating reagent carbonyl fluoride in situ by the thermal decomposition of **31f** and was able to provide fluorophosphine oxide **28a** in a high yield of 81%.[60] The advantage of Chen's method is the ability of the chemist to avoid directly working with hazardous carbonyl fluoride, which is generated in situ.

Scheme 2.3 Electrophilic Fluorination for P-F Bond Construction

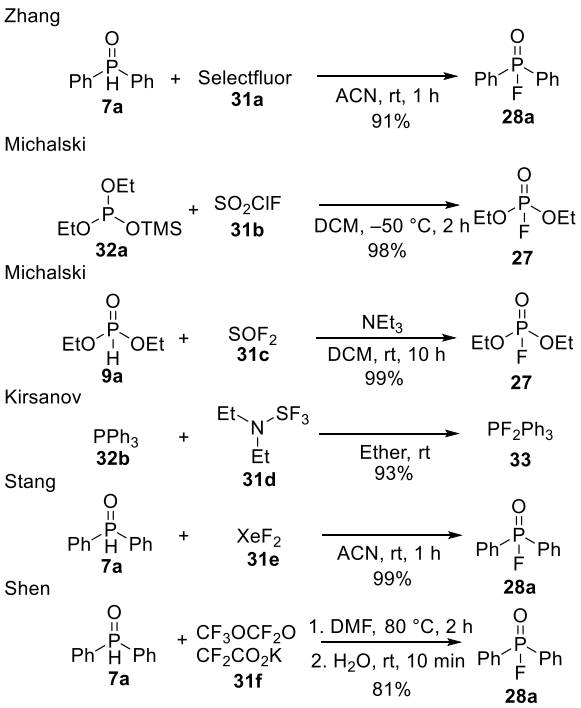

Electrochemistry is a powerful technique where electricity is used as the driving force for synthetic transformations. Electrons in the form of electricity are considered green and take the place of traditional metal catalysts used in ionic synthesis. While lone pairs of electrons are involved in ionic synthesis, electrochemistry uses a single electron in the form of a free radical. Strong oxidants or reductants are not necessary as oxidation (loss of electrons) occurs at the anode and reduction (gain of electrons) happens at the cathode.

Scheme 2.4 Famous Named Reactions in Electrochemistry

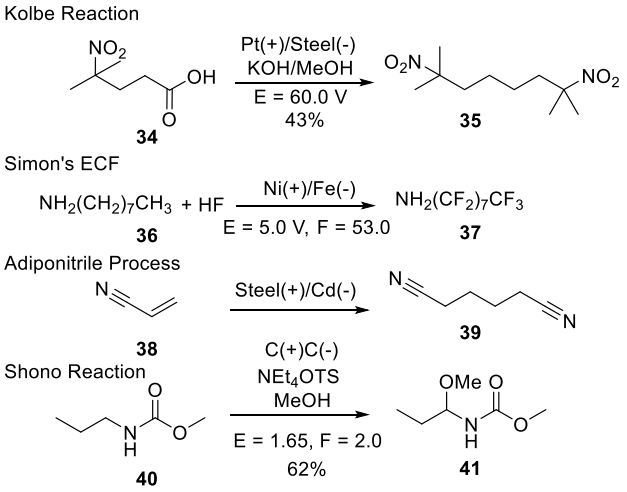

Some of the most prominent advances in electrochemistry are the Kolbe reaction, electrochemical fluorination (ECF), adiponitrile process, and the Shono oxidation (**Scheme 2.4**). In 1847, Kolbe introduced Kolbe electrolysis which involves the decarboxylative dimerization of a carboxylic acid under a constant current to form a new C-C bond.[61] For example,

Langkammerer used carboxylic acid **34** with itself to generate dinitro alkyl compound **35** in a moderate yield of 43% (**Scheme 2.4**).[62] Simons discovered the ECF process which involves the fluorination of an alkyl organic compound in the presence of HF under a constant voltage to turn all aliphatic C-H bonds into C-F bonds. Primary amine **36** can be transformed into perfluorinated amine **37** in high yields using the ECF process (**Scheme 2.4**).[63] This method requires dangerous HF and high voltage. ECF has been used to make PFAS (polyfluorinated alkyl substances) which have found much use in consumer items as a resistant polymeric coating.[64] Later in 1964, Monsanto introduced the Monsanto adiponitrile process which was an electrochemical coupling reaction of **38** used to make adiponitrile **39** on a process scale (**Scheme 2.4**).[65] Adiponitrile is an important feedstock chemical for the polymerization of nylon.[66] The Shono reaction is another famous electrochemical reaction where an acyl amine is oxidized at the anode to form a stable iminium ion. The iminium ion is then captured by an anionic nucleophile that is generated at the cathode by reduction reaction.[67] Shono treated alkyl amine **40** and methanol under electrochemical conditions to give **41** in a moderate yield of 62%.[68]

Electrochemical functionalization of organophosphorus compounds is an emerging area of interest. P-C, P-O, P-S, and P-N bond formation has been developed by electrochemical P-H bond activation.[21, 69-76] Lee developed electrochemical conditions to form a P-S bond by reacting phosphite **9a** with thiophenol **42** in the presence of iodine to form thiophosphate **43** in a low yield of 30% (**Scheme 2.5**).[77] Wang formed a P-N bond under electrochemical conditions by reacting diphenyl phosphine oxide **7a** and morpholine **44** in the presence of an iodine salt to form azaphosphine oxide **45** in a high yield of 86% (**Scheme 2.5**).[69] Han adopted the same

strategy and developed reaction conditions to accommodate an oxygen nucleophile. Diphenyl phosphine oxide **7a** and methanol are reacted under electrochemical conditions in the presence of TBAI to form phosphinate **8** in a high yield of 92% (**Scheme 2.5**).[21] Lastly, Ding utilized a Shono-type reaction of secondary amine **46** and phosphite **9a** under weakly basic conditions to form alpha amino phosphonate **47** in a high yield of 88% (**Scheme 2.5**).[70] Many of these methods use an iodine mediator to facilitate the reaction. Iodine has a low reduction potential and is easily oxidized at the anode, forming an iodide radical. The iodide radical will react with the P(V) compound through radical coupling to form a highly reactive phosphorous halogen bond, which can be functionalized by nucleophilic substitution.

Scheme 2.5 Electrochemical Phosphorous Heteroatom Bond Formation Methods

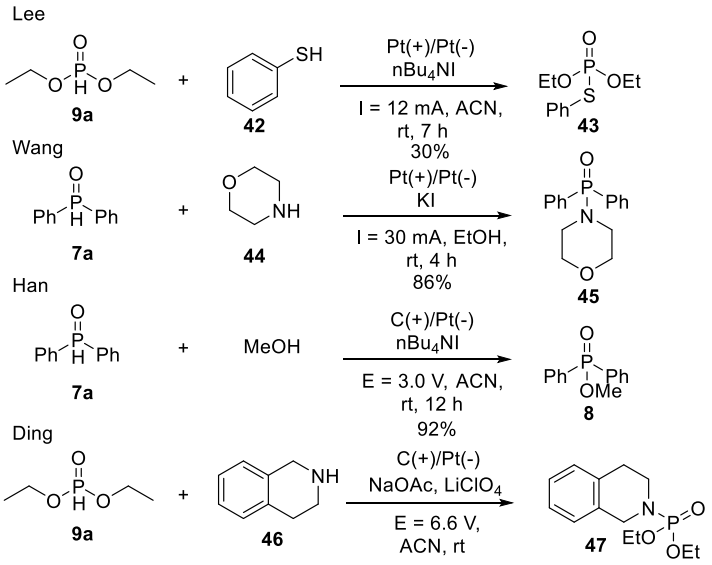

In 2023, Chen and coworkers developed electrochemical fluorination of secondary phosphine oxides using triethyl amine trihydrofluoride as the fluorinating agent. Diphenyl phosphine oxide **7a** is fluorinated under electrochemical conditions to give fluorophosphine oxide **28a** in a moderate yield of 65% (**Scheme 2.6**). Chen's method suffers from low to moderate yields and uses a hazardous fluorinating reagent. Triethyl amine trihydrofluoride can potentially give off hydrogen fluoride gas as a combustion product. Therefore, a safer and green fluorinating agent is still highly desired.

Scheme 2.6 Electrochemical P-F Bond Formation

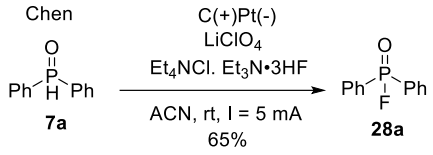

2.2 Specific Aim

To develop a new electrochemical P-F bond formation strategy, the electrochemical strategy will avoid the use of oxidizers/reductants and use a simple iodine mediator to facilitate the reaction. The challenges of the fluoride atoms' low nucleophilicity and cell overpotential will be studied to develop an effective reaction. A safe and easy-to-handle fluorinating agent will also be investigated.

2.3 Electrochemical P-F Bond Formation

We hypothesized that a P-I bond can be formed through anodic oxidation of secondary phosphine oxide and reacted with a metal fluoride nucleophile to form a fluorophosphine oxide. Simple metal fluoride salts are bench-stable and easy to handle. Thus, they are an attractive choice for a fluorinating agent. This strategy offers an attractive and green alternative to conventional methods by avoiding the use of metal catalysts, harsh chlorinating agents, exotic electrophilic fluorinating reagents, and unwanted HF byproduct generation.

Table 2.1 Optimization of Metal Fluoride[a]

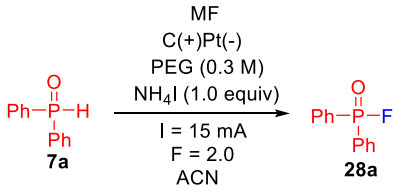

entry	MF	Yield[b]
1	KF (3.0 equiv)	26%
2	TBAF (3.0 equiv)	0%
3	KF (6.0 equiv)	0%
4	KF (1.5 equiv)	42%
5	KF (1.0 equiv)	52%
6	CsF (1.0 equiv)	52%

[a]Reaction conditions: Carbon anode, Platinum cathode at a constant current of 15 mA, **7a** (0.2 mmol), Metal fluoride (MF), Polyethylene glycol (PEG) (1.5 mmol), and NH_4I (0.2 mmol.) in ACN (5.0 mL) at room temperature. [b]Crude ^{19}F NMR yield using fluorobenzene as an internal standard.

Electrochemical synthesis requires the control of many variables such as total charge, electrode material, electrolyte, current, and concentration. The project began with the standard conditions from entry 1, which generated the product in 26% yield. The product yield was analyzed by ^{19}F NMR spectroscopy using fluorobenzene as an internal standard (**Table 2.1**, entry 1). The reaction was systematically optimized by running multiple reactions with one parameter being manipulated at a time to understand and optimize each experimental variable.

The first parameter was the metal fluoride. Metal fluorides are sparingly soluble in organic solvents in the absence of additives.[78] To proactively overcome this solubility problem, all reactions were performed with a polyethylene glycol (PEG) 200 additive. The role of this additive is to increase the solubility of the metal fluoride and raise its nucleophilicity by chelating the metal cation and freeing the fluoride anion to participate in the desired reaction.

The cation effect comes into play with larger cations, such as cesium, having more ionic character than cations like sodium.[79] Tetrabutyl ammonium fluoride was screened but it did not form any product (**Table 2.1**, entry 2). Next, the molar equivalence of the nucleophile was examined and no product was formed with a large excess (**Table 2.1**, entry 3). This can be explained by anode passivation. The excess of metal fluoride formed a visible coat over the anode which prevented the desired charge transfer reaction and greatly raised the potential of the cell. Learning from this experimental outcome, the opposite direction was pursued by lowering the equivalence of the nucleophile. This can prevent anodic passivation and increase the faradic efficiency of the reaction. When the equivalence of the metal fluoride was decreased to 1.5, the product yield was increased to 42% (**Table 2.1**, entry 4). Since this change was beneficial, the equivalence of metal fluoride was further decreased to 1.0 equivalence. It

increased the product yield to 52% (**Table 2.1**, entry 5). Then the cation effect was tested by replacing KF with CsF. The expected result was the yield would be greater with CsF due to having a weaker ionic bond and lower lattice energy than KF.[80] However, no positive effect was observed, and the crude yield remained the same at 52% (**Table 2.1**, entry 5).

Table 2.2 Optimization of Solvent, Electrolyte, and Electrode Material[a]

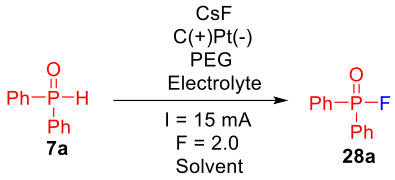

entry	Iodine Source	Anode	Cathode	Solvent	Yield[b]
1	NH_4I 100%	C	Pt	Acetone	57%
2	NH_4I 100%	C	Pt	DMF	35%
3	NH_4I 100%	RVC	Pt	Acetone	53%
4	NH_4I 300%	C	Pt	Acetone	62%

[a]Reaction conditions: Constant current of 15 mA, **7a** (0.2 mmol), CsF (0.2 mmol), PEG (1.5 mmol), and electrolyte in solvent (5.0 mL) at room temperature. [b]Crude ^{19}F NMR yield using fluorobenzene as an internal standard.

The solvent effect was then tested with other solvents such as acetone and DMF. An increase in yield was observed when running the reaction in acetone (**Table 2.2**, entry 1). This can be attributed to the oxygen atom in acetone acting as a Lewis base and solvating the metal cation to increase the reactivity of the fluoride anion. DMF gave inferior results compared to acetone and acetonitrile (**Table 2.2**, entry 2). Next, the effect of increasing surface area was

tested with a reticulated vitreous carbon (RVC) working electrode. The RVC electrode has a surface area of 2184 mm^2 and the graphite electrode has a surface area of 2164 mm^2. However, increasing the surface area of the working electrode did not improve product yield (**Table 2.2**, entry 3). Then, the electrolyte loading was evaluated. Increasing the electrolyte loading to 3.0 equivalents gave an increase of yield to 62% (**Table 2.2**, entry 4). This outcome contributes to the decreased resistance in the cell and increased faradaic efficiency.

Table 2.3 Optimization of Iodine Source, Reaction Time, and Molar Equivalence[a]

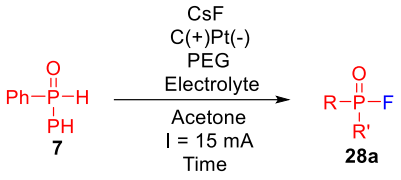

entry	7a	Iodine Source	F/Mol	Current	Additive	Yield[b]
1	1.0 equiv	KI 300%	2.0	15 mA	0.3 M PEG	0%
2	1.0 equiv	TBAI 300%	2.0	15 mA	0.3 M PEG	0%
3	1.0 equiv	NH_4I 300%	4.0	15 mA	0.3 M PEG	72%
4	1.0 equiv	NH_4I 300%	6.0	15 mA	0.3 M PEG	62%
5	1.0 equiv	NH_4I 300%	4.0	15 mA	0.1 M PEG	65%
6	2.0 equiv	NH_4I 300%	4.0	15 mA	0.3 M PEG	90%

[a]Reaction conditions: Carbon anode, Platinum cathode at a constant current of 15 mA, **7a**, CsF (0.2 mmol), PEG (1.5 mmol), and electrolyte (0.6 mmol.) in acetone (5.0 mL) at room temperature. [b]Crude ^{19}F NMR yield using fluorobezene as an internal standard.

Furthermore, the iodine source was evaluated. It was found that other iodine sources like KI and TBAI did not afford any product (**Table 2.3**, entries 1-2). The reaction time was then doubled to four faradays of charge to give a yield of 72% (**Table 2.3**, entry 3). Neither increasing the

reaction time nor lowering the concentration of PEG 200 increased the product yield (**Table 2.3**, entries 4-5). Finally, the product yield increased to 90% when two equivalents of secondary phosphine oxide was used (**Table 2.3**, entry 7). Presumably the increase in yield is due to the formation of more diphenyphosphinic iodide reactive intermediate.

Table 2.4 Deviation from Standard Conditions Control Experiments[a]

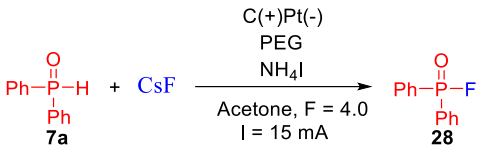

entry	Deviation from Standard Conditions	Yield
1	None	72%
2	No Electricity	0%
3	Bu_4NBF_4 instead of NH_4I	0%
4	No PEG additive	36%
5	ACN	50%
6	3.0 equiv **7a**	64%
7	1.0 equiv **7a**	56%
8	C(+)C(-)	68%
9	I = 5.0 mA	52%
10	F = 2.0/Mol	39%
11	F = 6.0/Mol	67%
12	1.0 equiv TEMPO	16%

[a]Reaction conditions: Carbon anode, Platinum cathode at a constant current of 15 mA, **7a** (0.4 mmol), CsF (0.2 mmol), PEG (1.5 mmol), and NH_4I (0.6 mmol.) in acetone (5.0 mL) at room temperature. Isolated yield.

A series of control experiments were conducted to further understand this electrochemical P-F bond forming reaction. Control experiments were then performed without electricity and an iodine salt. These experiments revealed that electricity and an iodine salt are

necessary for product formation (**Table 2.4**, entry 2-3). The role of polyethylene glycol was then investigated. Reaction without any polyethylene glycol additive gave a much lower yield of 36% (**Table 2.4**, entry 4). Polyethylene glycol serves as an additive to lower the resistivity of the cell and increase the nucleophilicity of the metal fluoride through chelation effects.[81] Acetonitrile did not improve product yield compared to acetone (**Table 2.4**, entry 1 vs entry 5). Changing the molar equivalence of **7** did not have a positive effect on reaction yield (**Table 2.4**, entry 6-7). Carbon cathode can be used giving a comparable yield of 68% (**Table 2.4**, entry 8). A low current of 5 mA did not increase product yield (**Table 2.4**, entry 9). A variation of reaction time from the standard (F = 4.0) did not increase the product yield (**Table 2.4**, entry 10-11). However, the yield of product **28a** was dramatically reduced when a radical scavenger was used. This outcome implies that the reaction occurs by a free radical mechanism (**Table 2.4**, entry 12).

With the optimized conditions in hand, various secondary phosphine oxides with steric and electronic differences were tested (**Table 2.5**). 2-methoxy diphenyl phosphine oxide **7b** generated the product **28b** in a moderate yield of 44%. The lower yield may be due to the methoxy group. It can induce intramolecular hydrogen bonding and raise the reduction potential of the P-H bond. Secondary phosphine oxides **7c** and **7d** containing electron-donating groups (4-MeO and 4-Me) provided the desired products **28c** and **28d** in a moderate yield of 70% and 58%; respectively. Next, sterically hindered phosphine oxides **7e-7g** (4-tBu, dimesityl, and 4-diphenyl) were tested and they furnished the products **28e-28g** in a moderate yield of 73-63%. A polycyclic secondary phosphine oxide **7h** afforded the product **28h** in a moderate yield of 65%. Alkyl secondary phosphine oxides **7i** and **7j** (dibenzyl and dihexyl) were also tolerated, giving **28i** and **28j** in yields of 53% and 58%, respectively. In addition, halogenated secondary

phosphine oxide **7k** gave the corresponding product **28k** in a moderate yield of 67%. Mixed secondary phosphine oxides **7l** and **7m** were also successfully fluorinated to form products **28l** and **28m** in yields of 51% and 60%, respectively. Based on the results from the substrate scope study the nucleophilic fluorination reaction tolerates steric and electronic effects (**Table 2.5**).

Table 2.5 Scope of Secondary Phosphine Oxide[a]

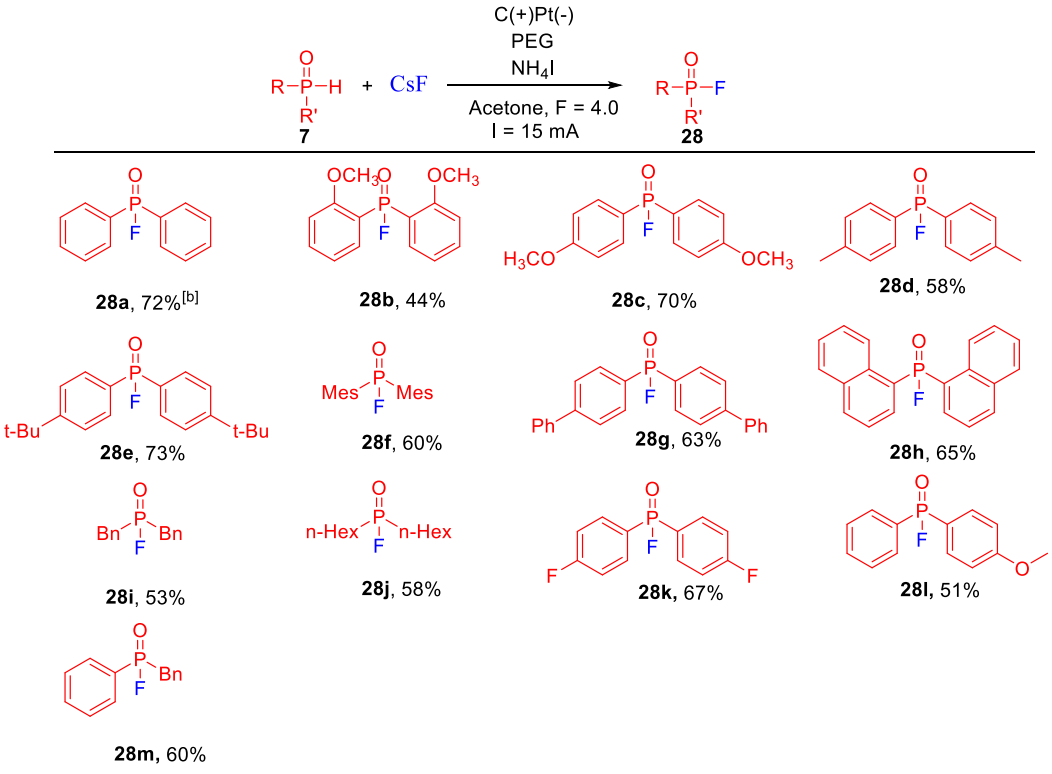

[a]Reaction conditions: Carbon anode, Platinum cathode at a constant current of 15 mA, **7** (0.4 mmol), CsF (0.2 mmol), PEG (1.5 mmol), and NH_4I (0.6 mmol.) in acetone (5.0 mL) at room temperature.[b]Isolated yield.

2.4 Cyclic Voltammetry Study

Figure 2.1 Cyclic Voltammetry Measurements

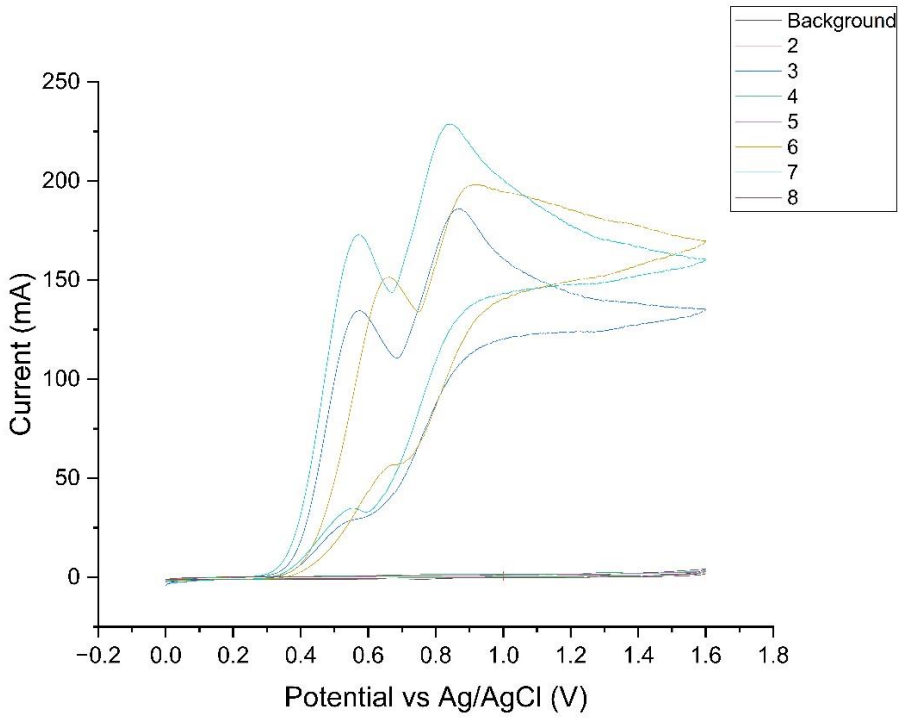

Cyclic voltammograms in IUPAC Convention of reagents in 0.1M $LiClO_4/CH_3CN$ using a glassy carbon working electrode (diameter, 2.0 mm). Pt as counter electrode and Ag/AgCl as the reference electrode at 100 mV/s scan rate: 1) background, 2) **7a** (10 mmol/L), 3) **7a** (10 mmol/L) + NH_4I (10 mmol/L), 4) CsF (10 mmol/L), 5) CsF (10 mmol/L) + PEG (0.3 M), 6) **7a** (10 mmol/L), NH_4I (10 mmol/L), CsF (10 mmol/L), PEG (0.3 M), 7) **7a** (10 mmol/L), NH_4I (10 mmol/L), CsF (10 mmol/L), 8) **28a** (10 mmol/L).

Cyclic voltammetry (CV) measurements were then performed to gain insight into the redox behavior of the reagents (**Figure 2.1**). The background scan provided no signal, as

expected (**Figure 2.1**, run 1). Diphenyl phosphine oxide **7a** without any NH_4I mediator did not present any oxidation peak (**Figure 2.1**, run 2). However, with NH_4I mediator there were two oxidation peaks at 0.45V and 0.68V (**Figure 2.1**, run 3). The peaks at 0.45V and 0.68V correspond to the oxidation of I^- to I_3^- and I_3^- to I_2^-.[82] CsF by itself and in the presence of PEG additive did not display any oxidation peak, which means fluoride is not being oxidized at this potential range (**Figure 2.1**, runs 4-5). Fluoride has a high reduction potential due to its high electronegativity.[83] Furthermore, when all components of the mixture were included, an increase of current was observed compared to just the iodine source, which implies the chemical interaction of all reagents (**Scheme 2.6**, runs 6-7). Lastly, the fluorinated product did not display any oxidation peak which shows that the product **28a** does not undergo oxidation. (**Figure 2.1**, run 8)

Scheme 2.7 Proposed Electrochemical Fluorination Mechanism

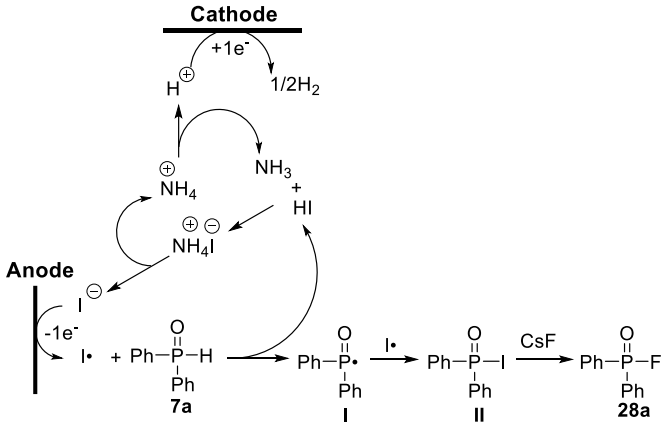

Based on CV results a plausible mechanism is proposed (**Scheme 2.7**). First, anodic oxidation of the iodide anion to the iodide radical occurs. Then, the iodide radical performs hydrogen atom transfer on **7a** to form HI and a phosphorous centered radical **I**. **I** and an iodide radical couple together to form **II**. **II** then reacts with cesium fluoride by a substitution reaction to furnish the product **28a**. Loss of hydrogen from ammonium forms ammonia and a proton. The proton is then reduced at the cathode to generate hydrogen gas, which can be visibly observed during the reaction.

2.5 Conclusion

Herein, we have developed an electrochemical fluorination reaction of secondary phosphine oxides. This reaction is catalyst-free as it is driven by electricity and uses a green, cheap, and bench-stable metal fluoride as a fluorinating agent. Furthermore, this method avoids the use of metal catalysts, the formation of HF byproducts, harsh chlorinating reagents, and expensive electrophilic fluorination reagents. Anodic passivation was prevented by having the metal fluoride as the limiting reagent. And the problem of low fluoride nucleophilicity is overcome by using a polyethylene glycol additive and a polar aprotic solvent.

2.6 Experimental Procedure

2.6.1 General Information

All reactions were carried out under air atmosphere in oven-dried glassware with magnetic stirring bar. Dry solvents (THF, toluene, ACN, diethyl ether, and DCM) were obtained by solvent purification system under argon. All commercially available reagents were used as received without further purification. IKA Electra Syn 2.0 and commercially available electrodes were used for the reactions. Purification of reaction products was carried out by flash column chromatography using silica gel 60 (230-400 mesh). Analytical thin layer chromatography was performed on 0.25 mm aluminum-backed silica gel 60-F plates. Visualization was accompanied with UV light and $KMnO_4$ solution. Concentration under reduced pressure refers to the removal of volatiles using a rotary evaporator attached to a dry diaphragm pump (10-15 mm Hg) followed by pumping to a constant weight with an oil pump (<300 mTorr). Infrared (IR) spectra were recorded on an IR spectrometer with KBr wafers or a film on KBr plate. High-resolution mass spectra (HRMS) were recorded on LCMS-IT-TOF mass spectrometer using ESI (electrospray ionization) or APCI (Atmospheric Pressure Chemical Ionization). ^1H NMR spectra were recorded in $CDCl_3$ on 400 MHz NMR spectrometer. The ^1H chemical shifts are referenced to residual solvent signals at δ 7.26 ($CHCl_3$) or δ 0.00 (TMS). ^1H NMR coupling constants (*J*) are reported in Hertz (Hz) and multiplicities are indicated as follows: s (singlet), bs (broad singlet), d (doublet), t (triplet), q (quartet), m (multiplet), dd (doublet of doublets), dt (doublet of triplets), td (triplet of doublets), tt (triplet of triplets). ^{13}C NMR spectra were proton decoupled and recorded in $CDCl_3$ on 100.5 MHz NMR spectrometer. The ^{13}C chemical shifts are referenced to solvent signals at δ 77.16 ($CDCl_3$). ^{31}P NMR spectra were proton decoupled and recorded in $CDCl_3$ on

162 MHz NMR spectrometer. ^{31}P chemical shifts are reported relative to 85% H_3PO_4 (0.00 ppm) as an external standard. ^{19}F chemical shifts are reported relative to the external standard (contained in a coaxial capillary) trifluoroacetic acid in $CDCl_3$: δ -76.55 ppm.

2.6.2 General Procedure Synthesis of Fluorophosphine Oxides

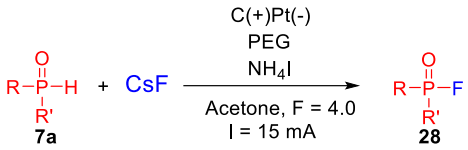

To a solution of PEG 200 (1.5 mmol) in acetone (5.0 mL) was added cesium fluoride (0.2 mmol), ammonium iodide (0.6 mmol), and phosphine oxide (0.4 mmol). Electrolysis was performed at a constant current of 15 mA with a platinum anode and carbon cathode on an Electrasyn 2.0. After electrolysis, the crude solution was directly purified by column chromatography.

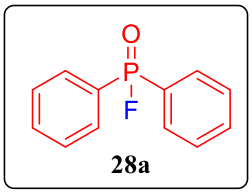

diphenylphosphinic fluoride (28a).[84] 31.8 mg, 72%; as a solid; **IR** ν (thin film, cm^{-1}) 3060, 2361, 1592, 1440, 1259, 1177, 837, 733; ^1H NMR (400 MHz, $CDCl_3$) δ 7.85-7.80 (m, 4H), 7.63-7.60 (m, 2H), 7.53-7.50 (m, 4H); ^{13}C NMR (100.5 MHz, $CDCl_3$): δ 133.3 (d, J = 2.9 Hz), 131.4 (dd, J = 2.3, 12.0 Hz), 128.8 (d, J = 14.1 Hz), 128.7 (dd, J = 22.6, 140.7 Hz); ^{31}P NMR (162 MHz, $CDCl_3$): δ 41.4 (d, J = 1019.2 Hz); ^{19}F NMR (376 MHz, $CDCl_3$): δ -75.1 (d, J = 1020.0 Hz).

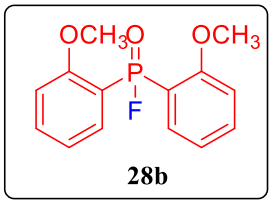

bis(2-methoxyphenyl)phosphinic fluoride (28b). 24.4 mg, 44%; as a solid, mp 84-86 °C; **IR** ν (thin film, cm^{-1}) 3053, 2943, 2306, 2033, 1592, 1433, 1258, 1097, 1019, 805, 729; ^1H NMR (400 MHz, $CDCl_3$) δ 7.90 (dd, J = 7.6, 1.6 Hz, 2H), 7.86 (dd, J = 7.2, 1.6 Hz, 2H), 7.53-7.51 (m, 2H), 7.07 (td, J = 7.6, 2.8 Hz, 2H), 6.88 (t, J = 7.6, 2H), 3.71 (s, 6H); ^{13}C NMR (100.5 MHz, $CDCl_3$): δ 161.2 (dd, J = 4.4, 1.5 Hz), 134.8

(d, *J* = 2.2 Hz), 134.0 (dd, *J* = 7.4, 2.2 Hz), 120.5 (d, *J* = 13.4 Hz), 118.6 (dd, *J* = 45.9, 19.3 Hz), 111.2 (d, *J* = 8.2 Hz), 55.7; ^{31}P NMR (162 MHz, $CDCl_3$): δ 38.0 (d, *J* = 1009.2 Hz); ^{19}F NMR (376 MHz, $CDCl_3$): δ -78.4 (d, *J* = 1009.2 Hz); HRMS(ESI): m/z calcd. For $C_{14}H_{14}FO_3P$ ([M+H]+): 281.0737; found 281.0729.

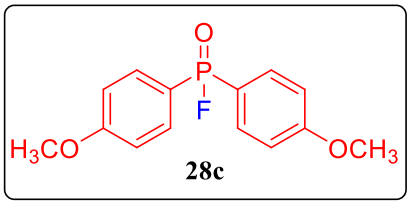

28c

Bis(4-methoxyphenyl)phosphinic fluoride (28c).[84] 39.1 mg, 70%; as a solid; **IR** ν (thin film, cm^{-1}) 3010, 2930, 1597, 1503, 1457, 1295, 1128, 947, 804, 719; ^{1}H NMR (400 MHz, $CDCl_3$) δ 7.76-7.71 (m, 4H), 7.00-6.97 (m, 4H), 3.84 (s, 3H); ^{13}C NMR (100.5 MHz, $CDCl_3$) δ 163.4 (d, *J* = 3.0 Hz), 133.4 (dd, *J* = 12.7, 1.5 Hz), 120.4 (dd, *J* = 148.8, 23.8 Hz) 114.3 (d, *J* = 14.9 Hz); ^{31}P NMR (162 MHz, $CDCl_3$): δ 42.5 (d, *J* = 1007.9 Hz); ^{19}F NMR (376 MHz, $CDCl_3$): δ -72.5 (d, *J* = 1007.6 Hz).

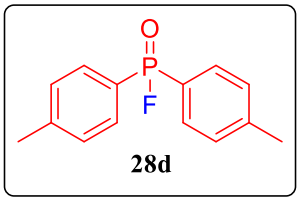

28d

Di-p-tolylphosphinic fluoride (28d).[84] 32.4 mg, 58%; as a solid; **IR** ν (thin film, cm^{-1}) 3023, 2921, 2250, 1604, 1447, 1174, 962, 808, 712, 637; ^{1}H NMR (400 MHz, $CDCl_3$) δ 7.70-7.65 (m, 4H), 7.29-7.27 (m, 4H), 2.38 (s, 6H); ^{13}C NMR (100.5 MHz, $CDCl_3$) δ 144.0 (d, *J* = 3.0 Hz), 131.4 (dd, *J* = 11.9, 1.5 Hz), 129.5 (d, *J* = 14.2 Hz), 125.7 (dd, *J* = 142.9, 22.4 Hz), 21.7; ^{31}P NMR (162 MHz, $CDCl_3$): δ 42.5 (d, *J* = 1014.4 Hz); ^{19}F NMR (376 MHz, $CDCl_3$): δ -74.3 (d, *J* = 1014.1 Hz).

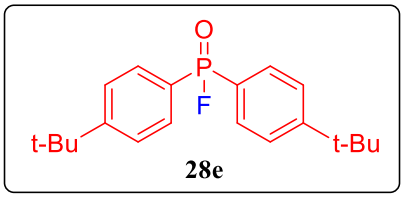

28e

Bis(4-(tert-butyl)phenyl)phosphinic fluoride (28e).[85] 48.7 mg, 73%; as a solid; **IR** ν (thin film, cm^{-1}) 3055, 2966, 1929, 1600, 1463, 1396, 1262, 1150, 825, 767; ^{1}H NMR (400 MHz, CDCl3) δ 7.76-7.74 (m, 4H), 7.53-7.51 (m, 4H), 1.33 (s, 18H); ^{13}C NMR (100.5 MHz, $CDCl_3$) δ 156.9 (d, *J* = 3.0 Hz), 131.3 (dd, *J* = 11.9, 2.2 Hz) 125.8 (d, *J* = 14.1 Hz), 125.7 (dd, *J* = 142.9, 22.3 Hz), 35.1,

31.0; ^{31}P NMR (162 MHz, $CDCl_3$): δ 42.2 (d, *J* = 1013.3 Hz); ^{19}F NMR (376 MHz, $CDCl_3$): δ 74.1 (d, *J* = 1016.0 Hz).

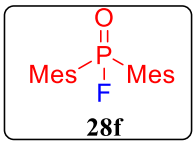

28f

dimesitylphosphinic fluoride (28f). 36.6 mg, 60%; as a solid; mp 169-171 °C; **IR** ν (thin film, cm^{-1}) 3053, 2943, 2306, 1592, 1480, 1251, 1149, 1018, 835, 715; ^{1}H NMR (400 MHz, $CDCl_3$) δ 6.88 (d, *J* = 4.4 Hz, 4H), 2.38 (d, *J* = 1.2 Hz, 12H), 2.28 (s, 6H); ^{13}C NMR (100.5 MHz, $CDCl_3$) δ 142.6 (d, *J* = 2.9 Hz), 124.1 (d, *J* = 11.1 Hz), 130.8 (d, *J* = 13.4 Hz), 126.2 (dd, *J* = 17.9, 134.0 Hz); ^{31}P NMR (162 MHz, $CDCl_3$): δ 47.1 (d, *J* = 1019.5 Hz); ^{19}F NMR: -56.9 (d, *J* = 1019.0 Hz); HRMS(ESI): m/z calcd. For $C_{18}H_{22}FOP$ ([M+H]+): 305.1465; found 305.1466.

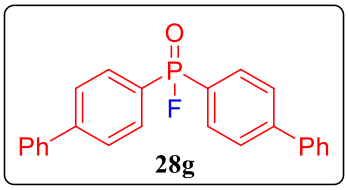

28g

di([1,1'-biphenyl]-4-yl)phosphinic fluoride (28g).[86] 46.8 mg, 63%; as a solid; **IR** ν (thin film, cm^{-1}) 3059,2924, 2345, 1597, 1483, 1396, 1250, 1120, 837, 762; ^{1}H NMR (400 MHz, $CDCl_3$) δ 7.96-7.90 (m, 4H), 7.74 (dd, *J* = 8.4, 3.2 Hz, 4H), 7.60-7.58 (m, 4H), 7.48-7.38 (m, 6H); ^{13}C NMR (100.5 MHz, $CDCl_3$): δ 146.2 (d, *J* = 2.3 Hz), 139.5, 132.0 (dd, *J* = 11.9, 2.2 Hz), 129.0, 128.5, 127.6, 127.5, 127.3; ^{31}P NMR (162 MHz, $CDCl_3$): δ 42.2 (d, *J* = 1013.3 Hz); ^{19}F NMR (376 MHz, $CDCl_3$): δ -74.1 (d, *J* = 1016.0 Hz).

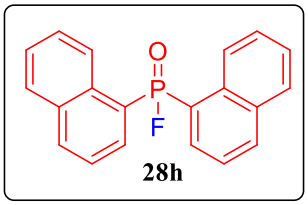

28h

di(naphthalen-1-yl)phosphinic fluoride (28h).[85] 41.4 mg, 65%; as a solid; **IR** ν (thin film, cm^{-1}) 3065, 2365, 1957, 1726, 1569, 1355, 1251, 1154, 1026, 804, 735; ^{1}H NMR (400 MHz, $CDCl_3$) δ 8.55-8.52 (m, 2H), 8.08 (d, *J* = 2.1 Hz, 2H), 8.04 (dd, *J* = 7.2, 1.2 Hz, 1H), 8.00 (dd, *J* = 7.2, 1.2 Hz, 1H), 7.92-7.89 (m, 2H), 7.57-7.47 (m, 6H); ^{13}C NMR (100.5 MHz, $CDCl_3$): δ 134.6 (d, *J* = 3.0 Hz), 133.8 (dd, *J* = 12.6,

4.4 Hz), 133.6 (d, *J* = 11.1 Hz), 132.7 (d, *J* = 11.1 Hz), 129.2 (d, *J* = 1.5 Hz), 128.0, 126.8, 126.2 (d, *J* = 5.2 Hz), 125.5 (dd, *J* = 19.4, 136.9 Hz), 124.5 (d, *J* = 16.4 Hz); ^{31}P NMR (162 MHz, $CDCl_3$): δ 44.9 (d, *J* = 1018.3 Hz); ^{19}F NMR (376 MHz, $CDCl_3$): δ -67.9 (d, *J* = 1018.2 Hz).

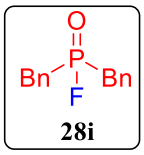

28i

Dibenzylphosphinic fluoride (28i).[19] 26.2 mg, 53%; as a solid; **IR** ν (thin film, cm^{-1}) 3027, 2951, 2350, 1453, 1259, 1127, 953, 709; ^{1}H NMR (400 MHz, $CDCl_3$) δ 7.29-7.22 (m, 6H), 7.18-7.14 (m, 4H), 3.15 (dd, *J* = 17.2, 1.6 Hz, 4H); ^{13}C NMR (100.5 MHz, $CDCl_3$) δ 128.8 (d, *J* = 5.2 Hz), 128.2 (dd, *J* = 7.5, 1.5 Hz), 128.0 (d, *J* = 3.0 Hz), 126.6 (d, *J* = 3.0 Hz), 33.7 (dd, *J* = 85.6, 14.2 Hz); ^{31}P NMR (162 MHz, $CDCl_3$): δ 58.9 (d, *J* = 1039.5 Hz); ^{19}F NMR (376 MHz, $CDCl_3$): δ -76.7 (d, *J* = 1041.5 Hz).

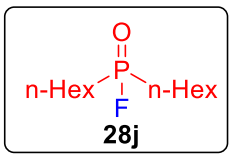

28j

dihexylphosphinic fluoride (28j).[19] 27.8 mg, 58%; as a solid; **IR** ν (thin film, cm^{-1}) 2922, 2351, 1466, 1263, 1150, 962, 705; ^{1}H NMR (400 MHz, $CDCl_3$) δ 1.86-1.79 (m, 4H), 1.68-1.61 (m, 4H), 1.43-1.38 (m, 4H), 1.34-1.25 (m, 8H), 0.91-0.86 (m, 6H); ^{13}C NMR (100.5 MHz, $CDCl_3$): δ 31.1, 30.2 (d, *J* = 14.9 Hz), 27.6 (dd, *J* = 87.1, 14.1 Hz), 22.2, 21.1 (d, *J* = 4.4 Hz), 13.9; ^{31}P NMR (162 MHz, $CDCl_3$): δ 71.1 (d, *J* = 1015.7 Hz); ^{19}F NMR (376 MHz, $CDCl_3$): δ -78.2 (d, *J* = 1016.3 Hz).

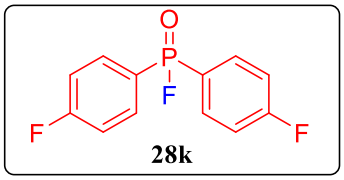

28k

Bis(4-fluorophenyl)phosphinic fluoride (28k).[19] 34.2 mg, 67%; as a solid; **IR** ν (thin film, cm^{-1}) 3072, 2922, 2361, 1494, 1499, 1399, 1229, 1130, 931, 669; ^{1}H NMR (400 MHz, $CDCl_3$) δ 7.87-7.81 (m, 4H), 7.24-7.20 (m, 4H); ^{13}C NMR (100.5 MHz, $CDCl_3$): δ 165.9 (dd, *J* = 256.1, 3.7 Hz), 134.1 (ddd, *J* = 12.6. 9.0, 1.5 Hz), 124.5 (ddd, *J* = 145.9, 23.9, 3.8 Hz), 116.5 (dd, *J* = 21.6, 14.9 Hz); ^{31}P NMR

(162 MHz, $CDCl_3$): δ 39.2 (d, *J* = 1018.6 Hz); ^{19}F NMR (376 MHz, $CDCl_3$): δ -72.9 (d, *J* = 1018.6 Hz), -103.3.

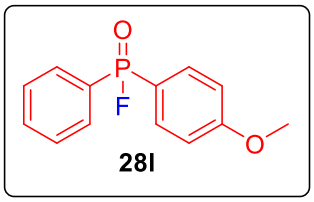

28l

(4-methoxyphenyl)(phenyl)phosphinic fluoride (28l).[84] 25.9 mg, 51%; as a solid; **IR** ν (thin film, cm^{-1}) 2963, 2920, 2359, 1598, 1505, 1133, 1024, 755, 693; ^1H NMR (400 MHz, $CDCl_3$) δ 7.81-7.73 (m, 4H), 7.62-7.58 (m, 1H), 7.52-7.47 (m, 2H), 7.02-6.98 (m, 2H), 3.86 (s, 3H); ^{13}C NMR (100.5 MHz, $CDCl_3$): δ 163.6 (d, *J* = 3.0 Hz), 133.6 (dd, *J* = 12.7, 1.5 Hz), 133.1 (d, *J* = 2.2 Hz), 131.2 (dd, *J* = 11.1, 2.2 Hz), 129.3 (dd, *J* = 23.1, 141.4 Hz), 128.8 (d, *J* = 14.1 Hz), 119.7 (dd, *J* = 148.1, 23.1 Hz), 114.4 (d, *J* = 14.9 Hz), 55.4; ^{31}P NMR (162 MHz, $CDCl_3$): δ 41.9 (d, *J* = 1014.7 Hz); ^{19}F NMR (376 MHz, $CDCl_3$): δ -73.8 (d, *J* = 1013.3 Hz).

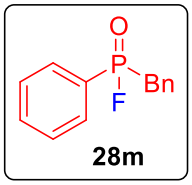

28m

Benzyl(phenyl)phosphinic fluoride (28m).[85] 28.2 mg; as a solid; **IR** ν (thin film, cm^{-1}) 3060, 2921, 1601, 1495, 1437, 1128, 965, 828, 695; ^1H NMR (400 MHz, $CDCl_3$) δ 7.64-7.57 (m, 3H), 7.47-7.42 (m, 2H), 7.28-7.23 (m, 3H), 7.14-7.10 (m, 2H), 3.48 (dd, *J* = 18.0, 5.2 Hz, 2H); ^{13}C NMR (100.5 MHz, $CDCl_3$): δ 133.5 (d, *J* = 3.0 Hz), 131.5 (dd, *J* = 10.4, 2.2 Hz), 129.9 (*J* = 6.0 Hz), 129.3 (dd, *J* = 7.4, 1.5 Hz), 128.7 (d, *J* = 3.0 Hz), 128.6 (d, *J* = 13.4 Hz), 127.4 (d, *J* = 3.8 Hz), 127.3 (dd, *J* = 132.5, 18.6 Hz), 37.1 (dd, *J* = 91.5, 18.6 Hz); ^{31}P NMR (162 MHz, $CDCl_3$): δ 49.7 (d, *J* = 1033.8 Hz); ^{19}F NMR (376 MHz, $CDCl_3$): δ -76.8 (d, *J* = 1034.0 Hz).

Chapter III

Synthetic Utility of Thiophosphoric Acid: Synthesis of Thiophosphate and Phosphorous Disulfide

3.1 Introduction and Background of Thiophosphate and Disulfide Synthesis

Thiophosphate-containing small molecules are of great interest to organic chemists because they have been used as antibacterial, anticancer, and anti-glaucoma agents (**Scheme 3.1**).[87-91] In addition, phosphorodithioate compounds have been utilized extensively in agricultural chemistry as herbicides and insecticides.[92] Therefore, much research has been dedicated to studying and synthesizing this important functional group.

Scheme 3.1 Applications of Thiophosphate and Phosphorodithioate

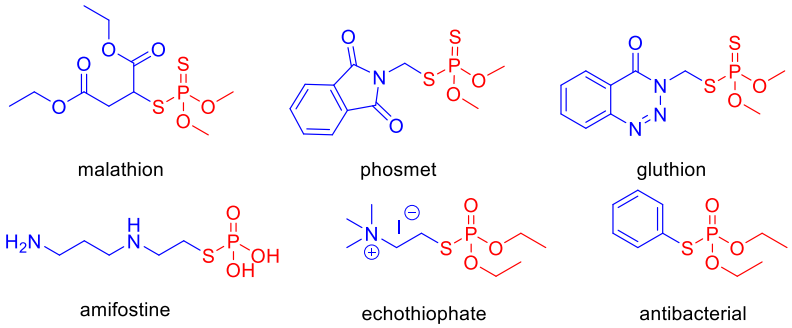

One of the most common approaches to synthesizing thiophosphate involves the reaction of P-Cl-containing compounds with thiols through nucleophilic substitution.[93] However, chlorophosphines are moisture-sensitive and challenging to handle. To circumvent this, the Xiao group reported a 1,3-dichloro-5,5-dimethylhydantoin (DCDMH) mediated thiophosphate synthesis using dipropyl phosphite **9b** and sterically hindered thiol **42b** to furnish **43b** in a high yield of 92% (**Scheme 3.2**).[94] Cross dehydrogenative coupling (CDC) reactions have also been used, which directly couple a thiol and a P(V) nucleophile under metal catalysis. CDC reactions are an attractive strategy for thiophosphate synthesis as they are direct coupling and catalytic reactions. Ni, Cu, Fe, Cs, Pd, n-chlorosuccinimide, H_2O_2, and sulfur salts have been used in CDC reactions to synthesize thiophosphate.[95-106]

Scheme 3.2 Synthetic Strategies for Thiophosphate Synthesis

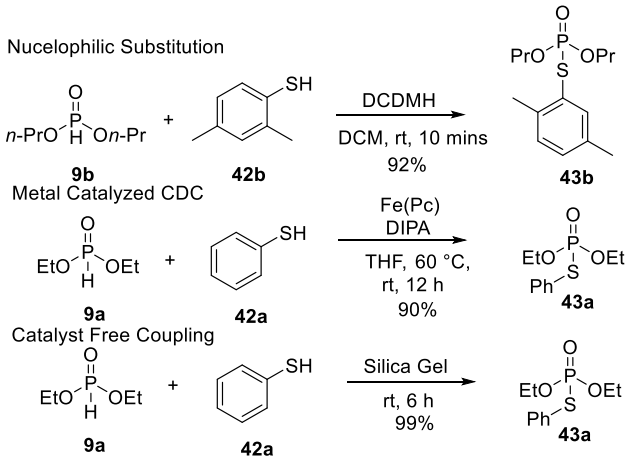

Our research group has previously developed a CDC reaction using diethyl phosphite **9**, thiolphenol **42a,** and an iron (II) catalyst to give thiophosphate **43a** in a high yield of 90% through a free radical mechanism (**Scheme 3.2**).[96] Badasara reported a catalyst-free approach by reacting diethyl phosphite **9a** and thiophenol **42a** with silica gel to synthesize **43a** in a high yield of 99% (**Scheme 3.2**).[107] Catalyst-free methods are currently limited to having a trivalent phosphorous tautomer as a nucleophile. Electrochemical and photochemical methods have also been reported for the synthesis of thiophosphate.[71, 108, 109]

Scheme 3.3 Thiophosphoric Acid as a Reagent for Thiophosphate Synthesis

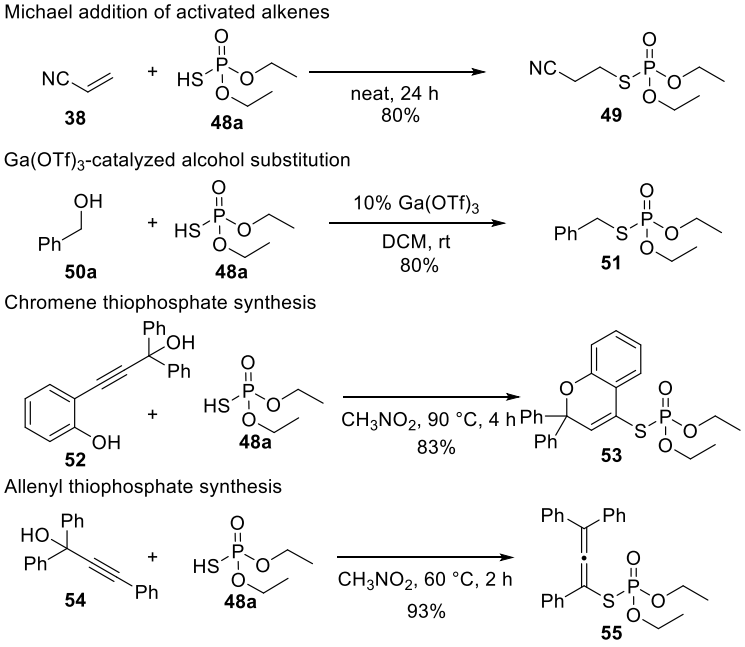

It can be envisioned that $(EtO)_2P(O)SH$ can pose as a pentavalent nucleophile and offer an alternative disconnection for synthesizing thiophosphates. The Mieloszynski group used a neat mixture of **48a** $(EtO)_2P(O)SH$ and acrylonitrile **38** to give β-functionalized thiophosphate **49** in 80% yield (**Scheme 3.3**).[110] This result proves that $(EtO)_2P(O)SH$ can serve as a Michael donor to highly activated Michael acceptors. The Wu group developed a catalytic approach to thiophosphates using a $Ga(OTf)_3$ catalyzed cross-coupling of benzyl alcohol **50a** and **48a** to give thiophosphate **51** in a high yield of 80% (**Scheme 2.3**).[111] The Xiao group used **48a** as a catalyst and Michael donor to synthesize chromene thiophosphate **53** and allenyl thiophosphate **55** in high yields from propargyl alcohols **52** and **54** (**Scheme 3.3**).[112, 113]

Orthoquinone methides (o-QM) are reactive intermediates in organic synthesis and biological systems. They can be generated by thermal, acidic, basic, or photochemical conditions and have been used as Michael acceptors for addition reactions.[114-121] For example, addition to the exocyclic double bond of a quinone methide will result in aromatization of the molecule, a thermodynamic driving force. Phosphorylation of o-QM, p-QM, and aza o-QM with trivalent phosphorous nucleophiles has been reported.[122-128] Our research group previously disclosed a nitrogen heterocyclic phosphorodiamidic acid catalyzed P-C bond-forming reaction of in situ formed o-QM with triethyl phosphite **57** and diaryl alcohol **56a** to give functionalized phosphonate **58** in a high yield of 91% (**Scheme 3.4**).[129] Thiophosphorylation of o-QM and the use of P(V) nucleophiles in o-QM chemistry remains underexplored.

Scheme 3.4 Nitrogen Heterocyclic Phosphorodiamidic Acid Catalyzed C-P Bond Formation

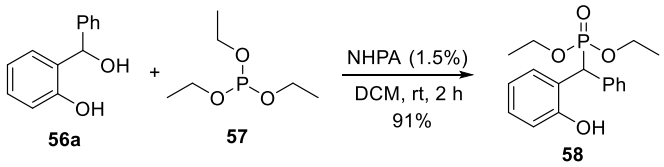

In addition to thiophosphates, disulfides have numerous applications in different areas of chemistry (**Scheme 3.5**).[130, 131] More specifically, disulfide bonds are prevalent in the human body as oxidized cysteine residues and play a vital role in stabilizing secondary and tertiary protein structures (**Scheme 3.5**).[132] Small molecule disulfides have many therapeutic applications such as anti-viral agents, anti-cancer reagents, and an anti-alcoholism drug (**Scheme 3.5**).[133-136] Disulfides naturally occurring in garlic have been studied and have been found to possess antithrombic, antimicrobial, and anticancer properties (**Scheme 3.5**).[137] Furthermore, they have been employed as a silane coupling agent to covalently link silica filler and rubber polymer in passenger car tires to provide better fuel economy, wear and tear, and wet traction (**Scheme 3.5**).[138] Therefore, many efforts have been dedicated to synthesizing symmetrical and unsymmetric disulfides.

Scheme 3.5 Selected Applications of Disulfide

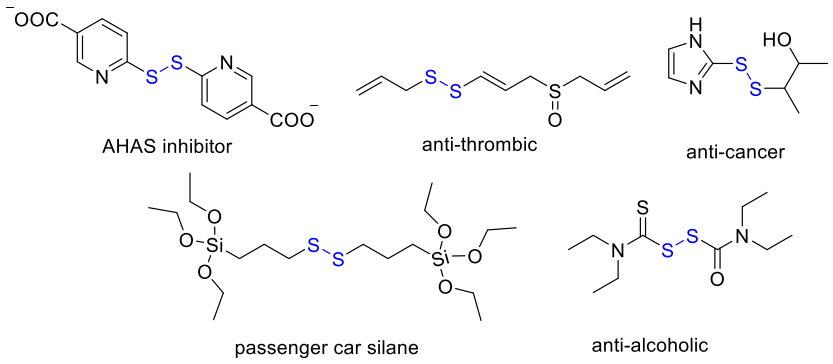

The synthesis of symmetrical disulfides is straightforward compared to the synthesis of unsymmetrical disulfides due to no side reactions. Symmetrical disulfides have been synthesized using molecular oxygen as the oxidizing agent with metal catalysts such as iron and cobalt.[139-141] Iodine and hydrogen peroxide are other commonly employed oxidizing agents for synthesizing symmetrical disulfides. In addition, disulfur chloride has been utilized as a bis-electrophile and reacted with two equivalents of thiol to produce symmetrical disulfides through nucleophilic substitution.[142] Other chlorinating agents, such as trimethylsilyl chloride (TMSCl) and cyanuric chloride with dimethyl sulfoxide (DMSO) as the oxidant, have also been used to synthesize symmetric disulfides.[143] Notably, the Harp group oxidized cubyl mercaptan **59** to cubyl disulfide **60** in high yield using molecular iodine as the oxidant (**Scheme 3.6**).[144]

Scheme 3.6 Synthesis of Disulfide by Oxidation

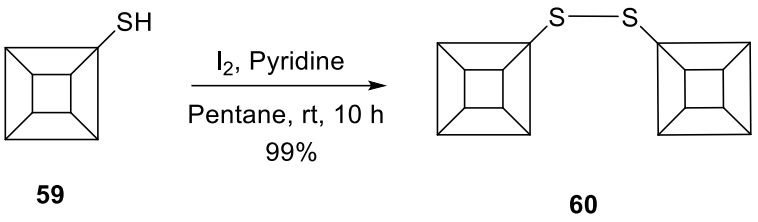

59 **60**

The synthesis of mixed disulfides poses more challenges due to a side reaction: the formation of thiol homodimers.[145] This competing reaction decreases the yield of the desired unsymmetrical disulfide. However, a direct coupling reaction between two distinct thiol reaction partners can be achieved by taking advantage of reactivity differences such as sterics and oxidation kinetics.[146, 147]

Scheme 3.7 Catalytic Mixed Disulfide Synthesis

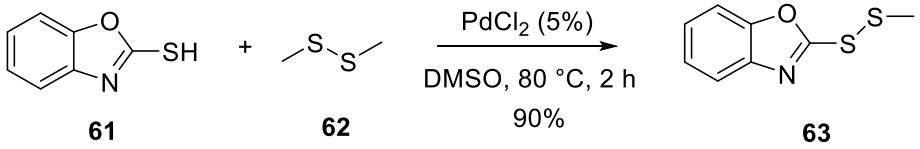

61 **62** **63**

Catalytic approaches to unsymmetric disulfide synthesis have been performed using Rh, Pd, and NFSI catalysts.[148-150] For example, the Xu group demonstrated a catalytic synthesis of unsymmetrical disulfide **63** by reacting thiol **61** with disulfide **62** through a palladium-catalyzed disulfide exchange reaction (**Scheme 3.6**).[149] A common approach to unsymmetric disulfide synthesis, which minimizes the formation of homodimers, uses an umpolung strategy. This method treats a thiol with a preactivated sulfur electrophile such as sulfenamides, thiosulfonate, mercaptobenzotriazole, mercaptobenzothiazole, phosphorous disulfide, 2-pyridyl disulfide, and Bunte salts.[151-159] The Paquer group used Bunte salt **64** as a sulfur electrophile to react with thiolate **65** to form unsymmetrical disulfide **66** in a high yield of 70% using an aqueous system. (**Scheme 3.8**).[154]

Scheme 3.8 Disulfide Synthesis by Preactivated Sulfur Electrophile

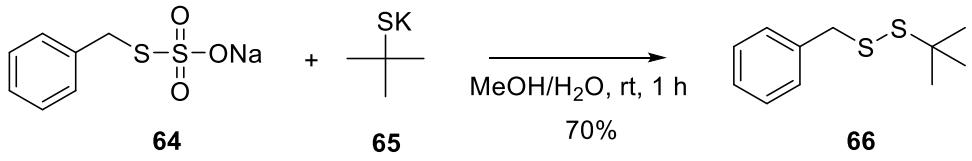

64 **65** **66**

Recently, the Jiang group released a Suzuki and Hiyama-type cross-coupling reaction to forge disulfides.[160, 161] They reacted boronic acid **67** with mixed disulfide **68** under catalytic conditions to generate disulfide **69** through a persulfide intermediate (**Scheme 3.9**).[160] In

addition, the Jiang group developed other disulfurating reagents containing reactive S-O bonds that can be readily substituted with soft nucelophiles.[162, 163] They have also been employed in a Sandmeyer and photocatalytic C-H functionalization reaction.[164, 165]

Scheme 3.9 Disulfide Synthesis by Disulfurating Reagent

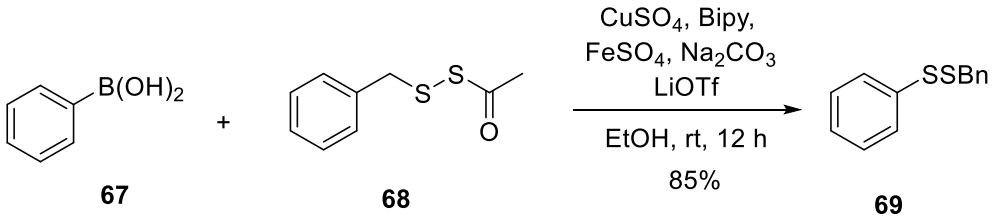

67 **68** **69**

A one-pot umpolung strategy to synthesize disulfides involves the formation of sulfenyl halides and subsequent reaction with thiol and has been recently realized.[166, 167] The logic behind this strategy is to reverse the polarity of the sulfur atom by installing an electronegative halogen. The Yang group has reacted 4-methyl thiophenol **70** with 2-mercaptopyridine **71** in the presence of a chlorinating agent to form unsymmetric disulfide **72** in a yield of 89% (**Scheme 3.10**).[168] Lei has also developed a direct electrochemical approach to disulfide synthesis without metals or oxidants but it requires a bulky thiol with a lower oxidation reaction rate to minimize homodimerization.[147]

Scheme 3.10 Disulfide Synthesis by Sulfenyl Chloride

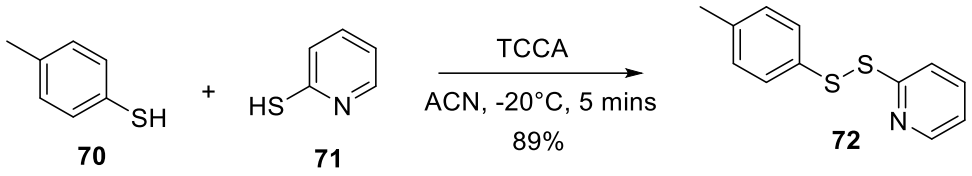

70 **71** **72**

Although many examples of unsymmetric and symmetrical disulfide synthesis are available, there has only been one precedent example of a synthetic method to access P(O)-S-S bond motifs. The Cao group demonstrated P(O)-S-S bond formation and synthesized **74** from dithioperoxate **73** and secondary phosphine oxide **7a** using ball milling and a diisopropylethylamine (DIPEA) additive (**Scheme 3.11**).[169] The substrate scope for this method is limited to alkyl dithioperoxate. When aryl dithioperoxates are used, an alternative reaction pathway is followed to give thiophosphate as the product.

Scheme 3.11 P(O)-S-S Bond Forming Reaction by Ball Milling

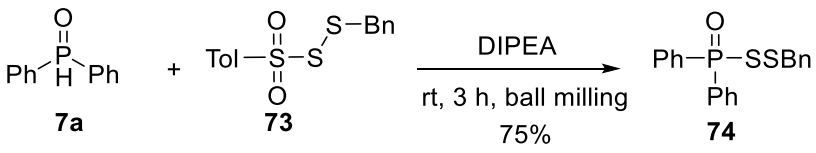

7a **73** **74**

As both thiophosphates and disulfides possess valuable properties, novel small molecules containing P(O)-S-S bonds would interest chemists in academia and industry. A dual role of $(EtO)_2P(O)SH$ can be harnessed to synthesize valuable thiophosphates and phosphorous disulfides.

3.2 Specific Aim

This project aims to explore the new reactivity of $(EtO)_2P(O)SH$. Develop a mild, atom-economical, catalyst-free, and additive-free synthesis of thiophosphates.[170] It also aims to develop a green synthesis of phosphorous disulfides that is additive-free, energy-neutral, uses renewable solvents, and avoids harsh reagents.

3.3 Green Synthesis of Thiophosphate

We hypothesized that $(EtO)_2P(O)SH$ **48a** could serve as a Brønsted acid and thiolate nucleophile. The Brønsted acidity will be able to activate certain reaction partners through an acid-base reaction, and the in-situ generated thiolate can serve as a strong nucleophile for subsequent addition or substitution reactions. To test our hypothesis, we used diaryl alcohol **56a** and $(EtO)_2P(O)SH$ **48a** as model substrates for reaction optimization. The reaction was first tested using a 1:1 ratio of **56a**:**48a,** and the product **75a** was generated in a yield of 37% (**Table 3.1**, entry 1). Next, the ratio of 1:1.5 of **56a**:**48a** was used, and the yield of **75a** increased significantly to 91% (**Table 3.1**, entry 2). Solvent effects were then analyzed, and it was found that the solvents THF, DCE, toluene, ACN, and ether gave inferior yields compared to DCM. (**Table 3.1**, entries 3-7). Next, the reaction was tested under neat conditions, and it provided a

yield of 44% (**Table 3.1**, entry 8). The decrease in yield is presumably due to the diminished intermolecular interaction since the reaction mixture is a heterogenous solution.

Table 3.1 Optimization of Thiophosphorylation Reaction Conditions[a]

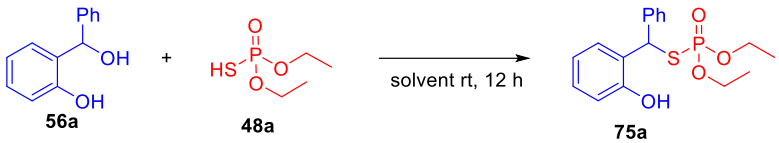

entry	**56a** :**48a**	solvent	yield (%)
1	1.0 : 1.0	DCM	37
2	1.0 : 1.5	DCM	91
3	1.0 : 1.5	THF	-
4	1.0 : 1.5	DCE	45
5	1.0 : 1.5	toluene	49
6	1.0 : 1.5	ACN	37
7	1.0 : 1.5	ether	24
8	1.0 : 1.5	neat	44

[a]Reaction conditions: **56a** and **48a** in solvent (0.5 mL) for 12 h. Isolated yield.

With the optimized conditions established, the scope of the diaryl alcohol reaction partner **56** was tested to see the steric and electronic effect on reaction outcome (**Table 3.2**). Halogenated diaryl alcohols (4-F, 4-Cl, 3,4 di-Cl) **56b-56d** gave the corresponding products **75b-75d** in yields of 63%-82%. Diaryl alcohols containing electron-donating substituents (4-Me, 2-MeO, and 3,5-tert-Bu) **56e**-**56g** were well tolerated giving the desired products **75e**-**75g** in high yields of 69%-81%. Bulky aromatic systems such as **56h** and **56i** (biphenyl and naphthyl) were also well tolerated, providing the target products **75h** and **75i** in 78% and 92% yields,

respectively. However, Alkyl substituted phenol **56j** generated the product **75j** in a low yield of 34%. The low yield is presumably due less stabilization of the o-QM intermediate.

Table 3.2 Scope of Thiophosphorylation Reaction[a]

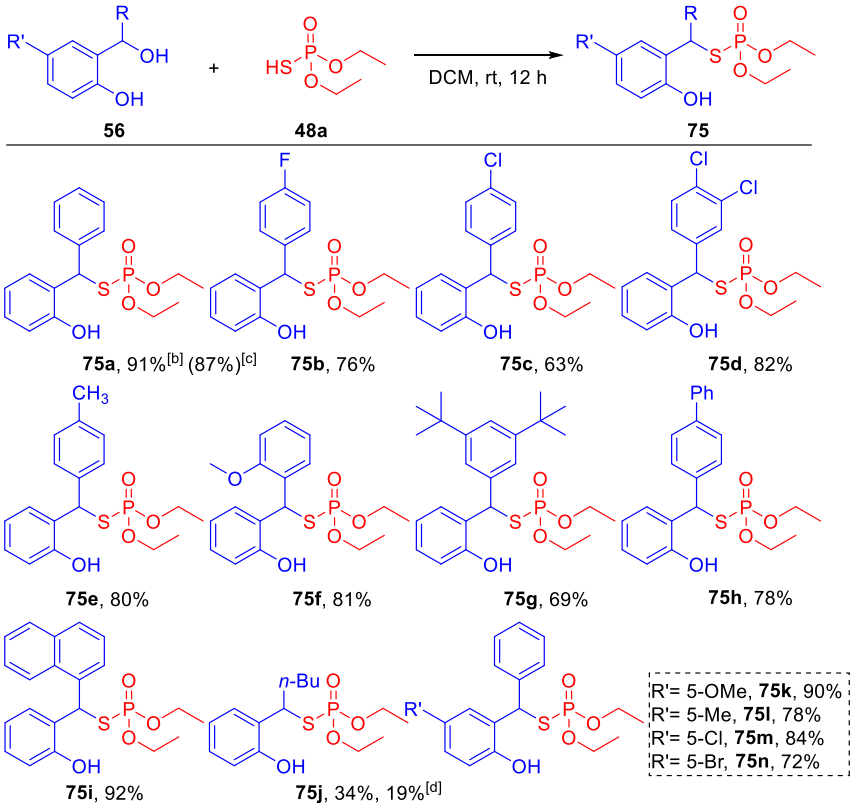

[a]Reaction conditions: **56** (0.1 mmol) and **48a** (0.15 mmol) in DCM (0.5 mL) for 12 h. [b]Isolated yield. [c]A gram-scale experiment with **56a** (3.0 mmol). [d]with 3Å molecular sieves.

Furthermore, the use of molecular sieves did not improve the yield of **75j**. This result implies that H_2O may help to stabilize the reactive intermediate through hydrogen bonding interactions.[171]

Next, the substrate variation on the phenol motif was explored. Electron donating groups such as **56k** and **56l** (5-MeO and 5-Me) on the phenol were tolerated to give **75k** and **75l** in high yields of 90% and 78%, respectively. Phenols containing halogenated substituents **56m** and **56n** (5-Cl and 5-Br) also furnished **76m** and **76n** in high yields of 84% and 72%, respectively. A scale-up experiment (3.0 mmol) was performed and gave product **75a** in a high yield of 87%. This experiment demonstrated that the reactivity is not compromised at a larger scale.

Table 3.3 Scope of Thiophosphoric Acid Nucleophile to Form Thiophosphate[a]

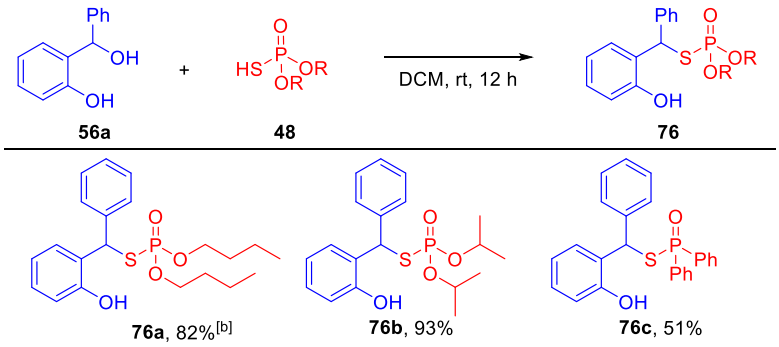

[a]Reaction conditions: **56a** (0.1 mmol) and **48** (0.15 mmol) in DCM (0.5 mL) for 12 h.[b]Isolated yield.

Phosphorous thioacids with different substituents **48** (alkoxy and aryl) were then tested to see their effects on reaction outcomes (**Table 3.3**). Alkoxy substituted thioacids **48b** and **48c** (n-Bu and i-Pr) effectively provided the target products **76a** and **76b** in high 82% and 93% yields, respectively. Aryl diphenyl thiophosphinic acid **48d** also afforded the product **76c** in a moderate yield of 51%. These results demonstrated that thioacid derivatives were well tolerated.

Table 3.4 Scope of Sulfonamido Thiophosphate Synthesis[a]

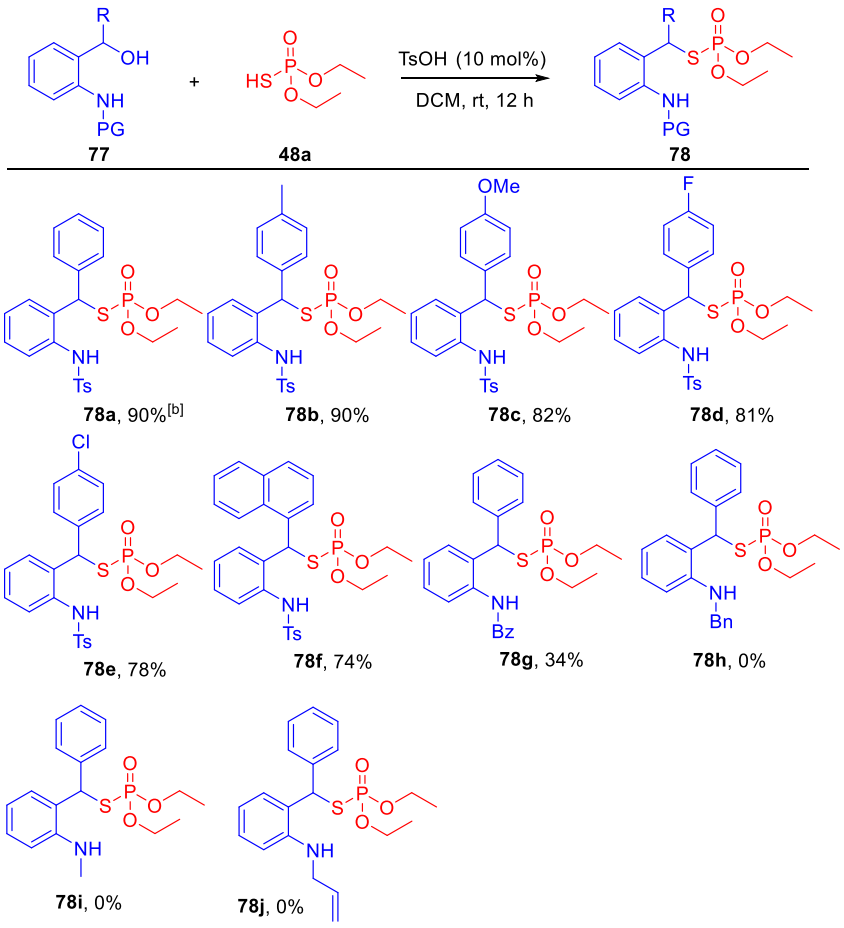

[a]Reaction conditions: **77** (0.1 mmol), **48a** (0.2 mmol), and TsOH (10 mol%) in DCM (0.5 mL) for 12 h.[b]Isolated yield.

Next, we wanted to expand the scope of this chemistry further and apply it to aza o-QM (**Table 3.4**). Aza o-QM has not been studied as much in the literature compared to o-QM due to the multistep preparation of the amino alcohol starting material. Our preliminary results found that thiophosphoric acid was not a strong enough acid to form the aza o-QM. However, when toluene sulfonic acid (TsOH) was used at a catalytic amount (10 mol%), the reaction proceeded to generate **78a** at a high yield of 90%. Other sulfonamido alcohols **77** were screened with different benzylic functionalization (**Table 3.4**). For example, sulfonamido alcohols containing electron-donating groups **77b** and **77c** (4-Me and 4-MeO) provided the target products **78b** and **78c** in high yields of 90% and 80%, respectively. Next, halogen-containing alcohols **77d** and **77e** (4-F and 4-Cl) were evaluated, and they also furnished the desired products **78d** and **78e** in high yields of 81% and 78%, respectively. In addition, sulfonamido alcohol containing a bulky naphthyl group **77f** provided the product **78f** in a high yield of 78%. The benzoyl nitrogen protecting group was investigated on amido alcohol **77g**. However, it provided the product **78g** in a low yield of 34%. This low yield is presumably due to the weak polarizability by the benzoyl group compared to the tosyl group.[172] Furthermore, alkyl-protecting groups were screened **77h-77j**. The final products were unstable and rapidly decomposed after isolation, preventing compound characterization. A possible explanation is an E1cB reaction to remove the stable thiophosphate group, which could be electronically promoted by having an electron-donating group, such as an alkyl group attached to the nitrogen atom.

Scheme 3.12 Proposed o-QM Addition Mechanism

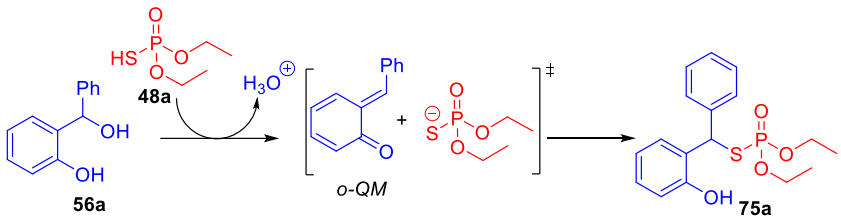

Based on the experimental observation and our previous work a plausible mechanism is proposed (**Scheme 3.12**).[129] Diaryl alcohol **56a** is protonated by **48a** and water is released to form o-QM intermediate and thiolate. Next, sulfa-Michael addition reaction of o-QM and thiolate provides product **75a**.

3.4 Mechanism Study Control Experiments

Some control experiments were performed to gain further insights into the reaction mechanism (**Scheme 3.13**). Diaryl alcohol **56a** was treated with thiophosphoric acid **48a** and phosphoric acid **79** in a stoichiometric amount, and the reaction outcome provided **75a** in an 83% yield. This competition experiment shows that the thiolate nucleophile is much more reactive than an oxygen nucleophile. Based on the experimental results, thiols are much better nucleophiles than oxygen nucleophiles in hard soft acid base theory and the Mayer reactivity scale.[173, 174] Furthermore, the reaction between **56a** and **79** yielded none of the desired products, which can be attributed to the lower acidity and nucleophilicity of **79**. **48a** has a pka of 1.0 (in H_2O), while **79** has a pka of 3.8 (in H_2O). The outcomes of the control experiment

support the dual role of **48a** as Brønsted acid and thiolate nucleophile. However, the reaction of **48a** with benzyl alcohol **50a** and diphenyl methanol **50b** provided no target compounds, which suggests that a reaction mechanism may not involve a carbocation. Instead, the mechanism may proceed through an o-QM intermediate.

Scheme 3.13 Thiophosphorylation Reaction Control Experiments

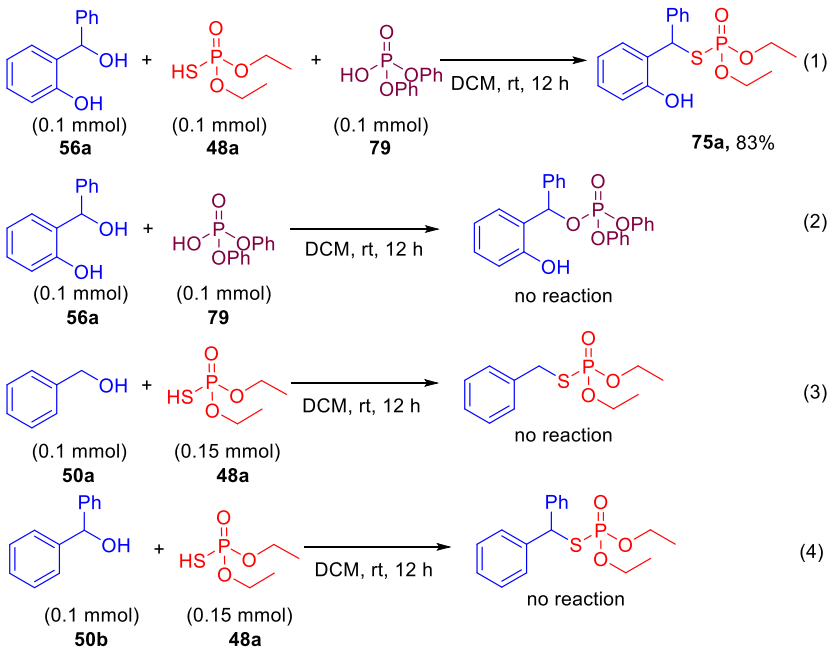

3.5 Green Synthesis of Phosphorous Disulfide

Table 3.5 Optimization of Phosphorous Disulfide Synthesis[a]

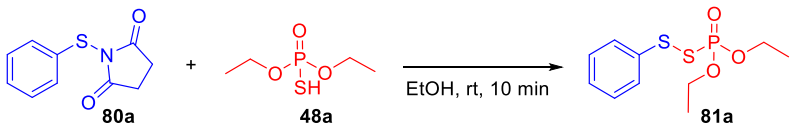

entry	solvent	Yield (%)
1	EtOH	95
2	DCM	94
3	Acetone	74
4	ACN	92
5	THF	92
6	Ether	94
7	Toluene	75

[a]Reaction conditions: **80a** (0.1 mmol) and **48a** (0.1 mmol) in solvent (0.5 mL) for 10 min. Isolated yield.

Based on our findings of the dual functionality of **48a**, we hypothesized that this reagent could be reacted with n-thiosuccinimides to form a P(O)-S-S bond.[170] Using N-thiosuccinimide **80a** and $P(O)(OEt)_2SH$ **48a** as model substrates in ethanol as the reaction solvent, the reaction completed in 10 minutes to give **81a** in an isolated yield of 95% (**Table 1**, entry 1). Next, the reaction was screened with other solvents to test solvent effects, they were well tolerated to provide the product with high yields (**Table 1**, entries 2-7). Ultimately, ethanol was chosen as the solvent because it is environmentally friendly and is readily available through biomass fermentation.[175] The reaction addresses many of the 12 principles of green chemistry as defined by the American Chemical Society.[176] The reaction is highly atom-economical as no additional additives or a molar excess of reagents are used. Additionally, the reaction is energy neutral as no heating is required. The use of safer solvents and renewable feedstocks is achieved by using ethanol as the solvent. Lastly, the synthesis avoids using transition metal catalysts and harsh chlorinating reagents, typically used for disulfide synthesis.

Table 3.6 Scope of Phosphorus Disulfide Synthesis[a]

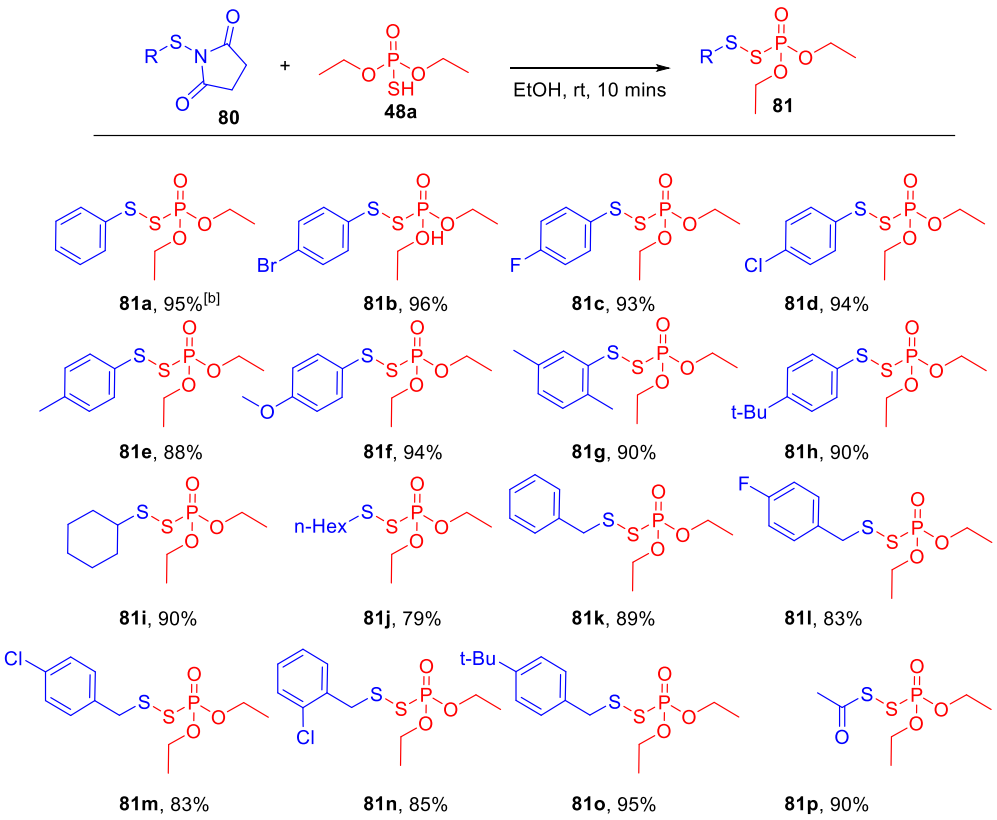

[a]Reaction conditions: **80** (0.1 mmol) and **48a** (0.1 mmol) in EtOH (0.5 mL) for 10 min.[b]Isolated yield.

With the optimized reaction conditions, the scope of N-thiosuccinimide electrophiles was tested to probe the steric and electronic effects on the reaction outcome (**Table 3.6**). The reaction provided the target products **82a-82p** in high yields of 74-96% and tolerated steric and electronic factors of the N-thiosuccinimide reaction partner **80** (**Table 3.6**). Aryl halogen containing N-thiosuccinimides **80b-80d** (4-Br, 4-F, and 4-Cl) generated the products **81b-81d** in high yields of 93-96%. Aryl N-thiosuccinimides bearing electron-donating groups **80e** and **80f** (4-

Me and 4-OMe) also provided the products **80e** and **80f** in high yields of 88% and 94%, respectively. Next, aryl N-thio succinimides **80g** and **80h** containing sterically demanding groups (2,5 dimethyl and 4-tertbutyl) provided the products **81g** and **81h** in a high yield of 90%. Akyl N-thiosuccinimides **80i** and **80j** (n-hexyl and cyclohexane) were also well tolerated, giving products **81i** and **81j** in high yields of 79% and 90%, respectively. Additionally, benzylic N-thiosuccinimide **80k** provided the product **81k** in a yield of 89%, and no competing substitution reactions at the benzylic carbon occurred. Benzylic N-thiosuccinimides containing halogens and electron donating groups **80l-80o** (4-fluoro, 4-chloro, 2-chloro, and 4-tertbutyl) generated the corresponding products **81l-81o** in high yields of 83-95%. Furthermore, acyl N-thiosuccinimides **80p** was also tolerated, giving the product **81p** with a high yield of 90%.

Table 3.7 Scope of Thiophosphoric Acid Nucleophile for Thiophosphorylation Reaction[a]

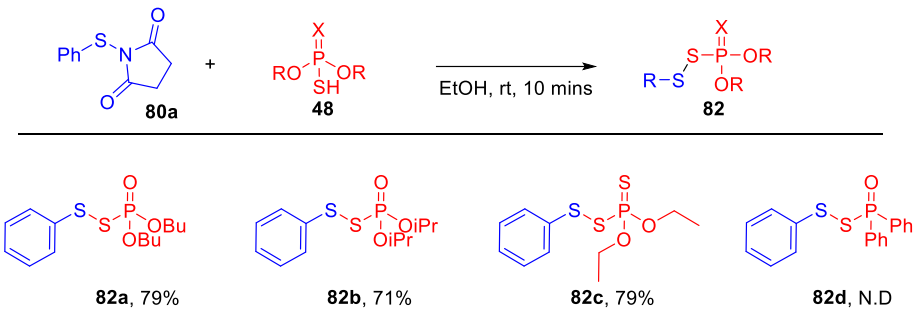

[a]Reaction conditions: **80a** (0.1 mmol) and **48** (0.1 mmol) in EtOH (0.5 mL) for 10 min. Isolated yield. N.D = not detected.

The scope of the thioacid nucleophile was then evaluated (**Table 3.7**). Thioacids with different alkoxy substituents **48b** and **48c** (butyl and isopropyl) were well tolerated, giving the products **82a** and **82b** in high yields of 79% and 71%, respectively. O,O-diethyl S-hydrogen phosphorodithioate **48d,** which bears a thiophosphoryl bond, was screened and provided the product **82c** in a high yield of 79%. However, Diphenylthiophosphinic acid **48d** did not provide the target product even at elevated temperatures.

3.6 Mechanism Study and Control Experiments

Scheme 3.14 Sulfurization Control Experiments

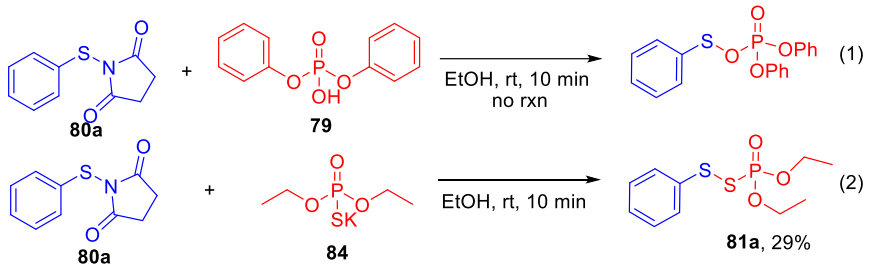

Control experiments were performed to gain insight into the reaction mechanism (**Scheme 3.14**). The reaction with diphenyl phosphoric acid **79** and **80a** did not give any desired product, which reveals that a stronger acid and more nucleophilic thiolate are required for the reaction. In addition, the role of the proton was investigated by using

the potassium salt **84**, which provided the desired product in a much lower yield compared to **48a**. This outcome suggests that a proton is necessary to increase the electrophilicity of **80a**.

Mechanistically, the nitrogen atom of **80a** is protonated by **48a** to form pyrrolidinium intermediate **I**. The electrophilic intermediate **I** undergoes substitution reaction with phosphorous thiolate intermediate **II** to generate the disulfide product **81a** by liberating the succinimide leaving group (**Scheme 3.15**).

Scheme 3.15 Proposed Mechanism of Phosphorous Disulfide Synthesis

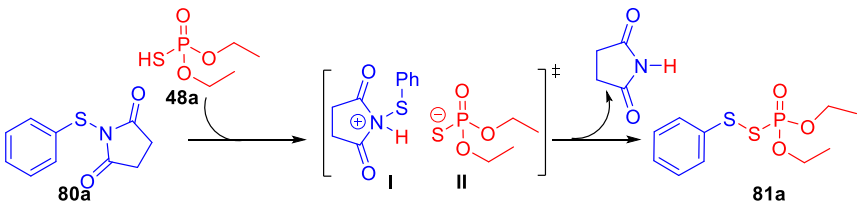

3.7 Conclusion

The series of control experiments support the dual functionality of **48a. 48a** can serve as a Brønsted acid, and thiolate nucleophile. Diaryl alcohols were activated in situ to form a reactive o-QM intermediate that was trapped to form desirable highly functionalized thiophosphates. This synthetic method allows for facile synthesis of thiophosphates and

sulfonamido thiophosphates. The method avoids metal catalysts, additives, increased temperature, and poor atom economics. Furthermore, we have developed a rapid and green synthetic method to access phosphorous disulfides that addresses the persistent homodimerization issues in unsymmetrical disulfide synthesis. The method's advantages are the short reaction time, green solvent, high atom economy, and avoidance of using harsh reagents such as oxidants, chlorinating reagents, and transition metal catalysts. Phosphorous disulfides are an emerging functional group that will greatly benefit medicinal and synthetic organic chemistry.

3.8 Experimental

3.8.1 General information

All reactions were carried out under air atmosphere in oven-dried glassware with magnetic stirring bar. Dry solvents (THF, toluene, ACN, diethyl ether, and DCM) were obtained by solvent purification system under argon. All commercially available reagents were used as received without further purification. The tubes used for the reaction are shown in **Figure S1**. Purification of reaction products was carried out by flash column chromatography using silica gel 60 (230-400 mesh). Analytical thin layer chromatography was performed on 0.25 mm aluminum-backed silica gel 60-F plates. Visualization was accompanied with UV light and $KMnO_4$ solution. Concentration under reduced pressure refers to the removal of volatiles using a rotary evaporator attached to a dry diaphragm pump (10-15 mm Hg) followed by pumping to a constant weight with an oil pump (<300 mTorr). Infrared (IR) spectra were recorded on an IR spectrometer with KBr wafers or a film on KBr plate. High-resolution mass spectra (HRMS) were

recorded on LCMS-IT-TOF mass spectrometer using ESI (electrospray ionization) or APCI (Atmospheric Pressure Chemical Ionization). ^{1}H NMR spectra were recorded in $CDCl_3$ on 400 MHz NMR spectrometer. The ^{1}H chemical shifts are referenced to residual solvent signals at δ 7.26 ($CHCl_3$) or δ 0.00 (TMS). ^{1}H NMR coupling constants (*J*) are reported in Hertz (Hz) and multiplicities are indicated as follows: s (singlet), bs (broad singlet), d (doublet), t (triplet), q (quartet), m (multiplet), dd (doublet of doublets), dt (doublet of triplets), td (triplet of doublets), tt (triplet of triplets). ^{13}C NMR spectra were proton decoupled and recorded in $CDCl_3$ on 100.5 MHz NMR spectrometer. The ^{13}C chemical shifts are referenced to solvent signals at δ 77.16 ($CDCl_3$). ^{31}P NMR spectra were proton decoupled and recorded in $CDCl_3$ on 162 MHz NMR spectrometer. ^{31}P chemical shifts are reported relative to 85% H_3PO_4 (0.00 ppm) as an external standard.

3.8.2 General procedure 1 Synthesis of Thiophosphate

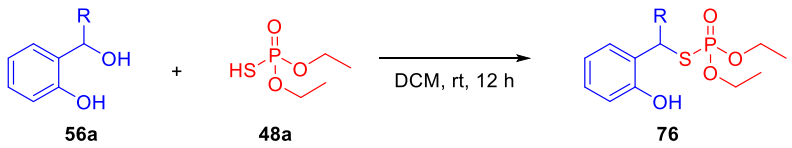

To a solution of O,O-diethyl S-hydrogen phosphorothioate **48a** (0.15 mmol) in DCM (0.5 mL) was added diaryl phenol **56** (0.10 mmol) at room temperature. The reaction mixture was stirred for 12 hours. After stirring for 12 hours at room temperature, the reaction mixture was subjected to column chromatography on silica gel to give the corresponding thiophosphate product **75**.

3.8.3 General Procedure 2 Synthesis of Thiophosphate

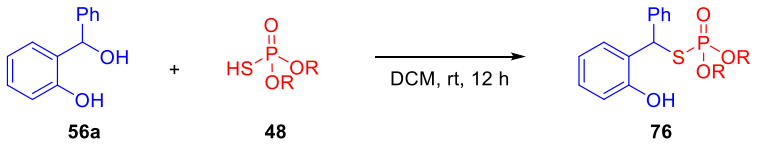

To a solution of thiophosphoric acid **48** (0.15 mmol) in DCM (0.5 mL) was added 2-(hydroxy(phenyl)methyl)-4-methylphenol **56a** (0.10 mmol) at room temperature. The reaction mixture was stirred for 12 h. After stirring for 12 hours at room temperature, the reaction mixture was subjected to column chromatography on silica gel to give the corresponding thiophosphate product **76**.

3.8.4 General Procedure Synthesis of Sulfonamido Thiophosphate 78

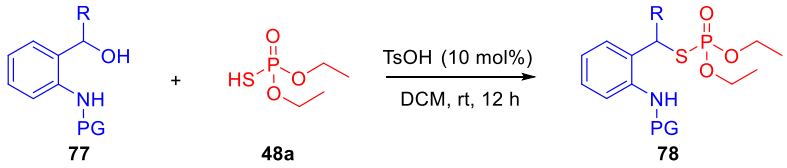

To a solution of thiophosphoric acid **48a** (0.2 mmol) and sulfonamido alcohol **77** (0.1 mmol) in DCM (0.5 mL) was added p-toluenesulfonic acid (0.01 mmol) at room temperatue. The reaction mixture was stirred for 12 hours at room temperature. After stirring for 12 hours at room temperature, the reaction mixture was subjected to column chromatography on silica gel to give the corresponding sulfonamido thiophosphate product **78**.

3.8.5 General Procedure 1 Synthesis of Phosphorous Disulfide

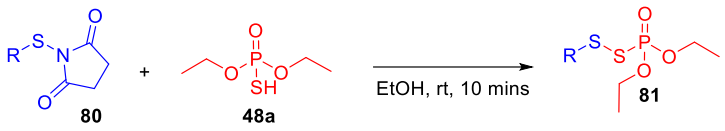

To a solution of thiophosphoric acid **48a** (0.10 mmol) in ethanol (0.5 mL) was added thiosuccinimide **80** (0.10 mmol) at room temperature. The reaction mixture was stirred for 10 minutes. After stirring for 10 minutes at room temperature, the reaction mixture was subjected to column chromatography on silica gel to give the corresponding phosphorous disulfide product **81**.

3.8.6 General procedure 2 Synthesis of Phosphorous Disulfide

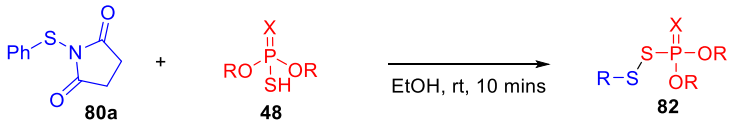

To a solution of thiophosphoric acid **48** (0.10 mmol) in ethanol (0.5 mL) was added thiosuccinimide **80a** (0.10 mmol) at room temperature. The reaction mixture was stirred for 10 minutes. After stirring for 10 minutes at room temperature, the reaction mixture was subjected to column chromatography on silica gel to give the corresponding phosphorous disulfide products **82**.

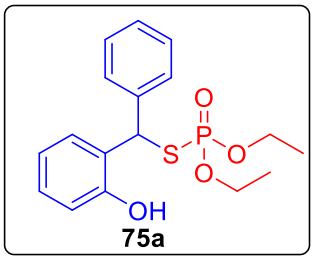

75a

O,O-diethyl S-((2-hydroxyphenyl)(phenyl)methyl) phosphorothioate (75a). 31.5 mg, 91%; as an oil; **IR** ν (thin film, cm^{-1}); 3322, 2986, 1597, 1480, 1450, 1226, 1018, 972, 756, 702; **^{1}H NMR** (400 MHz, $CDCl_3$) δ 7.47 (d, *J* = 8.0 Hz, 2H), 7.32-7.28 (m, 2H), 7.24-7.21 (m, 2H), 7.11-7.07 (m, 1H), 6.92 (d, *J* = 4.0 Hz, 1H), 6.83 (t, *J* = 7.2 Hz, 1H), 6.14 (d, *J* = 12.4 Hz, 1H). 4.07-3.91 (m, 3H), 3.90- 3.83 (m, 1H), 1.22-1.13 (m, 6H); **^{13}C NMR** (100.5 MHz, $CDCl_3$) δ 153.8, 140.7 (d, *J* = 5.2 Hz), 129.0, 128.8, 128.5 (d, *J* = 5.2 Hz), 128.4, 128.3, 127.3, 120.4, 117.2, 64.1 (d, *J* = 5.9 Hz), 64.0 (d, *J* = 5.9 Hz), 48.1 (d, *J* = 3.0 Hz), 15.7 (d, *J* = 7.4 Hz); **^{31}P NMR** (162 MHz, $CDCl_3$): δ 28.62; **HRMS** (ESI): m/z calcd. for $C_{17}H_{21}O_4PS$ ([M+Na]+): 375.0790; Found: 375.0769.

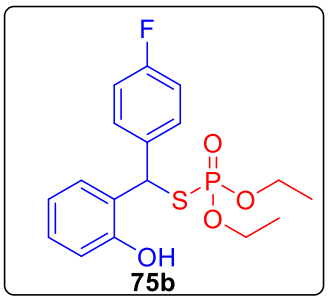

75b

O,O-diethyl S-((4-fluorophenyl)(2-hydroxyphenyl)methyl) phosphorothioate (75b). 28.2 mg, 76%; as an oil; **IR** ν (thin film, cm^{-1}); 3140, 2985, 1597, 1504, 1411, 1342, 1234, 1157, 1095, 702; 78%; **^{1}H NMR** (400 MHz, $CDCl_3$) δ 8.18 (br s, 1H), 7.45-7.42 (m, 2H), 7.20 (dd, *J* = 7.6 Hz, *J* = 1.6 Hz, 1H), 7.13-7.08 (m, 1H), 6.99-6.95 (m, 2H), 6.91 (dd, *J* = 8.4 Hz, *J* = 1.2 Hz, 1H), 6.84 (td, *J* = 7.6 Hz, *J* = 1.2 Hz, 1H), 6.14 (d, *J* = 12.4 Hz, 1H), 4.05-3.94 (m, 3H), 3.93-3.86 (m, 1H) 1.22-1.14 (m, 6H); **^{13}C NMR** (100.5 MHz, $CDCl_3$) δ 161.8 (d, *J* = 246.0 Hz), 153.7, 136.8, 136.7 (d, *J* = 5.9 Hz), 129.9 (d, *J* = 8.2 Hz), 128.8 (d, *J* = 16.4 Hz), 128.3 (d, *J* = 5.2 Hz), 120.2, 117.1, 115.2 (d, *J* = 20.8 Hz), 64.1 (ap t, *J* = 5.9 Hz), 47.3 (d, *J* = 12.0 Hz) 15.7 (d, *J* = 7.5 Hz); **^{31}P NMR** (162 MHz, $CDCl_3$): δ 28.03; **HRMS** (ESI): m/z calcd. for $C_{17}H_{20}O_4FPS$ ([M+Na]+): 393.0696; Found: 393.0688.

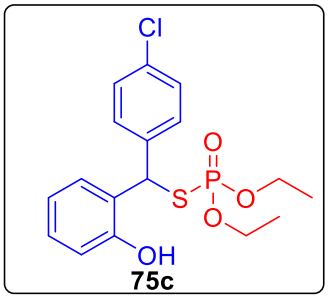

75c

S-((4-chlorophenyl)(2-hydroxyphenyl)methyl) O,O-diethyl phosphorothioate (75c). 24.2 mg, 63%; as an oil; **IR** ν (thin film, cm^{-1}); 3224, 1597, 1489, 1226, 1018, 756; **^{1}H NMR** (400 MHz, $CDCl_3$) δ 8.14 (br s, 1H), 7.42-7.38 (m, 2H), 7.28-7.25 (m, 2H), 7.21 (dd, *J* = 7.6 Hz, *J* =1.2 Hz, 1H), 7.13-7.09 (m, 1H), 6.90 (dd, *J* = 8.4 Hz, *J* =1.2 Hz, 1H), 6.84 (td, *J* = 8.4 Hz, *J* = 1.2 Hz, 1H), 6.12 (d, *J* = 12.8 Hz, 1H), 4.06-3.95 (m, 3H), 3.93-3.86 (m, 1H), 1.23-1.48 (m, 6H); **^{13}C NMR** (100.5 MHz, $CDCl_3$) δ 153.7, 139.5 (d, *J* = 5.2 Hz), 133.1, 129.6, 128.9, 128.7, 128.5, 128.1 (d, *J* = 5.2 Hz), 120.3, 117.2, 64.1 (ap t, *J* = 5.9 Hz), 47.4 (d, *J* = 2.9 Hz), 15.7 (d, *J* = 7.4Hz); **^{31}P NMR** (162 MHz, $CDCl_3$): δ 28.00; **HRMS** (ESI): m/z calcd. for $C_{17}H_{20}O_4ClPS$ ([M+Na]+): 409.0401; Found: 409.0378.

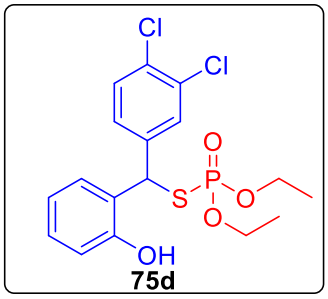

75d

S-((3,4-dichlorophenyl)(2-hydroxyphenyl)methyl) O,O-diethyl phosphorothioate (**75d**). 33.2 mg, 82%; as a white solid; mp 118-120 °C **IR** ν (thin film, cm^{-1}) 3224, 2985, 1597, 1458, 1226, 1018, 756; **^{1}H NMR** (400 MHz, $CDCl_3$) δ 7.57 (s, 1H), 7.35-7.24 (m, 3H), 7.14-7.10 (m, 1H), 6.91-6.84 (m, 2H), 6.12 (d, *J* = 12.4 Hz, 1H), 4.07-4.00 (m, 3H), 3.99-3.89 (m, 1H), 1.25-1.16 (m, 6H); **^{13}C NMR** (100.5 MHz, $CDCl_3$) δ 153.7, 141.5 (d, *J* = 5.3 Hz), 132.3, 131.3, 130.2 (*J* = 7.4 Hz), 129.1, 128.6, 127.7, 127.3, 127.2, 120.3, 116.8, 64.2 (ap t, *J* = 5.9 Hz), 46.8 (d, *J* = 3.0 Hz), 15.8 (d, *J* = 7.5 Hz); **^{31}P NMR** (162 MHz, $CDCl_3$): δ 27.34; **HRMS** (ESI): m/z calcd. for $C_{17}H_{19}O_4PSCl_2$ ([M+Na]+): 443.0011; Found: 443.0075.

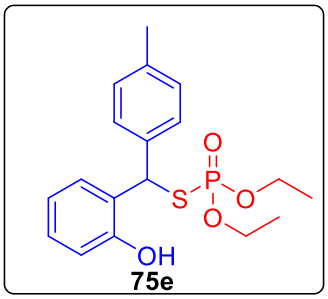

75e

O,O-diethyl S-((2-hydroxyphenyl)(p-tolyl)methyl) phosphorothioate (75e). 28.7 mg, 80%; as an oil; **IR** ν(thin film, cm^{-1}); 3232, 2985, 2924, 1597, 1504, 1450, 1219, 1018, 756; 80%; **^{1}H NMR** (400 MHz, $CDCl_3$) δ 7.93 (br s, 1H), 7.34 (d, *J* = 8.0 Hz, 2H), 7.18 (dd, *J* = 8.0 Hz, *J* =1.2 Hz, 1H), 7.13-7.09 (m, 2H), 7.08 (d, *J* = 1.6 Hz, 1H), 6.92 (dd, *J* = 8.0 Hz, *J* =1.2 Hz, 1H), 6.82 (td, *J* = 6.8 Hz, *J* =1.2 Hz, 1H), 6.07 (d, *J* = 12.4 Hz, 1H), 4.09-3.94 (m, 3H), 3.89-3.82 (m, 1H), 2.32 (s, 3H), 1.23-1.12 (m, 6H); **^{13}C NMR** (100.5 MHz, $CDCl_3$) δ 153.6, 137.5 (d, *J* = 6.0 Hz), 137.1, 129.2, 129.1, 129.0, 128.7, 128.1, 120.5, 117.7, 64.1 (d, *J* = 6.7 Hz), 64.0 (d, *J* = 5.9 Hz), 48.0 (d, *J* = 3.0 Hz), 21.0, 15.8 (d, *J* = 3.0 Hz), 15.7 (d, *J* = 3.0 Hz); **^{31}P NMR** (162 MHz, $CDCl_3$): δ 28.88; **HRMS** (ESI): m/z calcd. for $C_{18}H_{23}O_4PS$ ([M+Na]+): 389.0947; Found: 389.0926.

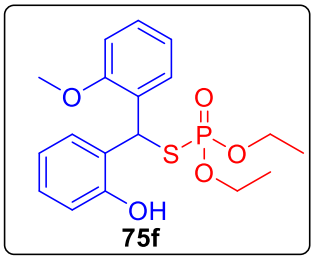

75f

O,O-diethyl S-((2-hydroxyphenyl)(2-methoxyphenyl)methyl) phosphorothioate (**75f**). 29.5 mg, 81%; as a white solid; mp 123-125 °C**; IR** ν(thin film, cm^{-1}); 3232, 2985, 1597, 1489, 1018, 756; **^{1}H NMR** (400 MHz, $CDCl_3$) δ 7.82 (br s, 1H), 7.60 (dd, *J* = 7.6, 1.6 Hz, 1H), 7.28-7.24 (m, 1H), 7.17 (dd, *J* = 8.0, *J* = 2.0 Hz, 1H), 7.11-7.07 (m, 1H), 6.99 (td, *J* = 8.0 Hz, *J* = 1.2 Hz, 1H), 6.91 (dd, *J* = 8.0 Hz, *J* = 1.2 Hz, 1H), 6.86 (dd, *J* = 8.4 Hz, *J* = 0.8 Hz, 1H), 6.78 (td, *J* = 7.6 Hz, *J* = 1.2 Hz, 1H), 6.27 (d, *J* = 14.0 Hz, 1H), 4.08-3.94 (m, 3H), 3.93-3.86 (m, 1H), 3.78 (s, 3H), 1.20-1.15 (m, 6H); **^{13}C NMR** (100.5 MHz, $CDCl_3$) δ 155.8, 155.3, 129.4, 129.0, 128.94, 128.90, 128.7, 128.6, 128.3, 128.2, 117.7, 111.0, 63.9 (ap t, *J* = 5.9 Hz), 42.8 (d, *J* = 3.0 Hz), 15.8 (d, *J* = 4.4 Hz), 15.7 (d, *J* = 4.5 Hz); **^{31}P NMR** (162 MHz, $CDCl_3$): δ 29.40; **HRMS** (ESI): m/z calcd. for $C_{18}H_{23}O_5PS$ ([M+Na]+): 405.0896; Found: 405.0885.

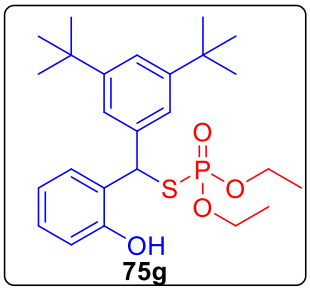

75g

S-((3,5-di-tert-butylphenyl)(2-hydroxyphenyl)methyl) O,O-diethyl phosphorothioate (**75g**). 46.4 mg, 69% as a white solid; mp 142-145 °C **IR** ν (thin film, cm^{-1}) 3224, 2962, 1597, 1458, 1226, 1018, 756; **^{1}H NMR** (400 MHz, $CDCl_3$) δ 7.30 (s, 3H), 7.18-7.16 (m, 1H), 7.11-7.07 (m, 1H), 6.94 (d, *J* = 8.4 Hz, 1H), 6.81 (t, *J* = 8.0 Hz, 1H), 6.05 (d, *J* = 12.8 Hz, 1H), 4.04-3.93 (m, 3H), 3.86- 3.82 (m, 1H), 1.29 (s, 18H), 1.18-1.09 (m, 6H); **^{13}C NMR** (100.5 MHz, $CDCl_3$) δ 153.7, 150.8, 139.3 (d, *J* = 5.9 Hz), 129.1 (d, *J* = 4.5 Hz), 129.0, 128.7, 122.7, 121.3, 120.4, 117.7, 64.1 (d, *J* = 5.9 Hz), 63.9 (d, *J* = 5.9 Hz), 49.0 (d, *J* = 2.9 Hz), 34.8, 31.4, 15.7 (d, *J* = 7.4 Hz); **^{31}P NMR** (162 MHz, $CDCl_3$): δ 29.35; **HRMS** (ESI): m/z calcd. for $C_{25}H_{37}NO_5PS$ ([M+Na]+): 487.2042; Found: 487.2024.

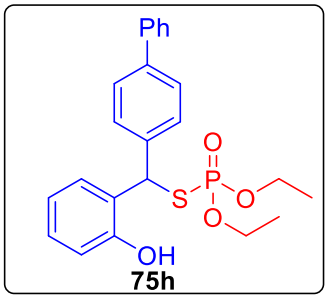

75h

S-([1,1'-biphenyl]-4-yl(2-hydroxyphenyl)methyl) O,O-diethyl phosphorothioate (75h). 32.5 mg, 78%; as a white solid; mp 128-130 °C; **IR** ν (thin film, cm^{-1}); 3209, 2978, 1597, 1481, 1220,1018, 750; **^{1}H NMR** (400 MHz, $CDCl_3$) δ 8.0 (br s, 1H), 7.77-7.51 (m, 6H), 7.44-7.39 (m, 2H), 7.35-7.31 (m, 1H), 7.27-7.15 (m, 1H), 7.14-7.11 (m, 1H), 6.94 (dd, *J* = 8.0 Hz, *J* =1.2 Hz, 1H), 6.86 (td, *J* = 7.6 Hz, *J* = 1.2 Hz, 1H), 6.17 (d, *J* = 12.8 Hz, 1H), 4.10-3.97 (m, 3H), 3.92-3.86 (m, 1H), 1.23-1.14 (m, 6H); **^{13}C NMR** (100.5 MHz, $CDCl_3$) δ 153.7, 140.4, 140.2, 139.6 (d, *J* = 5.9 Hz), 129.0, 128.9, 128.8 (d, *J* = 4.4 Hz), 128.76, 128.7, 127.3, 127.1, 127.0, 120.5, 117.6, 64.2 (d, *J* = 6.7 Hz), 64.1 (d, *J* = 6.0 Hz), 47.9 (d, *J* = 2.3 Hz), 15.8 (ap t, *J* = 2.2 Hz); **^{31}P NMR** (162 MHz, $CDCl_3$): δ 28.56; **HRMS** (ESI): m/z calcd. for $C_{23}H_{25}O_4PS$ ([M+Na]+): 451.1103; Found: 451.1097.

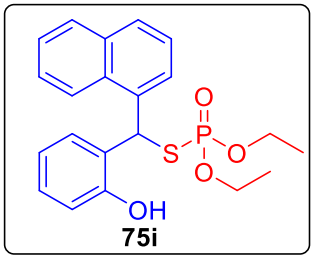

75i

O,O-diethyl S-((2-hydroxyphenyl)(naphthalen-1-yl)methyl) phosphorothioate (75i). 35.9 mg, 92%; as an oil; **IR** ν(thin film, cm^{-1}) 3217, 2985, 1597, 1458, 1219, 1018, 756; **^{1}H NMR** (400 MHz, $CDCl_3$) δ 8.52 (br s, 1H), 8.08-8.06 (m, 1H), 7.87 (d, *J* = 7.2 Hz, 1H), 7.84-7.79 (m, 2H), 7.53-7.49 (m, 1H), 7.44-7.40 (m, 2H), 7.12-7.05 (m, 2H), 7.0 (dd, *J* = 8.0 Hz, *J* = 1.2 Hz, 1H), 6.83 (d, *J* = 12.4 Hz, 1H), 6.75-6.71 (m, 1H), 4.14-3.81 (m, 4H), 1.21-1.09 (m, 6H); **^{13}C NMR** (100.5 MHz, $CDCl_3$) δ 153.2, 136.4 (d, *J* = 6.7 Hz), 133.7, 130.6, 129.4, 129.3, 129.0, 128.9, 128.6, 128.5, 126.7, 125.9, 124.8, 123.7, 120.7, 118.3, 64.3 (d, *J* = 6.7 Hz), 64.1 (d, *J* = 6.0 Hz), 45.7 (d, *J* = 2.3 Hz), 15.7 (ap t, *J* = 7.4 Hz); **^{31}P NMR** (162 MHz, $CDCl_3$): δ 29.29; **HRMS** (ESI): m/z calcd. for $C_{21}H_{23}O4PS$ ([M+Na]+): 425.0947; Found: 425.0927.

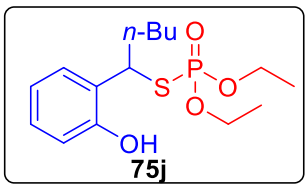

75j

O,O-diethyl S-(1-(2-hydroxyphenyl)pentyl) phosphorothioate (75j). 11.1 mg, 34%; as an oil; **IR** ν(thin film, cm^{-1}); 3224, 2954, 1597, 1458, 1219, 1018, 972, 756; **^{1}H NMR** (400 MHz, $CDCl_3$) δ 8.10 (br s, 1H), 7.27-7.25 (m, 2H), 7.16-7.11 (m, 1H), 6.96-6.91 (m, 2H), 4.73-4.66 (m, 1H), 4.23-4.10 (m, 2H), 3.83-3.67 (m, 2H), 2.08-2.00 (m, 2H), 1.44-1.24 (m, 6H), 1.12-1.07 (m, 3H), 0.90-0.85 (m, 3H); **^{13}C NMR** (100.5 MHz, $CDCl_3$) δ 153.7, 130.6, 128.6, 126.9, 121.2, 119.1, 64.1 (d, *J* = 6.7 Hz), 64.0 (d, *J* = 6.0 Hz), 44.9 (d, *J* = 3.7 Hz), 36.3 (d, *J* = 9.7 Hz), 29.8, 22.0, 15.9 (d, *J* = 7.4 Hz), 15.6 (d, *J* = 7.5 Hz), 13.8; **^{31}P NMR** (162 MHz, $CDCl_3$): δ 30.85; **HRMS** (ESI): m/z calcd. for $C_{15}H_{25}O_4PS$ ([M+Na]+): 355.1103; Found: 355.1087.

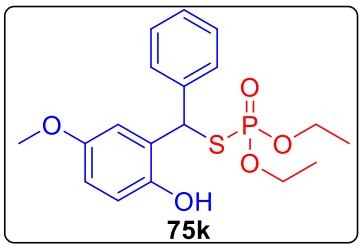

75k

O,O-diethyl S-((2-hydroxy-5-methoxyphenyl)(phenyl)methyl) phosphorothioate (**75k**). 34.3 mg, 90%; as a white solid; mp 119-121°C **IR** ν (thin film, cm^{-1}) 3248, 2985, 1597, 1435, 1103, 720; **^{1}H NMR** (400 MHz, $CDCl_3$) δ 7.47-7.45 (m, 2H), 7.34-7.30 (m, 2H), 7.27-7.25 (m, 1H), 6.88 (d, *J* = 8.4 Hz, 1H), 6.73 (d, *J* = 2.8 Hz, 1H), 6.69-6.66 (m, 1H), 6.07 (d, *J* = 12.0 Hz, 1H), 4.10-3.95 (m, 3H), 3.87-3.81 (m, 1H), 3.62 (s, 3H), 1.25-1.31 (m, 6H); **^{13}C NMR** (100.5 MHz, $CDCl_3$) δ 153.5, 147.4, 140.2 (d, *J* = 6.7 Hz), 130.4 (d, *J* = 3.7 Hz), 128.4, 128.1, 127.4, 118.9, 114.5, 114.0, 64.5 (d, *J* = 6.0 Hz), 64.2 (d, *J* = 6.7 Hz), 55.6, 48.2 (d, *J* = 3.0 Hz), 15.8 (d, *J* = 6.7 Hz), 15.7 (d, *J* = 7.5 Hz); **^{31}P NMR** (162 MHz, $CDCl_3$): δ 28.73; **HRMS** (ESI): m/z calcd. for $C_{18}H_{23}O_5PS$ ([M+Na]+): 405.0896; Found: 405.0886.

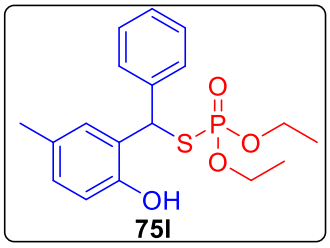

75l

O,O-diethyl S-((2-hydroxy-5-methylphenyl)(phenyl)methyl) phosphorothioate (75l). 27.4 mg, 78%; as an oil; **IR** ν (thin film, cm^{-1}) 3232, 2985, 1504, 1226, 1018, 810; **^{1}H NMR** (400 MHz, $CDCl_3$) δ 7.48-7.45 (m, 2H), 7.34-7.29 (m, 2H), 7.27-7.23 (m, 2H), 6.96-6.89 (m, 1H), 6.82 (d, *J* = 8.0 Hz, 1H), 6.06 (d, *J* = 12.8 Hz, 1H); 4.07-3.95 (m, 3H), 3.90-3.81 (m, 1H), 2.19 (s, 3H), 1.23-1.12 (m, 6H); **^{13}C NMR** (100.5 MHz, $CDCl_3$) δ 151.2, 140.5 (d, *J* = 6.0 Hz), 129.8, 129.5, 129.3, 128.8 (d, *J* = 3.7 Hz), 128.4, 128.2, 127.3, 117.7, 64.1 (d, *J* = 6.0 Hz), 64.0 (d, *J* = 5.9 Hz), 48.2 (d, *J* = 3.0 Hz), 20.6, 15.8 (d, *J* = 4.5 Hz), 15.7 (d, *J* = 4.4 Hz); **^{31}P NMR** (162 MHz, $CDCl_3$): δ 28.76; **HRMS** (ESI): m/z calcd. for $C_{18}H_{23}O_4PS$ ([M+Na]+): 389.0947; Found: 389.0935.

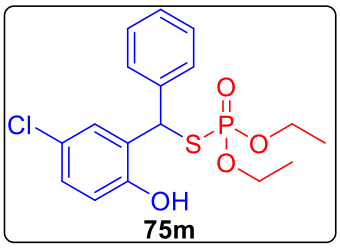

75m

S-((5-chloro-2-hydroxyphenyl)(phenyl)methyl) O,O-diethyl phosphorothioate (**75m**). 31.0 mg, 84%; as an oil; **IR** ν (thin film, cm^{-1}) 3201, 2985, 1597, 1489, 1219, 1018; **^{1}H NMR** (400 MHz, $CDCl_3$) δ 7.43 (d, *J* = 7.6 Hz, 2H), 7.31 (t, *J* = 8.0 Hz, 2H), 7.28-7.25 (m, 1H), 7.21 (d, *J* = 2.4 Hz, 1H), 7.03 (dd, *J* = 8.8 Hz, *J* = 2.8 Hz, 1H), 6.84 (d, *J* = 8.8 Hz, 1H), 6.09 (d, *J* = 12.4 Hz, 1H), 4.06-3.98 (m, 3H), 3.96-3.91 (m, 1H), 1.20 (q, *J* = 6.8 Hz, 6H); **^{13}C NMR** (100.5 MHz, $CDCl_3$) δ 152.6, 139.9 (d, *J* = 6.7 Hz), 130.5, 130.4, 128.7, 128.6, 128.1, 127.6, 124.7, 118.7, 64.3 (ap t, *J* = 6.7 Hz), 47.7 (d, *J* = 2.2 Hz), 15.7 (d, *J* = 7.5 Hz); **^{31}P NMR** (162 MHz, $CDCl_3$): δ 27.91; **HRMS** (ESI): m/z calcd. for $C_{17}H_{20}NO_4PSCl$ ([M+Na]+): 409.0401; Found: 409.0377.

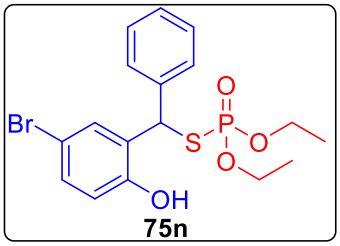

75n

S-((5-bromo-2-hydroxyphenyl)(phenyl)methyl) O,O-diethyl phosphorothioate (75n). 31.1 mg, 72%; as an oil; **IR** ν (thin film, cm^{-1}) 3170, 2985, 1589, 1489, 1219, 1018, 748; **^{1}H NMR** (400 MHz, $CDCl_3$) δ 7.43-7.41 (m, 2H), 7.39-7.25 (m, 4H), 7.16 (dd, *J* = 8.4 Hz, *J* = 2.4 Hz, 1H), 6.77 (d, *J* = 8.4 Hz, 1H), 6.11 (d, *J* = 12.4 Hz, 1H), 4.07-4.0 (m, 3H), 3.97-3.90 (m, 1H), 1.22-1.17 (m, 6H); **^{13}C NMR** (100.5 MHz, $CDCl_3$) δ 153.2, 140.0 (d, *J* = 6.7 Hz), 131.4, 130.72, 130.68, 128.6, 128.2, 127.6, 118.8, 111.7, 64.3 (ap t, *J* = 6.0 Hz), 47.6 (d, *J* = 3.0 Hz), 15.7 (d, *J* = 7.5 Hz); **^{31}P NMR** (162 MHz, $CDCl_3$): δ 28.01; **HRMS** (ESI): m/z calcd. for $C_{17}H_{20}O_4BrPS$ ([M+Na]+): 452.9895; Found: 452.9882.

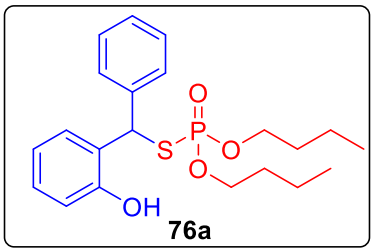

76a

O,O-dibutyl S-((2-hydroxyphenyl)(phenyl)methyl) phosphorothioate (76a). 33.4 mg, 82%; as an oil; **IR** ν (thin film, cm^{-1}) 3224, 2962, 1597, 1458, 1219, 1018, 748; **^{1}H NMR** (400

MHz, $CDCl_3$) δ 7.47-7.45 (m, 2H), 7.33-7.30 (m, 2H), 7.27-7.23 (m, 1H), 7.16 (dd, *J* = 7.6 Hz, *J* = 1.6 Hz, 1H), 7.12-7.09 (m, 1H), 6.94-6.92 (m, 1H), 6.82 (td, *J* = 7.6 Hz, *J* = 1.2 Hz, 1H), 6.11 (d, *J* = 12.8 Hz, 1H), 3.99-3.87 (m, 3H), 3.82-3.76 (m, 1H), 1.58-1.44 (m, 4H), 1.30-1.21 (m, 4H), 0.86-0.82 (m, 6H); **^{13}C NMR** (100.5 MHz, $CDCl_3$) δ 153.7, 140.5 (d, *J* = 6.0 Hz), 129.2, 129.1, 129.0, 128.8, 128.4, 128.2, 127.3, 126.8, 67.9 (d, *J* = 6.7 Hz), 67.7 (d, *J* = 6.0 Hz), 48.2 (d, *J* = 3.0 Hz), 31.9 (d, *J* = 2.2 Hz), 31.8 (d, *J* = 1.5 Hz), 18.5 (d, *J* = 3.0 Hz), 13.4; **^{31}P NMR** (162 MHz, $CDCl_3$): δ 29.29; **HRMS** (ESI): m/z calcd. for $C_{21}H_{29}O_4PS$ ([M+Na]+): 431.1416; Found: 431.1404.

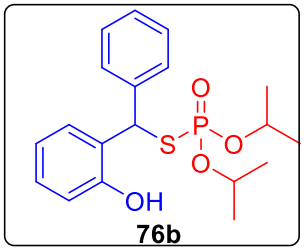

76b

S-((2-hydroxyphenyl)(phenyl)methyl) O,O-diisopropyl phosphorothioate (**76b**). 35.7 mg, 93%; as an oil; **IR** *ν* (thin film, cm^{-1}) 3217, 2978, 1597, 1458, 1219, 987, 748; **^{1}H NMR** (400 MHz, $CDCl_3$) δ 8.39 (br s, 1H), 7.46 (d, *J* = 7.2 Hz, 2H) 7.31 (t, *J* = 7.2 Hz, 2H), 7.24 (d, *J* = 5.6 Hz, 1H), 7.15 (d, *J* = 7.6 Hz, 1H), 7.12-7.07 (m, 1H), 6.94 (d, *J* = 8.0 Hz, 1H), 6.81 (d, *J* = 7.2 Hz, 1H), 6.14 (d, *J* = 13.2 Hz, 1H), 4.61-4.48 (m, 2H), 1.21-1.19 (m, 9H), 1.12 (d, *J* = 6.0 Hz, 3H); **^{13}C NMR** (100.5 MHz, $CDCl_3$) δ 153.9, 140.7 (d, *J* = 6.7 Hz), 129.3 (d, *J* = 3.8 Hz), 129.0, 128.7, 128.4, 128.3, 127.2, 120.3, 117.9, 73.5 (ap t, *J* = 6.7 Hz), 48.3 (d, *J* = 2.3 Hz); 23.6 (d, *J* = 3.7 Hz), 23.5 (d, *J* = 4.5 Hz), 23.4 (d, *J* = 2.2 Hz), 23.3 (d, *J* = 3.0 Hz); **^{31}P NMR** (162 MHz, $CDCl_3$): δ 26.76; **HRMS** (ESI): m/z calcd. for $C_{19}H_{25}O_4PS$ ([M+Na]+): 403.1103; Found: 403.1091.

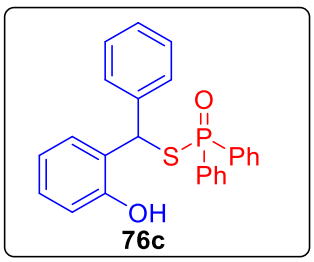

76c

S-((2-hydroxyphenyl)(phenyl)methyl) diphenylphosphinothioate (**76c**). 21.2 mg, 51%; as a white solid; mp 172-174°C; **IR** *ν* (thin film, cm^{-1}) 3062, 2990, 1450, 1382, 1220, 823, 761, 615; **^{1}H NMR** (400 MHz, DMSO-d6) δ 9.60 (br s, 1H), 7.72-7.66 (m, 4H), 7.57-7.53 (m,

2H), 7.47-7.43 (m, 4H), 7.31 (d, *J* = 7.6 Hz, 1H), 7.23-7.21 (m, 2H), 7.17-7.10 (m, 3H), 7.04-7.00 (m, 1H), 6.74-6.69 (m, 2H), 5.87 (d, *J* = 12.0 Hz, 1H); **^{13}C NMR** (100.5 MHz, DMSO-d6) δ 154.1, 142.1, (d, *J* = 3.0 Hz), 133.5 (d, *J* = 104.9 Hz), 132.8 (d, *J* = 3.0 Hz), 132.7 (d, *J* = 2.3 Hz), 131.4 (d, *J* = 6.0 Hz), 131.3 (d, *J* = 6.0 Hz), 129.2 (d, *J* = 72.9 Hz), 129.1 (d, *J* = 12.7 Hz) , 128.7, 128.3 (d, *J* = 17.8 Hz), 127.1, 119.4, 115.6, 46.3; **^{31}P NMR** (162 MHz, DMSO-d6): δ 35.91; **HRMS** (ESI): m/z calcd. for $C_{25}H_{21}O_2PS$ ([M+Na]+): 439.0892; Found: 439.0882.

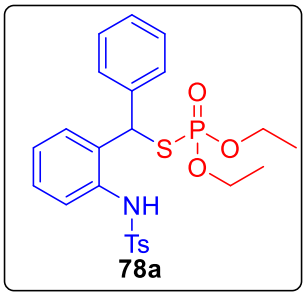

78a

O,O-diethyl S-((2-((4-methylphenyl)sulfonamido)phenyl)(phenyl)methyl) phosphorothioate (78a). 45.3 mg, 90%; as a white solid; mp 139-141°C ; **IR** ν (thin film, cm^{-1}) 3116, 2985, 1597, 1489, 1334, 1226, 1165, 1018, 748, 563; **^{1}H NMR** (400 MHz, $CDCl_3$) δ 8.82 (s, 1H), 7.71 (d, *J* = 8.4 Hz, 1H), 7.57 (d, *J* = 8.0 Hz, 1H), 7.24-7.17 (m, 4H), 7.17-7.12 (m, 2H), 7.08 (td, *J* = 8.4, *J* = 1.2 Hz, 1H), 7.03 (dd, *J* = 8.4 Hz, *J* = 1.6 Hz, 1H), 6.80 (dd, *J* = 8.4 Hz, *J* = 1.6 Hz, 2H), 5.59 (d, *J* = 12.8 Hz, 1H), 4.13-4.01 (m, 2H), 3.97-3.93 (m, 1H), 3.83-3.77 (m, 1H), 2.33 (s, 3H), 1.22-1.11 (m, 6H); **^{13}C NMR** (100.5 MHz, $CDCl_3$) δ 143.2, 139.1, 139.0, 137.6, 136.6, 136.5, 133.8, 129.6, 128.4, 128.2, 127.3, 127.2, 126.8, 126.5, 64.5 (d, *J* = 6.0 Hz), 64.2 (d, *J* = 6.7 Hz), 48.4 (d, *J* = 3.0 Hz), 21.4, 15.8 (d, *J* = 6.7 Hz), 15.7 (d, *J* = 7.5 Hz); **^{31}P NMR** (162 MHz, $CDCl_3$): δ 27.72; **HRMS** (ESI): m/z calcd. for $C_{24}H_{28}NO_5PS_2$ ([M+Na]+): 528.1039; Found: 528.1037.

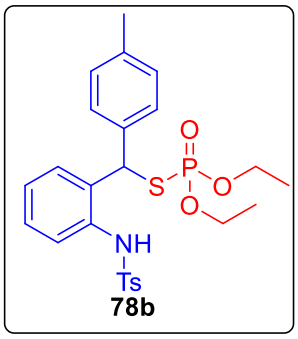

78b

O,O-diethyl S-((2-((4-methylphenyl)sulfonamido)phenyl)(p-tolyl)methyl) phosphorothioate (78b). 46.4 mg, 90%; as a white solid; mp 135-137 °C; **IR** ν (thin film, cm^{-1}) 3132, 2985, 1597, 1473, 1342, 1234, 1157, 1018, 756, 563; **^{1}H NMR** (400 MHz, $CDCl_3$) δ 7.72 (s, 1H), 7.64 (d, *J* = 8.4 Hz, 2H), 7.21 (d, *J* = 2.0 Hz, 1H), 7.16-7.12 (m, 5H), 7.10-7.02 (m, 4H), 5.48 (d, *J* = 12.0 Hz, 1H), 4.01-3.95 (m, 2H), 3.87-3.77 (m, 2H), 2.34 (s, 3H), 2.31 (s, 3H), 1.15-1.08 (m, 6H); **^{13}C NMR** (100.5 MHz, $CDCl_3$) δ 143.5, 142.7 (d, *J* = 5.2 Hz), 137.9 (d, *J* = 5.9 Hz), 137.3, 137.2, 136.1, 129.5, 129.3, 129.2, 127.9, 127.3, 124.4, 120.4, 119.8, 63.6 (d, *J* = 6.0 Hz), 53.5 (d, *J* = 2.9 Hz), 21.5, 21.0, 15.8 (d, *J* = 2.9 Hz), 15.7 (d, *J* = 3.0 Hz); **^{31}P NMR** (162 MHz, $CDCl_3$): δ 25.64; **HRMS** (ESI): m/z calcd. for $C_{25}H_{30}NO_5PS_2$ ([M+Na]+): 542.1195; Found: 542.1200.

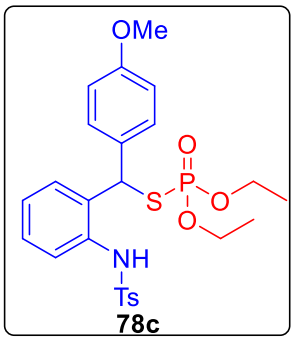

78c

O,O-diethyl S-((4-methoxyphenyl)(2-((4-methylphenyl)sulfonamido)phenyl)methyl) phosphorothioate (**78c**). 42.4 mg, 82% as a white solid; mp 145-148 °C **IR** ν (thin film, cm^{-1}) 3248, 2985, 1604, 1512, 1473, 1334, 1249, 1165, 1018; **^{1}H NMR** (400 MHz, $CDCl_3$) δ 7.63 (d, *J* = 8.4 Hz, 2H), 7.39 (br s, 1H), 7.20-7.14 (m, 6H), 7.10 (d, *J* = 8.0 Hz, 1H), 7.02 (dt, *J* = 8.0 Hz, *J* = .8 Hz, 1H), 6.80 (d, *J* = 8.8 Hz, 2H), 5.50 (d, *J* = 11.2 Hz, 1H), 4.01-3.96 (m, 2H), 3.95-3.80 (m, 2H). 3.78 (s, 3H), 2.38 (s, 3H), 1.16-1.10 (m, 6H); **^{13}C NMR** (100.5 MHz, $CDCl_3$) δ 158.8, 143.6, 142.9 (d, *J* = 5.2 Hz), 137.1, 136.0, 132.9 (d, *J* = 6.0 Hz), 129.5, 129.4, 129.2, 127.3, 124.5, 120.5, 119.3, 113.8, 63.5 (d, *J* = 5.9 Hz), 55.2, 53.3 (d, *J* = 3.0 Hz), 21.5, 15.8 (d, *J* = 3.7 Hz), 15.7 (d, *J* = 3.7 Hz); **^{31}P NMR** (162 MHz, $CDCl_3$): δ 25.54; **HRMS** (ESI): m/z calcd. for $C_{25}H_{30}NO_6PS_2$ ([M+Na]+): 558.1144; Found: 558.1117.

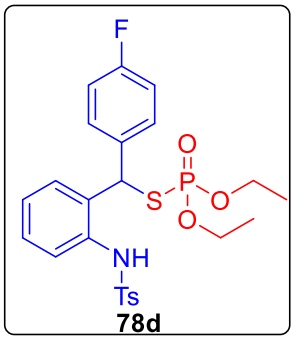

78d

O,O-diethyl S-((4-fluorophenyl)(2-((4-methylphenyl)sulfonamido)phenyl)methyl) phosphorothioate (**78d**). 42.7 mg, 81%; as an oil; **IR** ν (thin film, cm^{-1}) 3140, 2985, 1597, 1505, 1411, 1342, 1157, 702, 633 %; **^{1}H NMR** (400 MHz, $CDCl_3$) δ 7.70 (s, 1H), 7.63 (d, *J* = 8.4 Hz, 2H). 7.27-7.24 (m, 2H), 7.16 (d, *J* = 8.0 Hz, 4H), 7.09 (d, *J* = 6.8 Hz, 1H), 7.04-7.01 (m, 1H), 6.97-6.93 (m, 2H), 5.53 (d, *J* = 11.6 Hz, 1H), 4.01-3.95 (m, 2H), 3.89-3.82 (m, 2H), 2.35 (s, 3H), 1.16-1.15 (m, 6H); **^{13}C NMR** (100.5 MHz, $CDCl_3$) δ 161.9 (d, *J* = 245.6 Hz), 143.7, 142.3 (d, *J* = 6.0 Hz), 137.4, 136.8 (dd, *J* = 5.9 Hz, 3.7 Hz), 136.0, 129.8 (d, *J* = 8.2 Hz), 129.5 (d, *J* = 2.2 Hz), 127.9, 124.3, 120.3, 120.0, 115.4, 115.2, 63.8 (d, *J* = 3.0 Hz), 63.7 (d, *J* = 3.0 Hz), 52.9 (d, *J* = 2.9 Hz), 21.4, 15.8 (d, *J* = 2.3 Hz) 15.7 (d, *J* = 2.2 Hz); **^{31}P NMR** (162 MHz, $CDCl_3$): δ 25.17; **HRMS** (ESI): m/z calcd. for $C_{24}H_{27}NO_5FPS_2$ ([M+Na]+): 546.0944; Found: 546.0944.

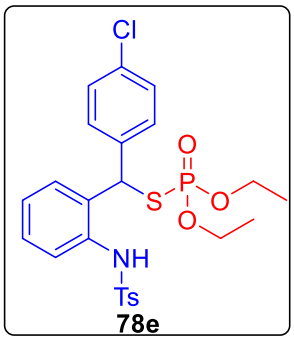

78e

S-((4-chlorophenyl)(2-((4-methylphenyl)sulfonamido)phenyl)methyl) O,O-diethyl phosphorothioate (78e). 42.3 mg, 78% as a white solid; mp 131-133 °C; **IR** ν (thin film, cm^{-1}) 3140, 2985, 1597, 1489, 1404, 1342, 1234, 1157, 1095, 1018; **^{1}H NMR** (400 MHz, $CDCl_3$) δ 7.63-7.60 (m, 2H), 7.54 (s, 1H), 7.25-7.20 (m, 4H), 7.15-7.13 (m, 4H), 7.08 (d, *J* = 8.0 Hz, 1H), 7.04-7.001 (m, 1H), 5.51 (d, *J* = 11.6 Hz, 1H), 4.02-3.96 (m, 2H), 3.89-3.83 (m, 2H), 2.36 (s, 3H), 1.17-1.12 (m, 6H); **^{13}C NMR** (100.5 MHz, $CDCl_3$) δ 143.7, 142.1 (d, *J* = 5.9 Hz), 139.6, 139.5, 137.3, 136.0, 133.3, 129.6, 129.5, 128.6, 127.2, 124.3, 120.2, 120.1, 63.8 (d *J* = 2.2 Hz), 63.7 (d, *J* = 2.3 Hz), 52.9 (d, *J* = 3.0 Hz), 21.4, 15.7 (ap t, *J* = 6.0 Hz); **^{31}P NMR** (162 MHz, $CDCl_3$): δ 25.01; **HRMS** (ESI): m/z calcd. for $C_{24}H_{27}NO_5PS_2Cl$ ([M+Na]+): 562.0649; Found: 562.0640.

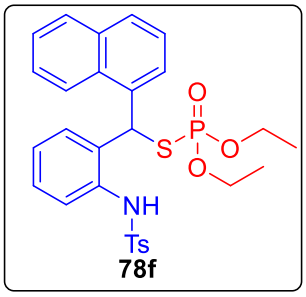

78f

O,O-diethyl S-((2-((4-methylphenyl)sulfonamido)phenyl)(naphthalen-1-yl)methyl) phosphorothioate (78f). 41.3 mg, 74% as a white solid; mp 175-178 °C; **IR** ν (thin film, cm^{-1}) 3140, 2985, 1597, 1473, 1334, 1234, 1165, 1018, 786; **^{1}H NMR** (400 MHz, $CDCl_3$) δ 8.06 (d, *J* = 8.0 Hz, 1H), 7.86 (d, *J* = 7.6 Hz, 1H), 7.79 (d, *J* = 8.0 Hz, 1H), 7.54 (d, *J* = 8.0 Hz, 1H), 7.49-7.42 (m, 4H), 7.41-7.39 (m, 1H), 7.28 (br s, 1H), 7.19-7.12 (m, 2H), 7.04-7.00 (m, 3H), 6.32 (d, *J* = 12.4 Hz, 1H), 4.03-3.96 (m, 2H), 3.95-3.82 (m, 2H), 2.29 (s, 3H), 1.13-1.07 (m. 6H); **^{13}C NMR** (100.5 MHz, $CDCl_3$) δ 143.5, 142.3 (d, *J* = 3.8 Hz), 137.2, 136.1 (d, *J* = 5.9 Hz), 135.9, 133.9, 130.3, 129.5, 129.4, 128.8, 128.6, 127.2, 126.8, 126.4, 125.8, 125.0, 124.8, 123.6, 120.8, 119.9, 63.8 (ap t, *J* = 6.0 Hz), 50.5, 21.4, 15.8 (d, *J* = 5.2 Hz), 15.7 (d, *J* = 6.0 Hz); **^{31}P NMR** (162 MHz, $CDCl_3$): δ 25.64; **HRMS** (ESI): m/z calcd. for $C_{28}H_{30}NO_5PS_2$ ([M+Na]+): 578.1195; Found: 578.1157.

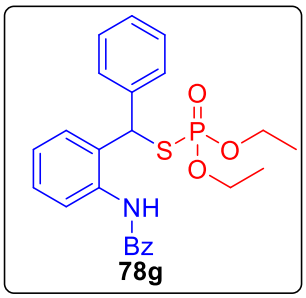

78g

S-((2-benzamidophenyl)(phenyl)methyl) O,O-diethyl phosphorothioate (78g). 15.3 mg, 34%; as an oil; **IR** ν (thin film, cm^{-1}) 3278, 2985, 1674, 1581, 1519, 1450, 1296, 1018, 748; **^{1}H NMR** (400 MHz, $CDCl_3$) δ 9.64 (br s, 1H), 8.09-8.07 (m, 2H), 7. 77 (d, *J* = 8.8 Hz, 1H), 7.56-7.44 (m, 3H), 7.42-7.34 (m, 3H), 7.30-7.23 (m, 3H), 7.21-7.17 (m, 2H), 6.08 (d, *J* = 10.4, 1H), 4.20-4.03 (m, 2H), 3.76-3.61 (m, 2H), 1.30-1.26 (m, 3H), 1.05-1.00 (m, 3H); **^{13}C NMR** (100.5 MHz, $CDCl_3$) δ 166.1, 139.4 (d, *J* = 8.9 Hz), 139.1 (d, *J* = 2.3 Hz), 134.7, 134.2, 131.7, 129.9, 128.6, 128.5, 128.2, 127.8, 127.7, 127.6, 126.9, 126.3, 64.3 (d, *J* = 6.0 Hz), 63.6 (d, *J* = 6.7 Hz), 48.8 (d, *J* = 3.0 Hz), 15.9 (d, *J* = 7.4 Hz), 15.6 (d, *J* = 8.2 Hz); **^{31}P NMR** (162 MHz, $CDCl_3$): δ 26.96; **HRMS** (ESI): m/z calcd. for $C_{24}H_{26}NO_4PS$ ([M+Na]+): 478.1212; Found: 478.1209.

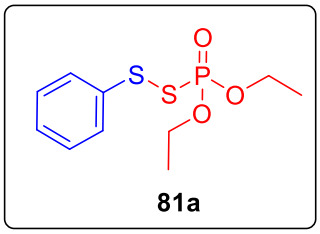

81a

O,O-diethyl SS-phenyl phosphoro(dithioperoxoate) (81a). 26.4 mg mg, 95%; as an oil; **IR** ν (thin film, cm^{-1}) 2981, 1577, 1477, 1438, 1390, 1255, 1162, 1024, 744, 688; ^{1}H NMR (400 MHz, $CDCl_3$) δ 7.66-7.63 (m, 2H), 7.38-7.30 (m, 3H), 4.20-4.10 (m, 2H), 4.02-3.92 (m, 2H), 1.26-1.22 (m, 6H); ^{13}C NMR δ 135.41 (d, J = 1.4 Hz), 130.82 (d, J = 1.5 Hz), 129.0, 128.5, 64.3 (d, J = 6.0 Hz), 15.8 (d, J = 7.4 Hz); ^{31}P NMR (162 MHz, $CDCl_3$): δ 23.15; HRMS(ESI): m/z calcd. for $C_{10}H_{15}O_3PS_2$ ([M+H]+): 278.0200; found 279.0279.

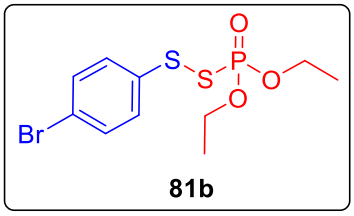

81b

SS-(4-bromophenyl) O,O-diethyl phosphoro(dithioperoxoate) (81b). 34.3 mg, 96%; as an oil; **IR** ν (thin film, cm^{-1}) 2981, 1471, 1386, 1255, 1161, 1010, 812, 750; ^{1}H NMR (400 MHz, $CDCl_3$) δ 7.53-7.51 (m, 2H), 7.48-7.47 (m, 2H), 4.21-4.14 (m, 2H), 4.06-3.99 (m, 2H), 1.29-1.25 (m, 6H); ^{13}C NMR (100.5 MHz, $CDCl_3$) δ 134.6, 132.2, 132.1, 122.8, 64.5 (d, J = 6.0 Hz), 15.9 (d, J = 6.7 Hz); ^{31}P NMR (162 MHz, $CDCl_3$): δ 22.80; HRMS (ESI): m/z calcd. for $C_{10}H_{14}O_3PS_2Br$ ([M+H]+): 355.9305; Found: 356.9366.

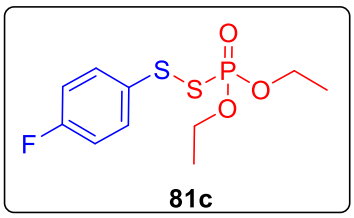

81c

O,O-diethyl SS-(4-fluorophenyl) phosphoro(dithioperoxoate) (81c). 26.8 mg, 93%; as an oil; **IR** ν (thin film, cm^{-1}) 2983, 1587, 1489, 1255, 1157, 1014, 833; ^{1}H NMR (400 MHz, $CDCl_3$) δ 7.69-7.66 (m, 2H), 7.07-7.02 (m, 2H), 4.20-4.12 (m, 2H), 4.03-3.96 (m, 2H), 1.30-1.26 (m, 6H); ^{13}C NMR (100.5 MHz, $CDCl_3$) δ 163.2 (d, J = 248.6 Hz), 134.2 (d, J = 8.2 Hz), 130.6 (d, J = 3.7 Hz), 116.3 (d, J = 22.3 Hz), 64.4 (d, J = 6.0 Hz), 15.9 (d, J = 6.6 Hz); ^{31}P NMR (162 MHz, $CDCl_3$): δ 23.29; HRMS (ESI): m/z calcd. for $C_{10}H_{14}O_3PS_2F$ ([M+H]+): 296.0106; Found: 297.0184.

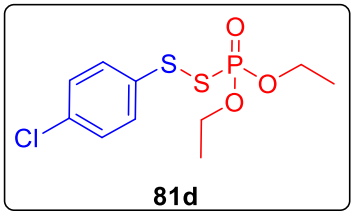

81d

SS-(4-chlorophenyl) O,O-diethyl phosphoro(dithioperoxoate) (81d). 29.2 mg, 82%; as an oil; **IR** ν(thin film, cm^{-1}) 2981, 1570, 1473, 1388, 1255, 1012, 815, 744; ^{1}H NMR (400 MHz, $CDCl_3$) δ 7.60 (d, *J* = 8.4 Hz, 2H), 7.32 (d, *J* = 8.4 Hz, 2H), 4.20-4.14 (m, 2H), 4.05-3.99 (m, 2H), 1.27 (t, *J* = 7.2 Hz, 6H); ^{13}C NMR (100.5 MHz, $CDCl_3$) δ 134.8, 133.9, 132.2, 129.2, 64.5 (d, *J* = 6.0 Hz), 15.9 (d, *J* = 7.4 Hz); ^{31}P NMR (162 MHz, $CDCl_3$): δ 22.86; HRMS (ESI): m/z calcd. for $C_{10}H_{14}O_3PS_2F$ ([M+H]+): 311.9810; Found: 312.9888.

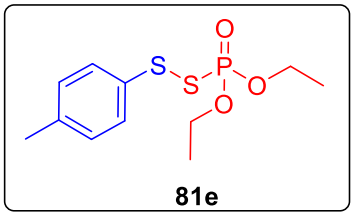

81e

O,O-diethyl SS-(p-tolyl) phosphoro(dithioperoxoate) (81e). 23.5 mg, 88%; as an oil; **IR** ν(thin film, cm^{-1}); 2981, 1720, 1489, 1392, 1255, 1014, 808, 750; ^{1}H NMR (400 MHz, $CDCl_3$) δ 7.55 (d, *J* = 8.0 Hz, 2H), 7.15 (d, *J* = 8.0 Hz, 2H), 4.18-4.12 (m, 2H), 4.00-3.93 (m, 2H), 2.35 (s, 3H), 1.25 (t, *J* = 7.6 Hz, 6H); ^{13}C NMR (100.5 MHz, $CDCl_3$) δ 139.2, 133.7, 131.2 (d, *J* = 1.5 Hz), 129.8, 64.2 (d, *J* = 6.0 Hz), 21.1, 15.9 (d, *J* = 7.4 Hz); ^{31}P NMR (162 MHz, $CDCl_3$): δ 23.58; HRMS (ESI): m/z calcd. for $C_{11}H_{17}O_3PS_2$ ([M+H]+): 389.0947; Found: 389.0926.

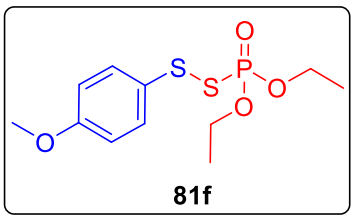

81f

O,O-diethyl SS-(4-methoxyphenyl) phosphoro(dithioperoxoate) (81f). 29.1 mg, 94%; as an oil; **IR** ν(thin film, cm^{-1}) 2981, 1589, 1492, 1390, 1253, 1014, 829, 752; ^{1}H NMR (400 MHz, $CDCl_3$) δ 7.64-7.62 (m, 2H), 6.88-6.85 (m, 2H), 4.18-4.12 (m, 2H), 4.00-3.93 (m, 3H), 3.81 (s, 3H), 1.30-1.26 (m, 6H); ^{13}C NMR (100.5 MHz, $CDCl_3$) δ 160.8, 135.1, 125.7, 114.6, 64.1 (d, *J* = 5.2 Hz), 55.4, 15.9 (d, *J* = 7.4 Hz); ^{31}P NMR (162 MHz, $CDCl_3$): δ 24.13; HRMS(ESI): m/z calcd. For $C_{11}H_{17}O_4PS_2$ ([M+H]+): 308.0306; found 309.0379.

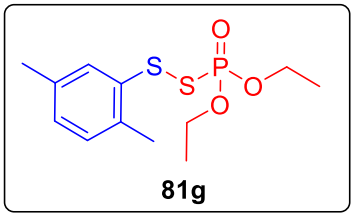

81g

SS-(2,5-dimethylphenyl) O,O-diethyl phosphoro(dithioperoxoate) (81g). 27.5 mg, 90%; as an oil; **IR** ν (thin film, cm^{-1}) 2980, 1600, 1390, 1255, 1016, 812; ^{1}H NMR (400 MHz, $CDCl_3$) δ 7.63 (d, *J* = 8.0 Hz, 1H), 7.04 (s, 1H), 7.01 (d, *J* = 8.0 Hz, 1H), 4.17-4.07 (m, 2H), 3.95-3.85 (m, 2H), 2.49 (s, 3H), 2.31 (s, 3H), 1.26-1.22 (m, 6H); ^{13}C NMR (100.5 MHz, $CDCl_3$) δ 140.7 (d, *J* = 1.5 Hz), 139.9, 134.1, 131.3, 130.3, 127.3, 64.0 (d, *J* = 5.2 Hz), 21.1, 20.5, 15.8 (d, *J* = 7.5 Hz); ^{31}P NMR (162 MHz, $CDCl_3$): δ 24.05; HRMS(ESI): m/z calcd. For $C_{12}H_{19}O_3PS_2$ ([M+H]+): 306.0513; found 307.0585.

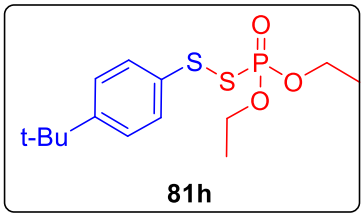

81h

SS-(4-(tert-butyl)phenyl) O,O-diethyl phosphoro(dithioperoxoate) (81h). 27.6 mg, 90% as an oil; **IR** ν (thin film, cm^{-1}) 2962, 1772, 1591, 1487, 1392, 1257, 1163, 1016, 827, 752; ^{1}H NMR (400 MHz, $CDCl_3$) δ 7.60-7.58 (m, 2H), 7.37-7.35 (m, 2H), 4.17-4.13 (m, 2H), 3.98-3.91 (m, 2H), 1.30 (s, 9H), 1.25-1.20 (m, 6H); ^{13}C NMR (100.5 MHz, $CDCl_3$) δ 152.3, 131.8, 131.5, 126.1, 64.2 (d, *J* = 5.6 Hz), 34.6, 31.1, 15.8 (d, *J* = 7.4 Hz); ^{31}P NMR (162 MHz, $CDCl_3$): δ 23.51; HRMS(ESI): m/z calcd. For $C_{14}H_{23}O_3PS_2$ ([M+H]+): 334.0826; found 335.0904.

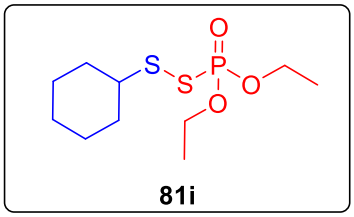

81i

SS-cyclohexyl O,O-diethyl phosphoro(dithioperoxoate) (81i). 25.6 mg, 90% as an oil; **IR** ν (thin film, cm^{-1}) 2929, 1444, 1390, 1255, 1016, 974, 790, 750; ^{1}H NMR (400 MHz, $CDCl_3$) δ 4.29-4.16 (m, 4H), 3.037-3.034 (m, 1H), 2.12-2.09 (m, 2H), 1.81-1.78 (m, 2H), 1.64-1.62 (m, 1H), 1.43-1.23 (m, 11H); ^{13}C NMR (100.5 MHz, $CDCl_3$) δ 64.3 (d, *J* = 6.0 Hz), 49.0, 32.2, 25.8, 25.5, 16.1 (d, *J* = 7.4 Hz); ^{31}P NMR (162 MHz, $CDCl_3$): δ 24.78; HRMS(ESI): m/z calcd. For $C_{10}H_{21}O_3PS_2$ ([M+H]+): 284.0670; found 285.0763.

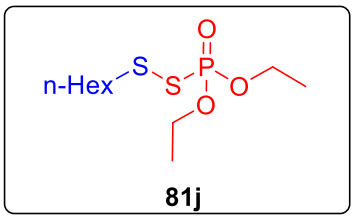

81j

O,O-diethyl SS-hexyl phosphoro(dithioperoxoate) (81j). 22.6 mg, 79%; as an oil; **IR** ν (thin film, cm^{-1}) 2927, 1454, 1255, 1016, 974, 750; ^{1}H NMR (400 MHz, $CDCl_3$) δ 4.29-4.17 (m, 4H), 2.88 (t, *J* = 7.2 Hz, 2H), 1.73-1.66 (m, 2H), 1.44-1.34 (m, 8H), 1.30-1.28 (m, 4H), 0.89 (t, *J* = 6.0 Hz, 3H); ^{13}C NMR (100.5 MHz, $CDCl_3$) δ 64.4 (d, *J* = 5.9 Hz), 38.7, 31.2, 28.5, 28.0, 22.4, 16.1 (d, *J* = 7.4 Hz), 13.9; ^{31}P NMR (162 MHz, $CDCl_3$): δ 24.88; HRMS(ESI): m/z calcd. For $C_{10}H_{23}O_3PS_2$ ([M+H]+): 286.0826; found 287.0896.

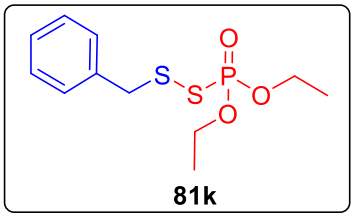

81k

SS-benzyl O,O-diethyl phosphoro(dithioperoxoate) (81k). 26.0 mg, 89%; as an oil; **IR** ν (thin film, cm^{-1}) 2981, 1494, 1390, 1257, 1016, 972, 765; ^{1}H NMR (400 MHz, $CDCl_3$) δ 7.35-7.26 (m, 5H), 4.31-4.18 (m, 4H), 4.14 (d, *J* = 2.0 Hz, 2H), 1.40 (t, *J* = 7.2 Hz, 6H); ^{13}C NMR (100.5 MHz, $CDCl_3$) δ 135.8, 129.4, 128.6, 127.8, 64.6 (d, *J* = 6.7 Hz), 43.1 (d, *J* = 5.6 Hz), 16.2 (d, *J* = 6.7 Hz); ^{31}P NMR (162 MHz, $CDCl_3$): δ 24.64; HRMS(ESI): m/z calcd. For $C_{11}H_{17}O_3PS_2$ ([M+H]+): 292.0357; found 293.0434.

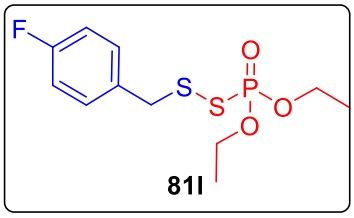

81l

O,O-diethyl SS-(4-fluorobenzyl) phosphoro(dithioperoxoate) (81l). 24.0 mg, 83%; as an oil; **IR** ν (thin film, cm^{-1}) 2981, 1598, 1508, 1255, 1222, 1014, 974, 839, 754; ^{1}H NMR (400 MHz, $CDCl_3$) δ 7.36-7.30 (m, 2H), 7.01 (t, *J* = 8.8 Hz, 2H), 4.29-4.18 (m, 4H), 4.15 (s, 2H), 1.42-1.36 (m, 6H); ^{13}C NMR (100.5 MHz, $CDCl_3$) δ 162.3 (d, *J* = 162.3 Hz), 131.7 (d, *J* = 3.0 Hz), 131.2 (d, *J* = 8.2 Hz), 115.5 (d, *J* = 21.5 Hz), 64.7 (d, *J* = 6.7 Hz), 42.2, 16.2 (d, *J* = 6.7 Hz); ^{31}P NMR (162 MHz, $CDCl_3$): δ 24.47; HRMS(ESI): m/z calcd. For $C_{11}H_{16}FO_3PS_2$ ([M+H]+): 310.0263; found 311.0336.

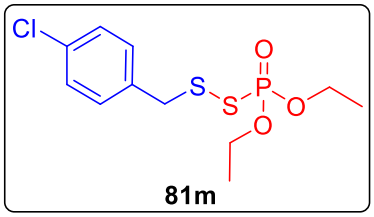

SS-(4-chlorobenzyl) O,O-diethyl phosphoro(dithioperoxoate) (81m). 26.9 mg, 83%; as an oil; **IR** ν (thin film, cm^{-1}) 2981, 1489, 1255, 1161, 1093, 1016, 808, 740; ^{1}H NMR (400 MHz, $CDCl_3$) δ 7.32-7.26 (m, 4H), 4.30-4.18 (M, 4H), 4.10 (d, *J* = 2.0 Hz, 2H), 1.41-1.38 (m, 6H); ^{13}C NMR (100.5 MHz, $CDCl_3$) δ 134.4, 133.7, 130.8, 128.7, 64.7 (d, *J* = 6.7 Hz), 42.2, 16.2 (d, *J* = 6.7 Hz); ^{31}P NMR (162 MHz, $CDCl_3$): δ 24.33; HRMS(ESI): m/z calcd. For $C_{11}H_{16}ClO_3PS_2$ ([M+H]+): 325.9967; found 327.0054.

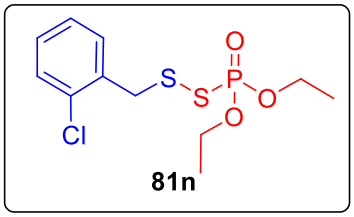

SS-(2-chlorobenzyl) O,O-diethyl phosphoro(dithioperoxoate) (81n). 27.6 mg, 85%; as an oil; **IR** ν (thin film, cm^{-1}) 2981, 1473, 1444, 1390, 1255, 1161, 1014, 759; ^{1}H NMR (400 MHz, $CDCl_3$) δ 7.41-7.38 (m, 2H), 7.27-7.23 (m, 2H), 4.32-4.20 (m, 6H), 1.44-1.37 (m, 6H); ^{13}C NMR (100.5 MHz, $CDCl_3$) δ 134.2, 133.8, 131.7, 129.8, 129.2, 126.7, 64.7 (d, *J* = 6.7 Hz), 40.6 (d, *J* = 1.5 Hz) 16.2 (d, *J* = 6.7 Hz); ^{31}P NMR (162 MHz, $CDCl_3$): δ 24.42; HRMS(ESI): m/z calcd. For $C_{11}H_{16}ClO_3PS_2$ ([M+H]+): 325.9967; found 327.0045.

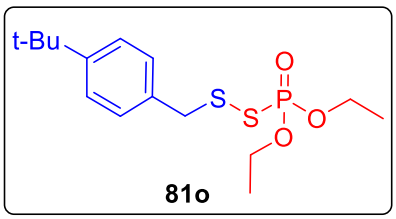

SS-(4-(tert-butyl)benzyl) O,O-diethyl phosphoro(dithioperoxoate) (81o). 34.4 mg, 95%; as an oil; **IR** ν (thin film, cm^{-1}) 2962, 1514, 1390, 1255, 1161, 1014, 974, 837, 790, 754; ^{1}H NMR (400 MHz, $CDCl_3$) δ 7.35 (d, *J* = 8.0 Hz, 2H), 7.27 (d, *J* = 8.4 Hz, 2H), 4.28-4.12 (m, 4H), 4.12 (d, *J* = 1.6 Hz, 2H), 1.42-1.38 (m, 6H), 1.30 (s, 9H); ^{13}C NMR (100.5 MHz, $CDCl_3$) δ 150.9, 132.7, 129.1, 125.6, 64.5 (d, *J* = 6.7 Hz), 42.9, 34.5, 32.1, 16.2 (d, *J* = 6.7 Hz); ^{31}P NMR (162 MHz, $CDCl_3$): δ 24.71; HRMS(ESI): m/z calcd. For $C_{15}H_{25}O_3PS_2$ ([M+H]+): 348.0983; found 349.1053.

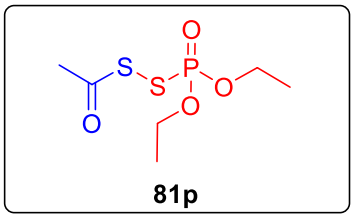

81p

acetic (diethyl phosphoric) dithioperoxyanhydride (81p). 21.6 mg, 90%; as an oil; **IR** ν (thin film, cm^{-1}) 2906, 1714, 1390, 1294, 1180, 1016, 790, 639; ^{1}H NMR (400 MHz, $CDCl_3$) δ 4.30-4.22 (m, 4H), 2.48 (s, 3H), 1.39-1.35 (m, 6H); ^{13}C NMR (100.5 MHz, $CDCl_3$) δ 191.0, 64.7 (d, J = 5.9 Hz), 28.8, 15.9 (d, J = 7.4 Hz); ^{31}P NMR (162 MHz, $CDCl_3$): δ 21.18 ; HRMS(ESI): m/z calcd. For $C_6H_{13}O_4PS_2$ ([M+H]+): 243.993; found 245.0083.

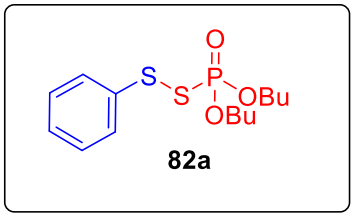

82a

O,O-dibutyl SS-phenyl phosphoro(dithioperoxoate) (82a). 26.4 mg, 79%; as an oil; **IR** ν (thin film, cm^{-1}) 2906, 1714, 1390, 1294, 1180, 1016, 790, 639; ^{1}H NMR (400 MHz, $CDCl_3$) δ 7.65-7.63 (m, 2H), 7.36-7.29 (m, 3H), 4.12-4.04 (m, 2H), 3.94-3.86 (m, 2H), 1.59-1.52 (M, 4H), 1.37-1.28 (m, 4H), 0.94-0.86 (m, 6H); ^{13}C NMR (100.5 MHz, $CDCl_3$) δ 135.5 (d, J = 1.5 Hz), 130.6, 129.0, 128.3, 68.1 (d, J = 7.4 Hz), 32.0 (d, J = 7.4 Hz), 18.5, 13.5; ^{31}P NMR (162 MHz, $CDCl_3$): δ 23.28 ; HRMS(ESI): m/z calcd. For $C_{14}H_{23}O_3PS_2$ ([M+H]+): 334.0826; found 335.0916.

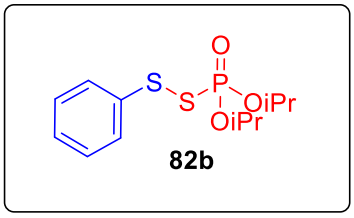

82b

O,O-diisopropyl SS-phenyl phosphoro(dithioperoxoate) (82b). 21.6 mg, 71%; as an oil; **IR** ν (thin film, cm^{-1}) 2980, 1465, 1384, 1255, 1101, 1008, 744, 688; ^{1}H NMR (400 MHz, $CDCl_3$) δ 7.65-7.63 (m, 2H), 7.35-7.26 (m, 3H), 4.76-4.71 (m, 2H), 3.88-3.82 (m, 2H), 1.36-1.31 (m, 6H), 1.22-1.20 (m, 6H); ^{13}C NMR (100.5 MHz, $CDCl_3$) δ 135.6, 130.3, 129.0, 128.1, 73.9 (d, J = 6.7 Hz), 23.8 (d, J = 3.8 Hz), 23.4 (d, J = 6.0 Hz); ^{31}P NMR (162 MHz, $CDCl_3$): δ 20.78; HRMS(ESI): m/z calcd. For $C_{12}H_{19}O_3PS_2$ ([M+H]+): 306.0513; found 307.0603.

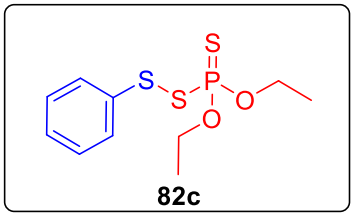

82c

O,O-diethyl SS-phenyl phosphoro(dithioperoxo)thioate (82c). 23.6 mg, 79%; as an oil; **IR** ν (thin film, cm^{-1}) 2980, 1475, 1438, 1159, 1010, 970, 829, 742, 648; ^{1}H NMR (400 MHz, $CDCl_3$) δ 7.63-7.60 (m, 2H), 7.35-7.29 (m, 3H), 4.19-4.12 (m, 2H), 3.88-3.82 (m, 2H), 1.27-1.18 (m, 6H); ^{13}C NMR (100.5 MHz, $CDCl_3$) δ 135.6, 130.6, 129.0, 128.3, 64.3 (d, J = 4.5 Hz), 15.5 (d, J = 8.9 Hz); ^{31}P NMR (162 MHz, $CDCl_3$): δ -44.52; HRMS(ESI): m/z calcd. For $C_{10}H_{15}O_2PS_3$ ([M+H]+): 295.0050; found 295.0047.

Chapter IV

Hydrothiolation of Alkenes using Hydrogen Persulfide

4.1 Introduction and Background of Hydrogen Persulfide Chemistry and Synthesis of Thioether

Hydrogen persulfides (RSSH) are an intriguing, emerging, and scarcely studied functional group. Hydrogen persulfides exist in biological systems and are biosynthesized by the reaction of thiol-containing amino acids with H_2S.[177] H_2S is one of the main three gasotransmitters and impacts essential physiological functions such as cytoprotection, circulation, brain function, and prevention of atherosclerosis.[178-180] In addition hydrogen persulfides are important for cell replication and survival through protection against reactive oxygen species.[181, 182]

Hydrogen persulfides have unique characteristics. For example, they possess both nucleophilic and electrophilic sulfur atoms.[183] Hydrogen persulfides have a lower pKa than the corresponding thiol. Pratt reported that the pKa of cumyl hydrogen persulfide is 7 while the pKa of cumyl thiol is greater than 10.[184]. Moreover, a computational study of cysteine hydrogen persulfide revealed a pKa of 4.3, which is much lower than regular cysteine.[185] The increased acidity indicates that highly ionized hydrogen persulfide will be formed under biological conditions, which may lead to increased reactivity.

The Pratt group has studied the kinetics of hydrogen atom transfer (HAT) reactions of hydrogen persulfides, and they reported that hydrogen persulfides possess stronger antioxidant properties than the corresponding thiols.[184] The HAT rates for carbon, oxygen, and sulfur-centered radicals were faster than the corresponding thiol. The low BDE of the RSS-H bond (70

kcal/mol) and the stability of the perthiyl radical make the HAT reaction exothermic and favorable.[184] Hydrogen persulfides also increases nucleophilicity due to the alpha effect.[183] A neighboring heteroatom with available lone pairs experiences enhanced reactivity. For example, hydrazine and peroxide a higher reactivity in S_N2 reactions compared to that of ammonia and hydroxide.[186] The sulfenyl sulfur of hydrogen persulfide serves as an electrophile and reacts with soft nucleophiles such as cyanide and triphenylphosphine.[187, 188]

The study of hydrogen persulfides is a challenging area of research due to their inherent instability, complex preparation, and analysis. Hydrogen persulfides are not stable because a disproportionation reaction can occur with itself to form various polysulfides.[189] Both sulfenyl and sulfhydryl sulfur atoms can act as leaving groups, and they can also be attacked by another molecule of hydrogen persulfide to form polysulfides. The conventional way to prepare benzyl hydrogen persulfide has a low overall yield and involves air-sensitive and volatile chemicals (**Scheme 4.1**).[190] For example, thioacetic acid **85** is transformed into thioacetic anhydride **86,** which is then chlorinated to form sulfenyl chloride **87**. Sulfenyl chloride **87** reacts with benzyl mercaptan through a nucleophilic substitution reaction to give disulfide **88**. Finally, alcoholysis of the acyl disulfide generates the persulfide **89a** and methyl acetate byproduct.

Scheme 4.1 Known Synthetic Route to Benzyl Hydrogen Persulfide

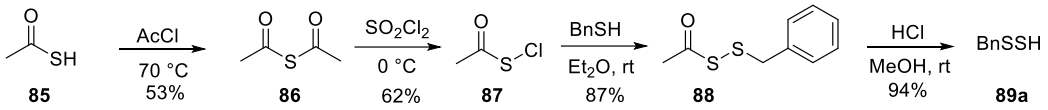

Analysis of hydrogen persulfides is also challenging because they have a similar structure to the corresponding thiol, except for an additional sulfur atom. It has been found that hydrogen persulfides have more downfield chemical shifts compared to the corresponding thiol in ^{1}H NMR spectroscopy.[191] Furthermore, IR spectroscopy shows the RSS-H stretch at around 2500 Hz.[191] Hydrogen persulfides can also be detected by indirect trapping methods such as trapping with phosphine, alkyl halides, or complexation to iron.[188, 192, 193]

Scheme 4.2 Known Hydrogen Persulfides

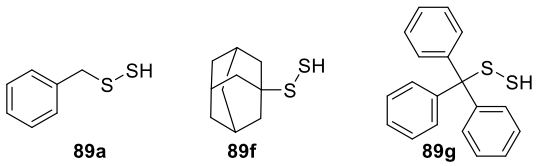

Three hydrogen persulfides have been synthesized and characterized. The three hydrogen persulfides are benzyl persulfide, trityl persulfide, and adamantyl persulfide **89** (**Scheme 4.2**).[194] They are sterically hindered to increase stability and slow down the disproportionation reaction leading to polysulfides. These persulfides have reacted with alkyl halides in a substitution reaction and activated alkenes in an addition reaction.[193, 195] The study of hydrogen persulfides has not been well explored due to their tedious synthesis and instability.

Scheme 4.3 Applications of Thioether Structural Motif

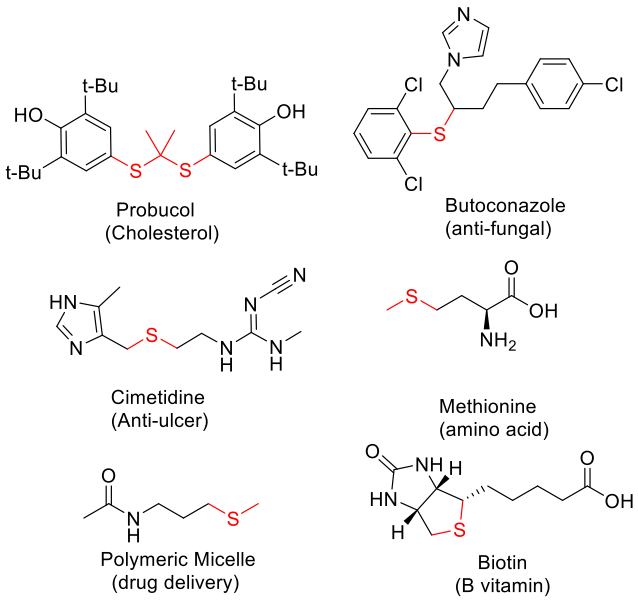

In addition, thioethers have been widely used in medicinal chemistry and chemical biology (**Scheme 4.3**).[196-201] For example, Probucol, Butoconazole, and Cimetidine were developed to treat high cholesterol, fungal infections, and stomach ulcers, respectively (**Scheme 4.3**).[196-198] Methionine is an amino acid that serves as a precursor to nonessential amino acids and antioxidants (**Scheme 4.3**).[199] In addition, thioethers have also been utilized to form micelles, aiding drug delivery (**Scheme 4.3**).[200] Furthermore, biotin is a B vitamin critical for metabolism and healthy hair and nails (**Scheme 4.3**).[201]

With the broad application of the thioether motif, synthetic methods to access thioethers have been well studied. They are synthesized by addition reactions, nucleophilic substitution reactions, and rearrangement reactions.[202-204]

Scheme 4.4 Thia-Michael Addition Reaction

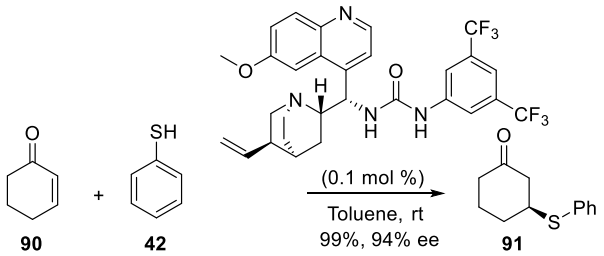

Sulfur is an excellent nucleophile for addition reactions due to its size and polarizability.[205, 206] Michael acceptors such as enones, nitroalkenes, and iminium ions have been utilized to form S-C bonds.[207-209] The Singh group has reacted cyclohexanone **90** with thiophenol **42** in the presence of a chiral thiourea catalyst to give chiral thioether product **91** in a high yield of 99% (**Scheme 4.4**).[210] Thiols can be used as nucleophiles in stereospecific reactions such as S_N2 and the Mitsunobu reaction to form thioethers. The Tunge group demonstrated a stereospecific S_N2 reaction of mesylate **92** with sodium thiophenoxide to give thioether **93** in a high yield of 99% (**Scheme 4.5**).[211]

Scheme 4.5 Stereospecific Thioether Synthesis by Nucleophilic Substitution

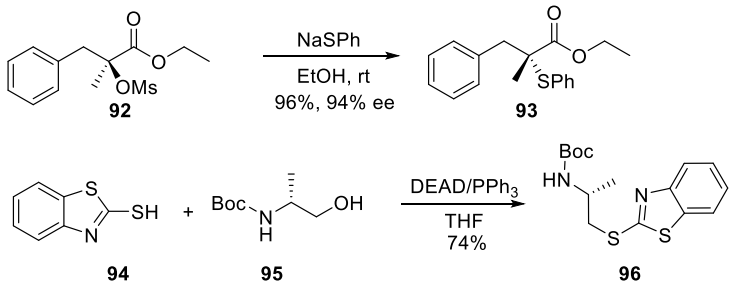

Furthermore, the Mitsunobu protocol is an activation strategy of alkyl alcohols using diethylazo dicarboxylate (DEAD) and triphenylphosphine.[212]The Sheardown group utilized this strategy by

treating primary alcohol **95** with DEAD/PPh_3 followed by thiol **94** to afford thioether **96** in a high yield of 74% (**Scheme 4.5**).[197]

Scheme 4.6 Odorless Synthesis of Thioether using Thiourea as Sulfur Source

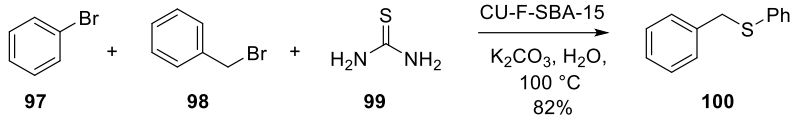

97 **98** **99** **100**

The downside of using thiols in organic synthesis is the pungent smell. Hence, a convenient alternative is to use an odorless synthetic equivalent such as thiourea. The Bhaumik group reacted thiourea **99**, benzyl bromide **98**, and aryl halide **97** in the presence of a copper-anchored mesoporous catalyst to form thioether **100** in a high yield of 82% (**Scheme 4.6**).[213]

Thiols are typically nucleophilic due to their large size and electron richness. However, umpolung reactivity, a reactivity reversal strategy, can be accessed by attaching a leaving group as an electron sink. Examples of these electrophilic sulfur reagents are thiosuccinimides, thiopthalimides, and thiosulfinates[202]. Sp^3 C-S bond formation has been achieved using electrophilic sulfur reagents with arenol, oxindole, and active methylene nucleophiles.[214-216] For example, Cheng reacted oxindole **101** with thiophthalimide **102** to form thioether **103** in a high yield of 98% (**Scheme 4.7**).[214]

Scheme 4.7 Thioether Synthesis via Electrophilic Sulfur Reagent

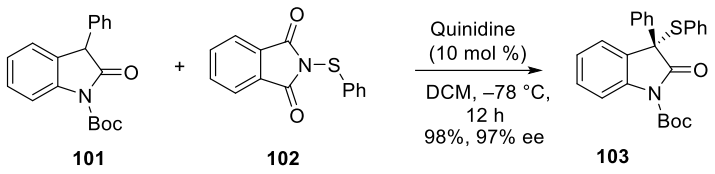

Rearrangement reactions such as the Pummerer and Smiles rearrangement are powerful strategies for accessing thioethers. The Nagao group achieved an enantioselective Pummer rearrangement with a 1,2 acetoxy shift by reacting chiral sulfoxide **104** with acetic anhydride using N-Methyl-2-pyrrolidone (NMP) solvent to give chiral thioether **105** in a 47% yield.[217] The Clayden group reacted amide **106** with a strong base to form chiral amide **107** through a Smiles-type rearrangement.[218]

Scheme 4.8 Rearrangement Reactions to Access Thioether

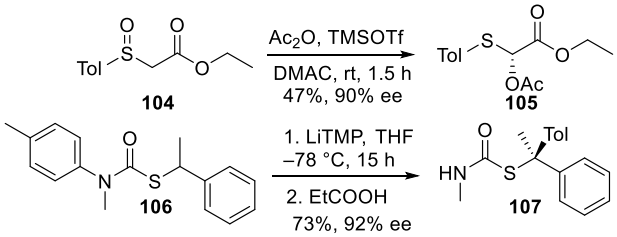

Furthermore, a hydrothiolation reaction is an attractive strategy to access thioethers from readily available alkene starting materials. A radical addition reaction to alkene systems will give anti-Markovnikov addition.[219] The Tanihuchi and Dunach group reported thioether synthesis from unactivated alkenes and achieved Markovnikov selectivity. The Taniguchi group reacted styrene **108** with benzyl mercaptan in the presence of a metal and acid cocatalytic system to form **109** in a high yield of 96% (**Scheme 4.9**). The Dunach group treated 4-methylthiophenol **70** with branched geminal alkene **110** to form thioether **111** in a high yield of 79%. However, both methods rely on metal catalysts and heating conditions (**Scheme 4.9**).

Despite the extensive study on thiol reactivity, the reactivity of hydrogen persulfide is not well known and the hydrothiolation of alkenes remains elusive to achieve under mild conditions.

Scheme 4.9 Hydrothiolation Strategies Requiring Metal Catalysts

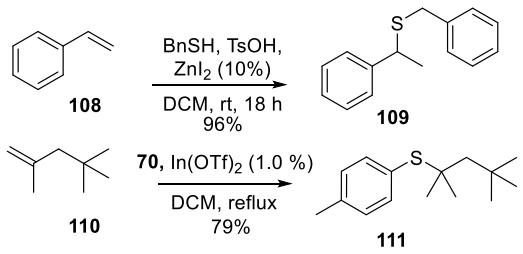

4.2 Specific Aim

This project aims to synthesize hydrogen persulfide and gain an understanding of the reactivity of hydrogen persulfide. It also aims to develop a green synthetic method to achieve Markovnikov addition to synthesize thioether products from hydrogen persulfides and unactivated alkenes. Furthermore, it aims to study the reaction mechanism.

4.3 Green Hydrothiolation of Alkenes using Hydrogen Persulfide

Scheme 4.10 Improved Hydrogen Persulfide Synthesis

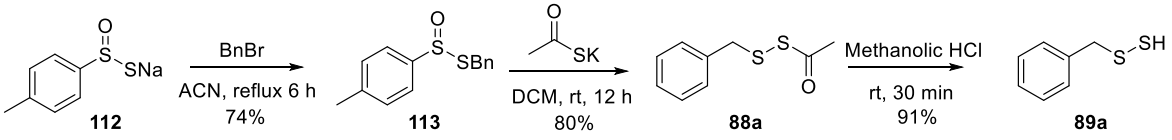

112 **113** **88a** **89a**

Benzyl hydrogen persulfide was synthesized in a three-step synthetic sequence from benzyl bromide. First, benzyl bromide was reacted with sodium thiolate **112** to form thiosulfinate **113**. Thiosulfinate was then treated with thioacetate via a disulfide exchange reaction to form disulfide **88a**. Finally, alcoholysis of **88a** generated persulfide **89a** in a high yield of 91%. All steps of this synthetic sequence are high-yielding and involve stable high molecular weight intermediates. The new route is an improvement of the known route in literature

(**Scheme 4.10** vs **Scheme 4.1**). Most notably, **88** is a stable solid that can be stored for long periods of time and used to access **89a** when needed. Benzyl hydrogen persulfide was shown to slowly react with itself through a disulfide exchange reaction to form a mixture of polysulfides. A challenge that needs to be overcome to use hydrogen persulfide is the minimization of the polysulfide byproducts. It was hypothesized that hydrogen persulfide could react with alkenes through an "ene" type of mechanism since the sulfhydryl bond of the hydrogen persulfide has low bond dissociation energy.

Table 4.1 Optimization of Hydrothiolation Reaction[a]

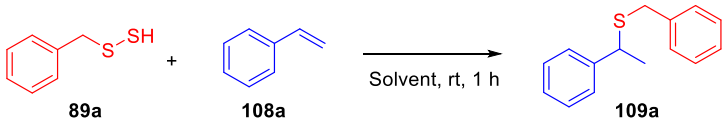

89a **108a** **109a**

entry	**89a** :**108a**	solvent	Yield (%)[b]
1	1.0 : 1.0	THF	47
2	1.0 : 1.0	Ether	61
3	1.0 : 1.0	EtOH	15
4	1.0 : 1.0	ACN	48
5	1.0 : 1.0	Toluene	51
6	1.0 : 1.0	DCM	73
7	1.0 : 1.0	Neat	77(77)[c]

[a]**89a** (0.1 mmol) and **108a** (0.1 mmol) in solvent for 1 h at rt.[b]Crude NMR yield determined by mesitylene internal standard.[c]Isolated yield.

To test our hypothesis, benzyl persulfide **89a** was treated with styrene **108**. The reaction was tested in THF and diethyl ether, and both gave a moderate crude yield of 47% and 61%, respectively (**Table 4.1**, entries 1-2). When the reaction was tested in ethanol, a low crude yield of 15% was generated (**Table 4.1**, entry 3). This could be due to the H-bonding solvation effects of the solvent with **89a**, which compromises the reactivity. Acetonitrile and toluene provided moderate crude yields of 48% and 51%, respectively (**Table 4.1**, entries 4-5). When the solvent was changed to DCM, a higher crude yield of 73% was generated (**Table 4.1**, entry 6). Lastly, neat conditions produced the target product in a yield of 77% (**Table 4.1**, entry 7).

The formation of polysulfides was observed in all crude mixtures after reaction completion and they were matched with known compounds reported in the literature.[220] However, the formation of polysulfides was suppressed when the reaction was performed neat. Presumably, the reaction rate of the hydrothiolation reaction is much faster than the rate at which polysulfides form from the intermolecular reaction of **89a** with itself when the reaction was performed under neat conditions.

With the optimized reaction conditions established, the reaction was tested with diverse styrenes to determine the steric and electronic effect on the reaction outcome (**Table 4.2**). Halogenated styrenes **108b-108d** (4-Br, 4-Cl, and 4-F) were well tolerated, giving **109b-109d** in high yields of 77%-82%. Styrenes with electron-donating groups **108e-108g** (4-Me, 2-Me, 4-OMe) showed increased reactivity providing **109e**-**109g** in high yields of 79%-89%. Styrene **108h** bearing a tertiary amine afforded **109h** in a moderate yield of 64%. This decreased yield is presumably due to the protonation of basic nitrogen and deactivation of styrene nucleophile. A

styrene **108i** with an electron-withdrawing group (4-CN), was well tolerated, giving **109i** in a high yield of 80%.

Table 4.2 Styrene Substrate Scope[a]

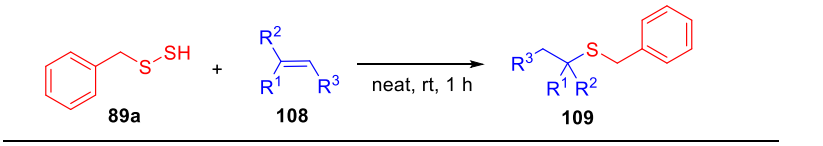

89a **108** **109**

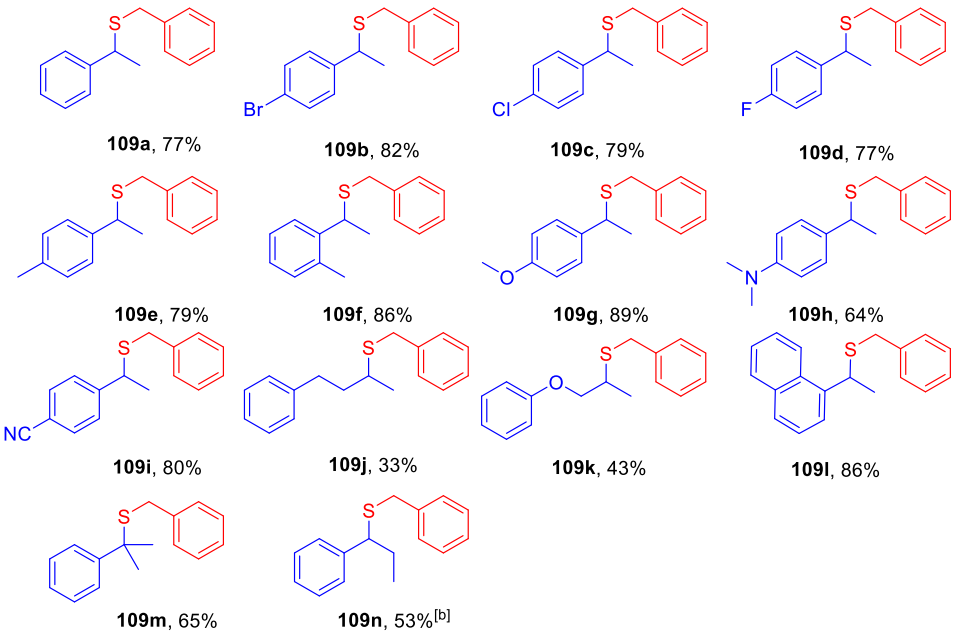

109a, 77% **109b**, 82% **109c**, 79% **109d**, 77%

109e, 79% **109f**, 86% **109g**, 89% **109h**, 64%

109i, 80% **109j**, 33% **109k**, 43% **109l**, 86%

109m, 65% **109n**, 53%[b]

[a]Reaction conditions: **89a** (0.1 mmol) and **108a** (0.1 mmol) stirred neat at room temperature for 1 h. Isolated yield. [b]heated for 12 h in toluene at 80 °C.

Next, the reaction was tested with alkyl terminal alkene **108j,** which provided **109j** in a low yield of 33%. The low yield is presumably due to the reduced nucleophilicity of **108j** because it is electron deficient compared to the electron-rich pi system of aryl styrene; also, the formed reactive carbocation intermediate lacks resonance stabilization. Allyl ether **108k** furnished product **109k,** and no cyclized product was formed. It is possible that **109k** could cyclize with neighboring group participation from the aryl group to give a substituted dihydrobenzofuran product. If this product were observed, it would provide insight into the possibility that the reactive intermediate is a three-membered bridged sulfonium ion that results from [2+1] cycloaddition reaction.[221] A bulky naphthyl styrene **108l** was well tolerated, giving **109l** in a high yield of 86%.

Next, the substituents on the styrene were changed to further test the steric effect on the reaction outcome. Alpha methyl styrene **108m** was well tolerated and gave **109m** in a moderate yield of 65%. Beta methyl styrene **108n** did not give any product under standard reaction conditions. However, under more forcing reaction conditions (overnight heating in toluene), **109n** was generated in a moderate yield of 53%. Overall, the hydrothiolation reaction was successful with styrenes bearing electron-donating and withdrawing groups, providing the desired products in high yields. A decrease in reactivity was observed when the reaction was tested with alkyl or sterically hindered olefins.

Some unsuccessful styrenes under the standard conditions are **108p**-**108s** (**Scheme 4.11**). Stilbene **108p** was unreactive, presumably due to steric bulk and no electronic difference. Cyclohexene **108q** seemed a suitable reaction partner because of internal alkene strain. The reaction can be driven by strain release and the rehybridization of sp^2 to sp^3. However,

cyclohexene showed no reactivity under the standard reaction conditions. A plausible explanation is that **108q** is a symmetrical alkene with no electronic difference, which makes the reaction unfavorable. Alkene **108r** also failed to provide the product, presumably due to steric hindrance. Vinyl pyridine **108s** was also an unsuccessful olefin. This experimental result supports that the styrene acts as a nucleophile, not as an electrophile.

Scheme 4.11 Unreactive Alkenes

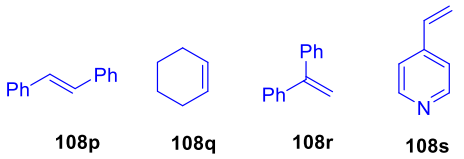

108p **108q** **108r** **108s**

Next, the hydrogen persulfide nucleophile reaction partner was tested. Methanolysis of disulfide **88** was used to generate new hydrogen persulfides (**Table 4.3**). The new hydrogen persulfides were characterized by ^{1}H NMR, ^{13}C NMR, and IR spectroscopy and they were consistent with the chemical shifts of hydrogen persulfides reported in the literature.[191] The alcoholysis of **88** provides the corresponding hydrogen persulfides **89b-89d** in high yields.

Table 4.3 Synthesis of New Hydrogen Persulfides via Methanolysis [a]

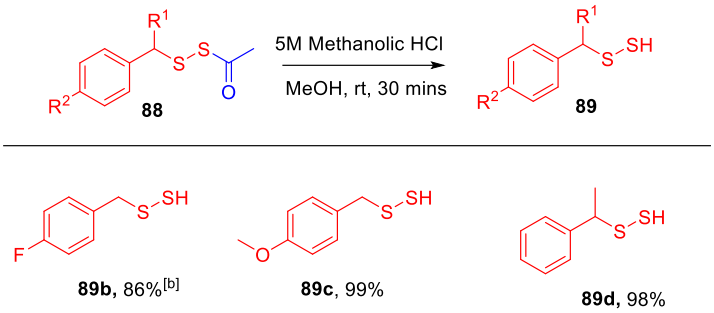

[a]Reaction conditions: **88** (0.3 mmol) and 5M methanolic HCl (1.5 mmol) in MeOH (0.5 mL) stirred at room temperature for 30 minutes.

[b]Isolated yield.

The three new hydrogen persulfides **89b-89d** (4-F, 4-MeO, and alpha-methyl) were then tested in the hydrothiolation reaction to see the electronic and steric effects on the reaction outcome (**Table 4.4**). All new hydrogen persulfides generated small amounts of polysulfide byproducts during the hydrothiolation reaction based on crude NMR analysis and thin-layer chromatography. Halogenated hydrogen persulfide **89b** provided product **114a** in a moderate yield of 67%. The reduced yield could be attributed to a slow benzylic radical coupling reaction of 4-fluorobenzyl hydrogen persulfide. When electron-rich benzyl hydrogen persulfide **89c** was employed, **114b** was formed in a high yield of 83%. The steric effect of hydrogen persulfide was investigated with **89d,** which provided symmetrical thioether **114c** in a moderate yield of 57%. Overall, a steric effect on both the alkene and hydrogen persulfide affects the success of the reaction.

Table 4.4 Scope of Hydrogen Persulfide Electrophile[a]

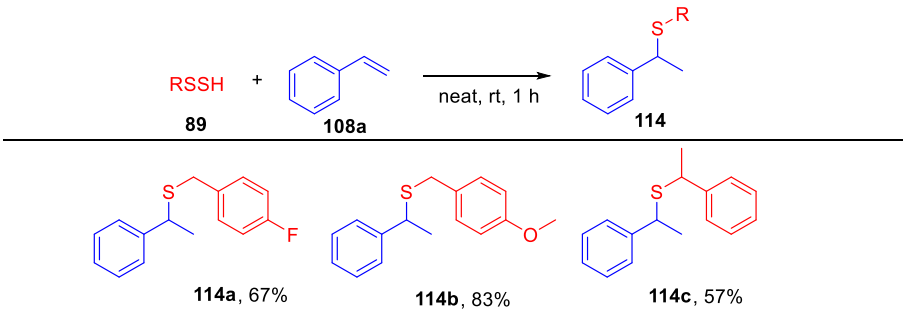

[a]Reaction conditions: **89** (0.1 mmol) and **108a** (0.1 mmol) stirred neat at room temperature for 1 h.[b]Isolated yield.

4.4 Control Experiments and Mechanism Study

Scheme 4.12 Deuterium Labeling Study

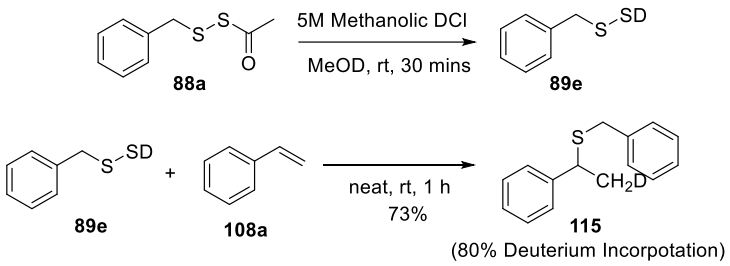

To study the reaction mechanism, control experiments were performed (**Scheme 4.12-4.16**). Deuterated hydrogen persulfide **89e** was synthesized by methanolysis in methanolic DCl. The deuterated hydrogen persulfide **89e** was treated with styrene **108a**, and the deuterium-incorporated product **115** was generated with a high yield of 73% and 80% deuterium incorporation. A similar yield was achieved when compared to the standard reaction. Product **115** showed a deuterium incorporation in the terminal position, consistent with the proposed Markovnikov addition mechanism.

Next, we were interested in where and how the polysulfide byproducts are generated. Persulfide **89a** was stirred in DCM solution for one hour, and ^{1}H NMR analysis showed the presence of hydrogen persulfide and polysulfide formation (**Scheme 4.13**). Therefore, polysulfide formation is presumably from the intermolecular reaction of hydrogen persulfide **89a** and is not generated from the reaction with styrene. Polysulfides can be produced from sulfenyl and sulfhydryl sulfur atoms, which can act as a leaving group, giving rise to polysulfide products.

Scheme 4.13 Decomposition of Benzyl Hydrogen Persulfide to Polysulfides in Solvent

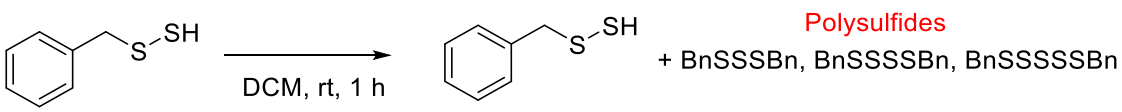

The possibility of a radical mechanism was investigated. Usually, radical addition reactions occur with anti-Markovnikov addition as a more substituted radical intermediate is favored.[222] The hydrothiolation reaction was tested with radical scavengers (2,2,6,6-Tetramethylpiperidin-1-yl)oxyl (TEMPO) and dibutylhydroxytoluene (BHT) **(Scheme 4.14**). The reaction of hydrogen persulfide **89a** and styrene **108a** with TEMPO did not form any product and generated a mixture of polysulfides. The experimental result suggests a free radical mechanism. Next, BHT was reacted with hydrogen persulfide **89a** and styrene **108a,** and the product **109a** was generated in a moderate yield of 66%. No BHT adducts were observed, and the yield was not significantly hampered. However, BHT may not be a sufficient radical trap to inhibit the reaction.

Scheme 4.14 Hydrothiolation Mechanism Study Control Experiments

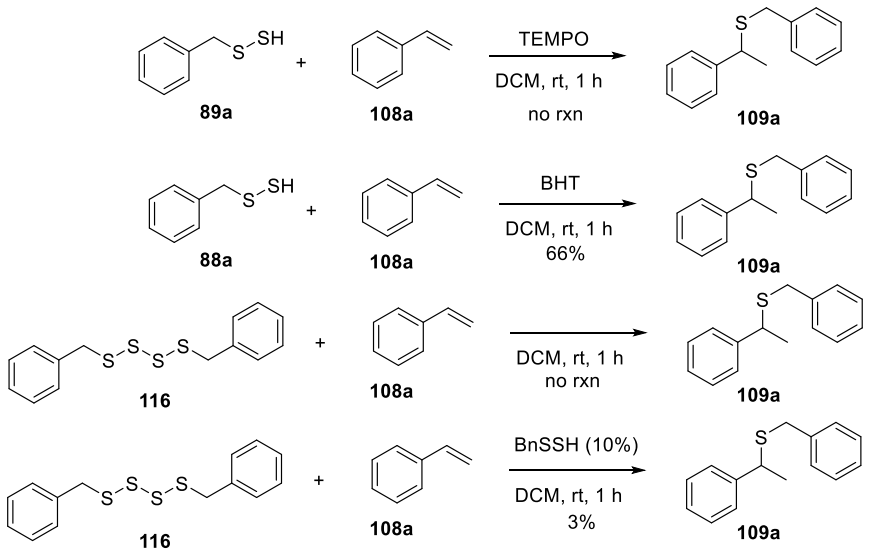

Furthermore, we wanted to see if the polysulfides were part of the reaction mechanism and involved in product formation. To test this, benzyl tetrasulfide **112** was reacted with styrene **108a**, but no product formation was observed (**Scheme 4.14**). A catalytic amount of hydrogen persulfide **89a** was also reacted with styrene **108a** and tetrasulfide, and a sub-catalytic amount of the product **109a** was formed (**Scheme 4.14**). These results tell us that polysulfides are a byproduct of the intermolecular reaction of hydrogen persulfide with itself and are not involved in the reaction mechanism.

Scheme 4.15 Disulfur Trapping Experiments

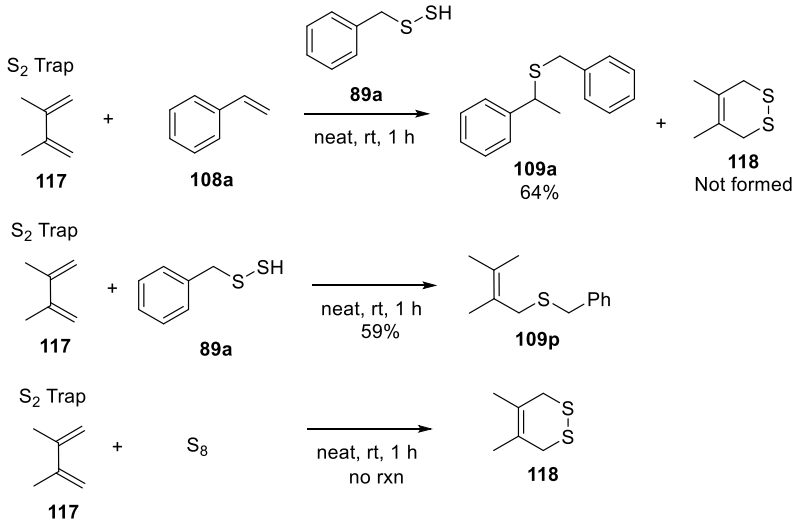

More mechanism study experiments were conducted to trap the reaction's byproducts. (**Scheme 4.15**). Elemental sulfur (S_8) and disulfur (S_2) are possible byproducts of the reaction. Diene **113** is a known trapping agent for S_2 and was employed under the standard reaction conditions.[223] The trapped product **118** was not formed under standard reaction conditions, and the major product formed was **109a**. Disulfur may be difficult to trap as it is a sensitive and short lived chemical species.[224] The reaction between **117** and **89a** formed allylic thioether **109p** in a moderate yield of 59%. This result shows a hydrothiolation reaction with dienes is also possible. Furthermore, another allotrope of sulfur (S_8) was reacted with butadiene **113**, and no reaction occurred, which eliminates the possibility that the trapped product **118** was formed from cyclization with S_8.

Next, we investigated the possibility of S_8 as a reaction byproduct (**Scheme 4.16**). Hydrogen persulfide **89a** was reacted with styrene **108g** under the standard conditions. The product **109g** and the trapped triphenyl phosphine sulfide **118b** were formed in a yield of 78%. This experiment result implies that S_8 is a major reaction byproduct.

Scheme 4.16 S_8 Trapping Experiment

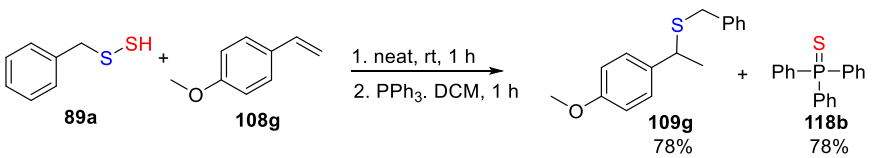

Based on the results of the control experiments, a plausible free radical reaction mechanism is proposed (**Scheme 4.17**). Styrene **108a** performs HAT on **89a** to form intermediate **I**. Intermediate **I** is desulfurized through a reaction with benzyl hydrogen persulfide **89a** via a radical mechanism to generate **109a**. The radical mechanism involves sulfur abstraction of **I** to form a Bn-S-S-S_8 radical. Homolytic bond cleavage of the Bn-S-S-S_8 radical liberates S_8 and a persulfide radical.

Scheme 4.17 Proposed Hydrothiolation Mechanism

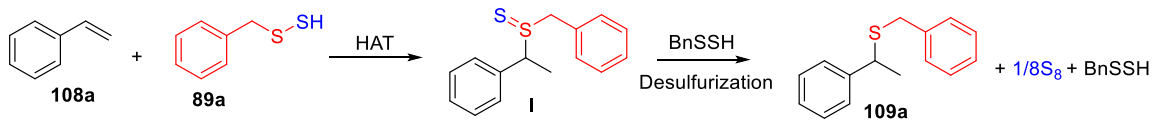

4.5 Conclusion

A highly atom economical, catalyst and metal free hydrothiolation of unactivated alkenes has been developed by using hydrogen persulfides. New hydrogen persulfides have been synthesized using a more straightforward synthetic method. Hydrogen persulfides have been shown to react with themselves to produce polysulfide byproducts, which are not involved in product formation. The optimized reaction conditions are solvent-free, suppressing the formation of polysulfide byproducts. The reaction follows a radical pathway with loss of S_8 to

give the thioether product. The reaction mechanism has been studied through deuterium labeling studies and control experiments. The hydrogen persulfide serves as the hydrogen atom transfer reagent for the synthetic transformation. The reaction is highly atom-economical and environmentally friendly because there is no solvent or molar excess of reagents. The only waste product is elemental sulfur.

4.6 Experimental Procedure

4.6.1 General information

All reactions were carried out under air atmosphere in oven-dried glassware with magnetic stirring bar. Dry solvents (THF, toluene, ACN, diethyl ether, and DCM) were obtained by solvent purification system under argon. All commercially available reagents were used as received without further purification. The tubes used for the reaction are shown in **Figure S1**. Purification of reaction products was carried out by flash column chromatography using silica gel 60 (230-400 mesh). Analytical thin layer chromatography was performed on 0.25 mm aluminum-backed silica gel 60-F plates. Visualization was accompanied with UV light and $KMnO_4$ solution. Concentration under reduced pressure refers to the removal of volatiles using a rotary evaporator attached to a dry diaphragm pump (10-15 mm Hg) followed by pumping to a constant weight with an oil pump (<300 mTorr). Infrared (IR) spectra were recorded on an IR spectrometer with KBr wafers or a film on KBr plate. High-resolution mass spectra (HRMS) were recorded on LCMS-IT-TOF mass spectrometer using ESI (electrospray ionization) or APCI (Atmospheric Pressure Chemical Ionization). ^1H NMR spectra were recorded in $CDCl_3$ on 400 MHz NMR spectrometer. The ^1H chemical shifts are referenced to residual solvent signals at δ

7.26 ($CHCl_3$) or δ 0.00 (TMS). ^1H NMR coupling constants (*J*) are reported in Hertz (Hz) and multiplicities are indicated as follows: s (singlet), bs (broad singlet), d (doublet), t (triplet), q (quartet), m (multiplet), dd (doublet of doublets), dt (doublet of triplets), td (triplet of doublets), tt (triplet of triplets). ^{13}C NMR spectra were proton decoupled and recorded in $CDCl_3$ on 100.5 MHz NMR spectrometer. The ^{13}C chemical shifts are referenced to solvent signals at δ 77.16 ($CDCl_3$). ^{31}P NMR spectra were proton decoupled and recorded in $CDCl_3$ on 162 MHz NMR spectrometer. ^{31}P chemical shifts are reported relative to 85% H_3PO_4 (0.00 ppm) as an external standard.

4.6.2 General Procedure 1 Hydrothiolation Reaction

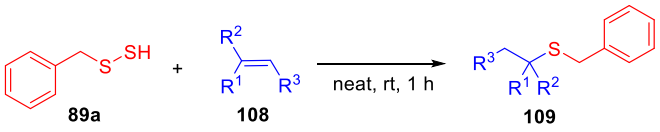

89a 108 109

Benzyl hydrogen persulfide **89a** (0.1 mmol) and alkene **108** (0.1 mmol), are stirred together under neat conditions for 1 hour at room temperature. The crude reaction is then directly purified by column chromatography to obtain **109**.

4.6.3 General Procedure 2 Hydrothiolation Reaction

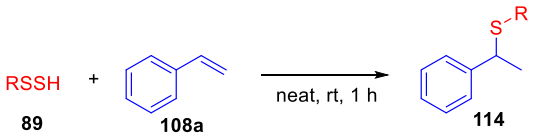

89 108a 114

Benzyl hydrogen persulfide **89** (0.1 mmol) and styrene **108a** (0.1 mmol), are stirred together under neat conditions for 1 hour at room temperature. The crude reaction is then directly purified by column chromatography to obtain **114**.

4.6.4 General Procedure Synthesis of Hydrogen Persulfide

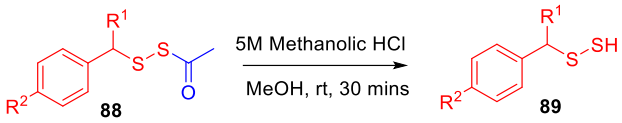

To a solution of **88** (0.3 mmol) in dry MeOH (0.5 mL) under inert conditions was added 5M methanolic HCl (1.5 mmol) dropwise. After addition the reaction was allowed to stir for 30 minutes. The reaction was then concentrated under reduced pressure to give hydrogen persulfide **89**.

4.6.5 Synthesis of Deuterated Hydrogen Persulfide

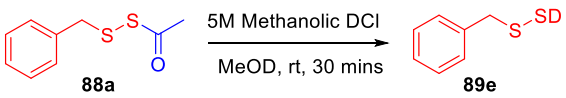

To a solution of **88a** (0.3 mmol) in dry MeOD (0.5 mL) under inert conditions was added 5M methanolic DCl (1.5 mmol) dropwise. After addition the reaction was allowed to stir for 30 minutes. The reaction was then concentrated under reduced pressure to give deuterated hydrogen persulfide **89e**.

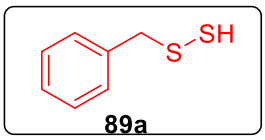

benzyldisulfane (89a).[191] 42.5 mg, 91%; as an oil; **IR** ν(thin film, cm^{-1}) 3027, 2502, 1601, 1493, 1452, 1232, 1070, 1028, 871, 764, 698; ^{1}H NMR (400 MHz, $CDCl_3$) δ 7.34-7.28 (m, 5H), 3.89 (s, 2H), 2.88 (s, 1H); ^{13}C NMR (100.5 MHz, $CDCl_3$): δ 136.6, 129.2, 128.5, 127.5, 44.7.

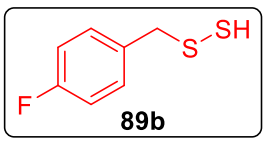

(4-fluorobenzyl)disulfane (89b). 48.9 mg, 86%; as an oil; **IR** ν(thin film, cm^{-1}) 3045, 2918, 2499, 1602, 1511, 1223, 1154, 1091, 1016, 833; ^{1}H

NMR (400 MHz, $CDCl_3$) δ 7.29-7.26 (m, 2H), 7.04-7.00 (m, 2H), 3.86 (s, 2H), 2.86 (s, 1H); ^{13}C NMR (100.5 MHz, $CDCl_3$): δ 161.2 (d, *J* = 244.9 Hz), 134.4 (d, *J* = 3.0 Hz), 130.8 (d, *J* = 8.2 Hz), 115.4 (d, *J* = 21.6 Hz), 43.8.

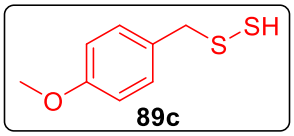

89c

(4-methoxybenzyl)disulfane (89c). 56.0 mg, 99%; as an oil; **IR** ν (thin film, cm^{-1}) 3030, 2953, 2501, 1608, 1510, 1460, 1247, 1172, 1103, 1031, 873, 829; ^1H NMR (400 MHz, $CDCl_3$) δ 7.25.7.21 (m, 2H), 6.87-6.85 (m, 2H), 3.85 (s, 2H), 3.80 (s, 3H), 2.87 (s, 1H); ^{13}C NMR (100.5 MHz, $CDCl_3$): δ 159.0, 130.4, 128.6, 113.9, 55.2, 44.3.

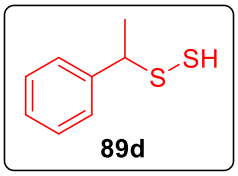

89d

(1-phenylethyl)disulfane (89d). 50.0 mg, 98%; as an oil; **IR** ν (thin film, cm^{-1}) 3026, 2964, 2501, 1492, 1452, 1371, 1209, 1043, 763, 696; ^1H NMR (400 MHz, $CDCl_3$) δ 7.36-7.24 (m, 5H), 4.03 (q, *J* = 6.8 Hz, 1H), 2.77 (s, 1H), 1.68 (d, *J* = 6.8 Hz); ^{13}C NMR (100.5 MHz, $CDCl_3$): δ 141.4, 128.4, 127.6, 127.5, 50.4, 20.0.

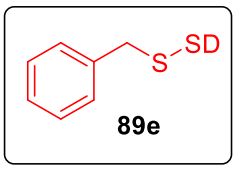

89e

1-benzyldisulfane-2-d (89e). 45.5 mg, 96%; as an oil; **IR** ν (thin film, cm^{-1}) 3026, 2956, 1946, 1492, 1230, 1122, 1070, 761, 696; ^1H NMR (400 MHz, $CDCl_3$) δ 7.36-7.24 (m, 5H), 3.88 (s, 2H); ^{13}C NMR (100.5 MHz, $CDCl_3$): δ 136.7, 129.2, 128.5, 127.5, 44.7.

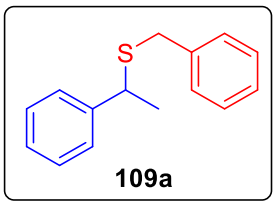

109a

benzyl(1-phenylethyl)sulfane (109a). 17.5 mg, 77%; as an oil; **IR** ν (thin film, cm^{-1}) 3060, 2966, 2922, 1601, 1492, 1452, 1222, 1026, 764, 699; ^1H NMR (400 MHz, $CDCl_3$) δ : 7.38-7.31 (m, 3H), 7.29-7.19 (m, 5H), 3.81 (q, *J* = 7.2 Hz, 1H), 3.53 (d, *J* = 13.6 Hz, 1H), 3.44 (d, *J* = 13.6 Hz, 1H), 1.52 (d, *J* = 6.8 Hz, 3H); ^{13}C NMR (100.5 MHz, $CDCl_3$): δ 143.8, 138.4, 128.8, 128.5, 128.3, 127.4, 127.0, 126.8, 43.5, 35.7, 22.5; HRMS(ESI): m/z calcd. For $C_{15}H_{16}S$ ([M+H]+): 229.1051; found 229.1049.

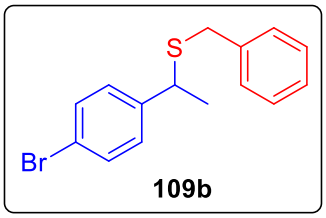

benzyl(1-(4-bromophenyl)ethyl)sulfane (109b). 25.2 mg, 82%; as an oil; **IR** ν (thin film, cm^{-1}) 3027, 2967, 1601, 1486, 1452, 1403, 1072, 1009, 825, 721, 721; ^{1}H NMR (400 MHz, $CDCl_3$) δ 7.45-7.42 (m, 2H), 7.30-7.17 (m, 7H), 3.74 (q, *J* = 7.2 Hz, 1H), 3.53 (d, *J* = 13.6 Hz, 1H), 3.42 (d, *J* = 13.6 Hz, 1H), 1.48 (d, *J* = 7.2 Hz, 3H); ^{13}C NMR (100.5 MHz, $CDCl_3$): δ 142.9, 138.1, 131.5, 129.1, 128.8, 128.4, 126.9, 120.6, 42.9, 35.7, 22.4; HRMS(ESI): m/z calcd. For $C_{15}H_{15}BrS$ ([M+H]+): 307.0156; found 307.0169.

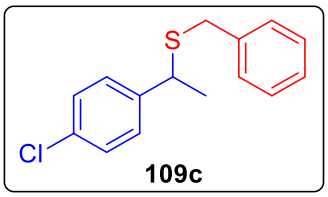

benzyl(1-(4-chlorophenyl)ethyl)sulfane (109c). 20.7 mg, 79%; as an oil; **IR** ν (thin film, cm^{-1}) 3027, 2967, 1601, 1492, 1407, 1091, 1014, 830, 698; ^{1}H NMR (400 MHz, $CDCl_3$) δ : 7.32-7.19 (m, 9H), 3.75 (q, *J* = 7.2 Hz, 1H), 3.53 (d, *J* = 13.2 Hz, 1H), 3.42 (d, *J* = 13.2 Hz, 1H), 1.49 (d, *J* = 7.2 Hz, 3H); ^{13}C NMR (100.5 MHz, $CDCl_3$): δ 142.3, 138.1, 132.6, 128.9, 128.8, 128.6, 128.4, 126.9, 42.8, 35.7, 22.5; HRMS(ESI): m/z calcd. For $C_{15}H_{15}ClS$ ([M+H]+): 263.0661; found 263.0640.

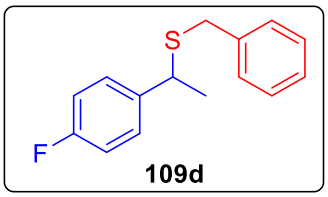

benzyl(1-(4-fluorophenyl)ethyl)sulfane (109d). 18.9 mg, 77%; as an oil; **IR** ν (thin film, cm^{-1}) 3029, 2967, 1601, 1508, 1452, 1223, 1156, 835, 702; ^{1}H NMR (400 MHz, $CDCl_3$) δ 7.33-7.20 (m, 6H), 7.03-6.98 (m, 2H), 3.78 (q, *J* = 7.2 Hz, 1H), 3.54 (d, *J* = 13.2 Hz, 1H), 3.43 (d, *J* = 13.2 Hz, 1H), 1.50 (d, *J* = 6.8 Hz, 3H); ^{13}C NMR (100.5 MHz, $CDCl_3$): δ 161.7 (d, *J* = 244.2 Hz), 139.5 (d, *J* = 3.0 Hz), 138.2, 128.9 (d, *J* = 7.2 Hz), 128.8, 128.4, 126.8, 115.2 (d, *J* = 21.6 Hz), 42.7, 35.7, 22.6; HRMS(ESI): m/z calcd. For $C_{15}H_{15}FS$ ([M+H]+): 247.0957; found 247.0969.

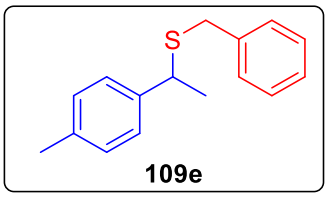

benzyl(1-(p-tolyl)ethyl)sulfane (109e). 20.2 mg, 79%; as an oil; **IR** ν (thin film, cm^{-1}) 3027, 2922, 1601, 1512, 1452, 1222, 1113, 818, 702; ^{1}H NMR (400 MHz, $CDCl_3$) δ 7.30- 7.20 (m, 6H), 7.13 (d, *J* = 8.0 Hz, 2H), 3.78 (q, *J* = 7.2 Hz, 1H), 3.53 (d, *J* = 13.6 Hz, 1H), 3.44 (d, *J* = 13.6 Hz, 1H), 2.34 (s, 3H), 1.51 (d, *J* = 7.2 Hz, 3H); ^{13}C NMR (100.5 MHz, $CDCl_3$): δ 140.7, 138.5, 136.6, 129.1, 128.8, 128.3, 127.3, 126.7, 43.2, 35.6, 22.5, 21.0; HRMS(ESI): m/z calcd. For $C_{16}H_{18}S$ ([M+H]+): 243.1207; found 243.1209.

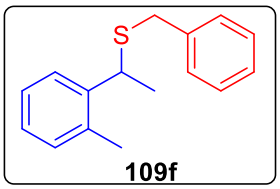

benzyl(1-(o-tolyl)ethyl)sulfane (109f). 20.8 mg, 86%; as an oil; **IR** ν (thin film, cm^{-1}) 3026, 2922, 1601, 1492, 1453, 1159, 1070, 762, 699; ^{1}H NMR (400 MHz, $CDCl_3$) δ 7.54 (d, *J* = 7.6 Hz, 1H), 7.29-7.18 (m, 5H), 7.14-7.08 (m, 2H), 4.02 (q, *J* = 6.8 Hz, 1H), 3.61 (d, *J* = 13.2 Hz, 1H), 3.52 (d, *J* = 13.2 Hz, 1H), 2.10 (s, 3H), 1.52 (d, *J* = 6.8 Hz, 3H); ^{13}C NMR (100.5 MHz, $CDCl_3$): δ 141.0, 138.3, 135.5, 130.3, 128.8, 128.3, 126.8, 126.7, 126.6, 126.4, 38.7, 35.6, 21.6, 18.9; HRMS(ESI): m/z calcd. For $C_{16}H_{18}S$ ([M+H]+): 243.1207; found 243.1205.

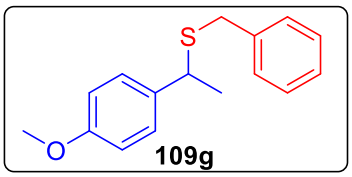

(4-methoxybenzyl)(1-phenylethyl)sulfane (109g). 21.4 mg, 83%; as an oil; **IR** ν (thin film, cm^{-1}) 3027, 2924, 1610, 1511, 1452, 1300, 1248, 1174, 1035, 830, 764, 699; ^{1}H NMR (400 MHz, $CDCl_3$) δ 7.32-7.23 (m, 5H), 7.13 (d, *J* = 8.8 Hz, 2H), 6.81 (d, *J* = 8.8 Hz, 2H), 3.81-3.78 (m, 4H), 3.49 (d, *J* = 13.2 Hz, 1H), 3.40 (d, *J* = 13.2 Hz, 1H), 1.52 (d, *J* = 6.8 Hz, 3H); ^{13}C NMR (100.5 MHz, $CDCl_3$): δ 158.4, 143.9, 130.3, 129.9, 128.4, 127.4, 127.0, 113.7, 55.2, 43.4, 35.0, 22.5; HRMS(ESI): m/z calcd. For $C_{16}H_{18}OS$ ([M+H]+): 259.1157; found 259.1155.

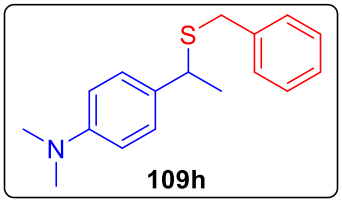

4-(1-(benzylthio)ethyl)-N,N-dimethylaniline (109h). 17.6 mg, 64%; as an oil; **IR** ν (thin film, cm^{-1}) 3027, 2921, 1613, 1521, 1452, 1348, 1164, 1062, 946, 818, 699; ^{1}H NMR (400 MHz, $CDCl_3$) δ 7.28-7.22 (m, 5H), 7.19 (d, *J* = 8.8 Hz, 2H), 6.71 (d, *J* = 8.8 Hz, 2H), 3.77 (q, *J* = 6.8 Hz, 1H), 3.53 (d, *J* = 13.6 Hz, 1H), 3.44 (d, *J* = 13.6 Hz, 1H), 2.94 (s, 6H), 1.50 (d, *J* = 7.2 Hz, 3H); ^{13}C NMR (100.5 MHz, $CDCl_3$): δ 149.7, 138.8, 131.3, 128.9, 128.3, 128.1, 126.6, 112.5, 43.0, 40.6, 35.6, 22.6; HRMS(ESI): m/z calcd. For $C_{17}H_{21}NS$ ([M+H]+): 272.1473; found 272.1479.

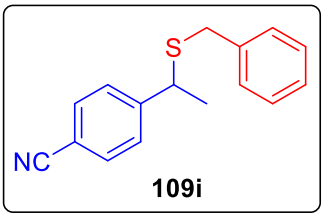

4-(1-(benzylthio)ethyl)benzonitrile (109i). 20.3 mg, 80%; as an oil; **IR** ν (thin film, cm^{-1}) 3029, 2227, 1605, 1495, 1452, 1222, 840, 700; ^{1}H NMR (400 MHz, $CDCl_3$) δ 7.60 (d, *J* = 6.8 Hz, 2H), 7.40 (d, *J* = 8.4 Hz, 2H), 7.30-7.17 (m, 5H), 3.80 (q, *J* = 7.2 Hz, 1H), 3.56 (d, *J* = 13.6 Hz, 1H), 3.42 (d, *J* = 13.6 Hz, 1H), 1.51 (d, *J* = 7.2 Hz, 3H); ^{13}C NMR (100.5 MHz, $CDCl_3$): δ 149.5, 137.6, 132.3, 128.6, 128.5, 128.2, 127.1, 118.8, 110.8, 43.2, 35.8, 22.2; HRMS(ESI): m/z calcd. For $C_{16}H_{15}NS$ ([M+H]+): 254.1003; found 254.100.

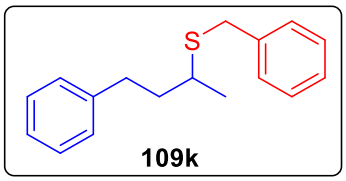

benzyl(4-phenylbutan-2-yl)sulfane (109k). 8.5 mg, 33%; as an oil; **IR** ν (thin film, cm^{-1}) 3026, 2921, 1601, 1495, 1453, 1236, 746, 698; ^{1}H NMR (400 MHz, $CDCl_3$) δ 7.29-7.22 (m, 6H), 7.18-7.15 (m, 1H), 7.12-7.10 (m, 2H), 3.7 (s, 2H), 2.70-2.63 (m, 3H), 1.90-1.73 (m, 2H), 1.30 (d, *J* = 6.8 Hz, 3H); ^{13}C NMR (100.5 MHz, $CDCl_3$): δ 141.9, 138.7, 128.8, 128.5, 128.4, 128.3, 126.8, 125.7, 38.7, 38.4, 34.8, 33.0, 21.2; HRMS(ESI): m/z calcd. For $C_{17}H_{20}S$ ([M+H]+): 257.1364; found 257.1367.

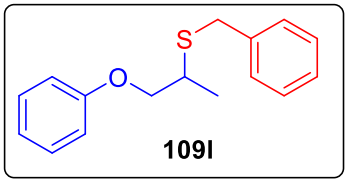

benzyl(1-phenoxypropan-2-yl)sulfane (109l). 11.3 mg, 43%; as an oil; **IR** ν (thin film, cm^{-1}) 3027, 2925, 1600, 1495, 1241, 1031, 745, 692; ^{1}H NMR (400 MHz, $CDCl_3$) δ 7.36-7.22 (m, 7H), 6.96-6.92 (m, 1H), 6.86-6.83 (m, 2H), 4.06-4.03 (m, 1H), 3.91-3.81 (m, 3H), 3.07-3.02 (m, 1H), 1.34 (d, *J* = 6.8 Hz, 3H); ^{13}C NMR (100.5 MHz, $CDCl_3$): δ 158.5, 138.4, 129.4, 128.8, 128.5, 127.0, 120.8, 114.5, 72.6, 38.4, 35.6, 18.1; HRMS(ESI): m/z calcd. For $C_{16}H_{18}OS$ ([M+Na]+): 281.0976; found 281.0972.

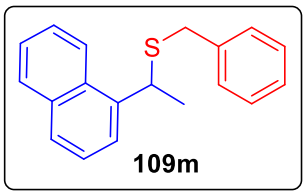

benzyl(1-(naphthalen-1-yl)ethyl)sulfane (109m). 24.0 mg, 86%; as an oil; **IR** ν (thin film, cm^{-1}) 3059, 3029, 2922, 1597, 1493, 1071, 1028, 798, 777, 699; ^{1}H NMR (400 MHz, $CDCl_3$) δ 7.86-7.83 (m, 2H), 7.75-7.72 (m, 2H), 7.48-7.39 (m, 4H), 7.28-7.22 (m, 2H), 7.19-7.16 (m, 2H), 4.62 (q, *J* = 6.8 Hz, 1H), 3.65 (d, *J* = 13.2 Hz, 1H), 3.55 (d, *J* = 13.2 Hz, 1H), 1.70 (d, *J* = 6.8 Hz, 3H); ^{13}C NMR (100.5 MHz, $CDCl_3$): δ 138.7, 138.3, 133.9, 131.0, 129.0, 128.9, 128.4, 127.6, 126.9, 125.8, 125.52, 125.5, 124.4, 123.0, 38.6, 35.9, 22.1; HRMS(ESI): m/z calcd. For $C_{19}H_{18}S$ ([M+H]+): 279.1207; found 297.1223.

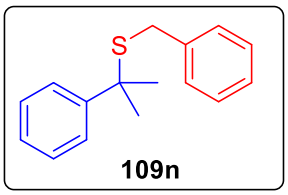

benzyl(2-phenylpropan-2-yl)sulfane (109n). 15.8 mg, 65%; as an oil; **IR** ν (thin film, cm^{-1}) 3029, 2964, 1601, 1493, 1453, 1133, 1098, 768, 696; ^{1}H NMR (400 MHz, $CDCl_3$) δ 7.59-7.56 (m, 2H), 7.36-7.3 (m, 2H), 7.25-7.16 (m, 3H), 7.13-7.11 (m, 2H), 3.39 (s, 2H), 1.72 (s, 6H); ^{13}C NMR (100.5 MHz, $CDCl_3$): δ 146.2, 138.1, 128.9, 128.3, 128.1, 126.7, 126.6, 126.5, 48.5, 34.5, 30.2; HRMS(ESI): m/z calcd. For $C_{16}H_{18}S$ ([M+Na]+): 265.1027; found 265.1049.

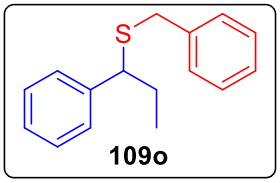

benzyl(1-phenylpropyl)sulfane (109o). 12.7 mg, 53%; as an oil; **IR** ν (thin film, cm^{-1}) 3027, 2928, 1601, 1493, 1452, 1238, 1070, 758, 698; ^{1}H NMR (400 MHz, $CDCl_3$) δ 7.34-7.19 (m, 9H), 3.56-3.52 (m, 2H), 3.41 (d, *J* = 13.2 Hz, 3H), 1.90-1.78 (m, 2H), 0.83 (t, *J* = 7.2 Hz, 3H); ^{13}C NMR (100.5 MHz, $CDCl_3$): δ 142.4, 138.5, 128.9, 128.4, 128.3, 128.1, 127.0, 126.7, 50.9, 35.3, 29.5, 12.2; HRMS(ESI): m/z calcd. For $C_{16}H_{18}S$ ([M+Na]+): 243.1207; found 243.1207.

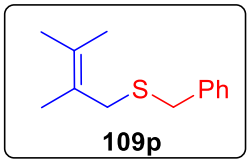

benzyl(2,3-dimethylbut-2-en-1-yl)sulfane (109p).[225] 12.2 mg, 59%; as an oil; **IR** ν (thin film, cm^{-1}) 3027, 2898, 2914, 1661, 1601, 1493, 1452, 1373, 1226, 1070, 762, 689; ^{1}H NMR (400 MHz, $CDCl_3$) δ 5.06 (s, 2H), 4.97 (s, 2H), 1.92 (s, 6H); ^{13}C NMR (100.5 MHz, $CDCl_3$): δ 137.6, 130.6, 129.3, 128.5, 127.3, 122.9, 43.8, 43.6, 20.9, 20.7, 18.1.

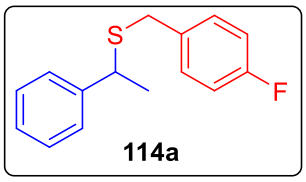

(4-fluorobenzyl)(1-phenylethyl)sulfane (114a). 16.5 mg, 67%; as an oil; **IR** ν (thin film, cm^{-1}) 3027, 2924, 1600, 1508, 1452, 1223, 1156, 834, 764, 699; ^{1}H NMR (400 MHz, $CDCl_3$) δ 7.35-7.28 (m, 5H), 7.26-7.22 (m, 2H), 7.18-7.14 (m, 2H), 3.79 (q, *J* = 6.8 Hz, 1H), 3.49 (d, *J* = 13.2 Hz, 1H), 3.41 (d, *J* = 13.2 Hz, 1H), 1.52 (d, *J* = 6.8 Hz, 3H); ^{13}C NMR (100.5 MHz, $CDCl_3$): δ 160.7 (d, *J* = 244.1 Hz), 143.6, 134.1 (d, *J* = 2.3 Hz), 130.3 (d, *J* = 8.2 Hz), 128.5, 127.4, 127.1, 115.2 (d, *J* = 21.6 Hz), 43.6, 34.9, 22.5; HRMS(ESI): m/z calcd. For $C_{15}H_{15}FS$ ([M+H]+): 247.0957; found 247.0963.

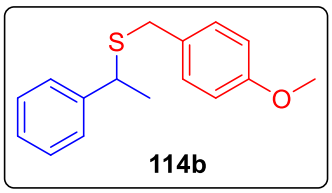

(4-methoxybenzyl)(1-phenylethyl)sulfane (114b). 21.4 mg, 83%; as an oil; **IR** ν (thin film, cm^{-1}) 3027, 2924, 1610, 1511, 1452, 1300, 1248, 1174, 1035, 830, 764, 699; ^{1}H NMR (400 MHz, $CDCl_3$) δ 7.32-

7.23 (m, 5H), 7.13 (d, *J* = 8.8 Hz, 2H), 6.81 (d, *J* = 8.8 Hz, 2H), 3.81-3.78 (m, 4H), 3.49 (d, *J* = 13.2 Hz, 1H), 3.40 (d, *J* = 13.2 Hz, 1H), 1.52 (d, *J* = 6.8 Hz, 3H); ^{13}C NMR (100.5 MHz, $CDCl_3$): δ 158.4, 143.9, 130.3, 129.9, 128.4, 127.4, 127.0, 113.7, 55.2, 43.4, 35.0, 22.5; HRMS(ESI): m/z calcd. For $C_{16}H_{18}OS$ ([M+H]+): 259.1157; found 259.1155.

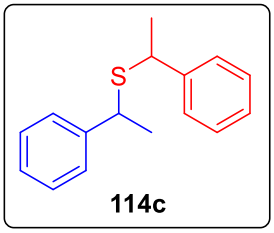

114c

bis(1-phenylethyl)sulfane (114c).[226] 13.9 mg, 57%; as an oil; **IR** ν (thin film, cm^{-1}) 3027, 2922, 1601, 1490, 1452, 1373, 1220, 1048, 1026, 764, 698; ^{1}H NMR (400 MHz, $CDCl_3$) δ 7.30-7.19 (m, 9H), 3.78 (q, *J* = 7.2 Hz, 2H), 1.55 (d, *J* = 7.2 Hz, 6H); ^{13}C NMR (100.5 MHz, $CDCl_3$): δ 143.6, 128.4, 127.2, 126.9, 43.5, 22.4.

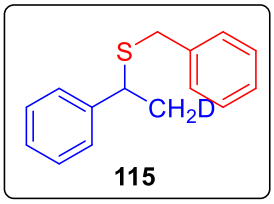

115

benzyl(1-phenylethyl-2-d)sulfane (115). 16.8 mg, 73%; as an oil; **IR** ν (thin film, cm^{-1}) 3027, 2928, 1601, 1492, 1452, 1071, 762, 698; ^{1}H NMR (400 MHz, $CDCl_3$) δ 7.37-7.19 (m, 9H), 3.80 (q, *J* = 6.8 Hz, 1H), 3.53 (d, *J* = 13.6 Hz, 1H), 3.44 (d, *J* = 13.6 Hz, 1H), 1.51 (dt, *J* = 6.8, 2.0 Hz, 3H); ^{13}C NMR (100.5 MHz, $CDCl_3$): δ 143.7, 138.4, 128.8, 128.4, 128.3, 127.4, 127.0, 126.8, 43.4, 35.7, 22.5 (d, *J* = 8.9 Hz), 22.2 (d, *J* = 20.1 Hz); HRMS(ESI): m/z calcd. For $C_{15}H_{15}DS$ ([M+H]+): 230.1109; found 230.1108.

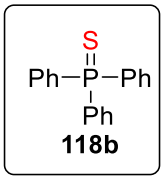

118b

Triphenyl phosphine sulfide (118b).[227] 23.2 mg, 78%; as a solid; ^{1}H NMR (400 MHz, $CDCl_3$) δ 7.75-7.69 (m, 6H), 7.52-7.48 (m, 3H), 7.46-7.41 (m, 6H); ^{13}C NMR (100.5 MHz, $CDCl_3$): δ 132.9 (d, *J* = 84.9 Hz), 132.3 (d, *J* = 11.2 Hz), 131.5 (d, *J* = 2.9 Hz), 128.5 (d, *J* = 12.7 Hz); ^{31}P NMR (162 MHz, $CDCl_3$): δ 43.8.

Chapter V

Catalytic Regioselective Alkylation of Beta Naphthol

5.1 Introduction and Background of Beta Naphthol Functionalization

Scheme 5.1 Selected Applications of Beta Naphthol Structural Motif

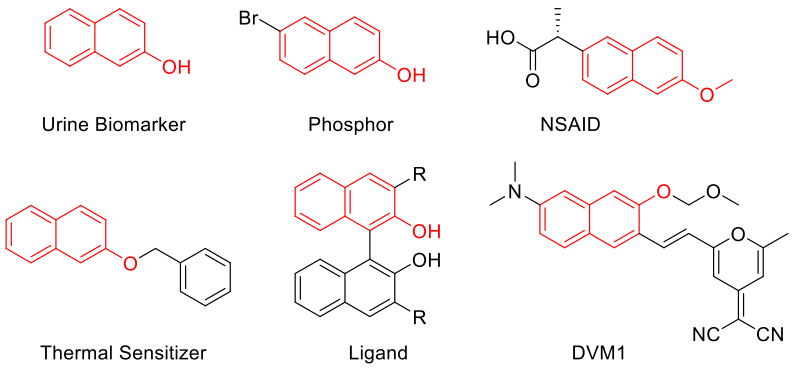

The Friedel-Craft reaction was discovered in 1877, and it has been used a method for installing new carbon-carbon bonds.[228] For example, the Friedel-Crafts alkylation reaction is commonly used for the electrophilic aromatic substitution of arenols. However, the Friedel-Crafts reaction requires metal catalysts and elevated temperatures.[229] In addition, the reaction produces a mixture of regioisomers.[230] Furthermore, the Friedel-Craft reaction involves a

carbocation intermediate which is prone to form rearrangement products.[230] To address these drawbacks, many efforts have been devoted to developing mild Friedel-Craft type reactions.[231]

The structural motif of beta naphthol and its derivatives have broad applications in asymmetric catalysis, bioimaging, and materials chemistry (**Scheme 5.1**).[232-239] Beta naphthol has been used as a urine biomarker.[232] Other derivatives of beta naphthol have been used for phosphors and the imaging of cancer cells.[233] Additionally, naproxen is an example of a nonsteroidal anti-inflammatory drug (NSAID), which treats pain and inflammation.[234] 2-(benzyloxy)naphthalene has been used in materials chemistry as a thermal sensitizer.[235] Furthermore, the beta naphthol structural motif has served as a ligand for asymmetric catalysis.[236-239]

Scheme 5.2 Metal-free Dehydrative Benzylation of Beta Naphthol

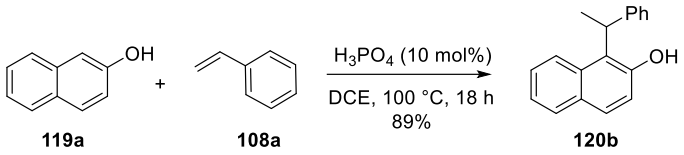

119a **108a** **120b**

Common approaches to functionalize beta naphthol involve alkylation, cyclization, and arylation. The alkylation strategies employ metals such as Rh, Cu, Ag, and Pd.[240-248] To develop a

metal-free approach, the Zhou group reacted beta naphthol **119a** with styrene **108a** in the presence of an acid catalyst to obtain the Markovnikov addition product **120b** in a high yield of 89% (**Scheme 5.2**).[249]

Cyclization strategies with beta naphthol have been extensively studied to construct valuable heterocycles such as benzoxazine, benzofuran, benzoindoline, dihydrofuran, and lactone.[250-255] More specifically, the Yin group has reported an annulation reaction of beta naphthol **119a** with phenylacetylene **121** to give benzohydrofuran product **122** in a high yield of 69% **(Scheme 5.3**).[252]

Scheme 5.3 Annulation of Beta Naphthol

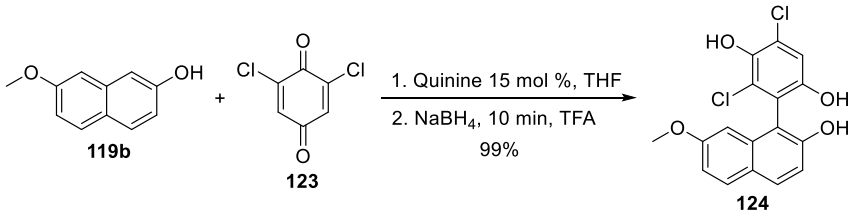

Arylation strategies have been studied to synthesize valuable BINOL ligands through metal catalysis or Lewis base organocatalysts.[256-261] A mild approach by the Bella group reacted beta naphthol **115b** and quinone **118** first in the presence of a quinine catalyst, followed by reduction with sodium borohydride to furnish chiral binol **124** in a yield of 99% (**Scheme 5.4**).[259]

Scheme 5.4 Arylation of Beta Naphthol

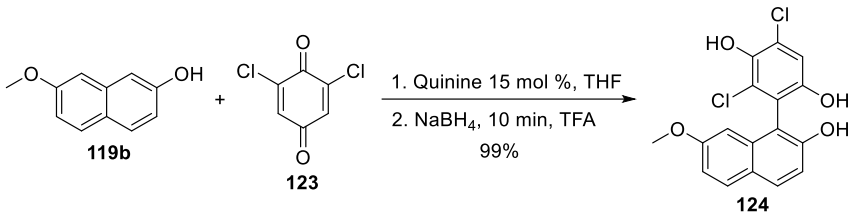

Furthermore, C-H functionalization by the Friedel-Crafts reaction with beta naphthol has been achieved using carbon electrophiles such as iminium, enone, and imine systems.[262-264] For example, the Zhao group has synthesized chiral lactone **126** from beta naphthol **119a** and oxindole **125** in a high yield of 97% (**Scheme 5.5**).[263]

Scheme 5.5 C-H Functionalization of Beta Naphthol by Friedel-Crafts Reaction

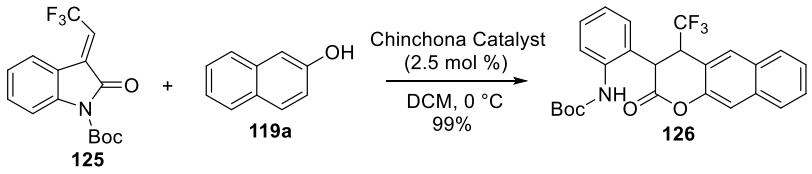

A dehydrative Friedel-Crafts reaction has been studied with primary and secondary alcohols, but it has not been applied to allylic alcohol systems (**Scheme 5.6**). [265-269] The Nakata group used an Sn catalyst to react beta naphthol **119a** with diphenyl methanol **50b** to form **120a** in a 96% yield.[268] On the other hand, the Yang group employed a phosphomolybdic catalyst to generate **120a** in a high yield of 99% (**Scheme 5.6**).[269] The Yaragorla group released a microwave-assisted method to give **120a** in a high yield of 90% (**Scheme 5.6**).[265] However, an elevated temperature of 140 °C was required. Furthermore, Muzart and Rodrigues have reported nucleophilic substitution reactions with allylic and benzylic alcohols; however, they have not explored the reaction with beta naphthol.[266, 267]

Allylic alcohol substrates are underexplored due to their instability and regioselectivity issues.[270-273] Activation of the hydroxyl group also poses difficulty as a hydroxyl group is a poor leaving group.[268, 274] Furthermore, there is potential deactivation of the heteroatom nucleophile reaction partner under acidic conditions. Nevertheless, indoles have been reacted with allylic alcohols through cobalt and ruthenium metal catalysis.[272, 273]

The Tsuji-Trost reaction involves an allylic system and a soft/hard nucleophile through a pi-allyl complex.[275] Regioselectivity is controlled by the electronics of the nucleophile. A Friedel Crafts type allylation can be a metal-free alternative to the traditional Tsuji-Trost reaction of arenols.[276-281] If allylic alcohols could participate in a Friedel-Crafts allylation of beta naphthol, it would provide new beta naphthol derivatives.

Scheme 5.6 Dehydrative Friedel-Crafts (FC) Reaction

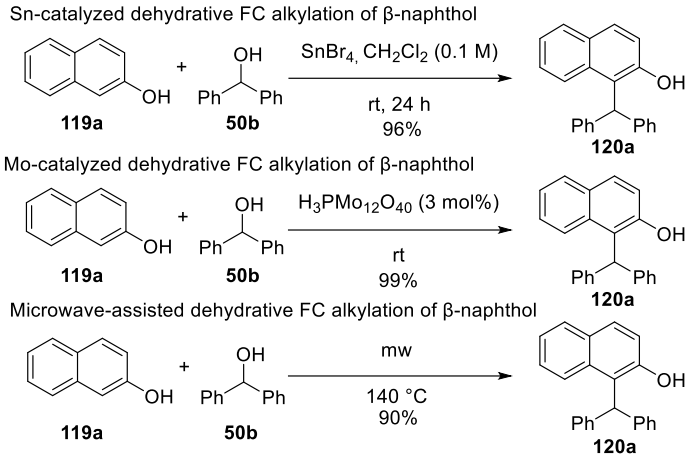

5.2 Specific Aim

This project aims to develop a catalytic and regioselectivity reaction of allylic alcohols with beta naphthol. The project also aims to overcome the poor leaving group ability of the hydroxyl group. It will also demonstrate the synthetic utility of new beta naphthol products.

5.3 Catalytic and Regioselective Allylation of Beta Naphthol

To achieve the aim, we treated allylic alcohol **127a** with beta naphthol **119a** as model substrates for reaction optimization (**Table 5.1**). Common Brønsted acids were initially evaluated (**Table 5.1**, entries 1-4). It was found that weaker Brønsted acids such as acetic acid, trifluoroacetic acid, and 4-nitrobenzoic acids, were unsuitable catalysts for this transformation, giving no product yield (**Table 5.1**, entries 1,2 and 4). However, when a stronger Brønsted acid such as TsOH was used, the product **128a** was generated in 84% yield (**Table 5.1**, entry 3).

Table 5.1 Allylation Reaction Optimization[a]

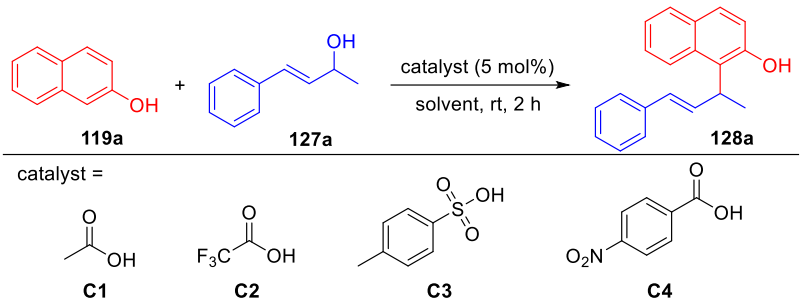

entry	catalyst	solvent	yield (%)[b]
1	C1	DCM	-
2	C2	DCM	-
3	C3	DCM	84
4	C4	DCM	-
5	C3	ACN	91
6	C3	Toluene	58
7	C3	THF	-
8	C3	Ether	-
9	C3	Ethanol	-
10	No catalyst	ACN	-

[a]Reaction conditions: **119a** (0.2 mmol), **127a** (0.2 mmol), catalyst (0.01 mmol) in solvent (1.0 mL) at room temperature for 2 h.

[b]Isolated yield.

Next, solvent effects were tested to optimize the reaction further. To our delight, when the reaction was run in acetonitrile, the yield increased to 91% (**Table 5.1**, entry 5). A nonpolar solvent such as toluene provided product **128a** in a moderate yield (**Table 5.1**, entry 6).

However, solvents that contain an oxygen heteroatom such as tetrahydrofuran, ether, and ethanol did not give any desired product (**Table 5.1**, entries 7-9). A possible explanation is that there is competition between solvent protonation and protonation of the allylic alcohol **127a**. Furthermore, a control experiment was performed without the catalyst, and no product was formed, revealing that a catalyst is necessary for this transformation (**Table 5.1**, entry 10).

With the optimized reaction conditions, the electronic and steric effects of the allylic alcohol **127** were tested (**Table 5.2**). Allylic alcohol with a bulky phenyl substituent **127b** formed the product **128b** with an 88% yield. Substrates containing an electron donating group **127c** and **127d** (4-Me, 4-MeO) gave the desired products **128c** and **128d** in high yields of 84% and 70%, respectively. Allylic alcohols with a halogen **127e** and **127f** (4-F, 4-Cl) were also tolerated to give **128e** and **128f** in a high yield of 89%.

When a primary allylic alcohol **127g** was tested, the corresponding product **128g** was formed with a moderate yield of 55%. This low yield is presumably due to the decreased stability of the primary allylic carbocation intermediate. Cycloalkyl allylic alcohol **127h** was also well tolerated, giving **128h** in a yield of 84%.

Next, we wanted to see if a complementary benzylation could be achieved. Diphenyl methanol **50b** was successful in forming **120a** in a high yield of 81%. A secondary alcohol with an aryl, alkyl substituent **50c** did not create any product under standard reaction conditions. However, when the reaction was heated at reflux for 12 hours, **120b** was formed in a moderate yield of 53%. This alkyl, aryl-substituted carbocation is much less stable than a diaryl carbocation. Other electronically distinct diaryl methanols **50d** and **50e** (4-Me and 4-Cl) also provided the products **120c** and **120d** in 92% and 77% yields, respectively. The synthesis of **128a** was performed on a larger scale (3.0 mmol) to demonstrate a scale-up reaction and gave a high yield of 78%.

Table 5.2 Substrate Scope of Allylic Alcohol Electrophile[a]

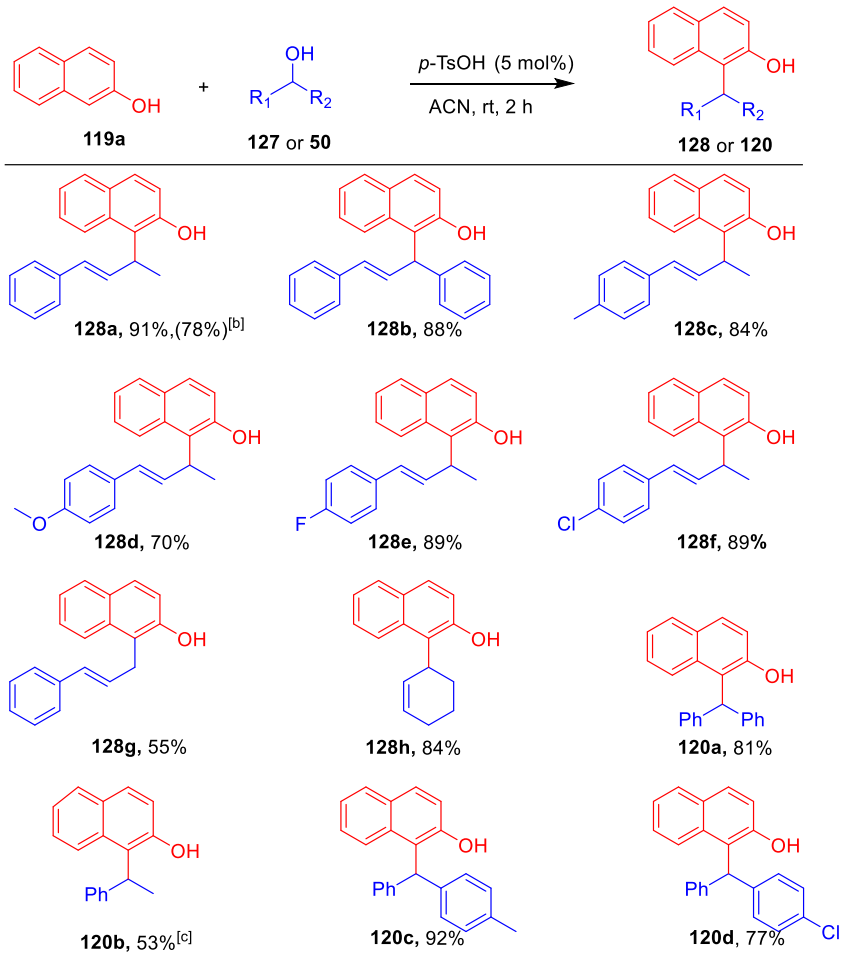

[a]Reaction conditions: **119a** (0.2 mmol), **127** or **50** (0.2 mmol), *p*-TsOH (0.01 mmol) in ACN (1.0 mL) at room temperature for 2 h. Isolated yield. [b]A scale-up experiment with **1a** (3.0 mmol). [c]Reflux for 12 h.

The scope of the arenol reaction partner was then tested (**Table 5.3**). Naphthol containing an electron donating group **115b** was tested and it generated **129a** in a high yield of 84%. Natural product seasamol **127c** also provided the product **129b** in a high yield of 96%. To control the regioselectivity of phenol, an ortho-blocked phenol **127d** was used to provide para-

substituted product **129c**. Lastly, alpha naphthol **115e** was tolerated to give **129d** in a moderate yield of 60%.

Table 5.3 Substrate Scope of Arenol Nucleophile[a]

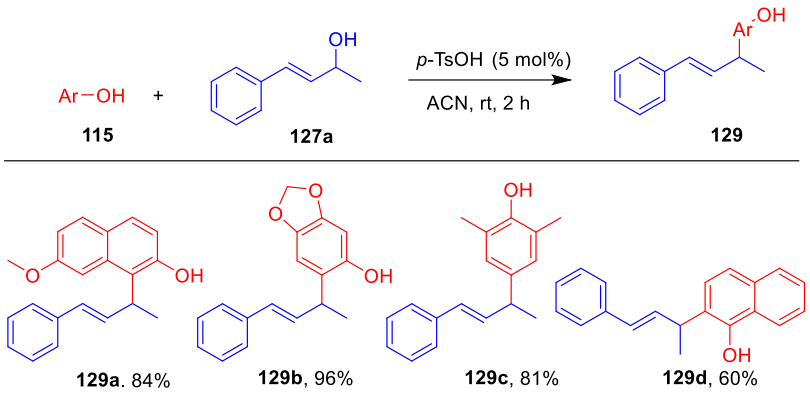

[a]Reaction conditions: **115** (0.2 mmol), **127a** (0.2 mmol), *p*-TsOH (0.01 mmol) in ACN (1.0 mL) at room temperature for 2 h. Isolated yield.

5.4 Synthetic Utility of Allylated Beta Naphthol

The synthetic utility of **128a** was explored under various reaction transformations (**Table 5.4**). Williamson ether synthesis was performed on **128a** to give benzyl naphthyl ether **130a** in a high yield of 84%. **130a** can serve as a thermal paper sensitizer.[235] In addition, the hydroxyl group was protected by reacting with diethyl chloroformate to generate **130b** in a high yield of 92%. Furthermore, a cyclization was achieved when **128a** was treated with n-thiosuccinimide in the presence of an acid catalyst to produce benzohydrofuran **130c** in a moderate yield of 65%.

Benzofurans are a valuable structural motif and have served as cytoprotective agents.[282] Lastly, phosphorylation of **128a** provided **130d** in a high yield of 71%. Phosphorylation has been shown to increase hydrophobicity and acidity for potential prodrug applications.[11] Overall this synthetic utility study demonstrated that the hydroxyl group and olefin of **128a** can be functionalized to give diverse products.

Table 5.4 Synthetic Utility of Beta Naphthol Motif

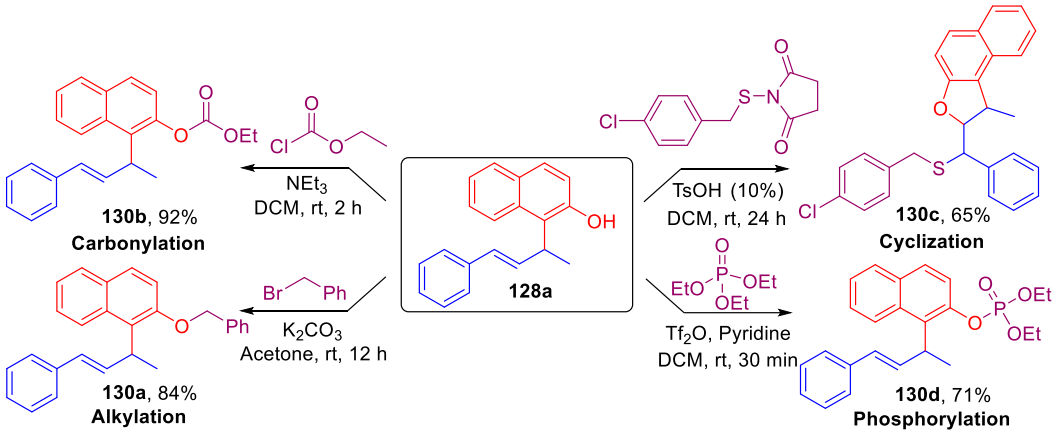

Based on the substrate scope study and information from the literature, this reaction involves an S_N1 mechanism (**Scheme 5.6)**.[283, 284] First, the hydroxyl group is protonated and leaves to form a secondary allylic carbocation intermediate **I**. Then, the high-energy carbocation

intermediate is reacted with beta naphthol **115a** at the alpha position. Finally, the catalyst is then regenerated by deprotonation of the Wheland complex **II** to give product **128a**.[285, 286]

Scheme 5.7 Proposed Dehydrative Allylation Mechanism

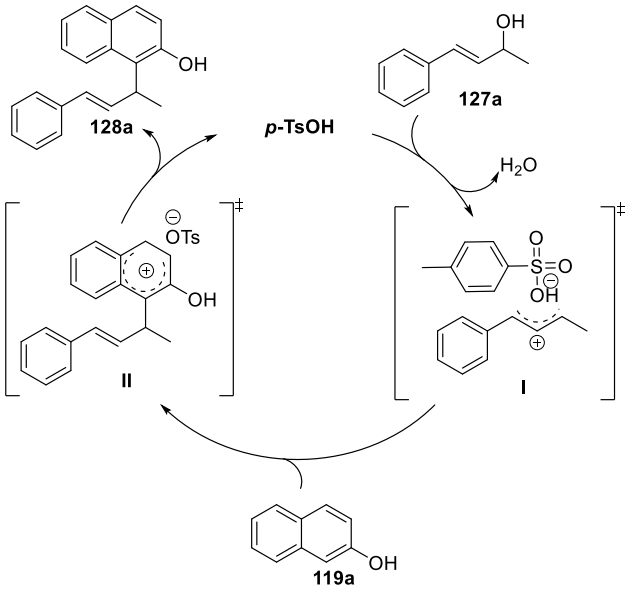

5.5 Conclusion

We have developed an allylation and benzylation strategy for beta naphthol. This transformation is regioselective, catalytic, and energy neutral. Toluene sulfonic acid is used as an inexpensive and readily available Brønsted acid catalyst. The substrate scope is tolerant of electronic and steric factors. Also, the synthetic utility of the novel naphthol products, such as

phosphorylation and cyclization, has been demonstrated. The developed methodology can serve as a general strategy for an allylation reaction of arenols.

5.6 Experimental Procedure

5.6.1 General information

All reactions were carried out under air atmosphere in oven-dried glassware with magnetic stirring bar. Dry solvents (THF, toluene, ACN, diethyl ether, and DCM) were obtained by solvent purification system under argon. All commercially available reagents were used as received without further purification. The tubes used for the reaction are shown in **Figure S1**. Purification of reaction products was carried out by flash column chromatography using silica gel 60 (230-400 mesh). Analytical thin layer chromatography was performed on 0.25 mm aluminum-backed silica gel 60-F plates. Visualization was accompanied with UV light and $KMnO_4$ solution. Concentration under reduced pressure refers to the removal of volatiles using a rotary evaporator attached to a dry diaphragm pump (10-15 mm Hg) followed by pumping to a constant weight with an oil pump (<300 mTorr). Infrared (IR) spectra were recorded on an IR spectrometer with KBr wafers or a film on KBr plate. High-resolution mass spectra (HRMS) were recorded on LCMS-IT-TOF mass spectrometer using ESI (electrospray ionization) or APCI (Atmospheric Pressure Chemical Ionization). ^1H NMR spectra were recorded in $CDCl_3$ on 400 MHz NMR spectrometer. The ^1H chemical shifts are referenced to residual solvent signals at δ 7.26 ($CHCl_3$) or δ 0.00 (TMS). ^1H NMR coupling constants (*J*) are reported in Hertz (Hz) and multiplicities are indicated as follows: s (singlet), bs (broad singlet), d (doublet), t (triplet), q (quartet), m (multiplet), dd (doublet of doublets), dt (doublet of triplets), td (triplet of

doublets), tt (triplet of triplets). ^{13}C NMR spectra were proton decoupled and recorded in $CDCl_3$ on 100.5 MHz NMR spectrometer. The ^{13}C chemical shifts are referenced to solvent signals at δ 77.16 ($CDCl_3$). ^{31}P NMR spectra were proton decoupled and recorded in $CDCl_3$ on 162 MHz NMR spectrometer. ^{31}P chemical shifts are reported relative to 85% H_3PO_4 (0.00 ppm) as an external standard.

5.6.2 General Procedure 1 Synthesis of Allylated or Benzylated Naphthol

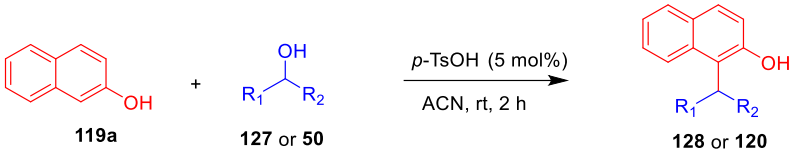

To a solution of alcohol **127** or **50** (0.2 mmol, 1.0 equiv) and beta naphthol **119a** (0.2 mmol, 1.0 equiv) in acetonitrile (1.0 mL) was added *p*-TsOH catalyst (1.7 mg, 0.01 mmol). The solution was stirred for 2 hours and then directly purified by column chromatography to give alkylated naphthol product **120** or **128**.

5.6.3 General Procedure 2 Synthesis of Allylated Arenol

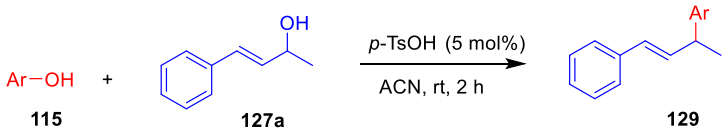

To a solution of allylic alcohol **127a** (0.2 mmol, 1.0 equiv) and aryl alcohol **115** (0.2 mmol, 1.0 equiv) in acetonitrile (1.0 mL) was added *p*-TsOH (1.7 mg, 0.01 mmol). The solution was stirred for 2 hours and then directly purified by column chromatography to give **129**.

5.6.4 Synthetic Utility: Alkylation, Carbonylation, Cycliczation, and Phosphorylation

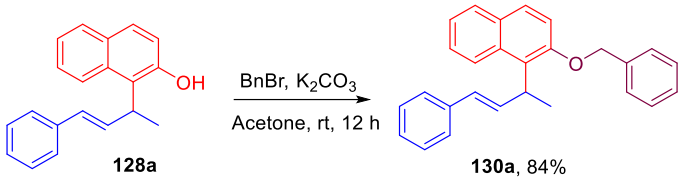

To a solution of **128a** (27.5 mg, 0.10 mmol, 1.0 equiv) and K_2CO_3 (41.5 mg, 0.30 mmol, 3.0 equiv) in acetone (0.25 mL) was added benzyl bromide (18 µL, 0.15 mmol, 1.5 equiv). The solution was stirred for 12 hours. The crude reaction mixture was filitered and then directly purified by column chromatography (85:15 hexane/DCM) to give **130a** (30.6 mg, 84%) as a clear oil.

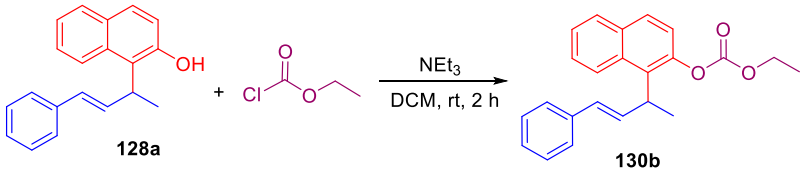

To a solution of **128a** (27.4 mg, 0.1 mmol, 1.0 equiv), and ethyl chloroformate (14 µL, 0.15 mmol, 1.5 equiv) was slowly added triethyl amine (28 µL, 0.20 mmol, 2.0 equiv). The solution was stirred for 2 hours, and then directly purified by column chromatography (6:4 Hexane/DCM) to give **130b** (33.0 mg, 92%) as a yellow oil.

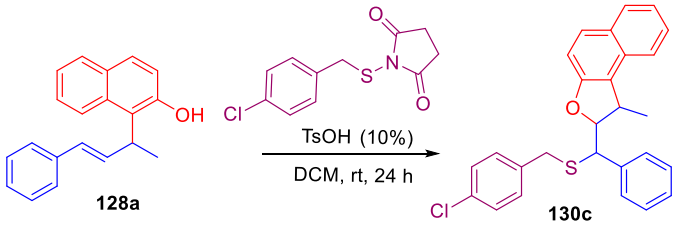

To a solution of **128a** (27.6 mg, 0.1 mmol, 1.0 equiv), and n-thiosuccinimide (38.7 mg, 0.15 mmol, 1.5 equiv) was added TsOH (1.7 mg, 0.01 mmol, 0.01 equiv). The reaction was stirred for 24 hours and then directly purified by column chromatography (7:3 hexane/ DCM) to give **130c** (28.2 mg, 65%), as a white solid.

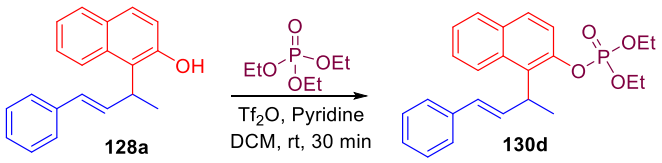

To a solution of triethyl phosphate (18.2 mg, 0.1 mmol, 1.0 equiv) was added Tf_2O (26 µL, 0.15 mmol, 1.5 equiv), and pyridine (16 µL, 0.20 mmol, 2.0 equiv). After stirring for 10 minutes, a solution of **128a** (55.0 mg, 0.2 mmol, 2.0 equiv) in DCM (200 µL), was added. After stirring for 30 minutes, the reaction was directly purified by column chromatography (7:3 hexane/ethyl acetate) to give phosphate **130d** (29.1 mg, 71%) as a clear oil.

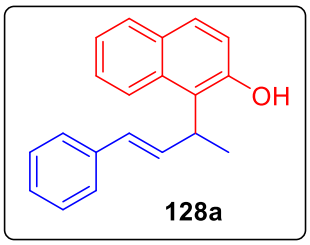

(E)-1-(4-phenylbut-3-en-2-yl)naphthalen-2-ol (128a).[279] 49.6 mg, 91%; as an oil; **IR** ν (thin film, cm^{-1}) 3452, 3056, 2964, 1666, 1620, 1511, 1258, 965, 815, 746, 695; ^{1}H NMR (400 MHz, $CDCl_3$) δ 8.04 (d, *J* = 8.4 MHz, 1H), 7.79 (d, *J* = 8.4 MHz, 1H), 7.67 (d, *J* = 8.8 MHz, 1H), 7.50-7.46 (m, 1H), 7.40-7.39 (m, 2H), 7.36-7.28 (m, 3H), 7.25-7.21 (m, 1H), 7.06 (d, *J* = 8.8 MHz, 1H), 6.75-6.74 (m, 2H), 5.84 (s, 1H), 4.63 (q, *J* = 6.8 MHz, 1H), 1.63 (d, *J* = 6.8 MHz, 3H); ^{13}C NMR (100.5 MHz, $CDCl_3$) δ 152.3, 136.6, 133.5, 132.5, 130.5, 129.6, 128.9, 128.8, 128.7, 127.7, 126.5, 126.3, 123.0, 122.3, 121.2, 119.2, 33.4, 17.2.

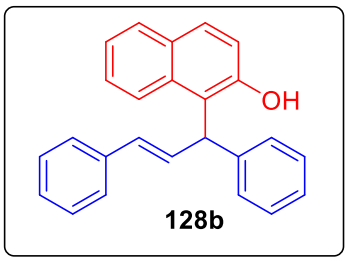

(E)-1-(1,3-diphenylallyl)naphthalen-2-ol (128b).[280] 58.9 mg, 88%; as a solid; mp 48-50 °C; **IR** ν (thin film, cm^{-1}) 3498, 3056, 1620, 1511, 1258, 965, 815, 746; ^{1}H NMR (400 MHz, $CDCl_3$) δ 7.98 (d, *J* = 8.4 MHz, 1H), 7.80 (d, *J* = 8.0 MHz, 1H), 7.73 (d, *J* = 8.8 MHz, 1H), 7.45-7.41 (m, 1H), 7.38-7.19 (m, 11H), 7.10 (d, *J* = 8.8 MHz, 1H), 6.94 (dd, *J* = 15.6, 6.4 MHz, 1H), 6.50 (d, *J* = 16.4 MHz, 1H), 5.87 (d, *J* = 6.8 MHz, 1H), 5.48 (s, 1H); ^{13}C NMR (100.5 MHz, $CDCl_3$) δ 152.3, 141.4, 136.7, 133.2, 132.9, 129.9, 129.7, 129.4, 128.9, 128.8, 128.5, 128.0, 127.6, 126.9, 126.7, 126.4, 123.2, 122.9, 119.5, 119.2, 45.2.

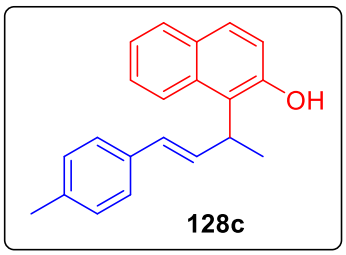

(E)-1-(4-(p-tolyl)but-3-en-2-yl)naphthalen-2-ol (128c).[279] 48.1 mg, 84%, as an oil; **IR** ν (thin film, cm^{-1}) 3412, 2964, 1602, 1511, 1246, 1172, 959, 815, 746; ^{1}H NMR (400 MHz, $CDCl_3$) δ 8.02 (d, *J* = 8.4 MHz, 1H), 7.77 (d, *J* = 8.4 MHz, 1H), 7.65 (d, *J* = 8.8 MHz, 1H), 7.48-7.44 (m, 1H), 7.34-7.26 (m, 3H), 7.18-7.09 (m, 2H), 7.05 (d, *J* = 8.8 MHz, 1H), 6.70-6.69 (m, 2H), 5.94 (s, 1H), 4.60 (q, *J* = 7.2 MHz, 1H), 2.31 (s, 3H), 1.60 (d, *J* = 7.2 MHz, 3H); ^{13}C NMR

(100.5 MHz, $CDCl_3$) δ 152.4, 137.6, 133.8, 132.5, 132.4, 130.5, 129.6, 129.4, 128.9, 128.7, 126.5, 126.3, 123.0, 122.4, 121.3, 119.3, 33.4, 21.2, 17.2.

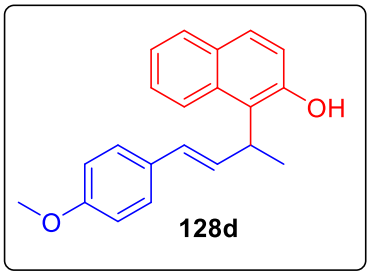

128d

(E)-1-(4-(4-methoxyphenyl)but-3-en-2-yl)naphthalen-2-ol (128d).[279] 42.3 mg, 70%; as an oil; **IR** ν (thin film, cm^{-1}) 3435, 2964, 1602, 1298, 1252, 1177, 999, 815, 741; ^1H NMR (400 MHz, $CDCl_3$) δ 8.03 (d, *J* = 8.4 MHz, 1H), 7.78 (d, *J* = 8.0 MHz, 1H), 7.66 (d, *J* = 8.8 MHz, 1H), 7.49-7.45 (m, 1H), 7.35-7.30 (m, 3H), 7.06 (d, *J* = 8.8 MHz, 1H), 6.85-6.82 (m, 2H), 6.70 (dd, *J* = 16.4, 2.0 MHz, 1H), 6.60 (dd, *J* = 16.4, 3.6 MHz, 1H), 6.01 (s, 1H), 4.62-4.58 (m, 1H), 3.79 (s, 3H), 1.60 (d, *J* = 7.2 MHz, 3H); ^{13}C NMR (100.5 MHz, $CDCl_3$) δ 159.3, 152.4, 132.5, 131.0, 130.1, 129.6, 129.3, 128.9, 128.7, 127.5, 126.5, 123.0, 122.3, 121.3, 119.3, 114.1, 55.3, 33.3, 17.2.

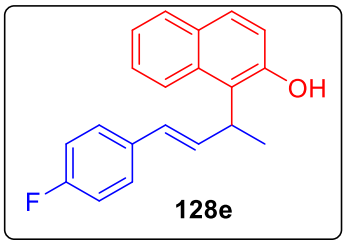

128e

(E)-1-(4-(4-fluorophenyl)but-3-en-2-yl)naphthalen-2-ol (128e).[279] 52.7 mg, 89%; as an oil; **IR** ν (thin film, cm^{-1}) 3452, 2970, 1620, 1511, 1258, 970, 815, 746; ^1H NMR (400 MHz, $CDCl_3$) δ 8.03 (d, *J* = 8.4 MHz, 1H), 7.79 (d, *J* = 8.0 MHz, 1H), 7.67 (d, *J* = 8.8 MHz, 1H), 7.50-7.46 (m, 1H), 7.36-7.31 (m, 3H), 7.05 (d, *J* = 8.8 MHz, 1H), 7.00-6.96 (m, 2H), 6.68-6.64 (m, 2H), 5.77 (s, 1H), 4.63-4.60 (m, 1H), 1.32 (d, *J* = 7.2 MHz, 3H); ^{13}C NMR (100.5 MHz, $CDCl_3$) δ 162.1 (d, *J* = 245.6 MHz), 152.1, 133.4, 132.8 (d, *J* = 3.7 MHz), 132.4, 129.6, 129.2, 128.9, 128.8, 127.9 (d, *J* = 8.2 MHz), 126.5, 123.1, 122.4, 121.2, 119.2, 115.5 (d, *J* = 21.6 MHz), 33.4, 17.3.

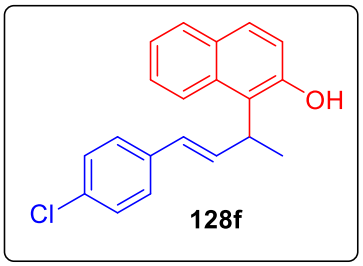

128f

(E)-1-(4-(4-chlorophenyl)but-3-en-2-yl)naphthalen-2-ol (128f).[279] 54.6 mg, 89%; as an oil; **IR** ν (thin film, cm^{-1}) 3452, 2964, 1666, 1258, 1149, 965, 810, 746; ^{1}H NMR (400 MHz, $CDCl_3$) δ 8.03 (d, *J* = 8.8 MHz, 1H), 7.80 (d, *J* = 7.6 MHz, 1H), 7.68 (d, *J* = 9.2 MHz, 1H), 7.50-7.46 (m, 1H), 7.36-7.24 (m, 5H), 7.06 (d, *J* = 8.8 MHz, 1H), 6.73 (dd, *J* = 16.4, 4.0 MHz, 1H), 6.65 (dd, *J* = 16.4, 2.0 MHz, 1H), 5.67 (s, 1H), 4.64-4.61 (m, 1H), 1.63 (d, *J* = 7.2 MHz, 3H); ^{13}C NMR (100.5 MHz, $CDCl_3$) δ 152.0, 135.2, 134.4, 133.2, 132.4, 129.6, 129.1, 128.9, 128.8, 128.7, 127.5, 126.5, 123.1, 122.4, 121.1, 119.1, 33.5, 17.3.

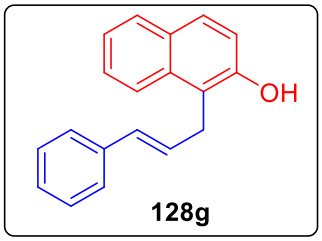

128g

1-cinnamylnaphthalen-2-ol (128g).[279] 28.6 mg, 55%; as an oil; **IR** ν (thin film, cm^{-1}) 3539, 3056, 2918, 1625, 1511, 1263, 956, 810, 741; ^{1}H NMR (400 MHz, $CDCl_3$) δ 7.95 (d, *J* = 8.8 MHz, 1H), 7.78 (d, *J* = 8.4 MHz, 1H), 7.67 (d, *J* = 8.8 MHz, 1H), 7.50-7.46 (m, 1H), 7.35-7.31 (m, 1H), 7.29-7.21 (m, 4H), 7.17-7.15 (m, 1H), 7.09 (d, *J* = 8.8 MHz, 1H), 6.43-6.42 (m, 2H), 5.05 (s, 1H), 3.97 (d, *J* = 3.2 MHz, 2H). ^{13}C NMR (100.5 MHz, $CDCl_3$) δ 151.1, 137.1, 133.2, 130.9, 129.4, 128.6, 128.5, 128.4, 127.5, 127.1, 126.6, 126.1, 123.2, 123.0, 117.9, 117.1, 28.4.

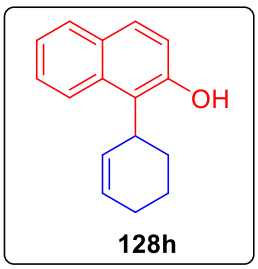

128h

1-(cyclohex-2-en-1-yl)naphthalen-2-ol (128h).[279] 37.7 mg, 84%; as an oil; **IR** ν (thin film, cm^{-1}) 3441, 3056, 2930, 1620, 1258, 1154, 982, 815, 741; ^{1}H NMR (400 MHz, $CDCl_3$) δ 7.92 (d, *J* = 8.8 MHz, 1H), 7.76 (d, *J* = 8.0 MHz, 1H), 7.64 (d, *J* = 8.8 MHz, 1H), 7.45 (t, *J* = 7.2 MHz, 1H), 7.32-7.28 (m, 1H), 7.08 (d, *J* = 8.8 MHz, 1H), 6.58 (s, 1H), 6.24 (s, 1H), 6.07 (d, *J* = 9.2 MHz, 1H), 4.30 (s, 1H), 2.27-2.19 (m, 2H), 2.12-2.08 (m, 1H), 1.96-1.90 (m, 1H), 1.81-1.72 (m, 2H); ^{13}C NMR (100.5 MHz,

$CDCl_3$) δ 153.1, 133.3, 132.6, 130.3, 129.3, 128.8, 128.5, 126.4, 122.9, 121.9, 120.6, 119.4, 34.4, 28.7, 25.1, 22.0.

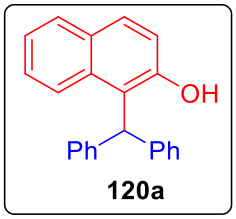

1-benzhydrylnaphthalen-2-ol (120a).[280] 50.2 mg, 81%, as a solid; mp 109-111 °C; **IR** ν (thin film, cm^{-1}) 3493, 3062, 2918, 1620, 1465, 1252, 1177, 1057, 907, 856, 741; ^1H NMR (400 MHz, $CDCl_3$) δ 7.98 (d, *J* = 8.8 MHz, 1H), 7.77 (d, *J* = 7.6 MHz, 1H), 7.73 (d, *J* = 8.8 MHz, 1H), 7.42-7.38 (m, 1H), 7.34-7.27 (m, 11H), 7.06 (d, *J* = 8.8 MHz, 1H), 6.40 (s, 1H), 5.13 (s, 1H); ^{13}C NMR (100.5 MHz, $CDCl_3$) δ 152.8, 141.5, 133.4, 129.7, 129.6, 129.1, 129.0, 128.7, 127.2, 126.8, 123.2, 122.7, 120.1, 119.8, 48.6.

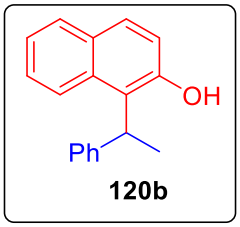

1-(1-phenylethyl)naphthalen-2-ol (120b).[287] 26.4 mg, 53%; as an oil; **IR** ν (thin film, cm^{-1}) 3498, 3027, 2970, 1620, 1493, 1258, 930, 810, 746; ^1H NMR (400 MHz, $CDCl_3$) δ 8.04 (d, *J* = 8.8 MHz, 1H), 7.79 (d, *J* = 8.4 MHz, 1H), 7.66 (d, *J* = 8.8 MHz, 1H), 7.46 (t, *J* = 7.2 MHz, 1H), 7.39-7.31 (m, 5H), 7.26-7.21 (m, 1H), 6.99 (d, *J* = 8.8 MHz, 1H), 5.19-5.14 (m, 1H), 4.83 (s, 1H), 1.78 (d, *J* = 6.8 MHz, 3H); ^{13}C NMR (100.5 MHz, $CDCl_3$) δ 151.5, 143.6, 132.8, 129.7, 129.0, 128.8, 128.7, 127.1, 126.8, 126.6, 123.8, 123.1, 122.6, 119.4, 34.8, 17.1.

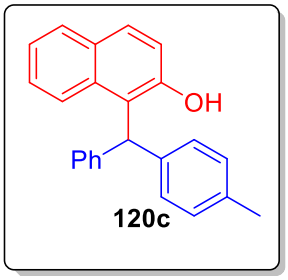

1-(phenyl(p-tolyl)methyl)naphthalen-2-ol (120c). 59.7 mg, 92%; as a sticky solid; **IR** ν (thin film, cm^{-1}) 3487, 3056, 3027, 1620, 1493, 1396, 1252, 1206, 1137, 959, 741; ^1H NMR (400 MHz, $CDCl_3$) δ 7.98 (d, *J* = 8.8 Hz, 1H), 7.76 (d, *J* = 8.0 Hz, 1H), 7.72 (d, *J* = 9.2 Hz, 1H), 7.41-7.37 (m, 1H), 7.33-7.21 (m, 6H), 7.23-7.21 (m, 4H), 7.06 (d, *J* = 8.8 Hz, 1H), 6.35 (s, 1H), 5.21 (s, 1H), 2.31 (s, 3H); ^{13}C NMR (100.5 MHz, $CDCl_3$) δ 152.8, 141.6, 138.5, 137.0, 133.4, 129.9, 129.7, 129.6,

129.1, 129.0, 128.8, 128.7, 127.1, 126.8, 123.2, 122.7, 120.2, 119.9, 48.3, 21.0; HRMS(ESI): m/z calculated for $C_{24}H_{20}O$ ([M+Na]+): 347.1412; found 347.1411.

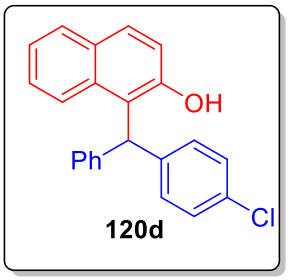

120d

1-((4-chlorophenyl)(phenyl)methyl)naphthalen-2-ol (120d).[288] 52.9 mg, 77%; as a sticky solid; **IR** ν (thin film, cm^{-1}) 3498, 3062, 3027, 1620, 1488, 1396, 1252, 1206, 1091, 907, 735; ^1H NMR (400 MHz, $CDCl_3$) δ 7.91 (d, *J* = 7.6 Hz, 1H), 7.77 (d, *J* = 8.0 Hz, 1H), 7.71 (d, *J* = 8.0 Hz, 1H), 7.41-7.37 (m, 1H), 7.33-7.17 (m, 10H), 7.04 (d, *J* = 8.8 Hz, 1H), 6.36 (s, 1H), 5.05 (s, 1H); ^{13}C NMR (100.5 MHz, $CDCl_3$) δ 152.6, 141.4, 140.0, 133.3, 132.9, 130.5, 129.9, 129.7, 129.2, 129.1, 128.9, 128.8, 127.4, 126.9, 123.3, 122.7, 119.8, 119.7, 47.9.

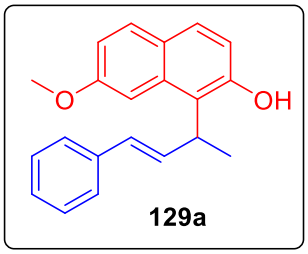

129a

(E)-7-methoxy-1-(4-phenylbut-3-en-2-yl)naphthalen-2-ol (129a).[279] 51.3 mg, 84%; as an oil; **IR** ν (thin film, cm^{-1}) 3447, 3022, 2964, 1625, 1516, 1459, 1258, 1034, 970, 833, 746; ^1H NMR (400 MHz, $CDCl_3$) δ 7.68 (d, *J* = 8.8 MHz, 1H), 7.57 (d, *J* = 8.4 MHz, 1H), 7.39-7.36 (m, 3H), 7.29 (t, *J* = 7.6 MHz, 2H), 7.23-7.20 (m, 1H), 7.01 (dd, *J* = 8.8, 2.4 MHz, 1H), 6.91 (d, *J* = 8.4 MHz, 1H), 6.74-6.73 (m, 2H), 5.80 (s, 1H), 4.56-4.53 (m, 1H), 3.88 (s, 3H), 1.63 (d, *J* = 7.2 MHz, 3H); ^{13}C NMR (100.5 MHz, $CDCl_3$) δ 158.3, 152.7, 136.7, 133.9, 133.8, 130.4, 130.2, 128.6, 128.4, 127.6, 126.3, 125.0, 120.4, 116.6, 114.9, 102.2, 55.2, 33.6, 17.0.

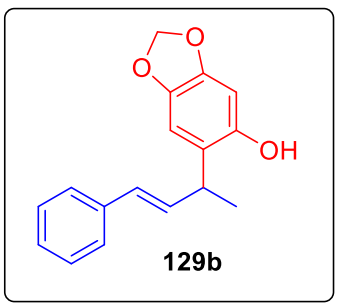

129b

(E)-4-(4-phenylbut-3-en-2-yl)benzo[d][1,3]dioxol-5-ol (129b).[279] 51.6 mg, 96%; as an oil; **IR** ν (thin film, cm^{-1}) 3481, 3022, 2964,1631, 1488, 1292, 1172, 1039, 936, 856, 752; ^1H NMR (400 MHz, $CDCl_3$) δ 7.36 (d, *J* = 1.6 MHz, 1H), 7.35 (s, 1H), 7.33-7.26 (m,

2H), 7.25-7.18 (m, 1H), 6.68 (s, 1H), 6.48 (dd, *J* = 16.0, 1.2 MHz, 1H), 6.41 (s, 1H), 6.35 (dd, *J* = 16.0, 6.4 MHz, 1H), 5.87 (s, 2H), 4.81 (s, 1H), 3.80-3.77 (m, 1H), 1.43 (d, *J* = 7.2 MHz, 3H); ^{13}C NMR (100.5 MHz, $CDCl_3$) δ 148.0, 146.3, 141.7, 136.9, 133.9, 129.3, 128.5, 127.3, 126.2, 122.6, 107.1, 101.0, 98.8, 36.4, 19.6.

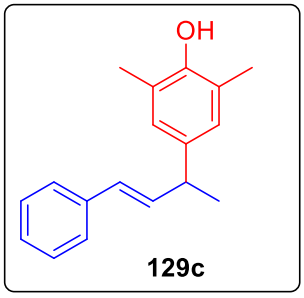

129c

(E)-2,6-dimethyl-4-(4-phenylbut-3-en-2-yl)phenol (129c).[281] 40.9 mg, 81%; as an oil; **IR** ν (thin film, cm^{-1}) 3573, 3022, 2964, 1602, 1488, 1195, 956, 746, 695; ^{1}H NMR (400 MHz, $CDCl_3$) δ 7.36-7.34 (m, 2H), 7.29-7.24 (m, 2H), 7.20-7.16 (m, 1H), 6.86 (s, 2H), 6.41-6.32 (m, 2H), 4.47 (s, 1H), 3.52-3.49 (m, 1H), 2.23 (s, 6H), 1.41 (d, *J* = 7.2 MHz, 3H); ^{13}C NMR (100.5 MHz, $CDCl_3$) δ 150.5, 137.6, 137.2, 135.7, 128.4, 127.9, 127.3, 126.9, 126.1, 122.9, 41.7, 21.3, 15.9.

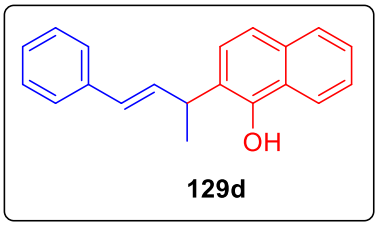

129d

(E)-2-(4-phenylbut-3-en-2-yl)naphthalen-1-ol (129d).[279] 28.6 mg, 60%; as an oil; **IR** ν (thin film, cm^{-1}) 3481, 3056, 2964, 1654, 1575, 1263, 970, 810, 752; ^{1}H NMR (400 MHz, $CDCl_3$) δ 8.15-8.13 (m, 1H), 7.79-7.77 (m, 1H), 7.48-7.42 (m, 3H), 7.37-7.20 (m, 6H), 6.61 (dd, *J* = 16.0, 1.2 MHz, 1H), 6.51 (dd, *J* = 16.0, 5.6 MHz, 1H), 5.67 (s, 1H), 3.98-3.95 (m, 1H), 1.59 (d, *J* = 6.8 MHz, 3H); ^{13}C NMR (100.5 MHz, $CDCl_3$) δ 148.8, 136.6, 133.5, 133.4, 130.0, 128.6, 127.6, 127.5, 126.3, 125.9, 125.8, 125.3, 125.0, 123.2, 121.3, 120.5, 37.7, 19.3.

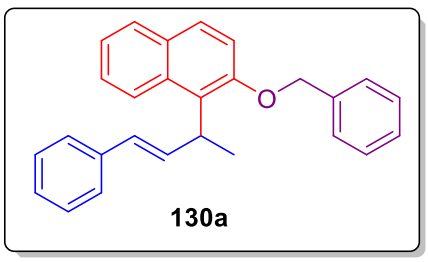

130a

(E)-2-(benzyloxy)-1-(4-phenylbut-3-en-2-yl)naphthalene (130a). 30.6 mg, 84%; as an oil; **IR** ν (thin film, cm^{-1}) 3056, 3027, 2964, 1620, 1597, 1453, 1258, 1022, 804, 746, 695; ^{1}H NMR (400 MHz, $CDCl_3$) δ 8.18 (d, *J* = 8.8 Hz, 1H), 7.78 (d, *J* =

8.0 Hz, 1H), 7.71 (d, *J* = 8.8 Hz, 1H), 7.72-7.21 (m, 12H), 7.16-7.12 (m, 1H), 6.73 (dd, *J* = 16.0, 5.2 Hz, 1H), 6.42 (dd, *J* = 16.0, 2.0 Hz, 1H), 5.20 (d, *J* = 4.0 Hz, 2H), 4.81-4.78 (m, 1H), 1.63 (d, *J* = 7.2 Hz, 3H); ^{13}C NMR (100.5 MHz, $CDCl_3$) δ 153.6, 138.0, 137.3, 135.8, 132.6, 130.0, 128.7, 128.5, 128.4, 128.3, 128.0, 127.9, 127.6, 127.5, 126.6, 126.0, 125.9, 124.3, 123.3, 115.6, 71.8, 33.8, 19.1; HRMS(ESI): m/z calculated for $C_{27}H_{24}O$ ([M+Na]+): 387.1725; found 387.1759.

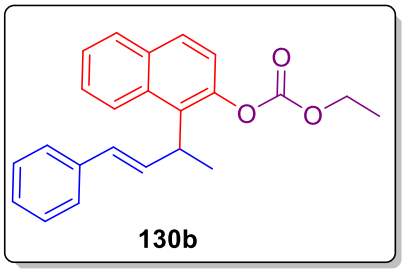

130b

(E)-ethyl (1-(4-phenylbut-3-en-2-yl)naphthalen-2-yl) carbonate (130b). 33.0 mg, 92%; as an oil; **IR** ν (thin film, cm^{-1}) 3055, 3024, 2978, 2931, 2873, 2137, 1759, 1242, 1215; ^{1}H NMR (400 MHz, $CDCl_3$) δ 8.22 (d, *J* = 8.4 Hz, 1H), 7.76 (d, *J* = 8.8 Hz, 1H), 7.77 (d, *J* = 9.2 Hz, 1H), 7.52-7.44 (m, 2H), 7.37-7.33 (m, 2H), 7.28-7.23 (m, 3H), 7.18-7.14 (m, 1H), 6.63 (dd, *J* = 16.0, 4.4 Hz, 1H), 6.51 (dd, *J* = 16.0, 1.6 Hz, 1H), 4.58-4.54 (m, 1H), 4.16-4.10 (m, 1H), 3.97-3.92 (m, 1H), 1.67 (d, *J* = 7.6 Hz, 3H), 1.21 (t, *J* = 6.8 Hz, 3H); ^{13}C NMR (100.5 MHz, $CDCl_3$) δ 153.8, 146.6, 137.5, 133.6, 132.5, 132.1, 131.6, 128.9, 128.5, 128.4, 128.3, 126.9, 126.3, 126.0, 125.3, 124.5, 121.9, 64.8, 34.0, 18.5, 14.0; HRMS(ESI): m/z calculated for $C_{23}H_{22}O_3$ ([M+Na]+): 369.1461; found 369.1411.

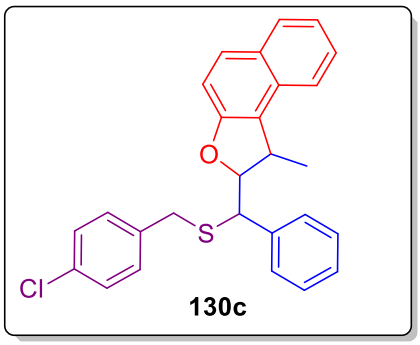

130c

2-(((4-chlorobenzyl)thio)(phenyl)methyl)-1-methyl-1,2-dihydronaphtho[2,1-b]furan (130c). 28.2 mg, 65%; as a white solid; mp 142-144°C; **IR** ν (thin film, cm^{-1}) 3062, 2968, 1623, 1600, 1489, 1400, 1229, 1088, 1014, 814, 741; ^{1}H NMR (400 MHz, $CDCl_3$) δ 7.81 (d, *J* = 8.4 Hz, 1H), 7.76 (d, *J* = 8.0 Hz, 1H), 7.62 (d, *J* = 9.2 Hz, 1H), 7.58-7.56 (m, 2H), 7.50-7.42 (m, 4H), 7.35-7.31 (m, 1H), 7.15 (d, *J* = 8.4 Hz, 2H), 7.08 (d, *J* = 8.8 Hz, 1H), 6.95 (d, *J* = 8.4 Hz, 2H), 5.27 (d, *J* = 11.2 Hz, 1H), 3.68 (q, *J* =

4.4 Hz, 1H), 3.11 (dd, *J* = 10.8, 4.8 Hz, 1H), 2.85 (d, *J* = 13.2 Hz, 1H), 2.67 (d, *J* = 13.2 Hz, 1H), 1.50 (d, *J* = 7.2 Hz, 3H); ^{13}C NMR (100.5 MHz, $CDCl_3$) δ 150.6, 139.7, 136.0, 132.8, 131.5, 130.1, 129.2, 128.8, 128.7, 128.5, 128.4, 128.3, 128.2, 126.6, 123.2, 121.7, 118.7, 118.6, 77.8, 48.3, 35.4, 32.2, 17.5; HRMS(ESI): m/z calculated for $C_{27}H_{23}ClOS$ ([M+H]+): 453.1056; found 453.1056.

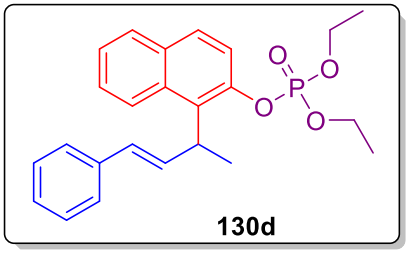

(E)-diethyl (1-(4-phenylbut-3-en-2-yl)naphthalen-2-yl) phosphate (130d). 29.1 mg, 71%; as an oil; **IR** ν (thin film, cm^{-1}) 3024, 2981, 1597, 1495, 1276, 1216, 1031, 976, 815, 749; ^{1}H NMR (400 MHz, $CDCl_3$) δ 8.23 (d, *J* = 8.0 Hz, 1H), 7.83 (d, *J* = 7.6 Hz, 1H), 7.74 (d, *J* = 8.8 Hz, 1H), 7.62 (d, *J* = 8.8 Hz, 1H), 7.46-7.39 (m, 2H), 7.34 (d, *J* = 6.8 Hz, 2H), 7.28-7.24 (m, 2H), 7.19-7.15 (m, 1H), 6.72 (dd, *J* = 16.0, 4.8 Hz, 1H), 6.50 (dd, *J* = 16.4, 2.0 Hz, 1H), 4.75-4.72 (m, 1H), 4.27-4.17 (m, 4H), 1.71 (d, *J* = 6.8 Hz, 3H), 1.35-1.30 (m, 6H); ^{13}C NMR (100.5 MHz, $CDCl_3$) δ 146.0, 137.6, 134.7, 132.3, 131.9, 130.0 (d, *J* = 7.4 Hz), 128.8, 128.7, 128.5, 128.4, 126.9, 126.1, 126.0, 125.2, 124.8, 119.8 (d, *J* = 1.5 Hz), 64.6 (d, *J* = 6.0 Hz), 33.8, 19.0, 16.2 (d, *J* = 3.7 Hz), 16.1 (d, *J* = 3.0 Hz); ^{31}P NMR (162 MHz, $CDCl_3$) δ -5.68; HRMS(ESI): m/z calculated for $C_{24}H_{27}O_4P$ ([M+H]+): 411.1725; found 411.1725.

Appendix

^{1}H NMR (400 MHz) in $CDCl_3$

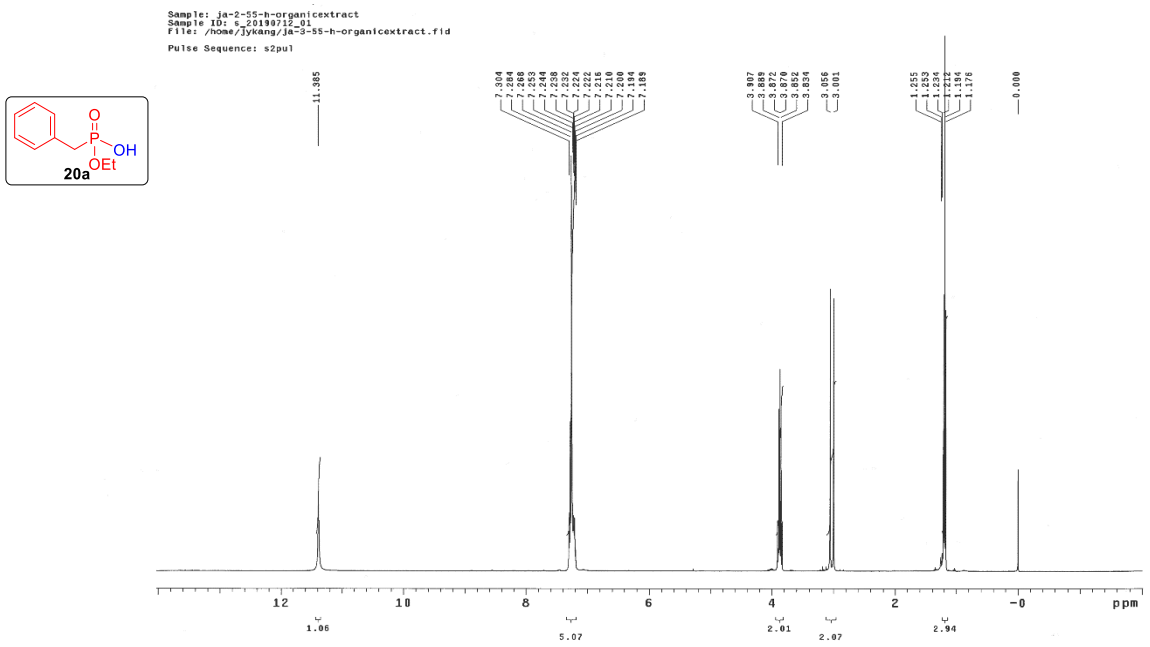

^{13}C NMR (100.5 MHz) in $CDCl_3$

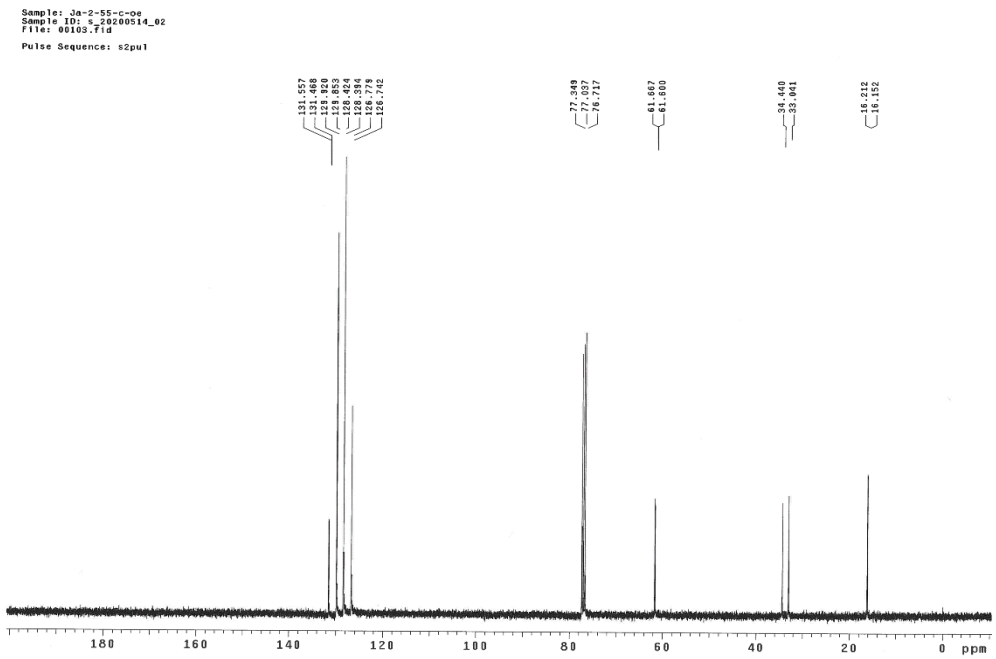

^{31}P NMR (162 MHz) in $CDCl_3$

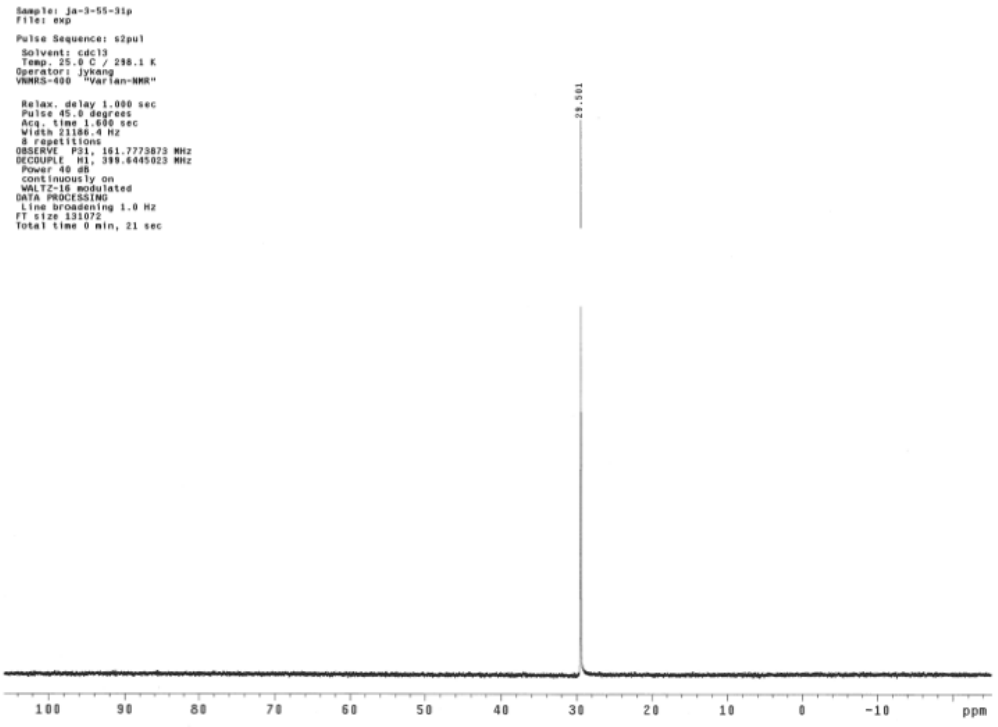

^{1}H NMR (400 MHz) in $CDCl_3$

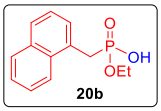

20b

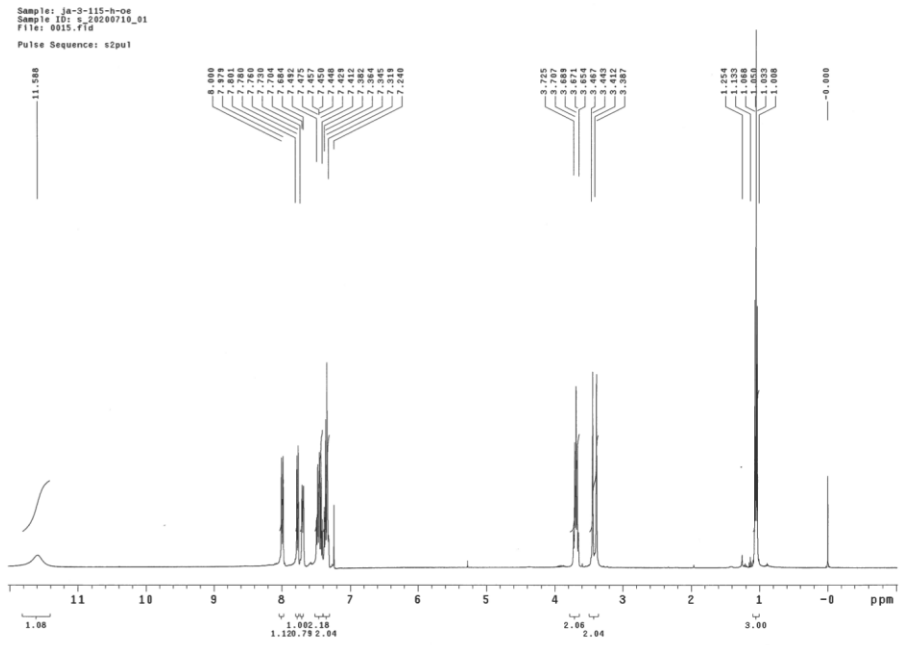

^{13}C NMR (100.5 MHz) in $CDCl_3$

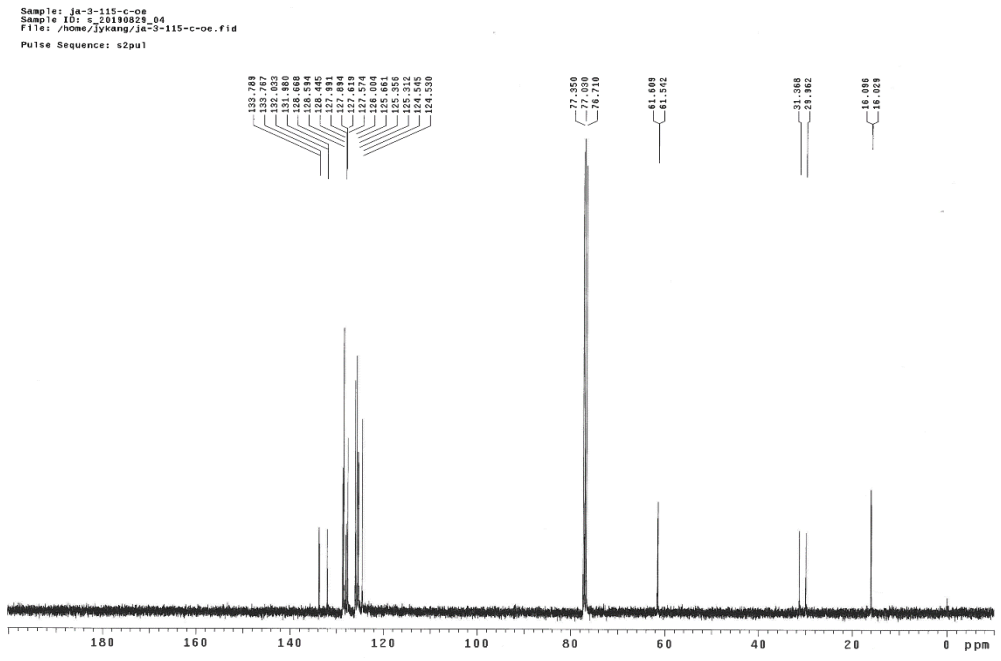

^{31}P NMR (162 MHz) in $CDCl_3$

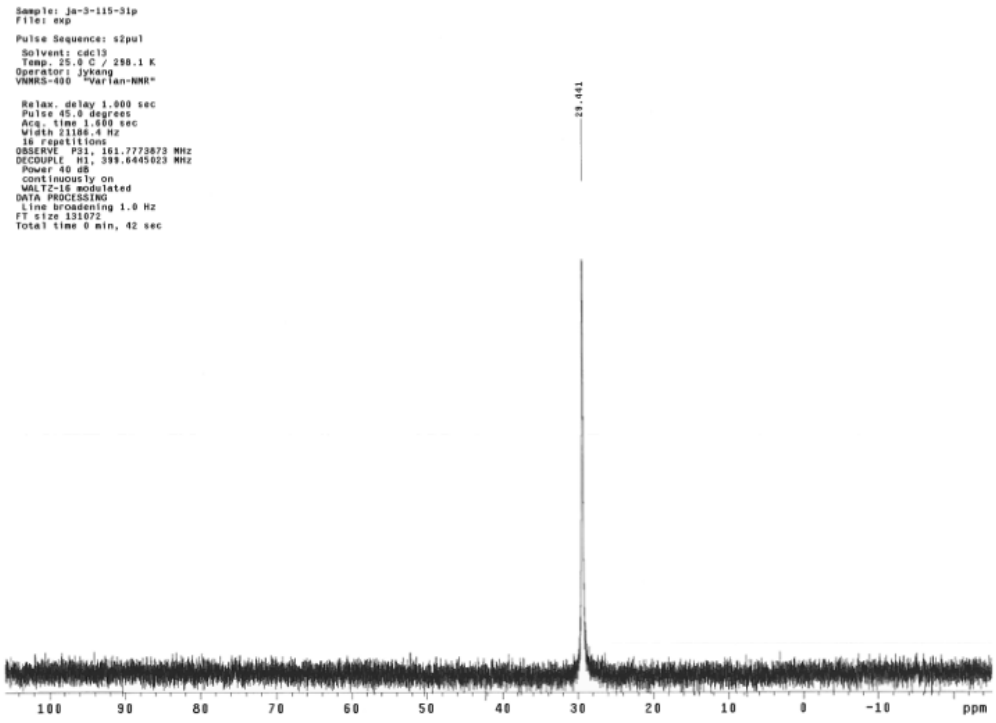

^{1}H NMR (400 MHz) in $CDCl_3$

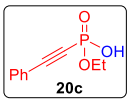

20c

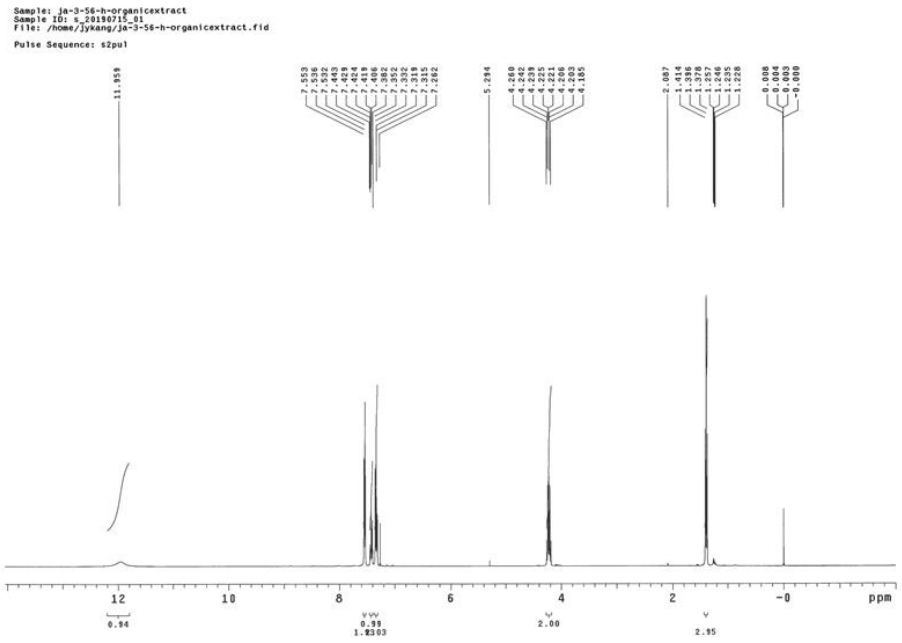

^{13}C NMR (100.5 MHz) in $CDCl_3$

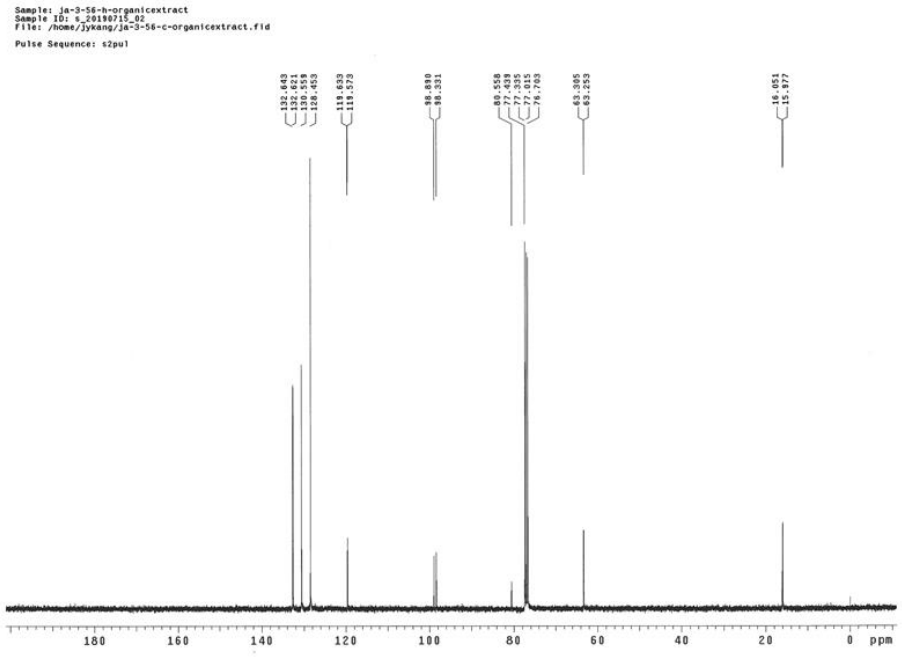

^{31}P NMR (162 MHz) in $CDCl_3$

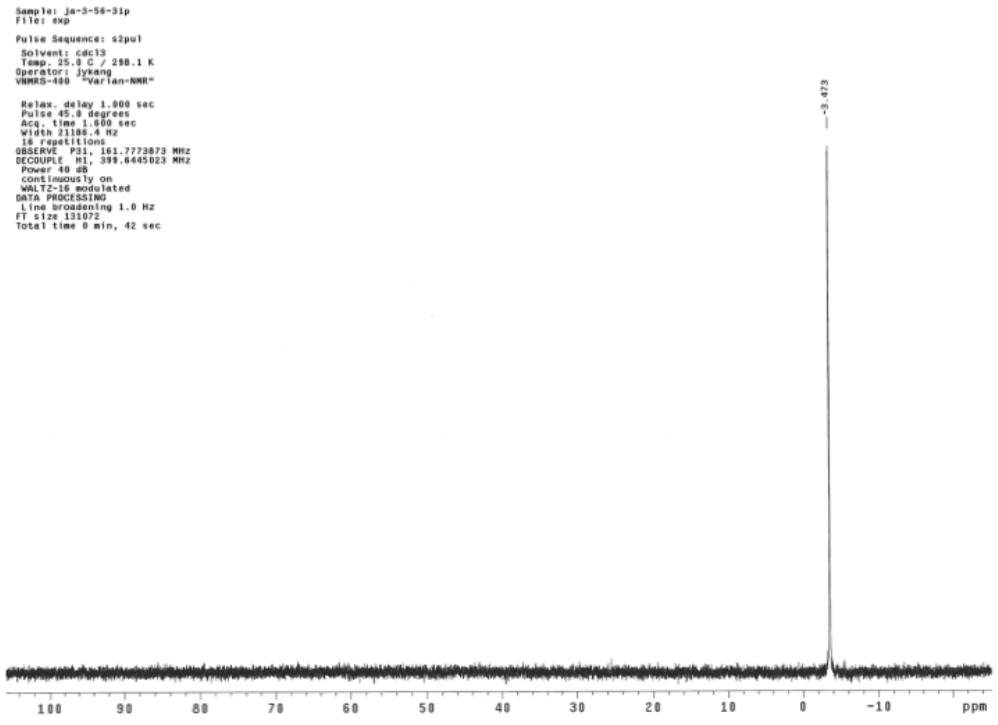

^{1}H NMR (400 MHz) in $CDCl_3$

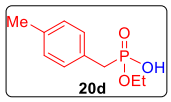

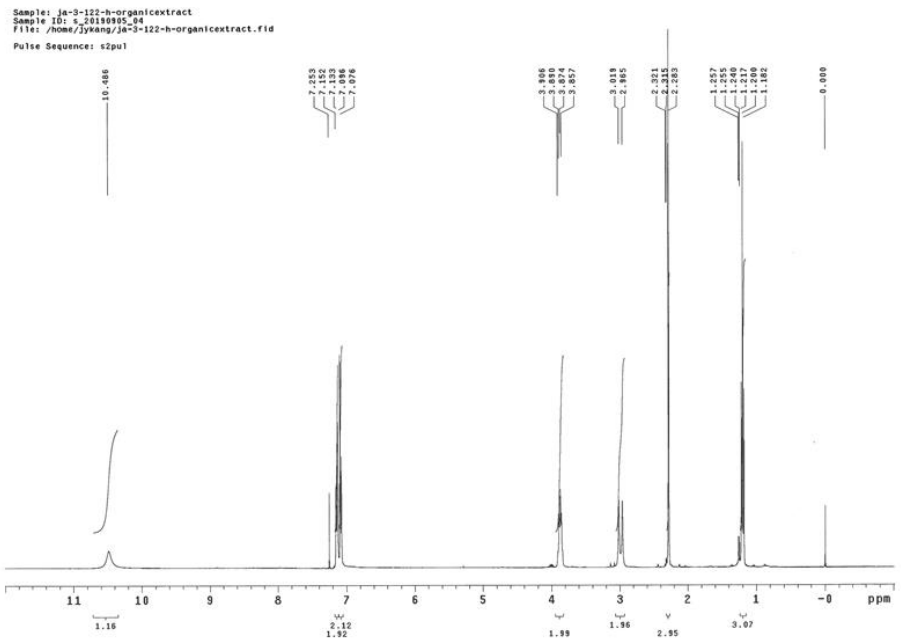

^{13}C NMR (100.5 MHz) in $CDCl_3$

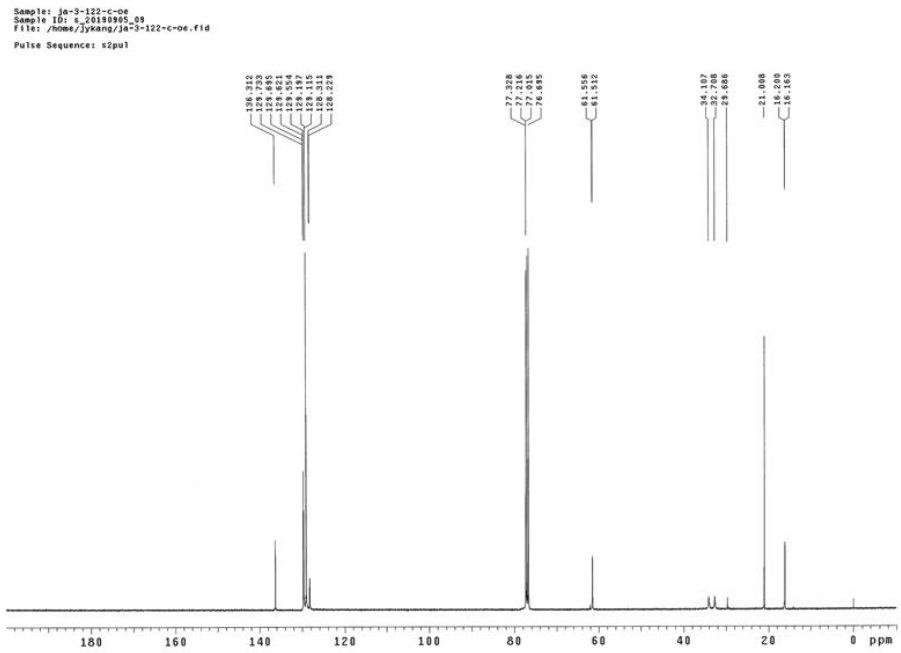

^{31}P NMR (162 MHz) in $CDCl_3$

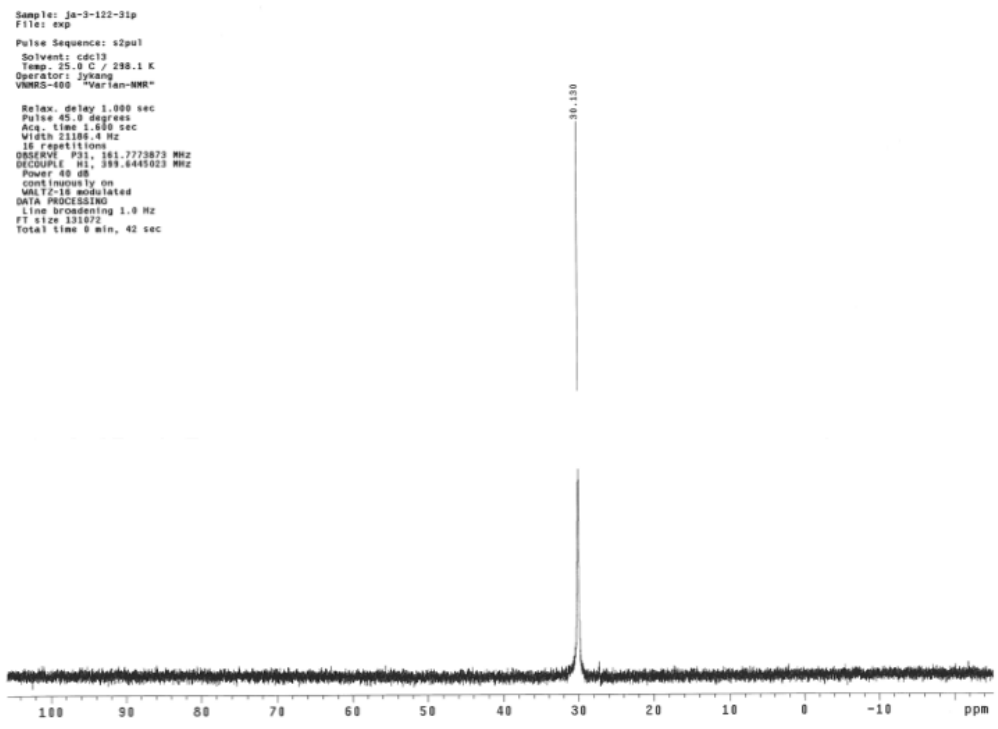

^{1}H NMR (400 MHz) in $CDCl_3$

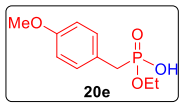

20e

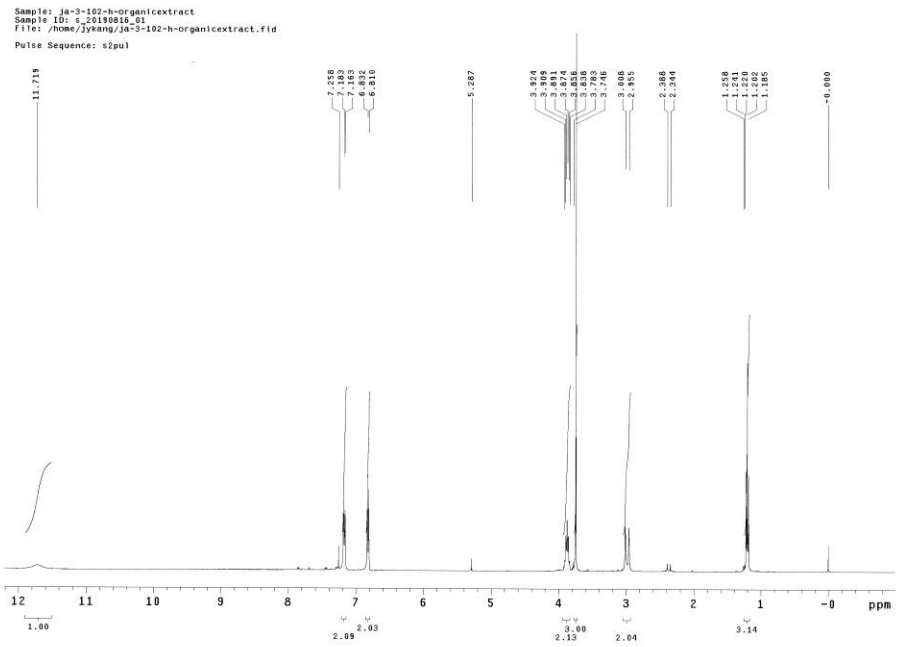

^{13}C NMR (100.5 MHz) in $CDCl_3$

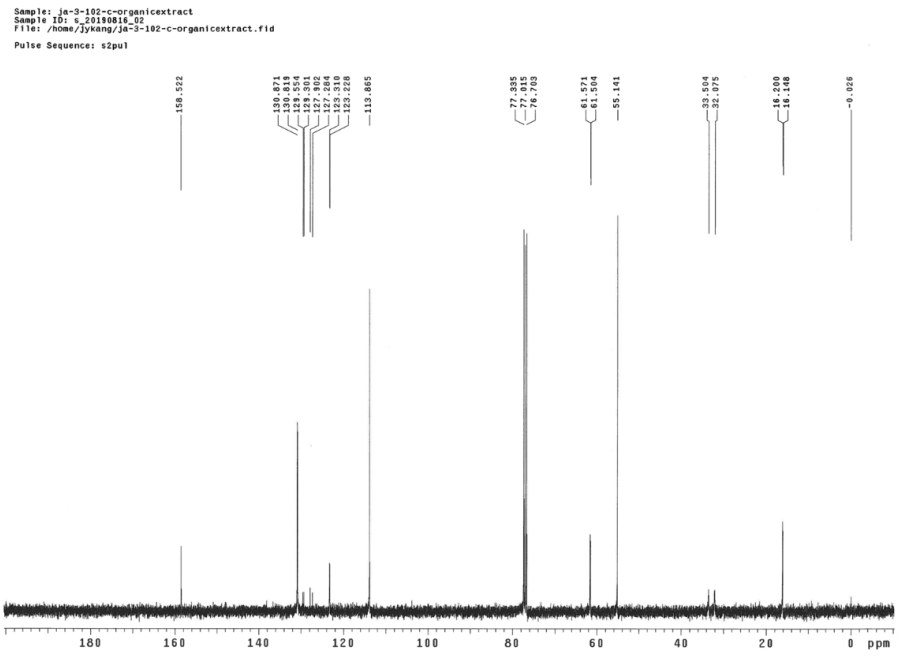

^{31}P NMR (162 MHz) in $CDCl_3$

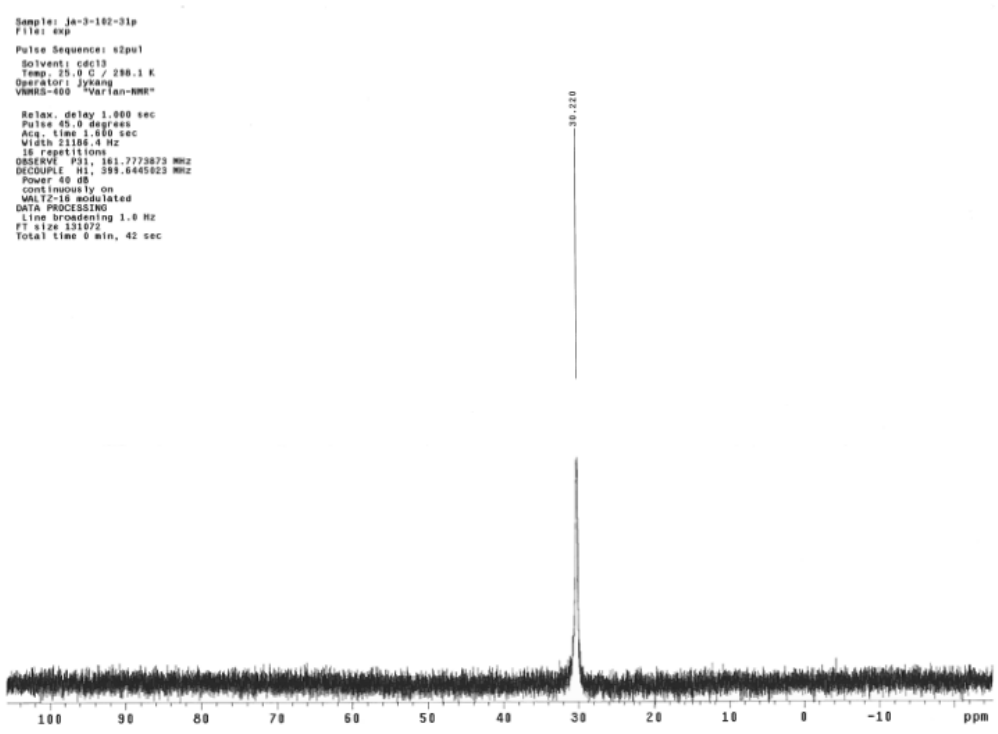

^{1}H NMR (400 MHz) in $CDCl_3$

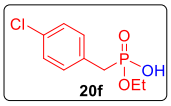

20f

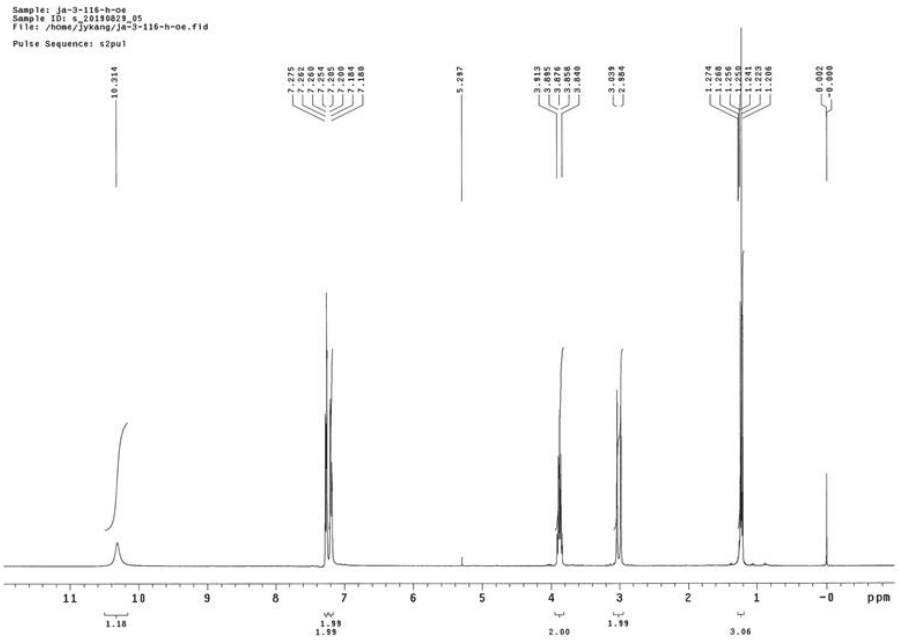

---

^{13}C NMR (100.5 MHz) in $CDCl_3$

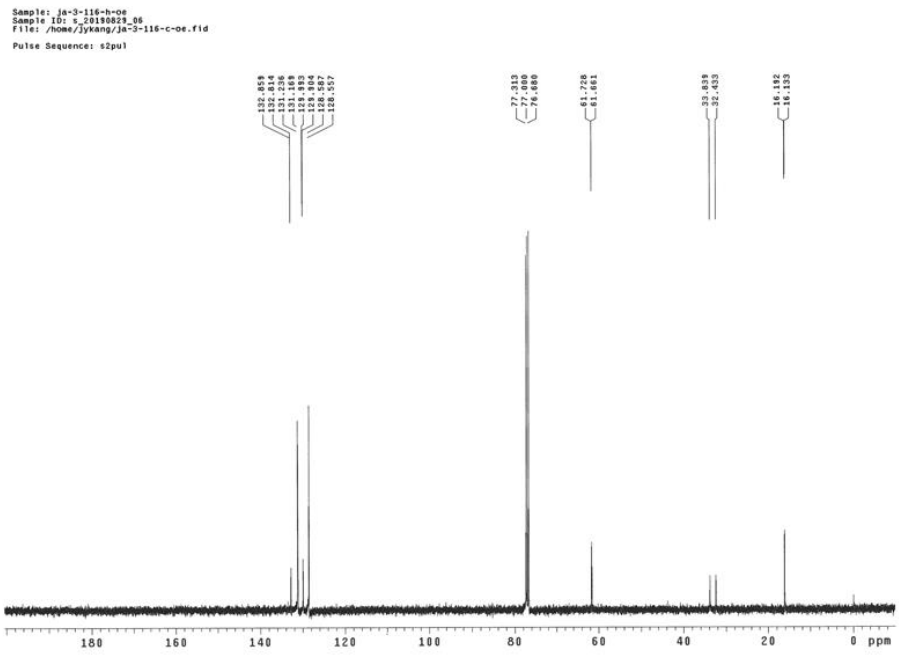

---

^{31}P NMR (162 MHz) in $CDCl_3$

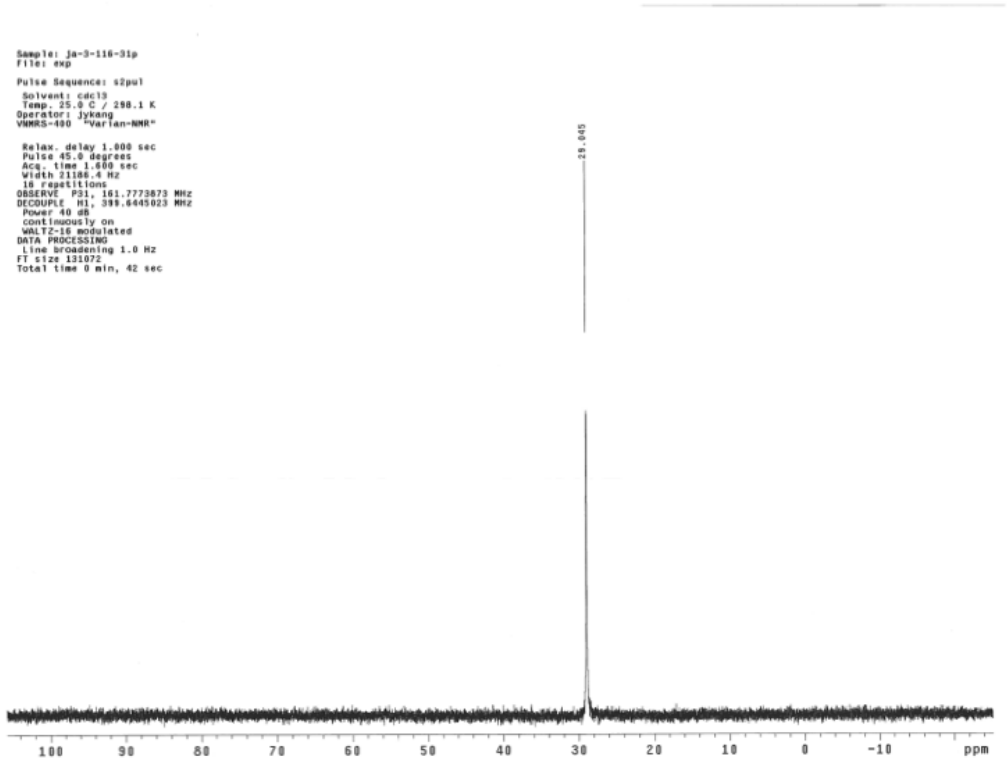

^{1}H NMR (400 MHz) in $CDCl_3$

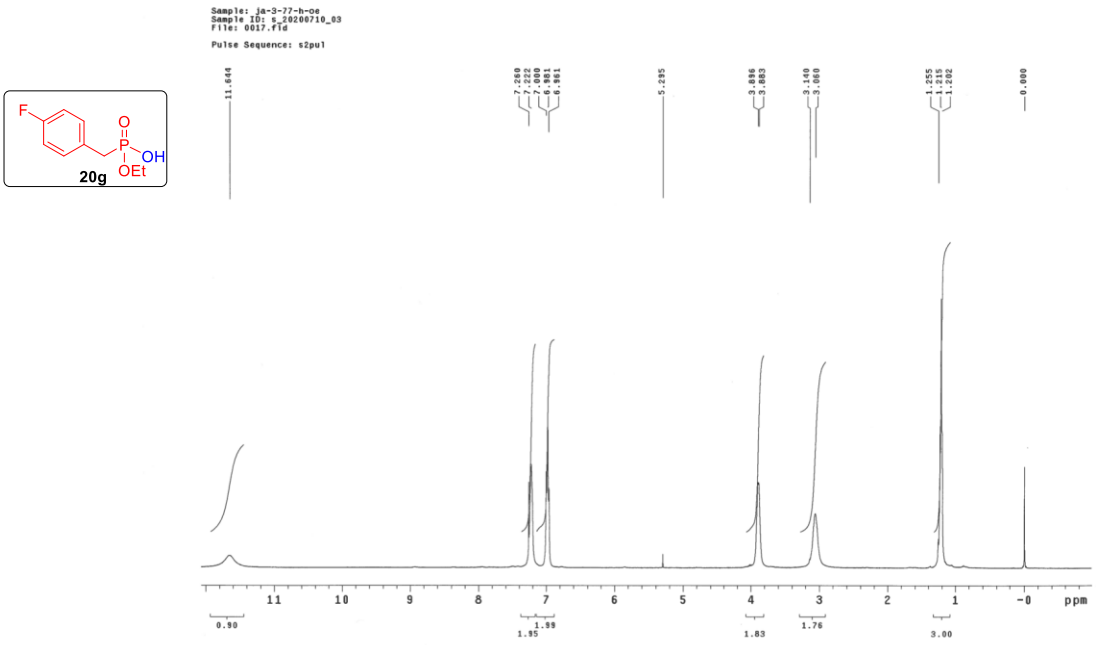

^{13}C NMR (100.5 MHz) in CD_3OD

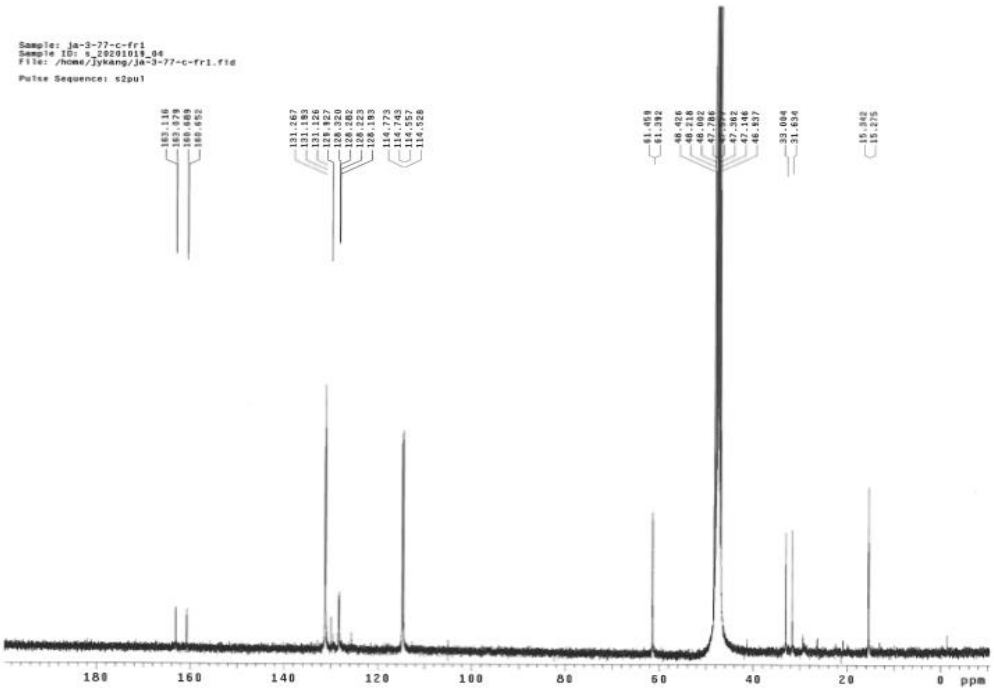

^{31}P NMR (162 MHz) in CD_3OD

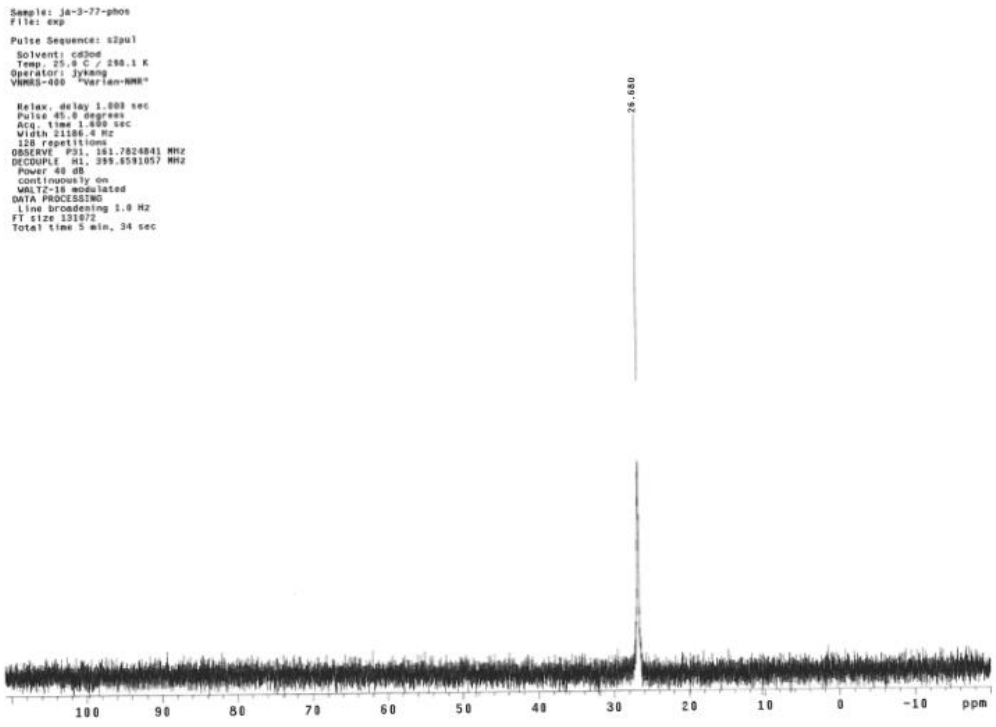

^{1}H NMR (400 MHz) in $CDCl_3$

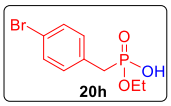

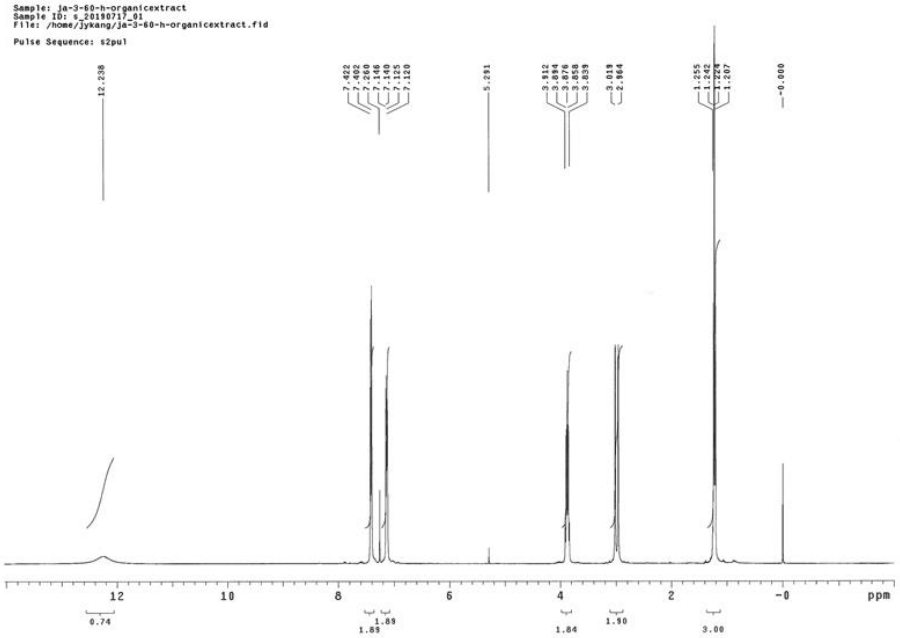

^{13}C NMR (100.5 MHz) in $CDCl_3$

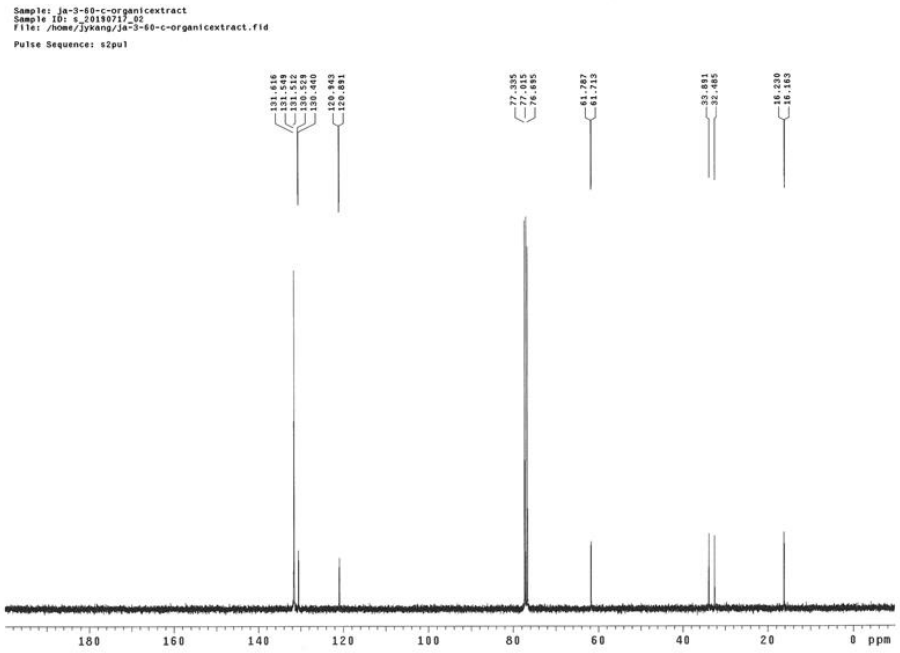

^{31}P NMR (162 MHz) in $CDCl_3$

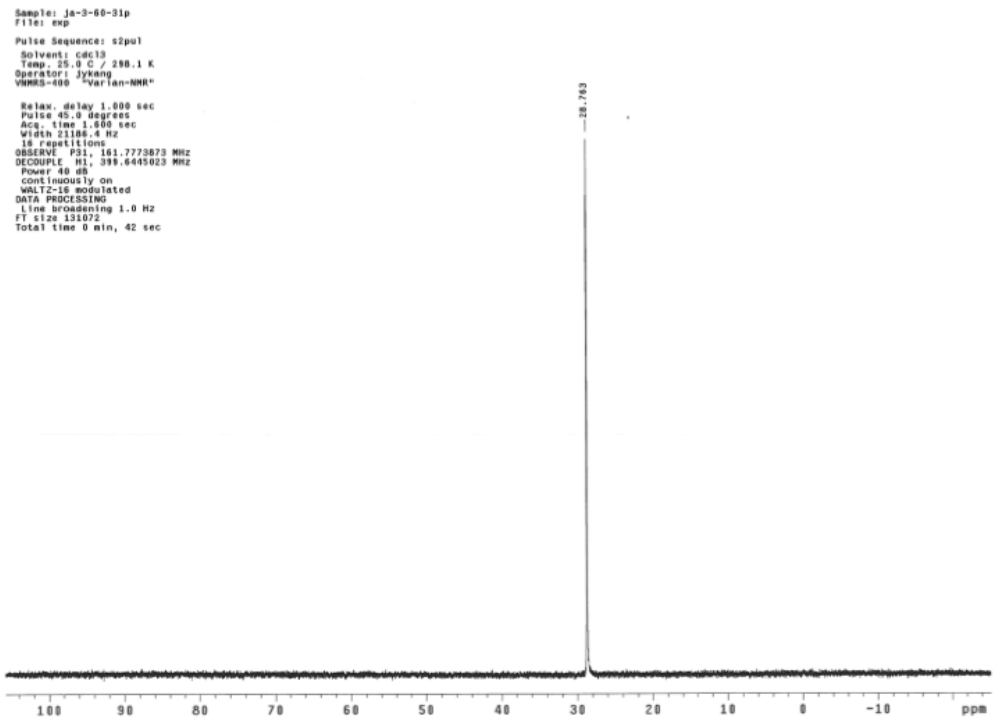

^{1}H NMR (400 MHz) in $CDCl_3$

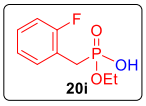

20i

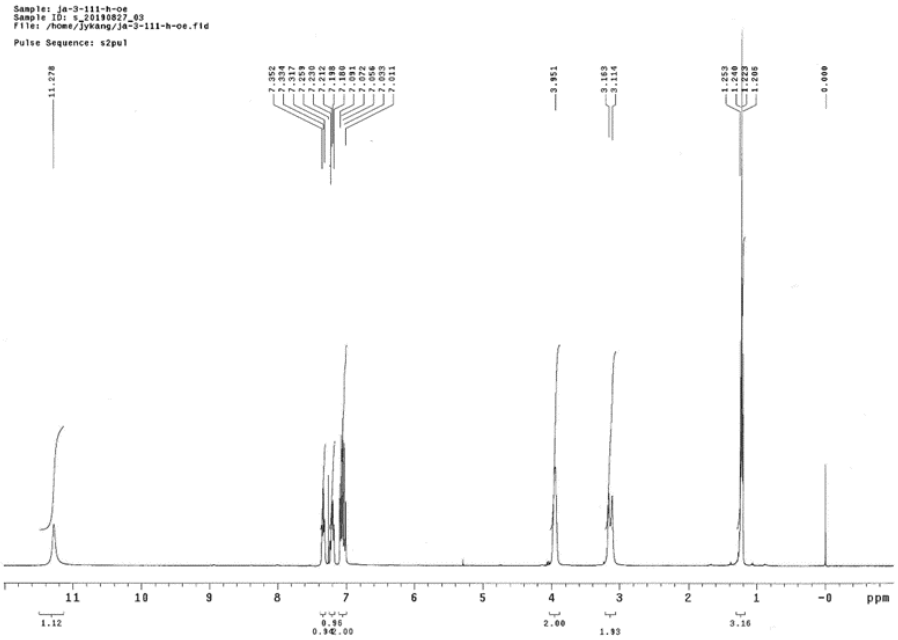

^{13}C NMR (100.5 MHz) in $CDCl_3$

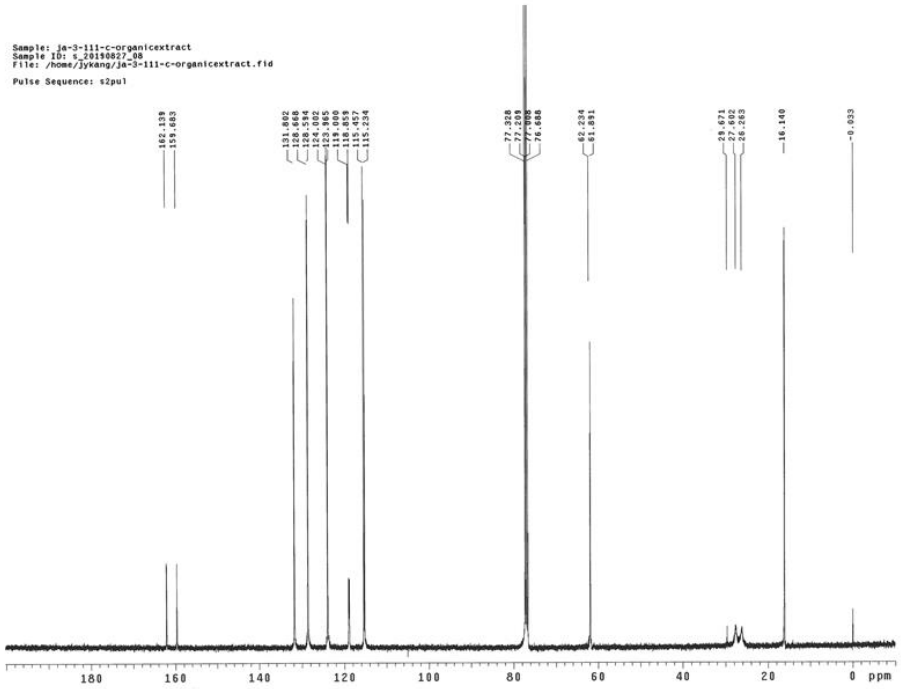

^{31}P NMR (162 MHz) in $CDCl_3$

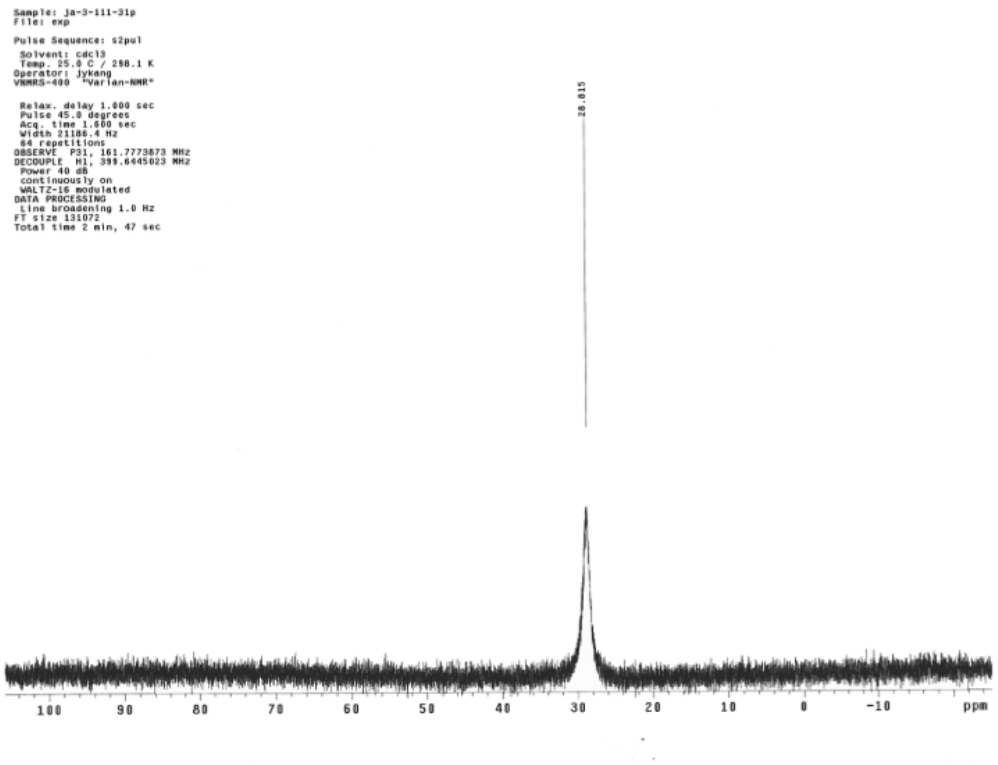

^{1}H NMR (400 MHz) in $CDCl_3$

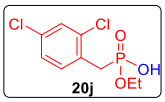

20j

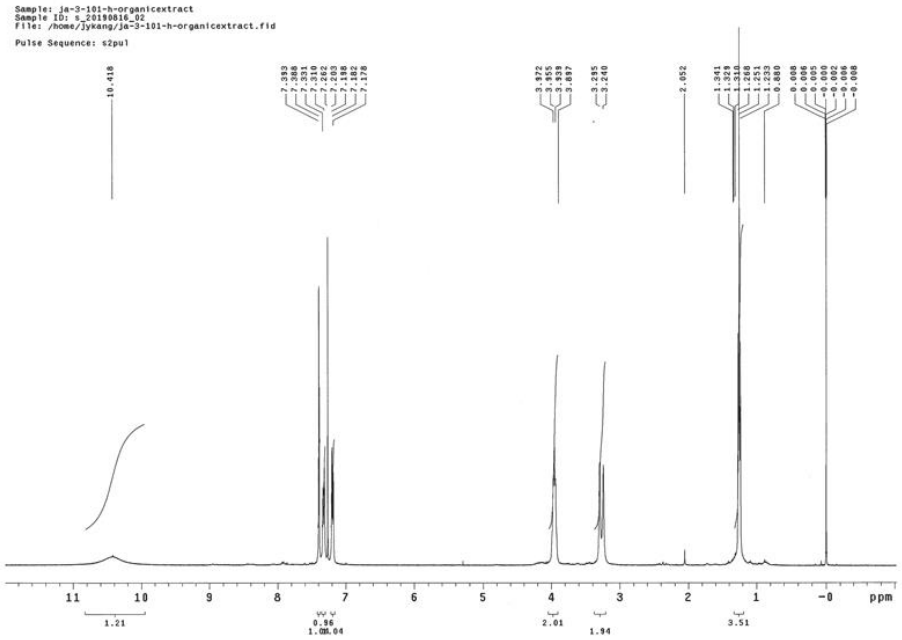

^{13}C NMR (100.5 MHz) in $CDCl_3$

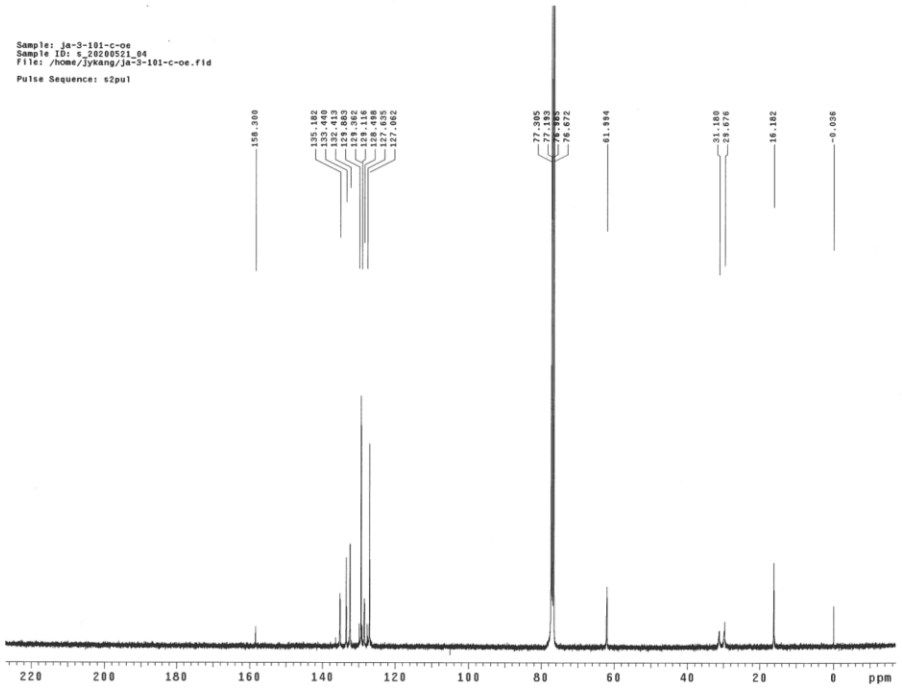

^{31}P NMR (162 MHz) in $CDCl_3$

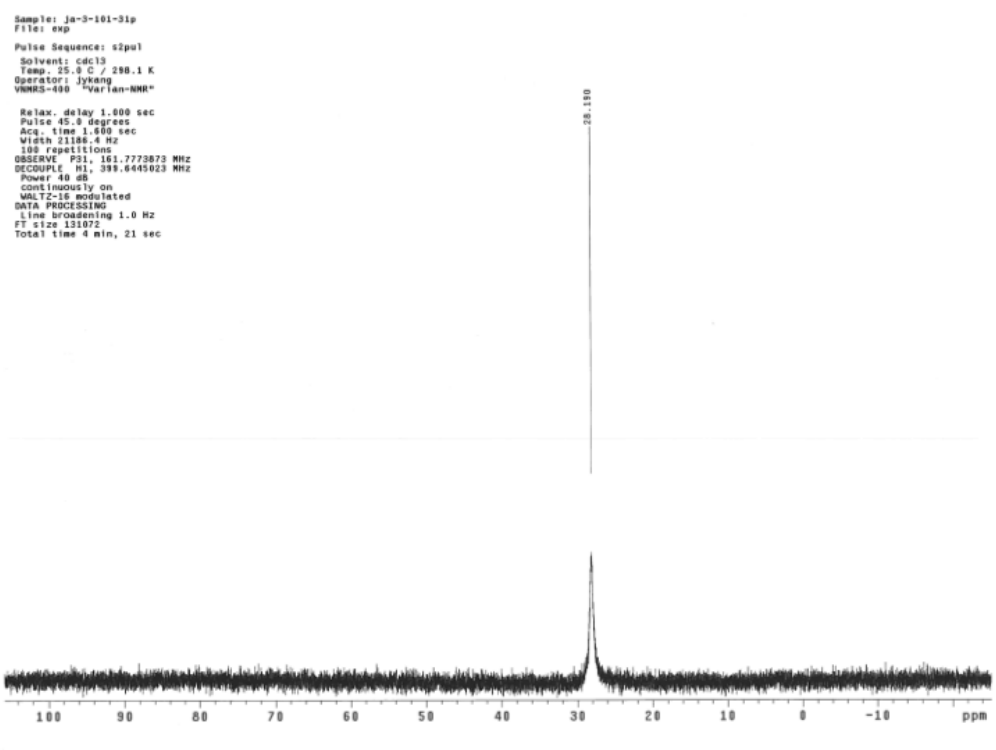

^{1}H NMR (400 MHz) in $CDCl_3$

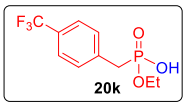

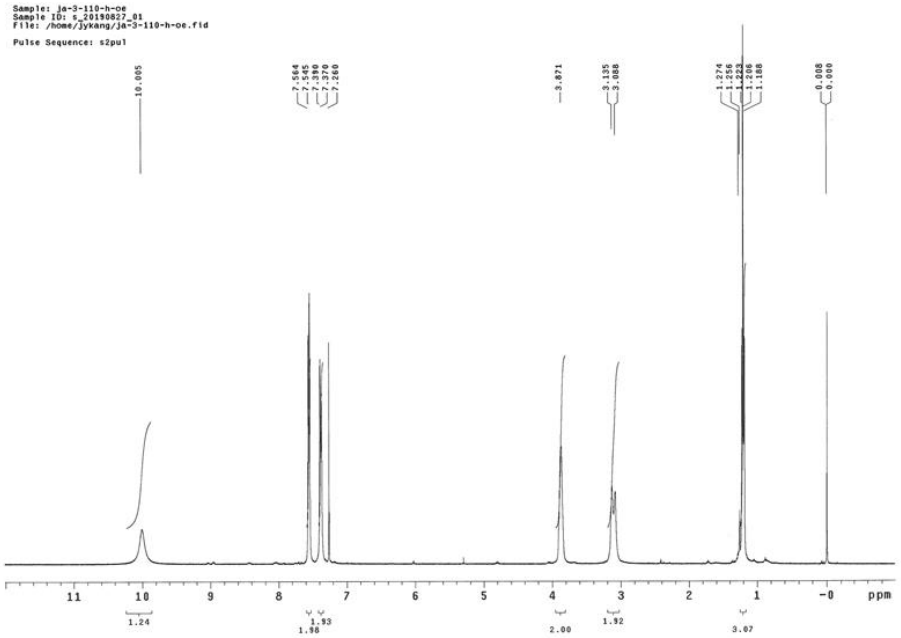

^{13}C NMR (100.5 MHz) in $CDCl_3$

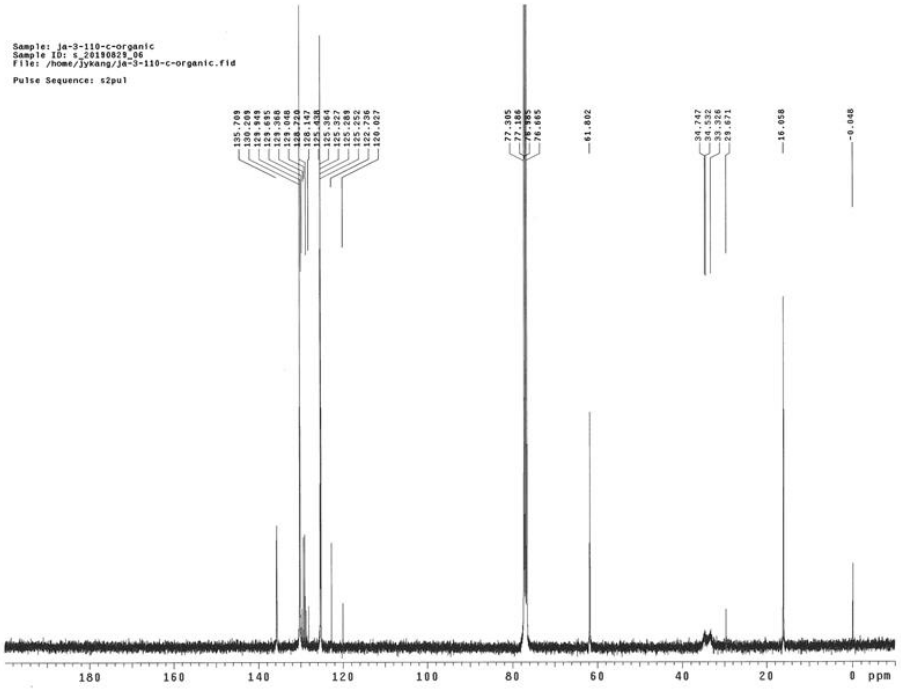

^{31}P NMR (162 MHz) in $CDCl_3$

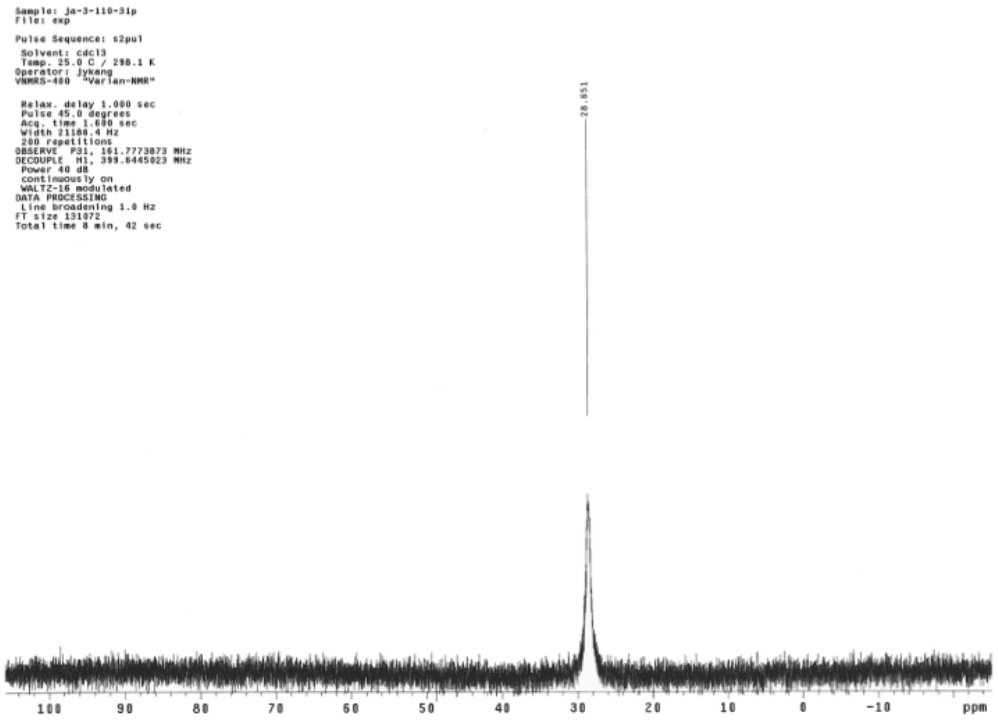

^{1}H NMR (400 MHz) in $CDCl_3$

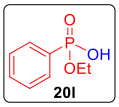

20l

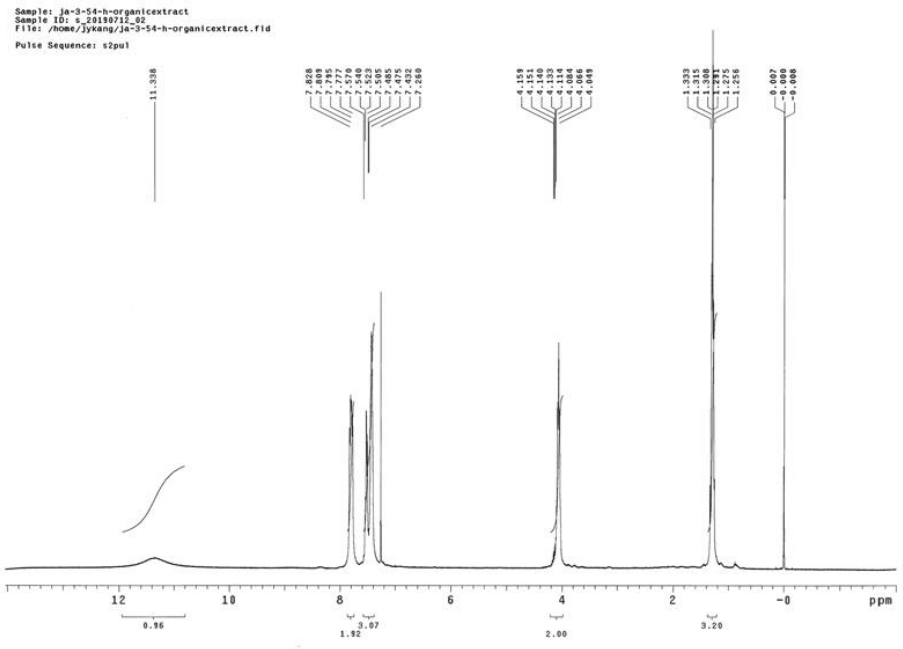

^{13}C NMR (100.5 MHz) in $CDCl_3$

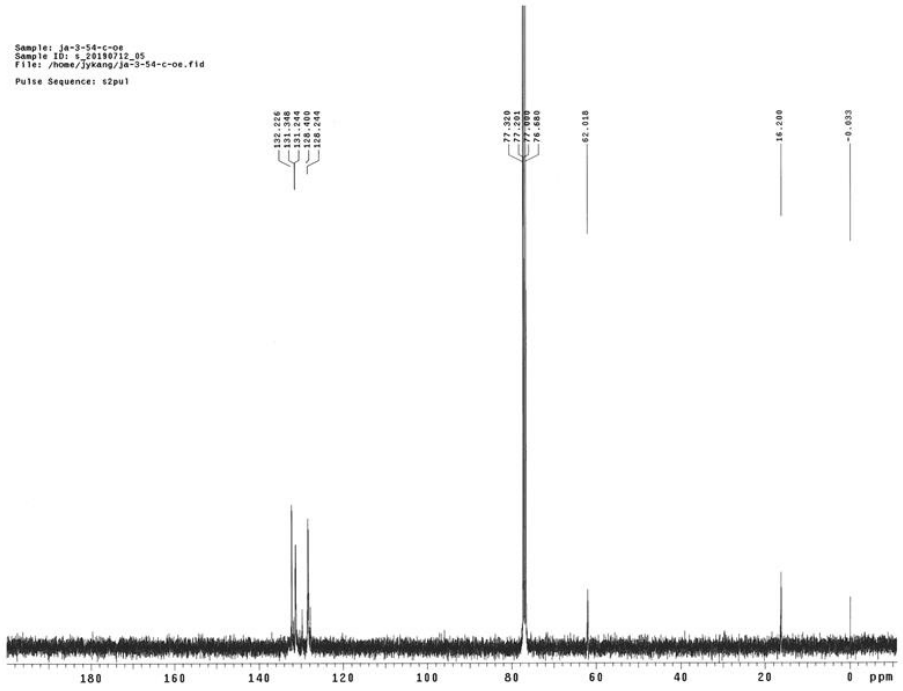

^{31}P NMR (162 MHz) in $CDCl_3$

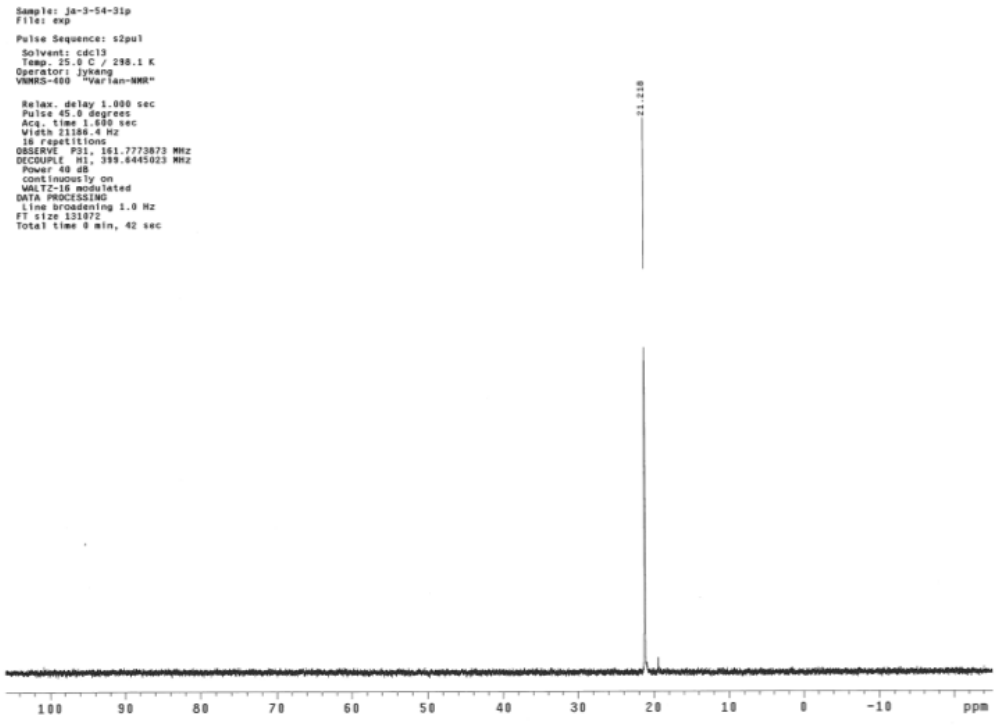

^{1}H NMR (400 MHz) in $CDCl_3$

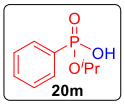

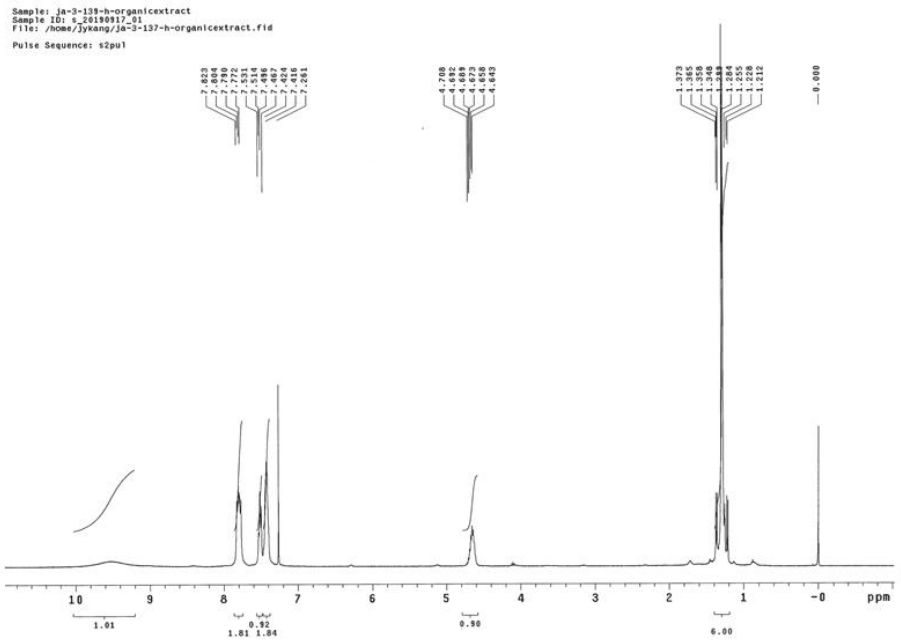

^{13}C NMR (100.5 MHz) in $CDCl_3$

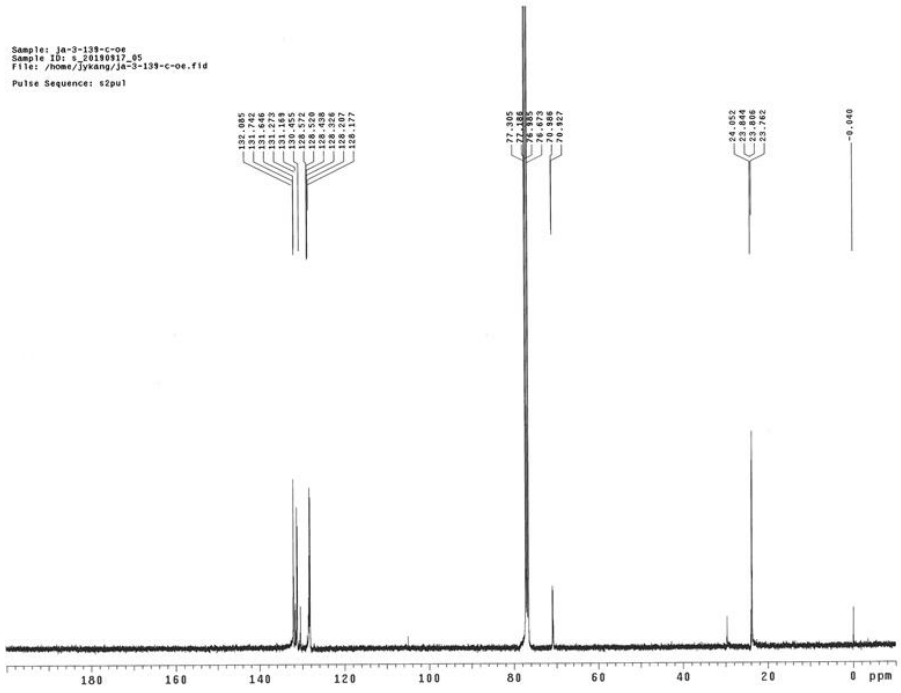

^{31}P NMR (162 MHz) in $CDCl_3$

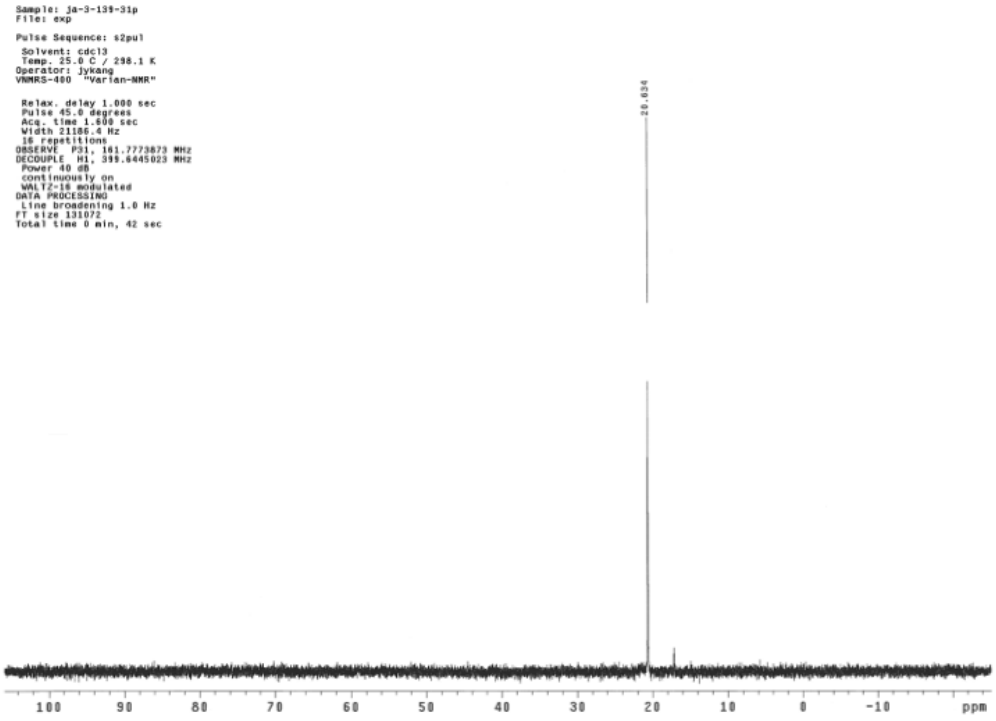

^{1}H NMR (400 MHz) in $CDCl_3$

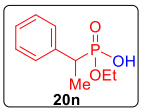

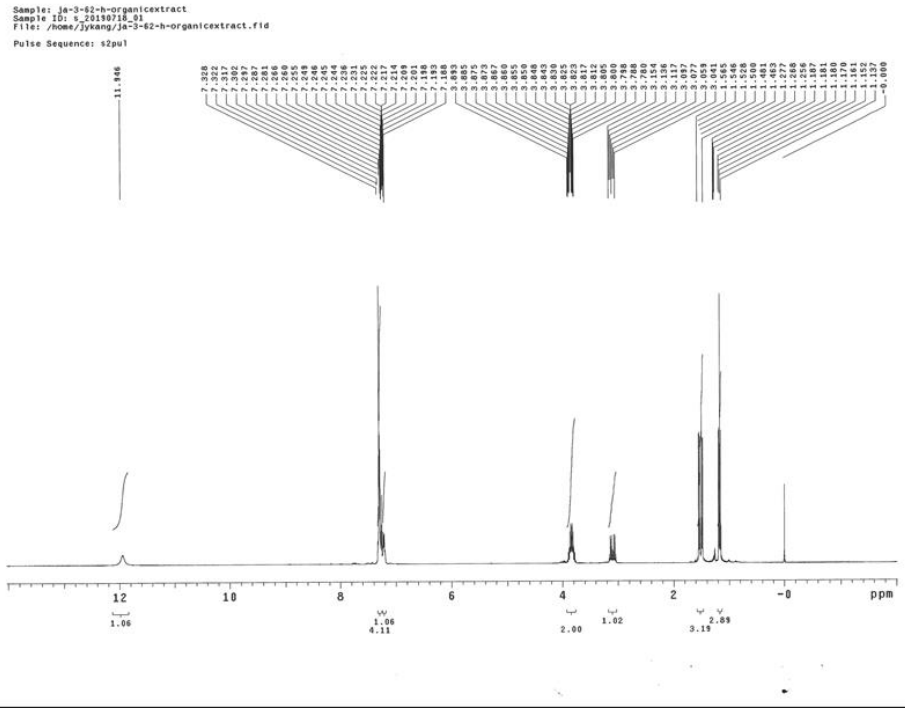

^{13}C NMR (100.5 MHz) in $CDCl_3$

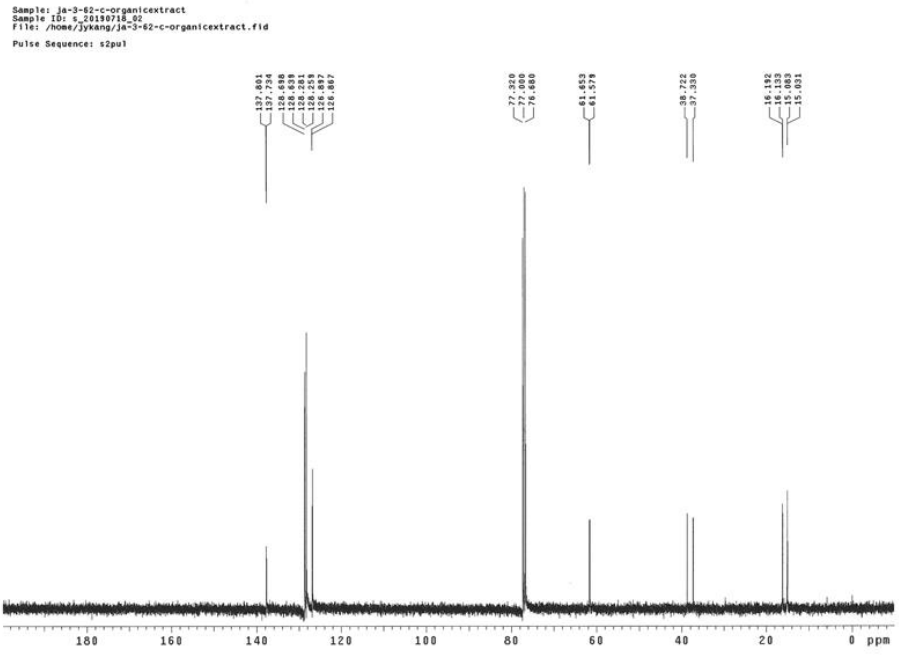

^{31}P NMR (162 MHz) in $CDCl_3$

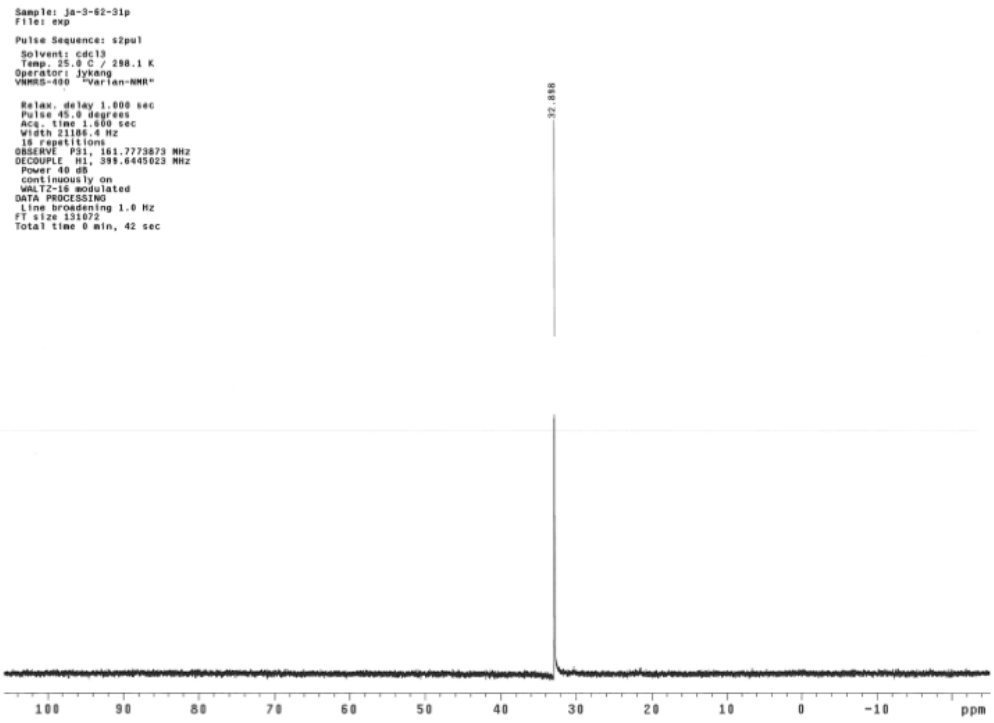

^{1}H NMR (400 MHz) in $CDCl_3$

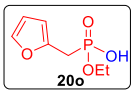

20o

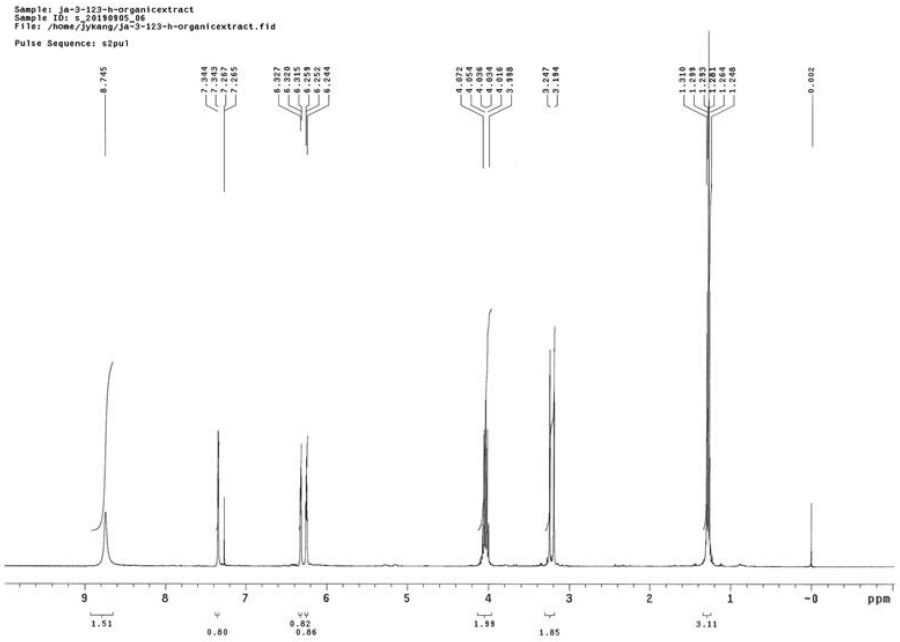

^{13}C NMR (100.5 MHz) in $CDCl_3$

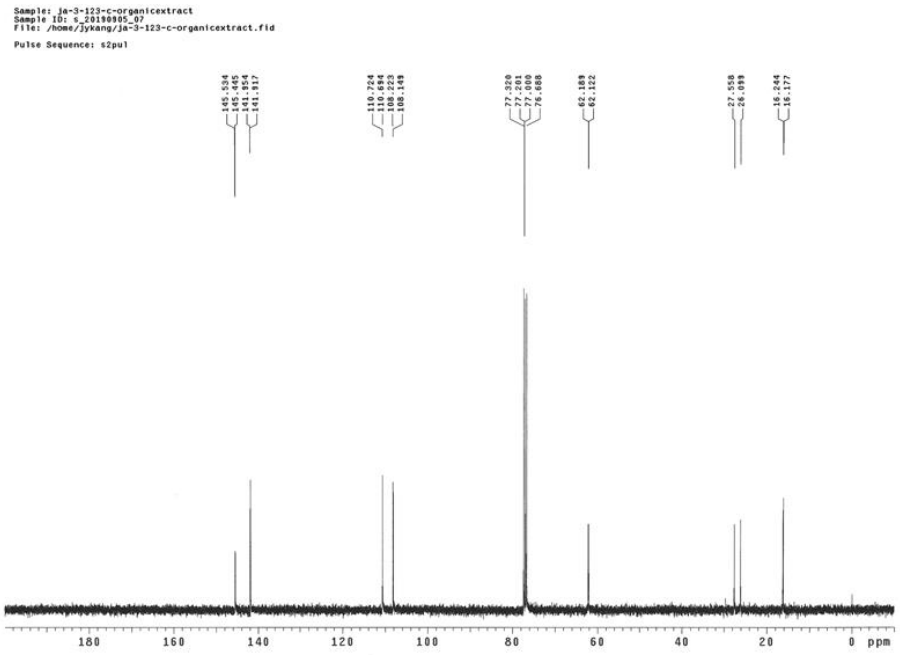

^{31}P NMR (162 MHz) in $CDCl_3$

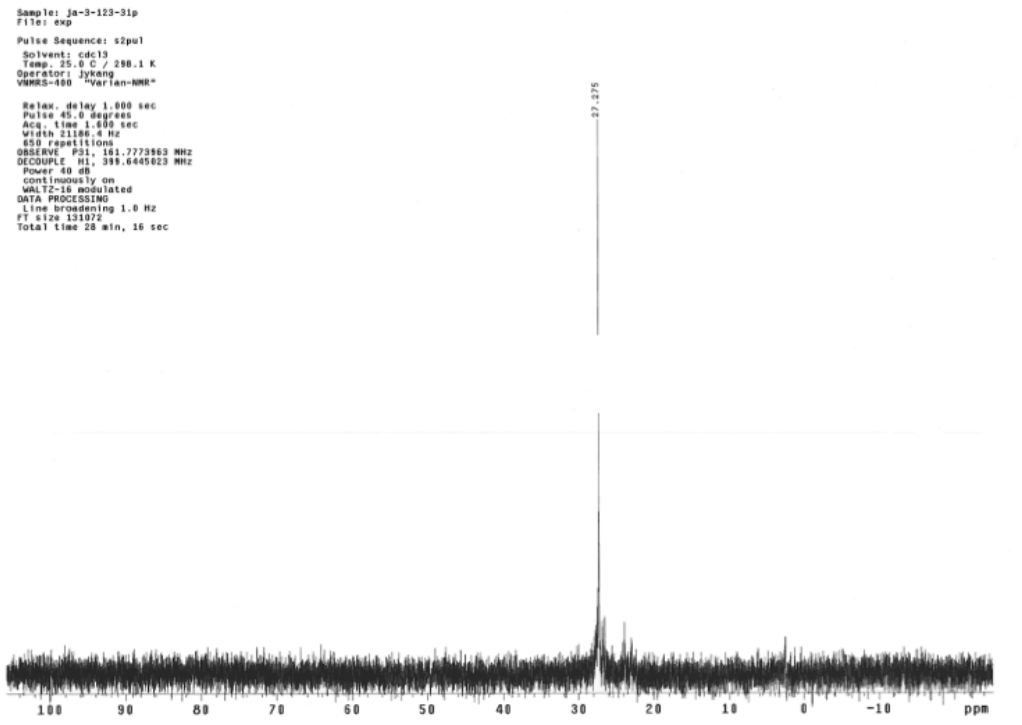

^{1}H NMR (400 MHz) in $CDCl_3$

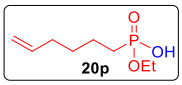

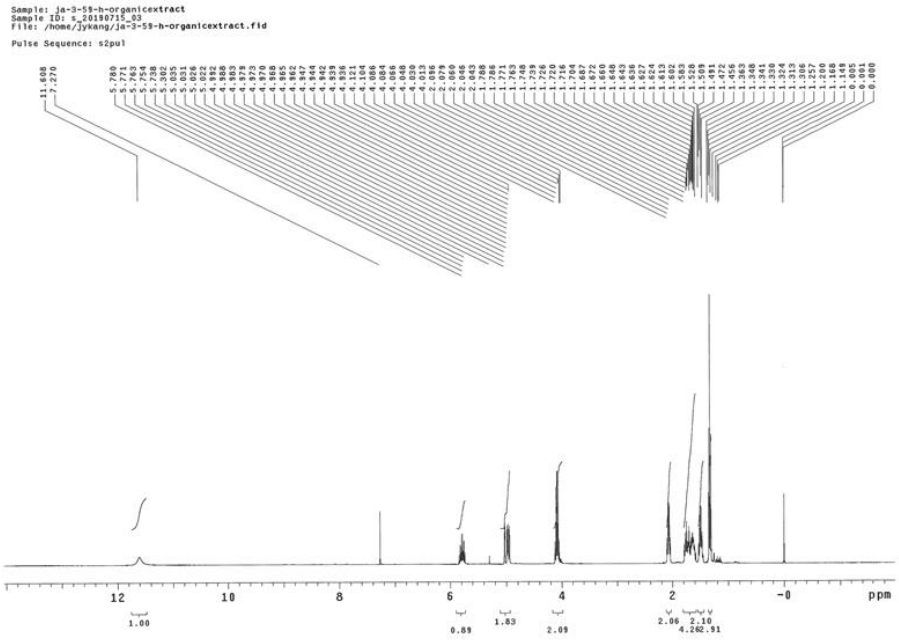

---

^{13}C NMR (100.5 MHz) in $CDCl_3$

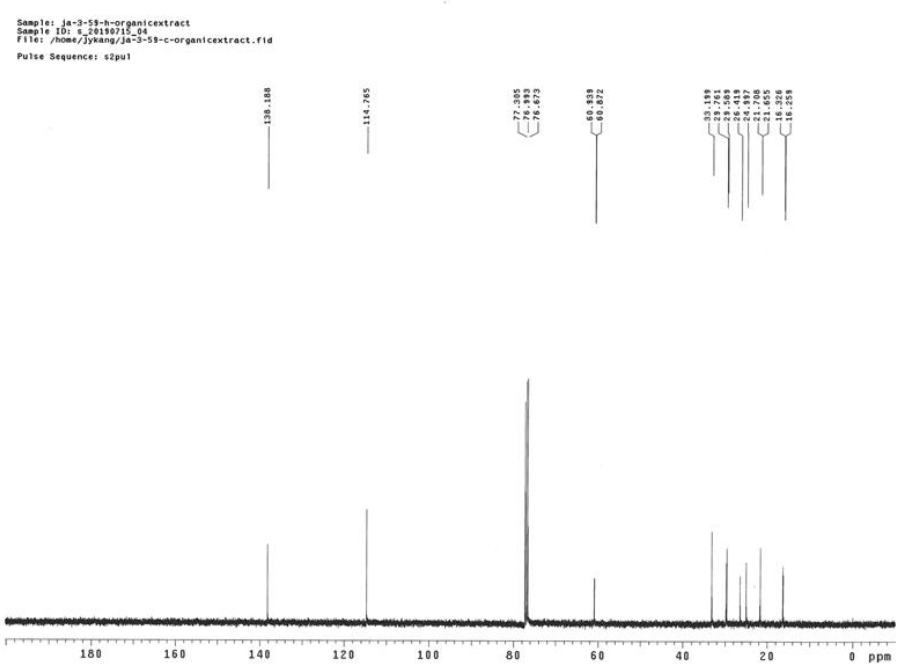

---

^{31}P NMR (162 MHz) in $CDCl_3$

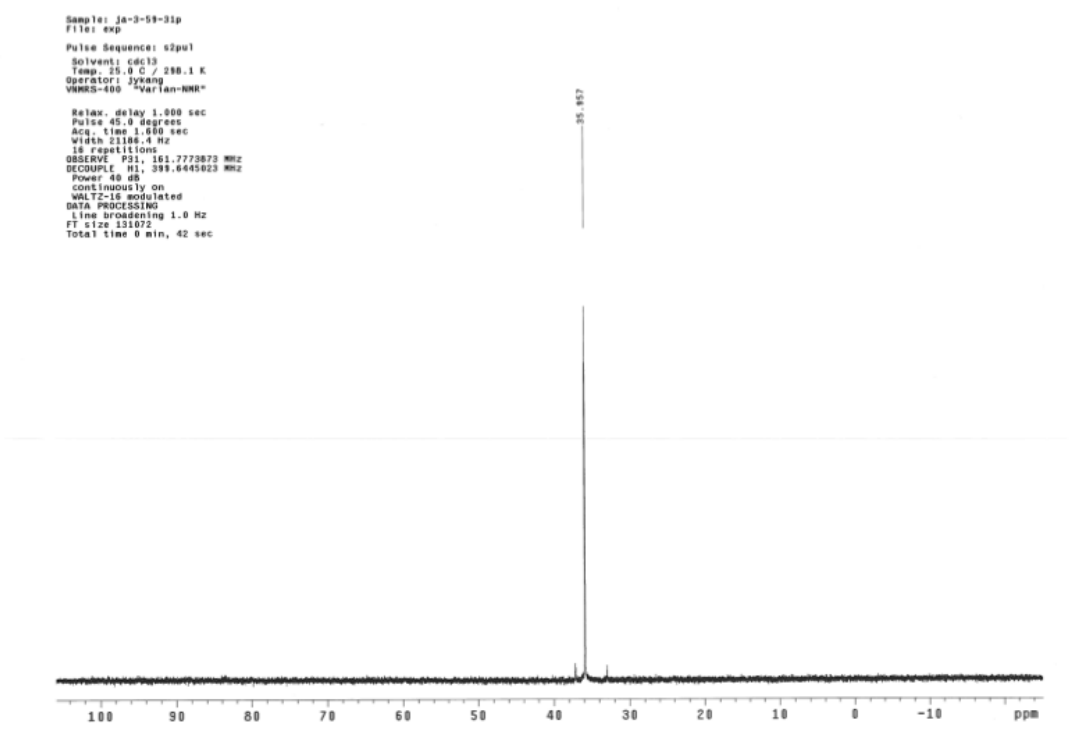

^{1}H NMR (400 MHz) in $CDCl_3$

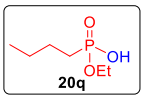

20q

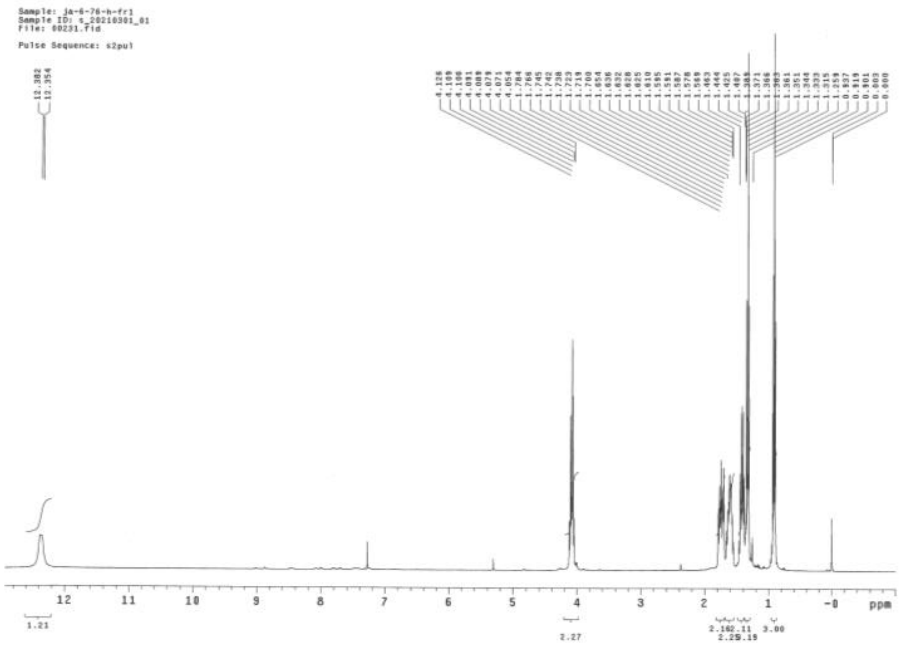

^{13}C NMR (100.5 MHz) in $CDCl_3$

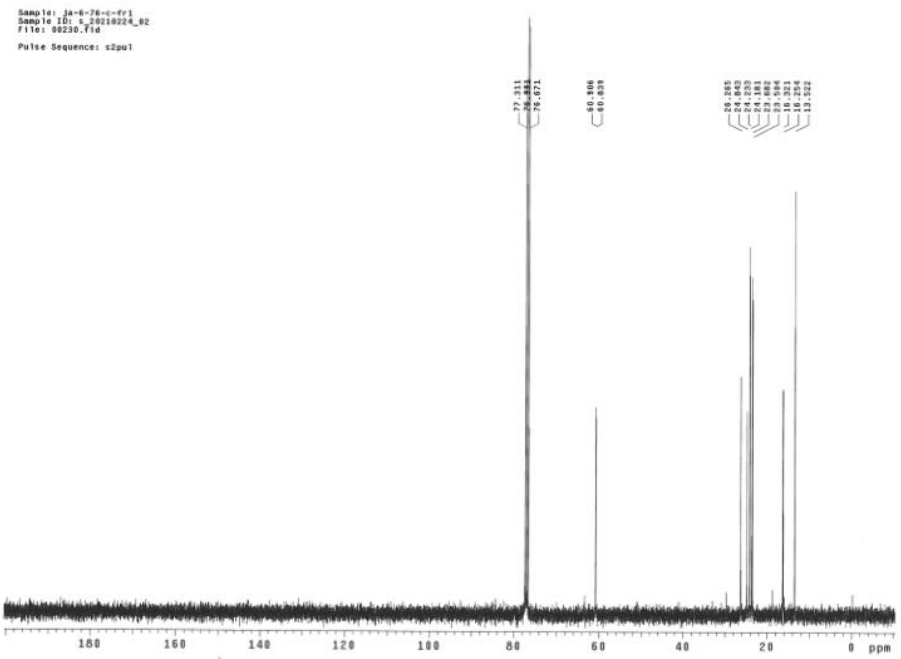

^{31}P NMR (162 MHz) in $CDCl_3$

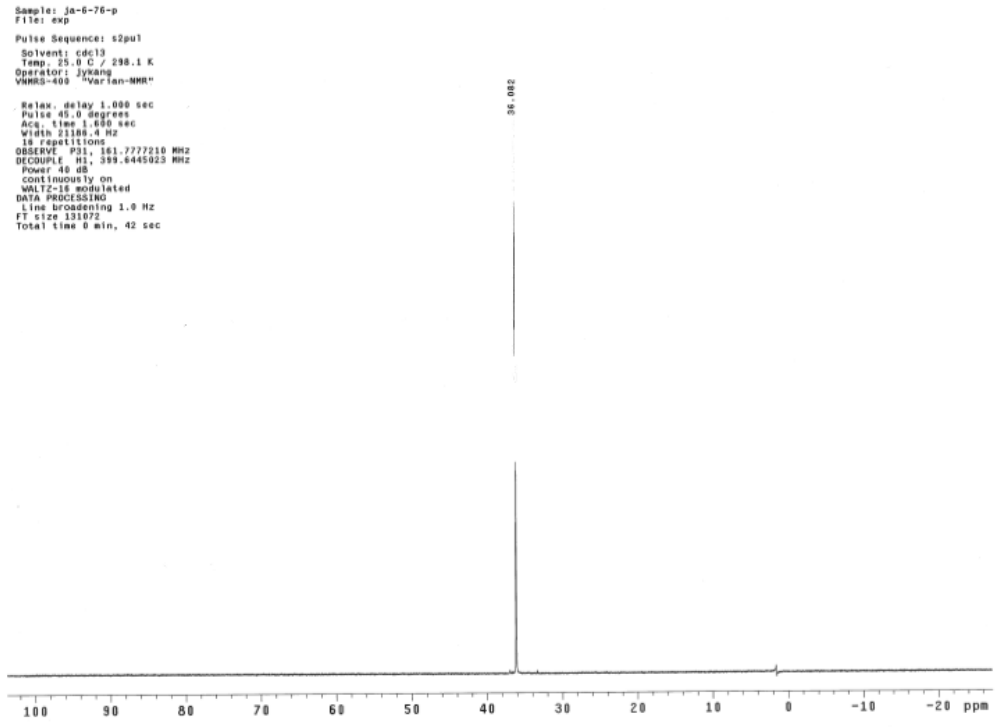

^{1}H NMR (400 MHz) in $CDCl_3$

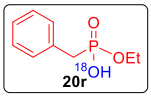

20r

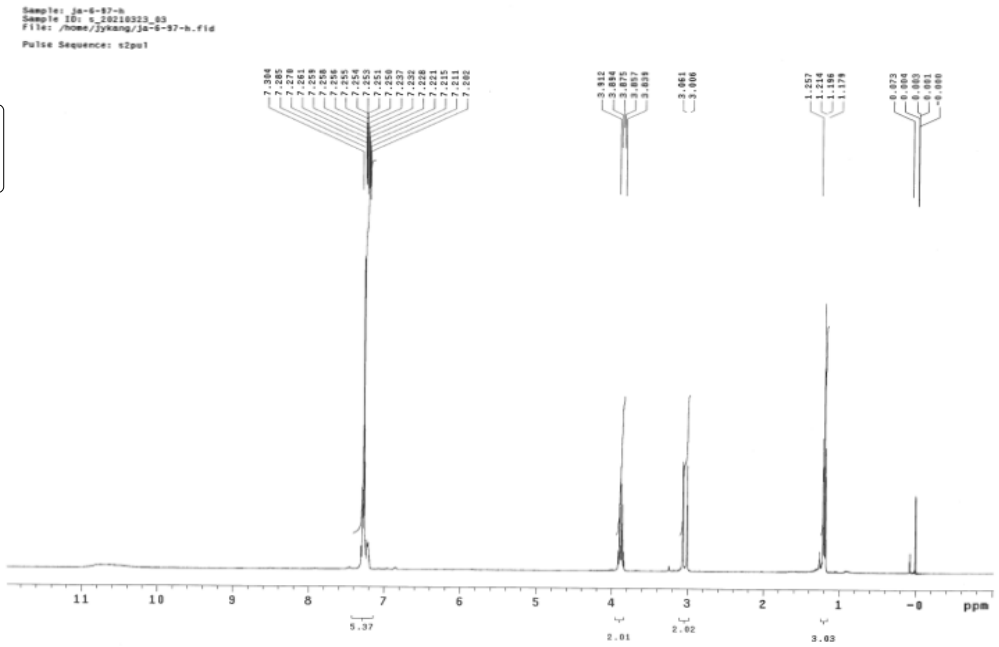

^{13}C NMR (100.5 MHz) in $CDCl_3$

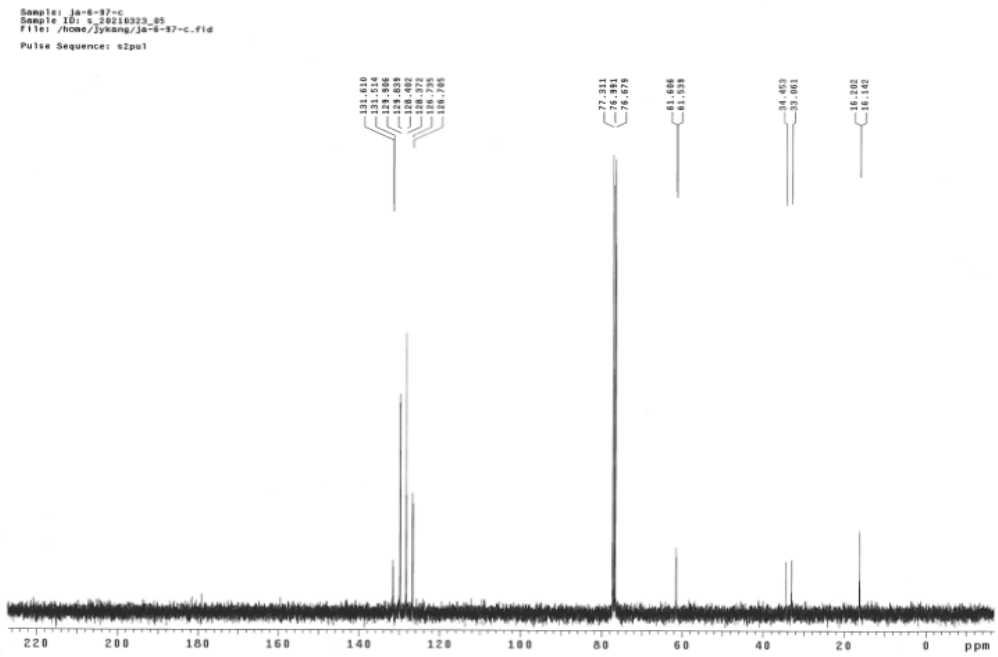

^{31}P NMR (162 MHz) in $CDCl_3$

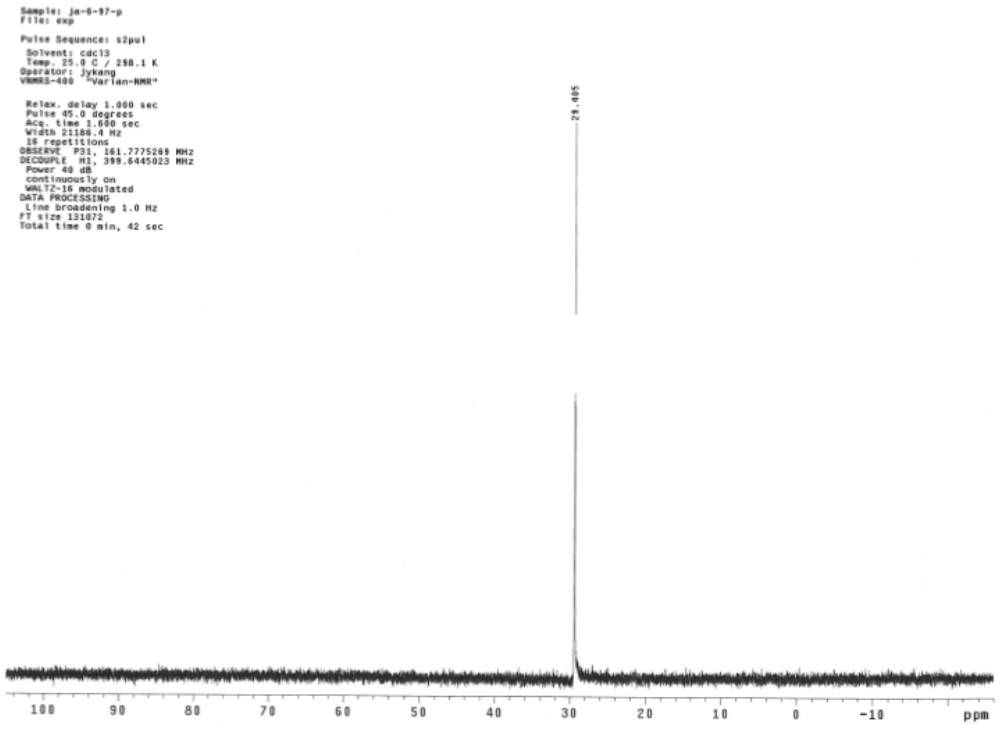

^{1}H NMR (400 MHz) in $CDCl_3$

26a

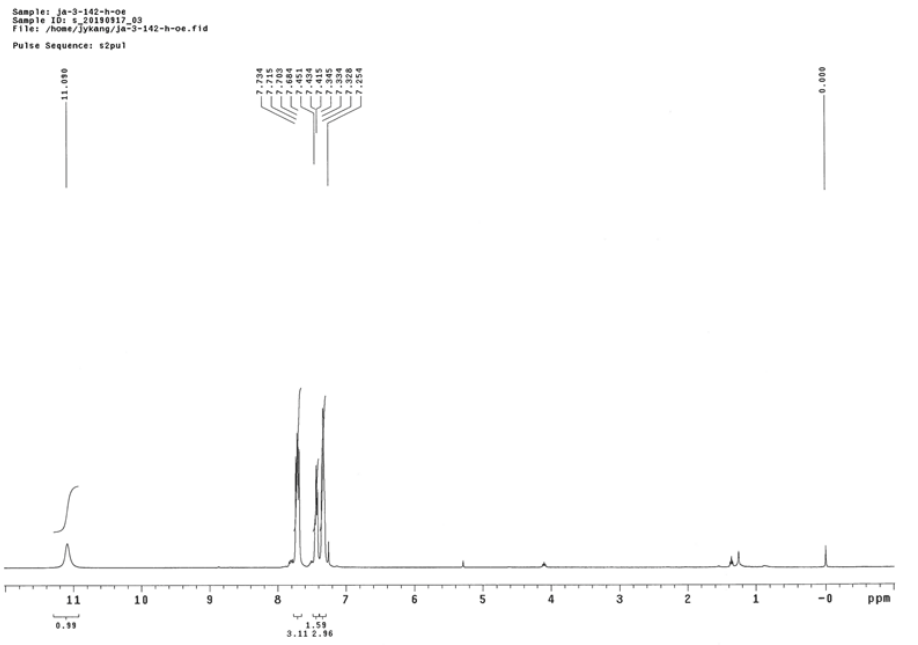

^{13}C NMR (100.5 MHz) in $CDCl_3$

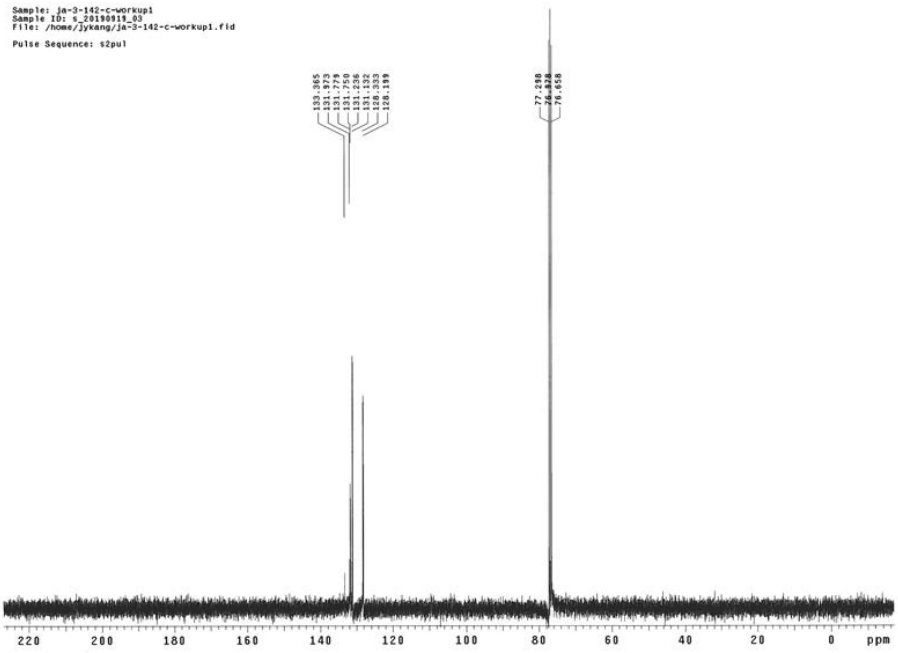

^{31}P NMR (162 MHz) in $CDCl_3$

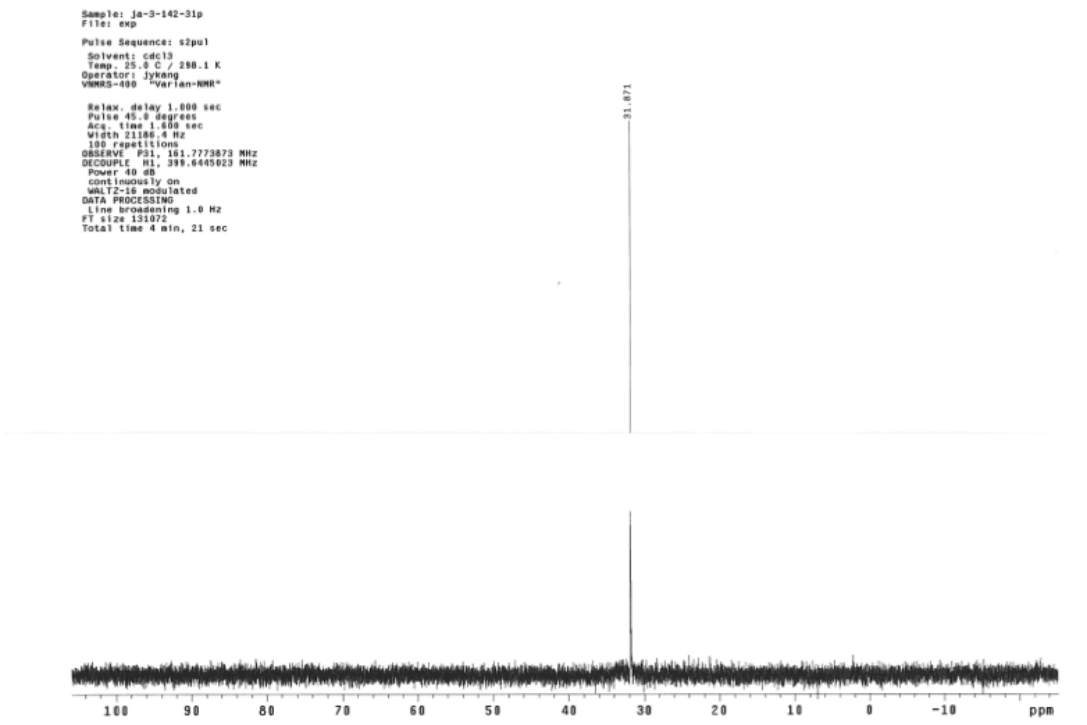

^{1}H NMR (400 MHz) in CD_3OD

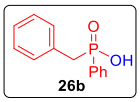

26b

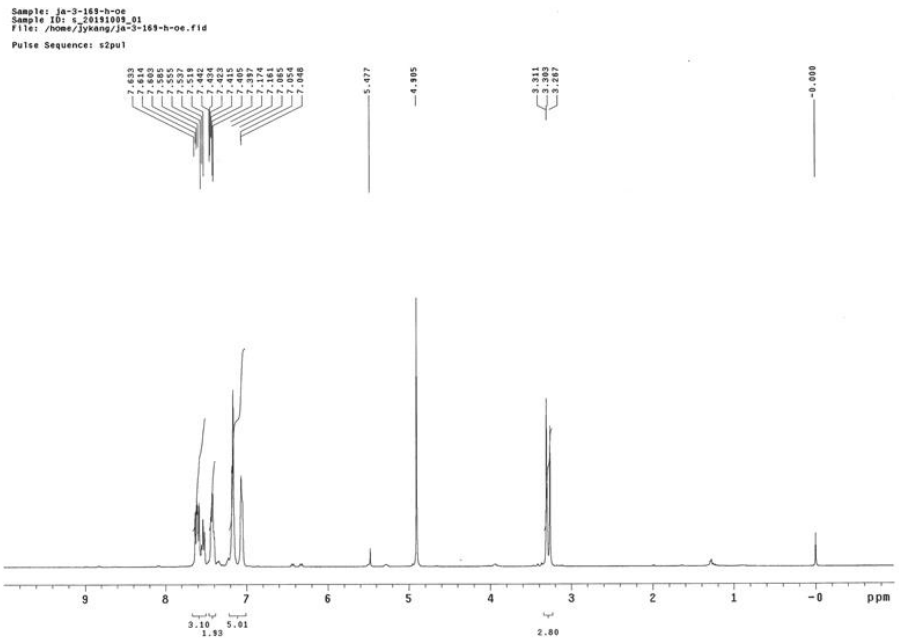

^{13}C NMR (100.5 MHz) in CD_3OD

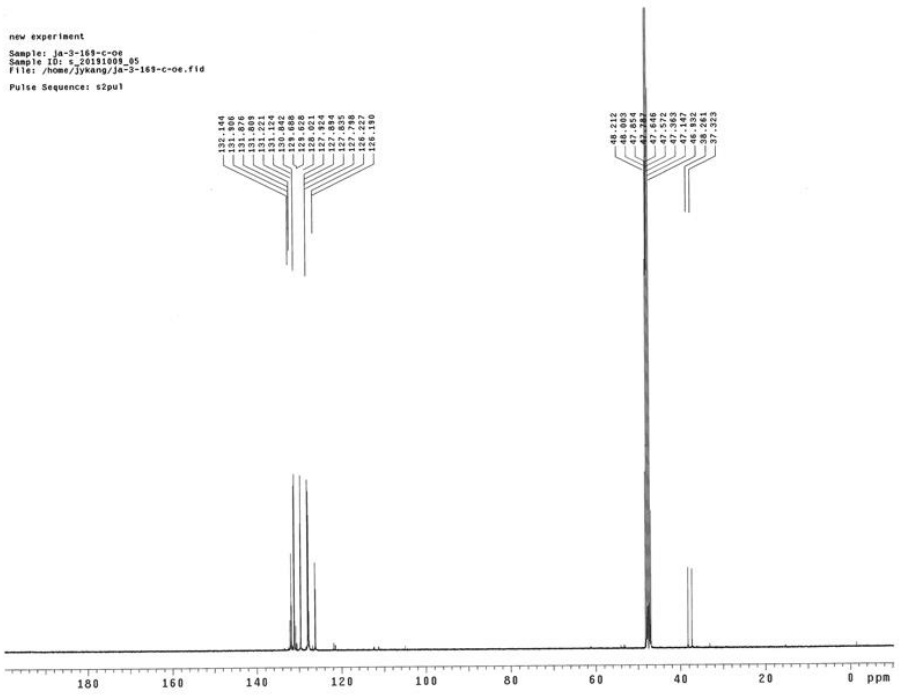

^{31}P NMR (162 MHz) in CD_3OD

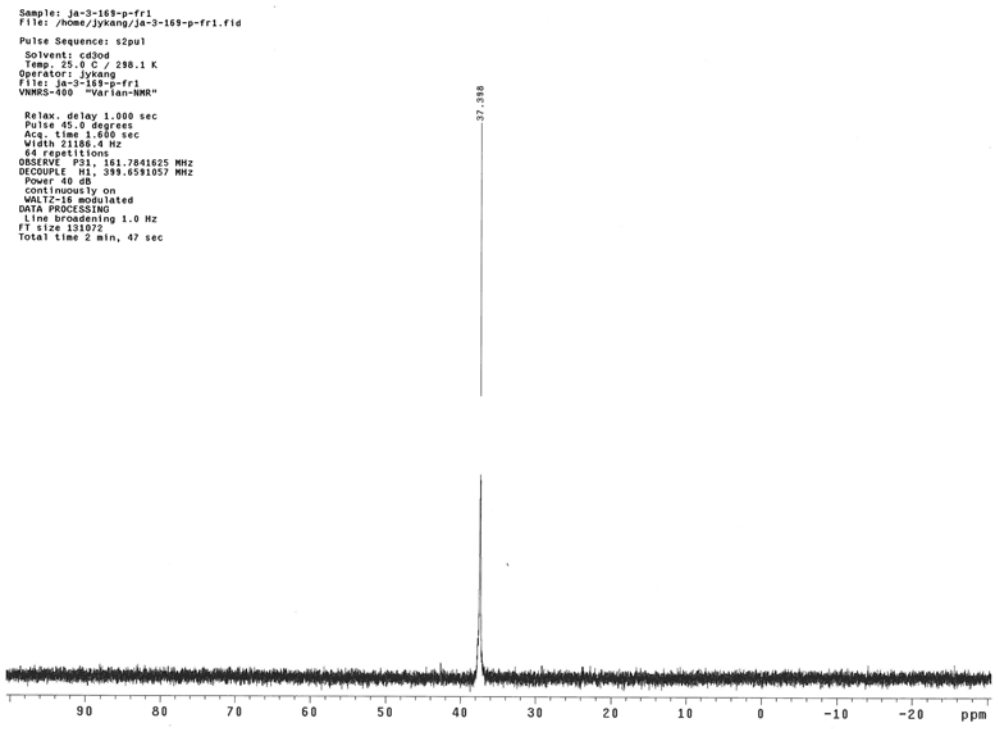

^{1}H NMR (400 MHz) in CD_3OD

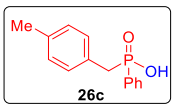

26c

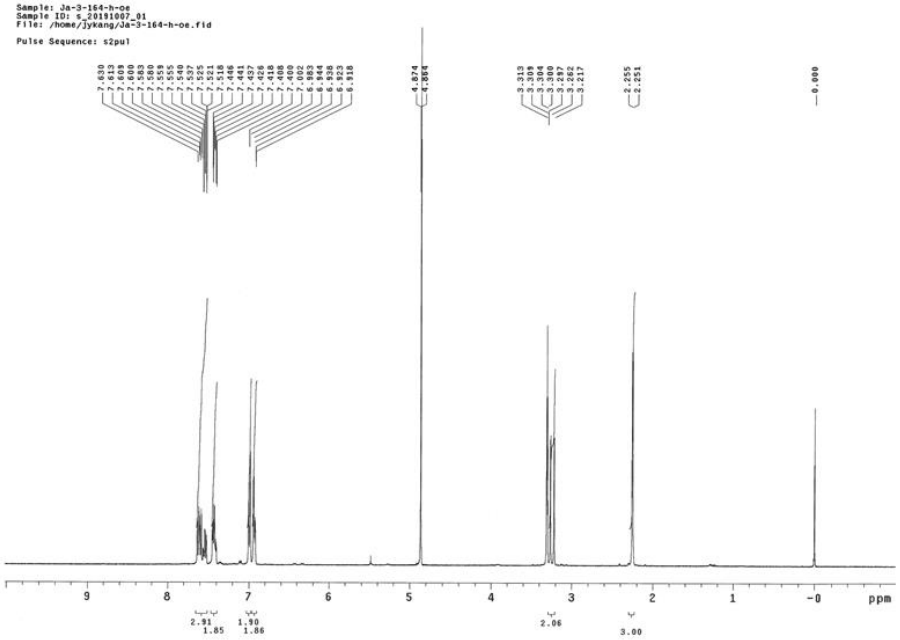

^{13}C NMR (100.5 MHz) in CD_3OD

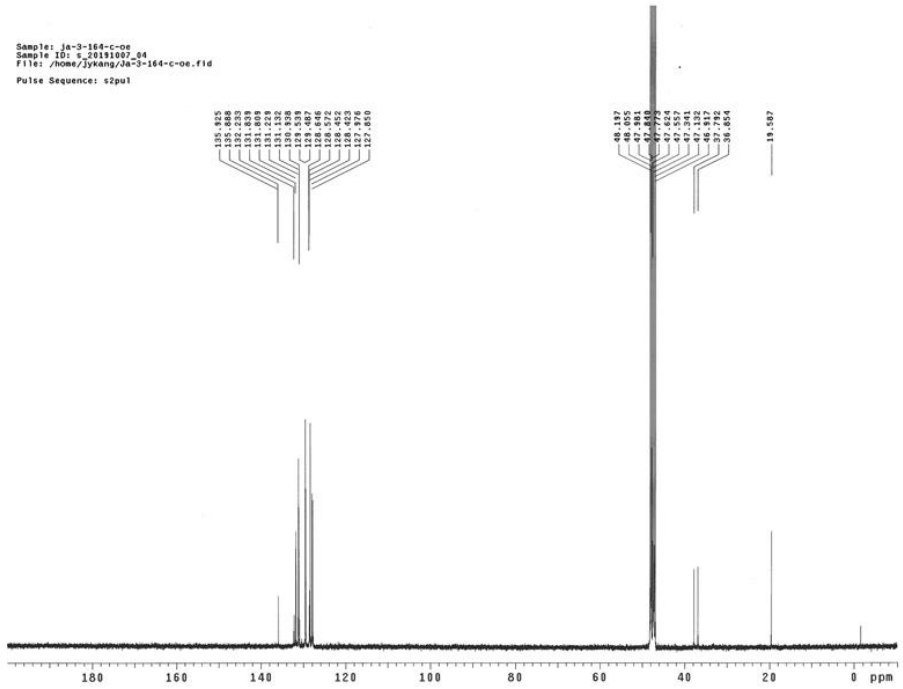

^{31}P NMR (162 MHz) in CD_3OD

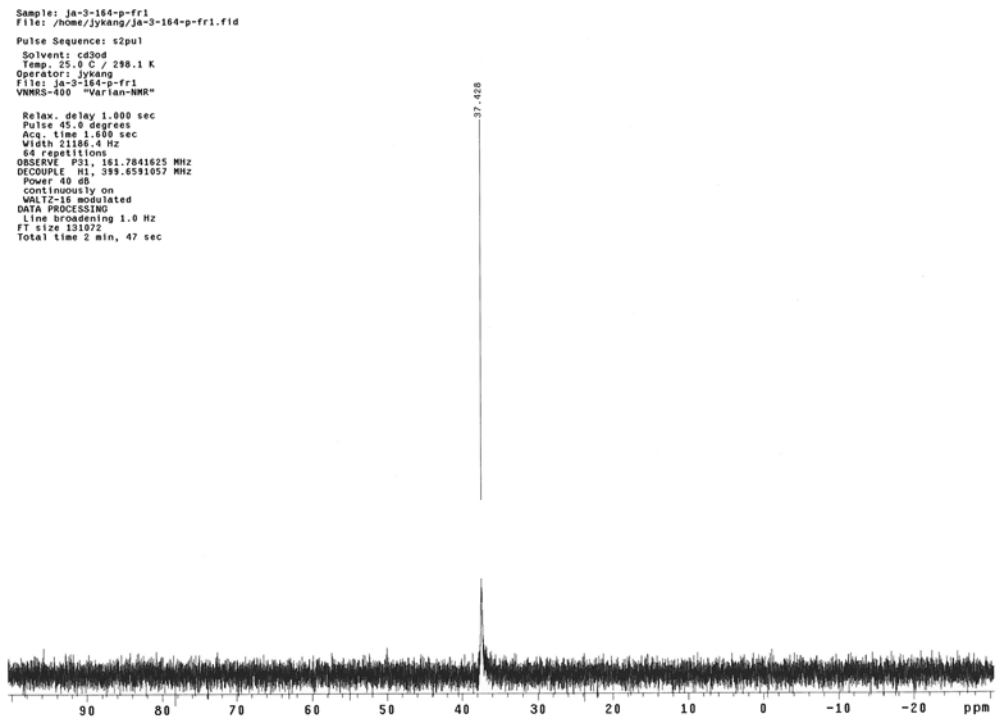

^{1}H NMR (400 MHz) in $CDCl_3$

26d

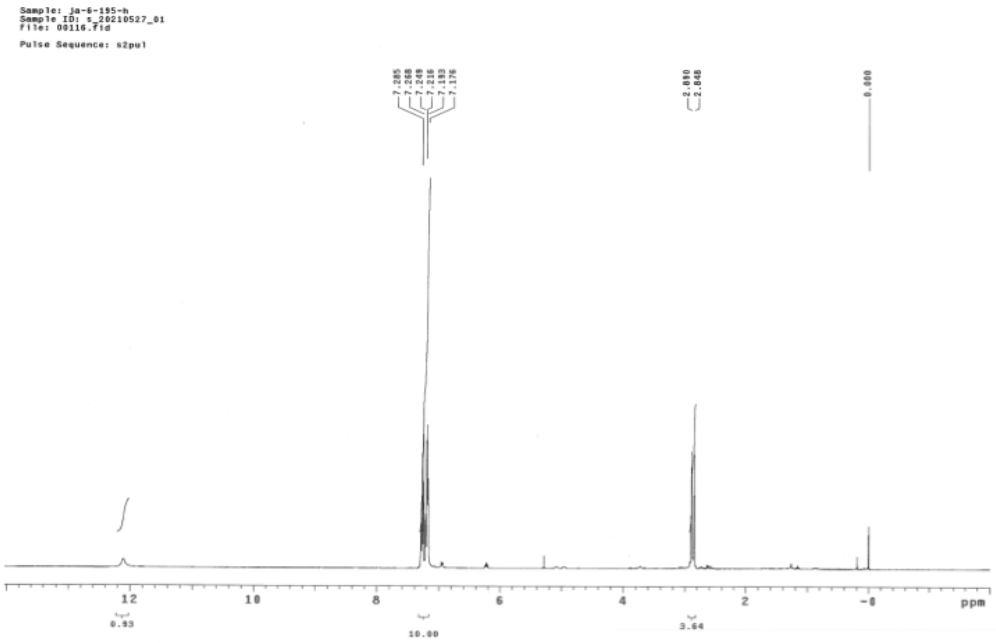

^{13}C NMR (100.5 MHz) in $CDCl_3$

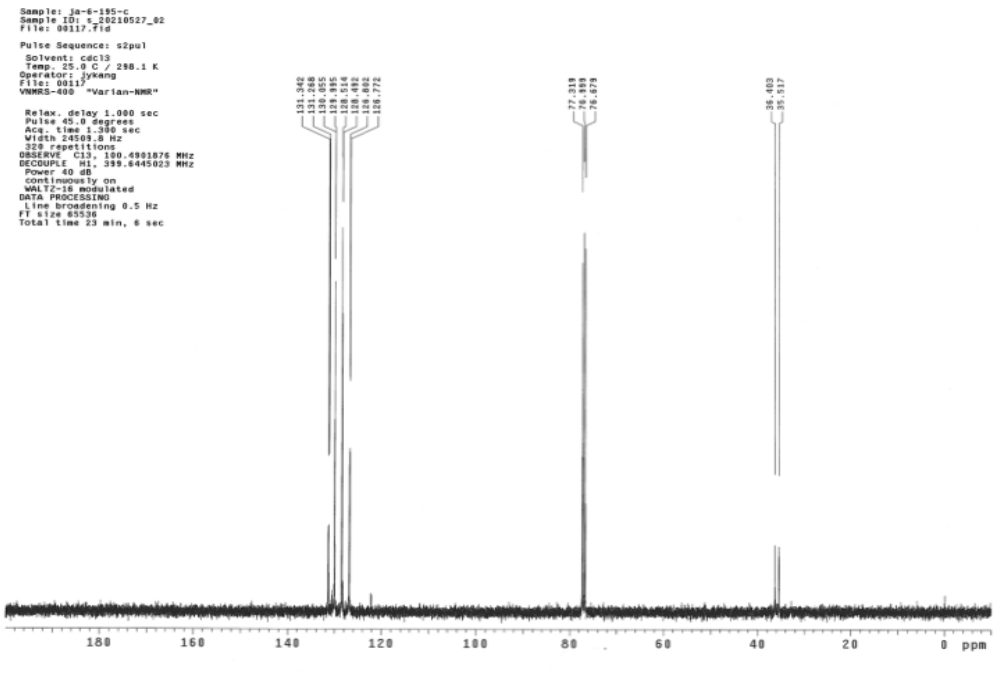

^{31}P NMR (162 MHz) in $CDCl_3$

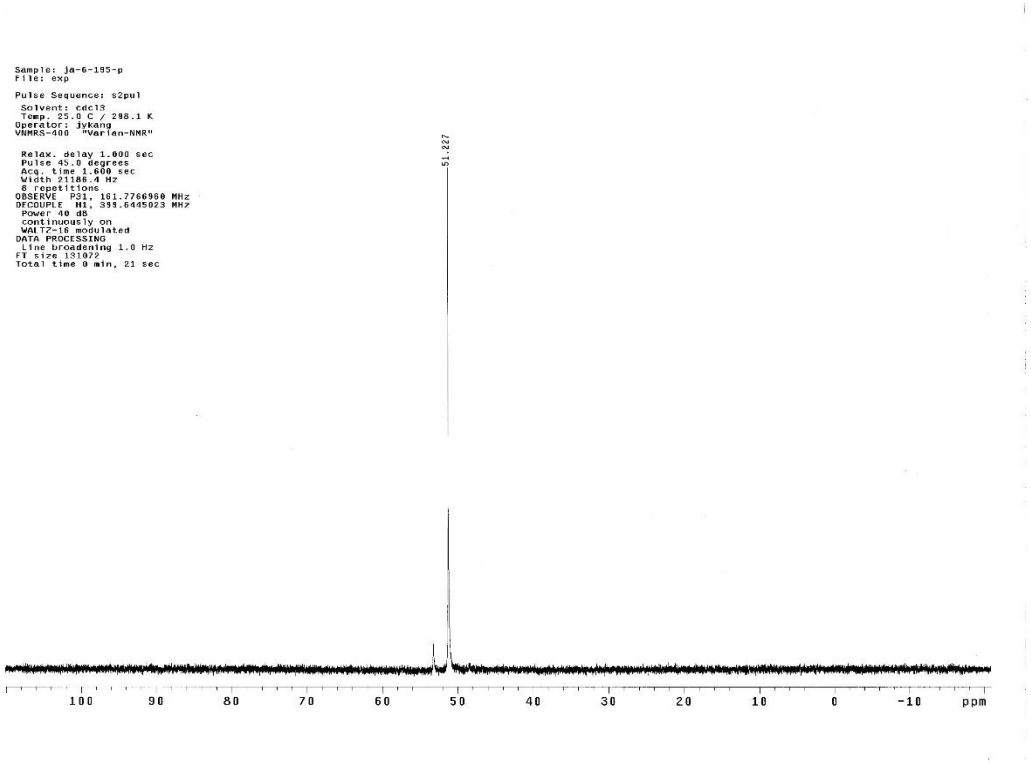

^{1}H NMR (400 MHz) in $CDCl_3$

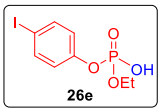

26e

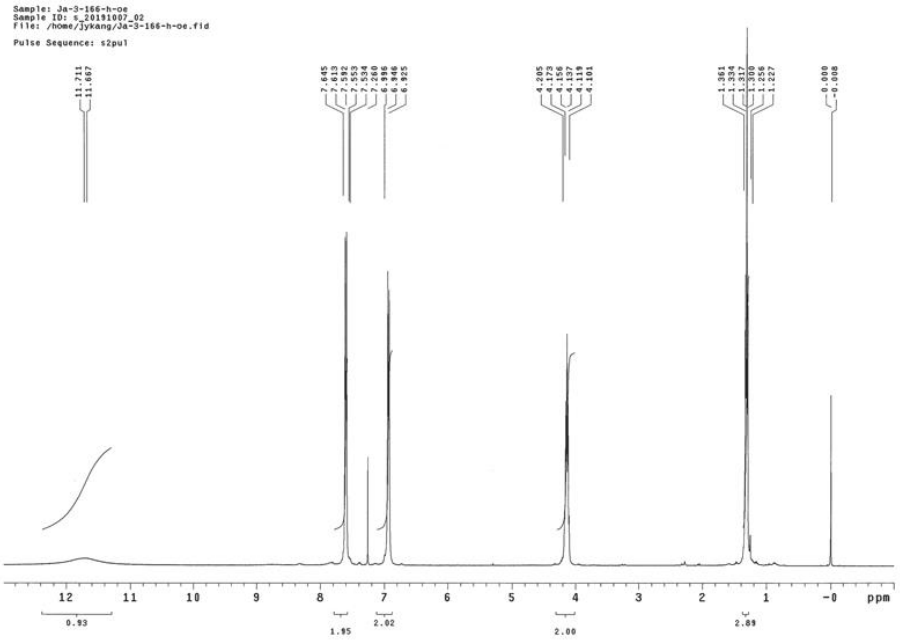

^{13}C NMR (100.5 MHz) in $CDCl_3$

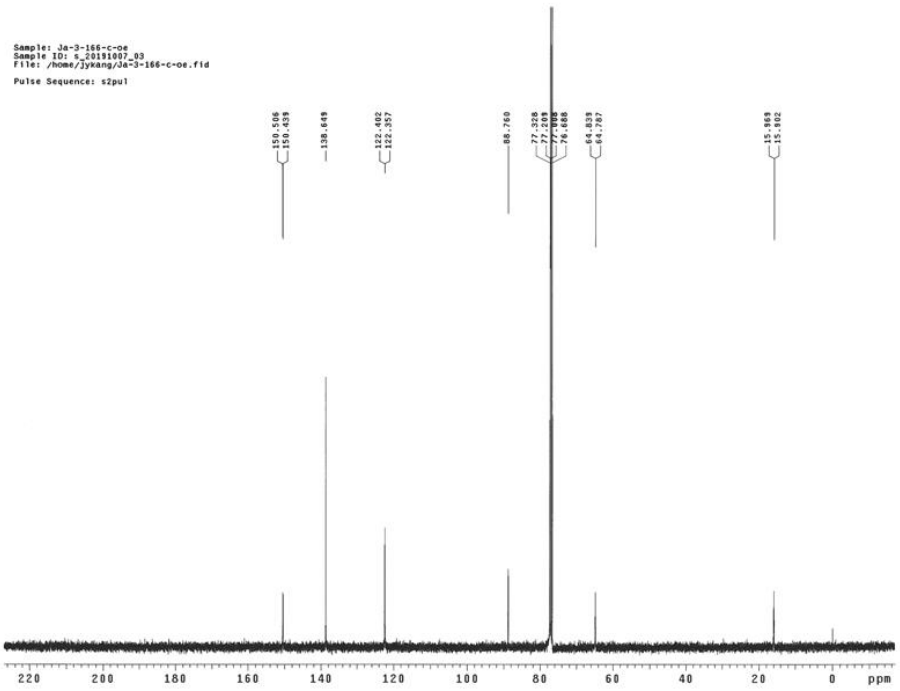

^{31}P NMR (162 MHz) in $CDCl_3$

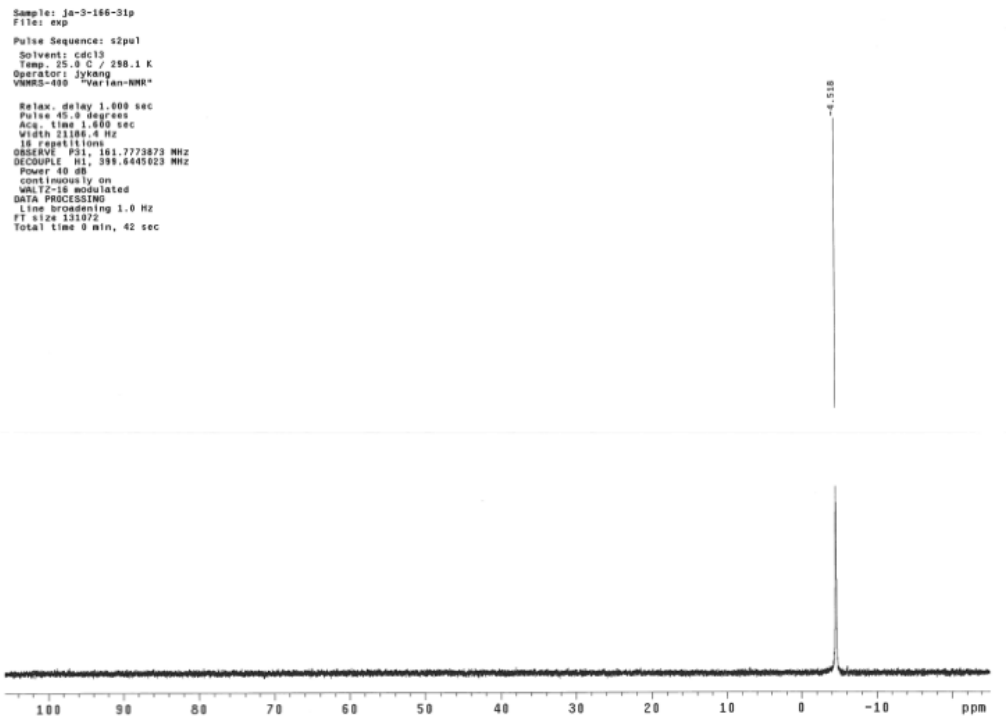

^{1}H NMR (400 MHz) in $CDCl_3$

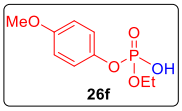

26f

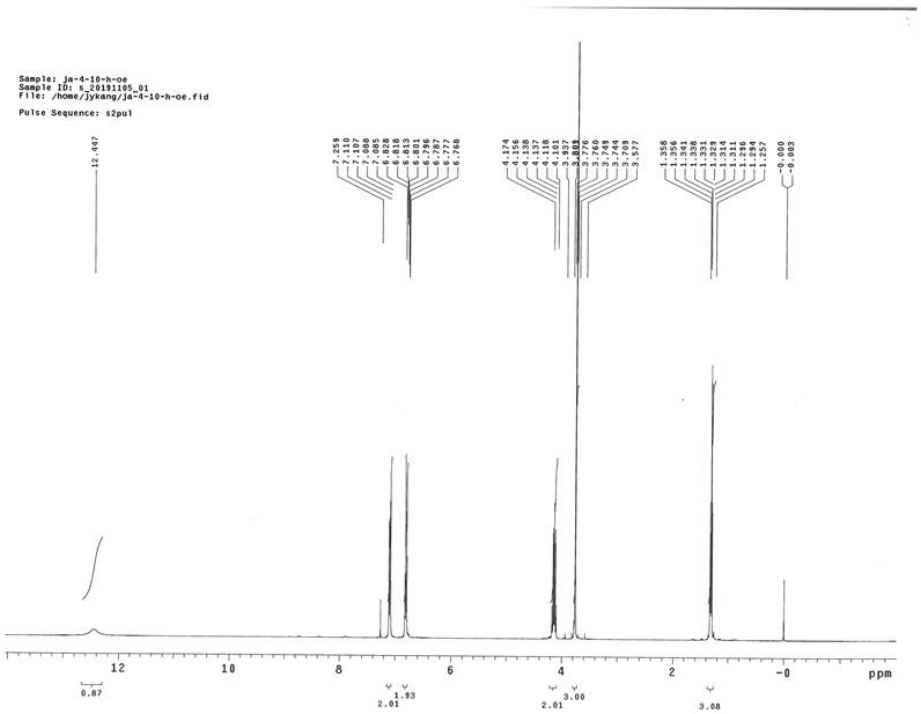

^{13}C NMR (100.5 MHz) in $CDCl_3$

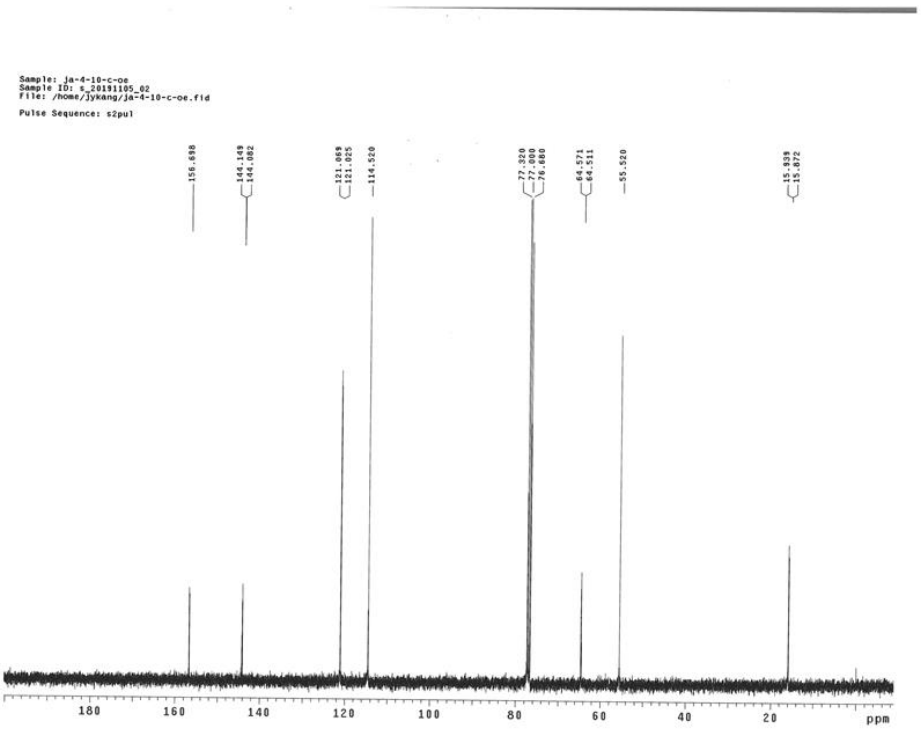

^{31}P NMR (162 MHz) in $CDCl_3$

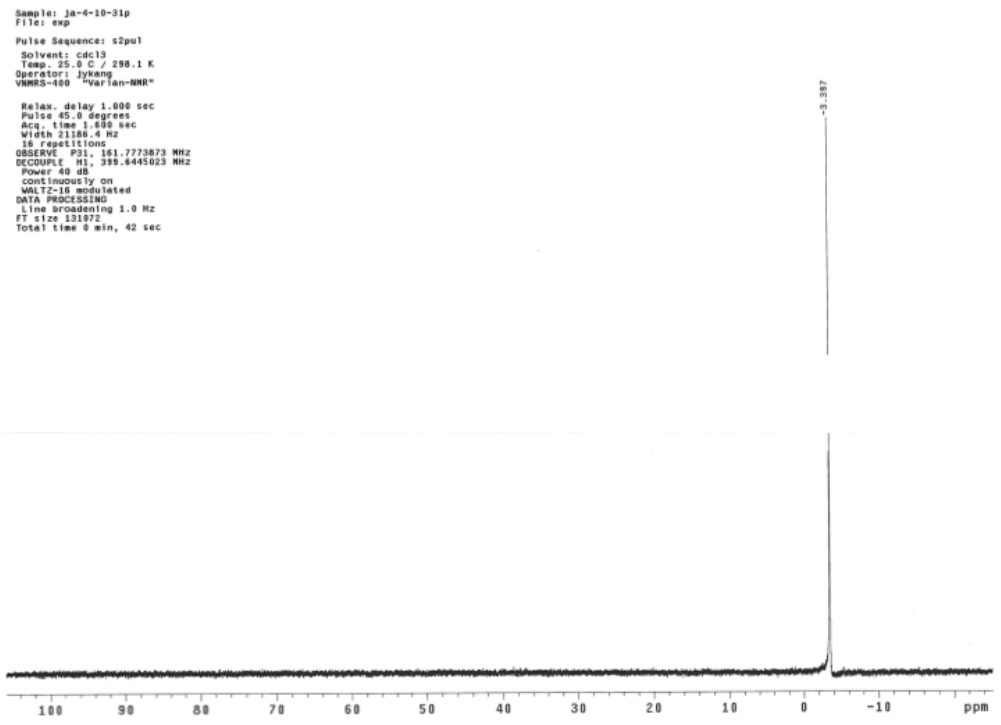

^{1}H NMR (400 MHz) in $CDCl_3$

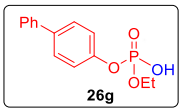

26g

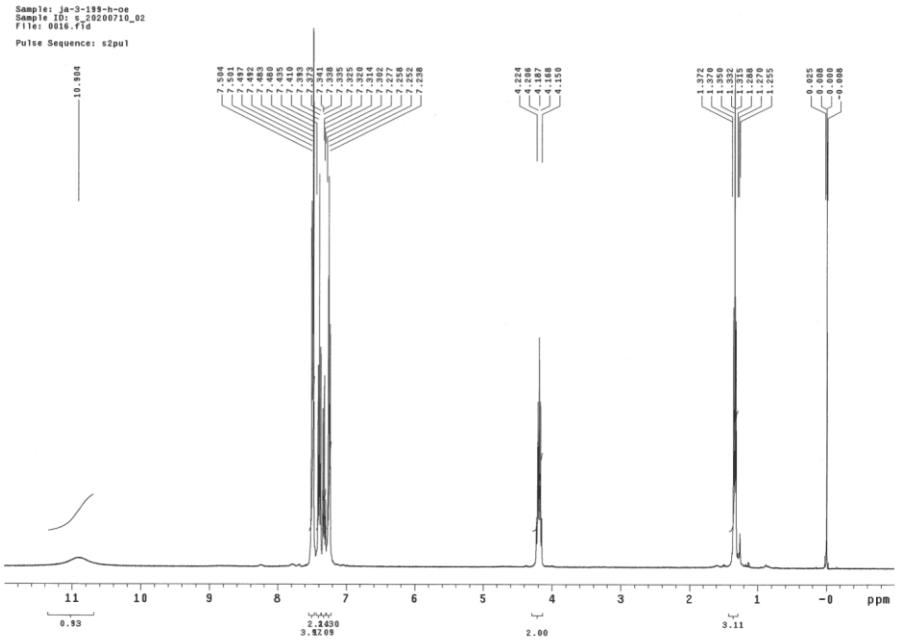

^{13}C NMR (100.5 MHz) in $CDCl_3$

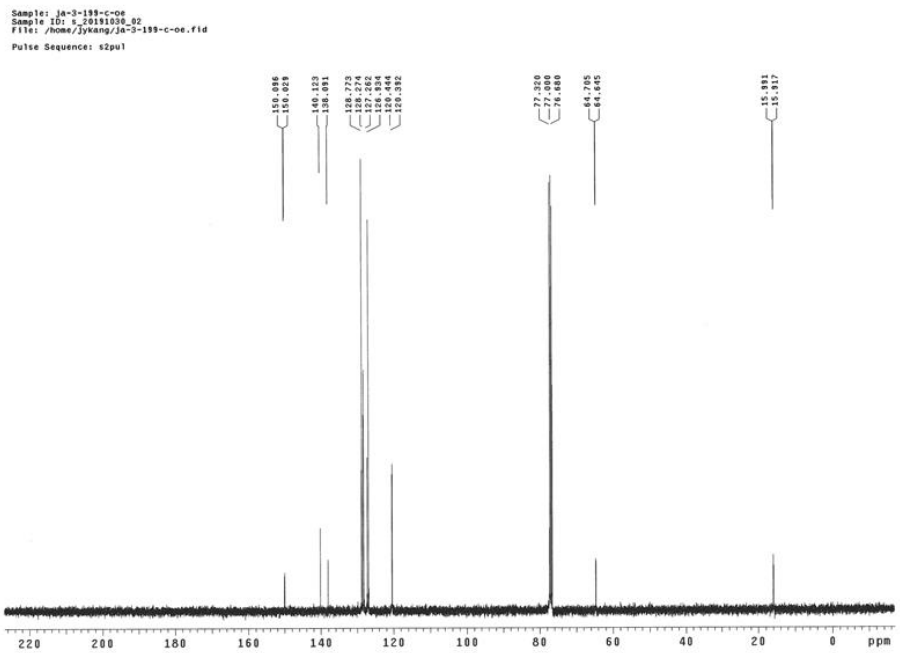

^{31}P NMR (162 MHz) in $CDCl_3$

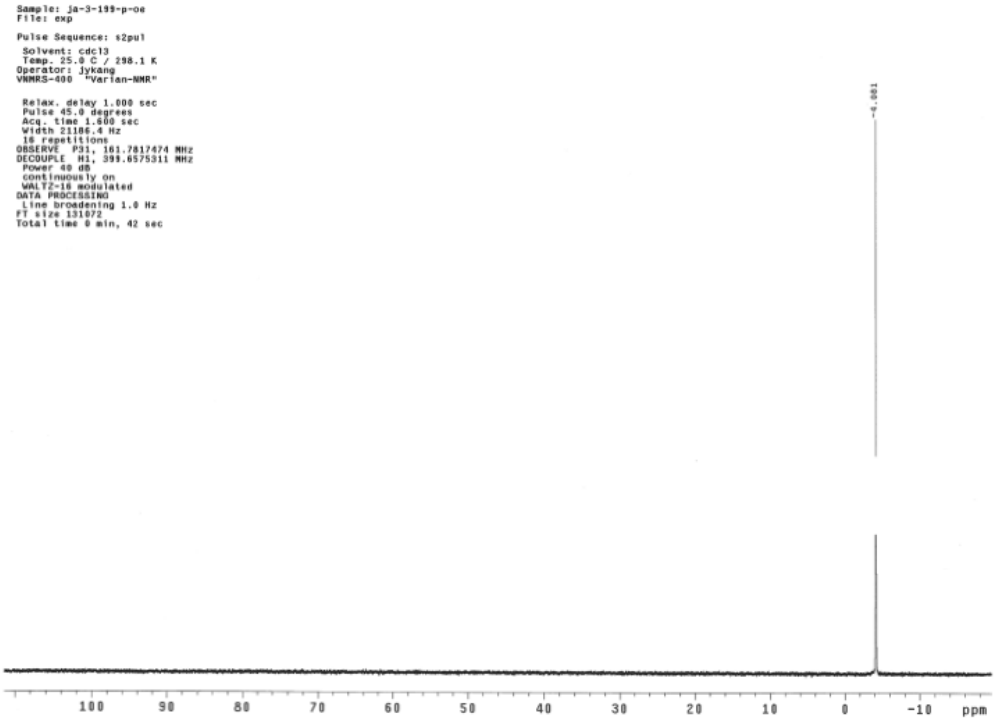

^{1}H NMR (400 MHz) in $CDCl_3$

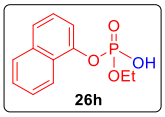

26h

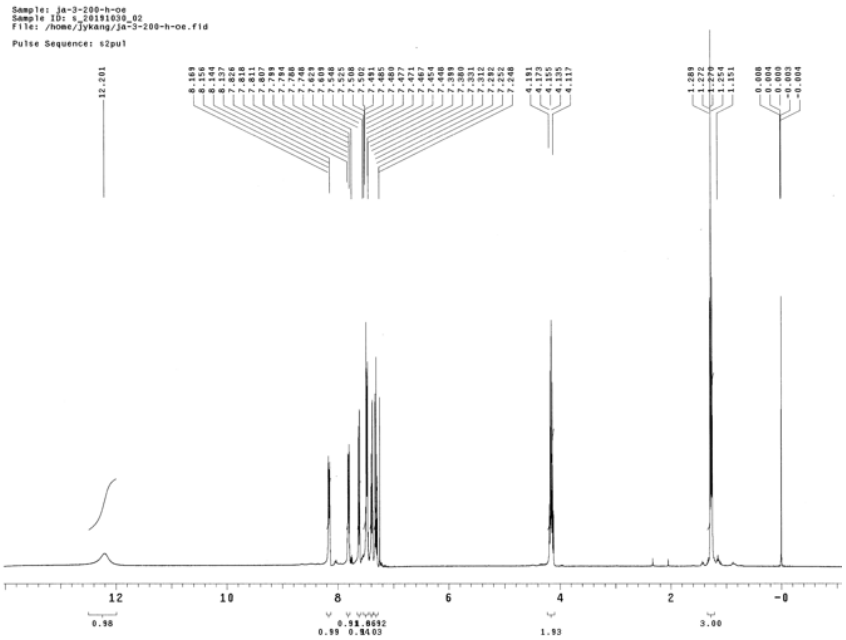

^{13}C NMR (100.5 MHz) in $CDCl_3$

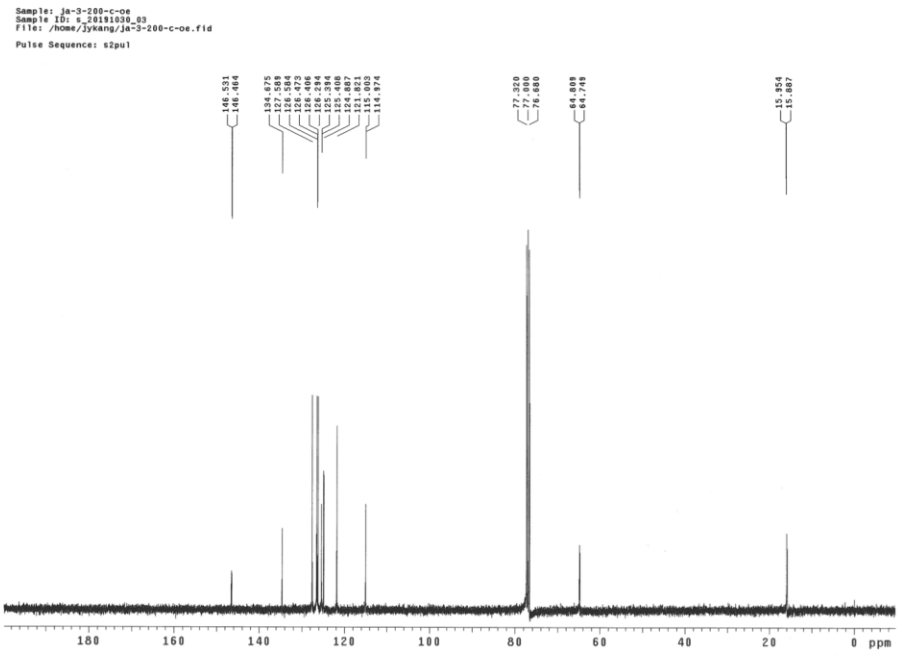

^{31}P NMR (162 MHz) in $CDCl_3$

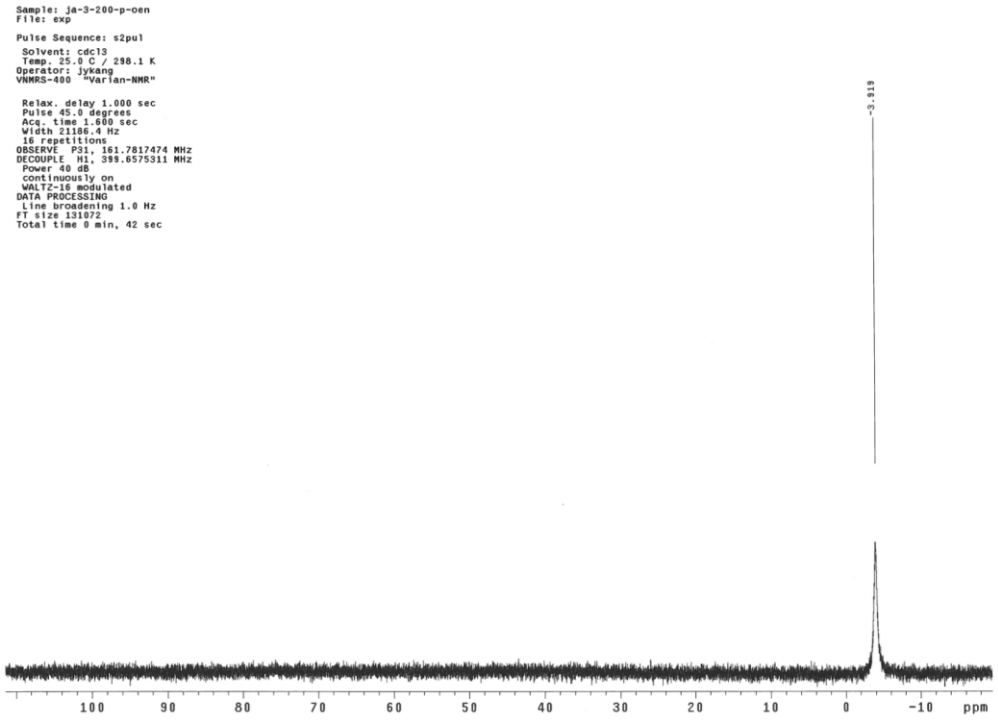

^{1}H NMR (400 MHz) in $CDCl_3$

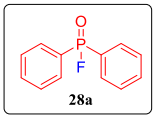

28a

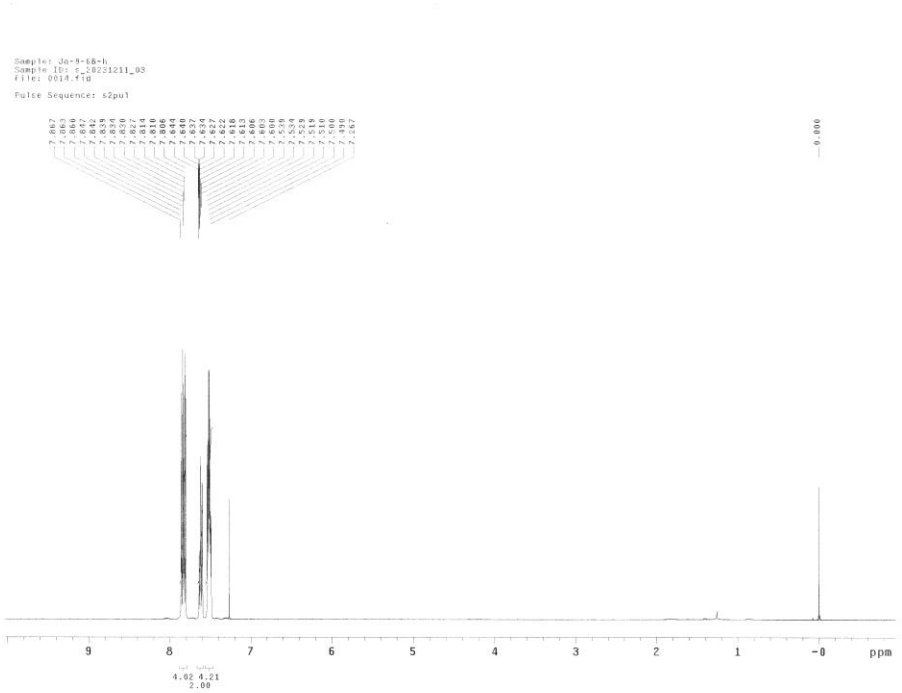

^{13}C NMR (100.5 MHz) in $CDCl_3$

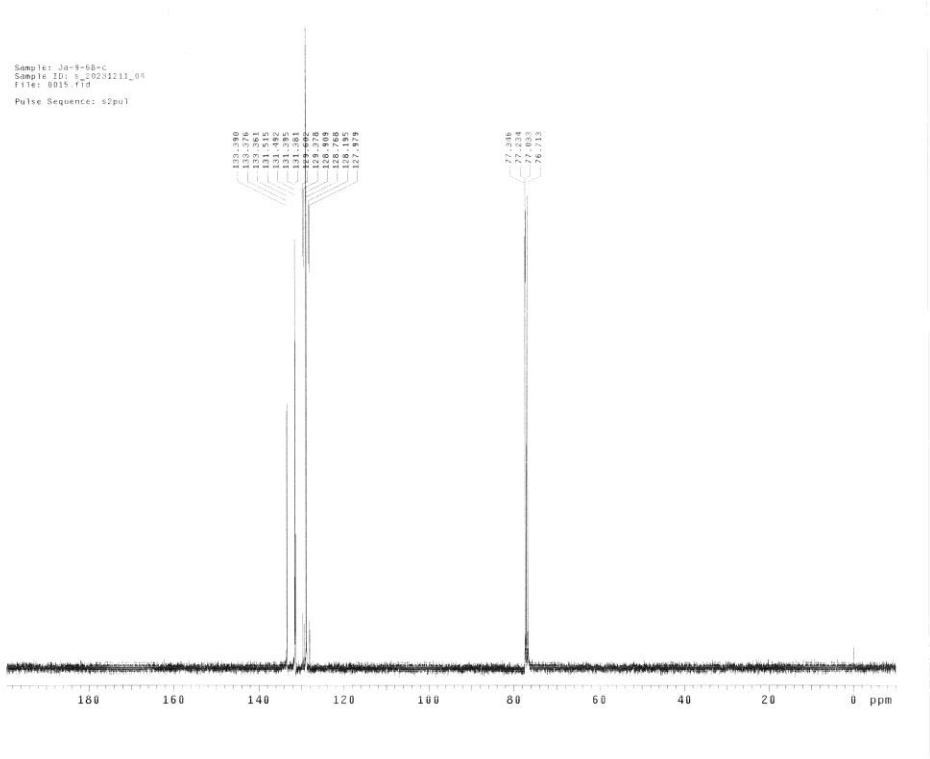

^{31}P NMR (162 MHz) in $CDCl_3$

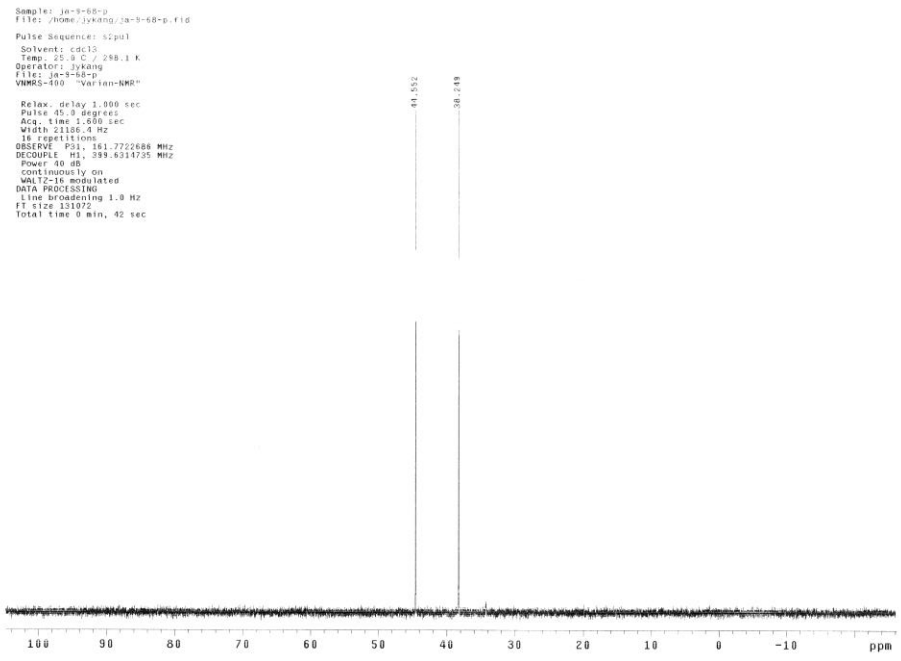

^{19}F NMR (376 MHz) in $CDCl_3$

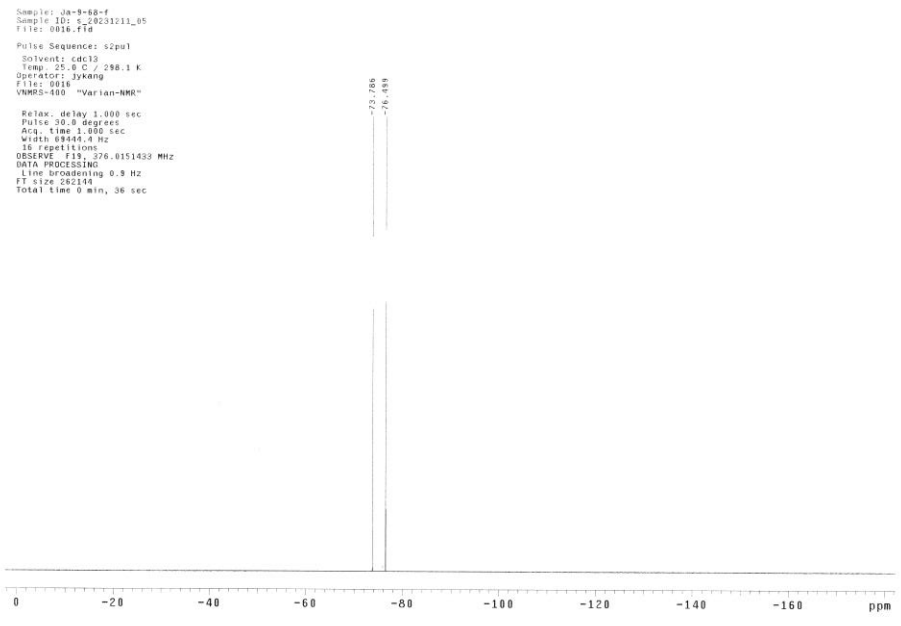

^{1}H NMR (400 MHz) in $CDCl_3$

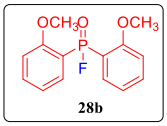

28b

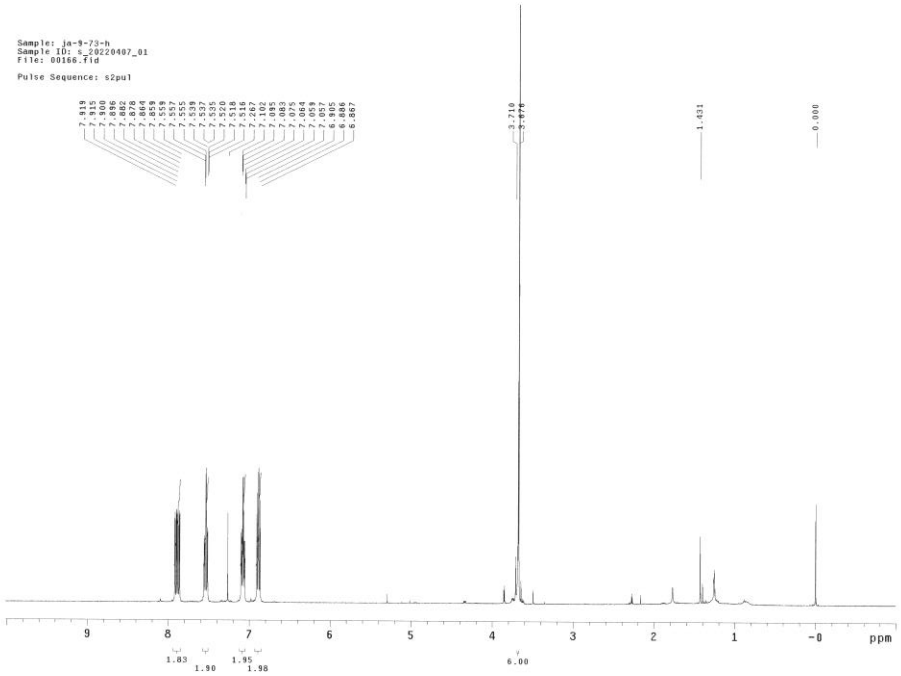

^{13}C NMR (100.5 MHz) in $CDCl_3$

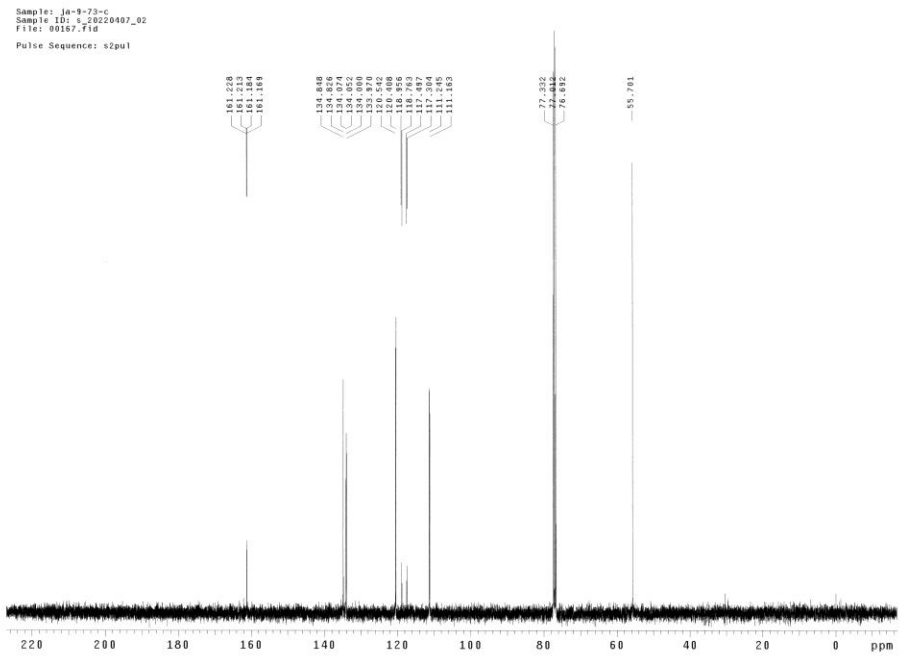

^{31}P NMR (162 MHz) in $CDCl_3$

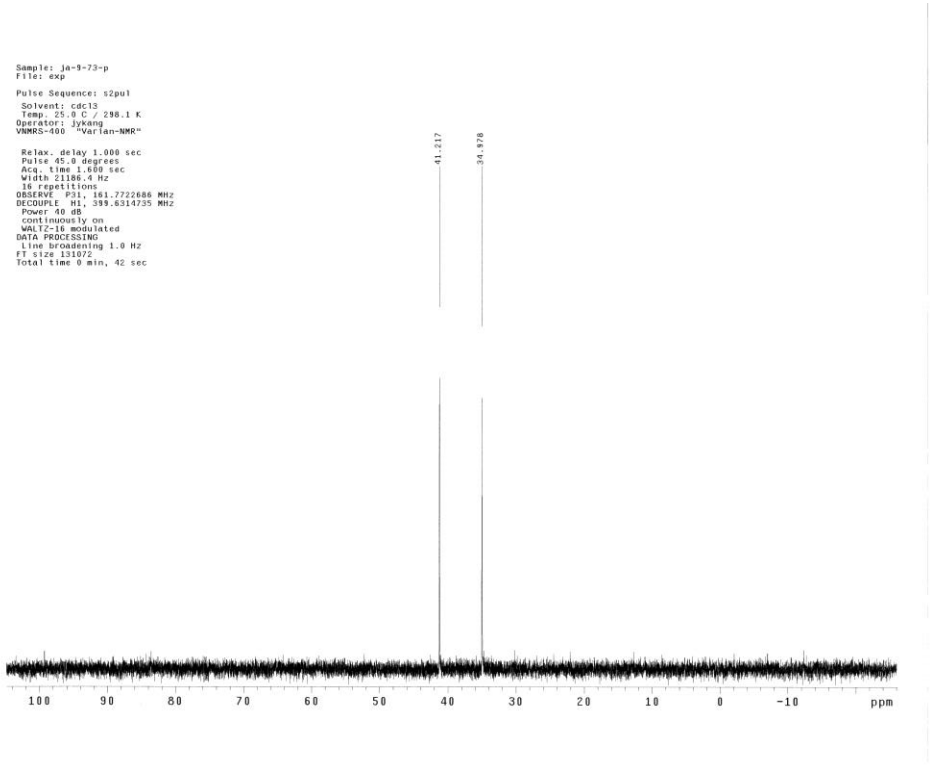

^{19}F NMR (376 MHz) in $CDCl_3$

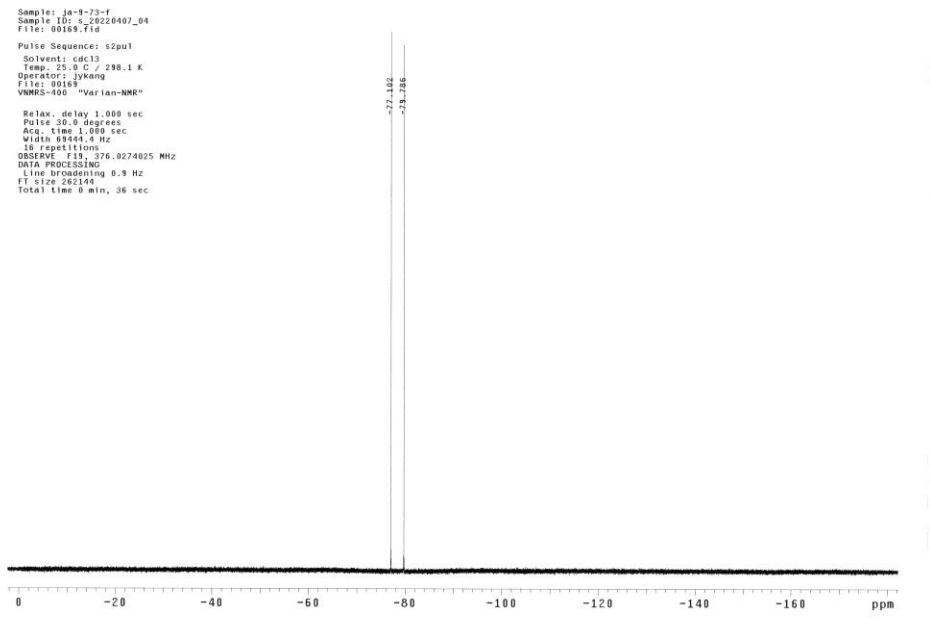

^{1}H NMR (400 MHz) in $CDCl_3$

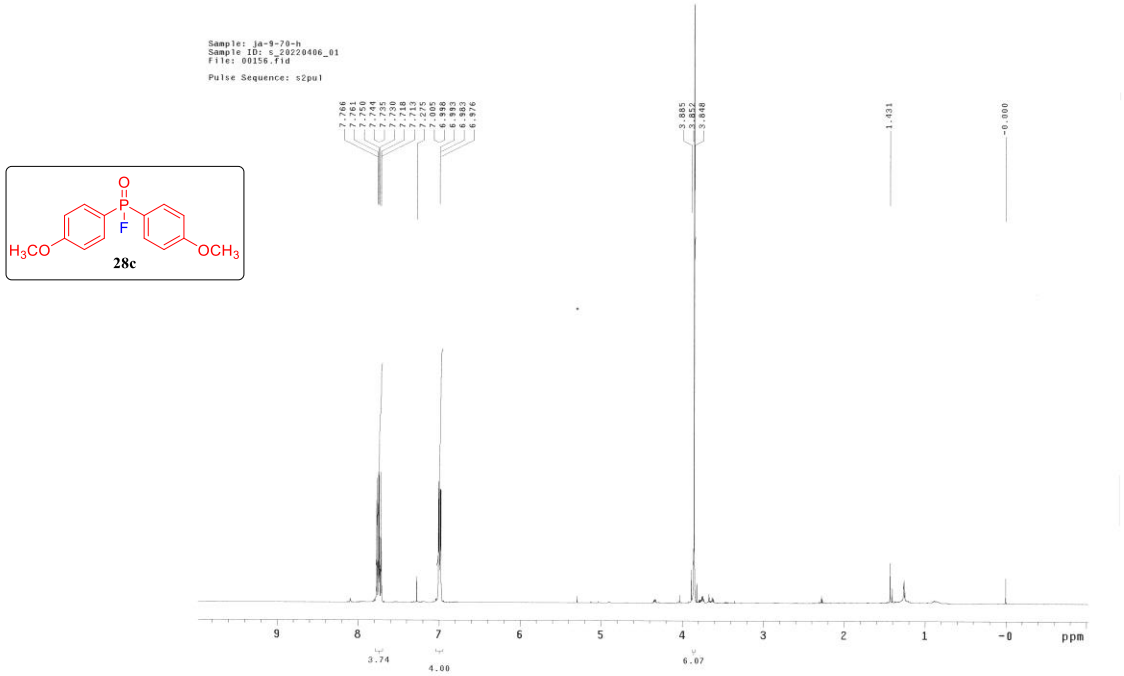

28c

^{13}C NMR (100.5 MHz) in $CDCl_3$

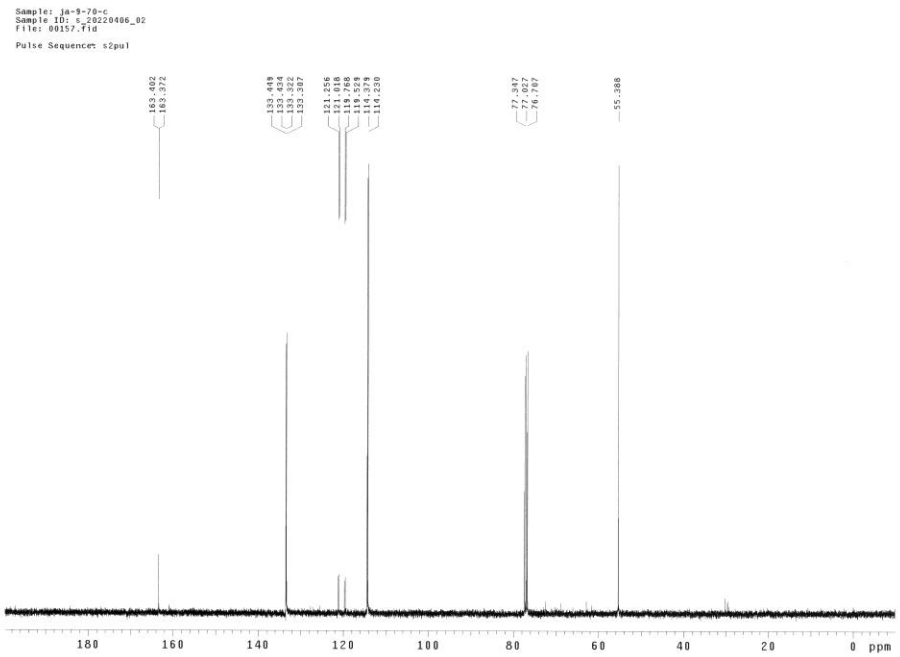

^{31}P NMR (162 MHz) in $CDCl_3$

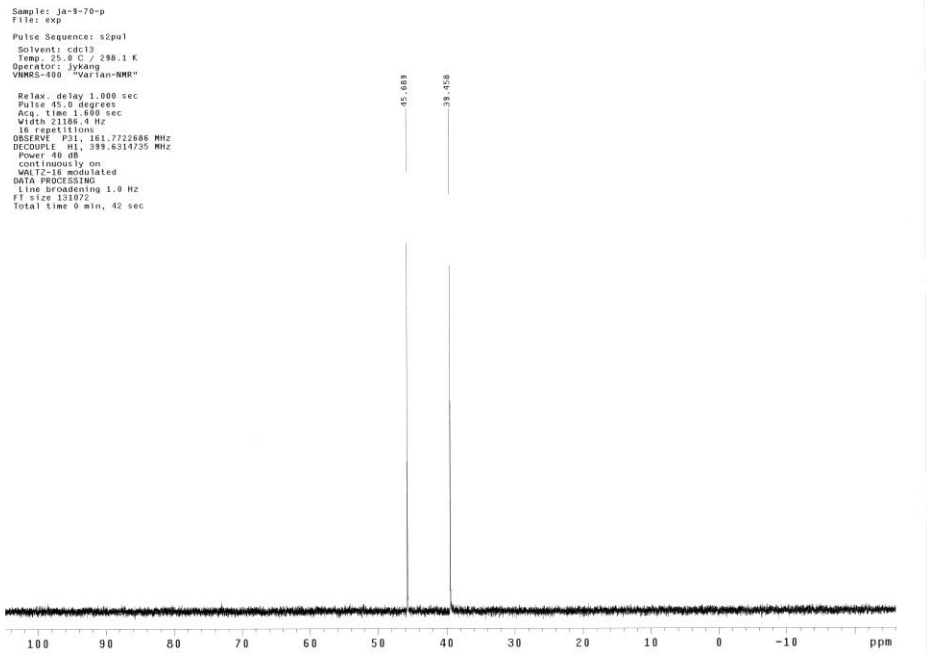

^{19}F NMR (376 MHz) in $CDCl_3$

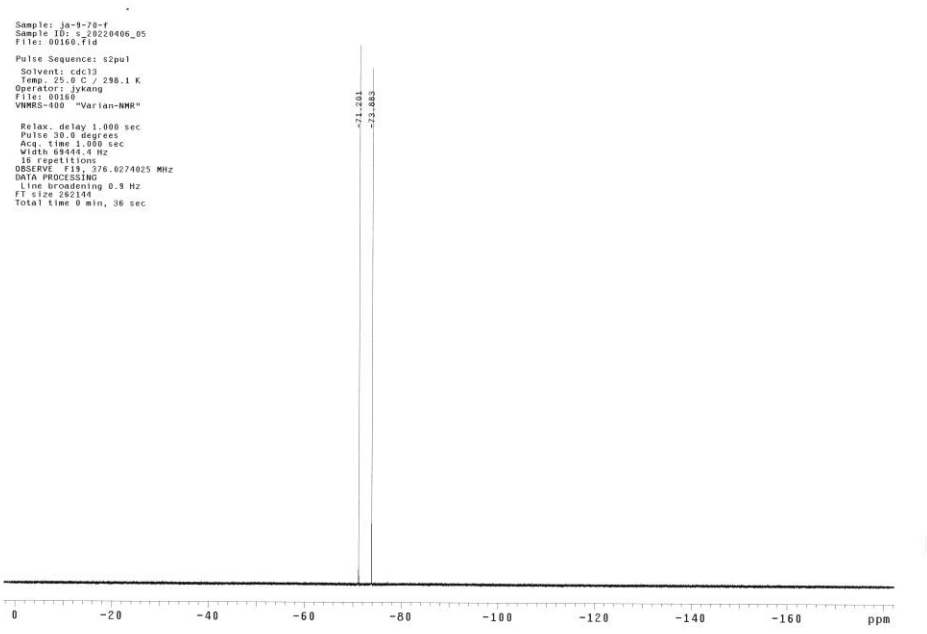

^{1}H NMR (400 MHz) in $CDCl_3$

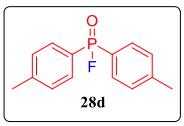

28d

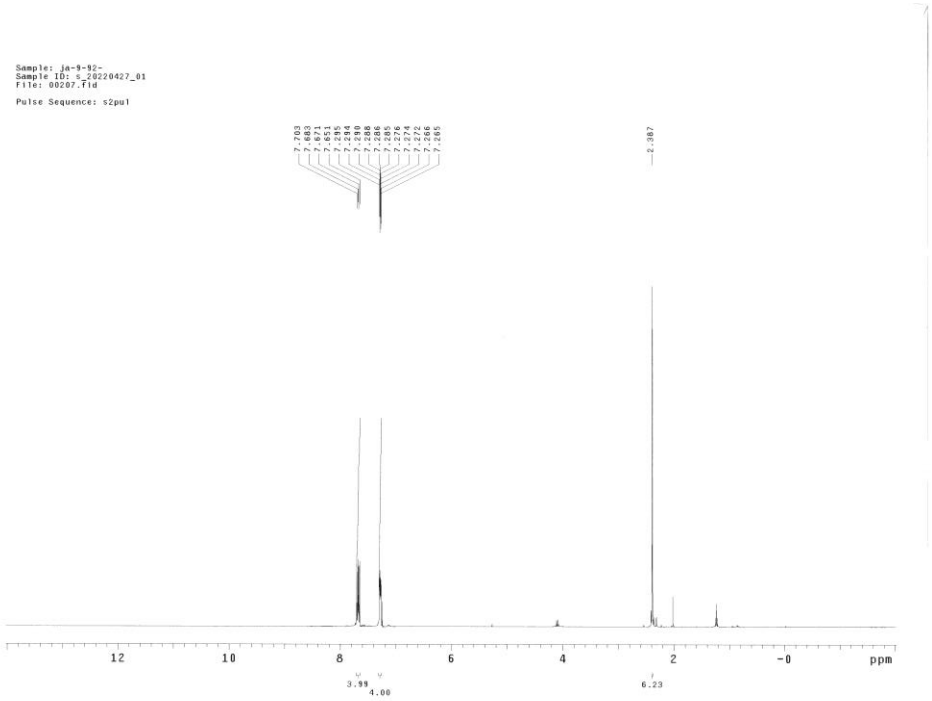

^{13}C NMR (100.5 MHz) in $CDCl_3$

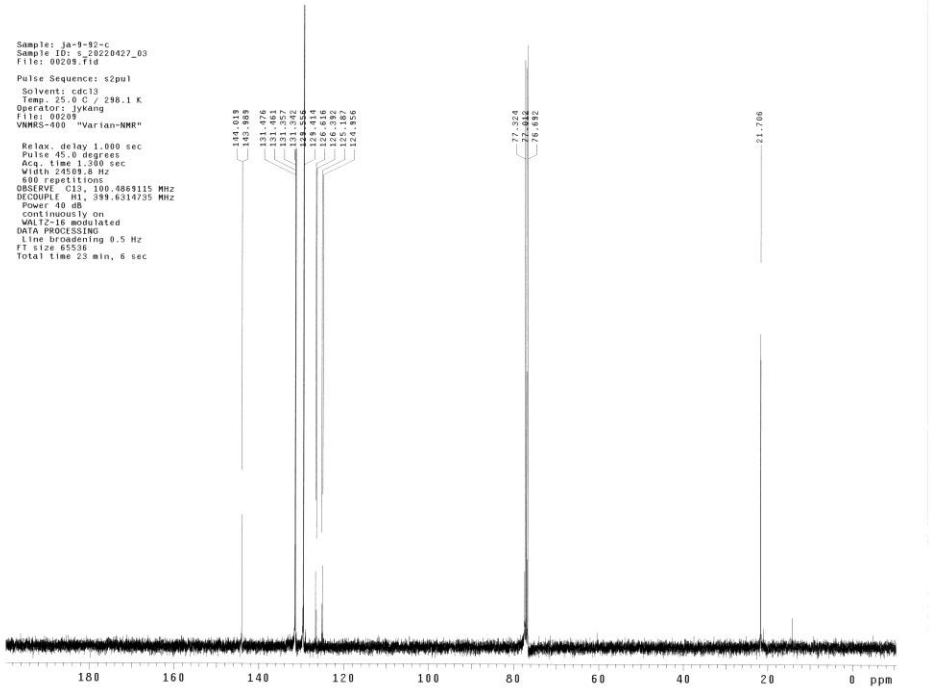

^{31}P NMR (162 MHz) in $CDCl_3$

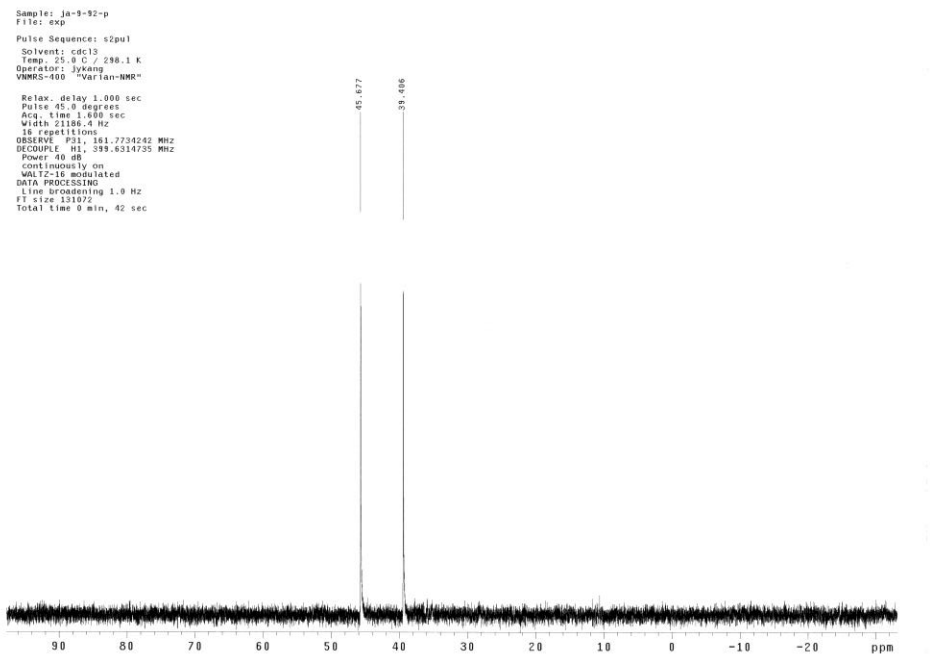

^{19}F NMR (376 MHz) in $CDCl_3$

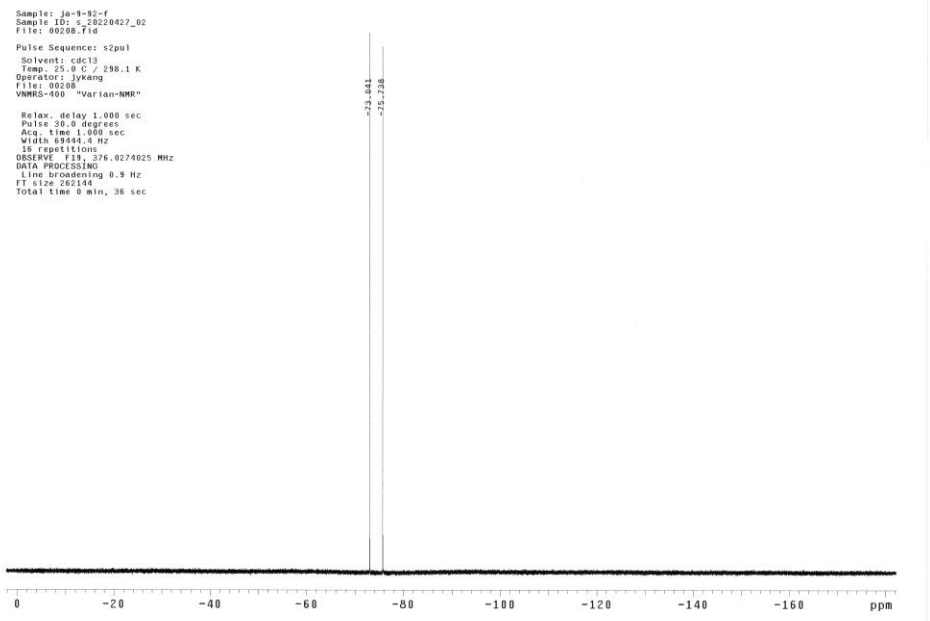

^{1}H NMR (400 MHz) in $CDCl_3$

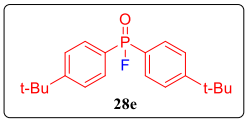

28e

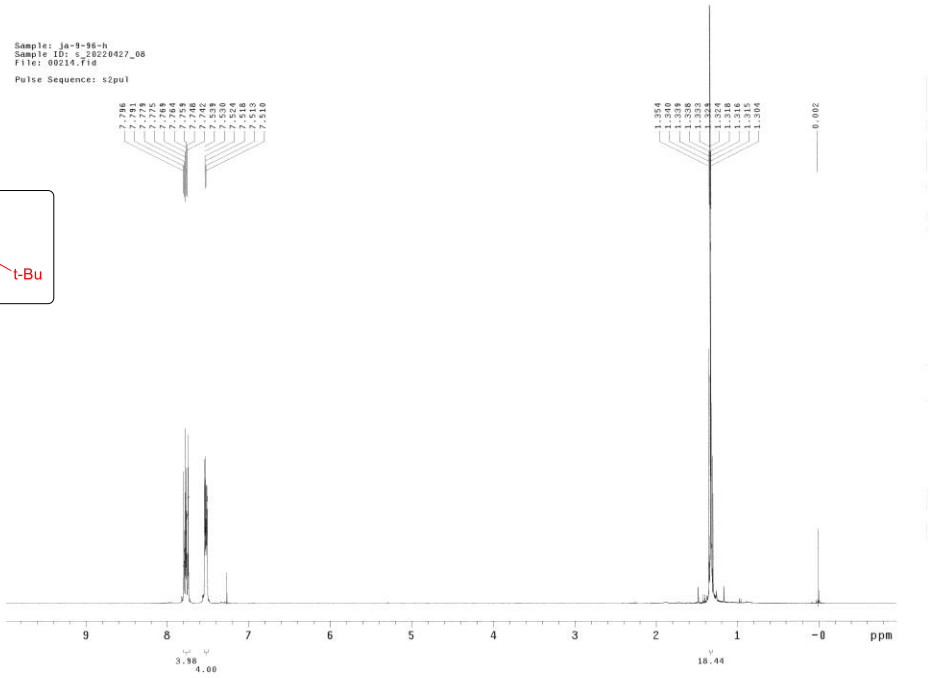

^{13}C NMR (100.5 MHz) in $CDCl_3$

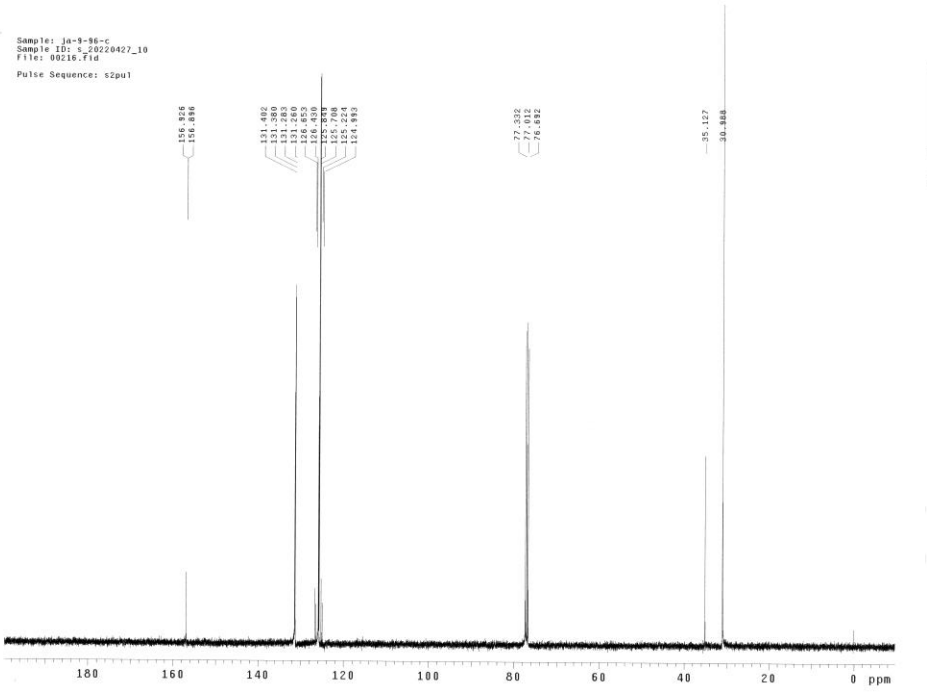

^{31}P NMR (162 MHz) in $CDCl_3$

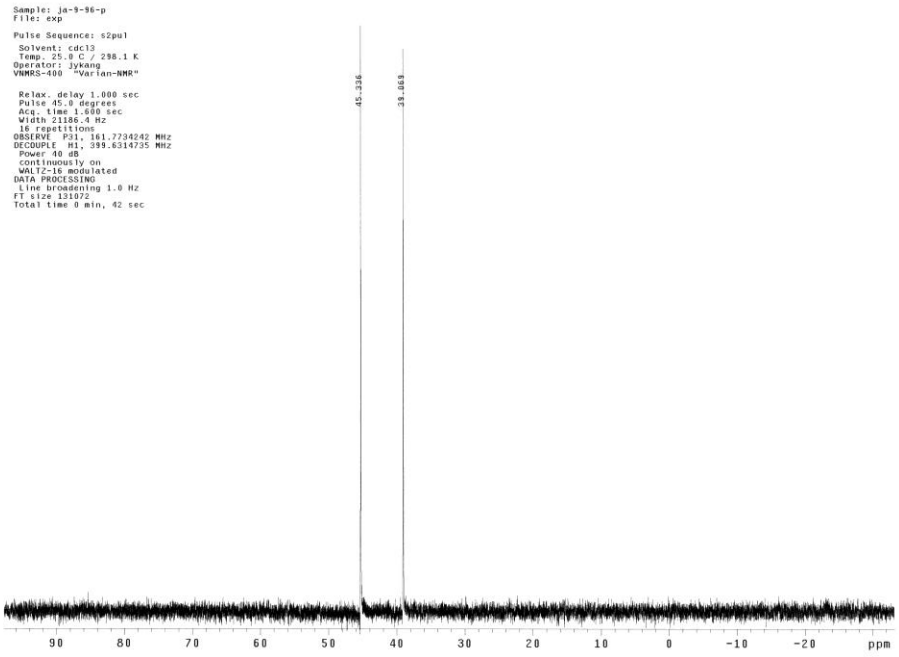

^{19}F NMR (376 MHz) in $CDCl_3$

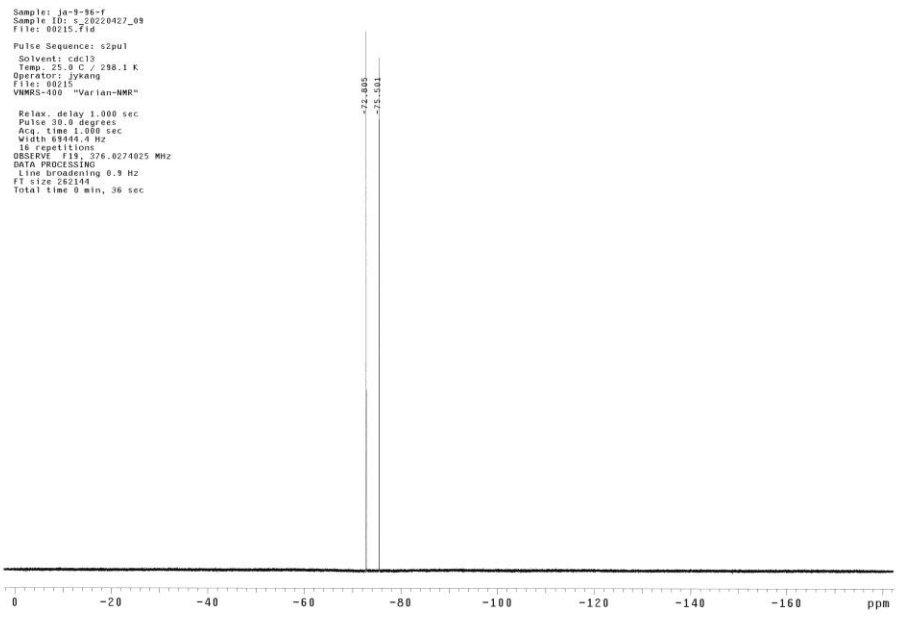

^{1}H NMR (400 MHz) in $CDCl_3$

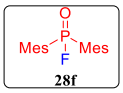

28f

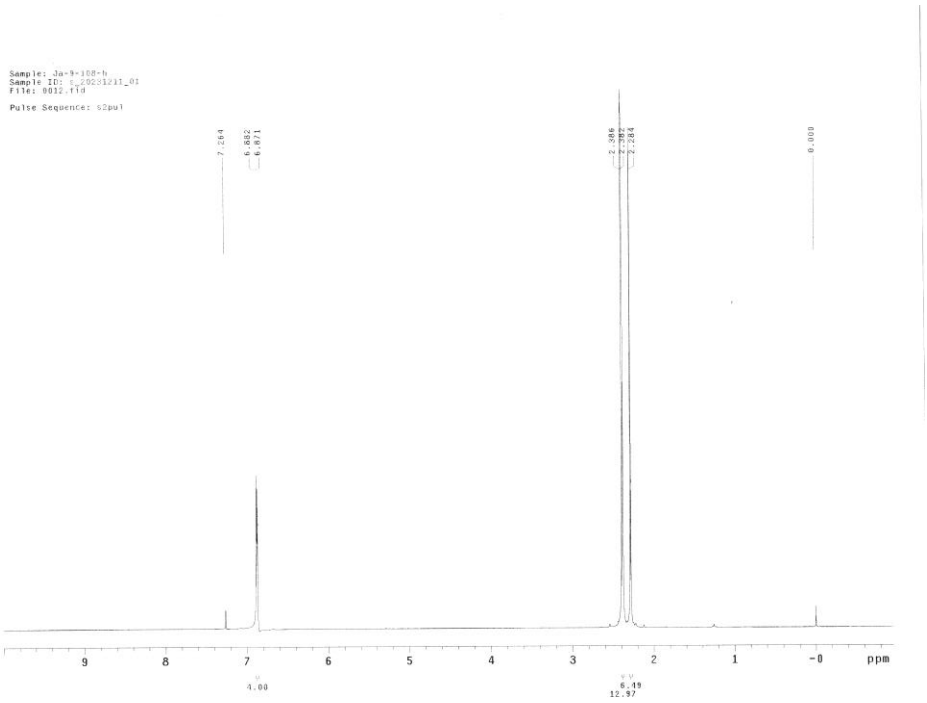

^{13}C NMR (100.5 MHz) in $CDCl_3$

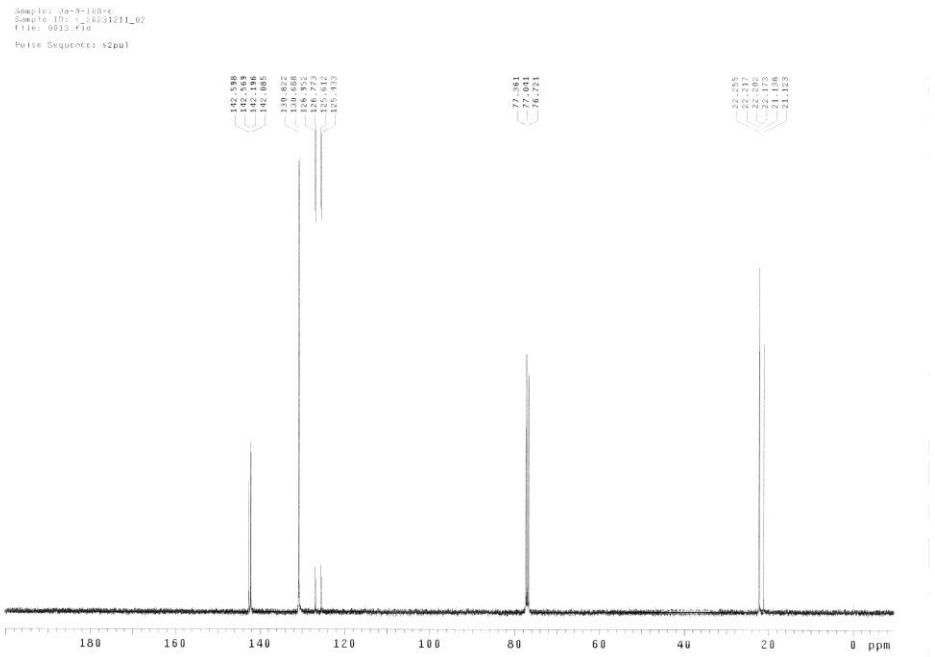

^{31}P NMR (162 MHz) in $CDCl_3$

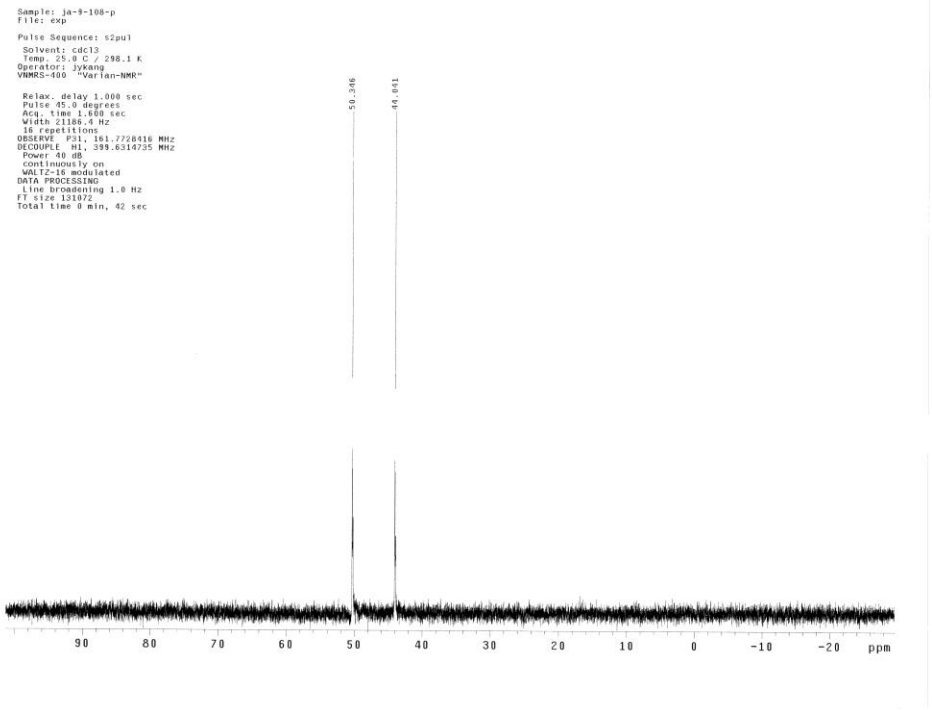

^{19}F NMR (376 MHz) in $CDCl_3$

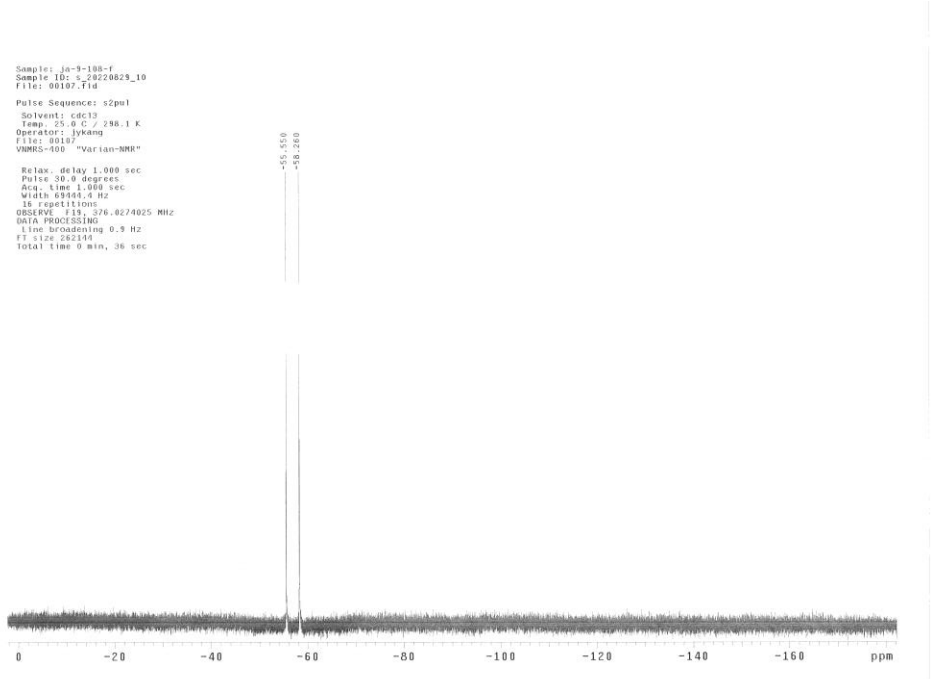

^{1}H NMR (400 MHz) in $CDCl_3$

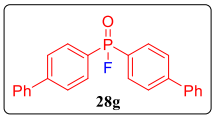

28g

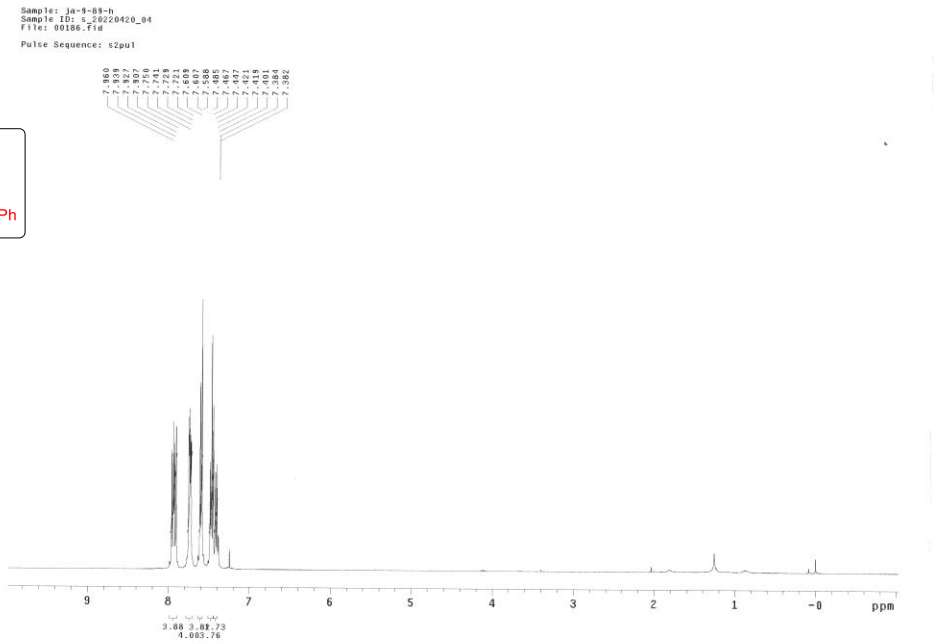

^{13}C NMR (100.5 MHz) in $CDCl_3$

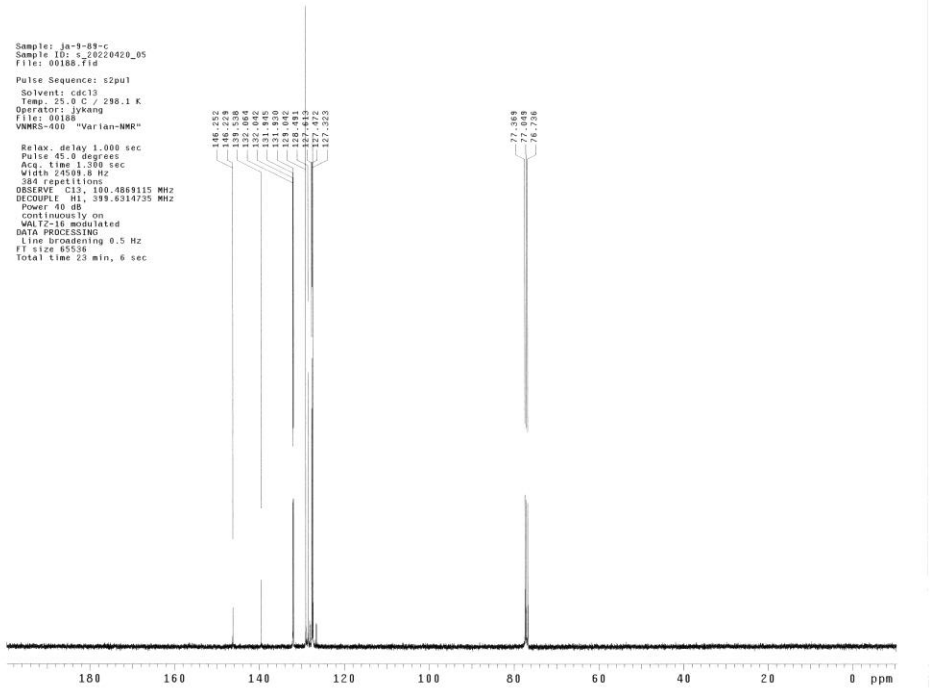

^{31}P NMR (162 MHz) in $CDCl_3$

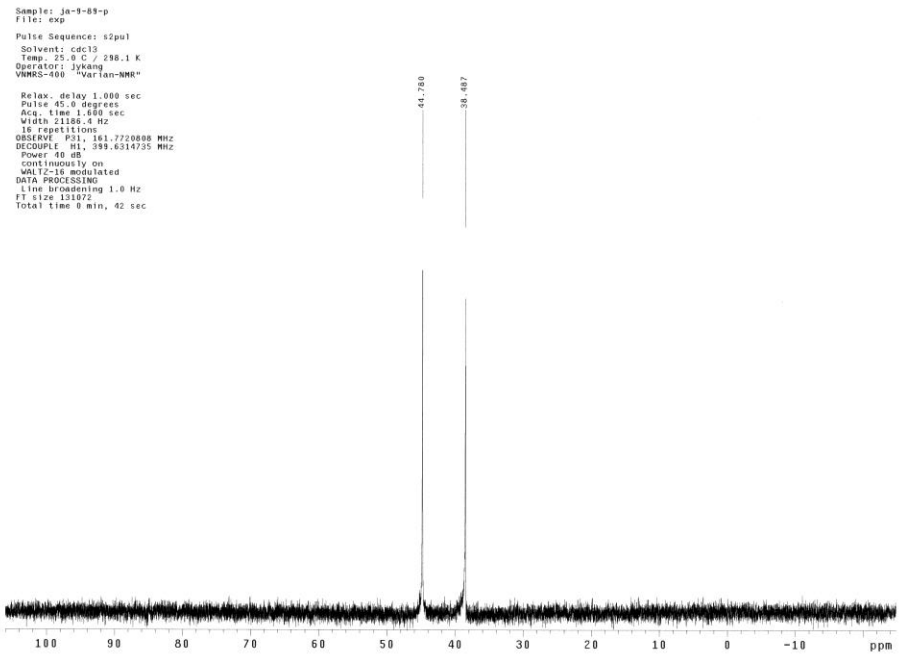

^{19}F NMR (376 MHz) in $CDCl_3$

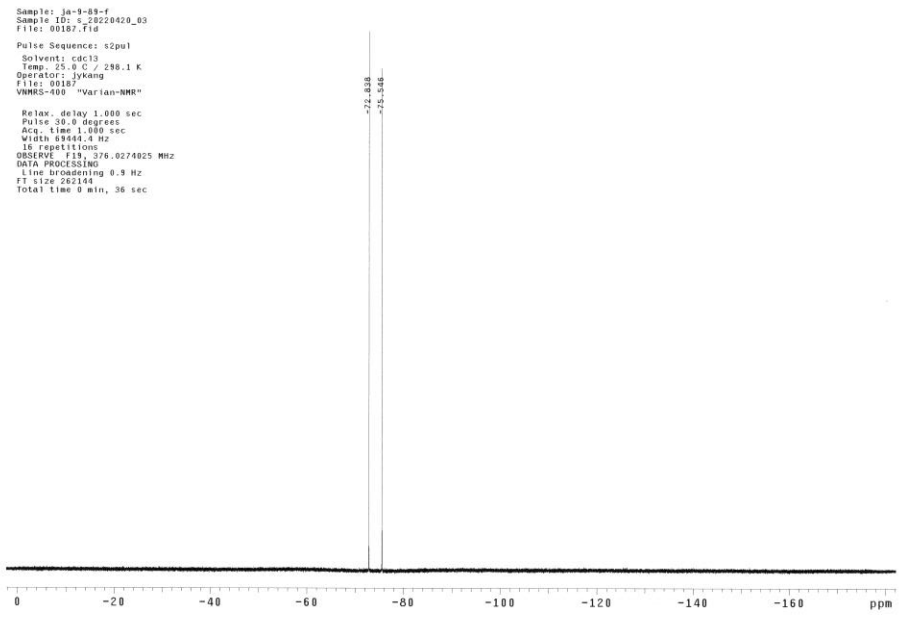

^{1}H NMR (400 MHz) in $CDCl_3$

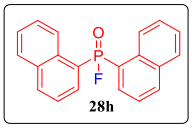

28h

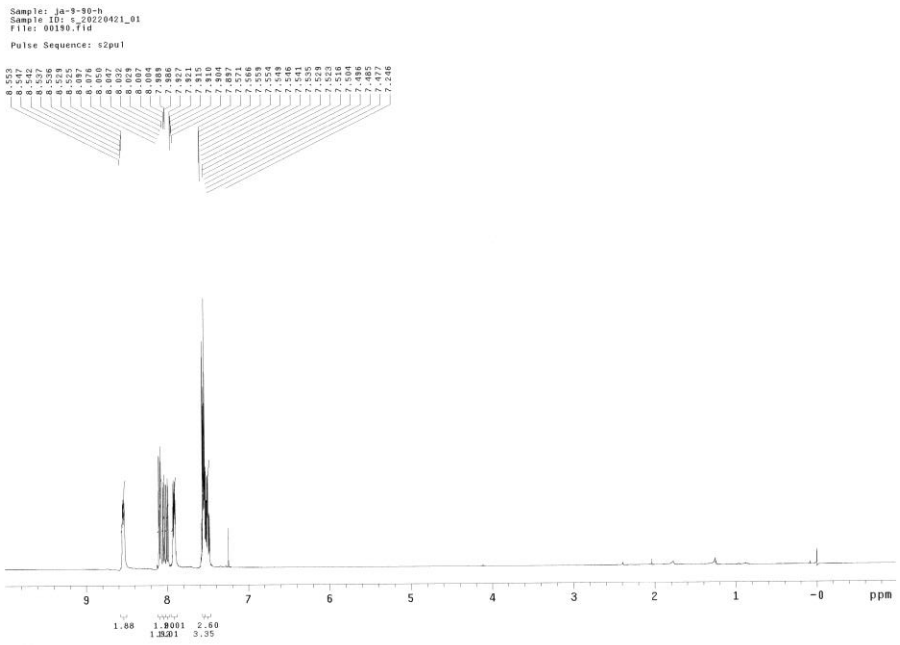

^{13}C NMR (100.5 MHz) in $CDCl_3$

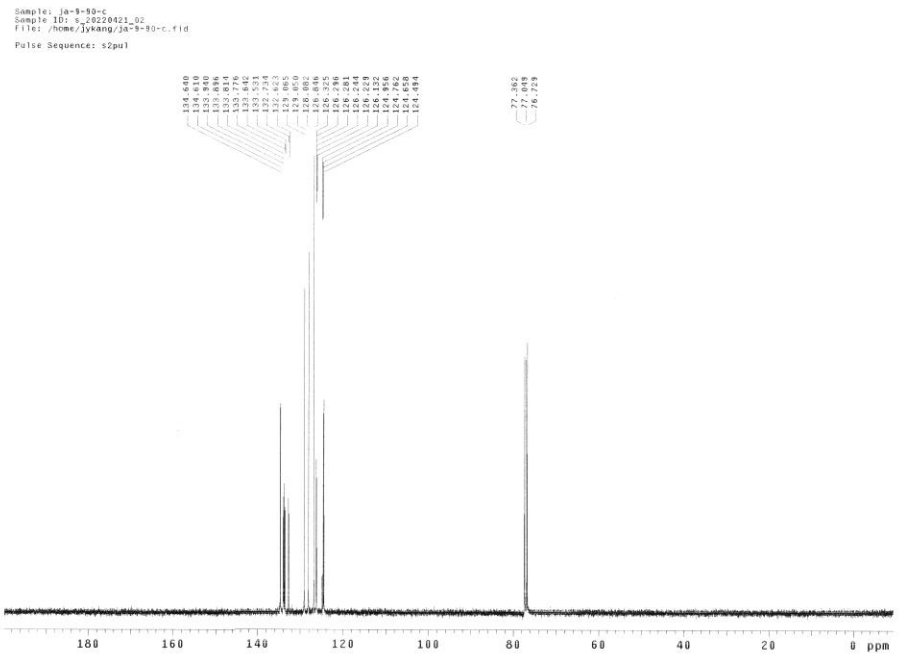

^{31}P NMR (162 MHz) in $CDCl_3$

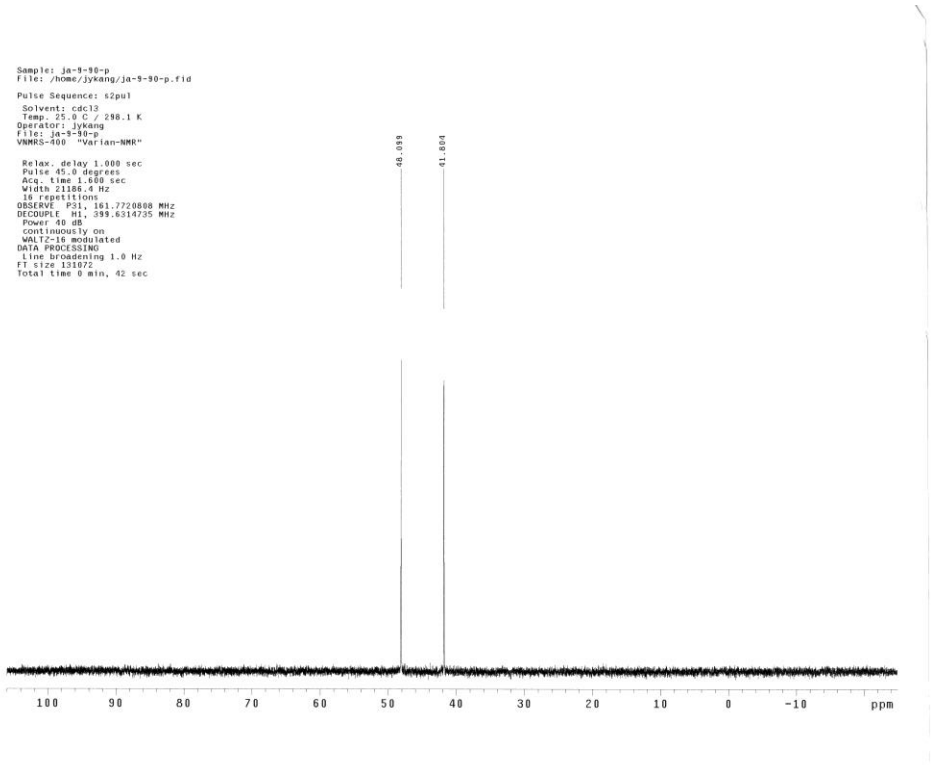

^{19}F NMR (376 MHz) in $CDCl_3$

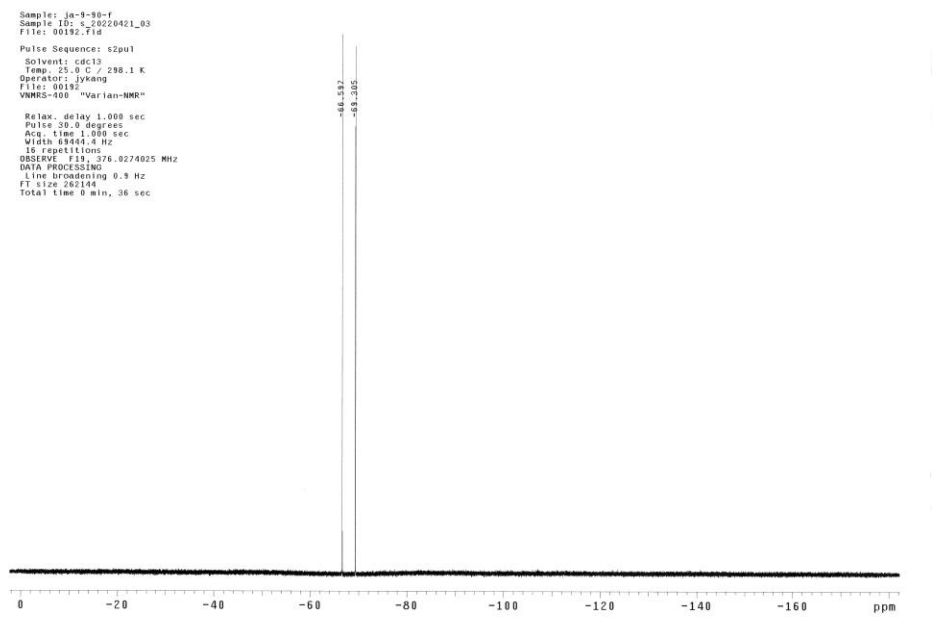

^{1}H NMR (400 MHz) in $CDCl_3$

28i

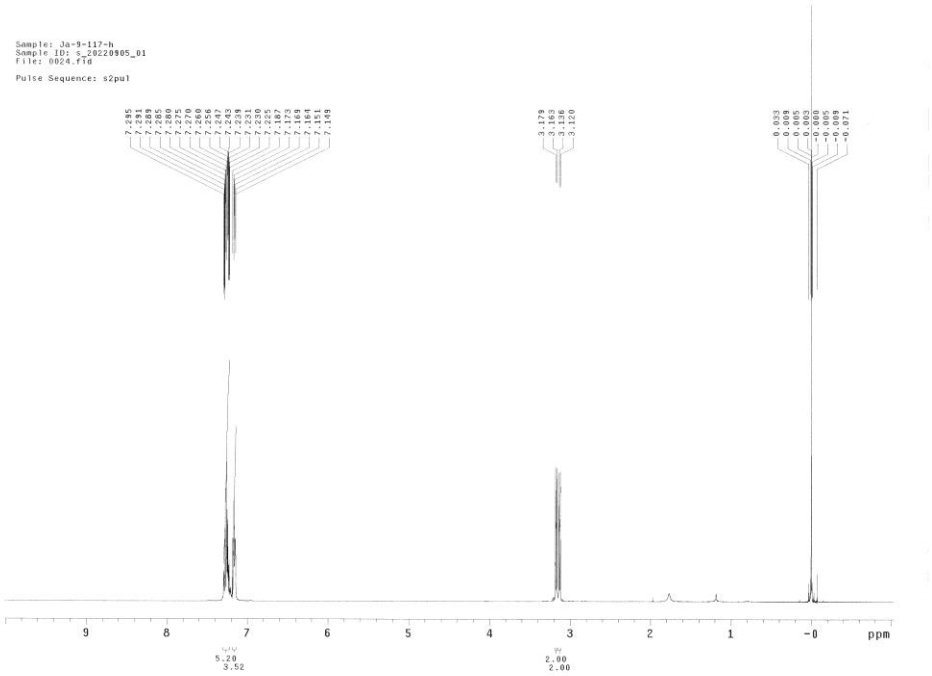

^{13}C NMR (100.5 MHz) in $CDCl_3$

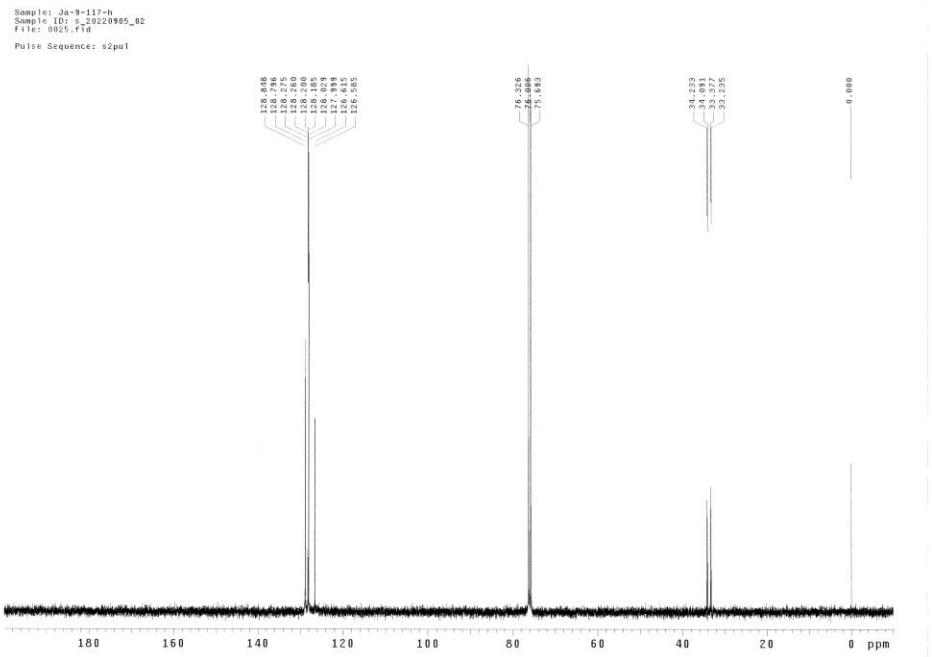

^{31}P NMR (162 MHz) in $CDCl_3$

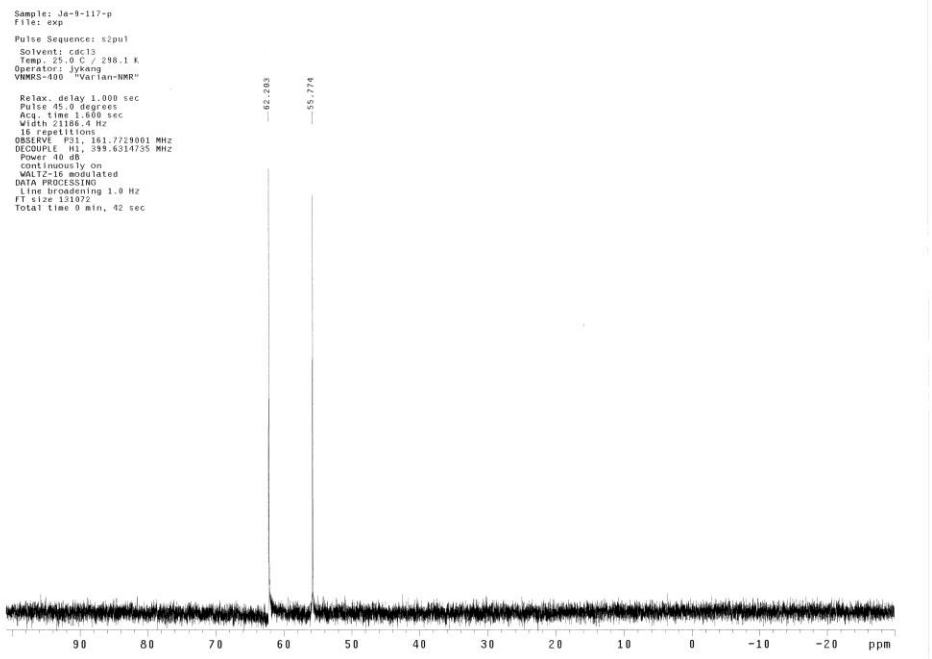

^{19}F NMR (376 MHz) in $CDCl_3$

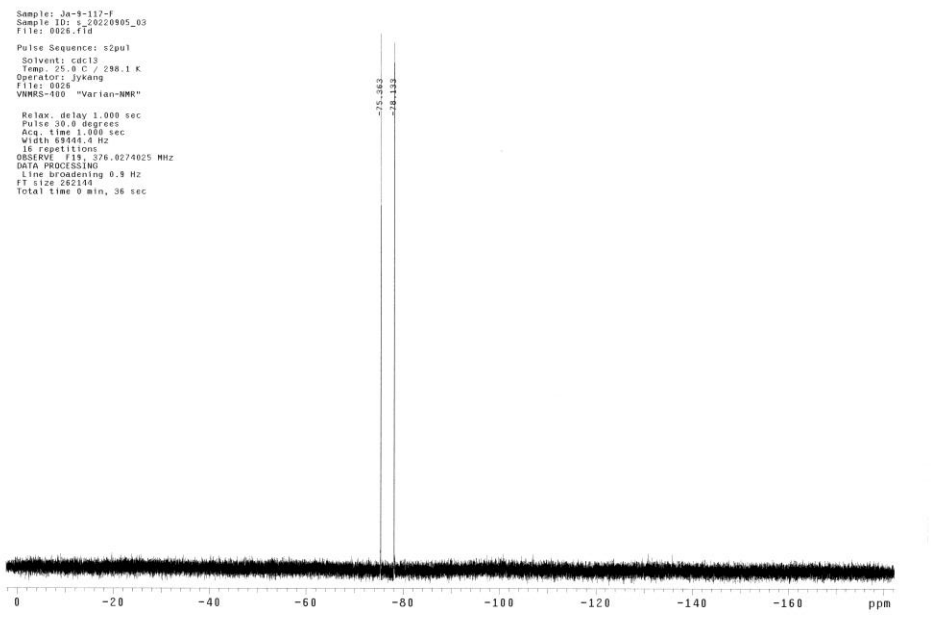

^{1}H NMR (400 MHz) in $CDCl_3$

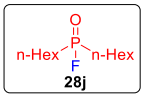

28j

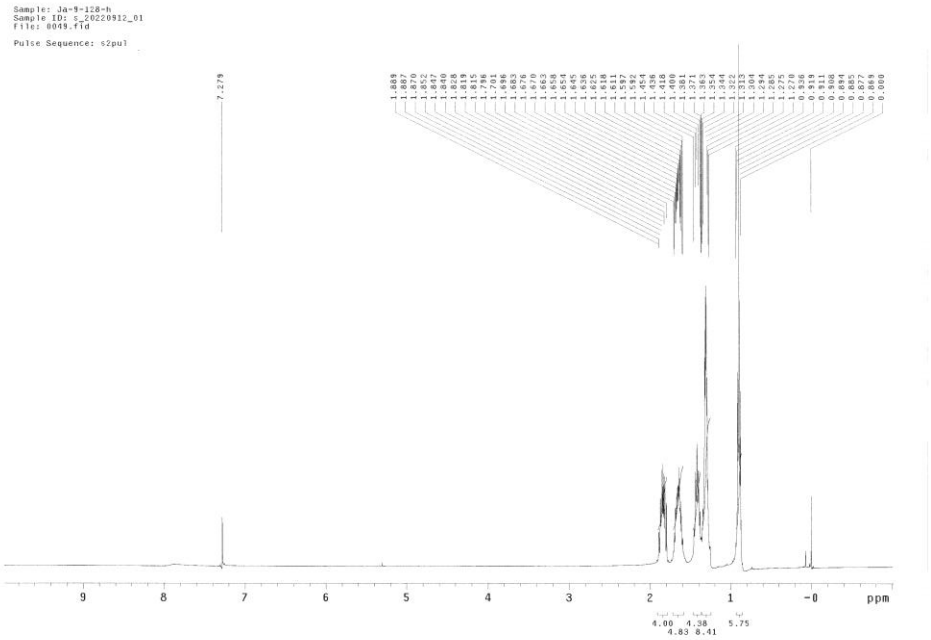

^{13}C NMR (100.5 MHz) in $CDCl_3$

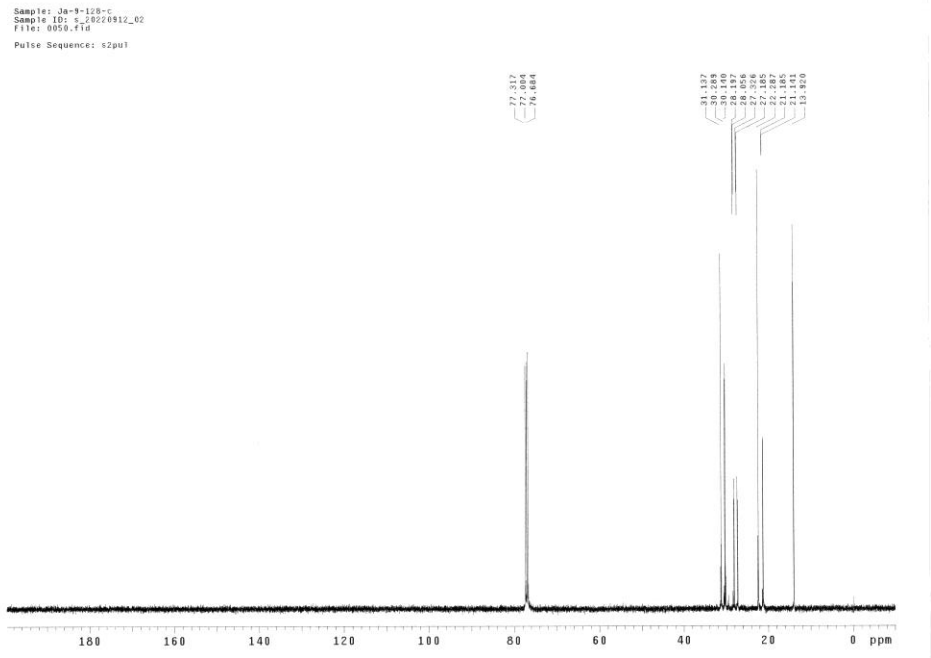

^{31}P NMR (162 MHz) in $CDCl_3$

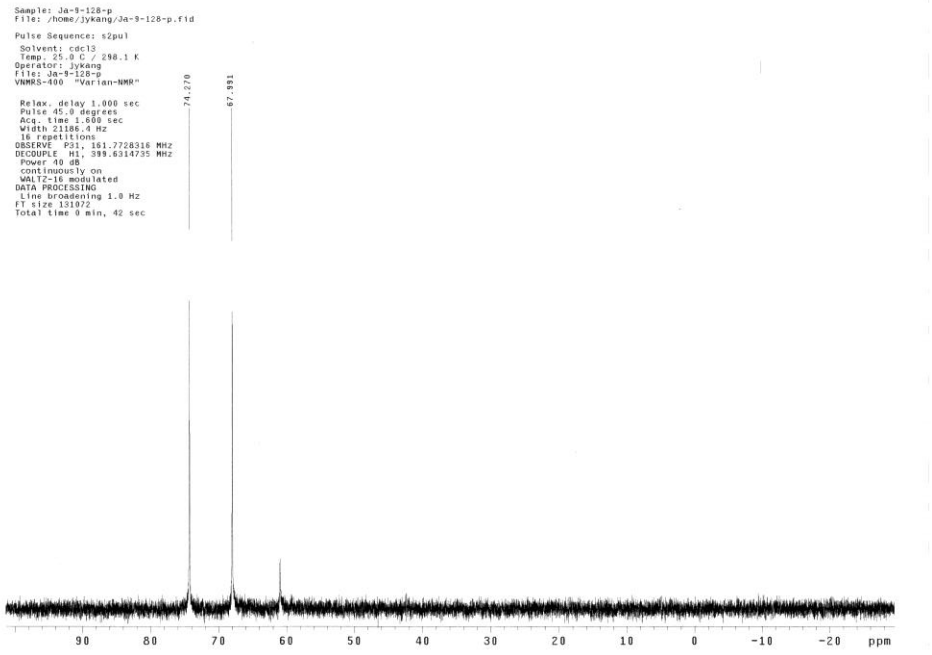

^{19}F NMR (376 MHz) in $CDCl_3$

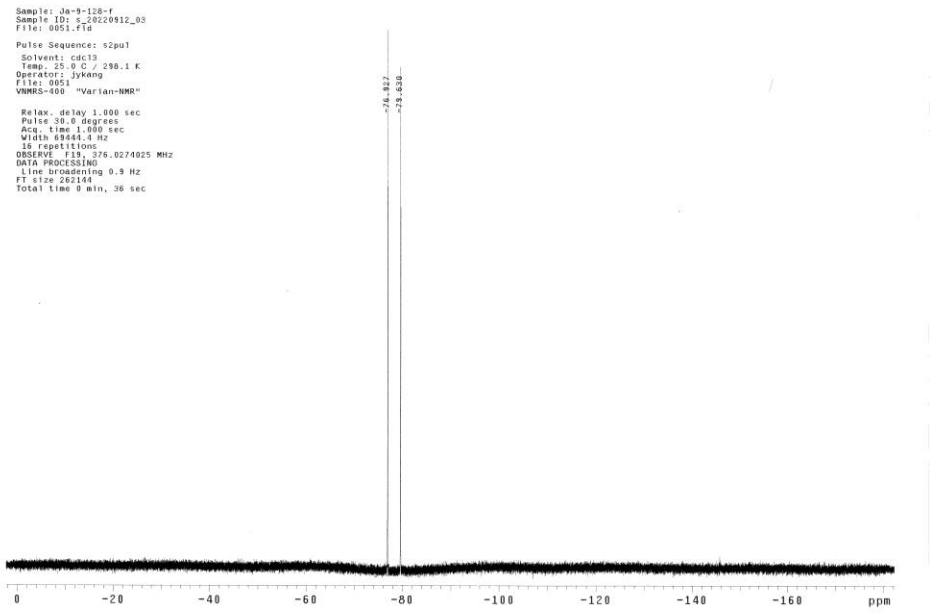

^{1}H NMR (400 MHz) in $CDCl_3$

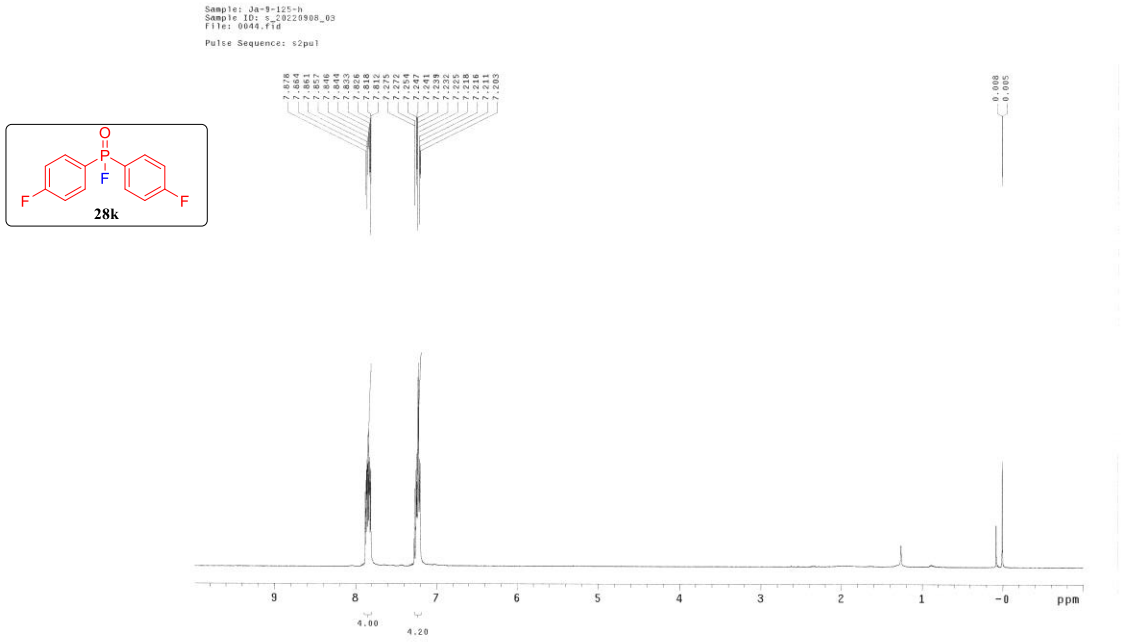

^{13}C NMR (100.5 MHz) in $CDCl_3$

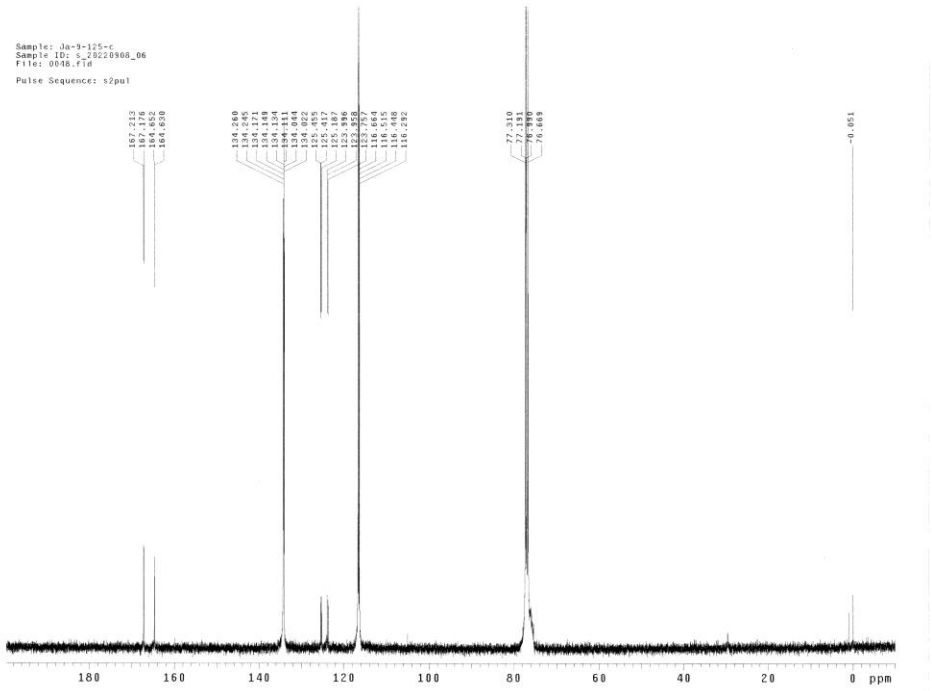

^{31}P NMR (162 MHz) in $CDCl_3$

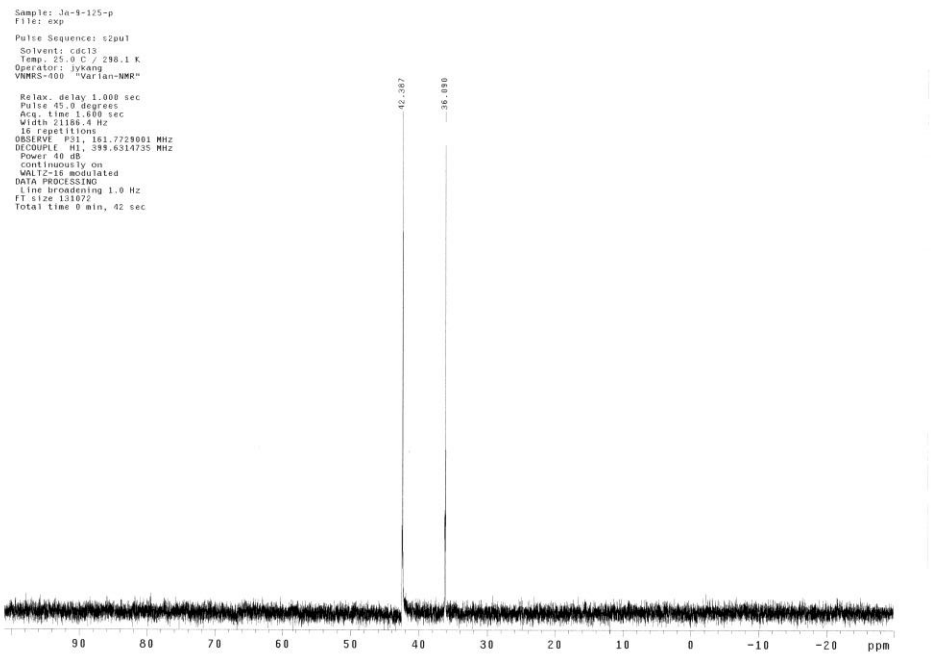

^{19}F NMR (376 MHz) in $CDCl_3$

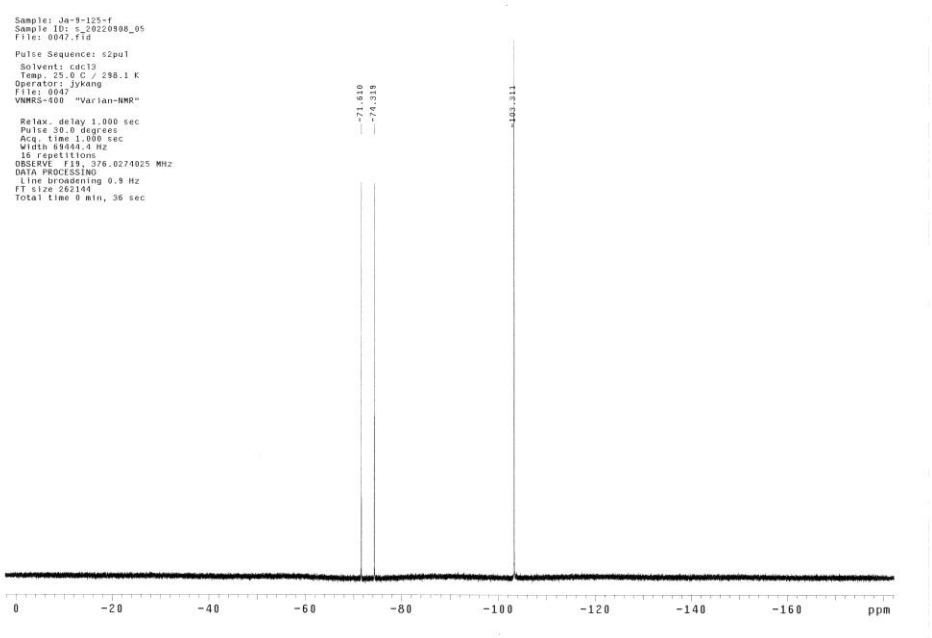

^{1}H NMR (400 MHz) in $CDCl_3$

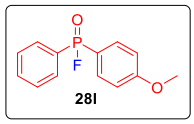

28l

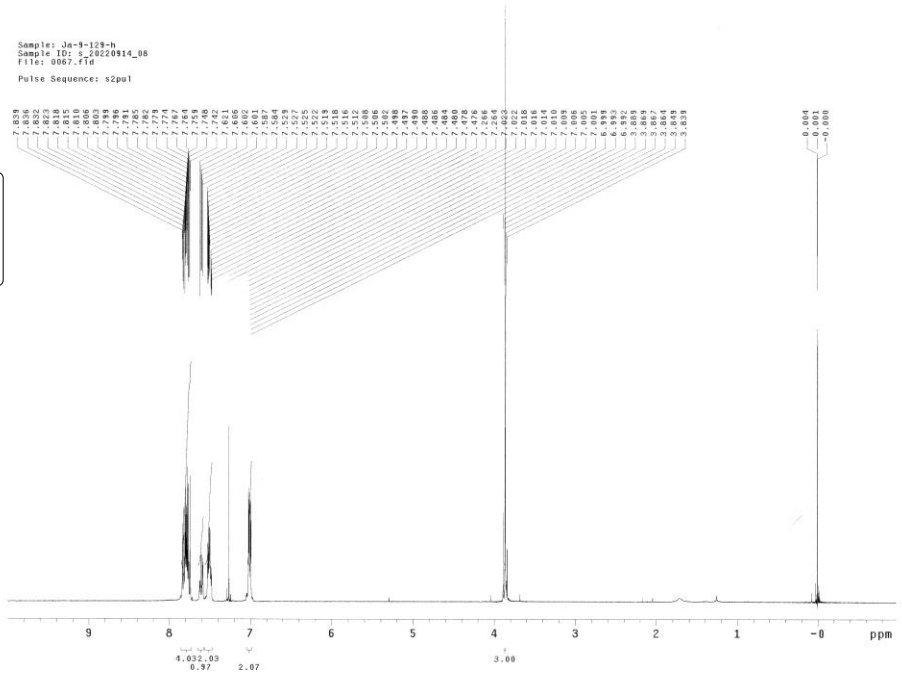

^{13}C NMR (100.5 MHz) in $CDCl_3$

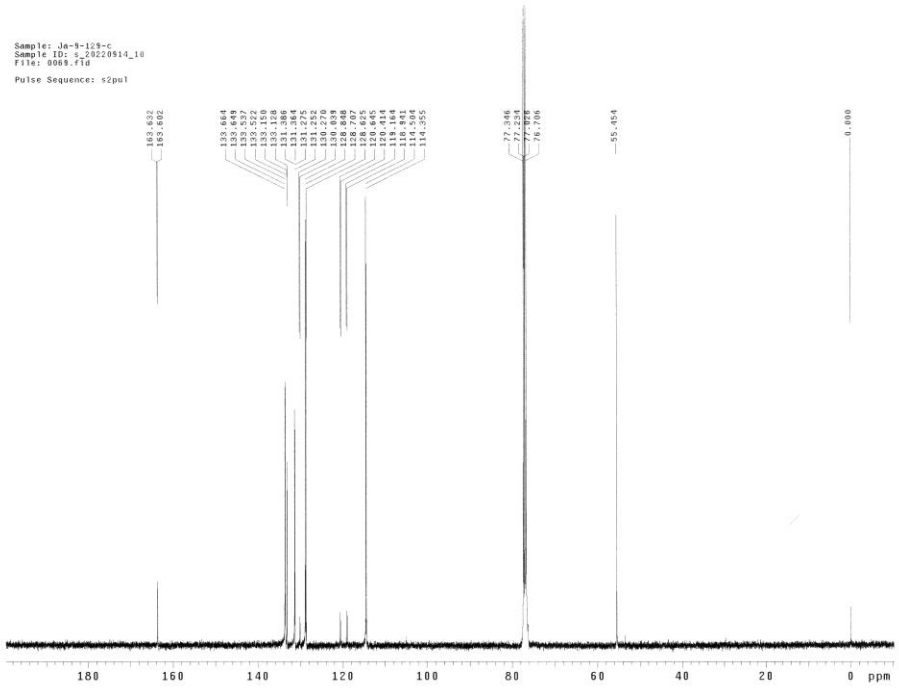

^{31}P NMR (162 MHz) in $CDCl_3$

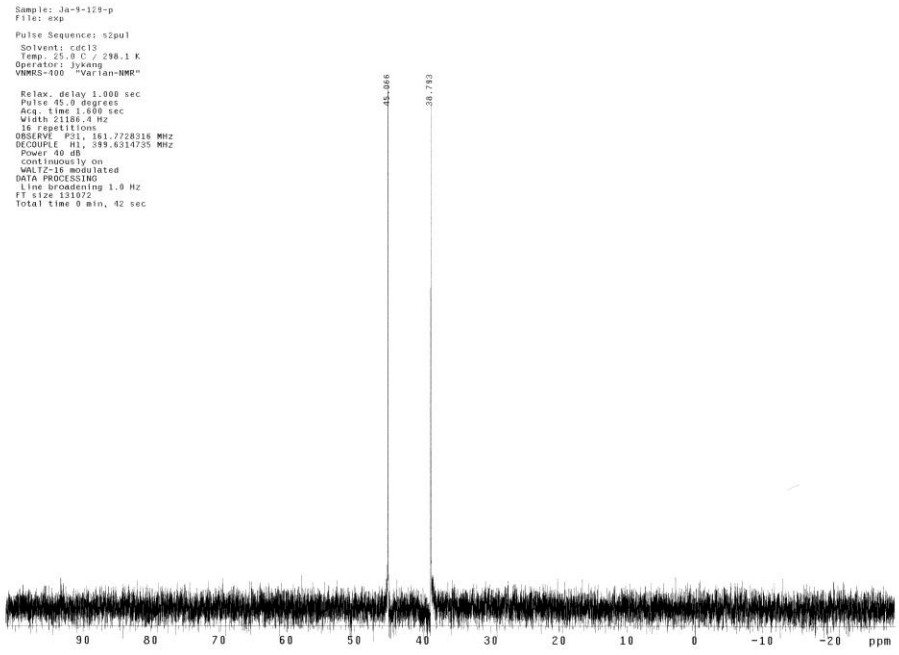

^{19}F NMR (376 MHz) in $CDCl_3$

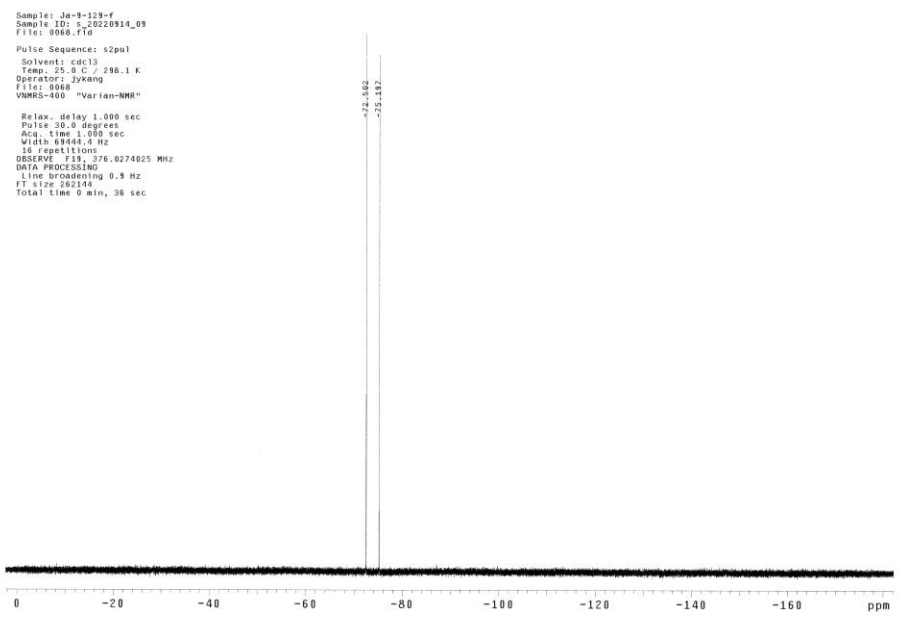

^{1}H NMR (400 MHz) in $CDCl_3$

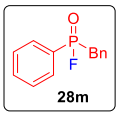

28m

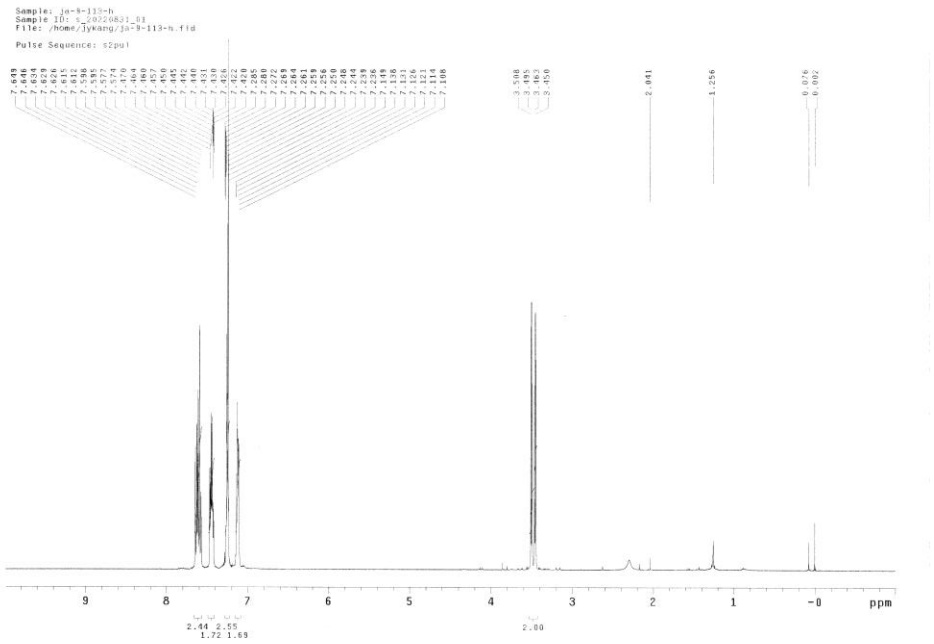

^{13}C NMR (100.5 MHz) in $CDCl_3$

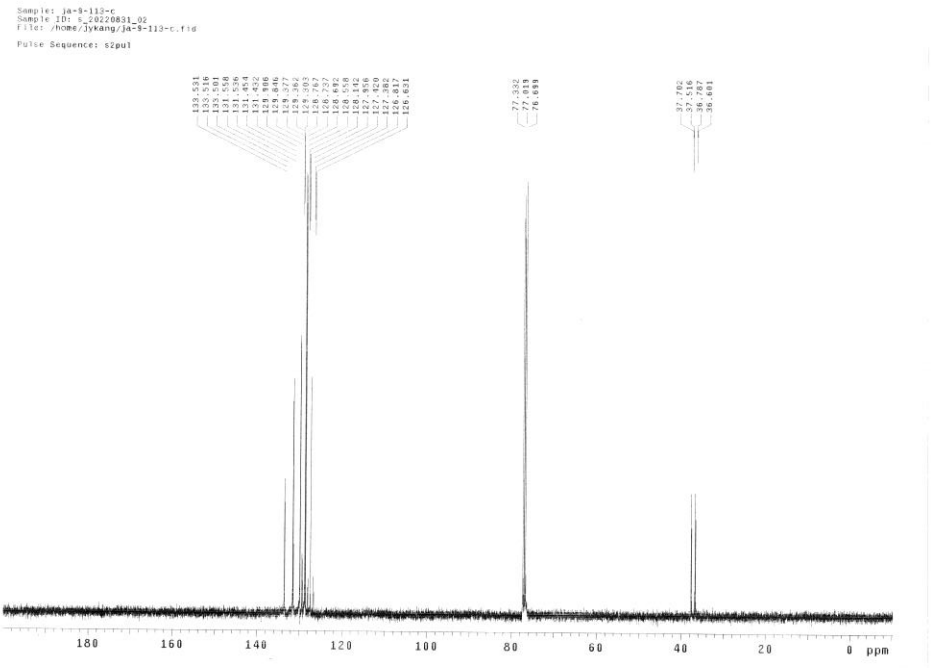

^{31}P NMR (162 MHz) in $CDCl_3$

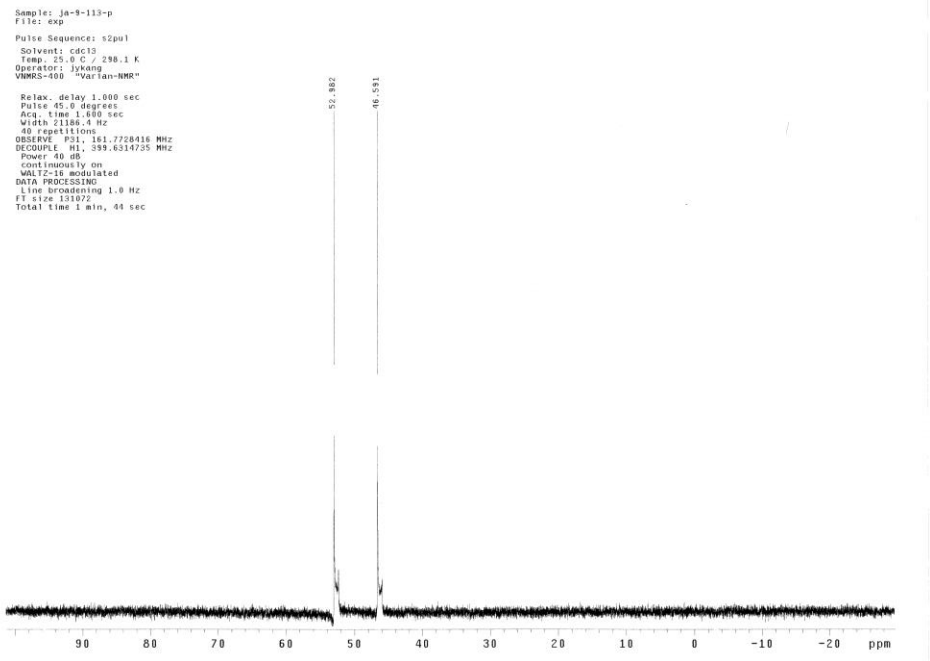

^{19}F NMR (376 MHz) in $CDCl_3$

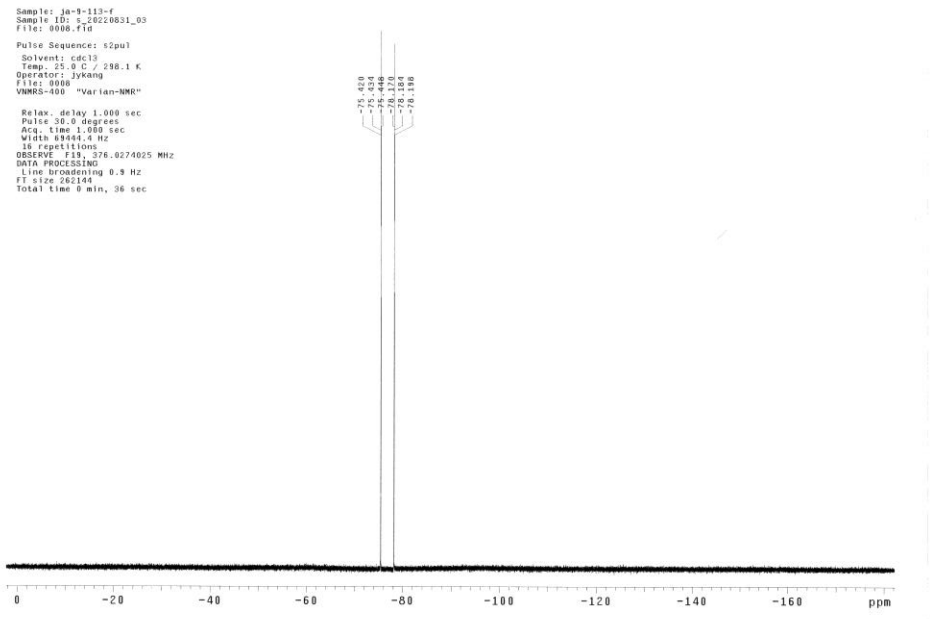

^{1}H NMR (400 MHz) in $CDCl_3$

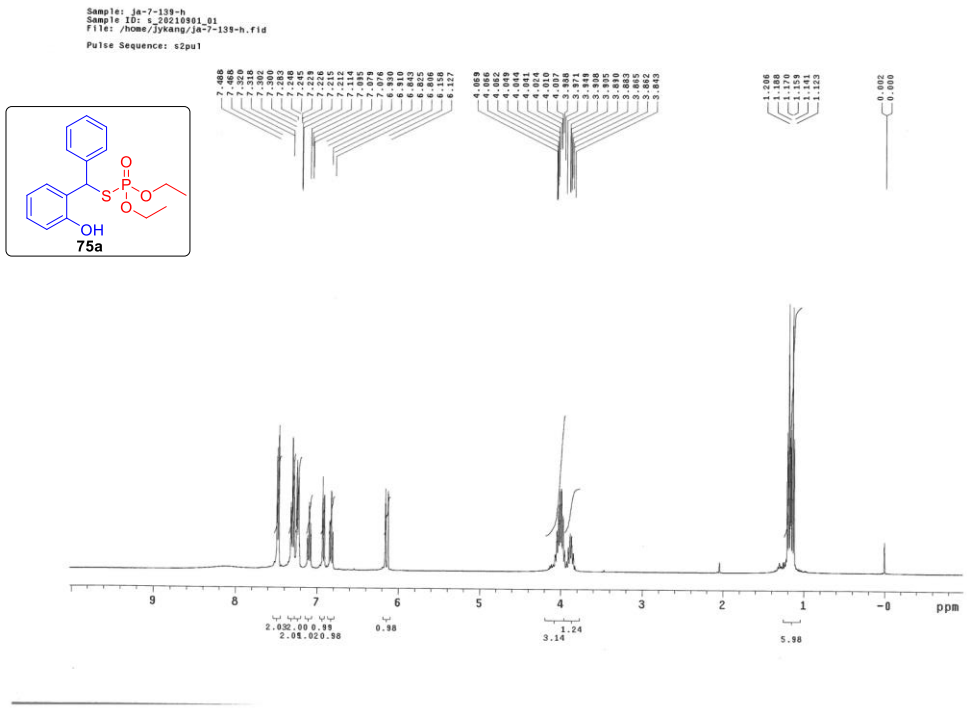

^{13}C NMR (100.5 MHz) in $CDCl_3$

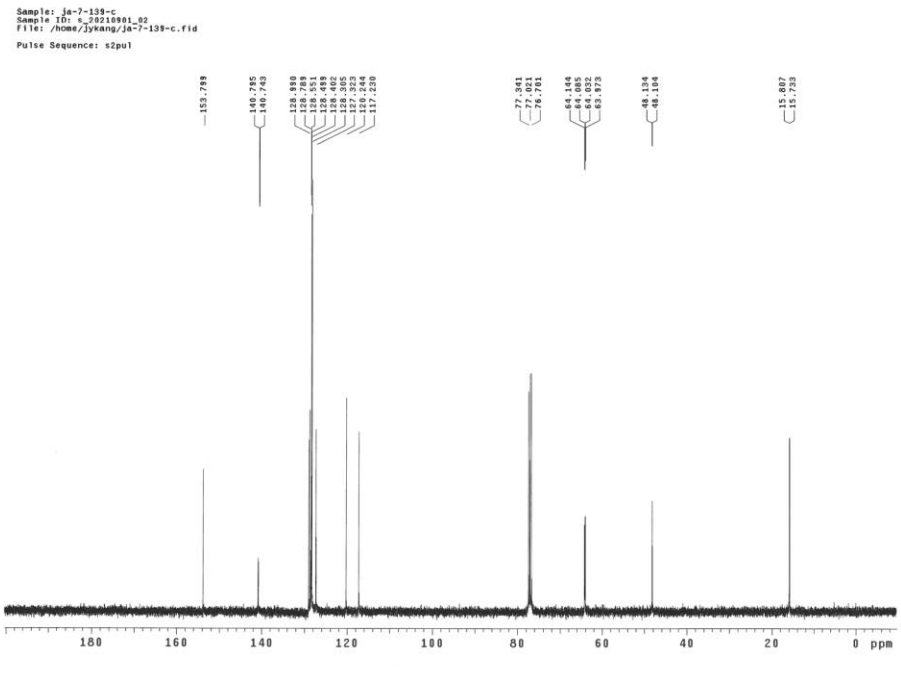

^{31}P NMR (162 MHz) in $CDCl_3$

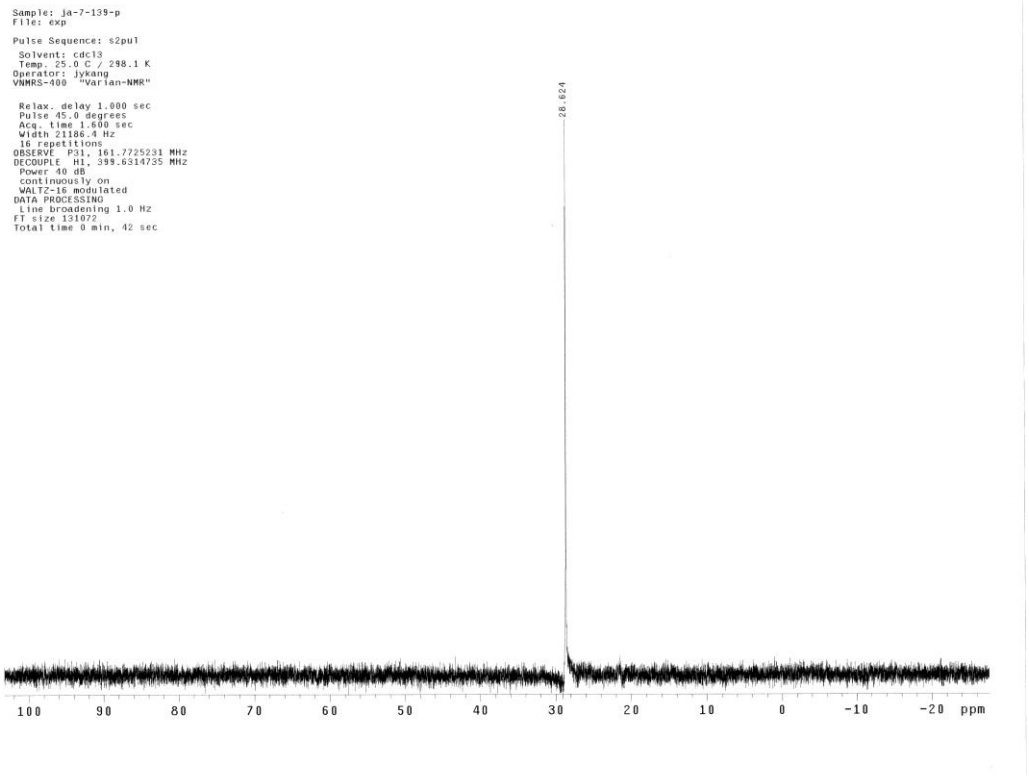

^{1}H NMR (400 MHz) in $CDCl_3$

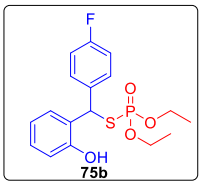

75b

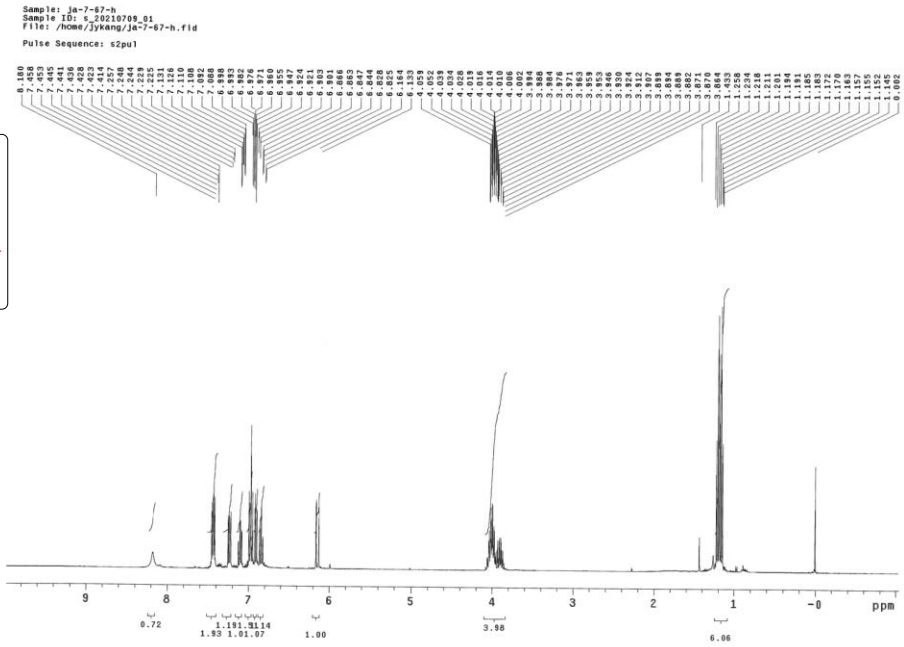

^{13}C NMR (100.5 MHz) in $CDCl_3$

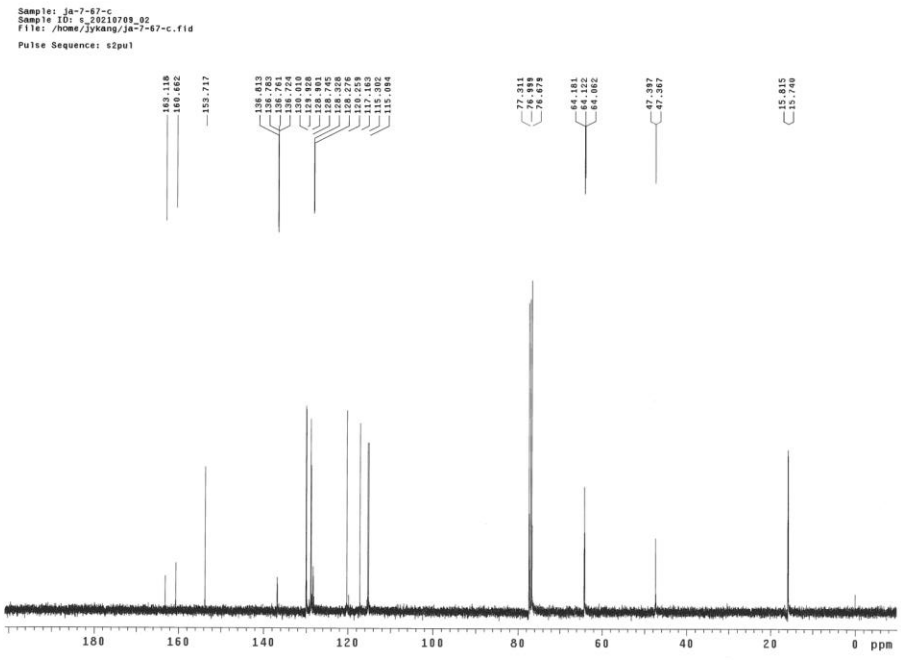

^{31}P NMR (162 MHz) in $CDCl_3$

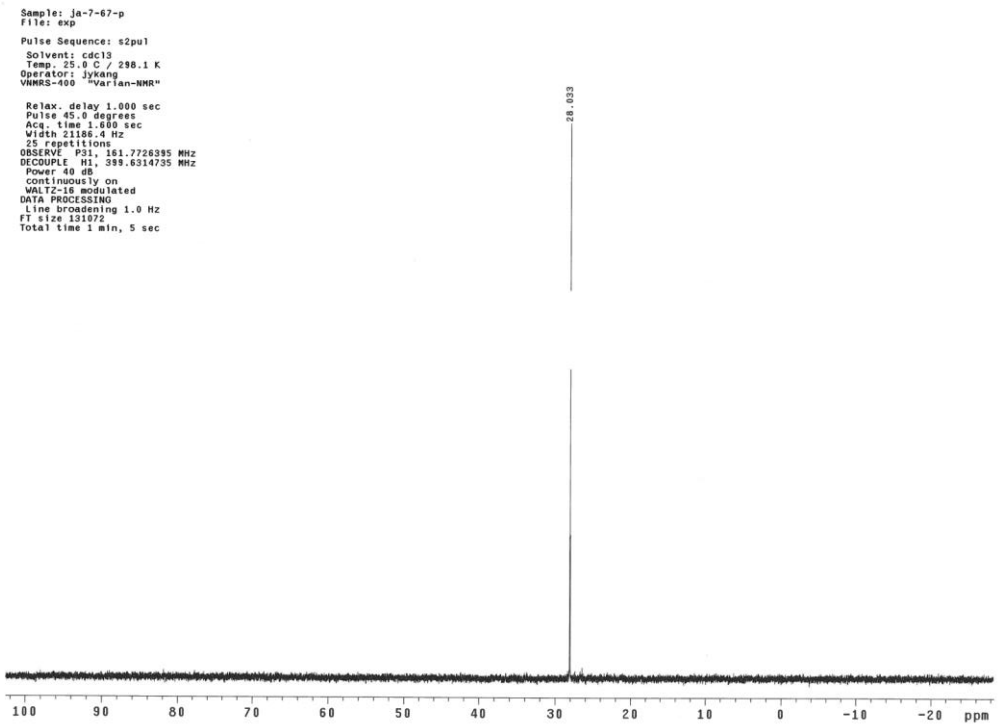

^{1}H NMR (400 MHz) in $CDCl_3$

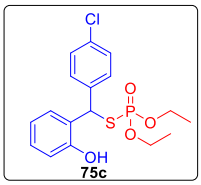

75c

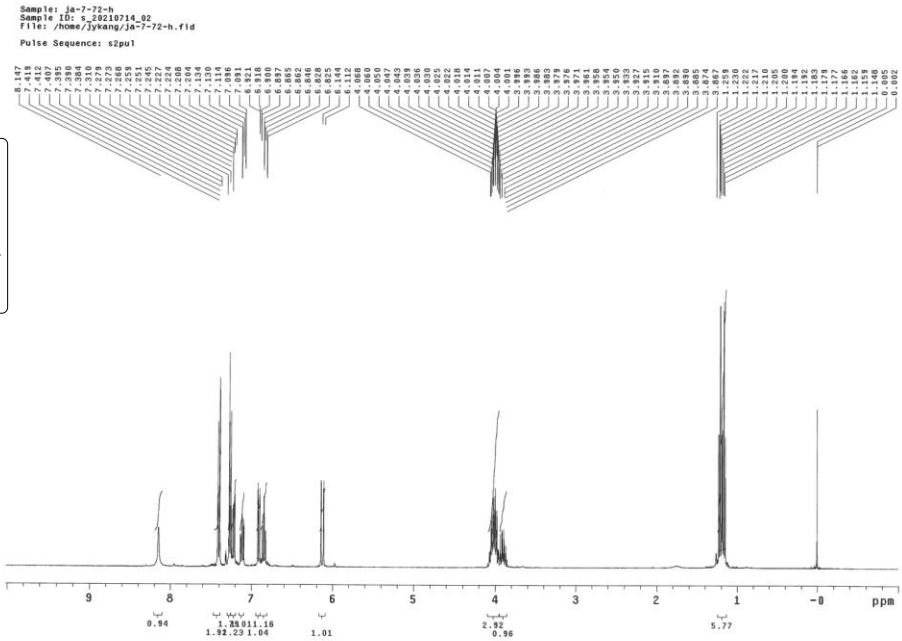

^{13}C NMR (100.5 MHz) in $CDCl_3$

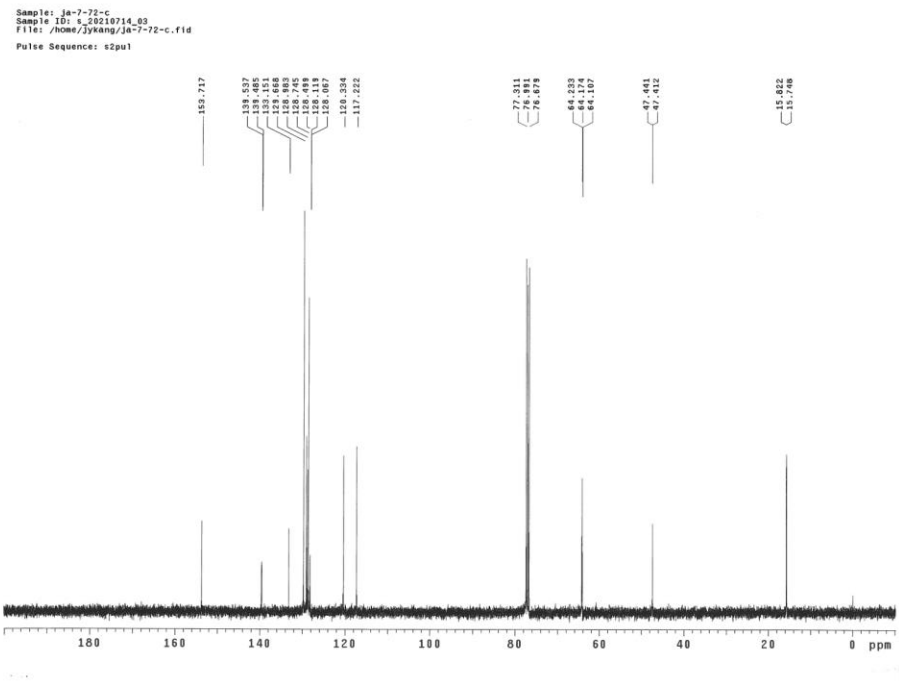

^{31}P NMR (162 MHz) in $CDCl_3$

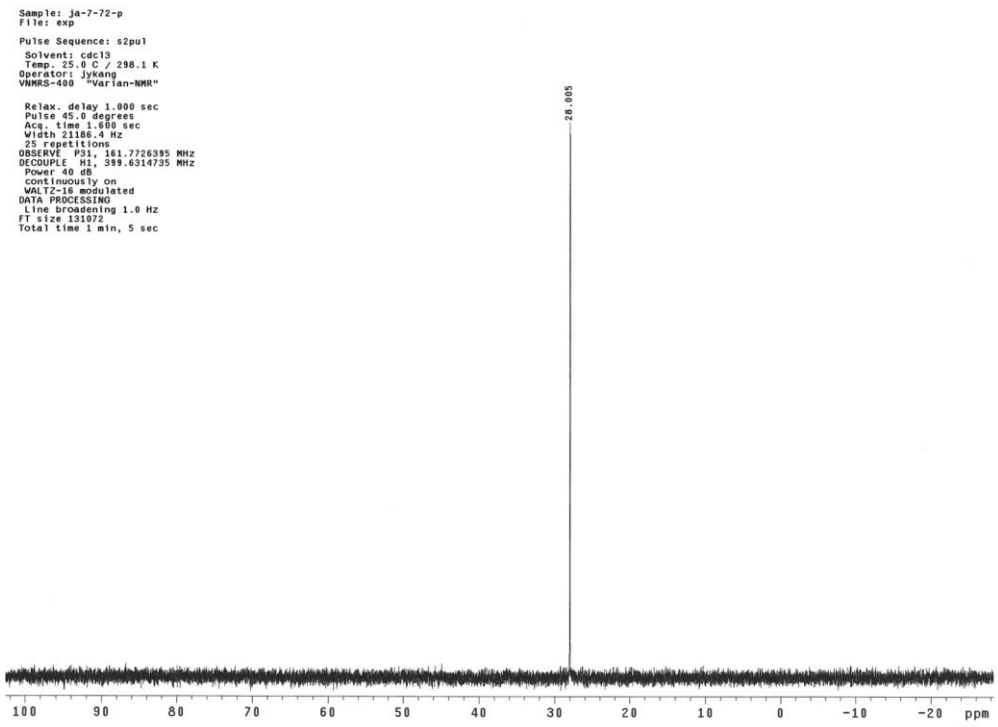

^{1}H NMR (400 MHz) in $CDCl_3$

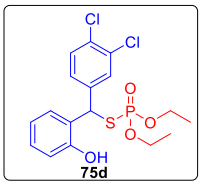

75d

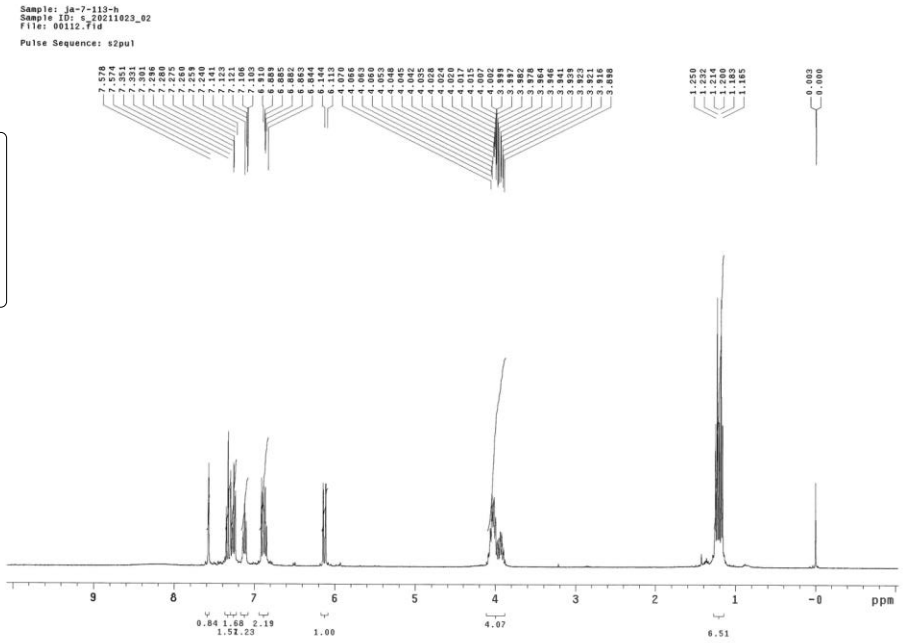

^{13}C NMR (100.5 MHz) in $CDCl_3$

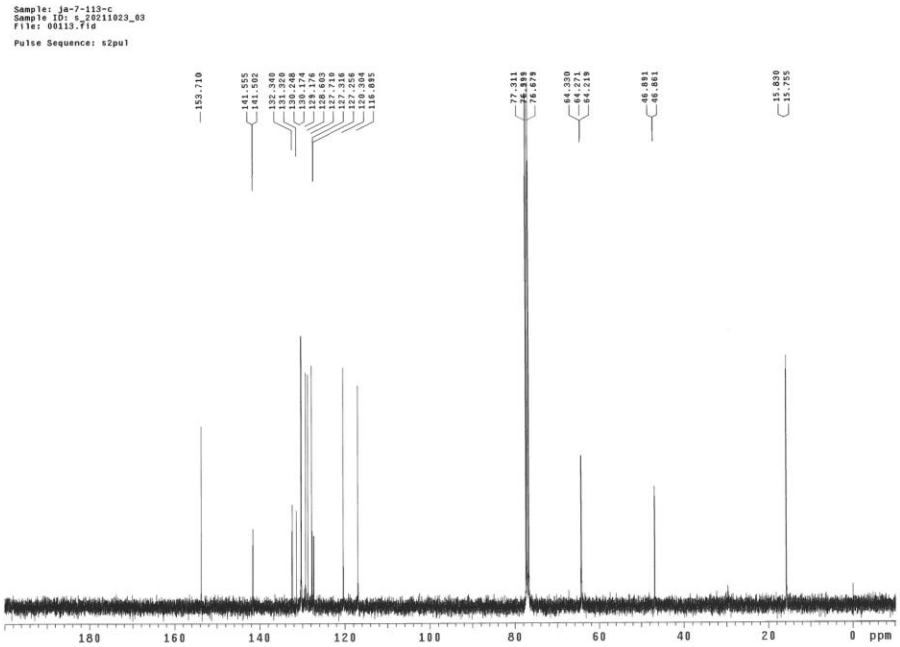

^{31}P NMR (162 MHz) in $CDCl_3$

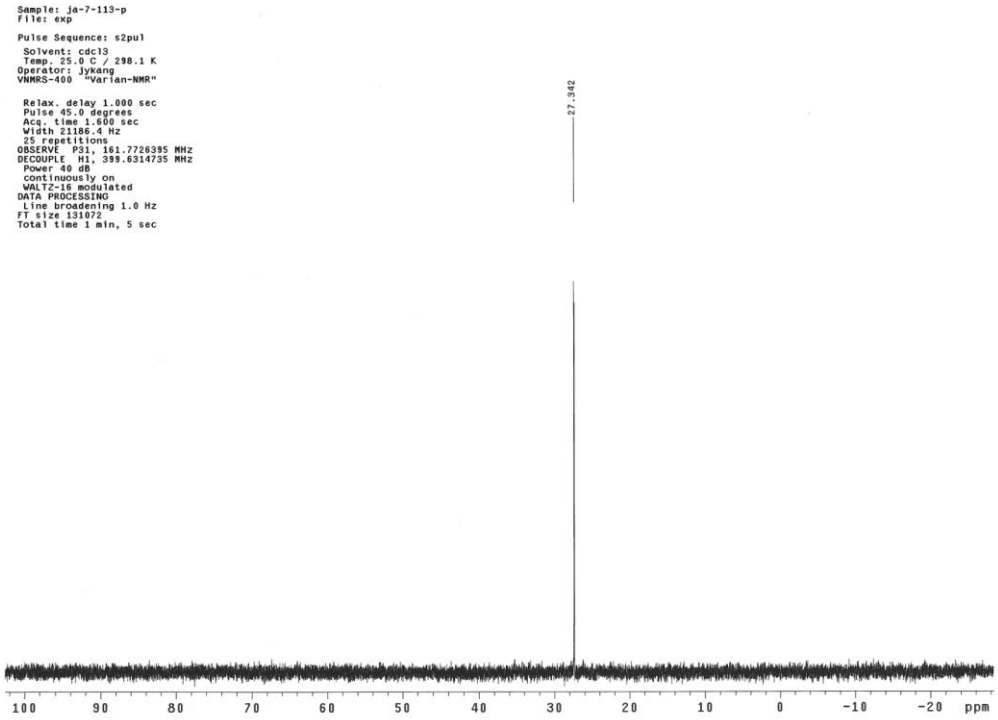

^{1}H NMR (400 MHz) in $CDCl_3$

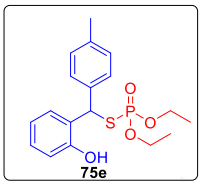

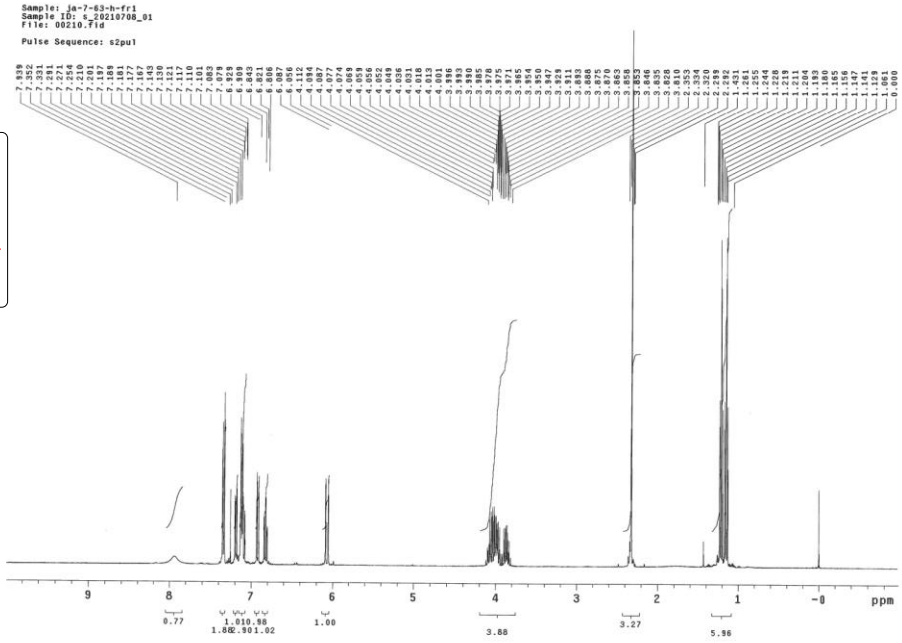

^{13}C NMR (100.5 MHz) in $CDCl_3$

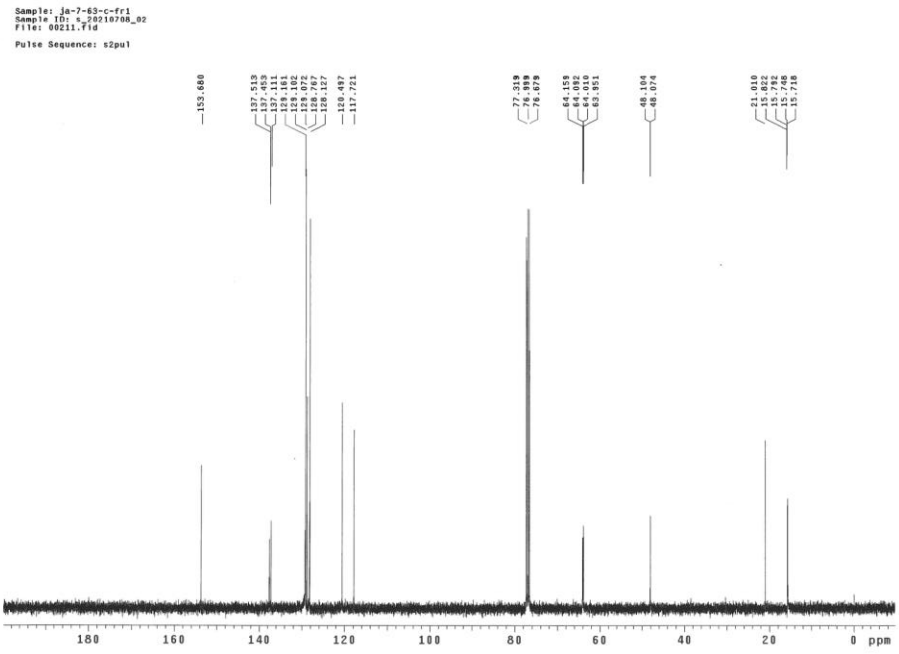

^{31}P NMR (162 MHz) in $CDCl_3$

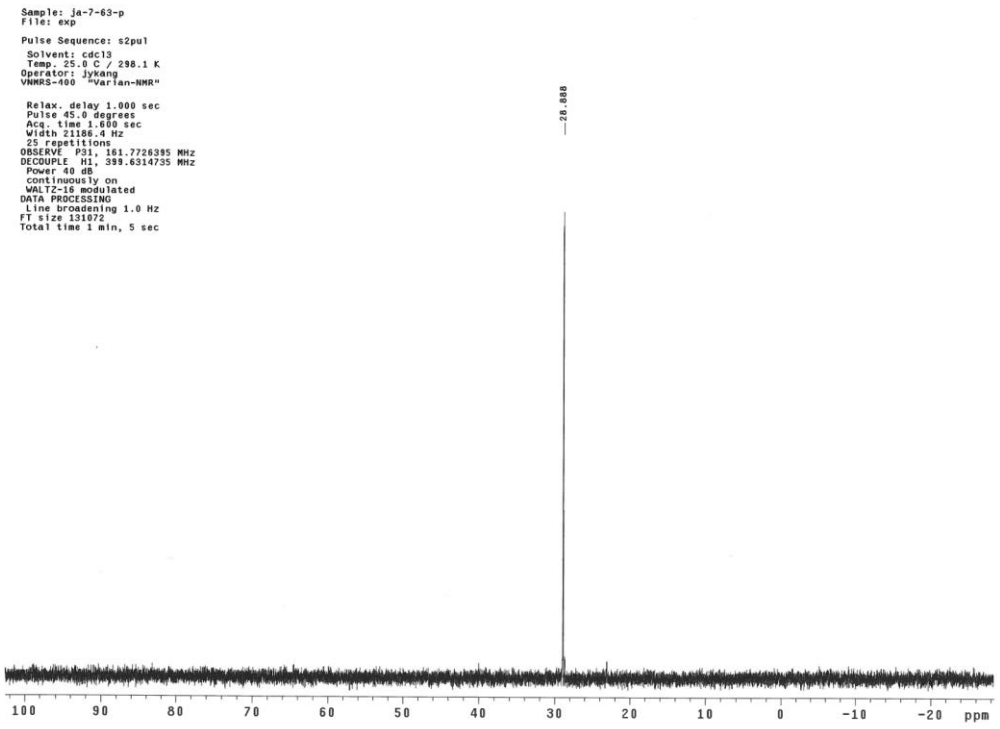

^{1}H NMR (400 MHz) in $CDCl_3$

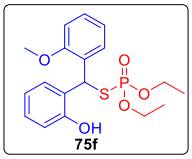

75f

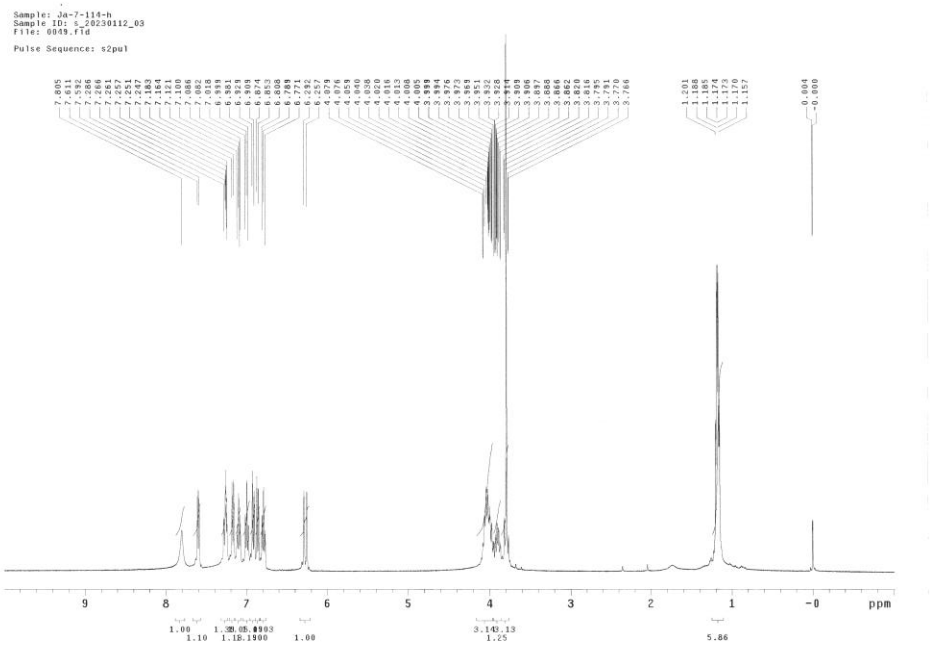

^{13}C NMR (100.5 MHz) in $CDCl_3$

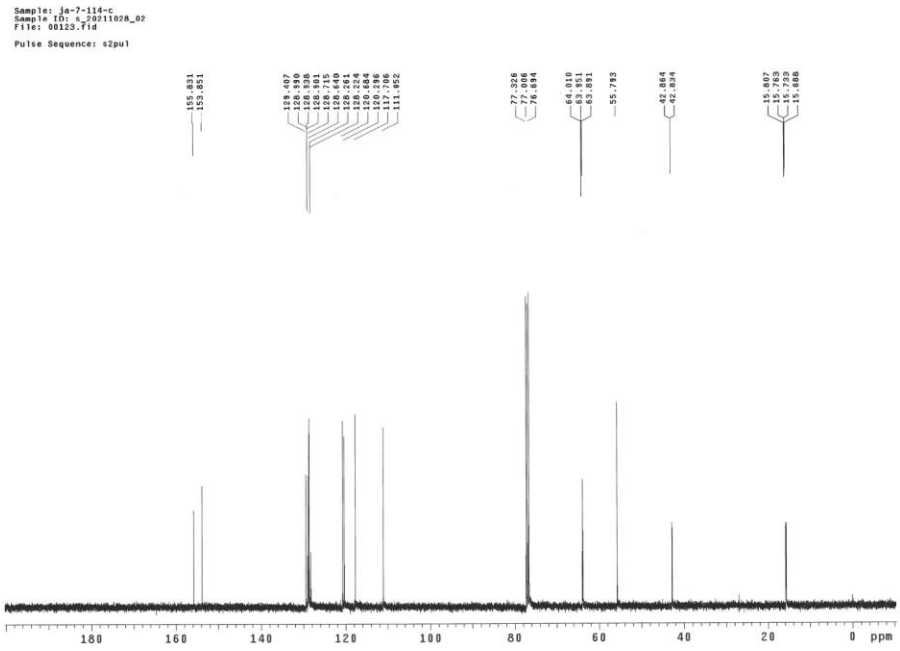

^{31}P NMR (162 MHz) in $CDCl_3$

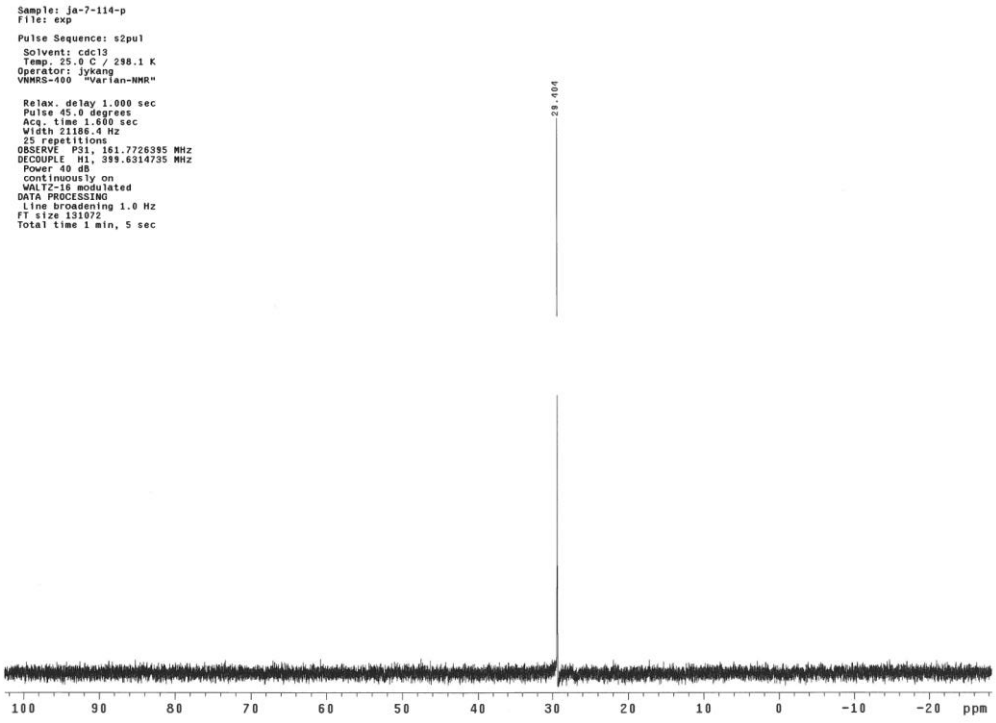

^{1}H NMR (400 MHz) in $CDCl_3$

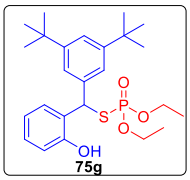

75g

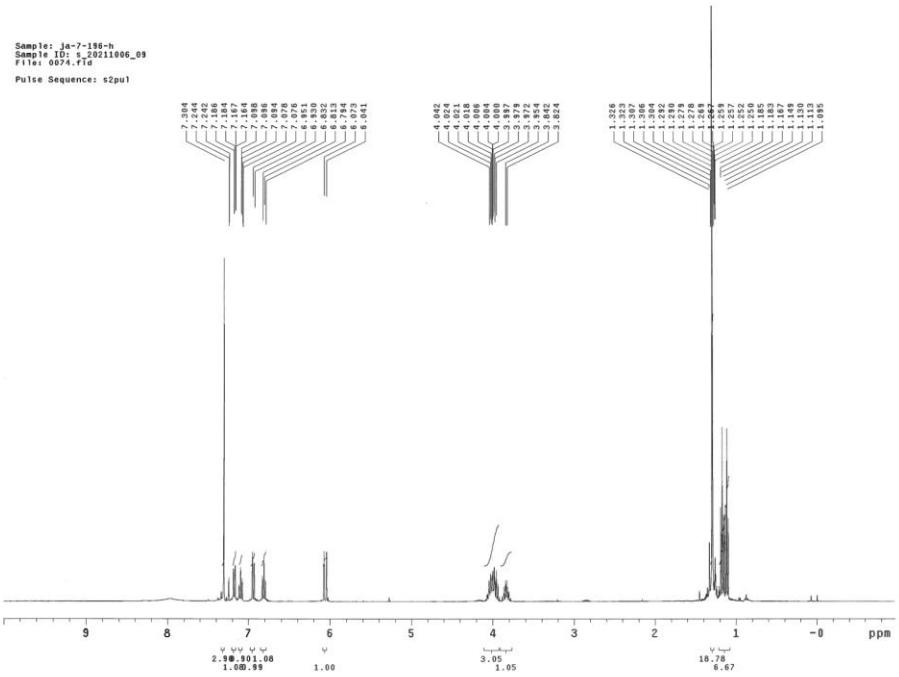

^{13}C NMR (100.5 MHz) in $CDCl_3$

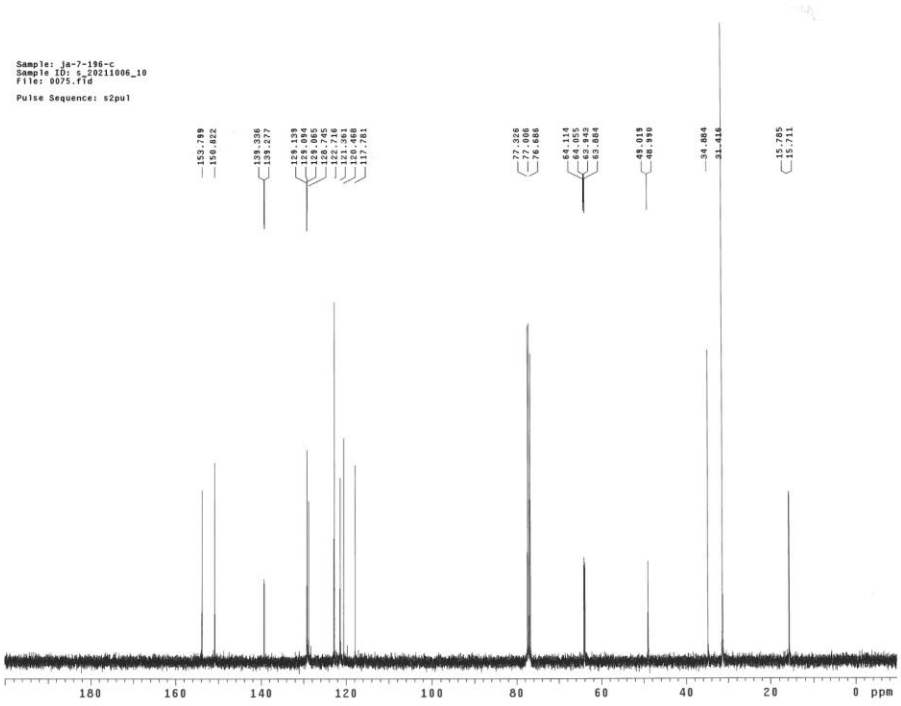

^{31}P NMR (162 MHz) in $CDCl_3$

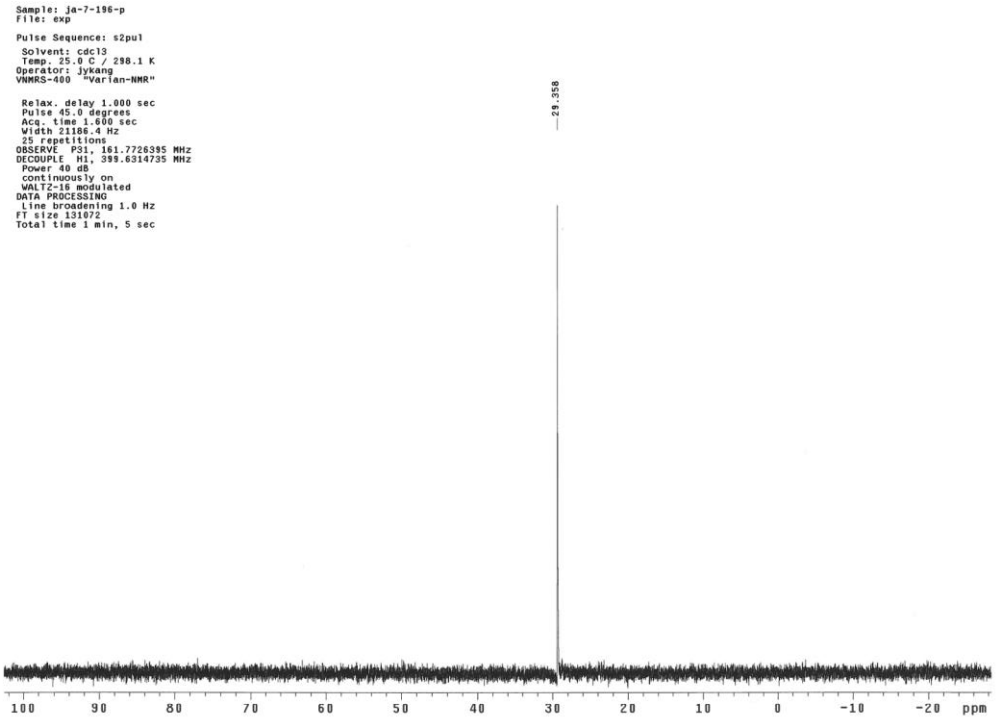

^{1}H NMR (400 MHz) in $CDCl_3$

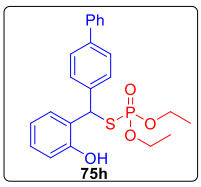

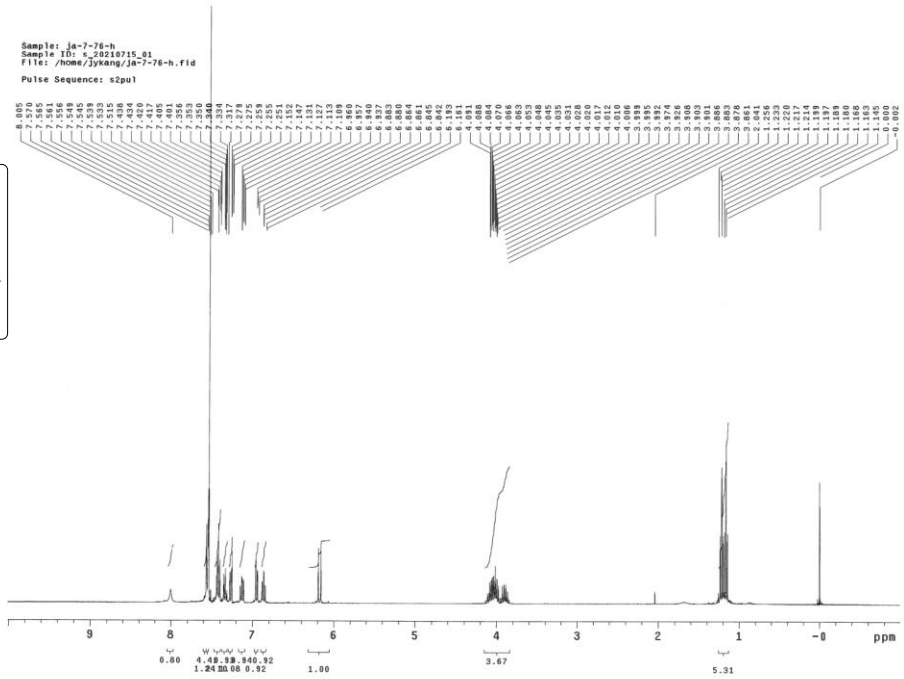

^{13}C NMR (100.5 MHz) in $CDCl_3$

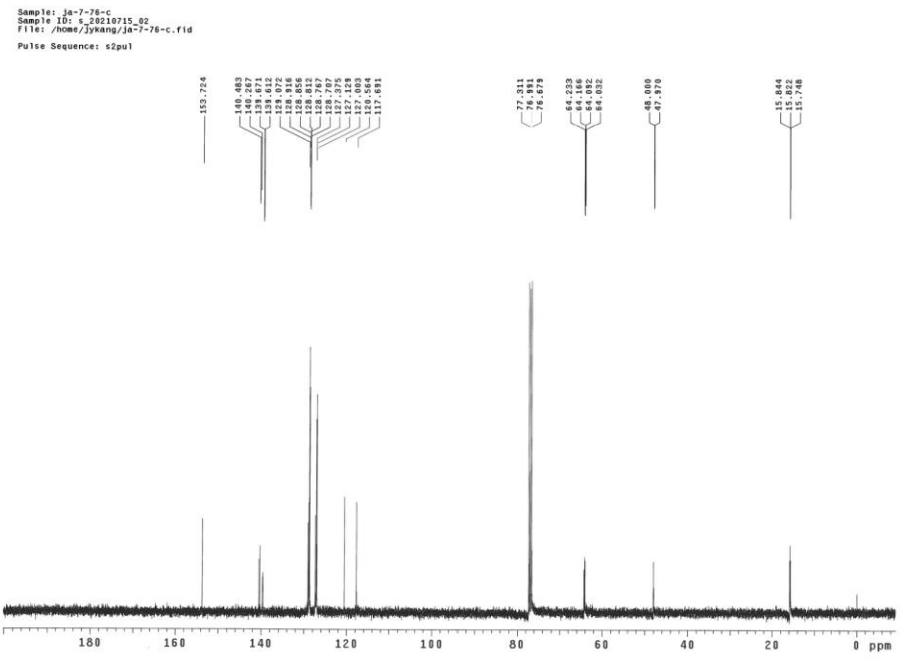

^{31}P NMR (162 MHz) in $CDCl_3$

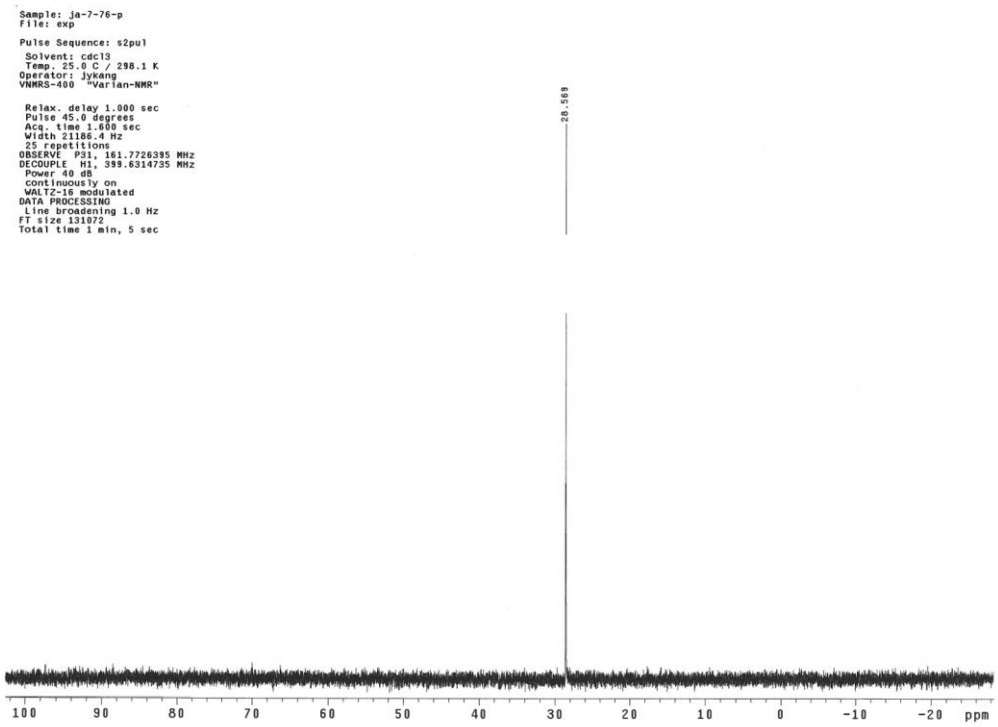

^{1}H NMR (400 MHz) in $CDCl_3$

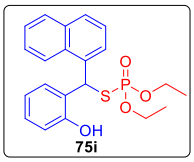

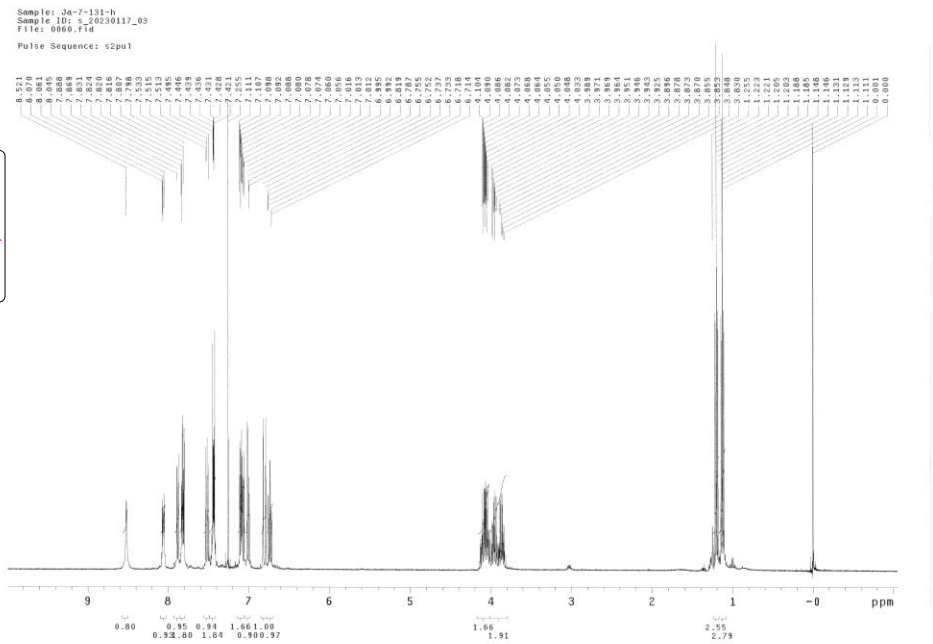

^{13}C NMR (100.5 MHz) in $CDCl_3$

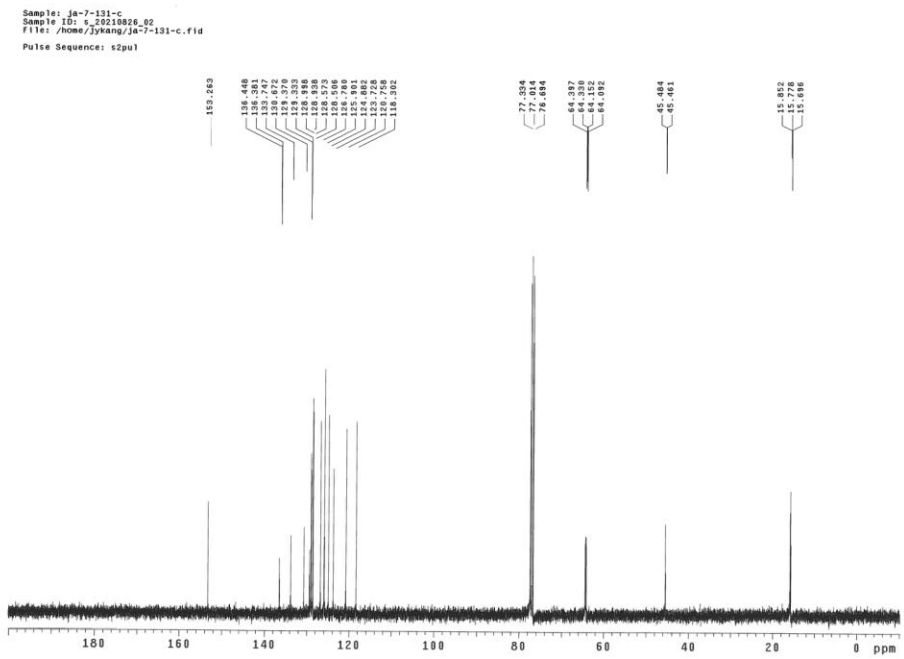

^{31}P NMR (162 MHz) in $CDCl_3$

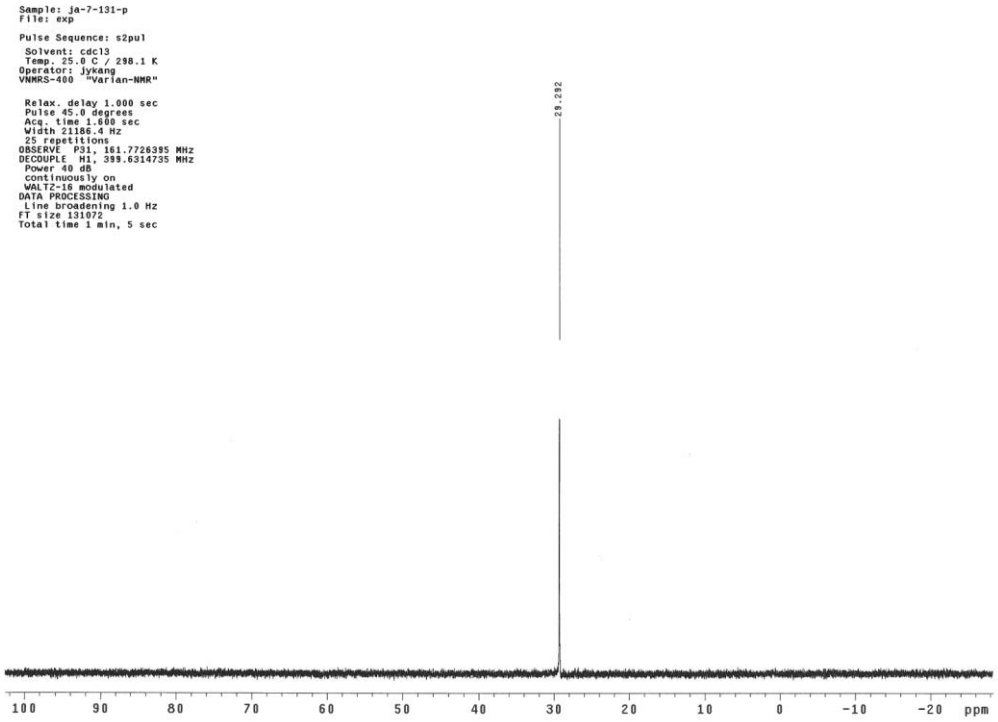

^{1}H NMR (400 MHz) in $CDCl_3$

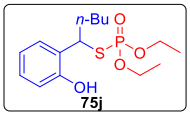

75j

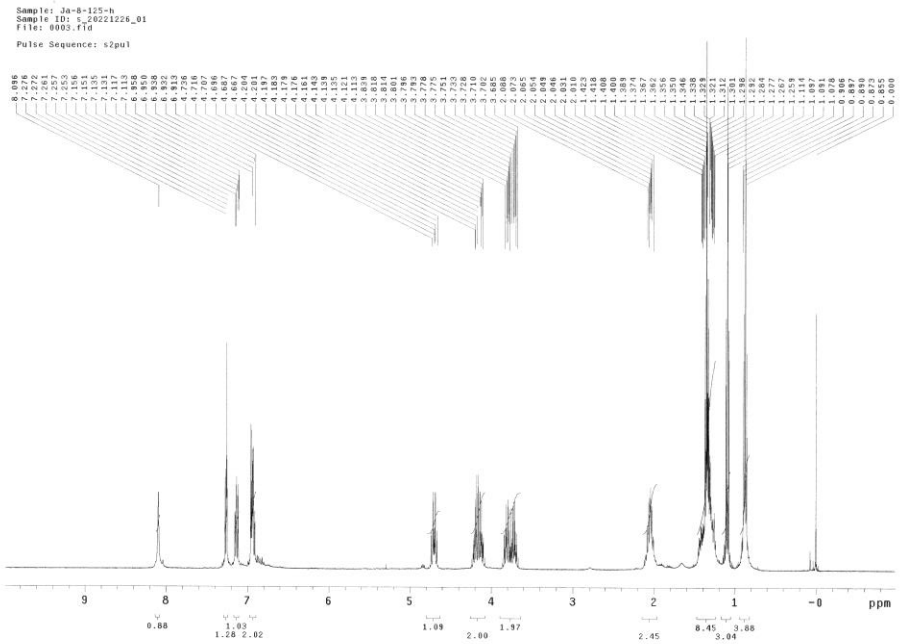

^{13}C NMR (100.5 MHz) in $CDCl_3$

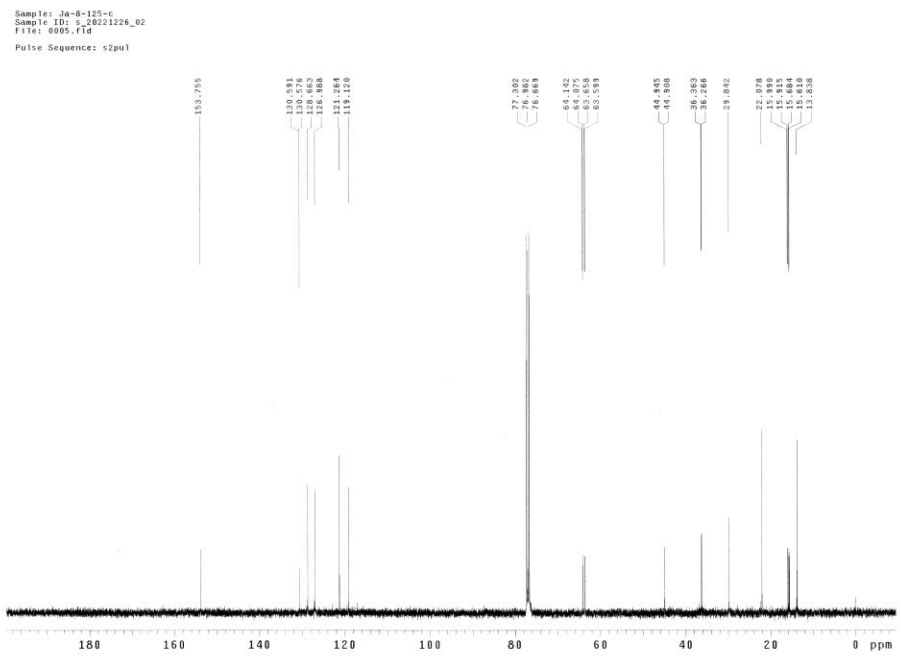

^{31}P NMR (162 MHz) in $CDCl_3$

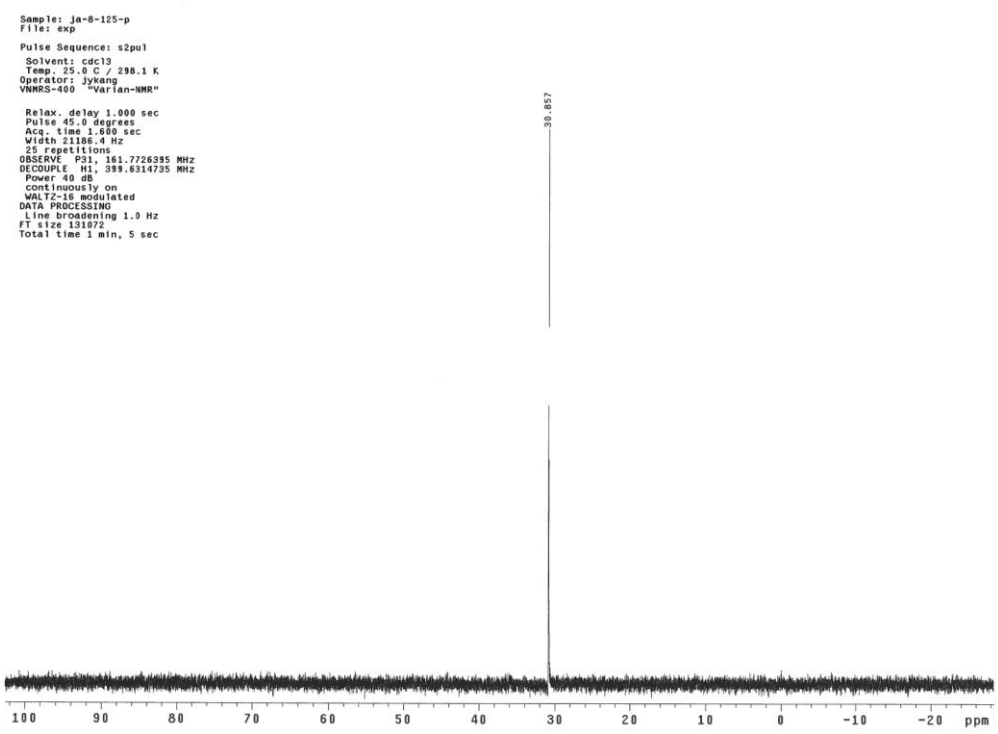

^{1}H NMR (400 MHz) in $CDCl_3$

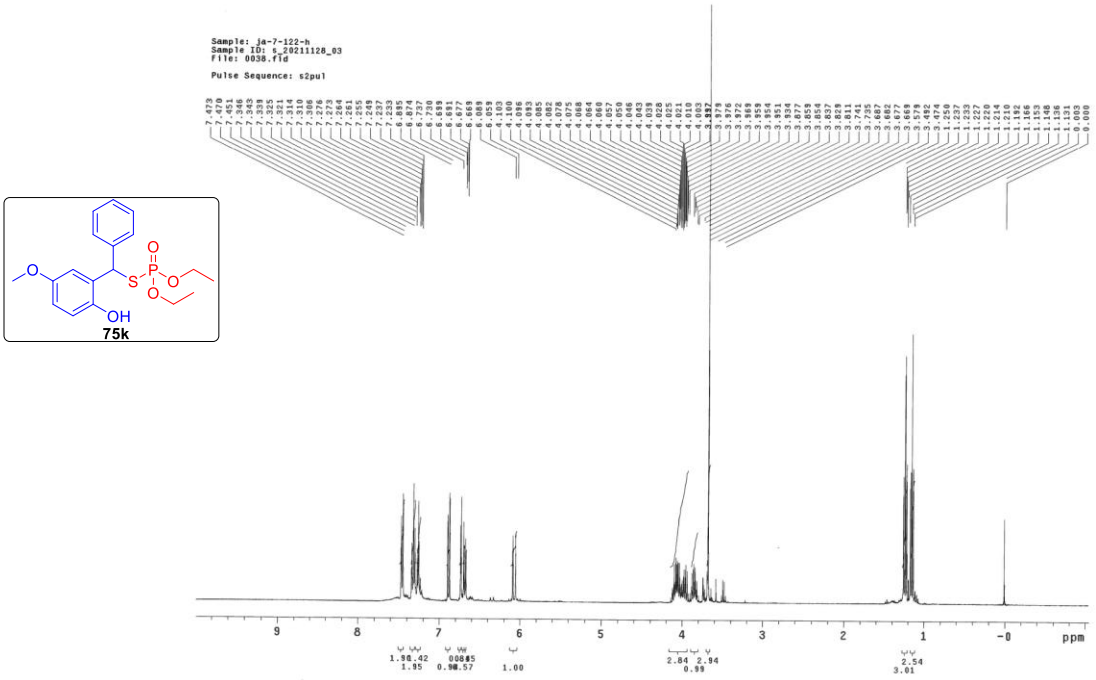

^{13}C NMR (100.5 MHz) in $CDCl_3$

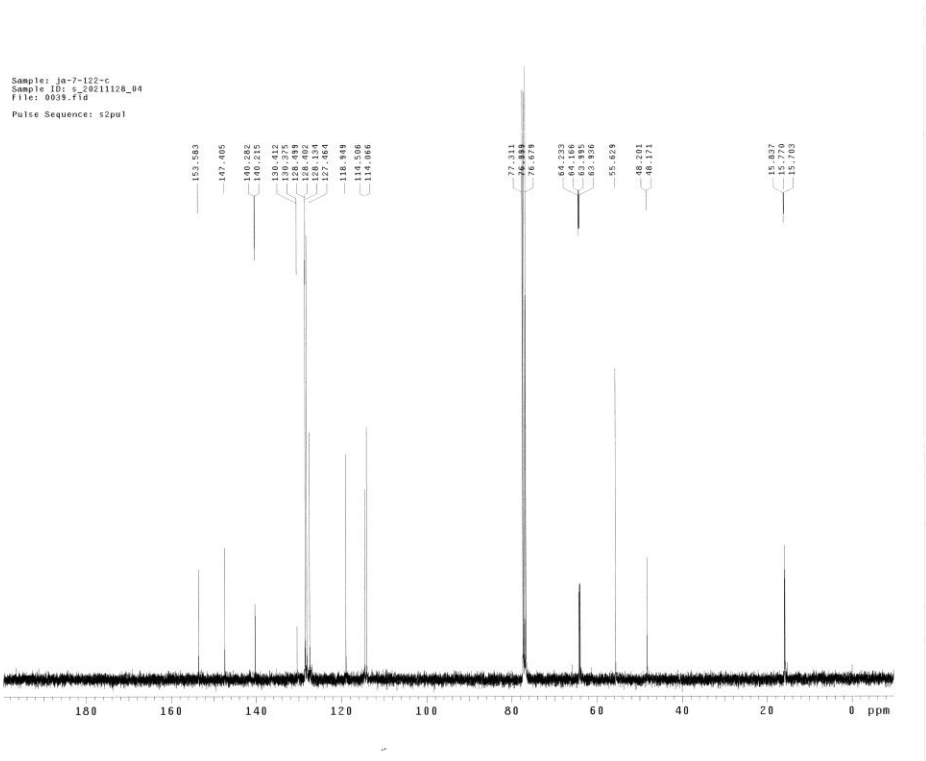

^{31}P NMR (162 MHz) in $CDCl_3$

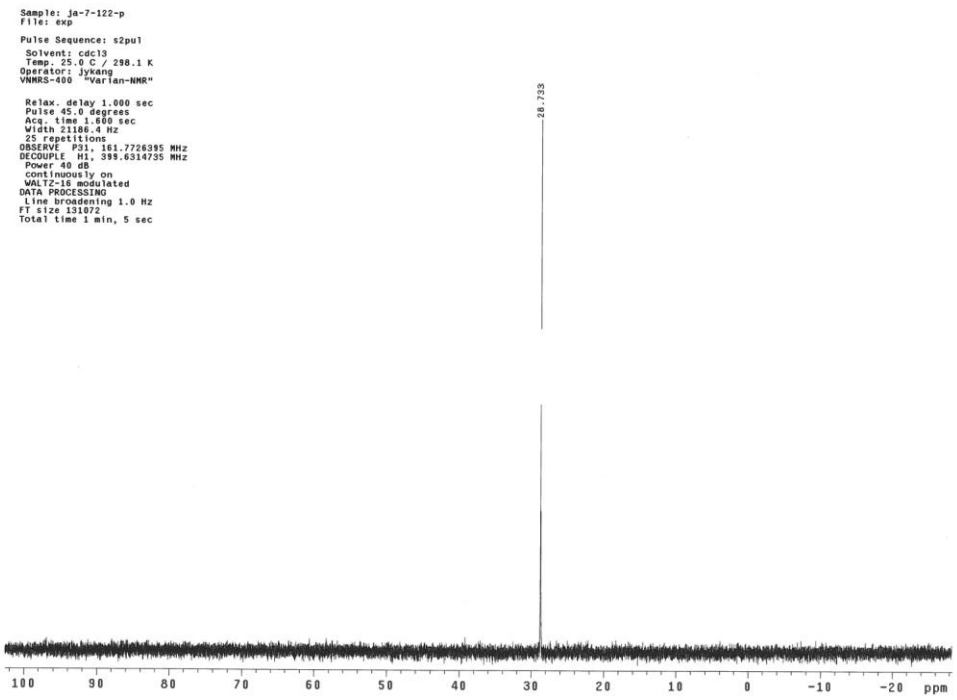

^{1}H NMR (400 MHz) in $CDCl_3$

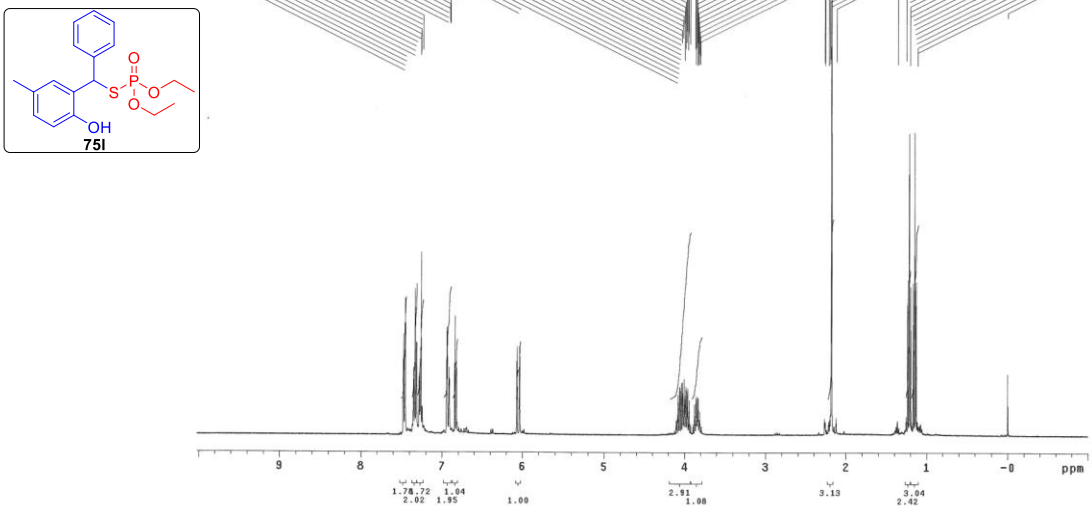

^{13}C NMR (100.5 MHz) in $CDCl_3$

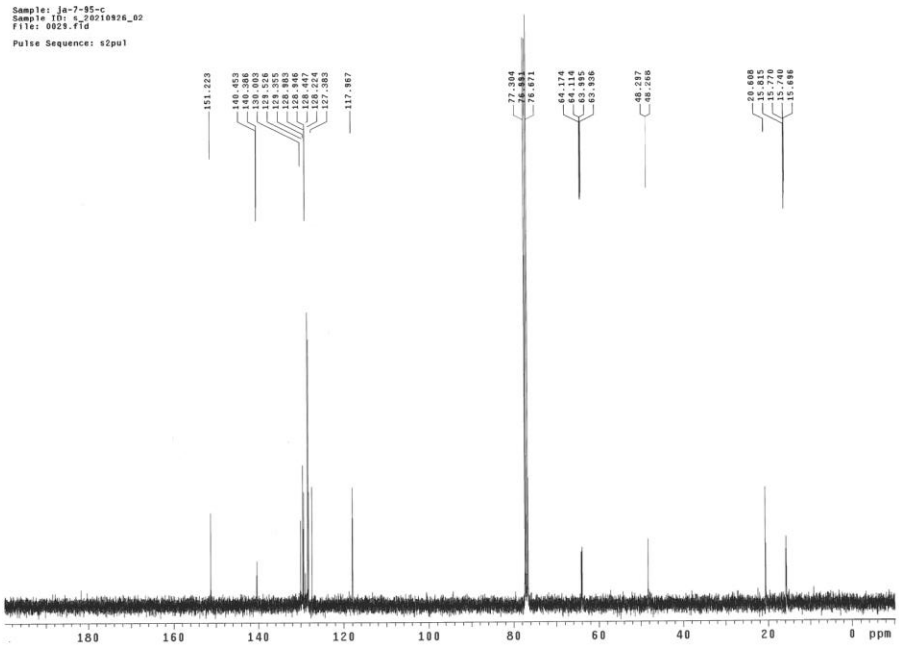

^{31}P NMR (162 MHz) in $CDCl_3$

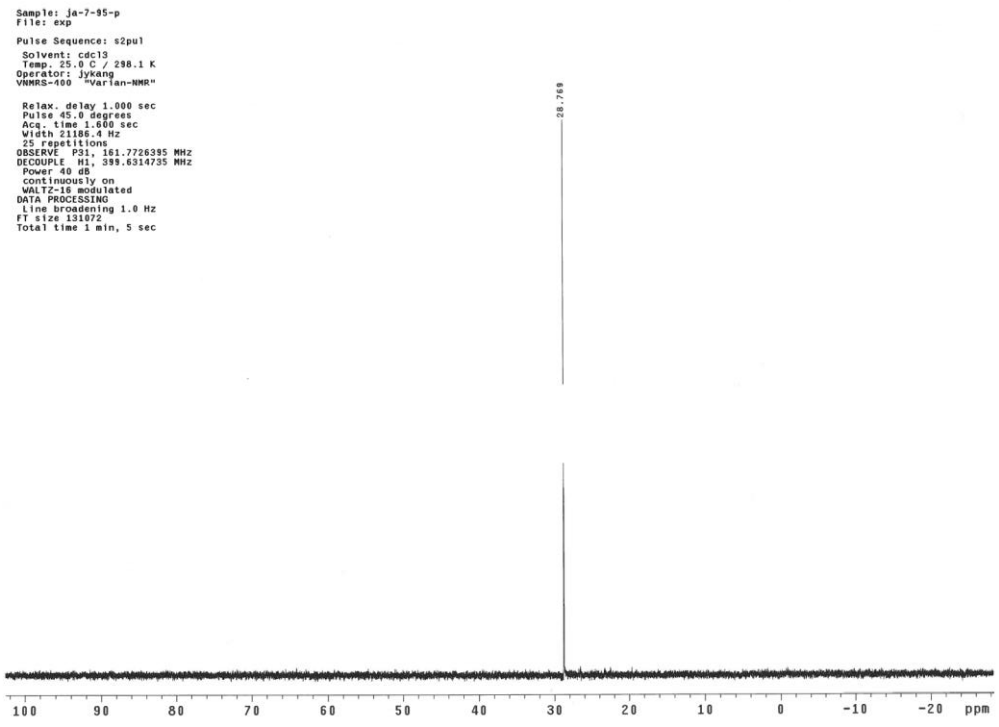

^{1}H NMR (400 MHz) in $CDCl_3$

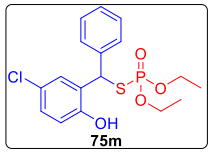

75m

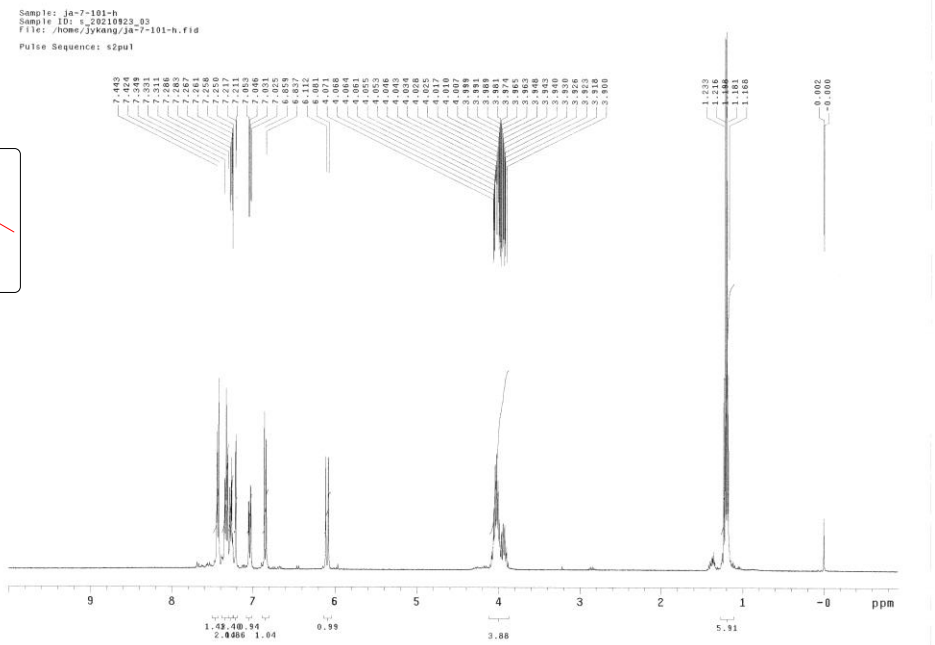

^{13}C NMR (100.5 MHz) in $CDCl_3$

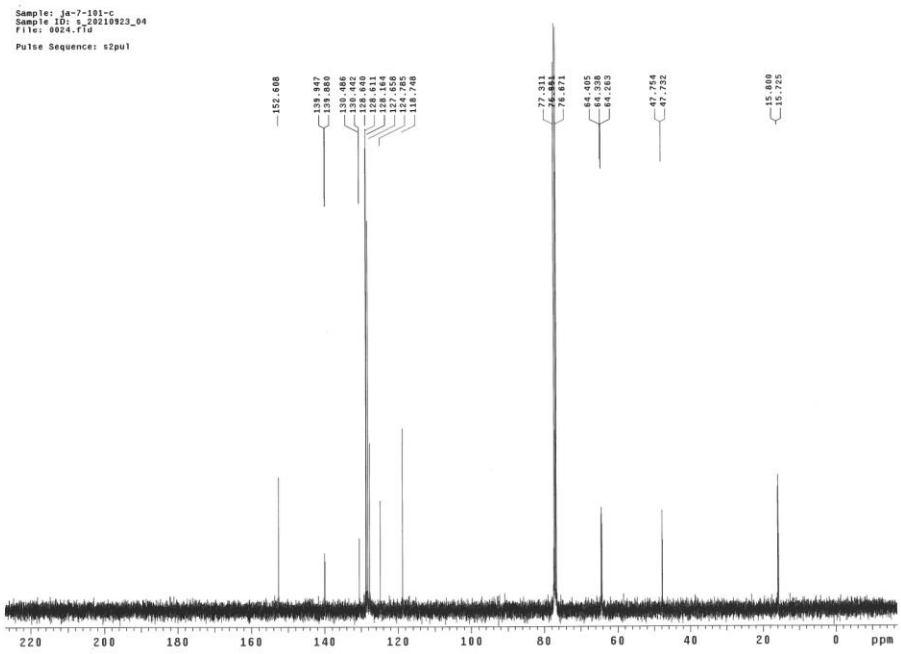

^{31}P NMR (162 MHz) in $CDCl_3$

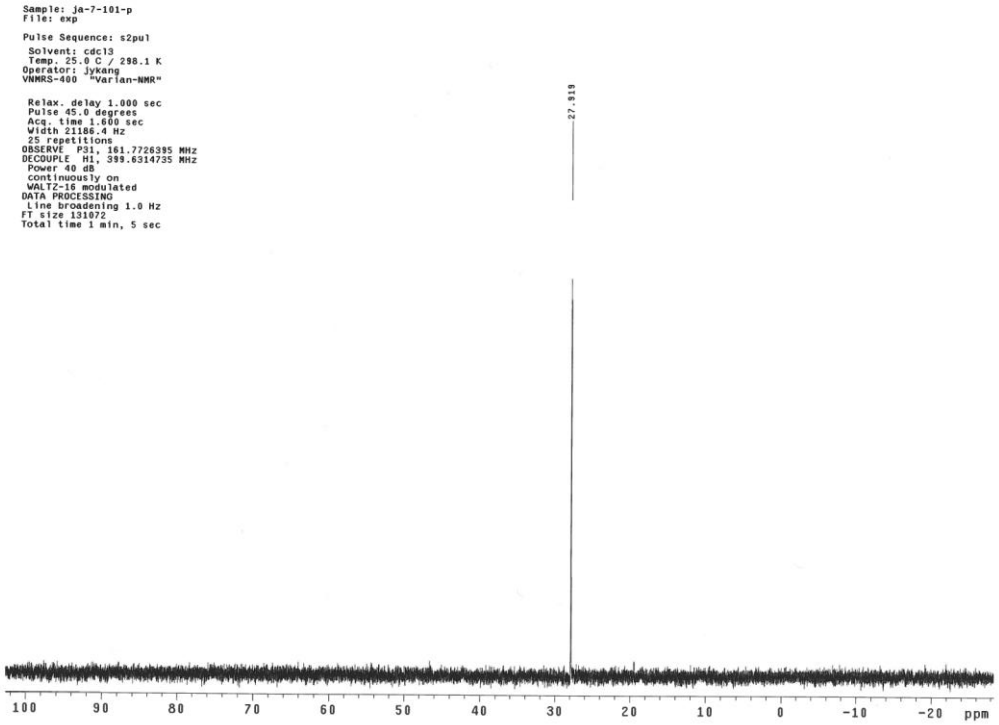

^{1}H NMR (400 MHz) in $CDCl_3$

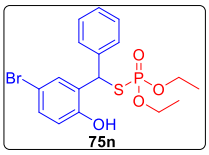

75n

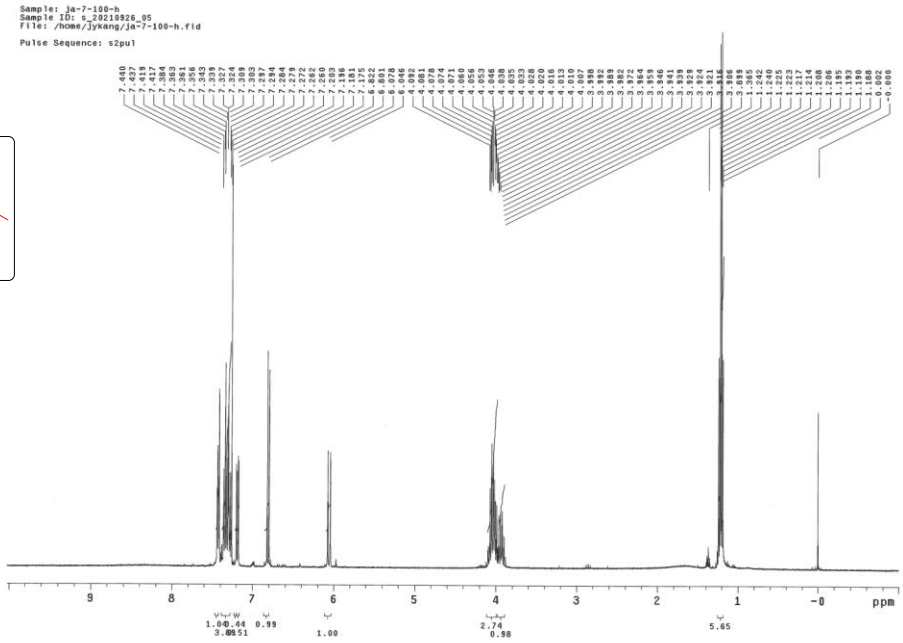

^{13}C NMR (100.5 MHz) in $CDCl_3$

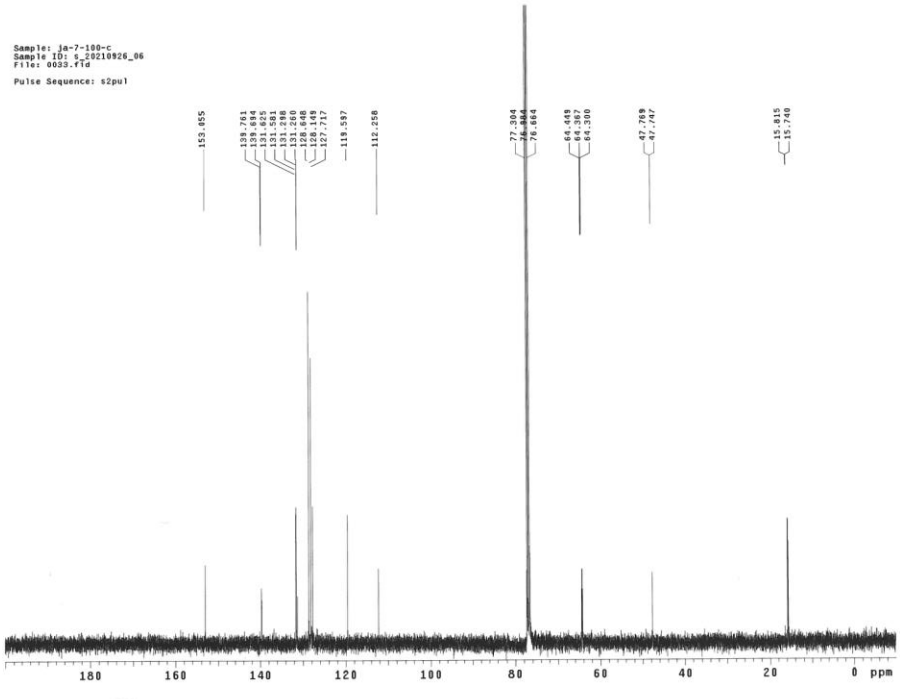

^{31}P NMR (162 MHz) in $CDCl_3$

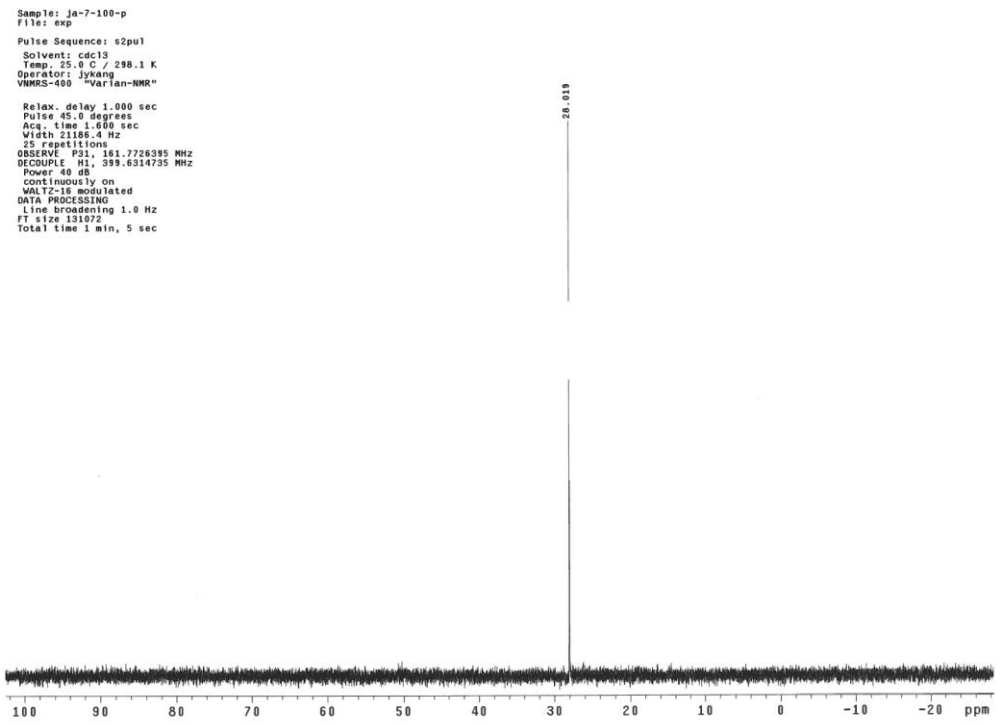

^{1}H NMR (400 MHz) in $CDCl_3$

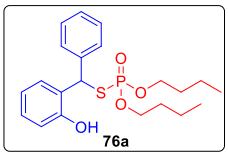

76a

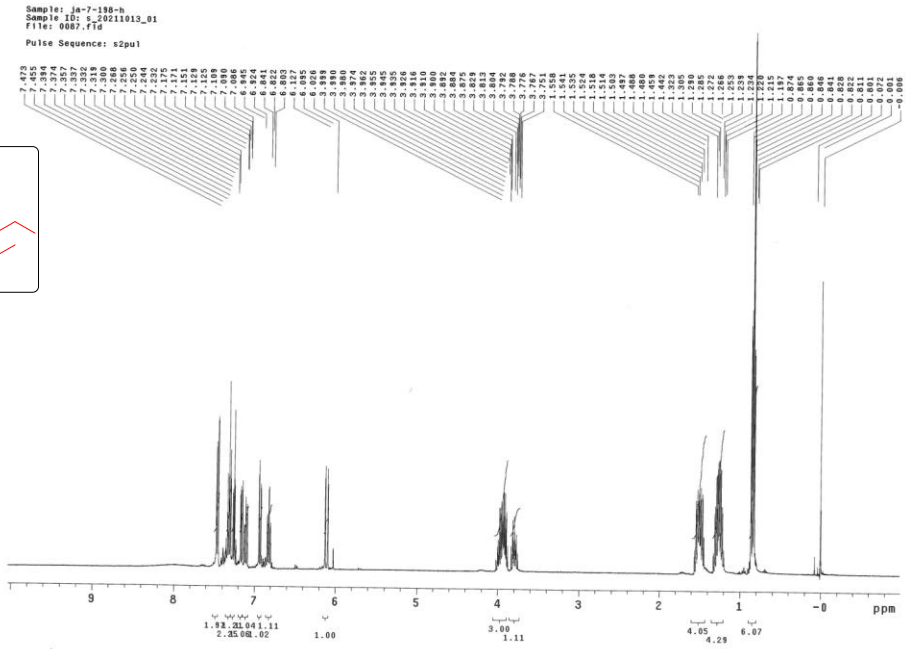

^{13}C NMR (100.5 MHz) in $CDCl_3$

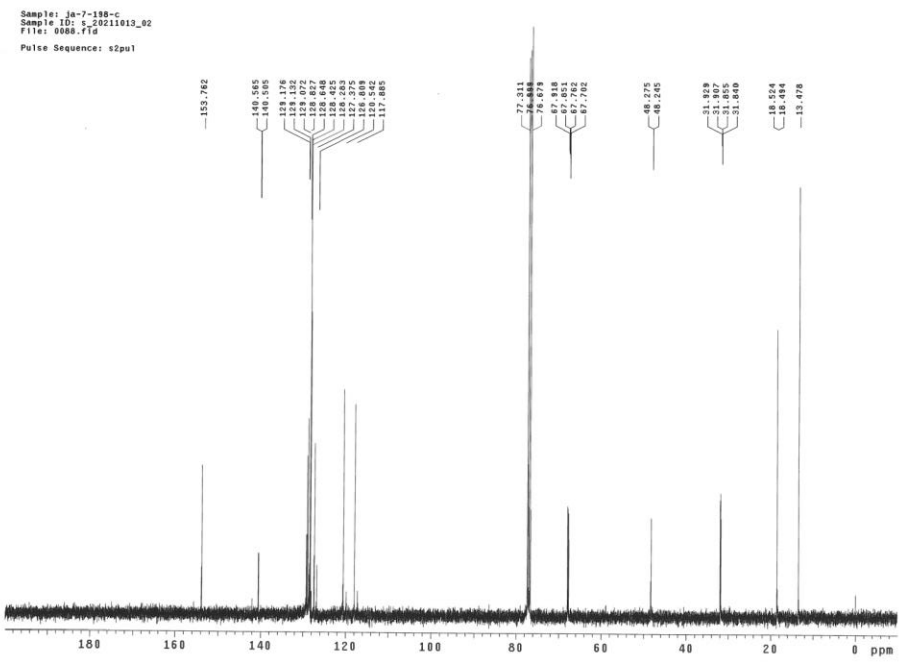

^{31}P NMR (162 MHz) in $CDCl_3$

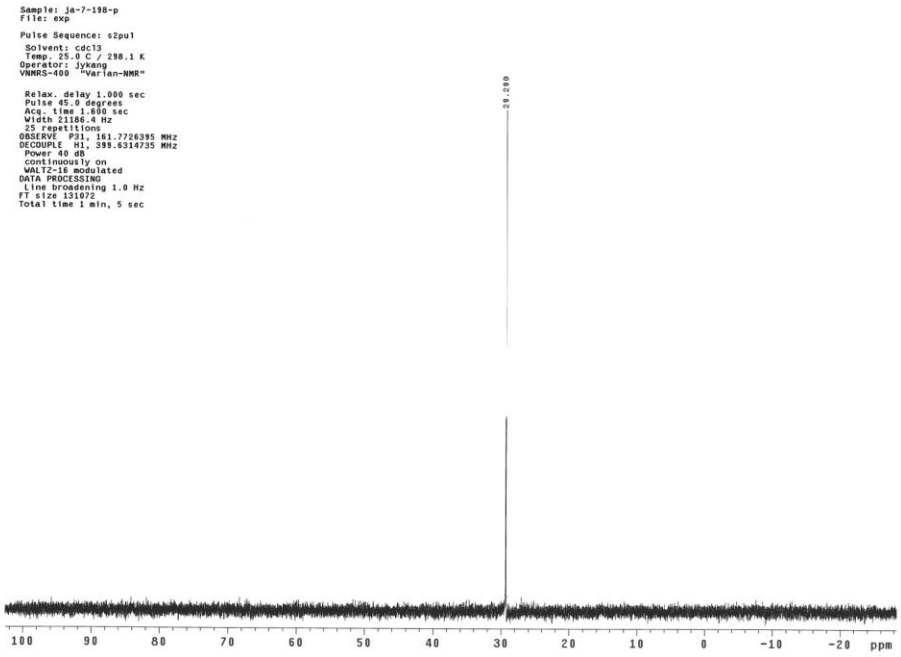

^{1}H NMR (400 MHz) in $CDCl_3$

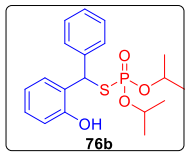

76b

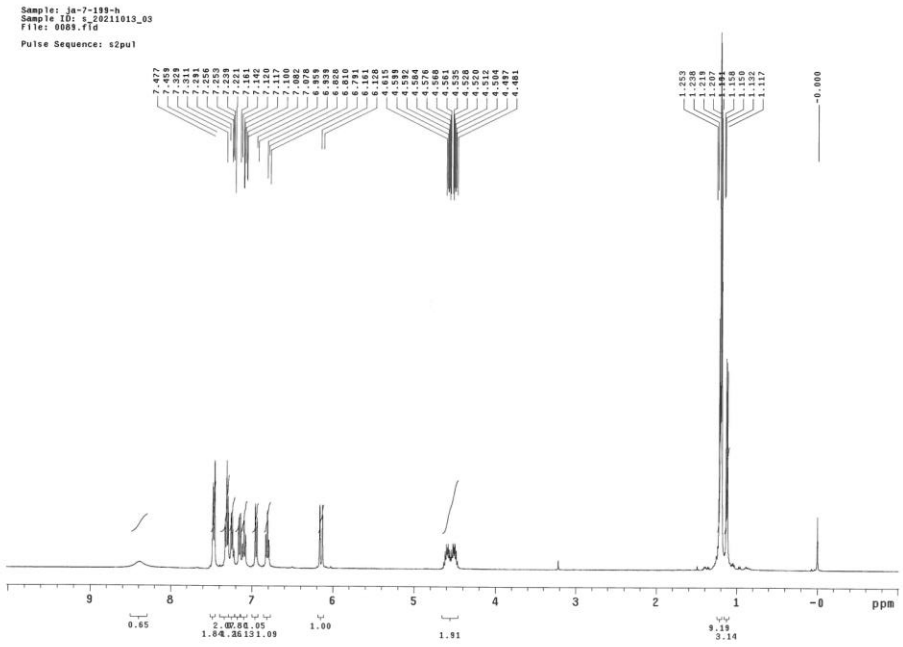

^{13}C NMR (100.5 MHz) in $CDCl_3$

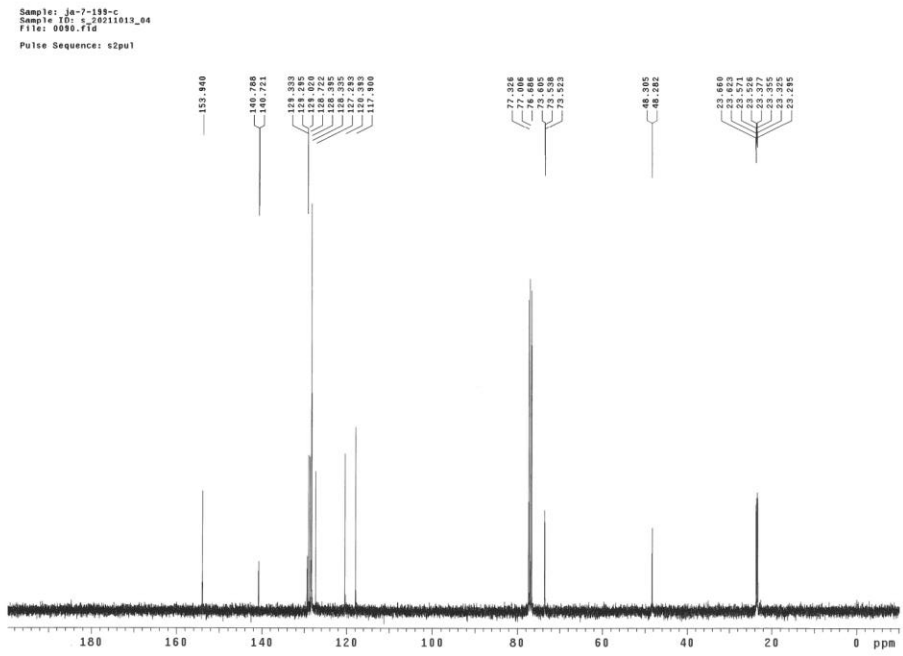

^{31}P NMR (162 MHz) in $CDCl_3$

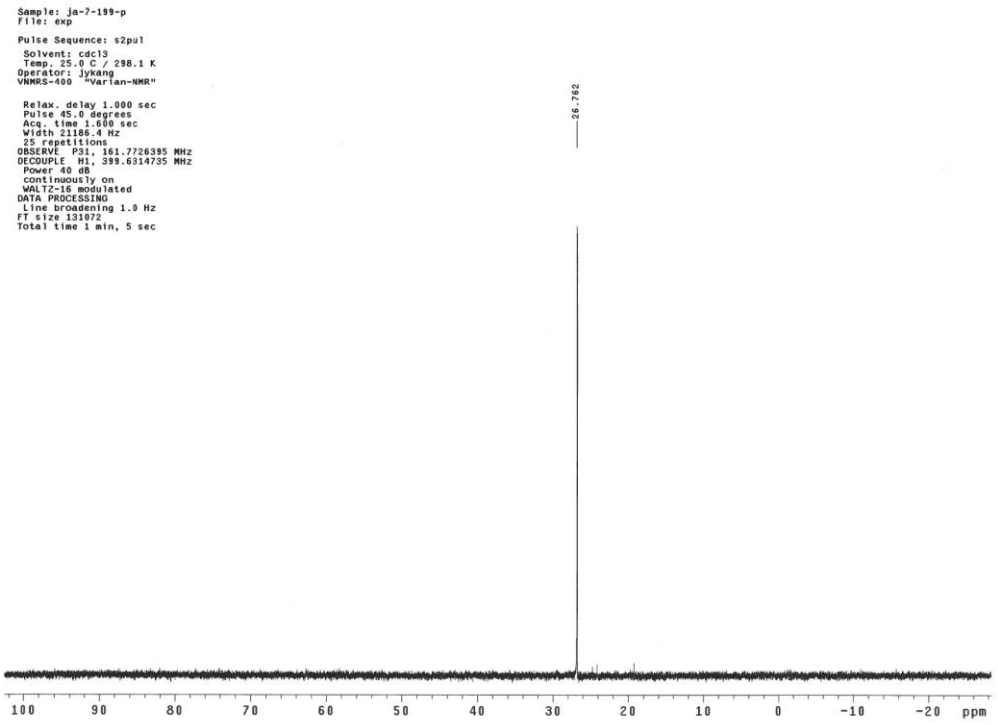

^{1}H NMR (400 MHz) in d6-DMSO

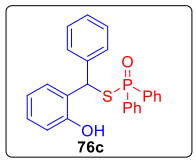

76c

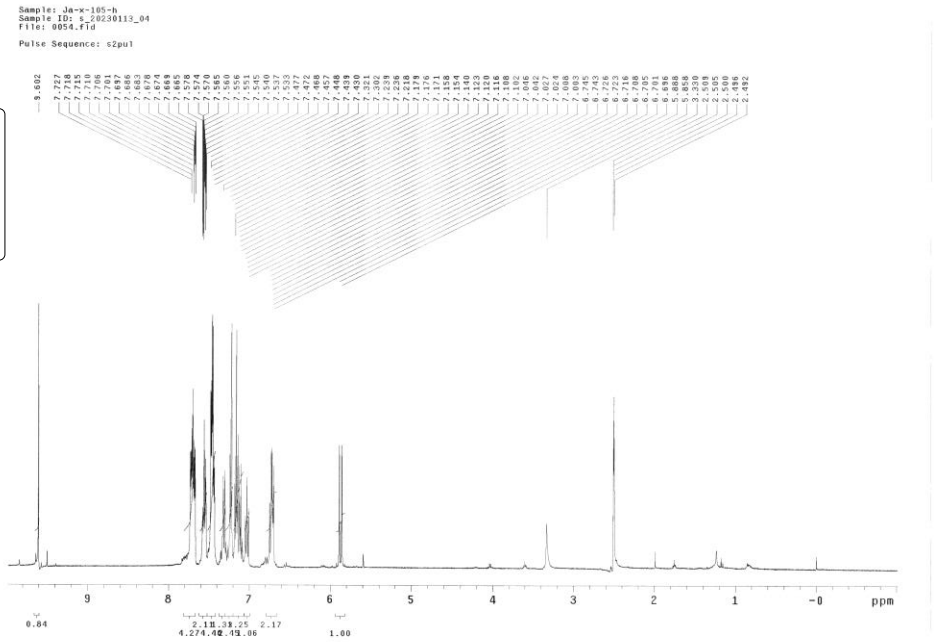

^{13}C NMR (100.5 MHz) in d6-DMSO

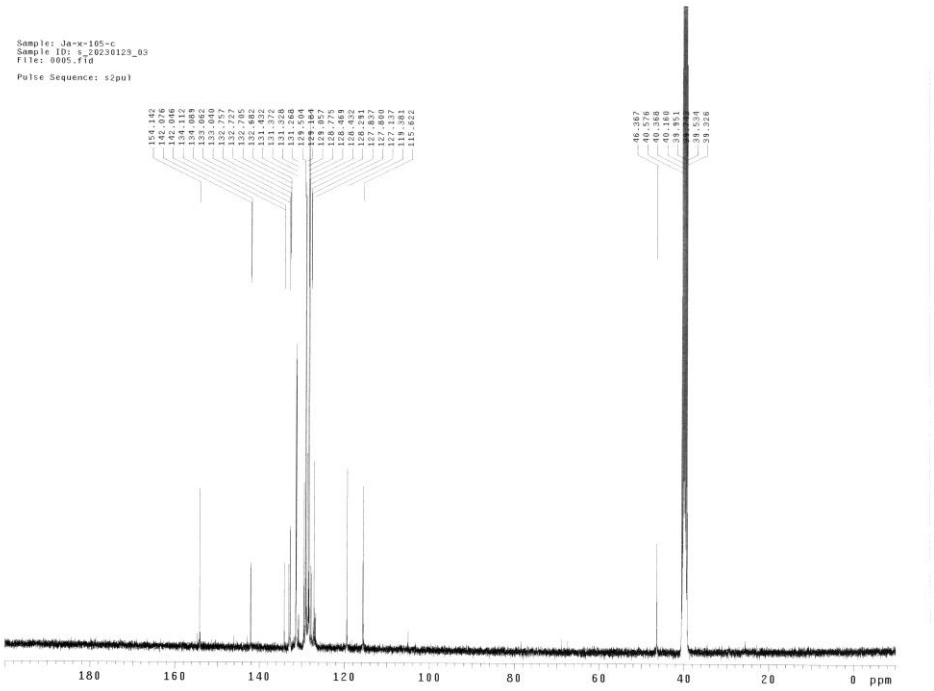

^{31}P NMR (162 MHz) in d6-DMSO

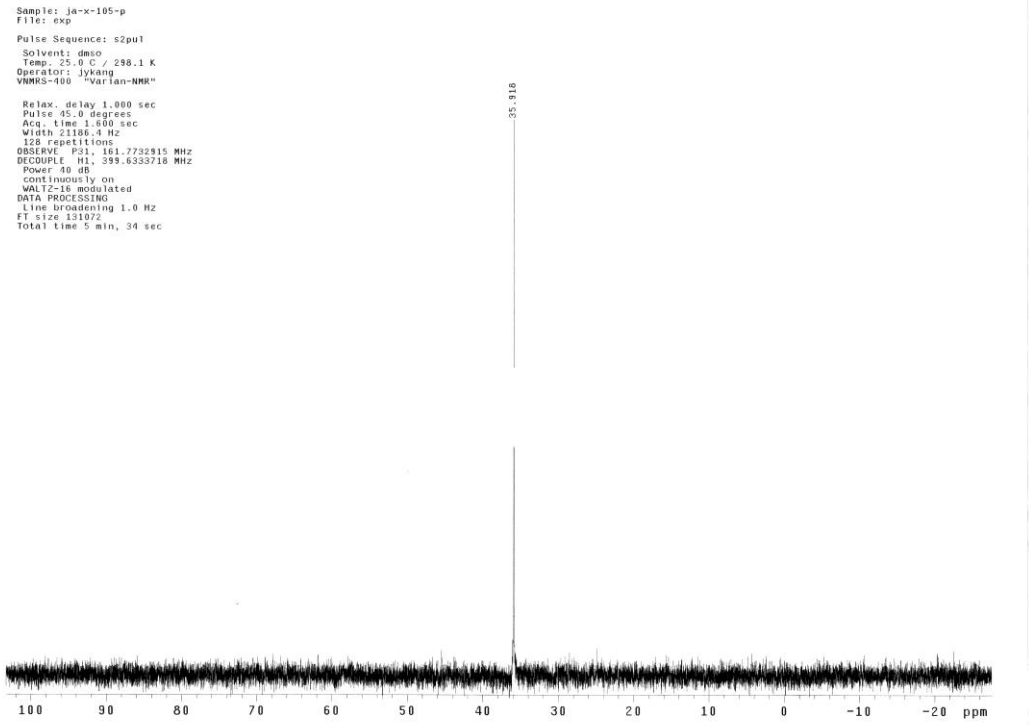

^{1}H NMR (400 MHz) in $CDCl_3$

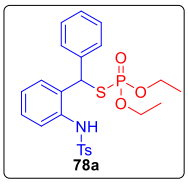

78a

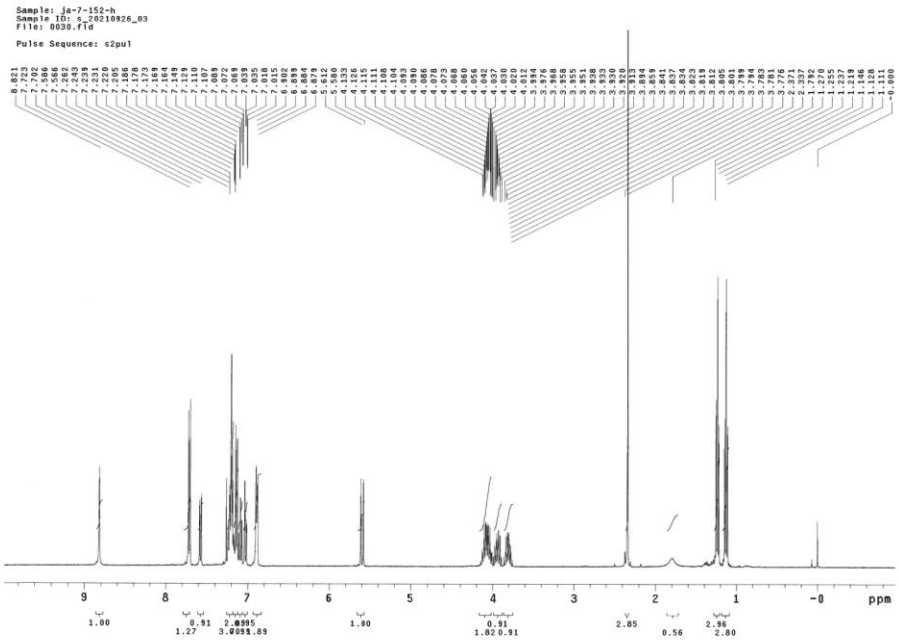

^{13}C NMR (100.5 MHz) in $CDCl_3$

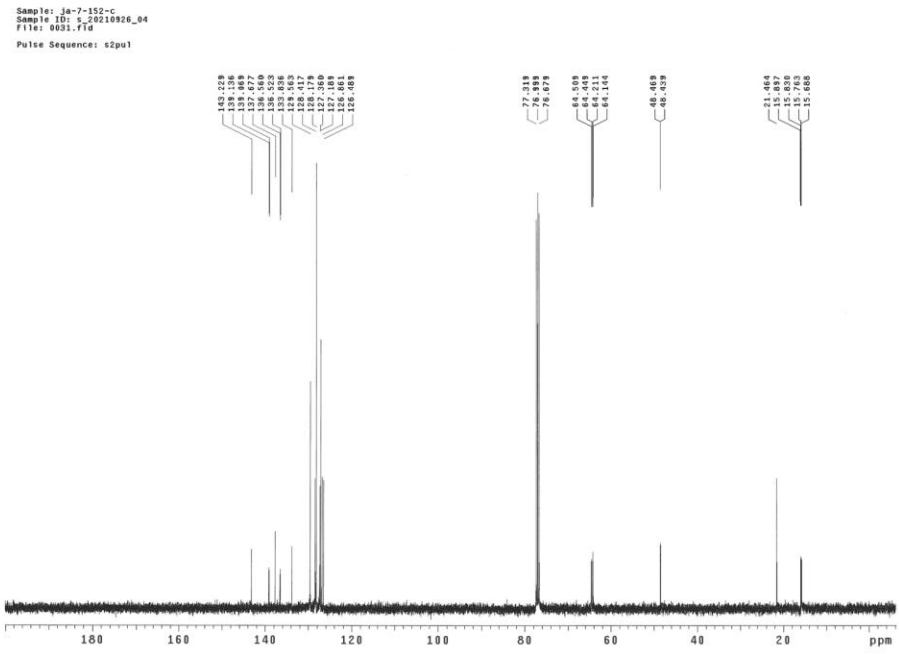

^{31}P NMR (162 MHz) in $CDCl_3$

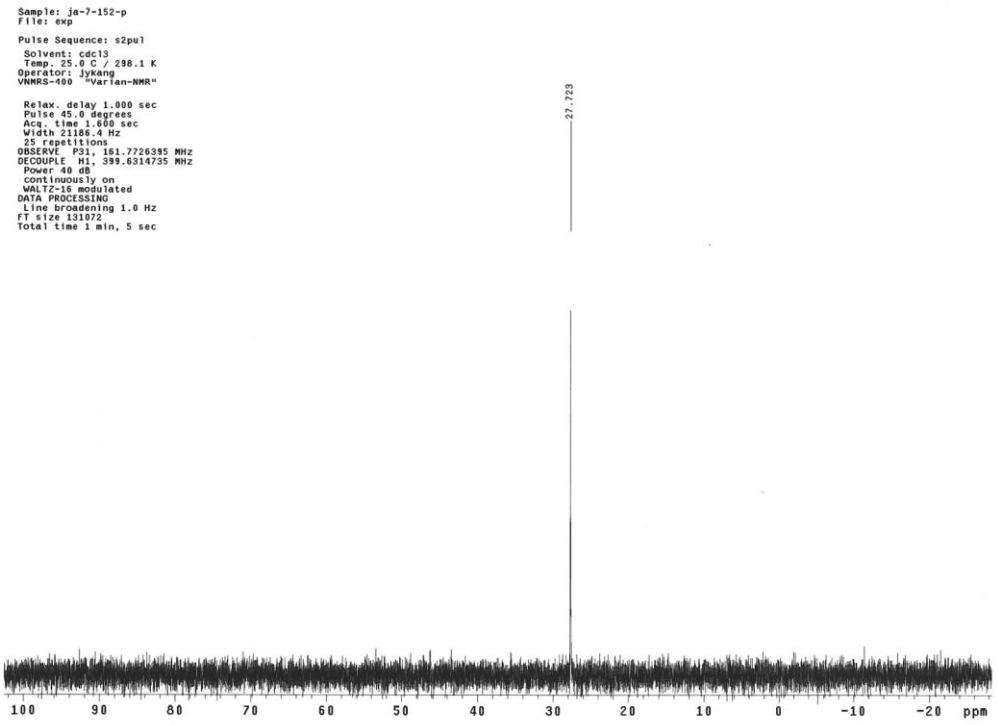

^{1}H NMR (400 MHz) in $CDCl_3$

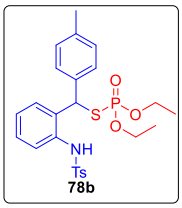

78b

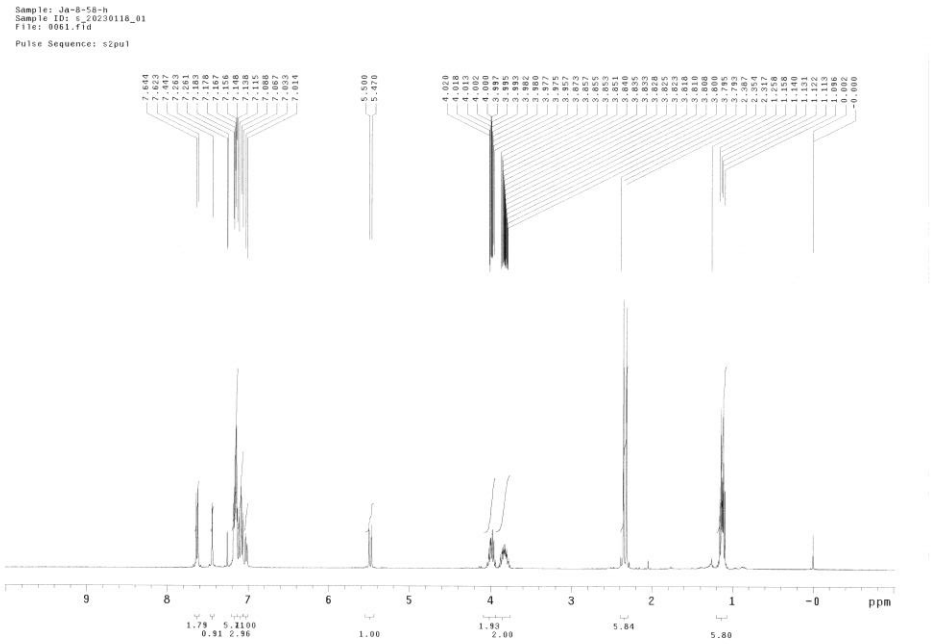

^{13}C NMR (100.5 MHz) in $CDCl_3$

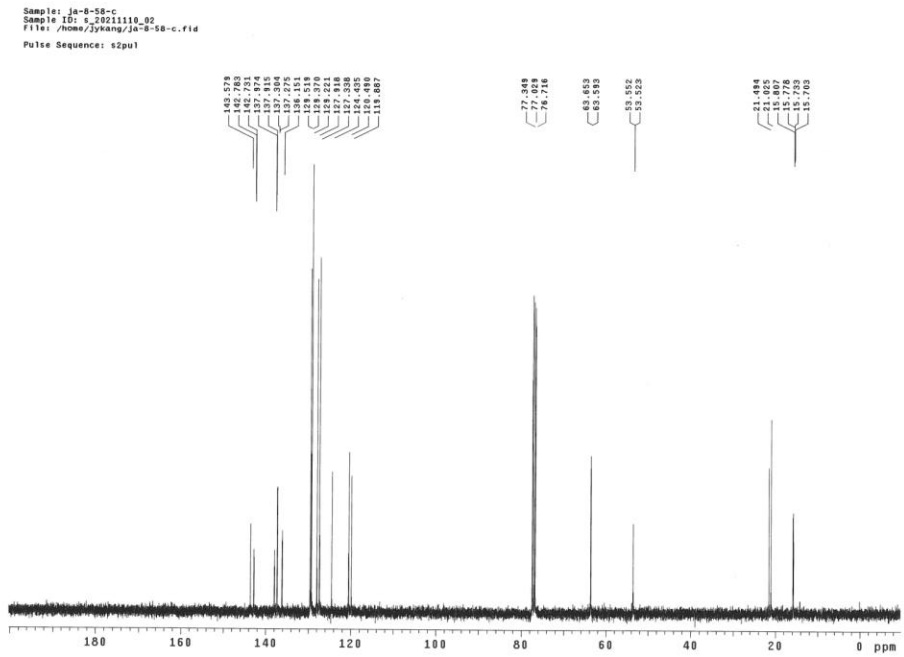

^{31}P NMR (162 MHz) in $CDCl_3$

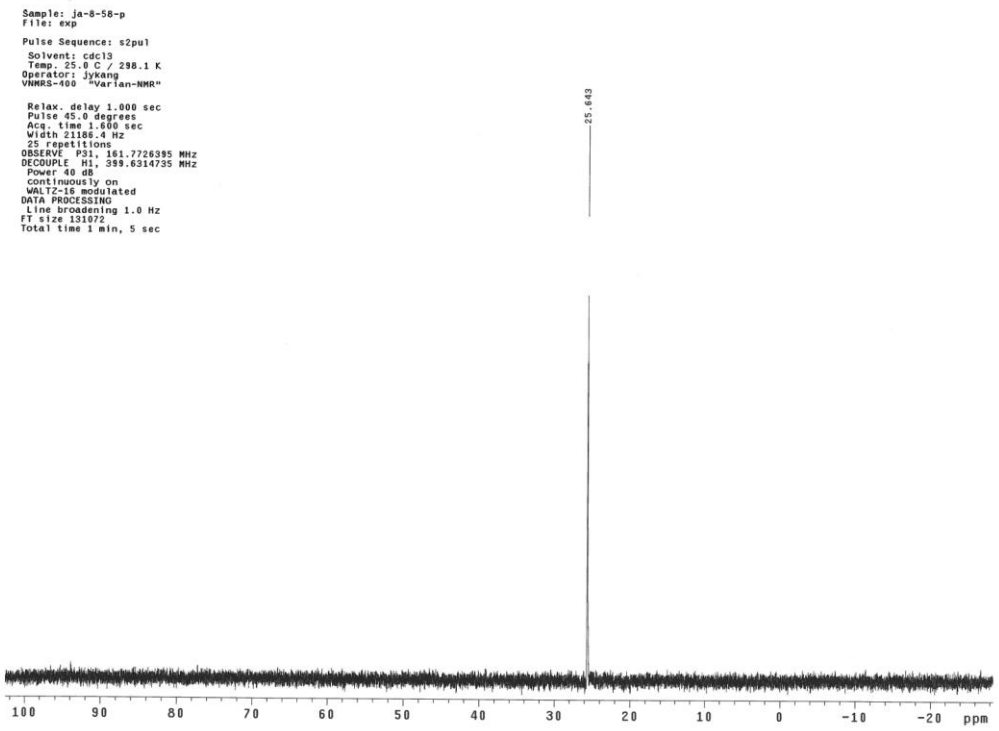

^{1}H NMR (400 MHz) in $CDCl_3$

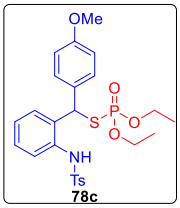

78c

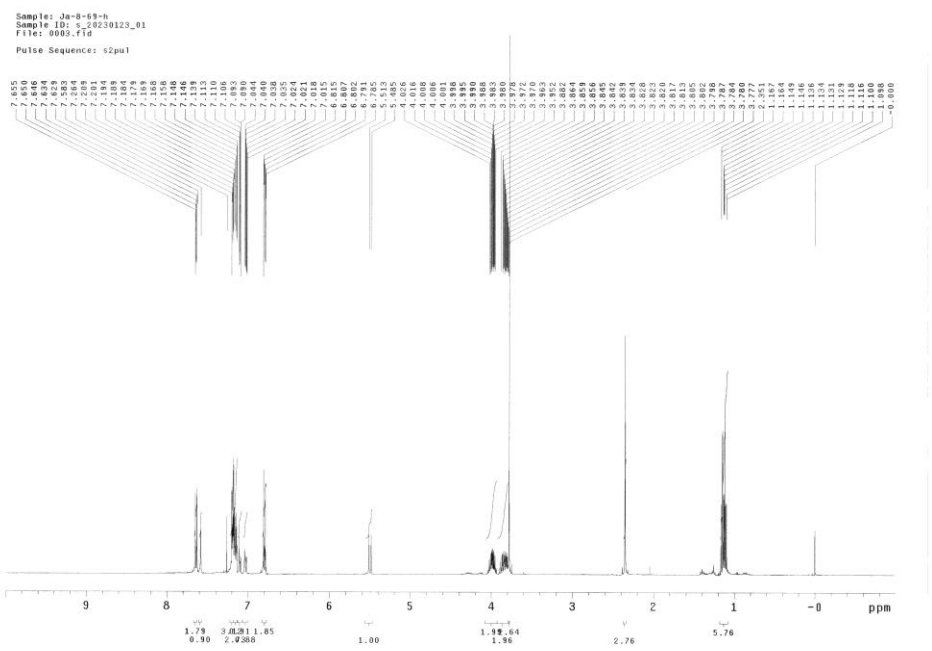

^{13}C NMR (100.5 MHz) in $CDCl_3$

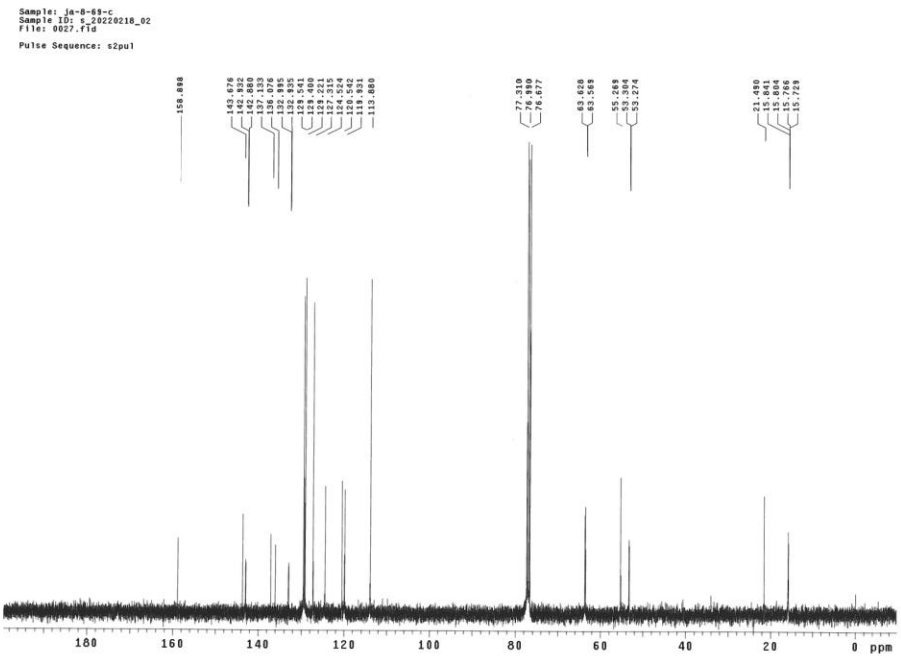

^{31}P NMR (162 MHz) in $CDCl_3$

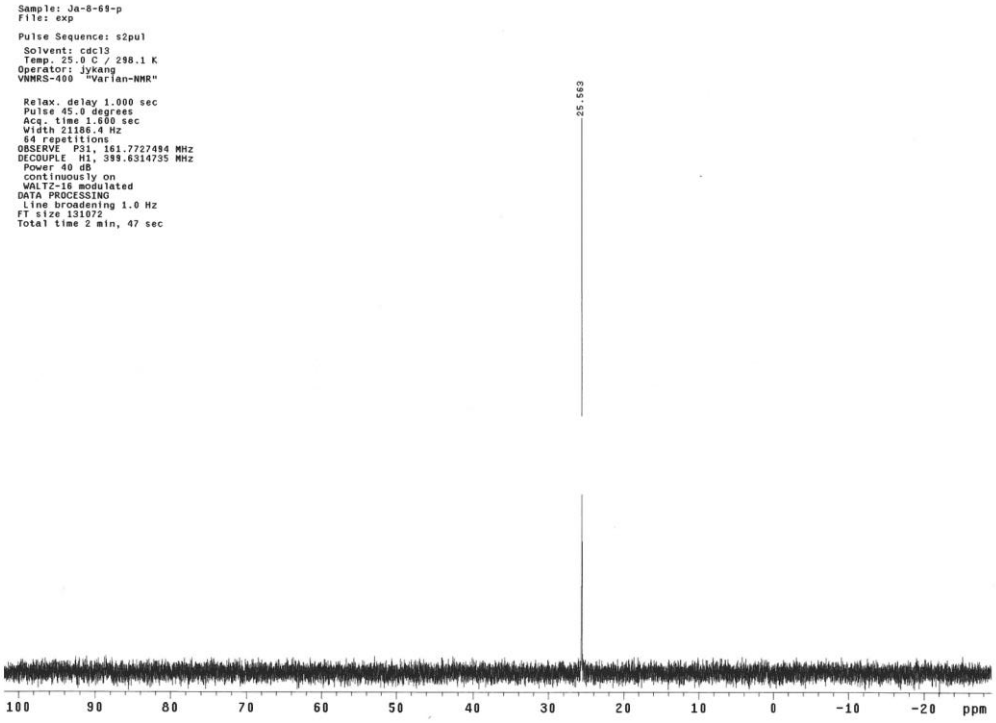

^{1}H NMR (400 MHz) in $CDCl_3$

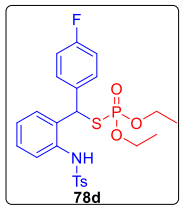

78d

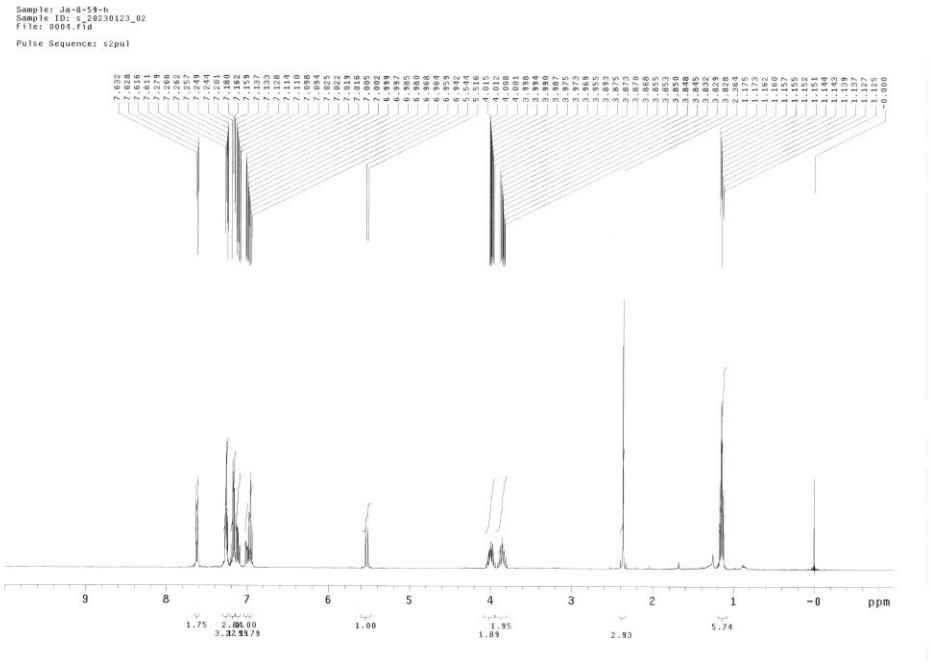

^{13}C NMR (100.5 MHz) in $CDCl_3$

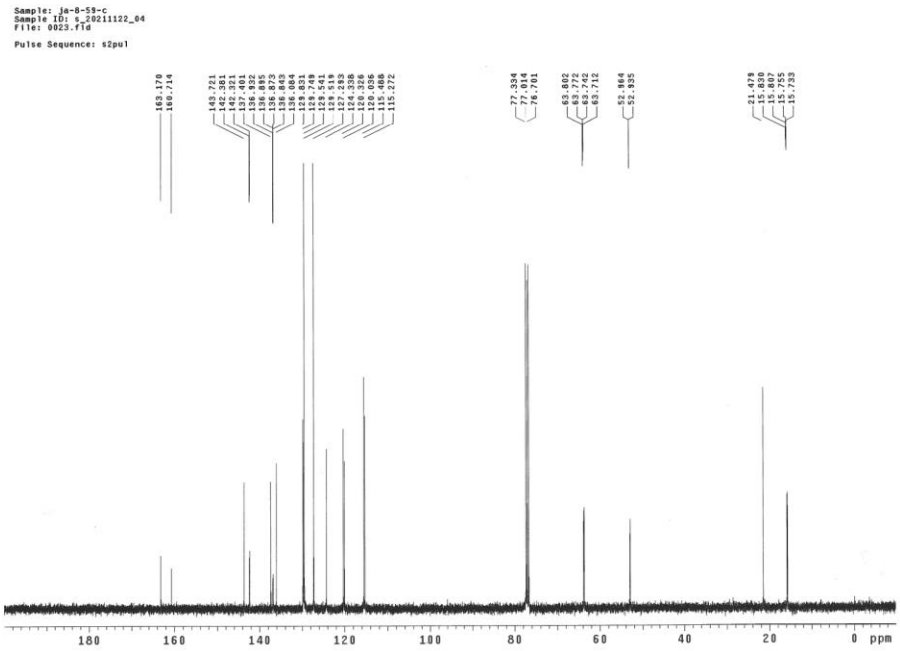

^{31}P NMR (162 MHz) in $CDCl_3$

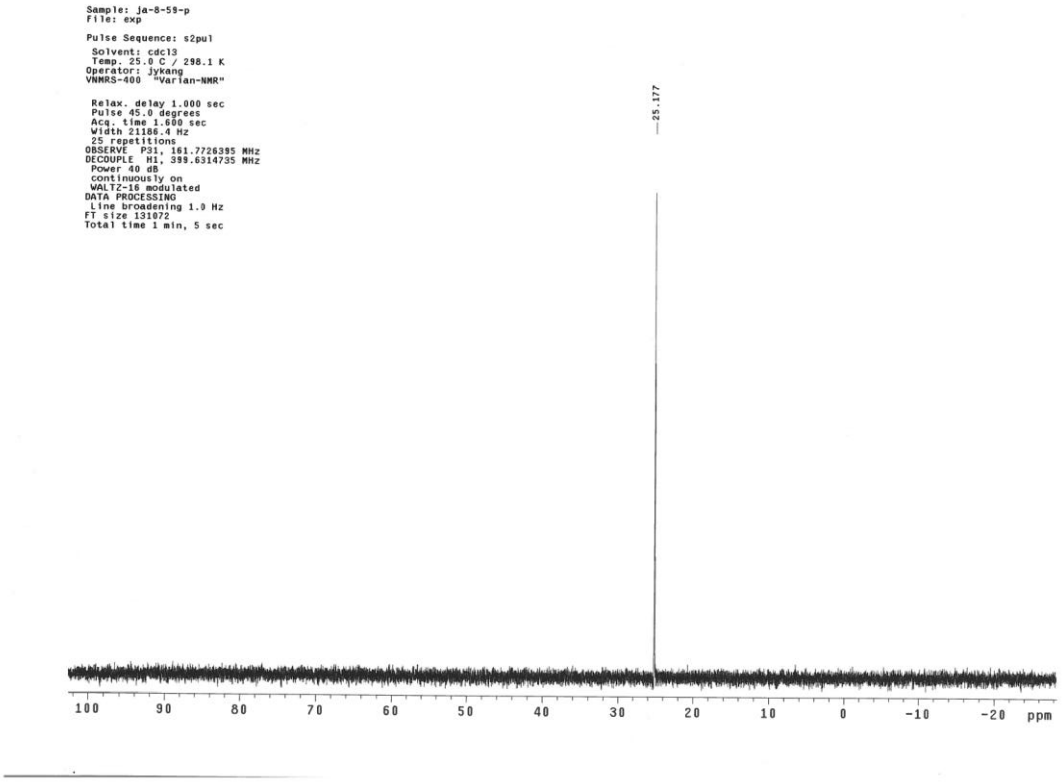

^{1}H NMR (400 MHz) in $CDCl_3$

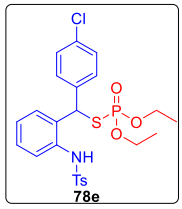

78e

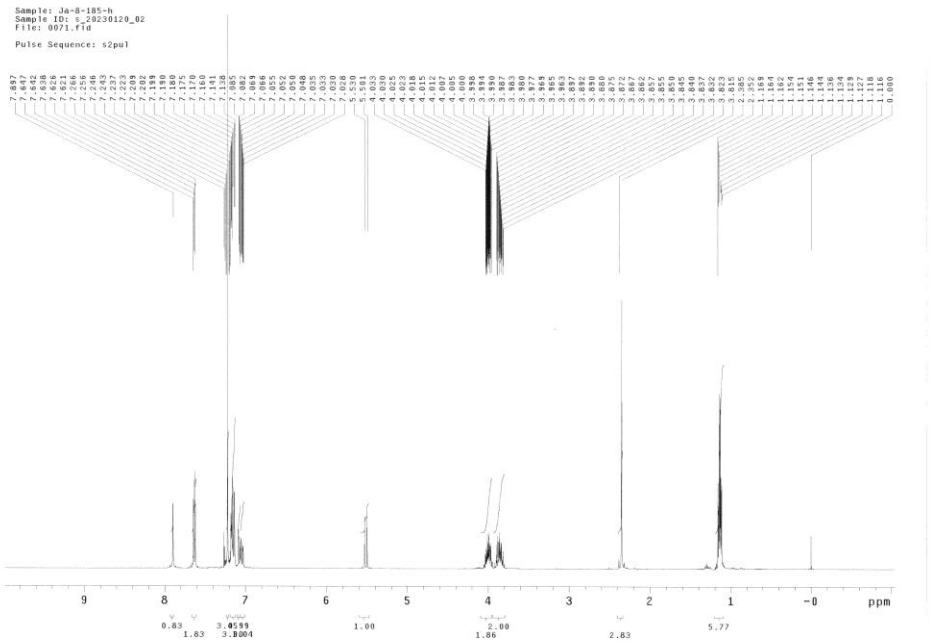

^{13}C NMR (100.5 MHz) in $CDCl_3$

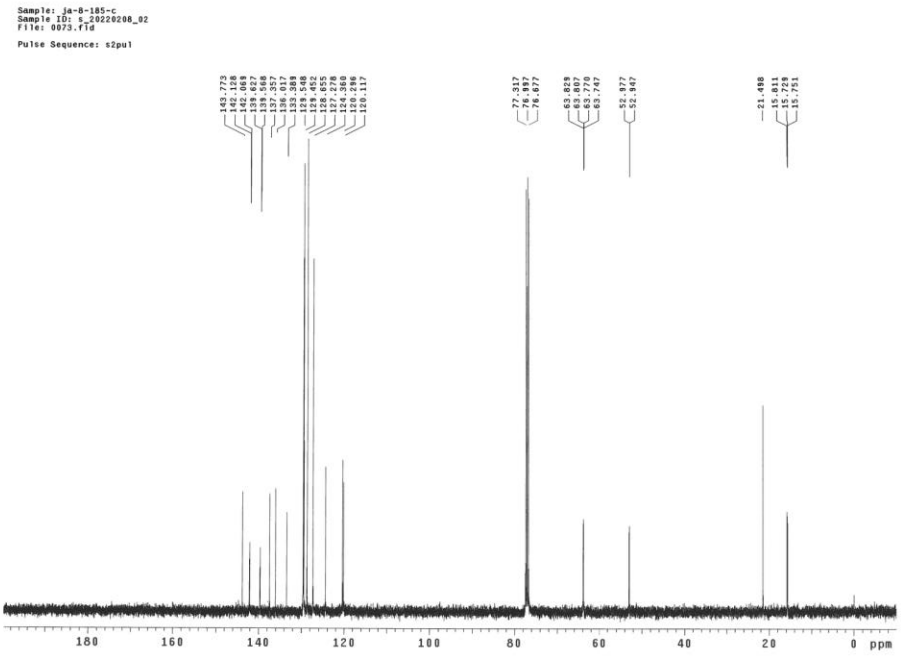

^{31}P NMR (162 MHz) in $CDCl_3$

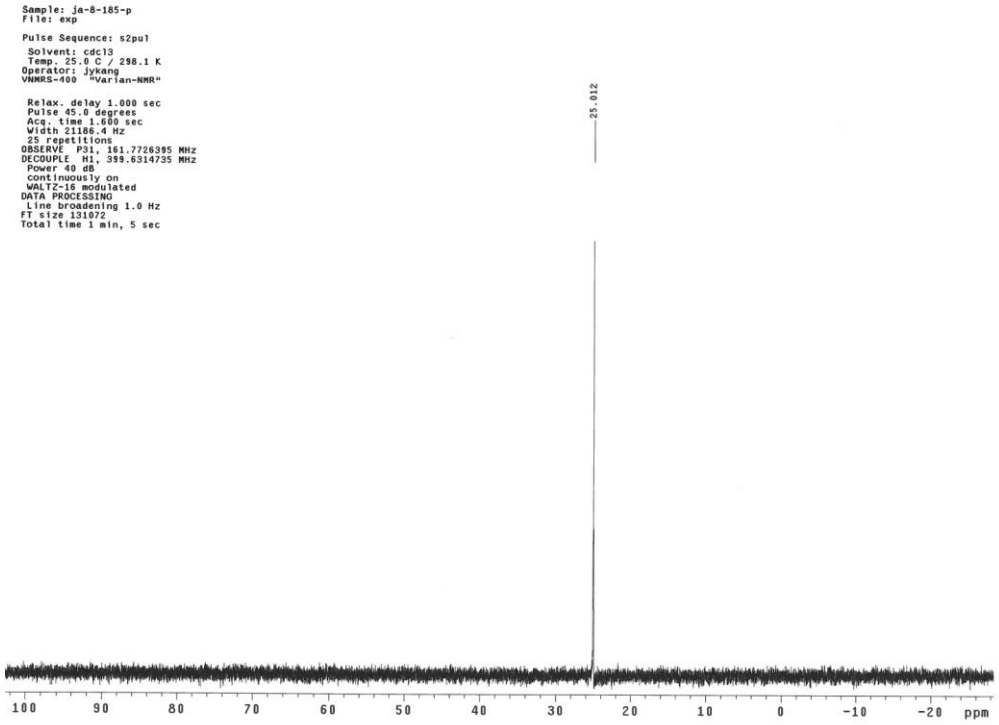

^{1}H NMR (400 MHz) in $CDCl_3$

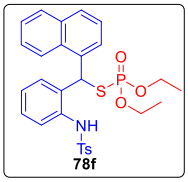

78f

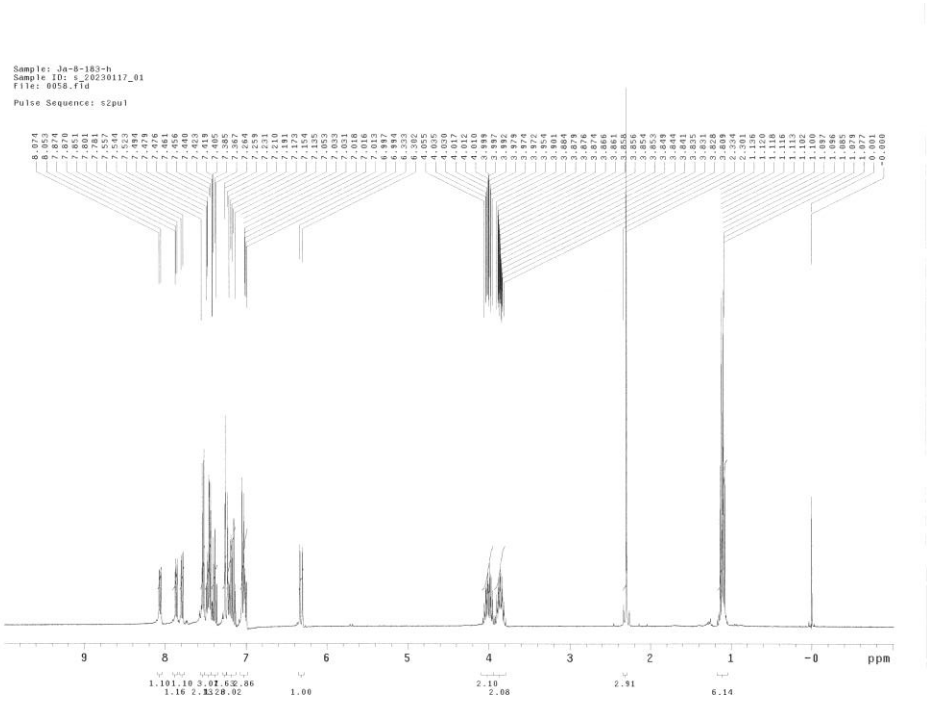

^{13}C NMR (100.5 MHz) in $CDCl_3$

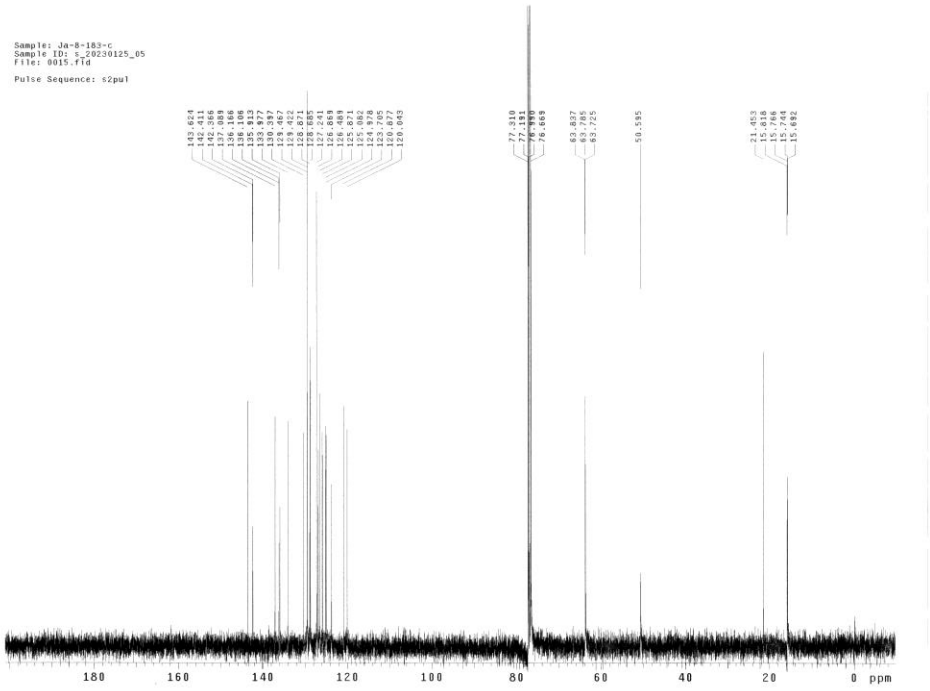

^{31}P NMR (162 MHz) in $CDCl_3$

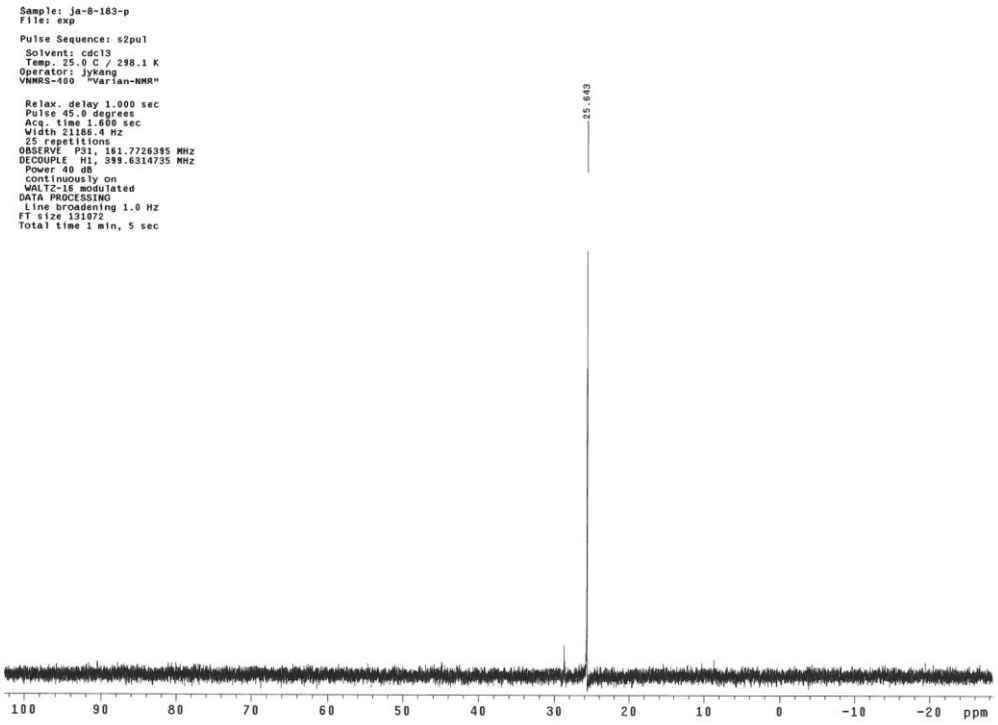

^{1}H NMR (400 MHz) in $CDCl_3$

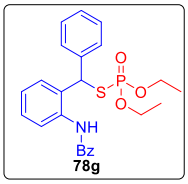

78g

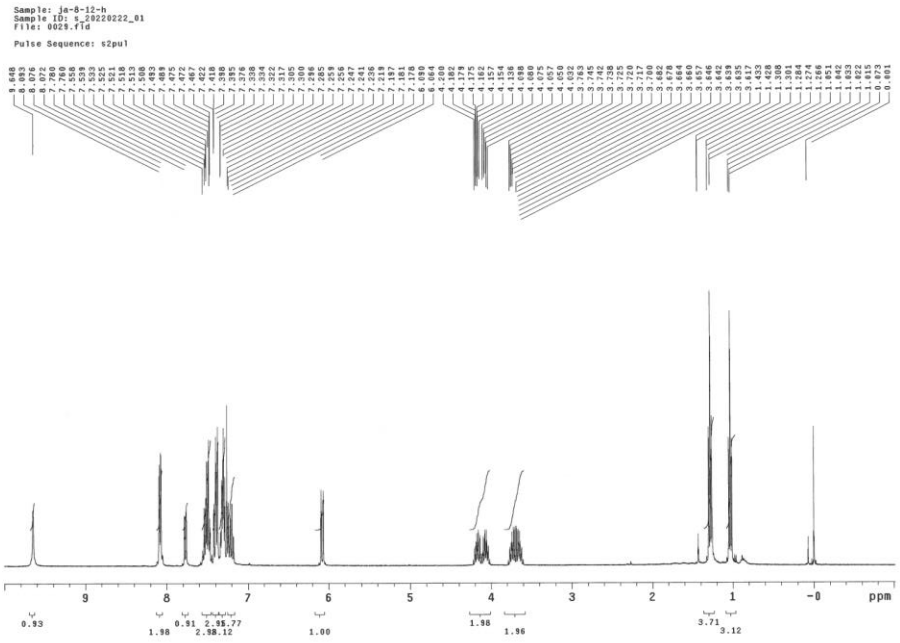

^{13}C NMR (100.5 MHz) in $CDCl_3$

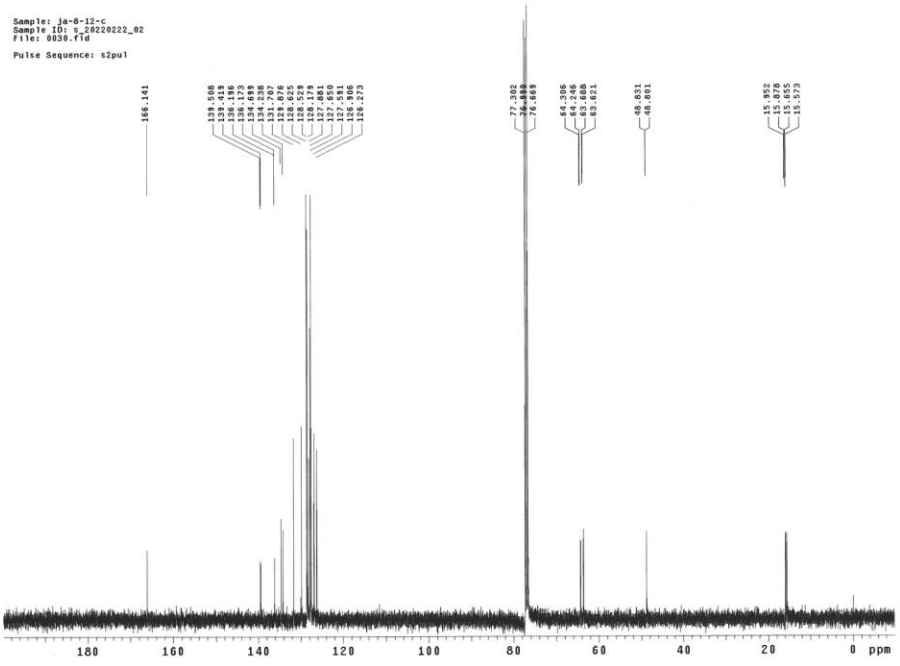

^{31}P NMR (162 MHz) in $CDCl_3$

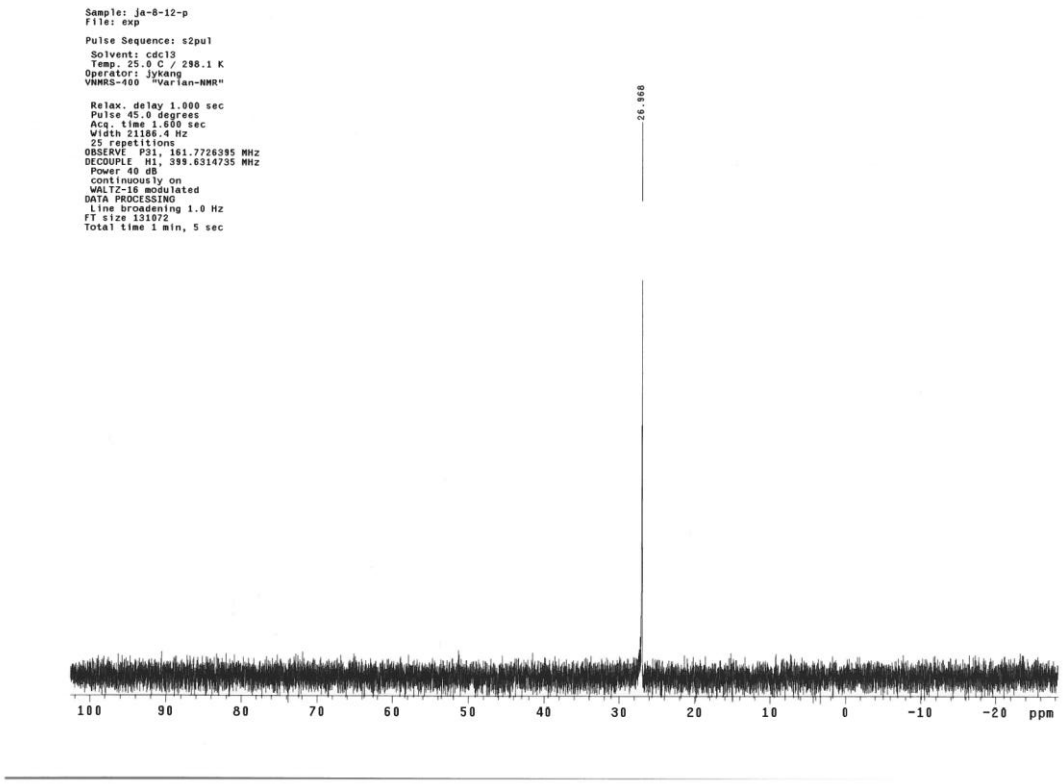

^{1}H NMR (400 MHz) in $CDCl_3$

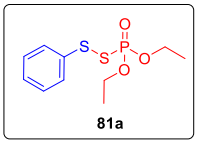

81a

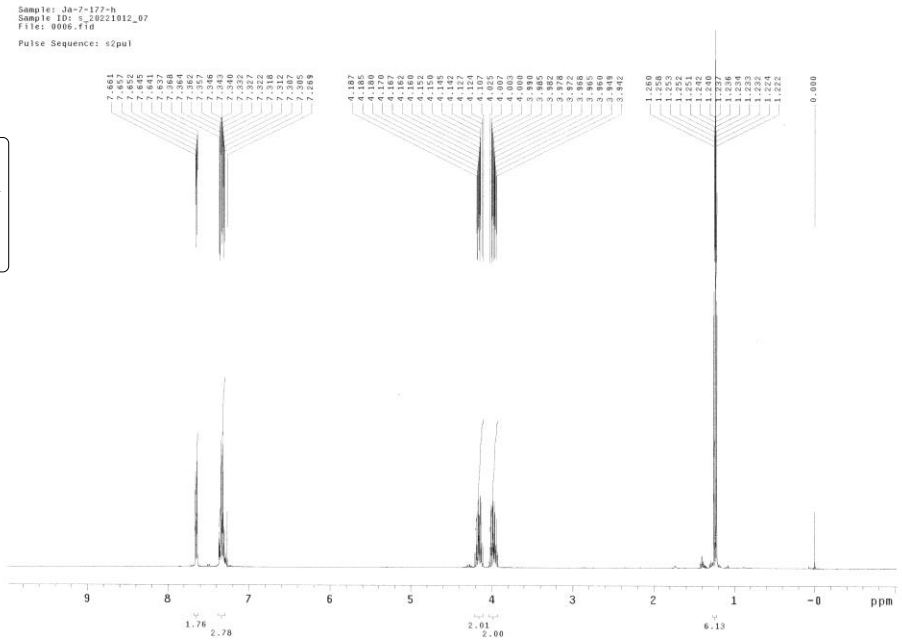

^{13}C NMR (100.5 MHz) in $CDCl_3$

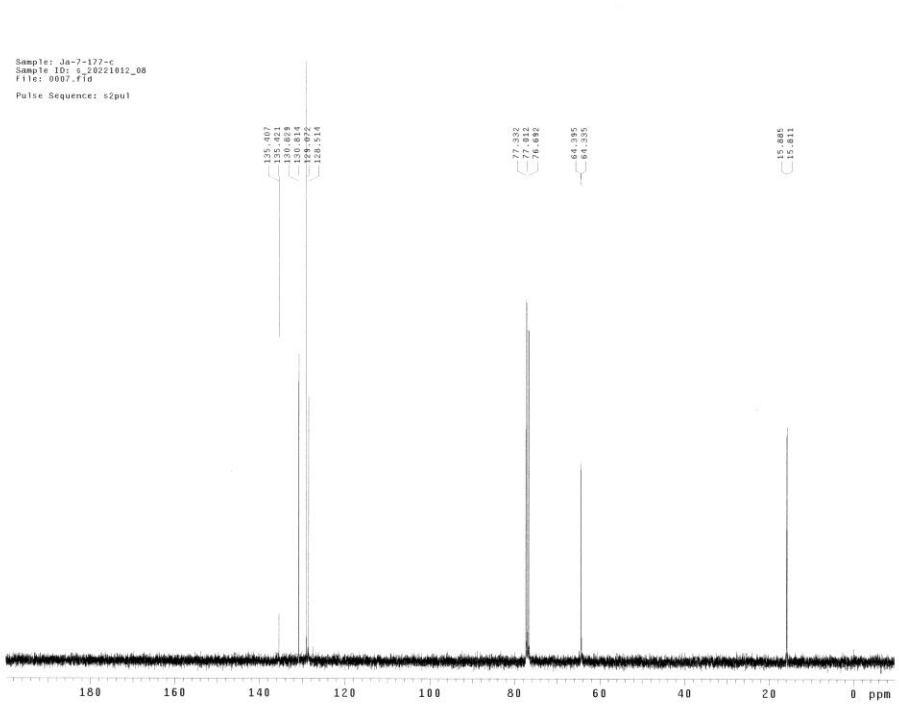

^{31}P NMR (162 MHz) in $CDCl_3$

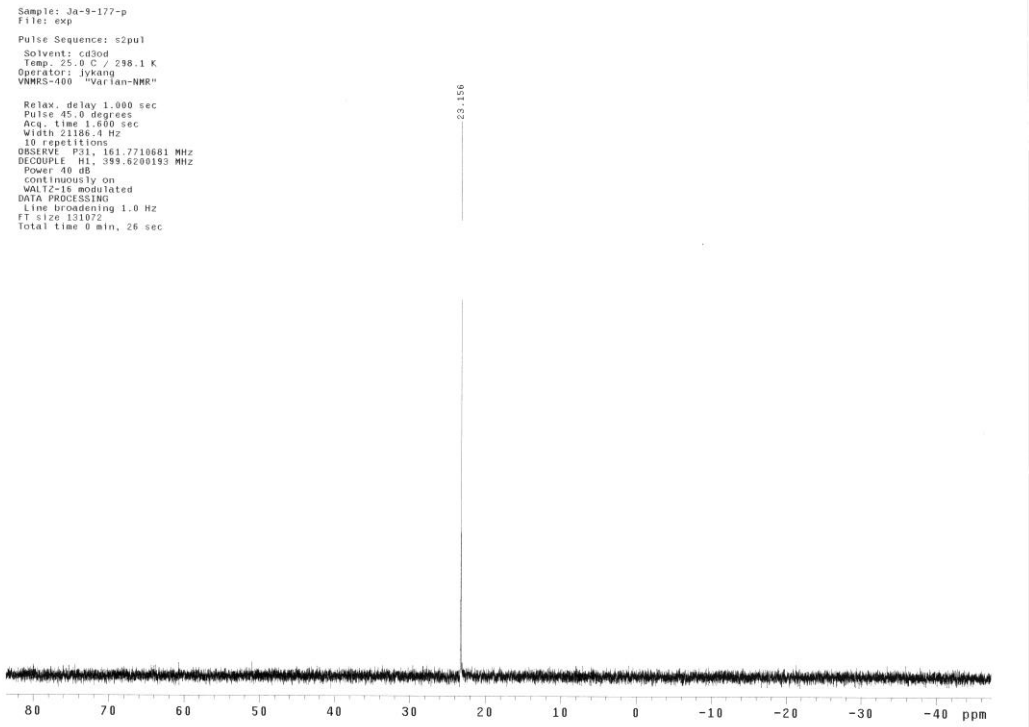

^{1}H NMR (400 MHz) in $CDCl_3$

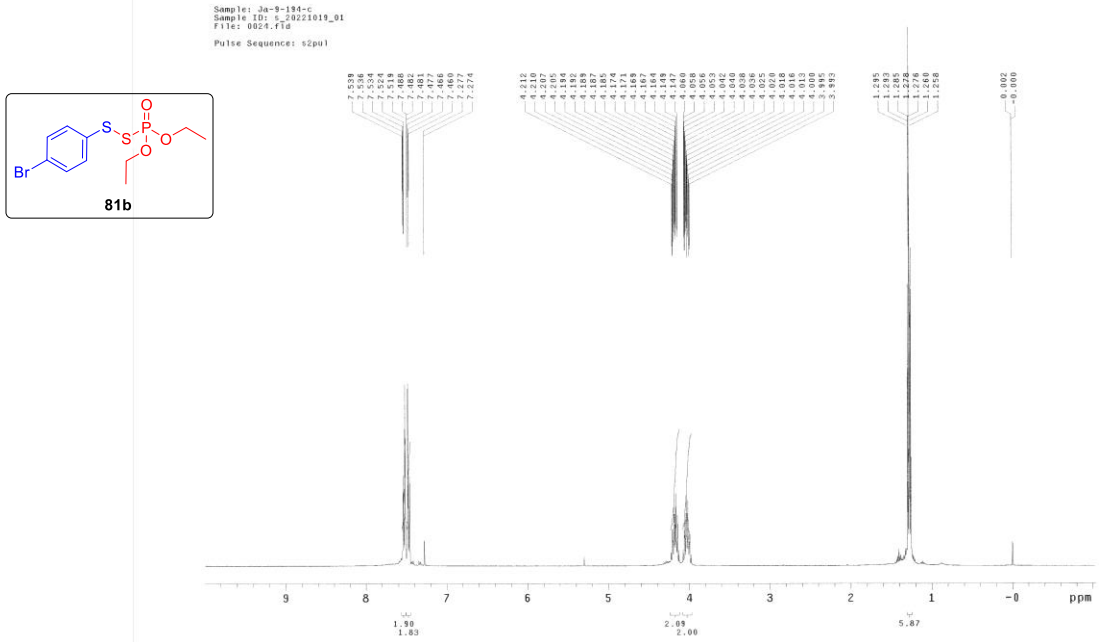

^{13}C NMR (100.5 MHz) in $CDCl_3$

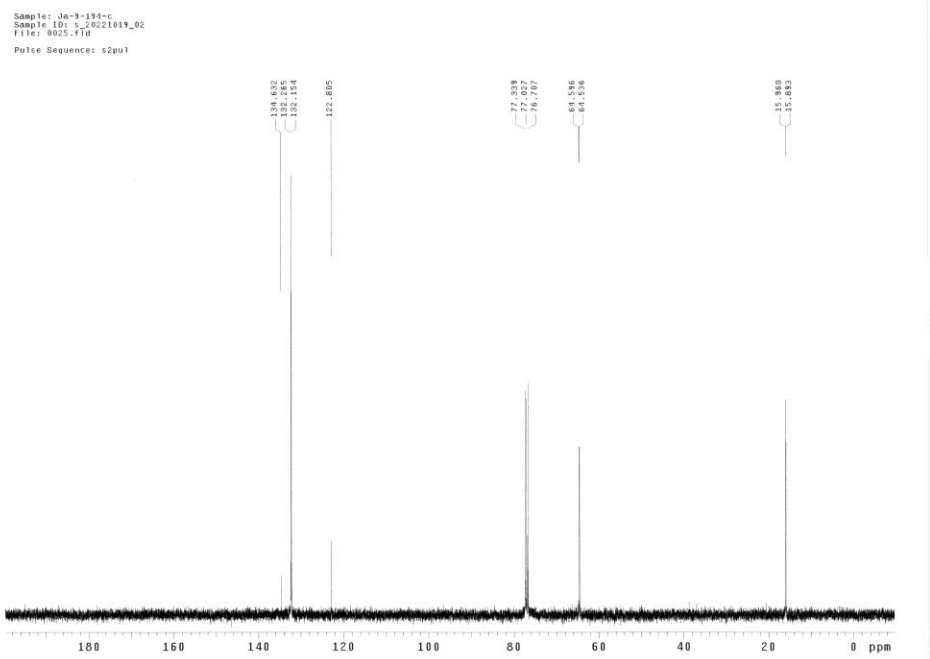

^{31}P NMR (162 MHz) in $CDCl_3$

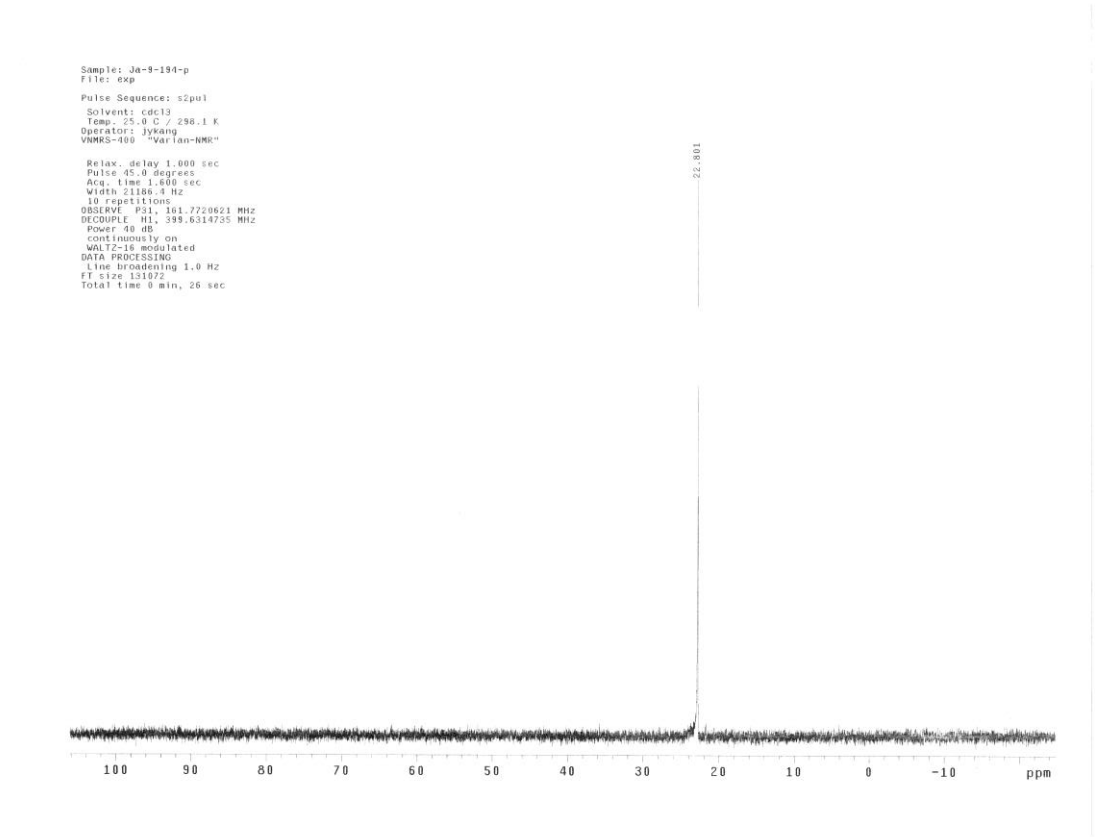

^{1}H NMR (400 MHz) in $CDCl_3$

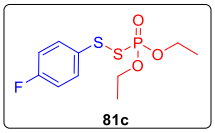

81c

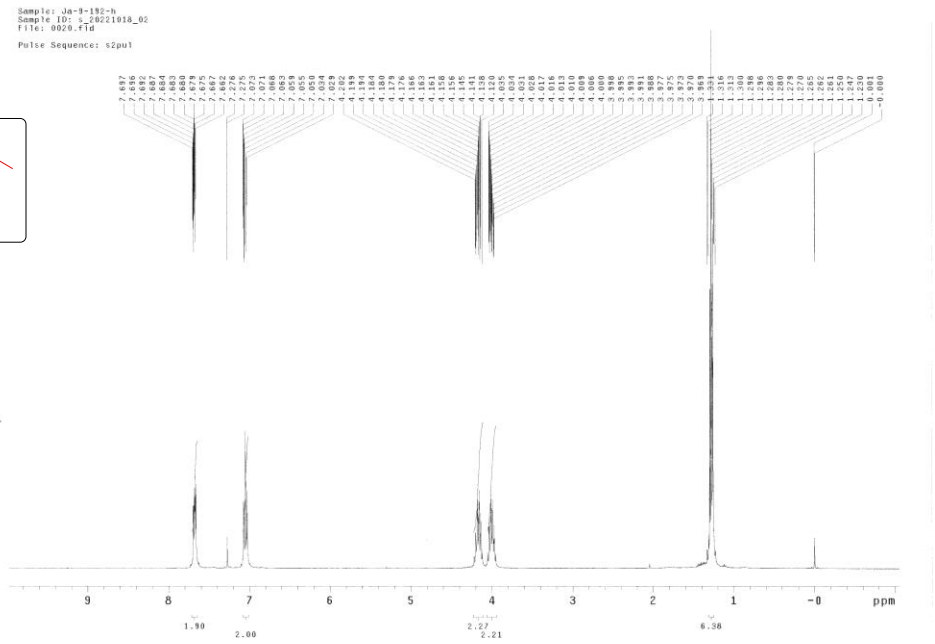

^{13}C NMR (100.5 MHz) in $CDCl_3$

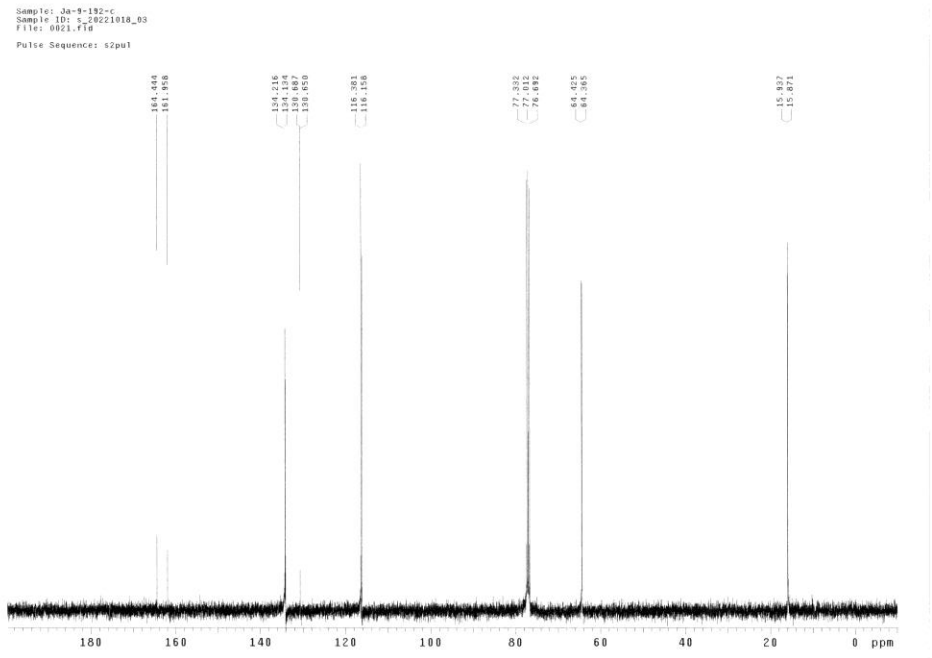

^{31}P NMR (162 MHz) in $CDCl_3$

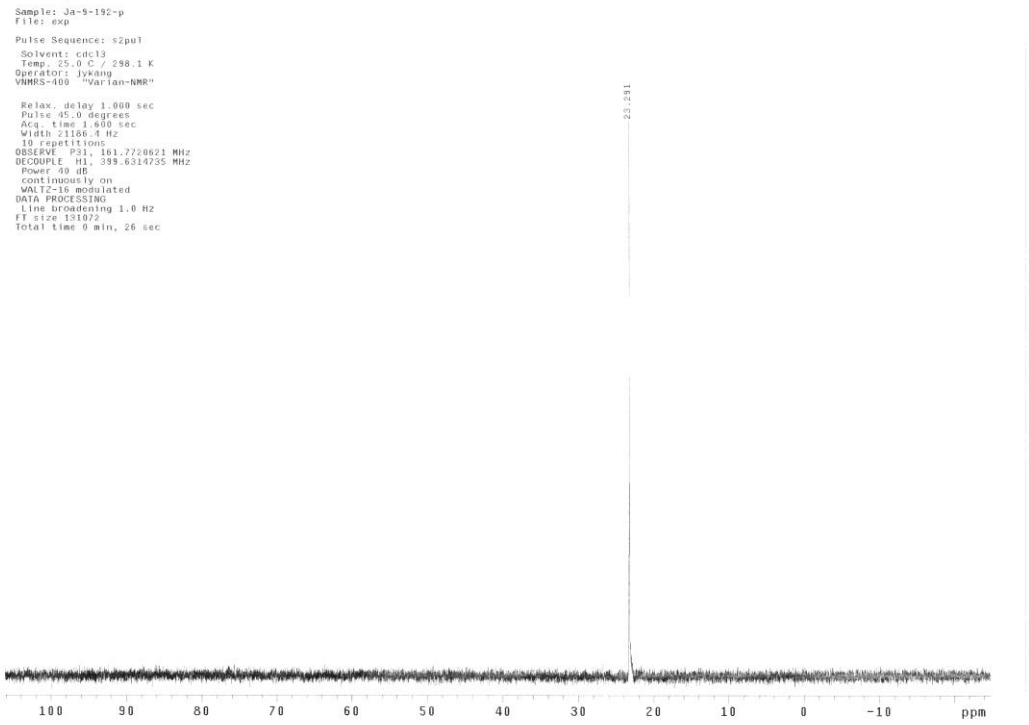

^{1}H NMR (400 MHz) in $CDCl_3$

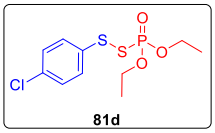

81d

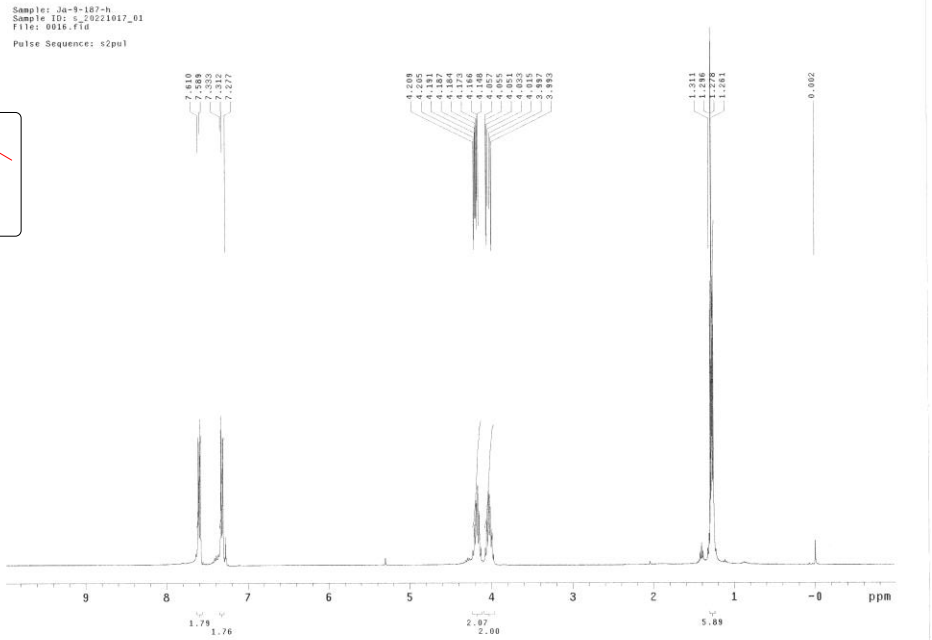

^{13}C NMR (100.5 MHz) in $CDCl_3$

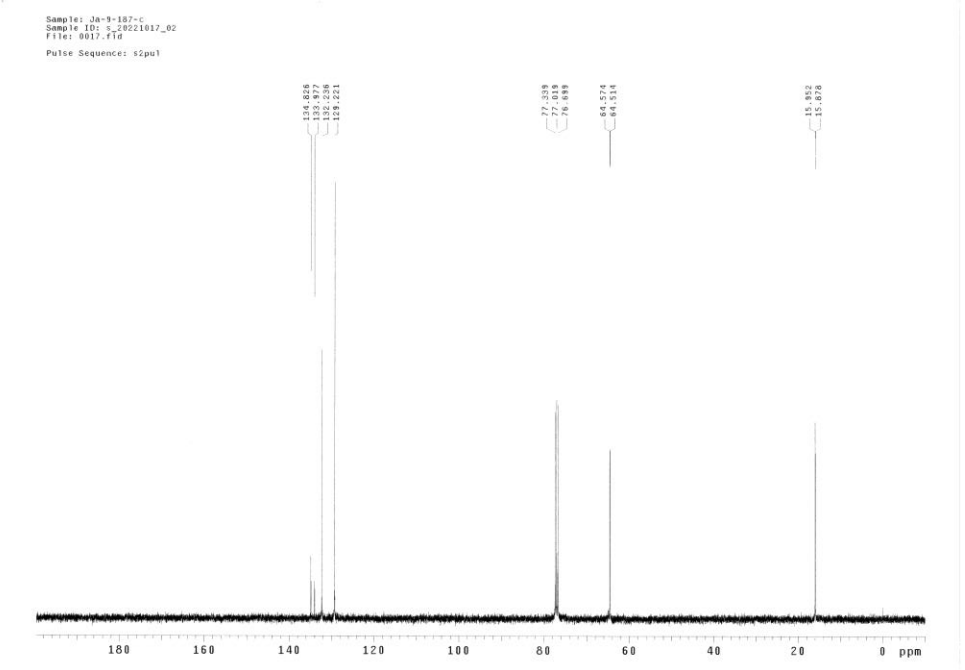

^{31}P NMR (162 MHz) in $CDCl_3$

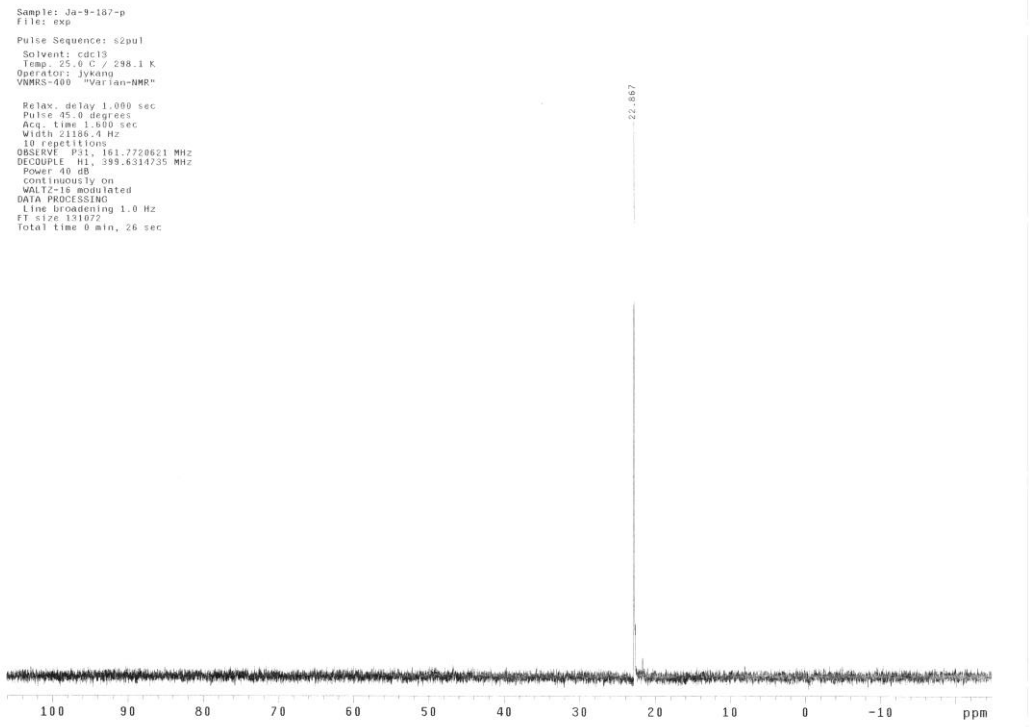

^{1}H NMR (400 MHz) in $CDCl_3$

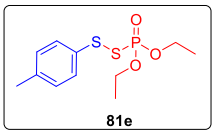

81e

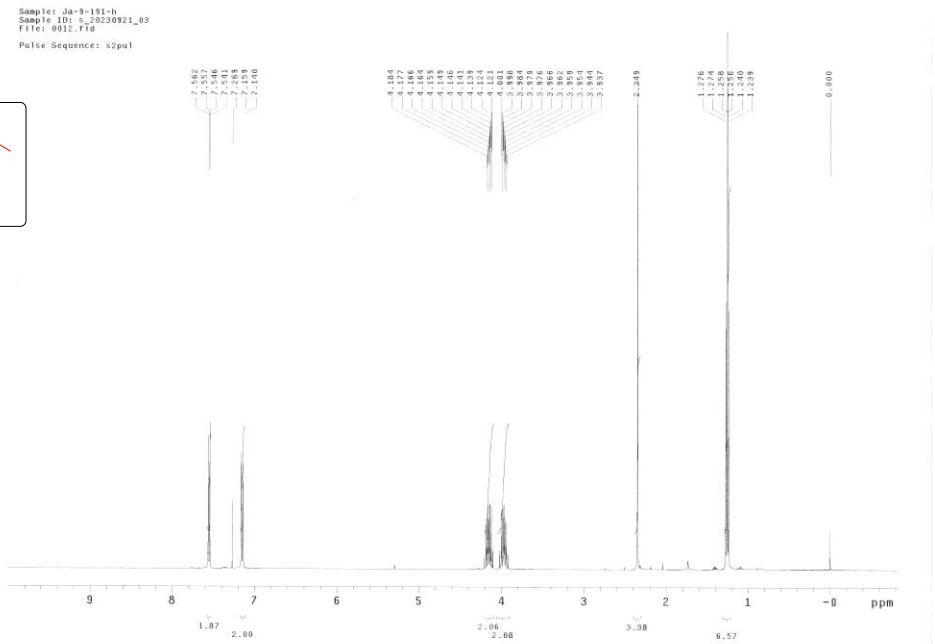

^{13}C NMR (100.5 MHz) in $CDCl_3$

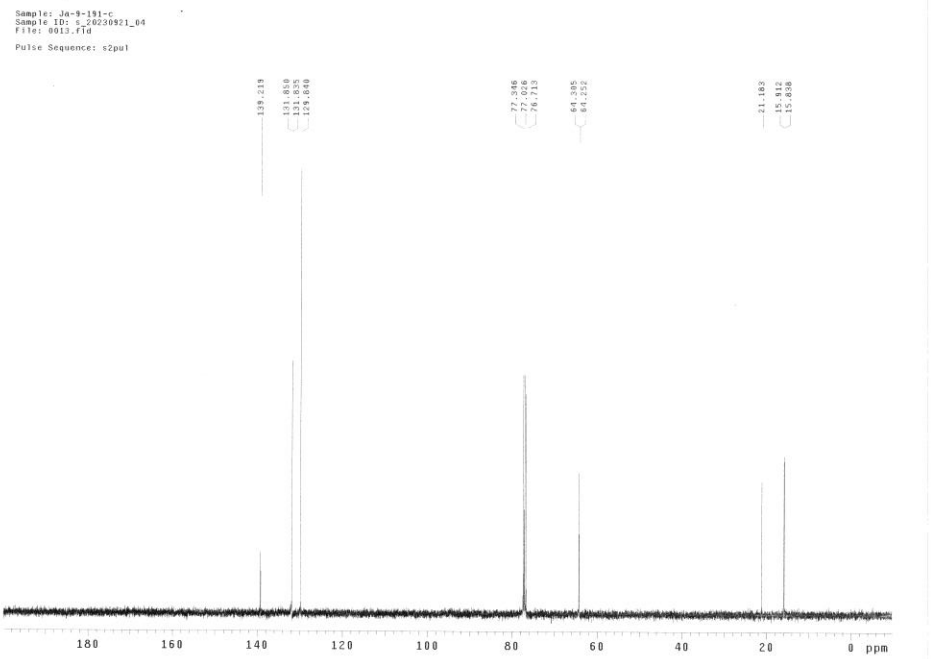

^{31}P NMR (162 MHz) in $CDCl_3$

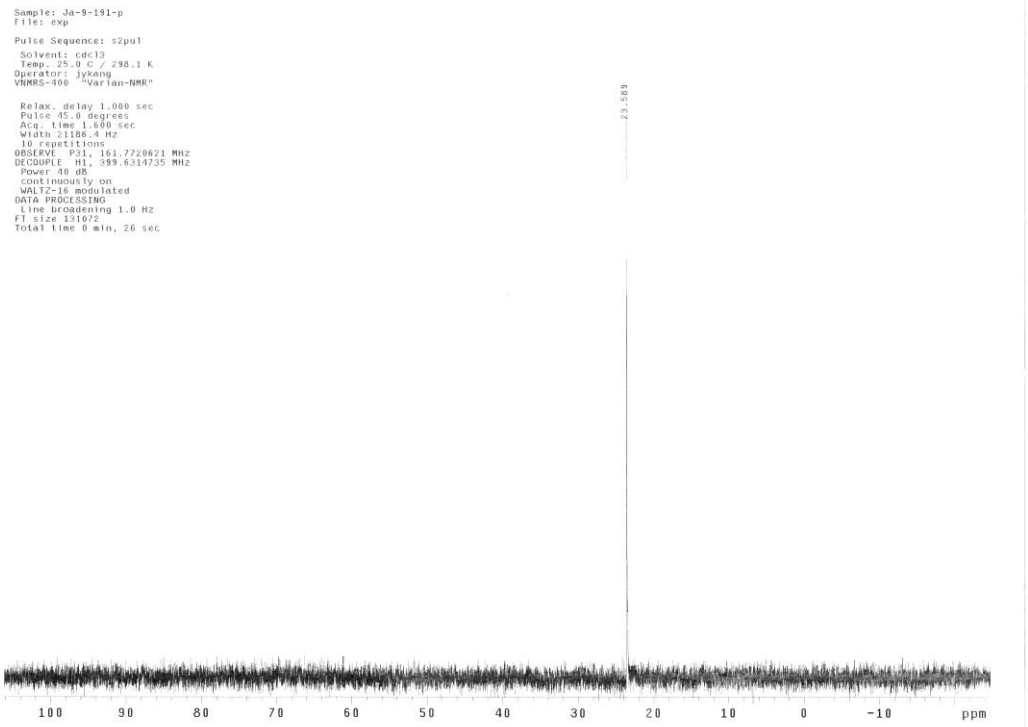

^{1}H NMR (400 MHz) in $CDCl_3$

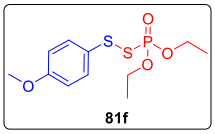

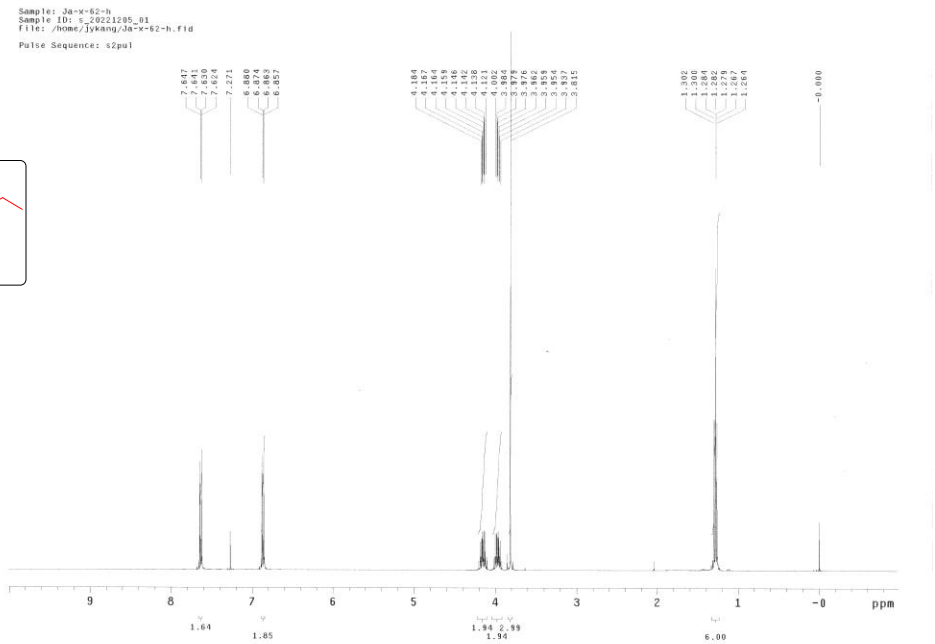

^{13}C NMR (100.5 MHz) in $CDCl_3$

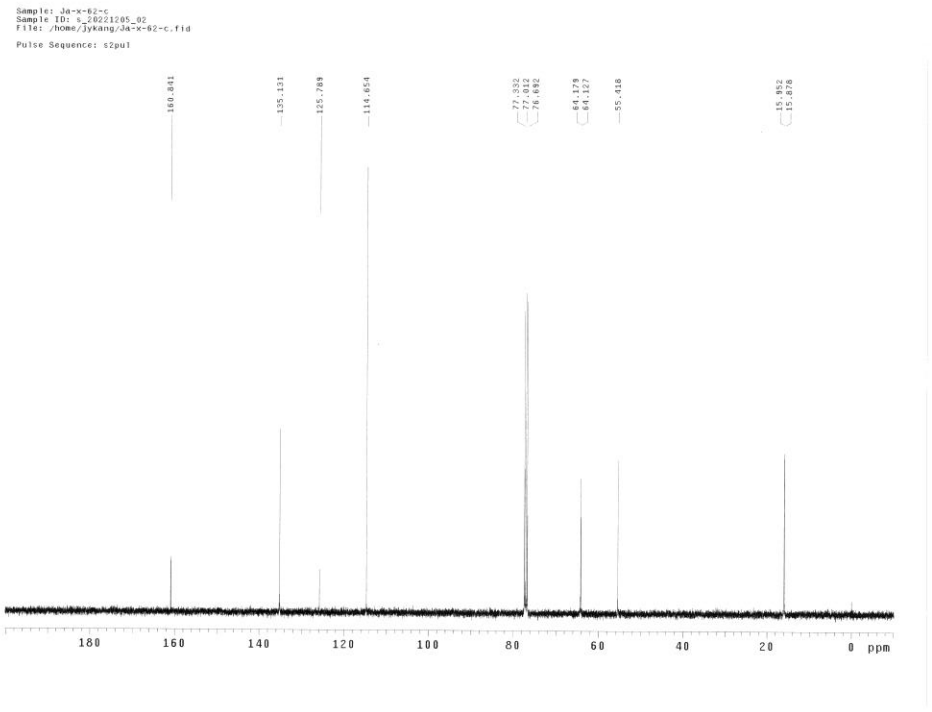

^{31}P NMR (162 MHz) in $CDCl_3$

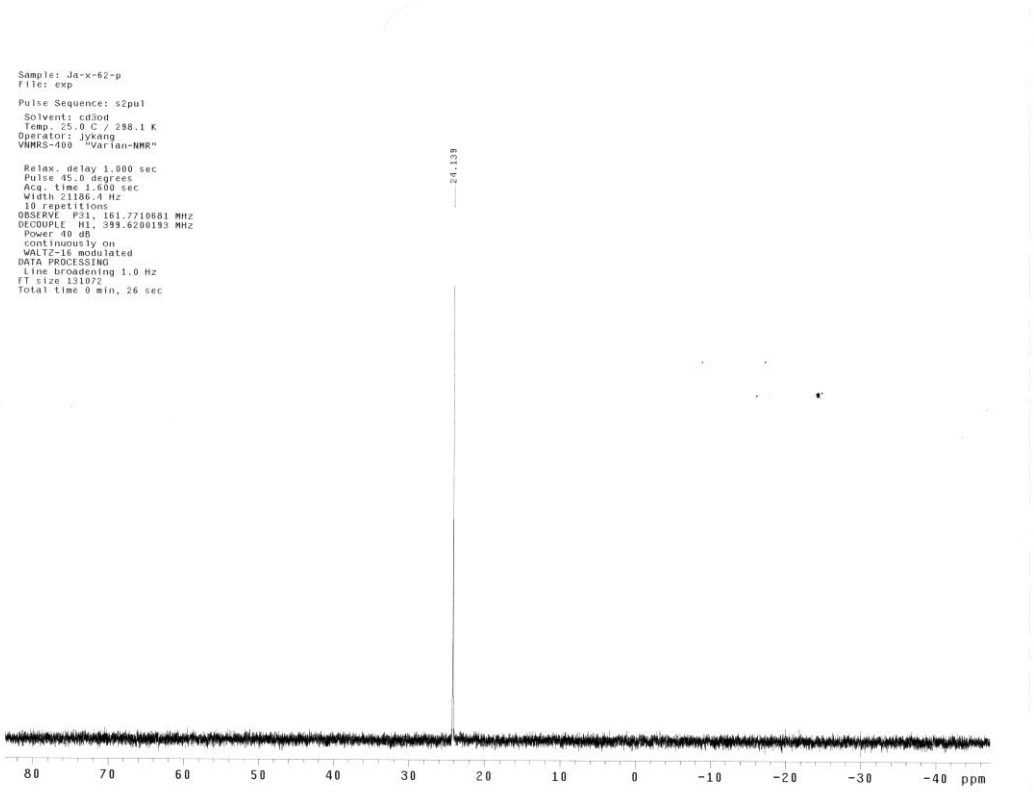

^{1}H NMR (400 MHz) in $CDCl_3$

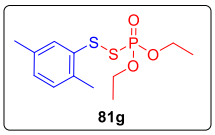

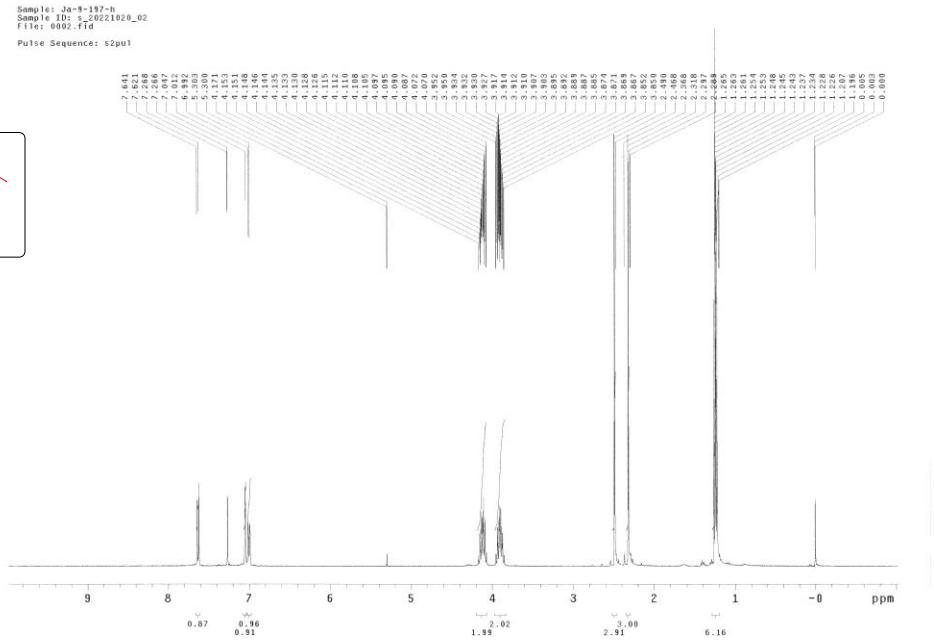

^{13}C NMR (100.5 MHz) in $CDCl_3$

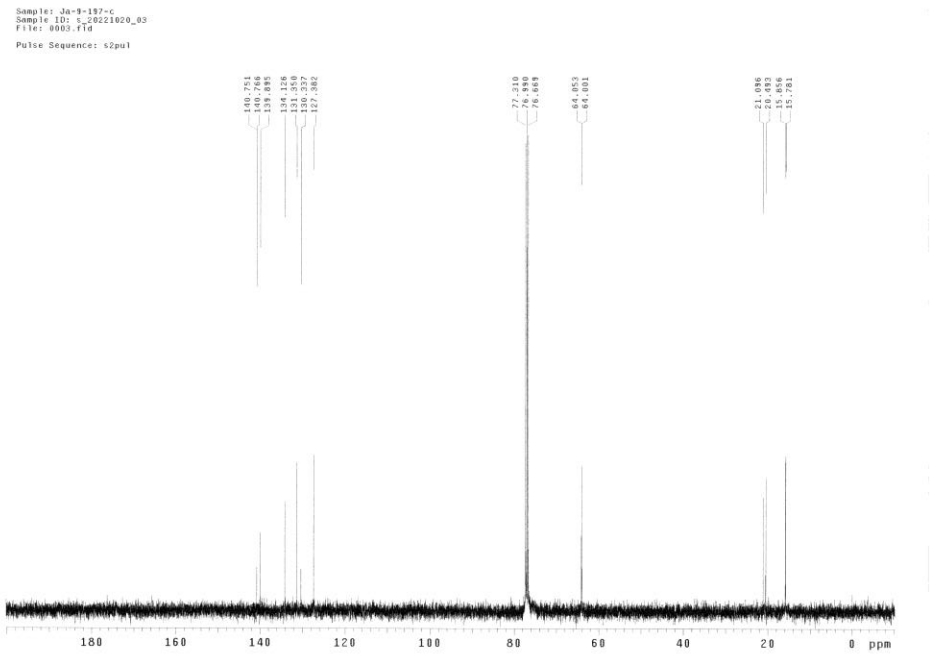

^{31}P NMR (162 MHz) in $CDCl_3$

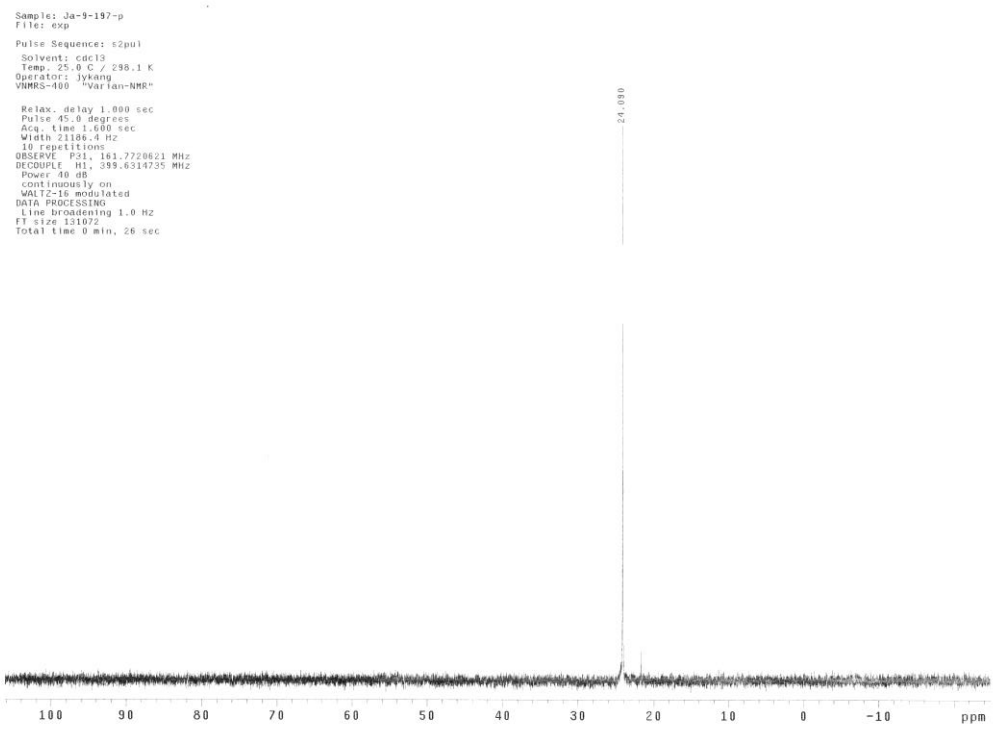

^{1}H NMR (400 MHz) in $CDCl_3$

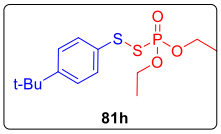

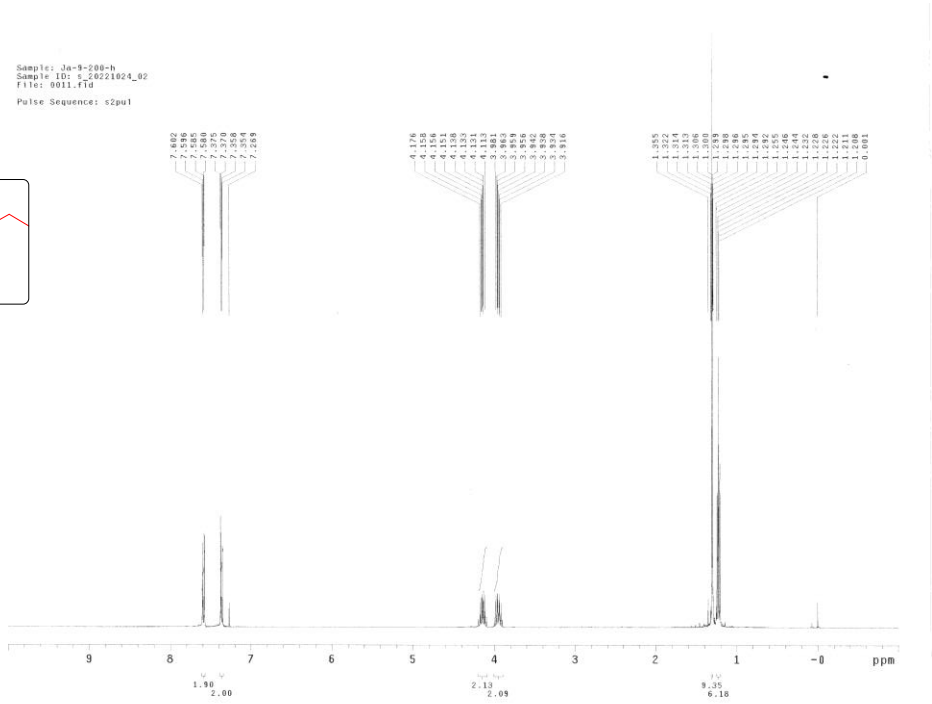

^{13}C NMR (100.5 MHz) in $CDCl_3$

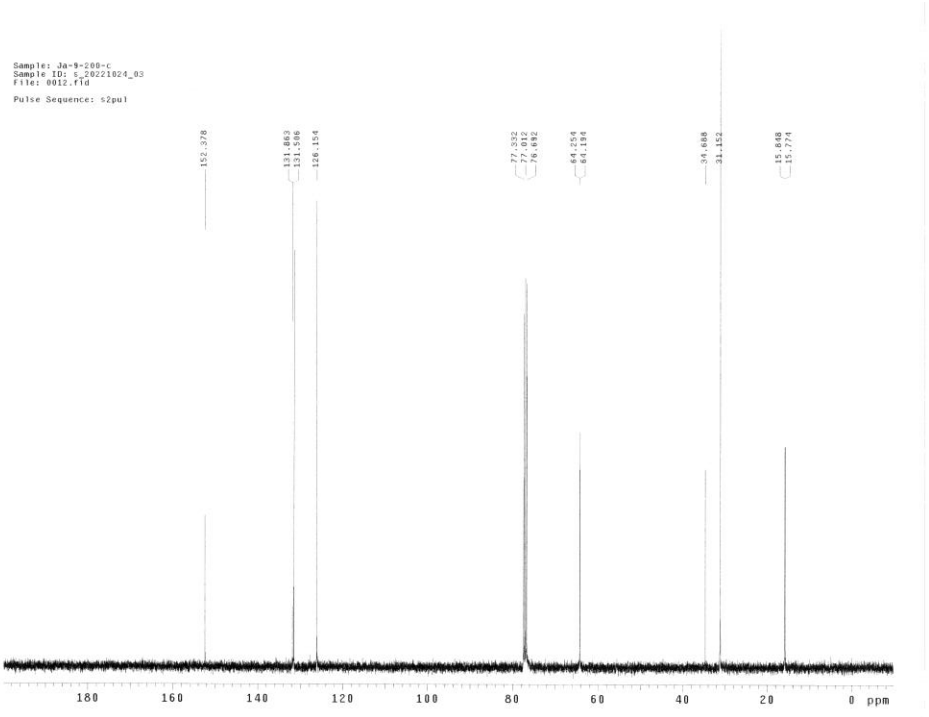

^{31}P NMR (162 MHz) in $CDCl_3$

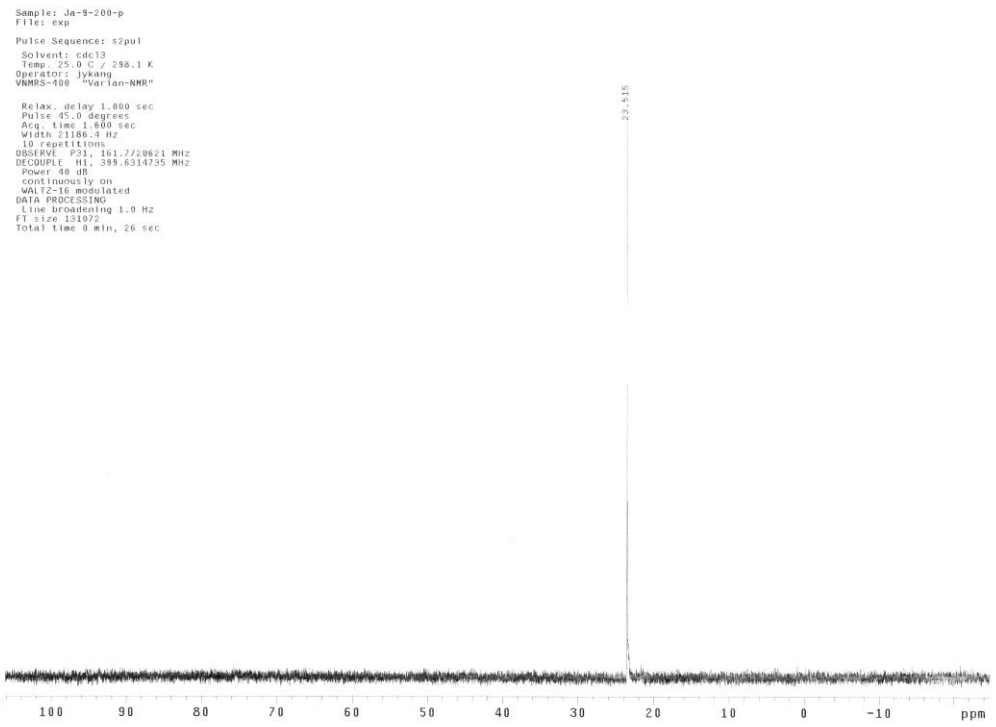

^{1}H NMR (400 MHz) in $CDCl_3$

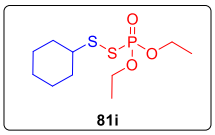

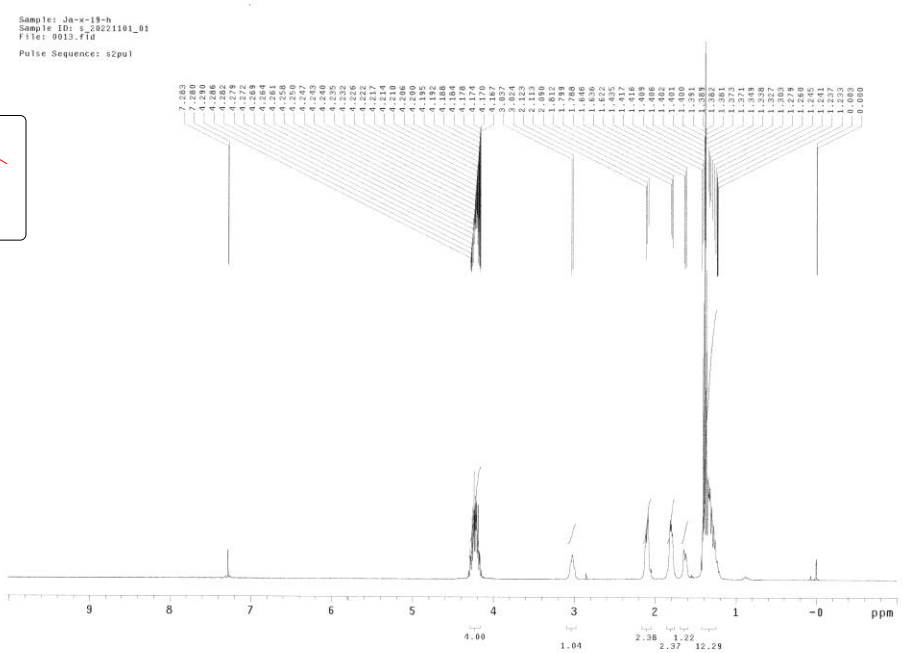

^{13}C NMR (100.5 MHz) in $CDCl_3$

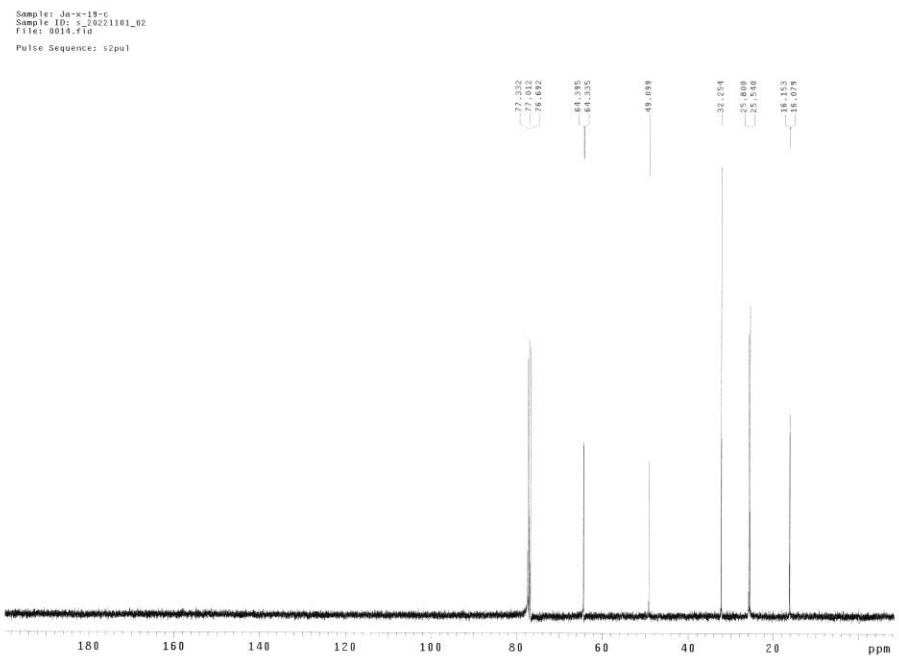

^{31}P NMR (162 MHz) in $CDCl_3$

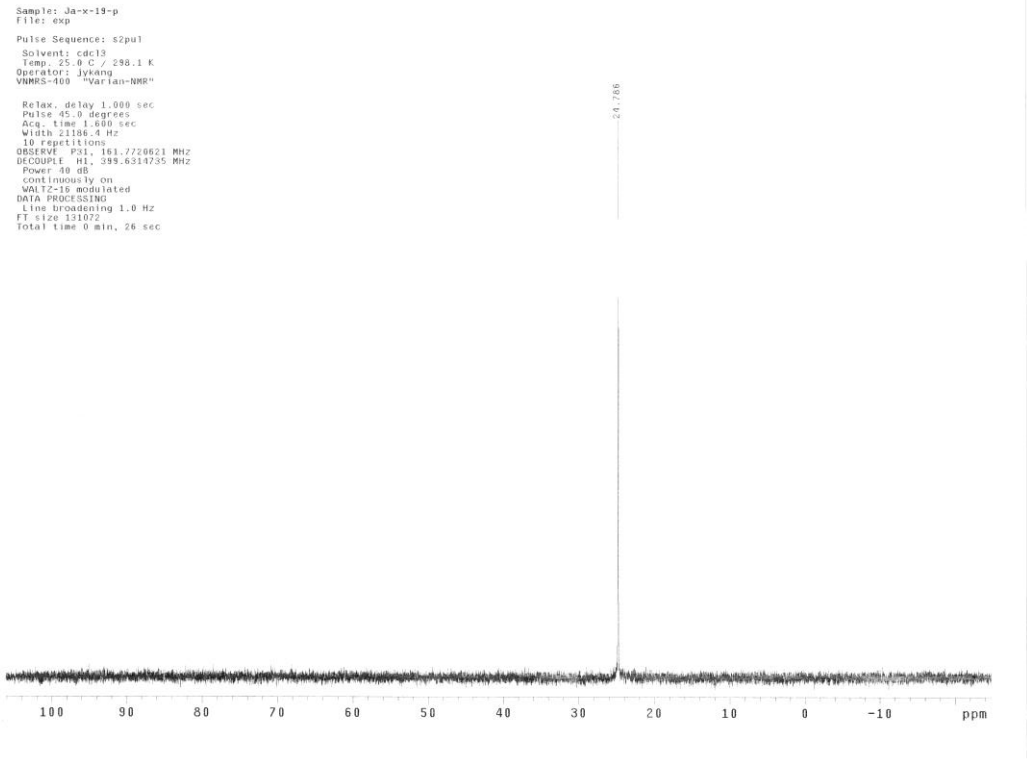

^{1}H NMR (400 MHz) in $CDCl_3$

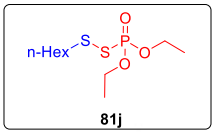

81j

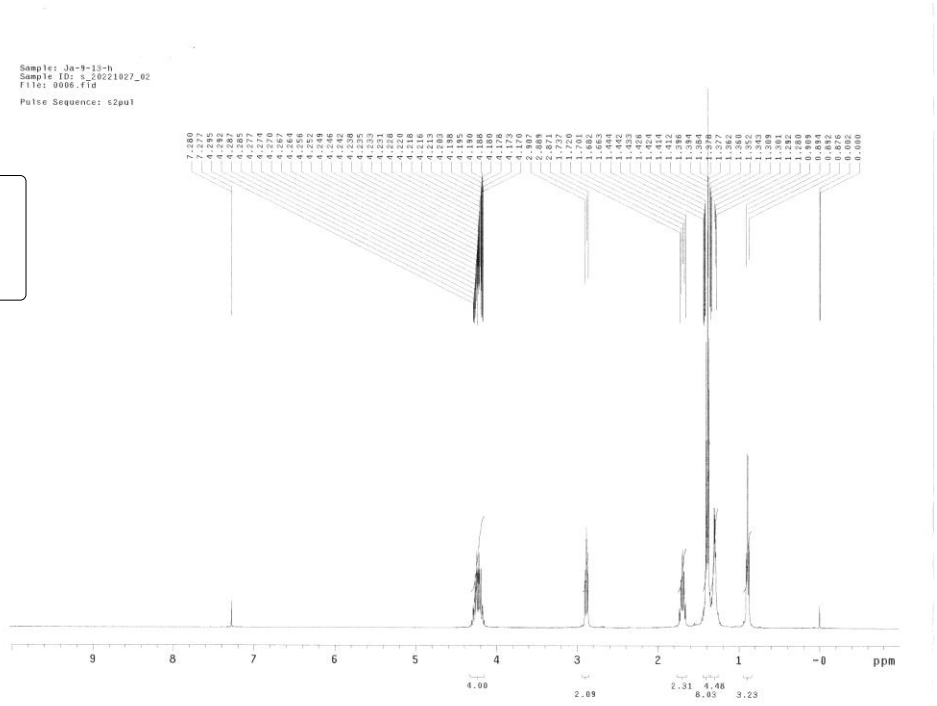

^{13}C NMR (100.5 MHz) in $CDCl_3$

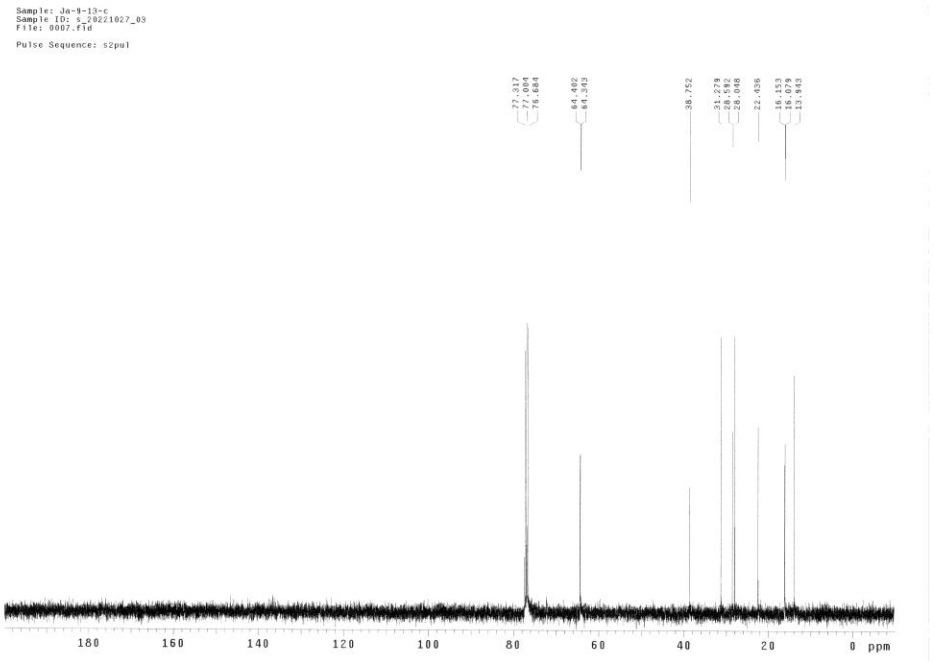

^{31}P NMR (162 MHz) in $CDCl_3$

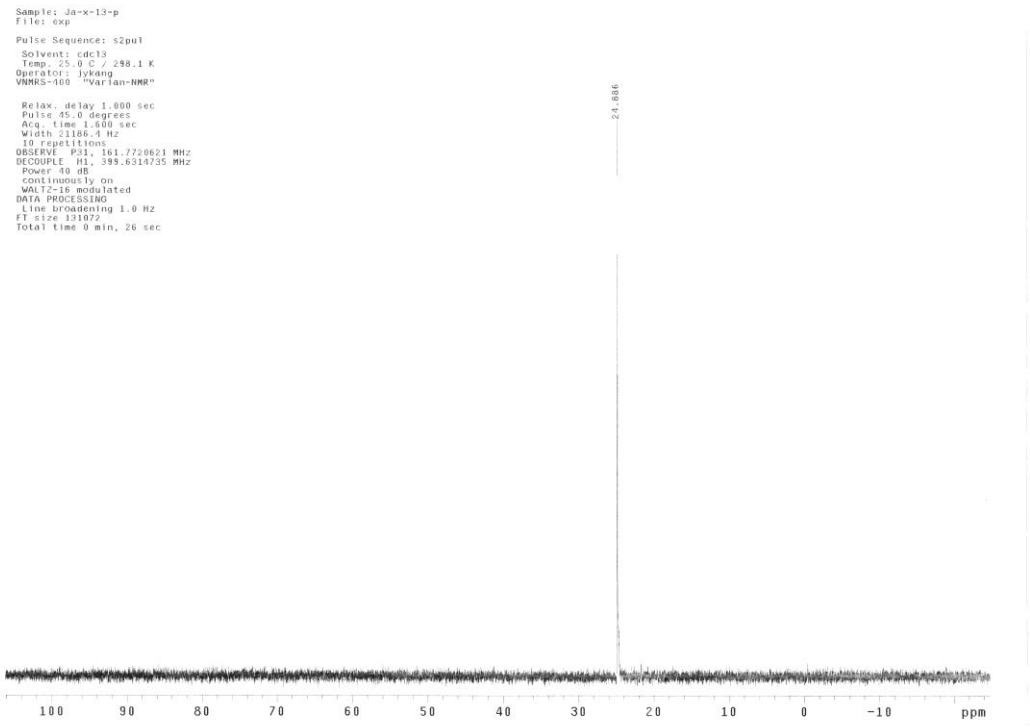

^{1}H NMR (400 MHz) in $CDCl_3$

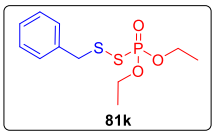

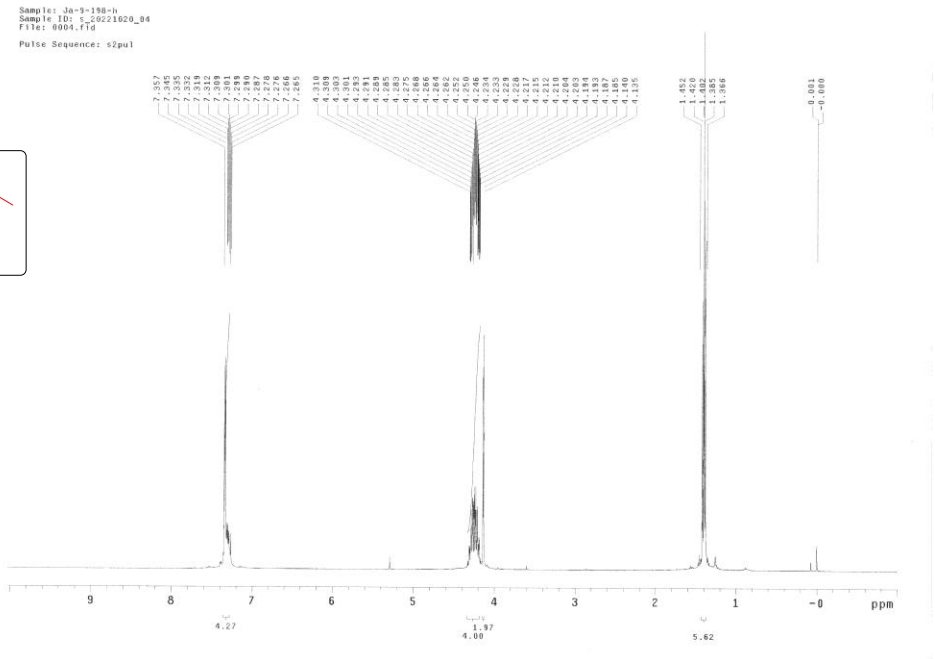

^{13}C NMR (100.5 MHz) in $CDCl_3$

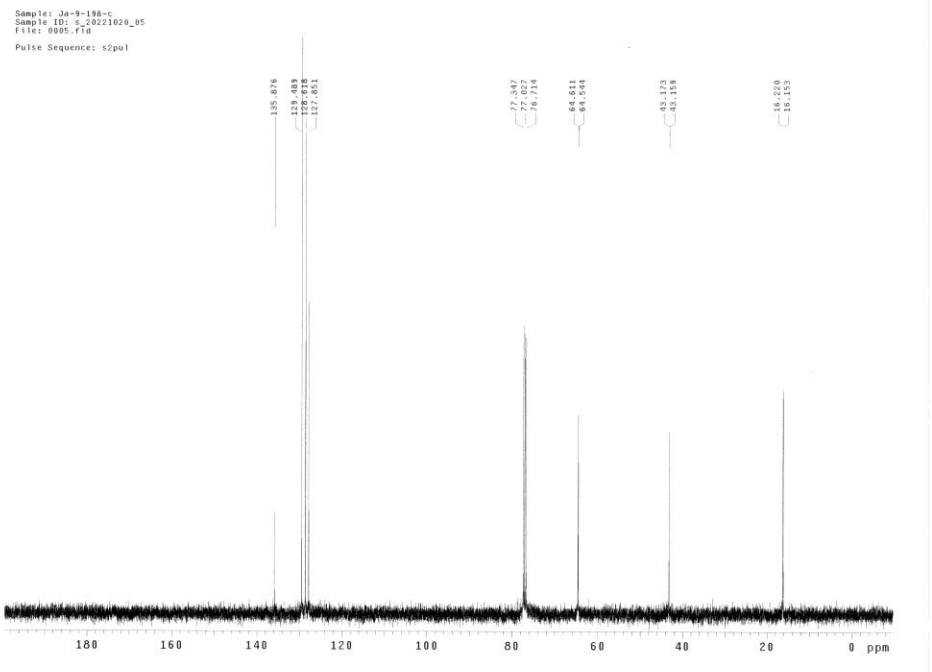

^{31}P NMR (162 MHz) in $CDCl_3$

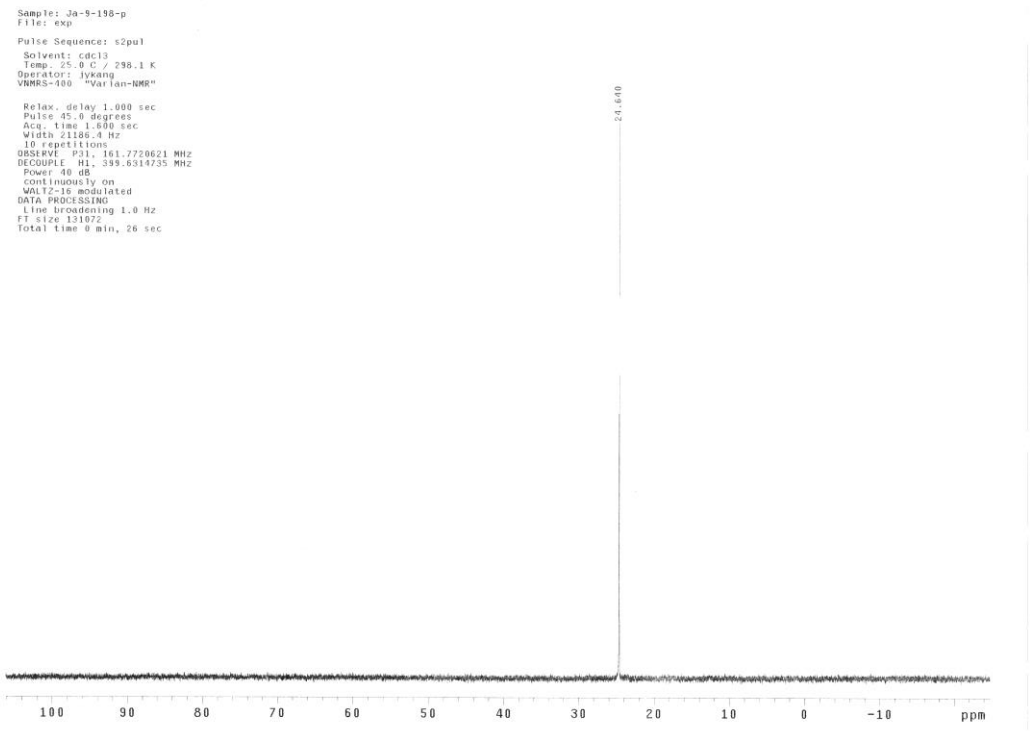

^{1}H NMR (400 MHz) in $CDCl_3$

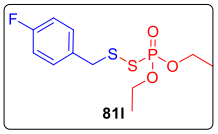

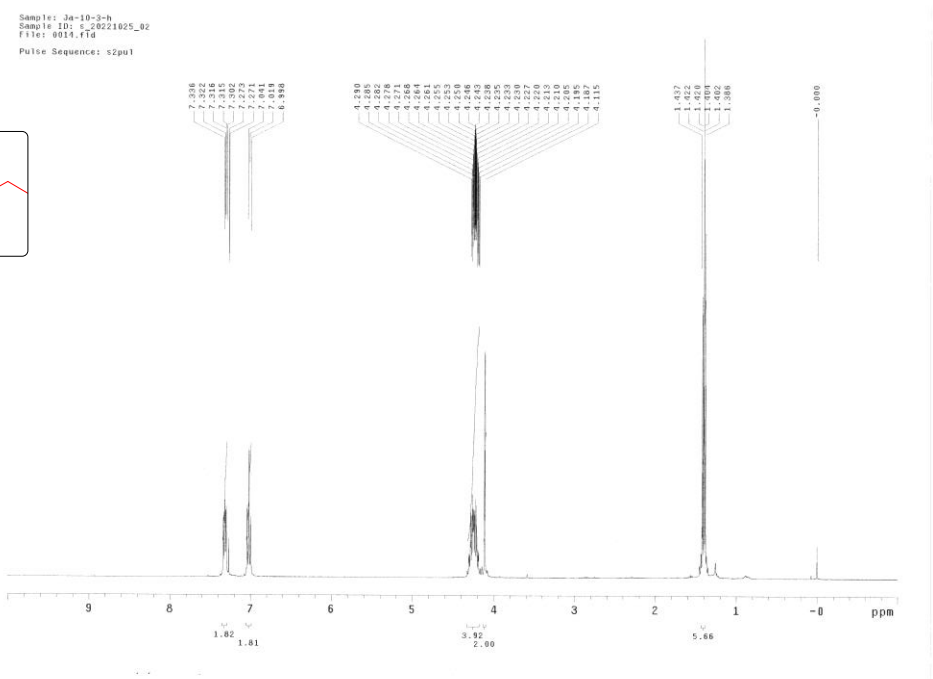

^{13}C NMR (100.5 MHz) in $CDCl_3$

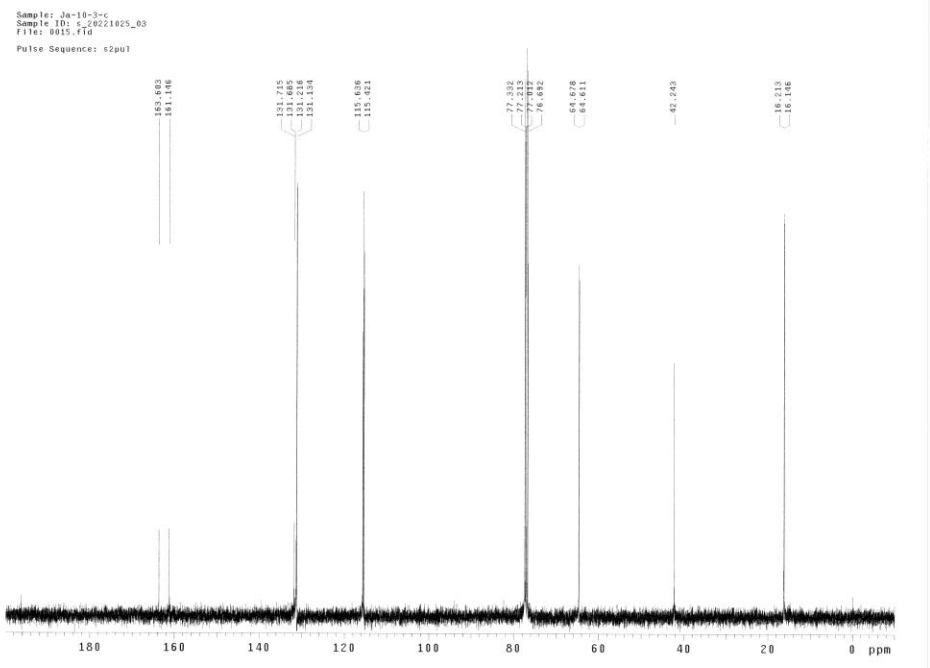

^{31}P NMR (162 MHz) in $CDCl_3$

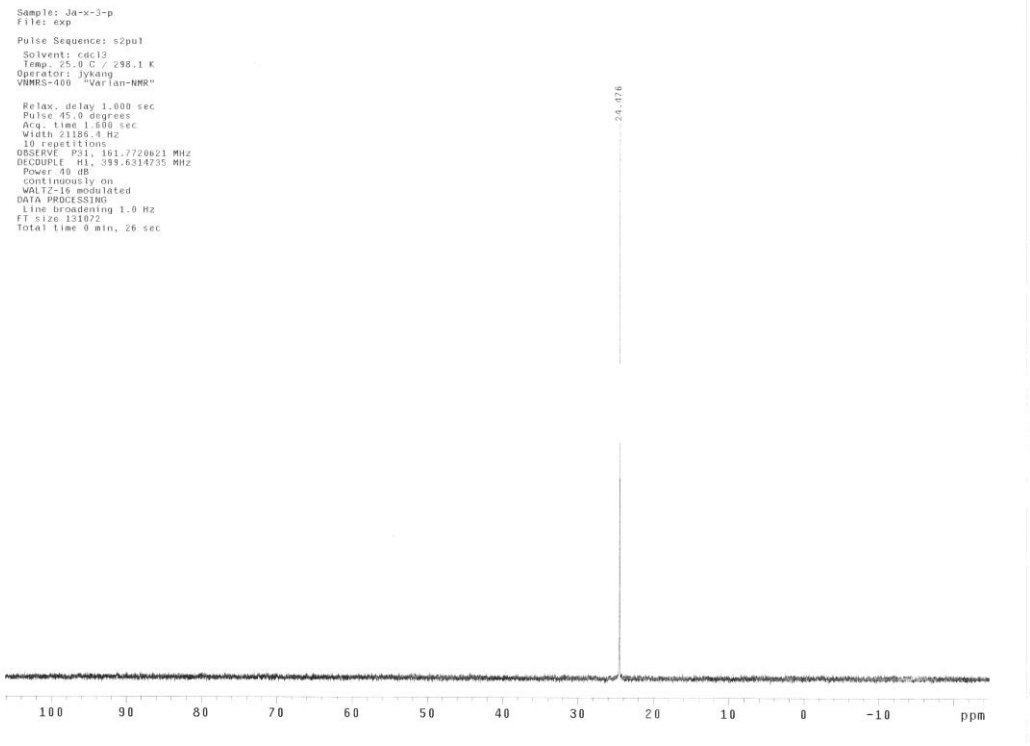

^{1}H NMR (400 MHz) in $CDCl_3$

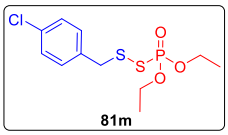

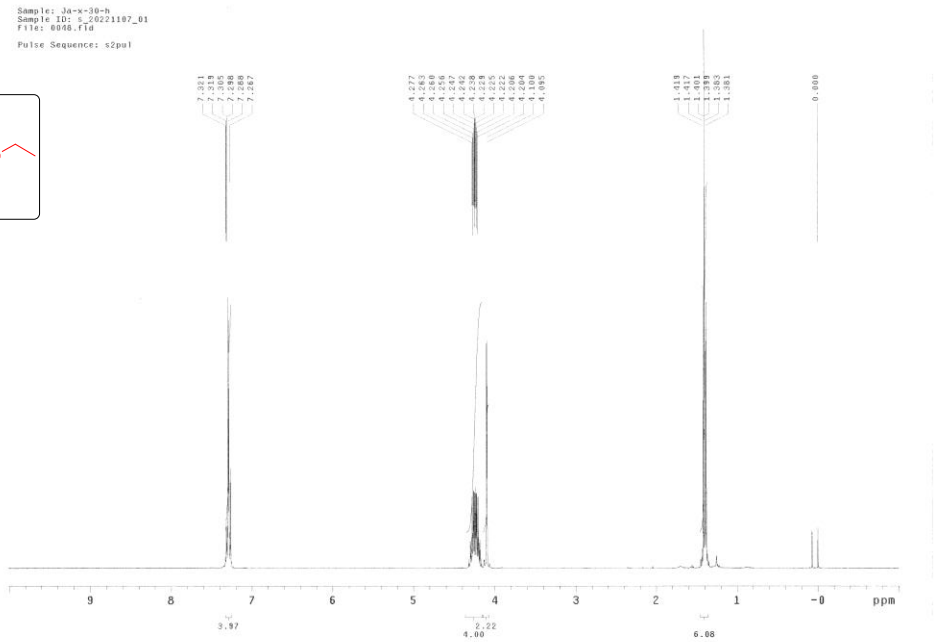

^{13}C NMR (100.5 MHz) in $CDCl_3$

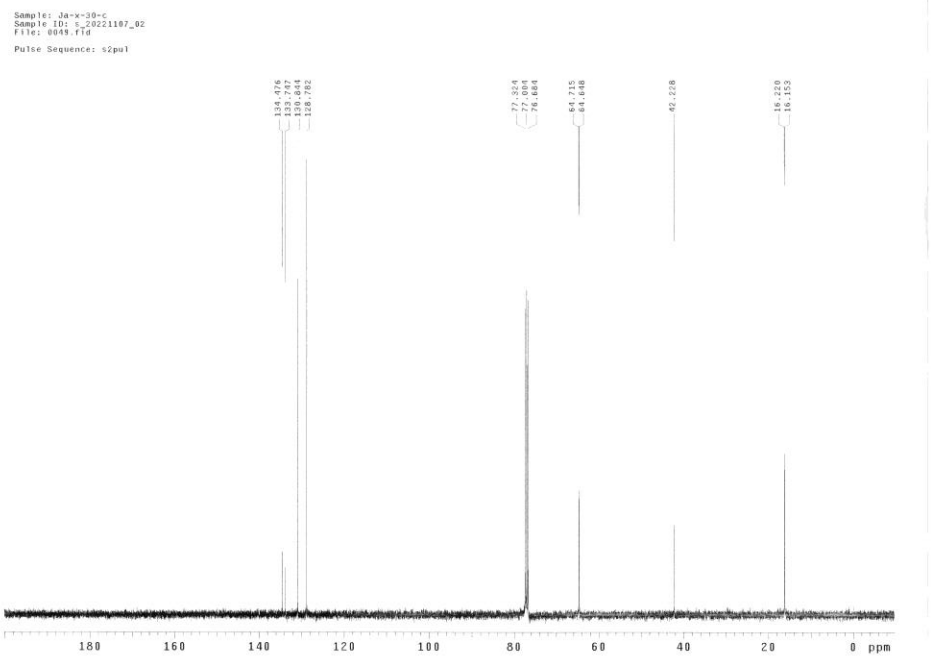

^{31}P NMR (162 MHz) in $CDCl_3$

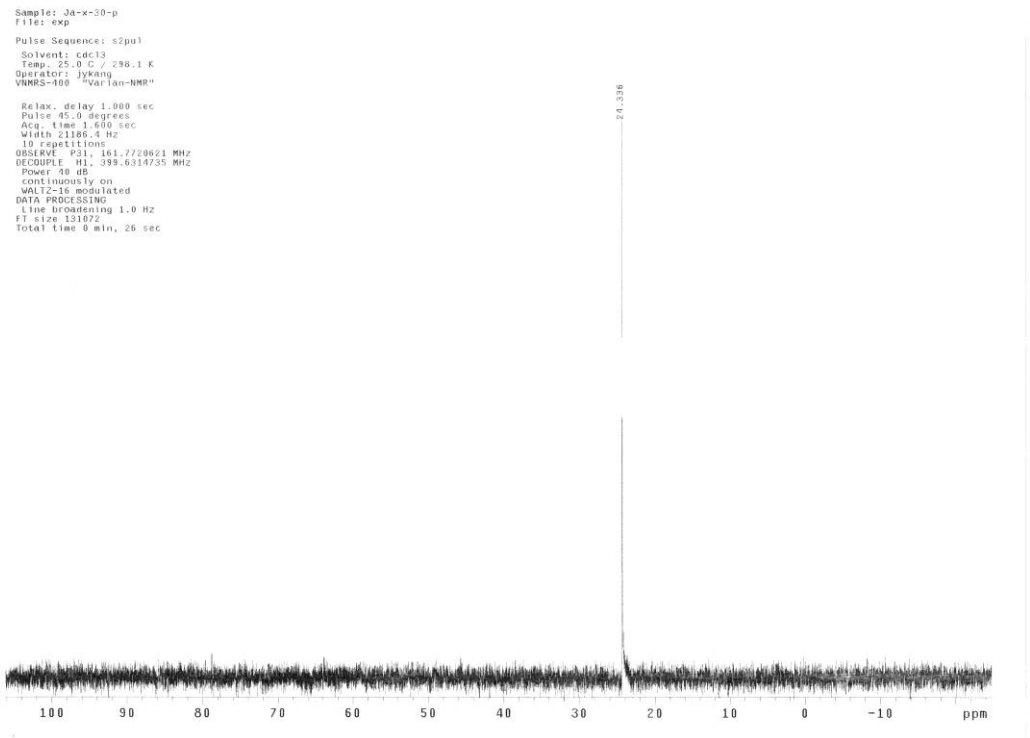

^{1}H NMR (400 MHz) in $CDCl_3$

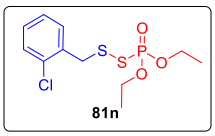

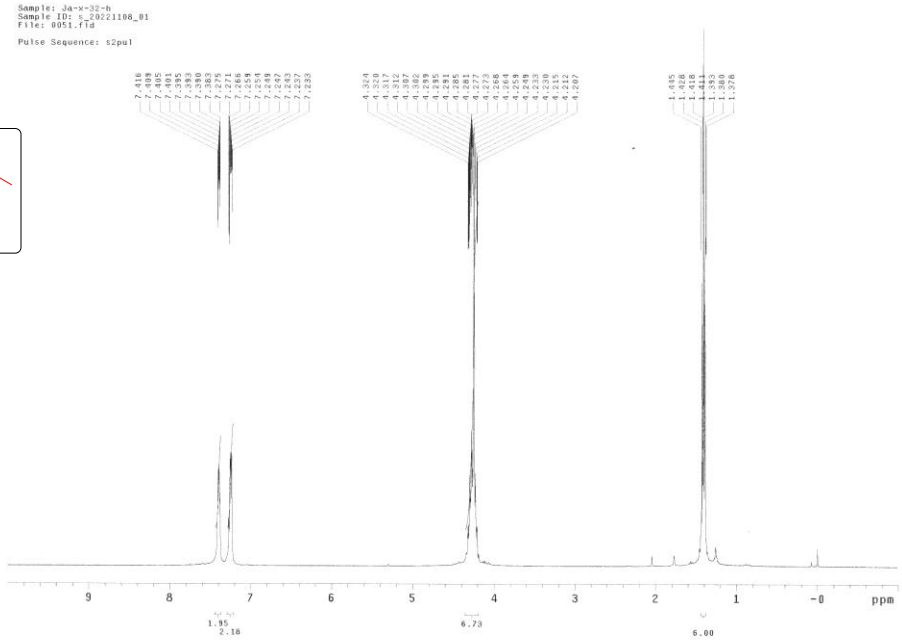

^{13}C NMR (100.5 MHz) in $CDCl_3$

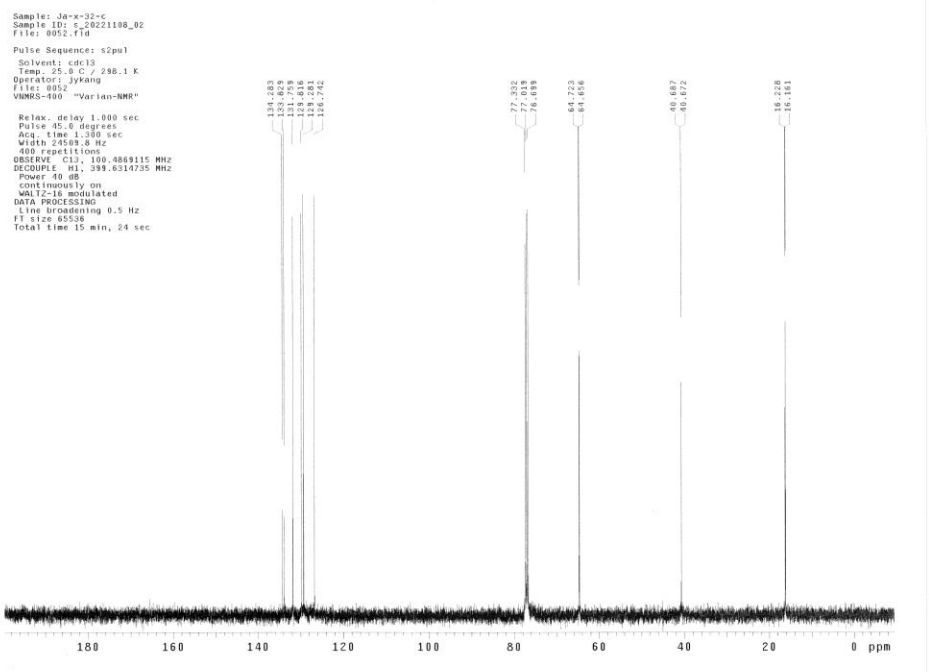

^{31}P NMR (162 MHz) in $CDCl_3$

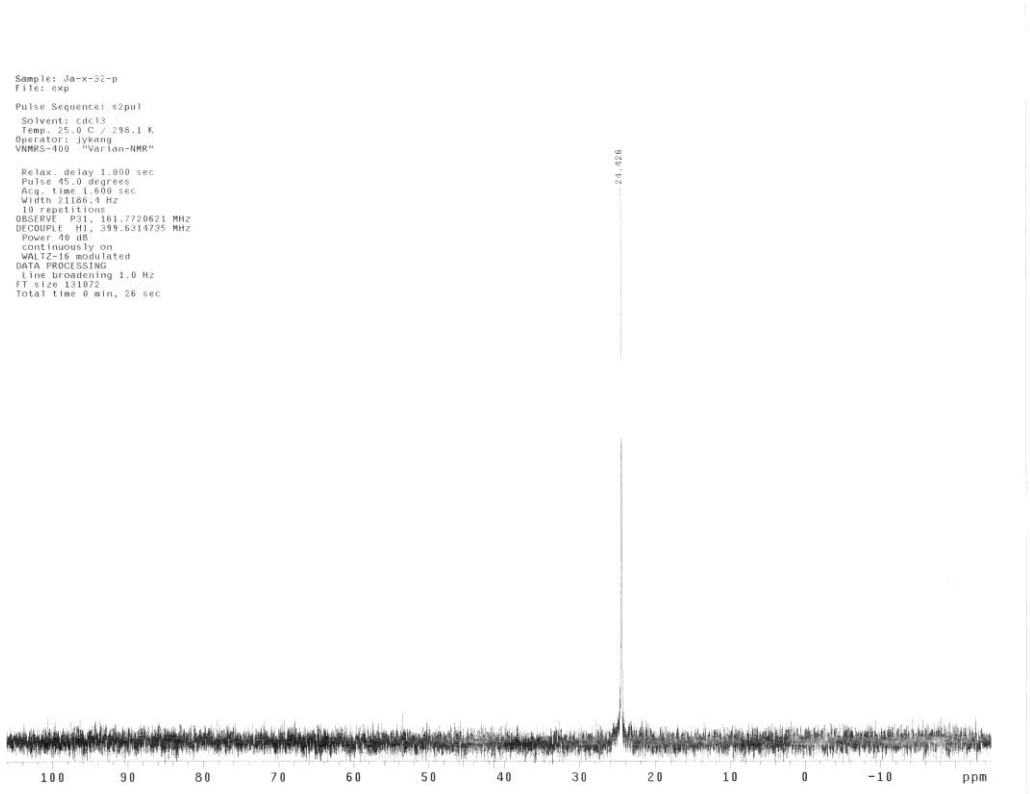

^{1}H NMR (400 MHz) in $CDCl_3$

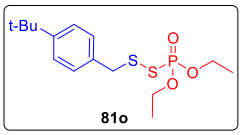

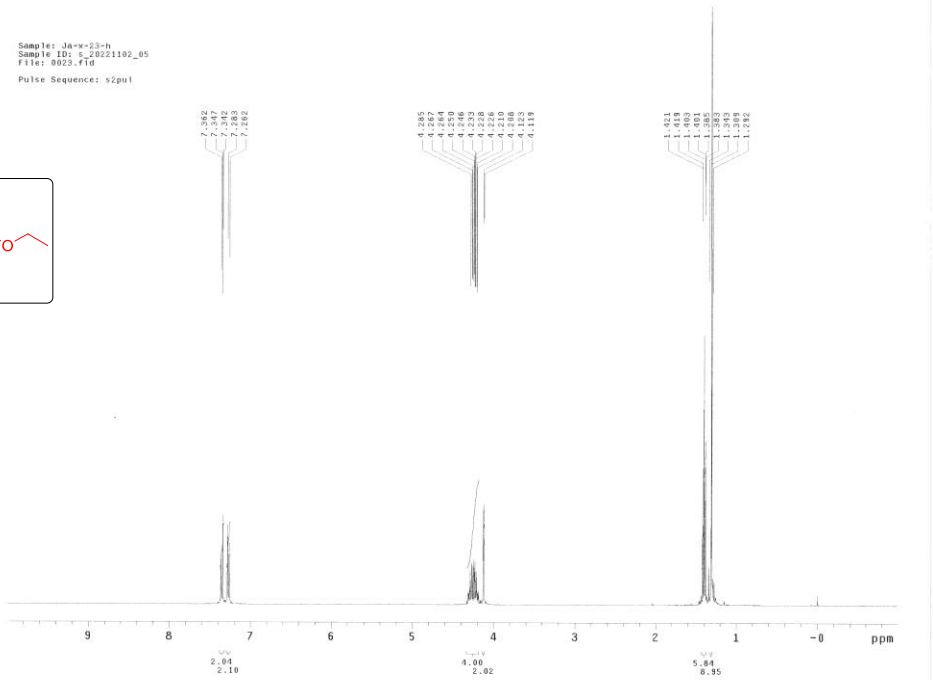

^{13}C NMR (100.5 MHz) in $CDCl_3$

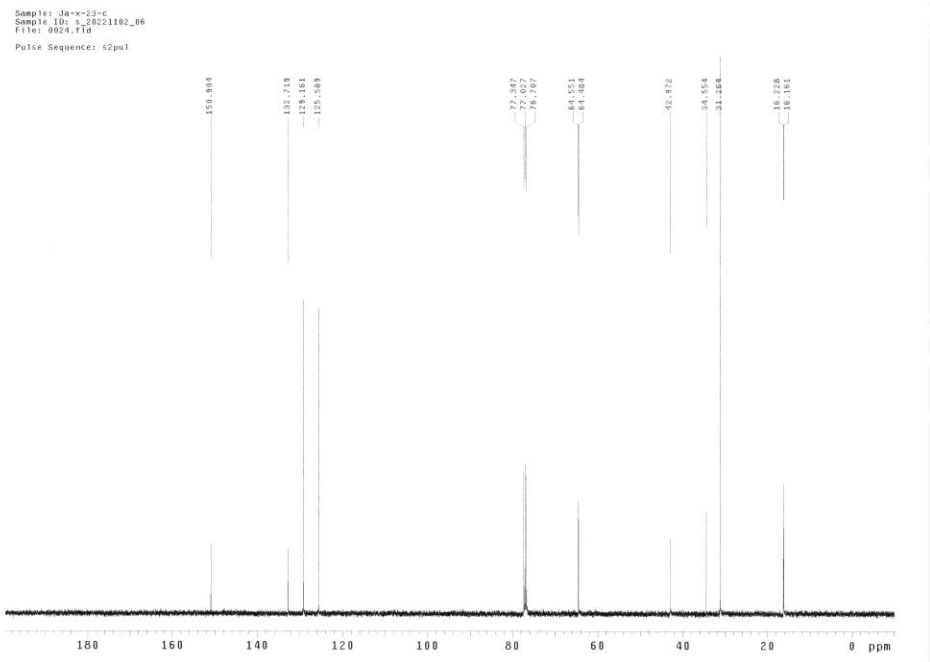

^{31}P NMR (162 MHz) in $CDCl_3$

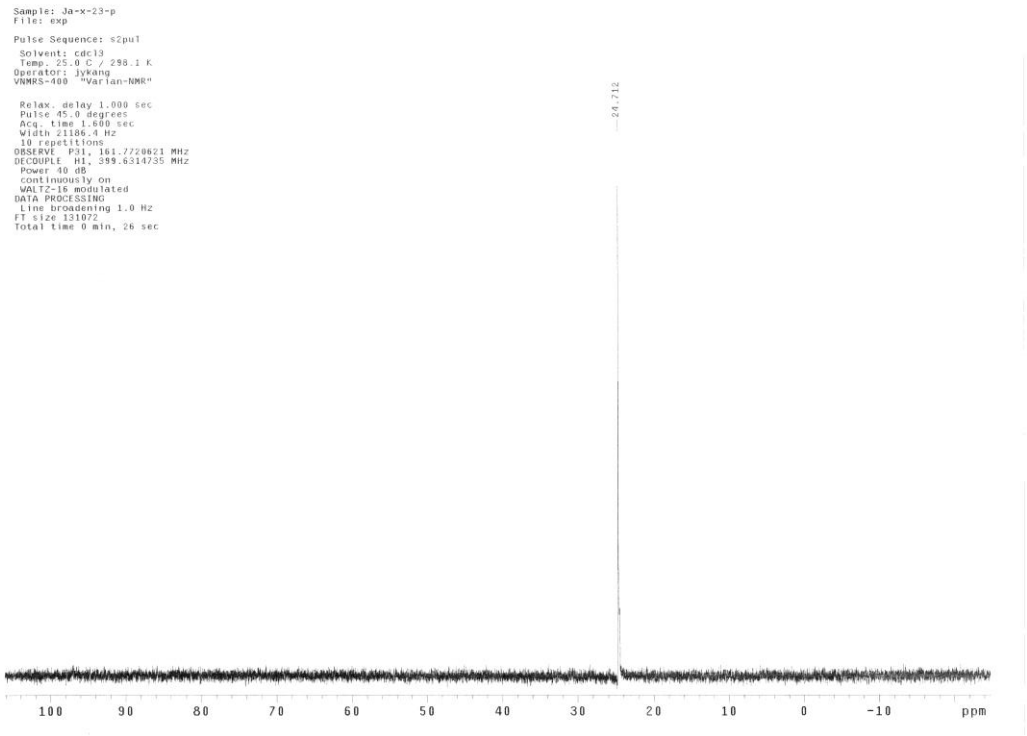

^{1}H NMR (400 MHz) in $CDCl_3$

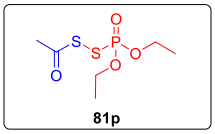

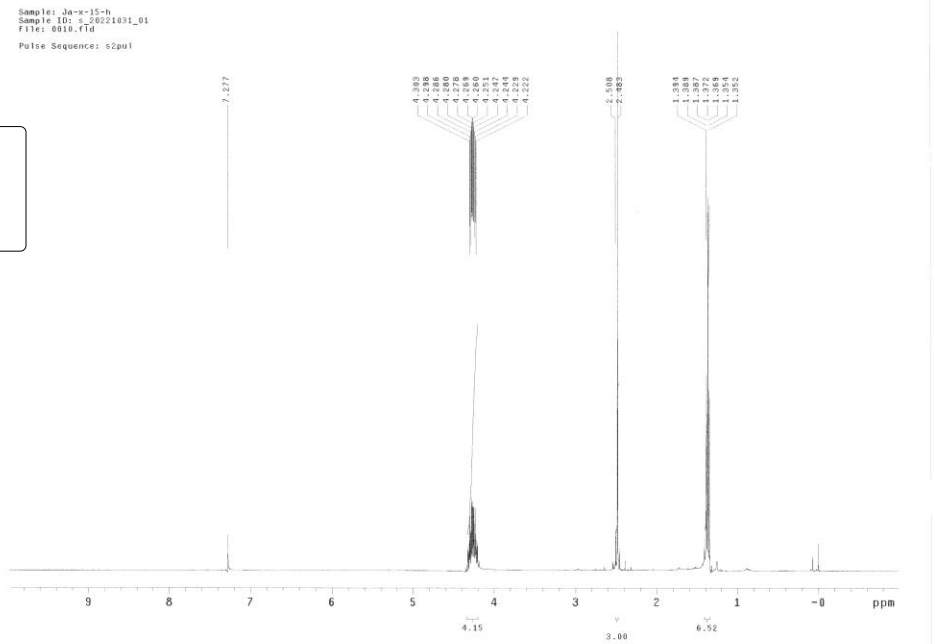

^{13}C NMR (100.5 MHz) in $CDCl_3$

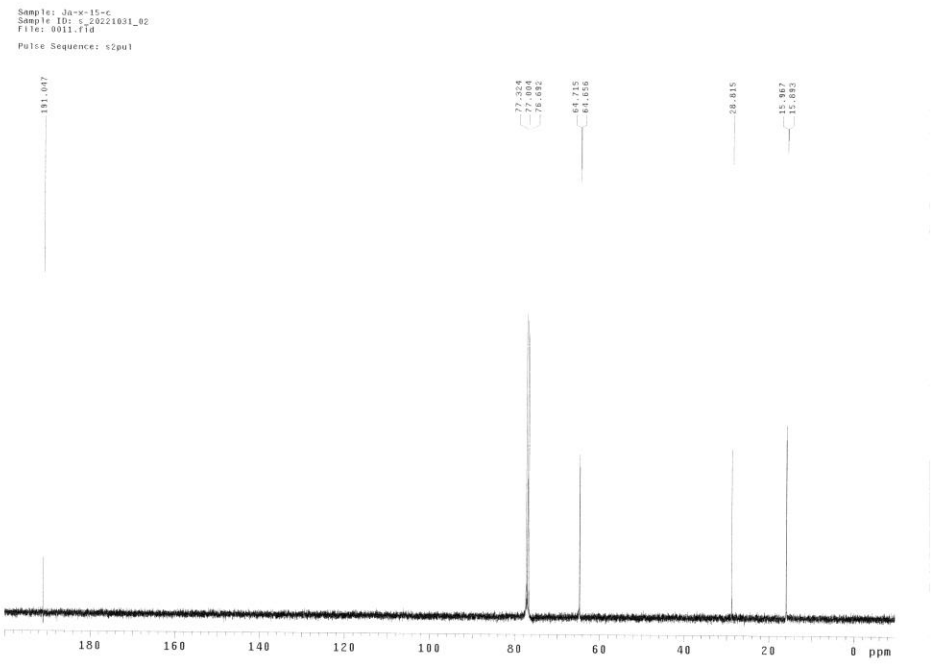

^{31}P NMR (162 MHz) in $CDCl_3$

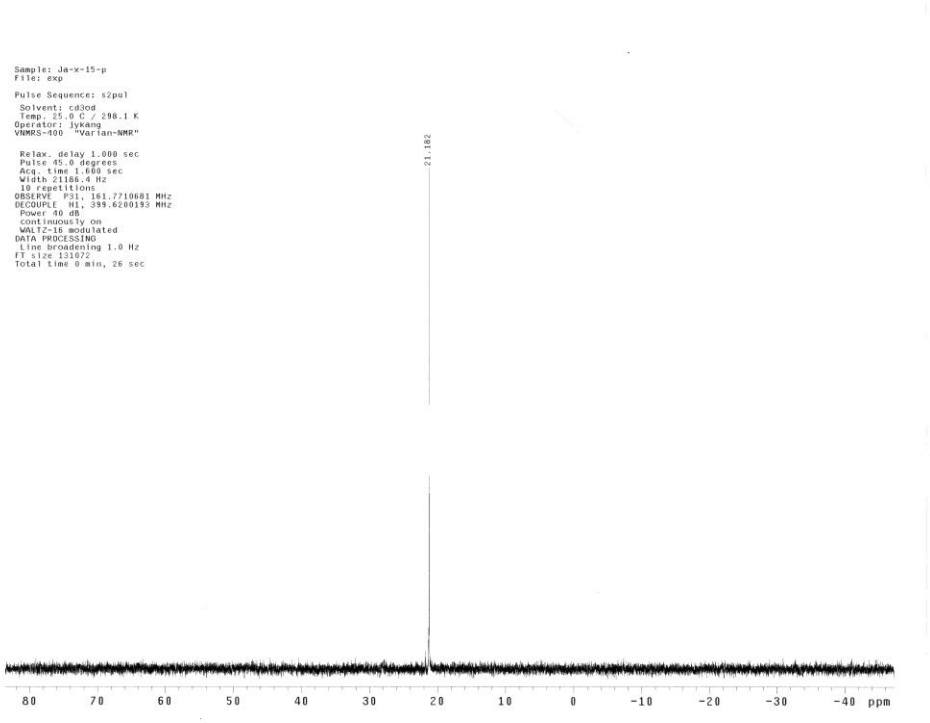

^{1}H NMR (400 MHz) in $CDCl_3$

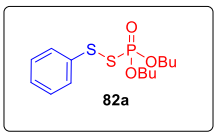

82a

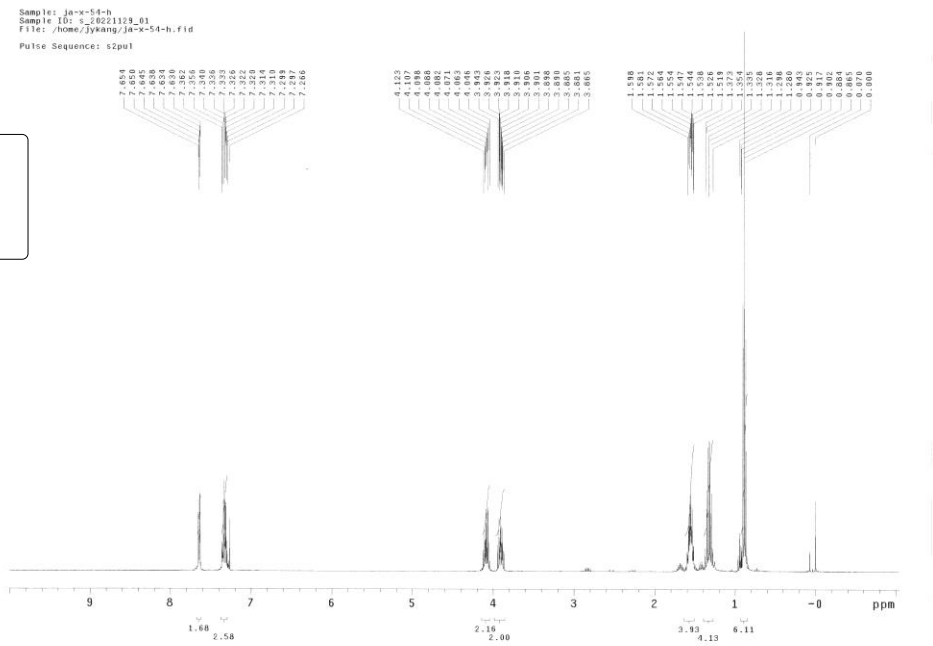

^{13}C NMR (100.5 MHz) in $CDCl_3$

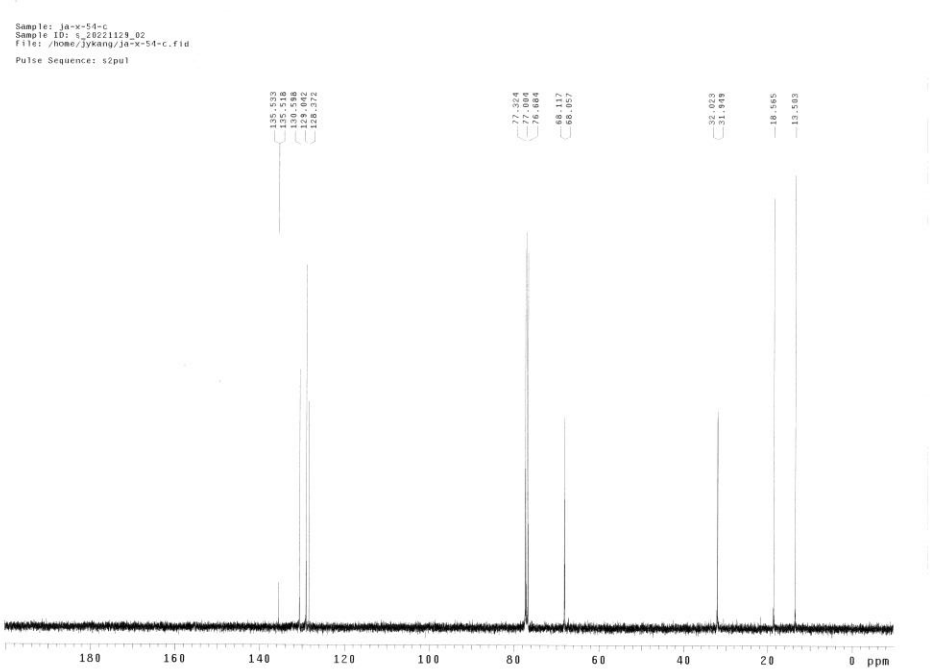

^{31}P NMR (162 MHz) in $CDCl_3$

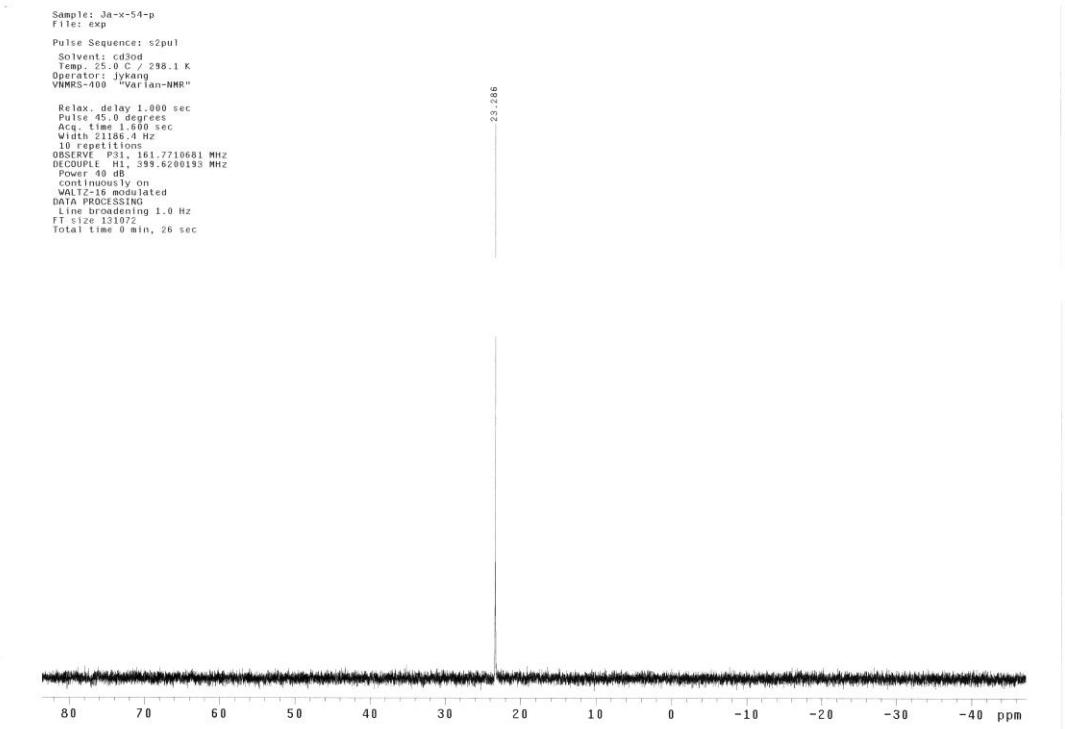

^{1}H NMR (400 MHz) in $CDCl_3$

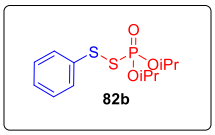

82b

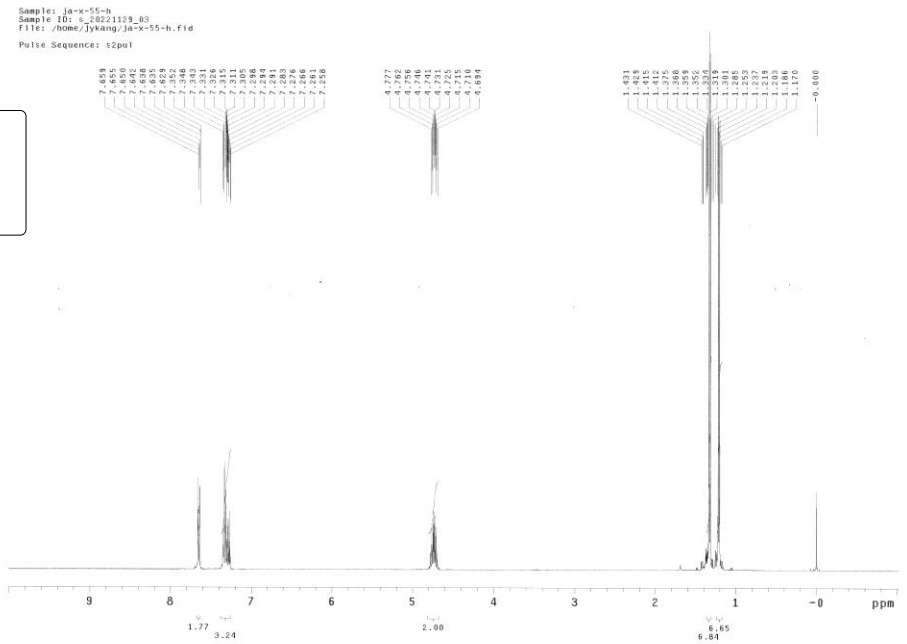

^{13}C NMR (100.5 MHz) in $CDCl_3$

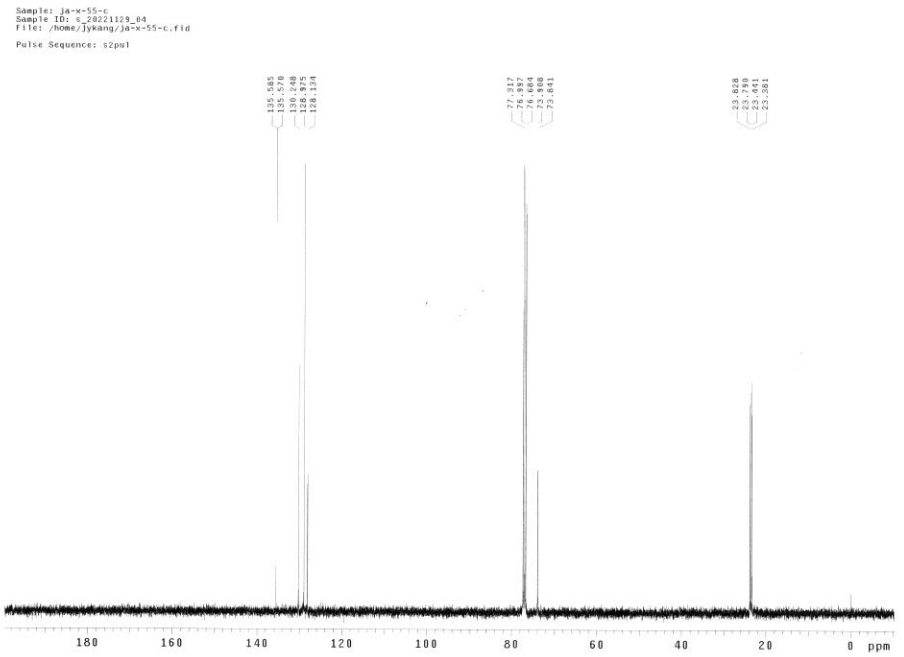

^{31}P NMR (162 MHz) in $CDCl_3$

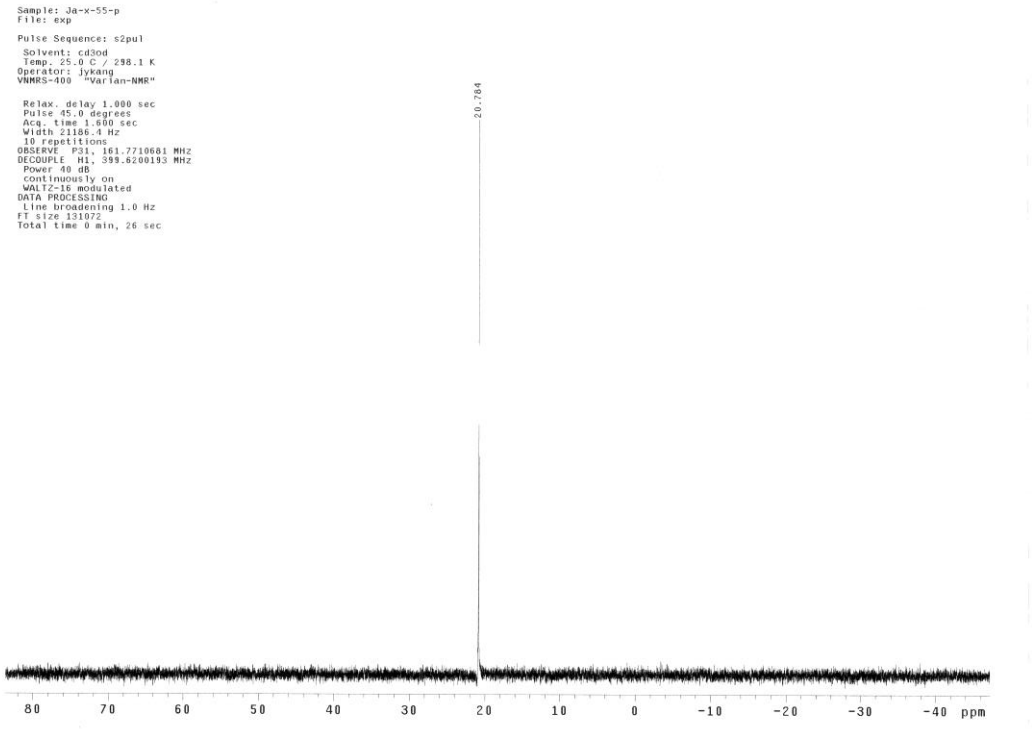

^{1}H NMR (400 MHz) in $CDCl_3$

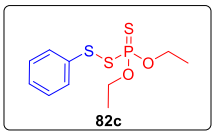

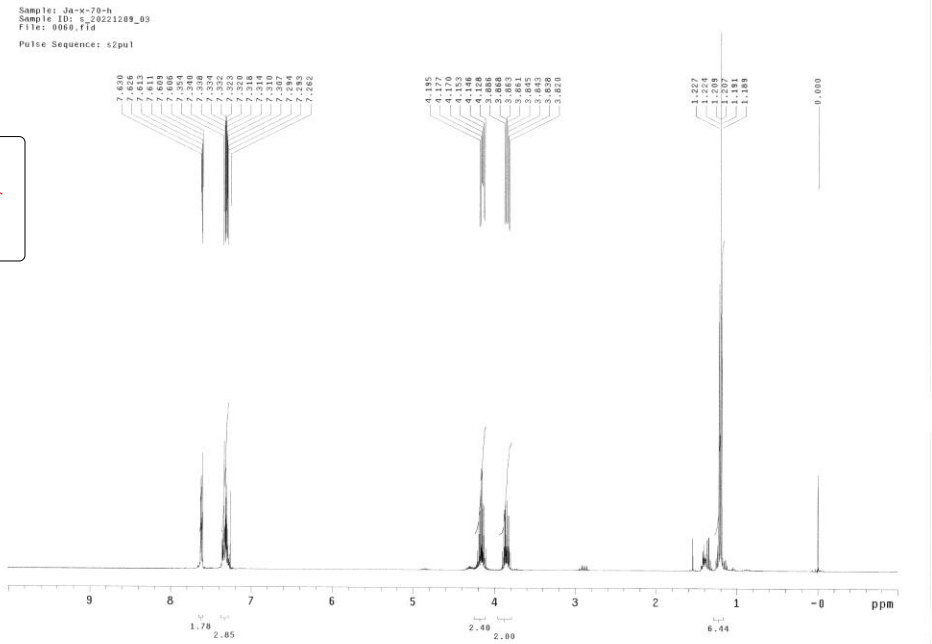

^{13}C NMR (100.5 MHz) in $CDCl_3$

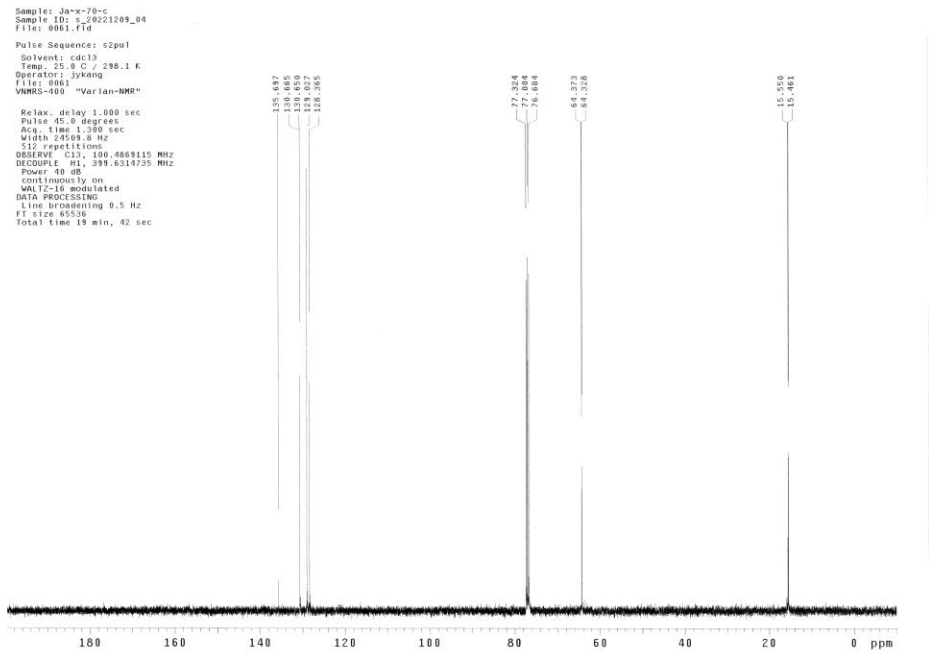

^{31}P NMR (162 MHz) in $CDCl_3$

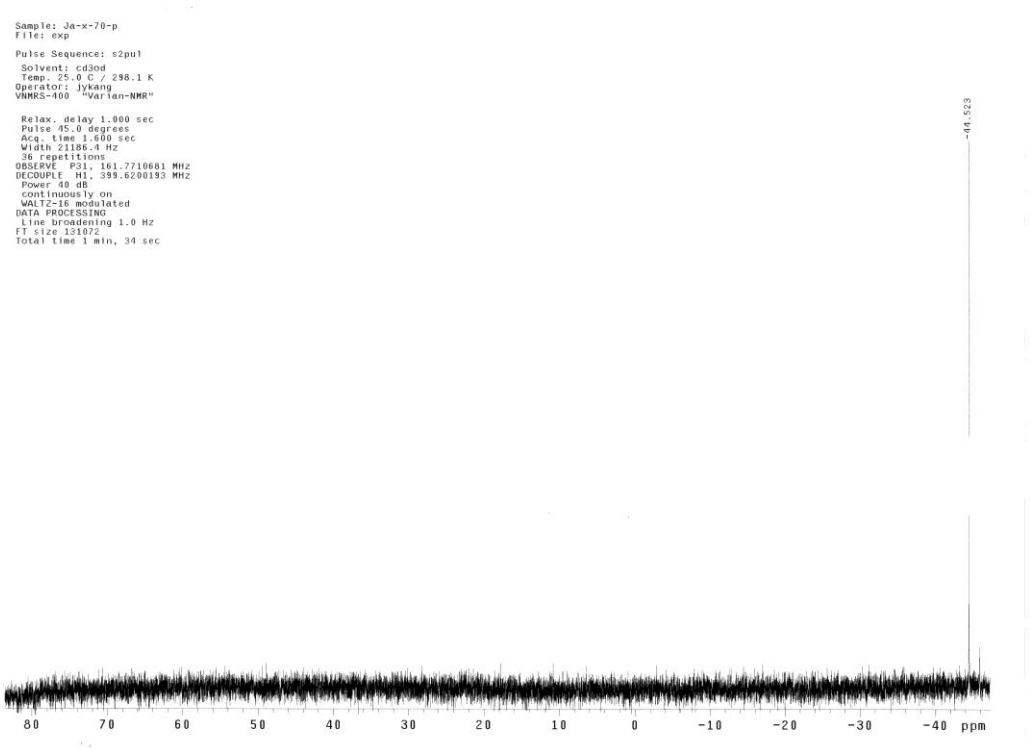

^{1}H NMR (400 MHz) in $CDCl_3$

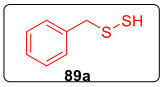

89a

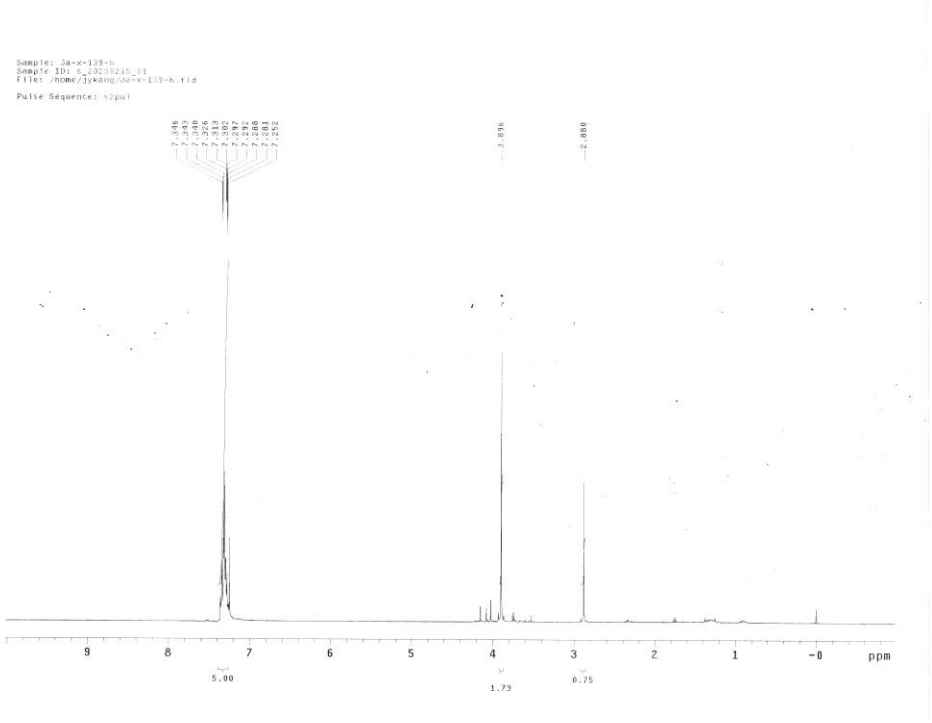

^{13}C NMR (100.5 MHz) in $CDCl_3$

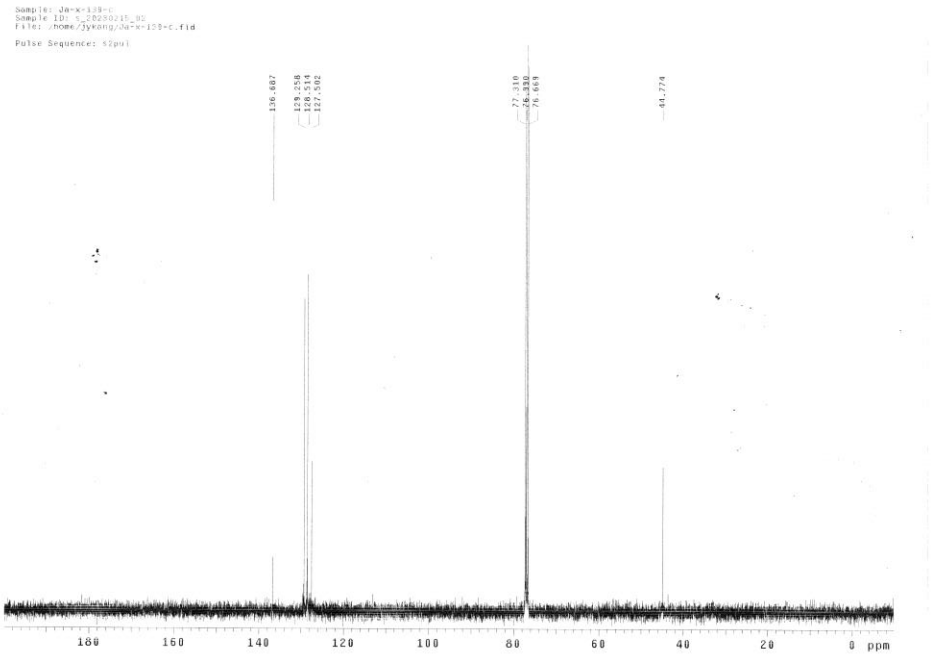

^{1}H NMR (400 MHz) in $CDCl_3$

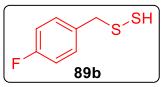

89b

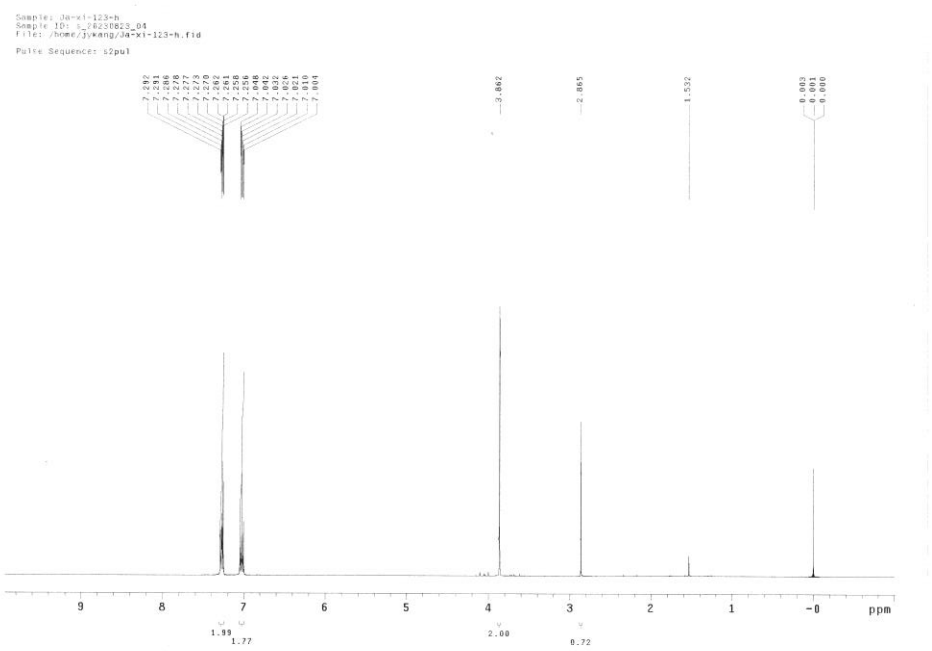

^{13}C NMR (100.5 MHz) in $CDCl_3$

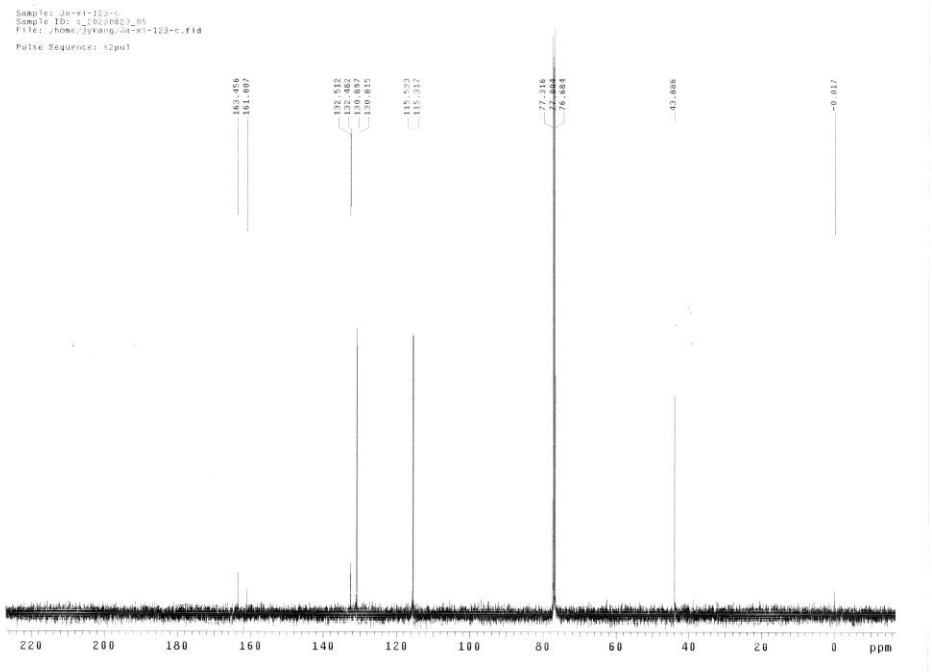

^{1}H NMR (400 MHz) in $CDCl_3$

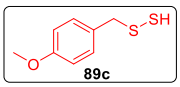

89c

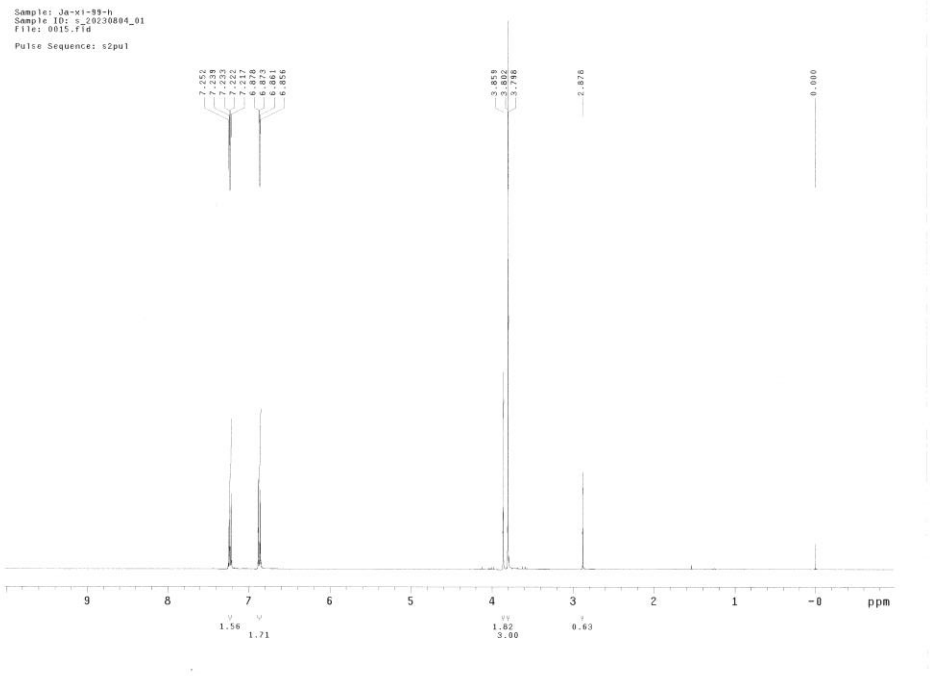

^{13}C NMR (100.5 MHz) in $CDCl_3$

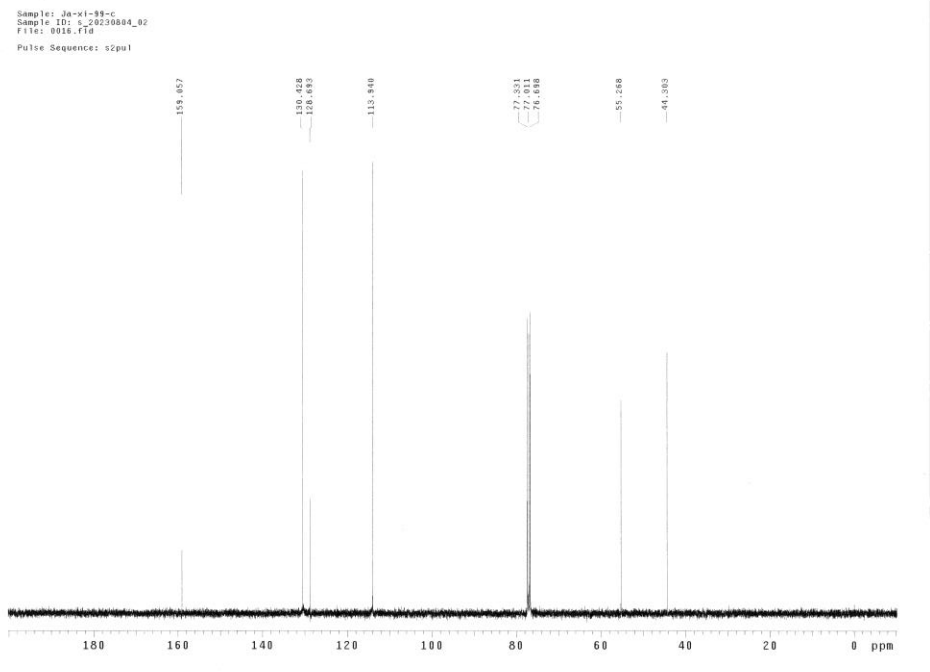

^{1}H NMR (400 MHz) in $CDCl_3$

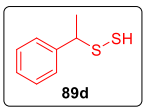

89d

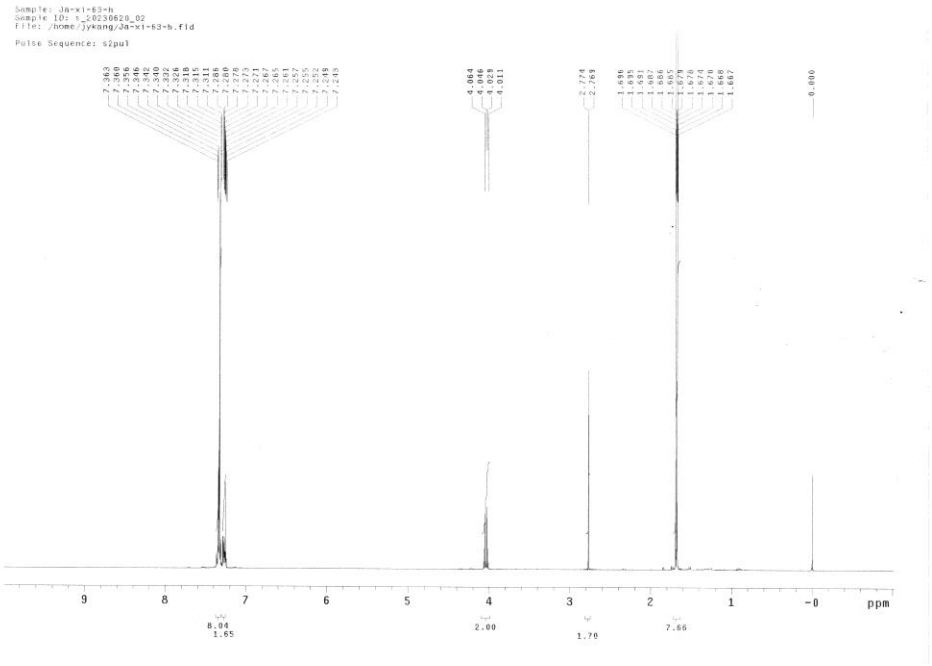

^{13}C NMR (100.5 MHz) in $CDCl_3$

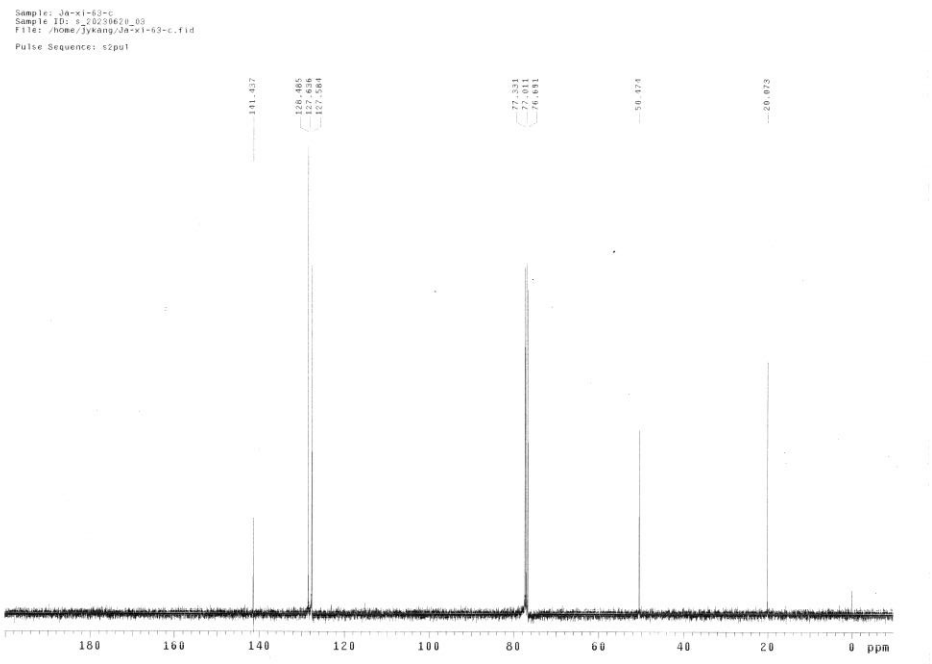

^{1}H NMR (400 MHz) in $CDCl_3$

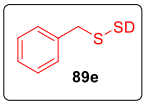

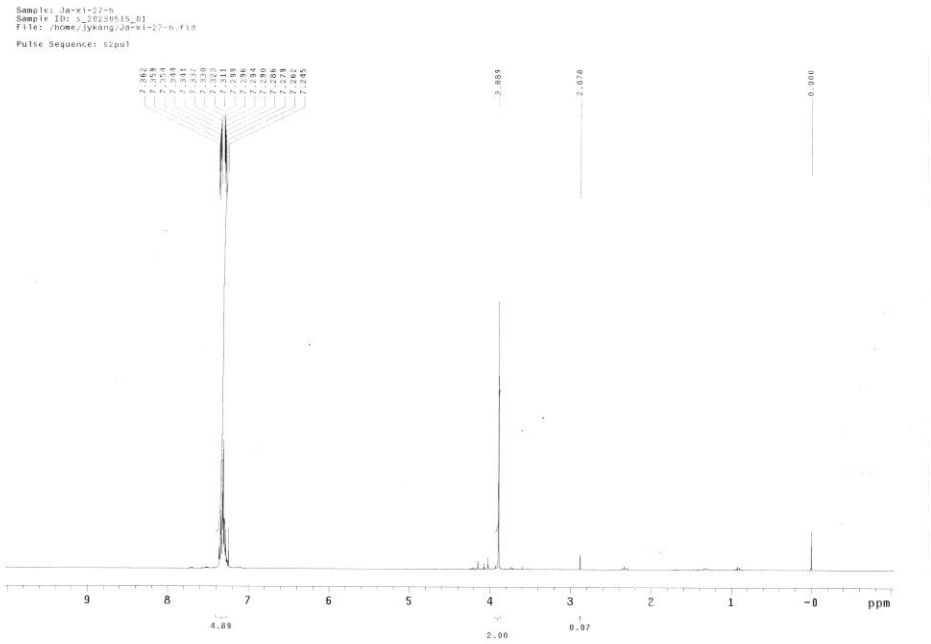

^{13}C NMR (100.5 MHz) in $CDCl_3$

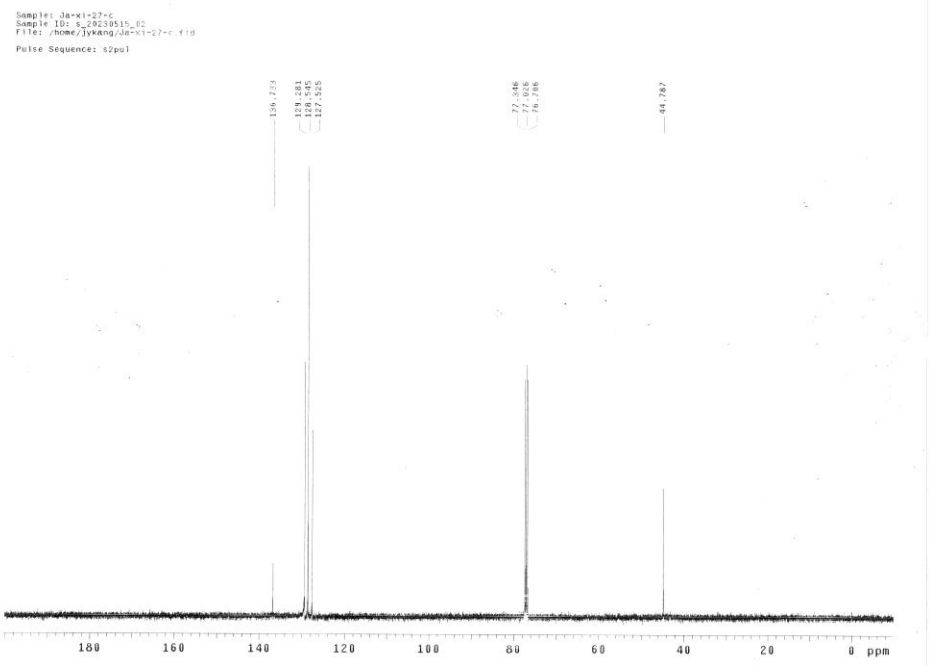

^{1}H NMR (400 MHz) in $CDCl_3$

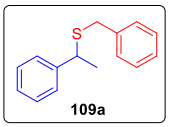

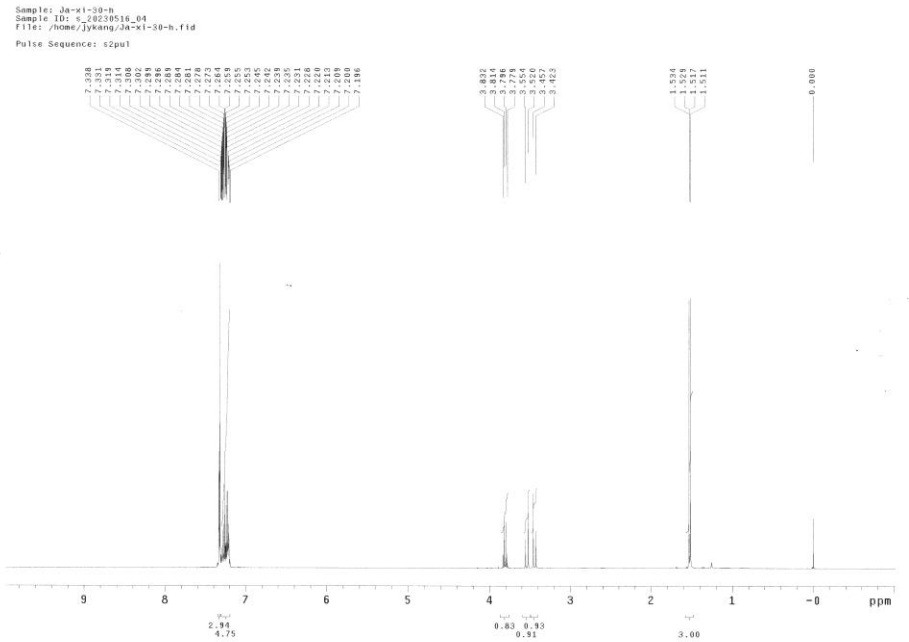

^{13}C NMR (100.5 MHz) in $CDCl_3$

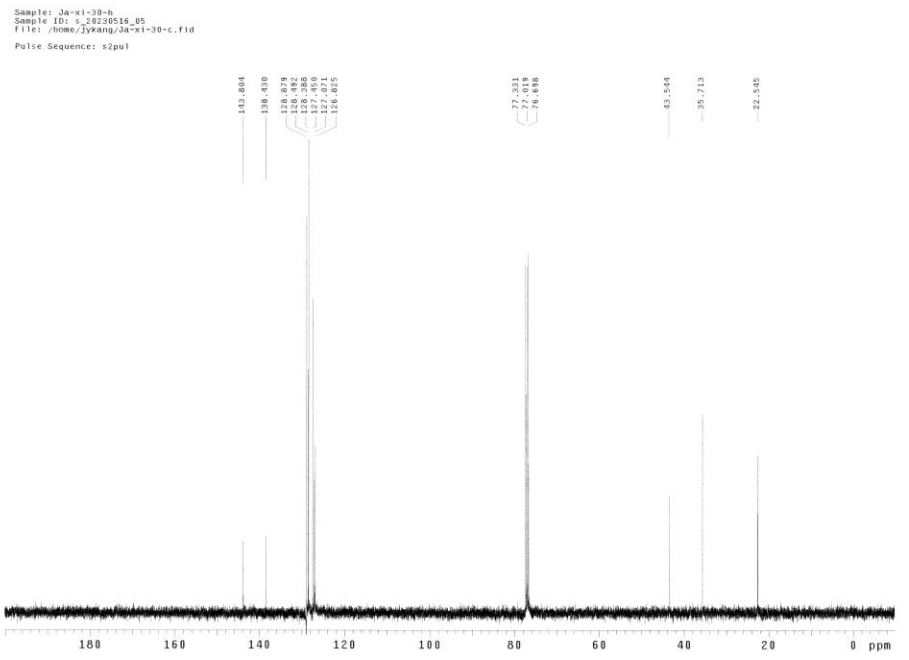

^{1}H NMR (400 MHz) in $CDCl_3$

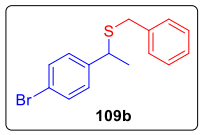

109b

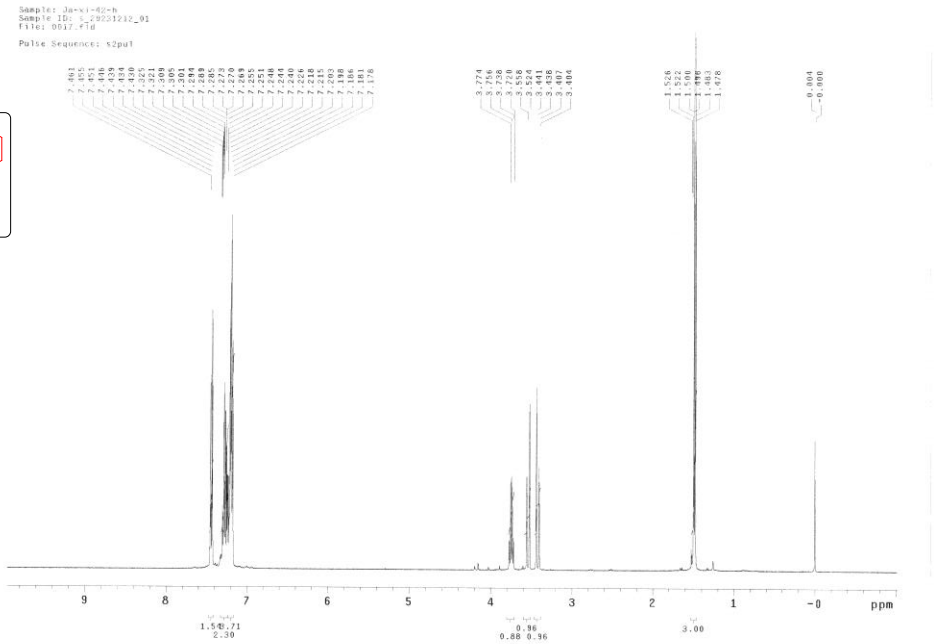

^{13}C NMR (100.5 MHz) in $CDCl_3$

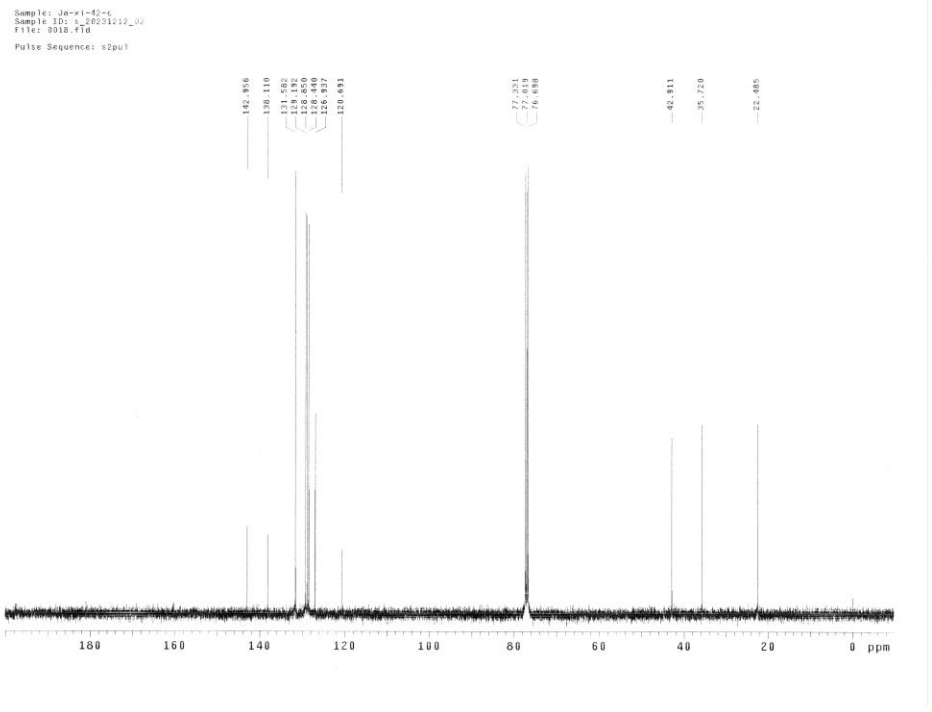

^{1}H NMR (400 MHz) in $CDCl_3$

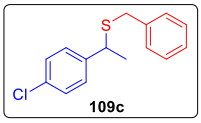

109c

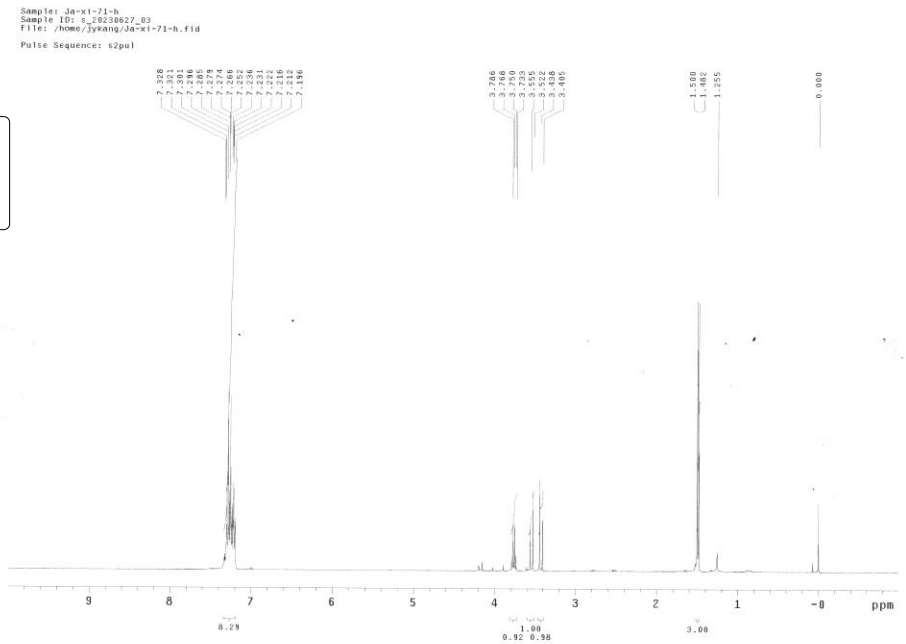

^{13}C NMR (100.5 MHz) in $CDCl_3$

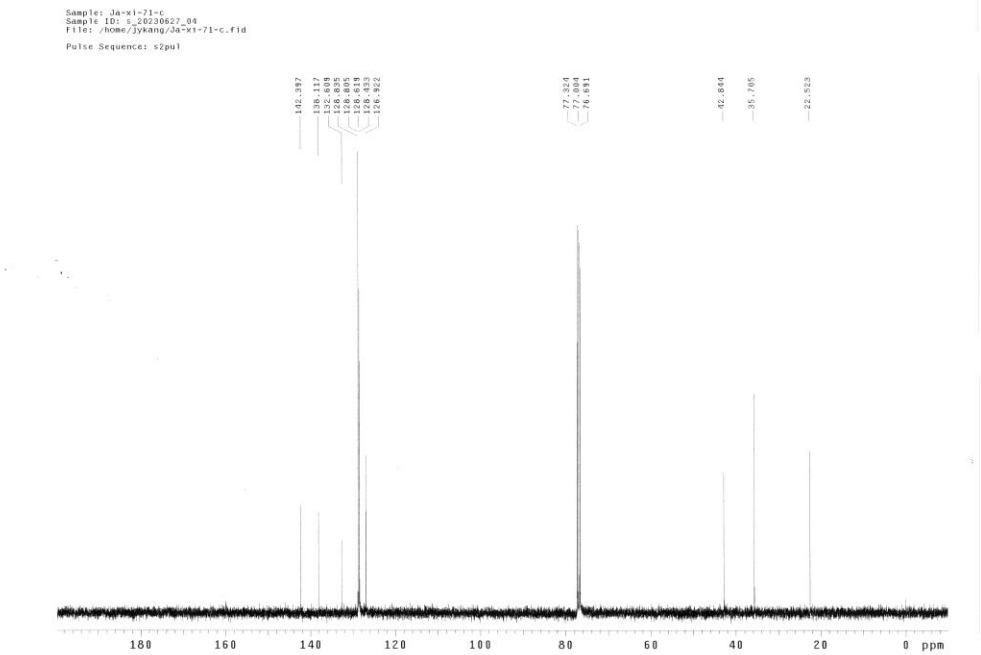

^{1}H NMR (400 MHz) in $CDCl_3$

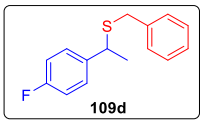

109d

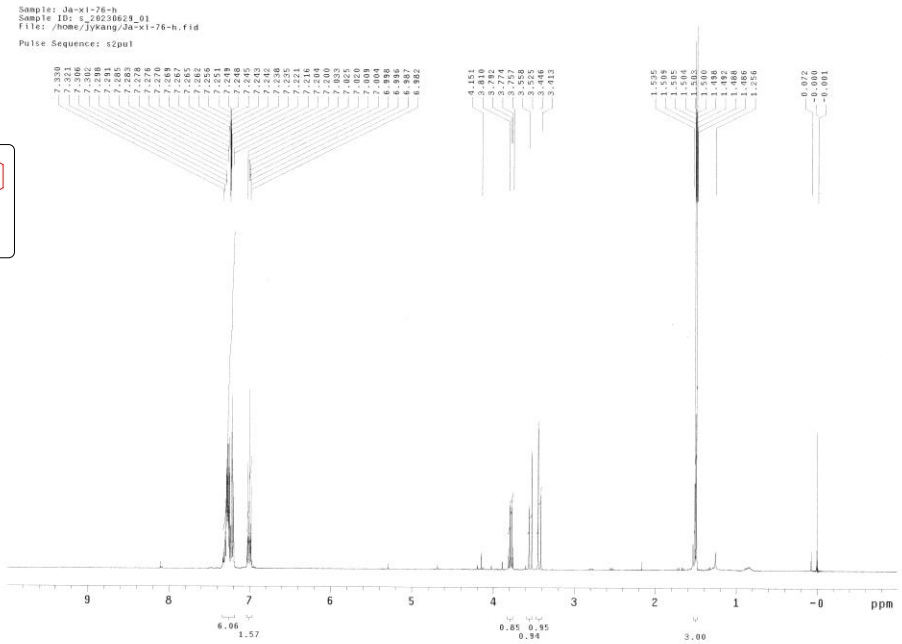

^{13}C NMR (100.5 MHz) in $CDCl_3$

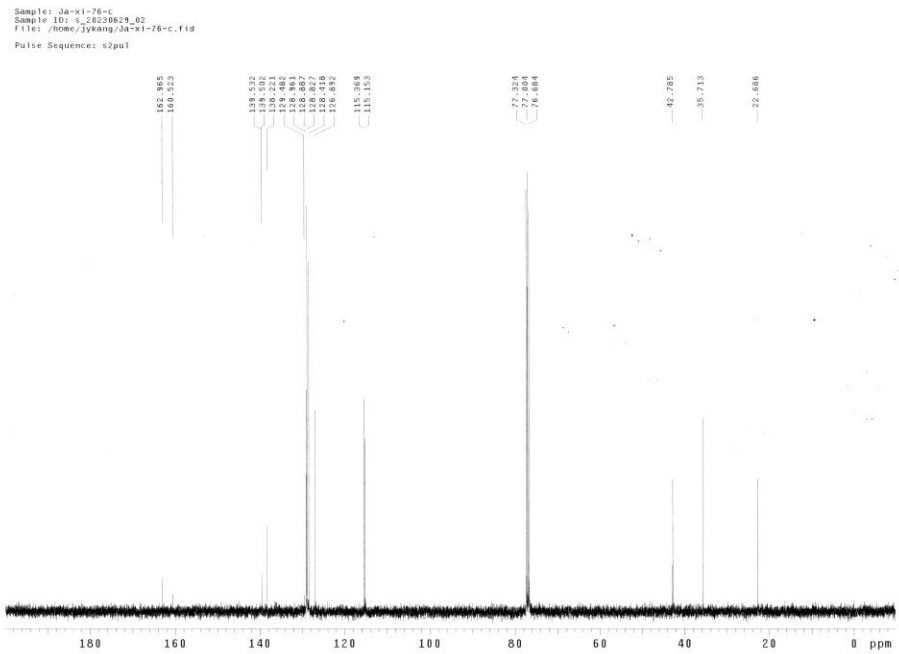

^{1}H NMR (400 MHz) in $CDCl_3$

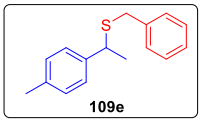

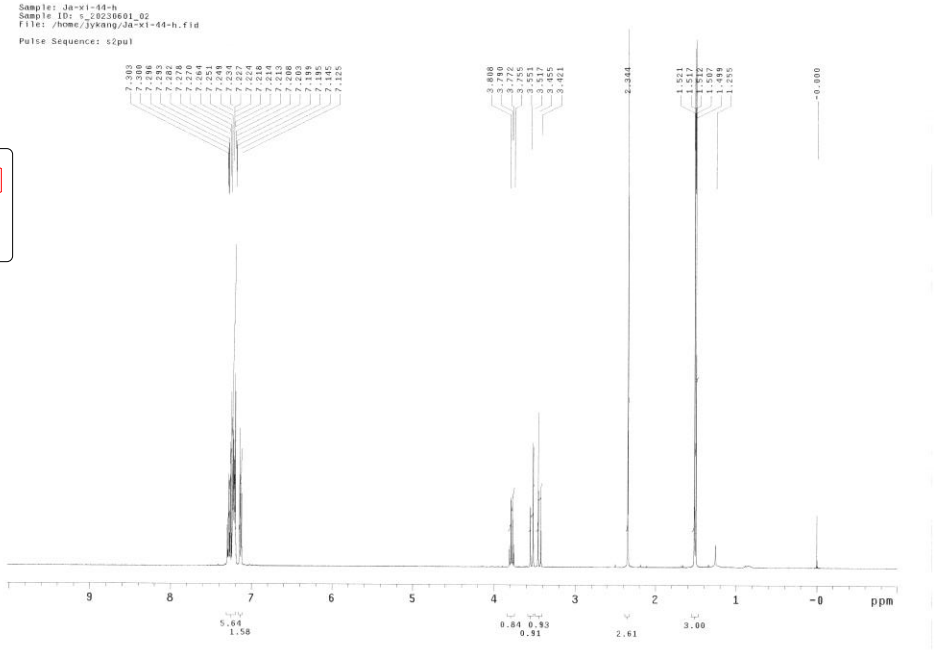

^{13}C NMR (100.5 MHz) in $CDCl_3$

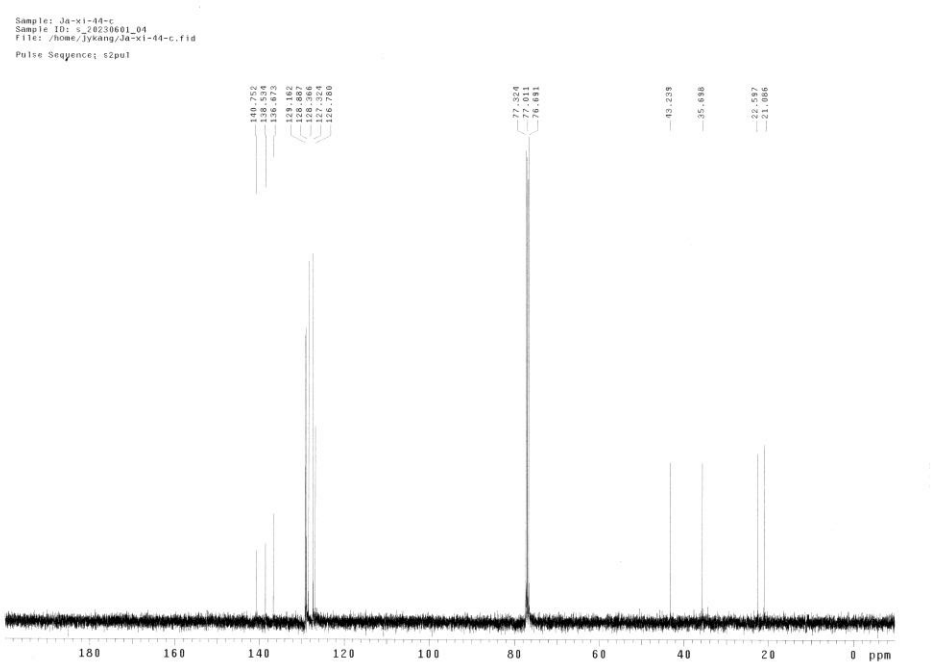

^{1}H NMR (400 MHz) in $CDCl_3$

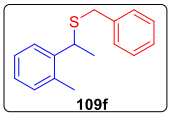

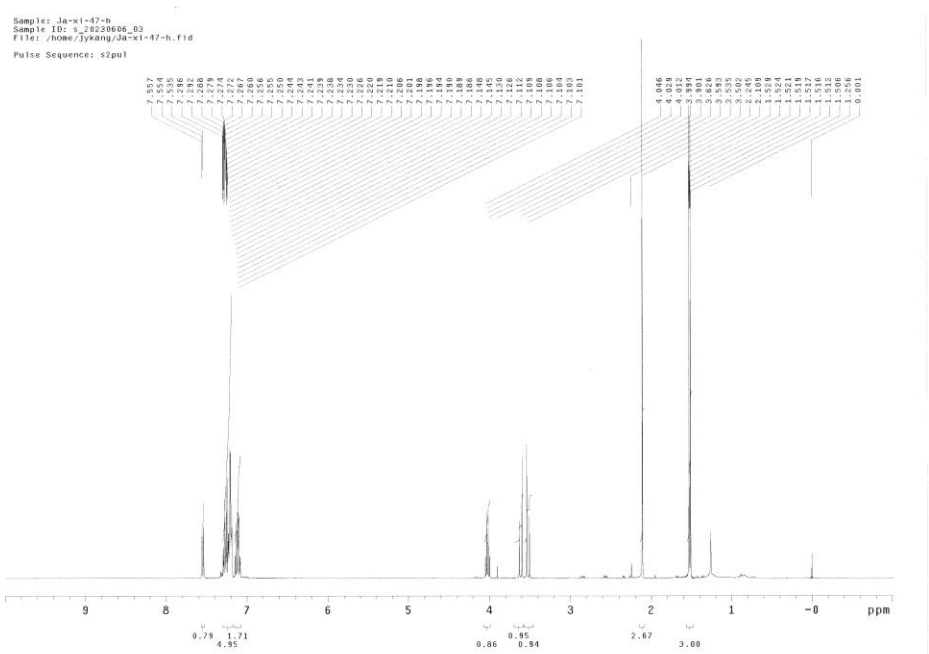

^{13}C NMR (100.5 MHz) in $CDCl_3$

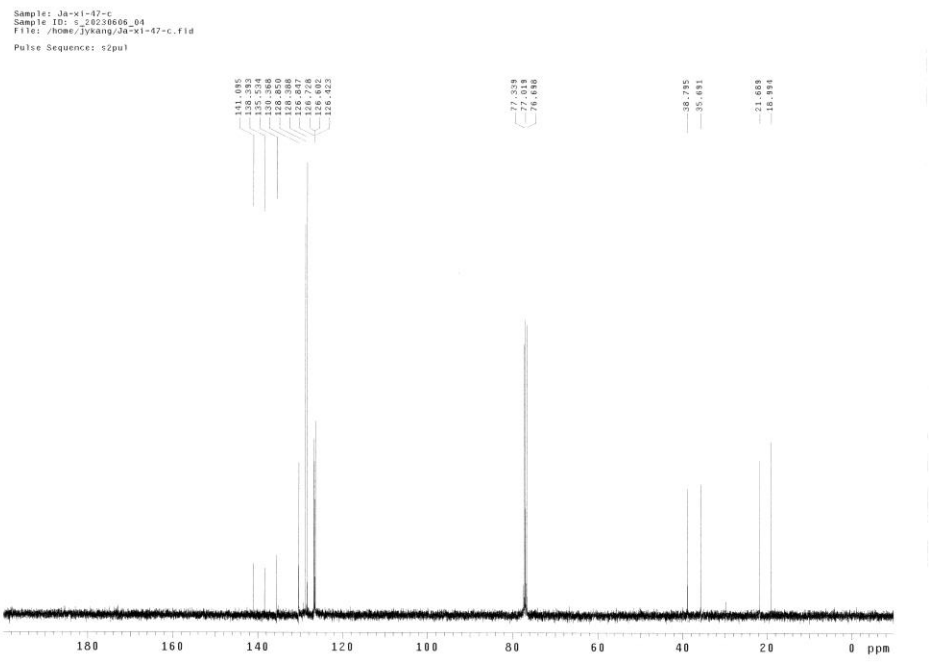

^{1}H NMR (400 MHz) in $CDCl_3$

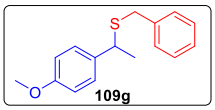

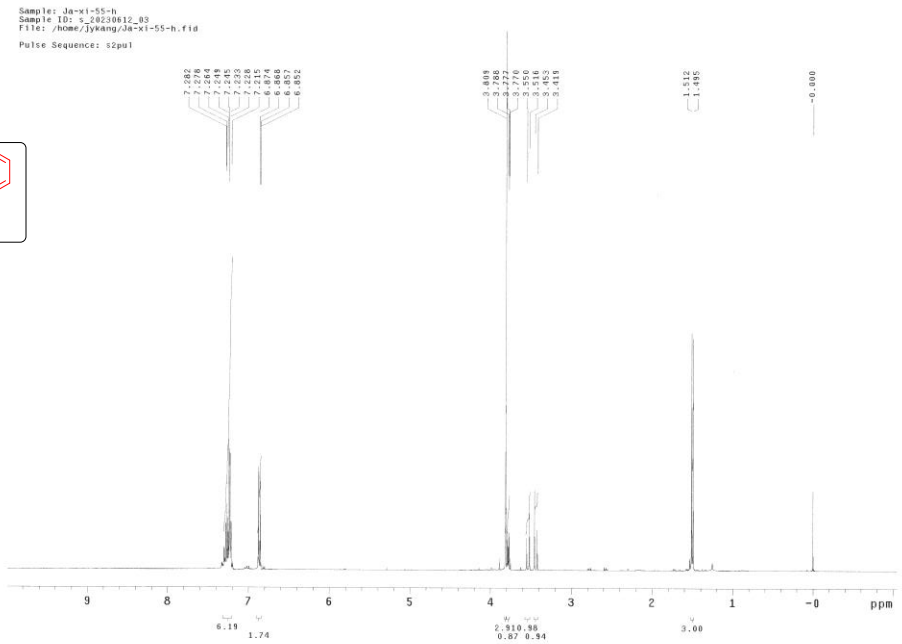

^{13}C NMR (100.5 MHz) in $CDCl_3$

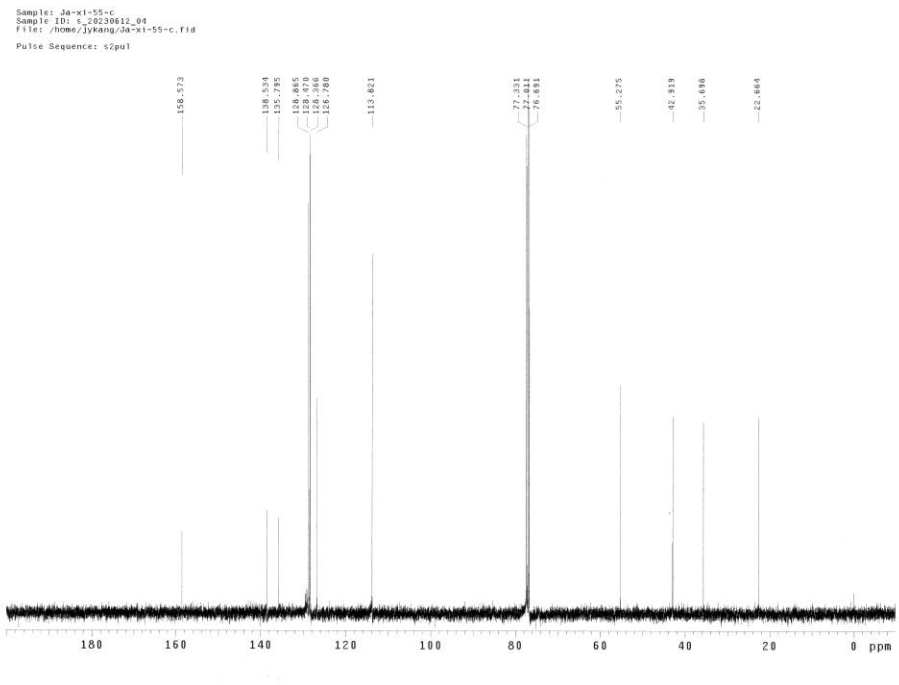

^{1}H NMR (400 MHz) in $CDCl_3$

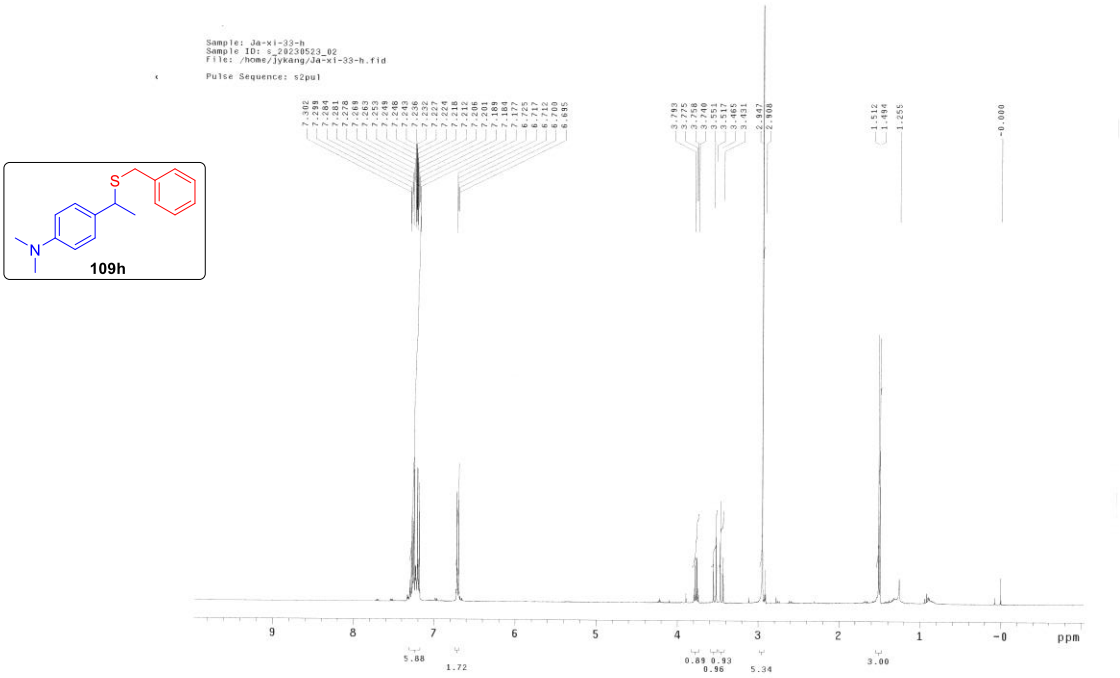

^{13}C NMR (100.5 MHz) in $CDCl_3$

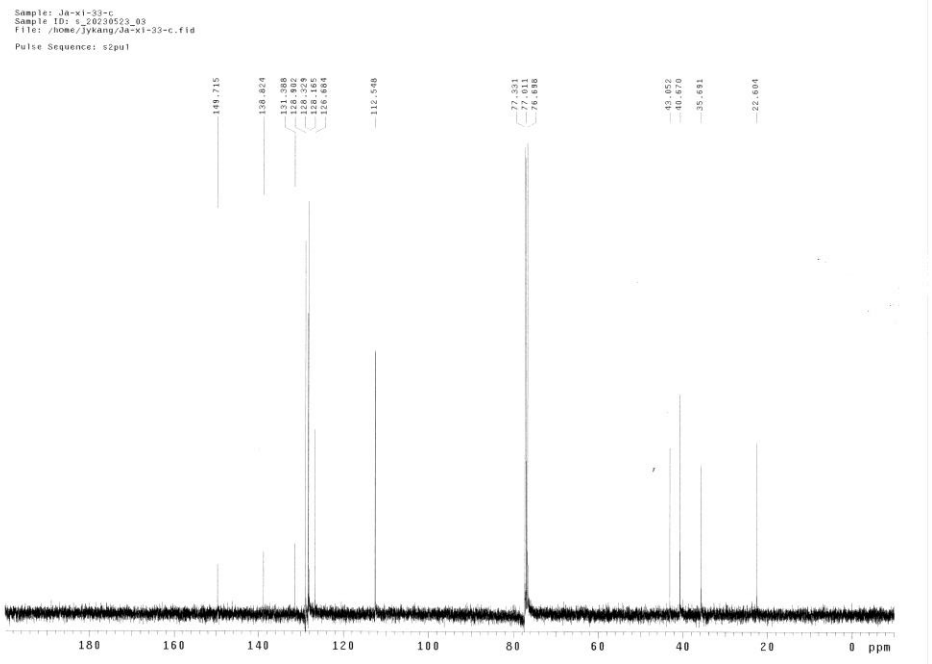

^{1}H NMR (400 MHz) in $CDCl_3$

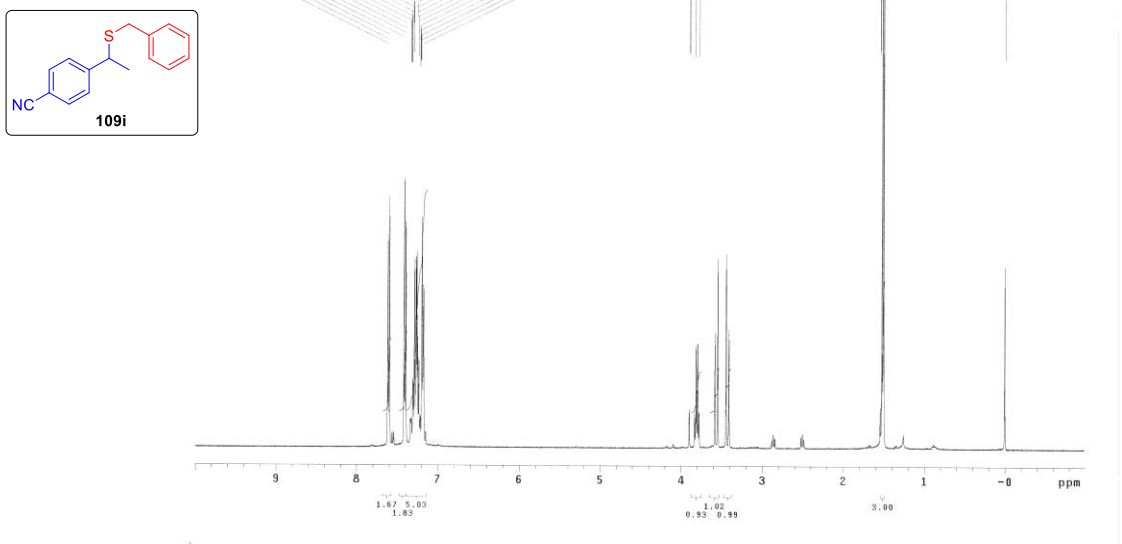

^{13}C NMR (100.5 MHz) in $CDCl_3$

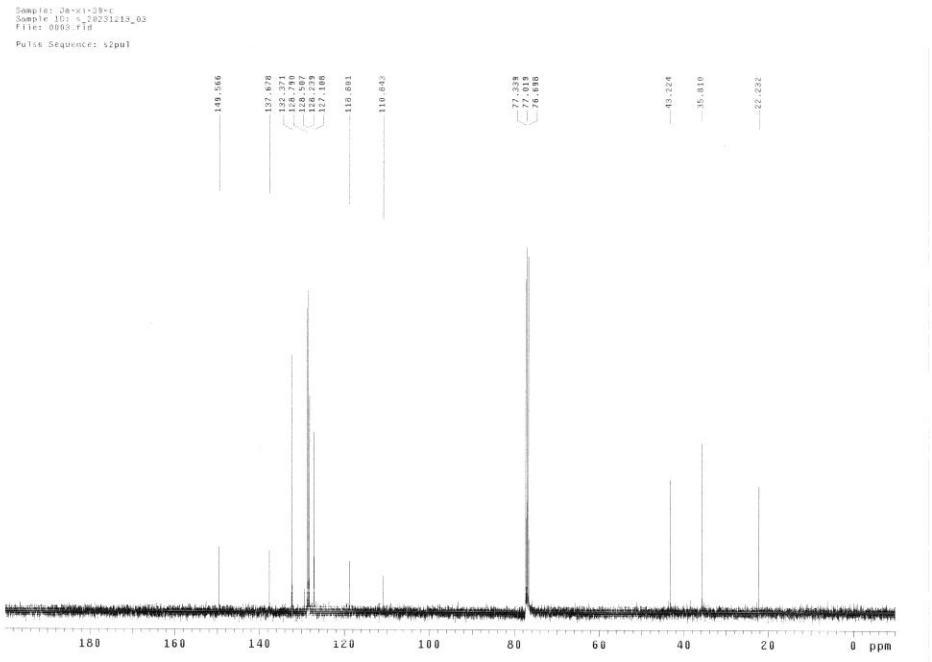

^{1}H NMR (400 MHz) in $CDCl_3$

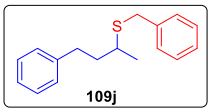

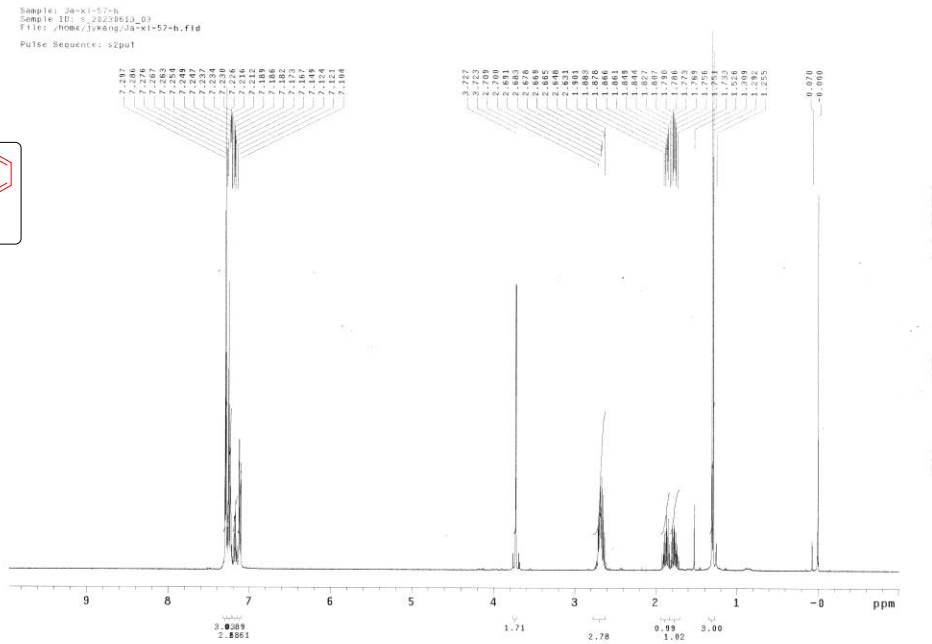

^{13}C NMR (100.5 MHz) in $CDCl_3$

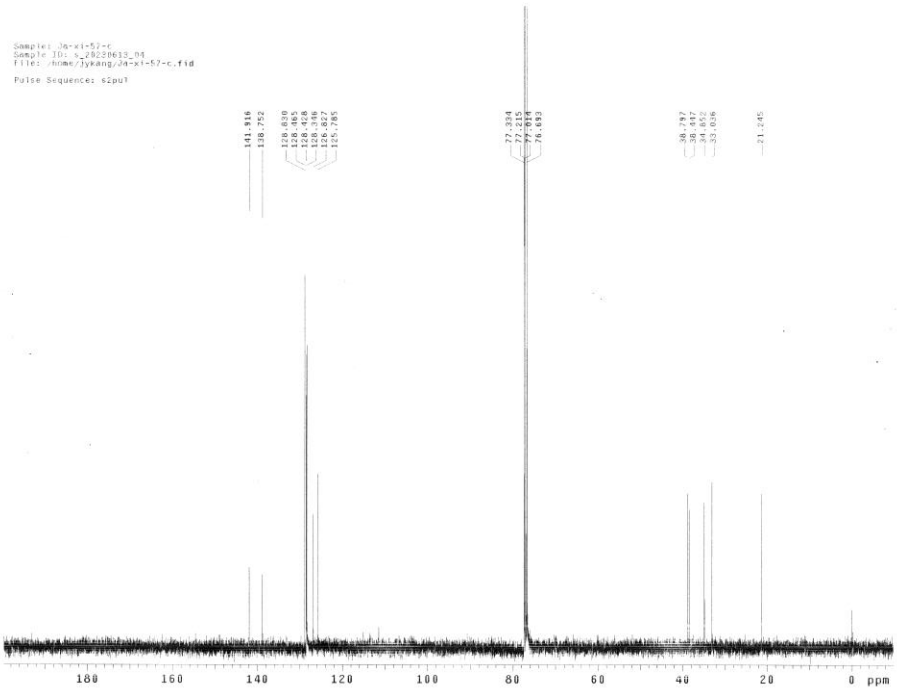

^{1}H NMR (400 MHz) in $CDCl_3$

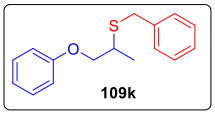

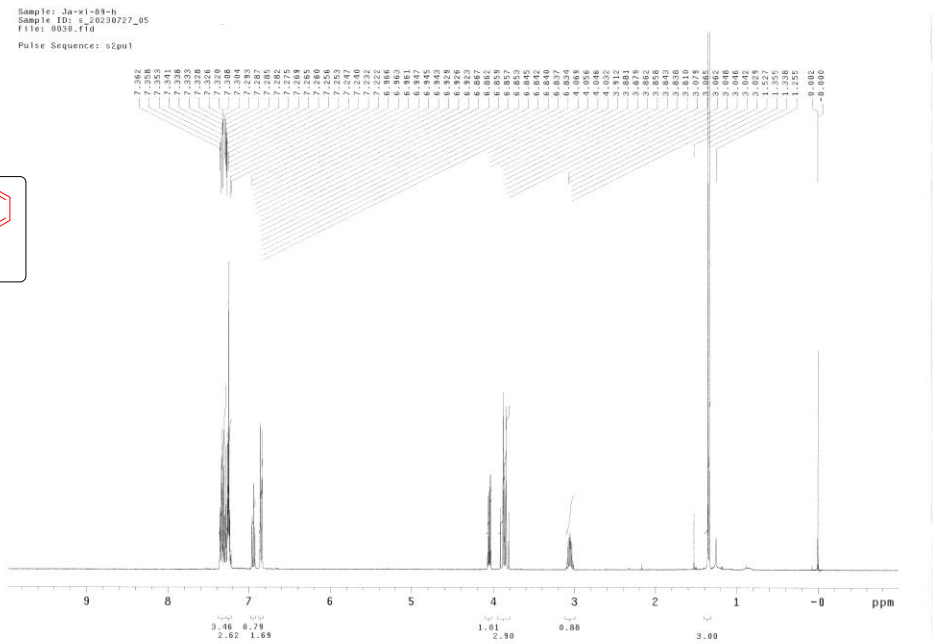

^{13}C NMR (100.5 MHz) in $CDCl_3$

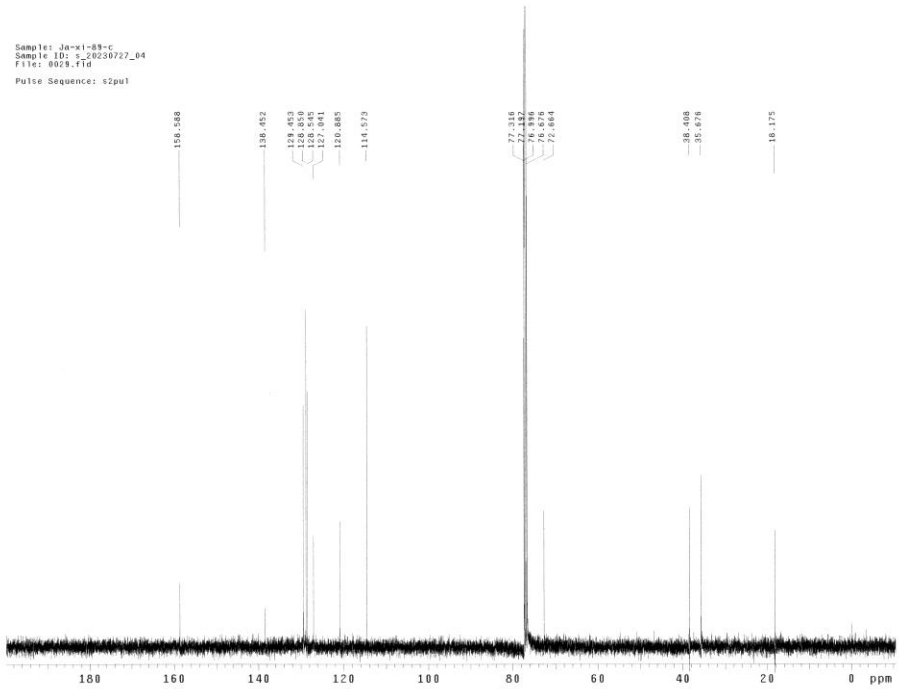

^{1}H NMR (400 MHz) in $CDCl_3$

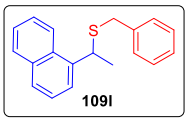

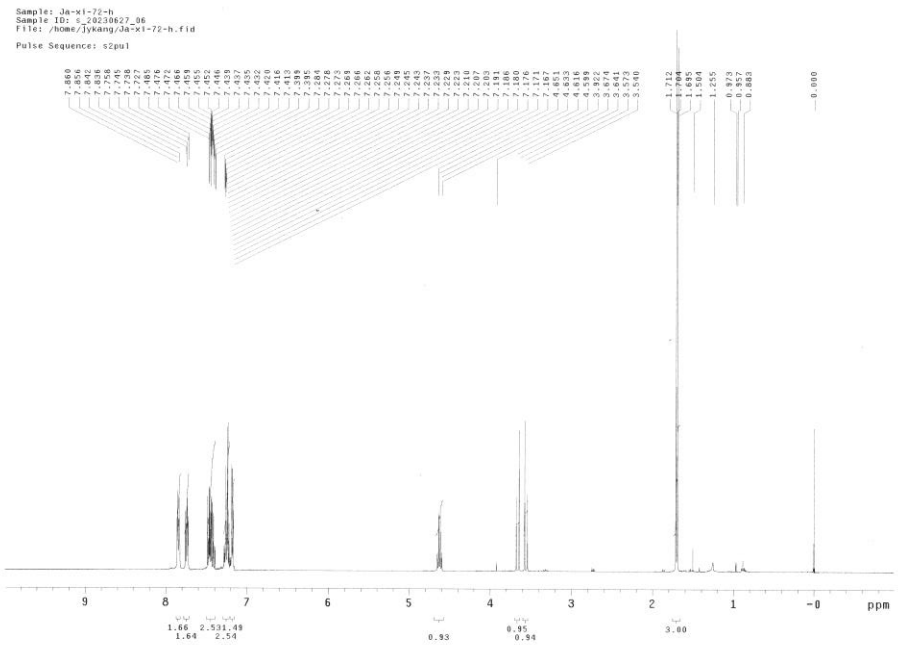

^{13}C NMR (100.5 MHz) in $CDCl_3$

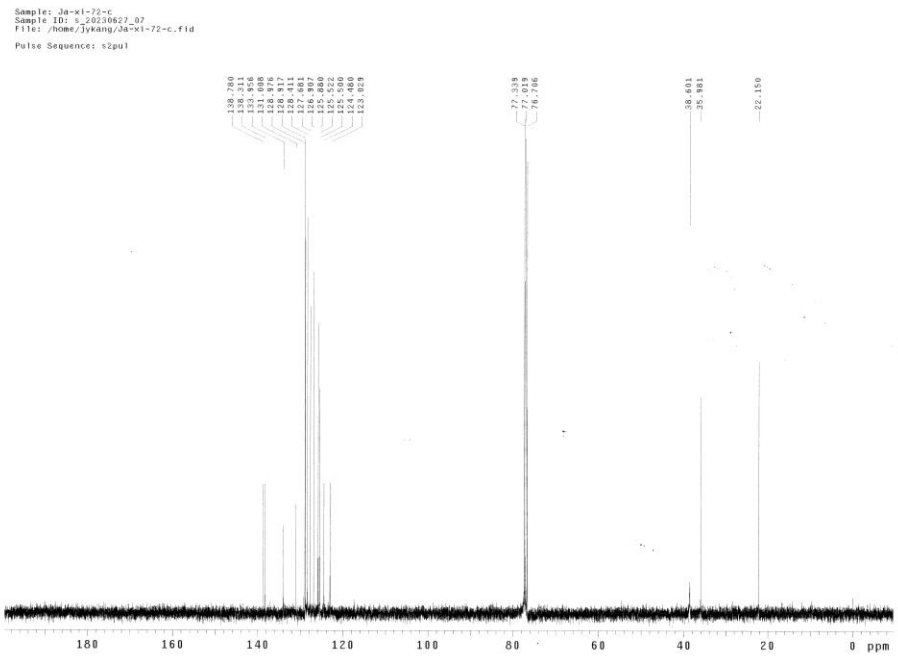

^{1}H NMR (400 MHz) in $CDCl_3$

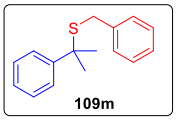

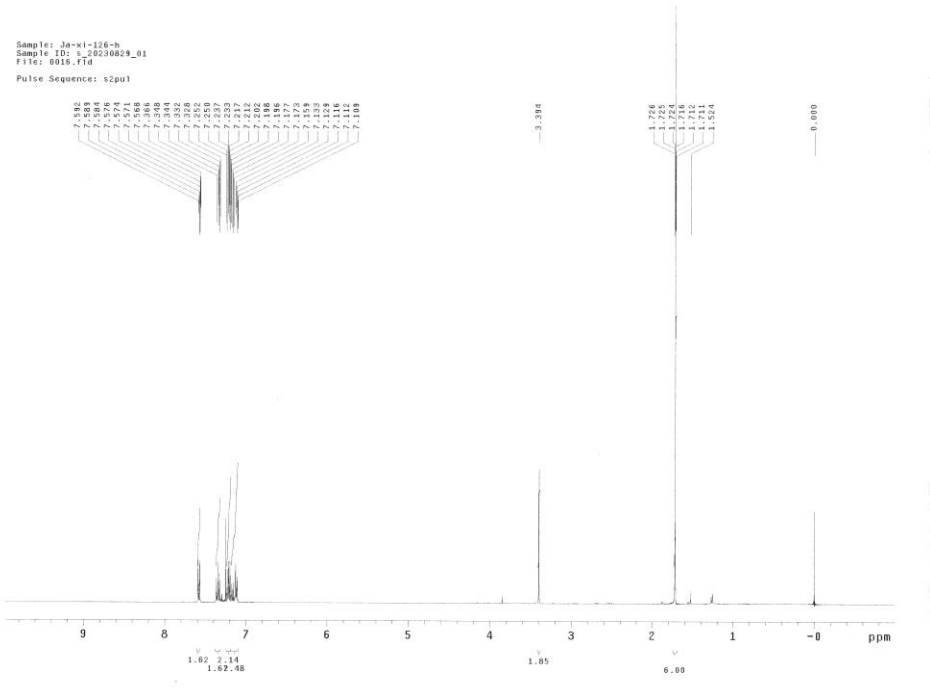

^{13}C NMR (100.5 MHz) in $CDCl_3$

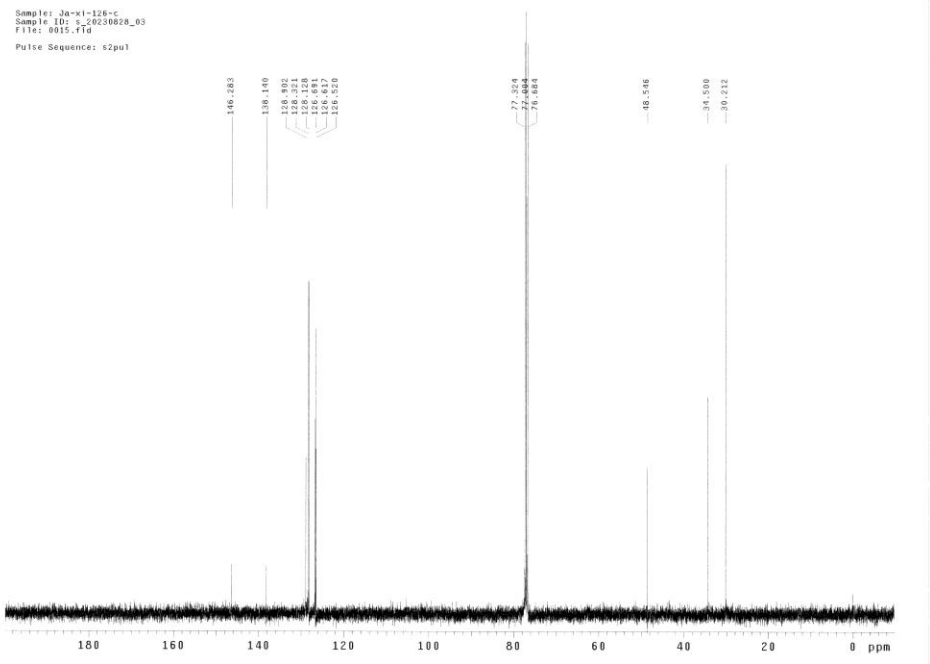

^{1}H NMR (400 MHz) in $CDCl_3$

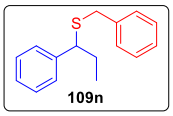

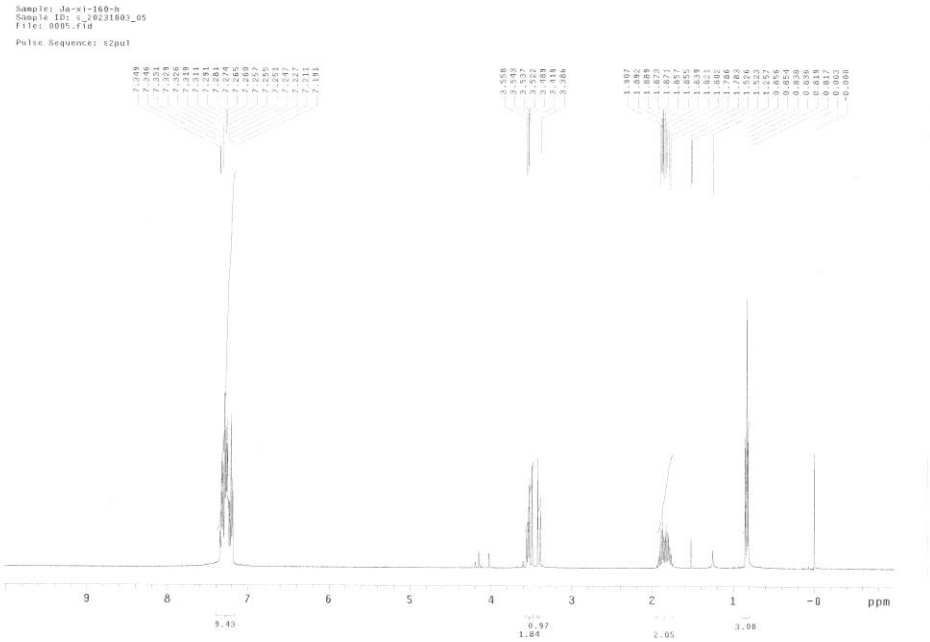

^{13}C NMR (100.5 MHz) in $CDCl_3$

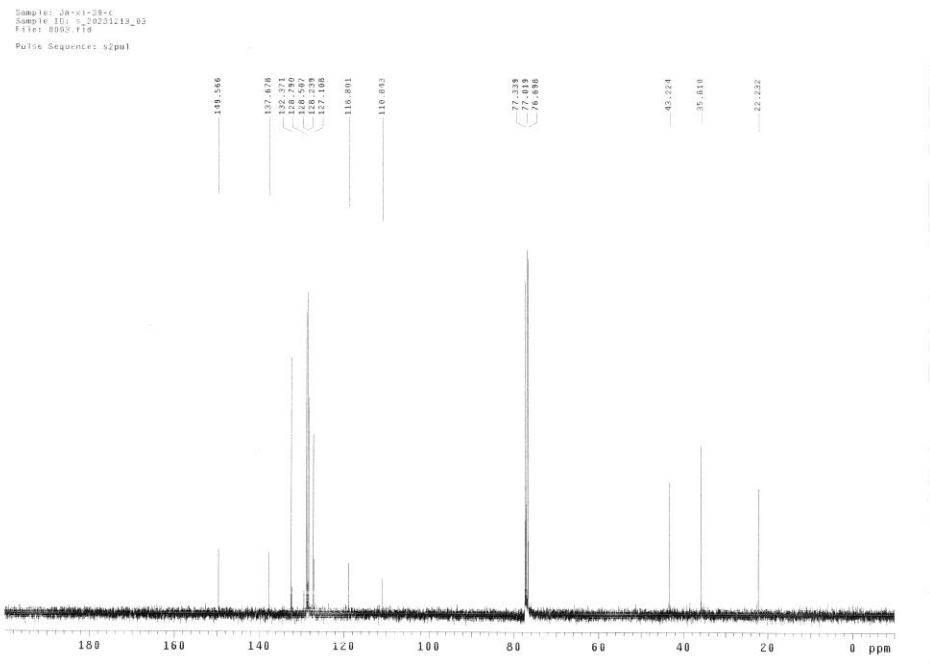

^{1}H NMR (400 MHz) in $CDCl_3$

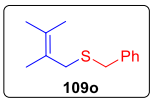

109o

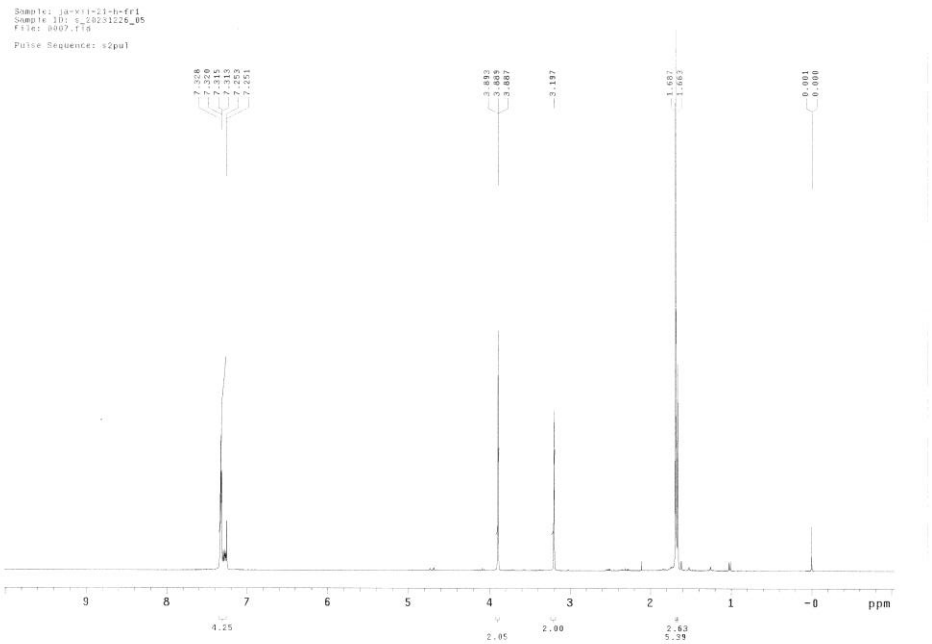

^{13}C NMR (100.5 MHz) in $CDCl_3$

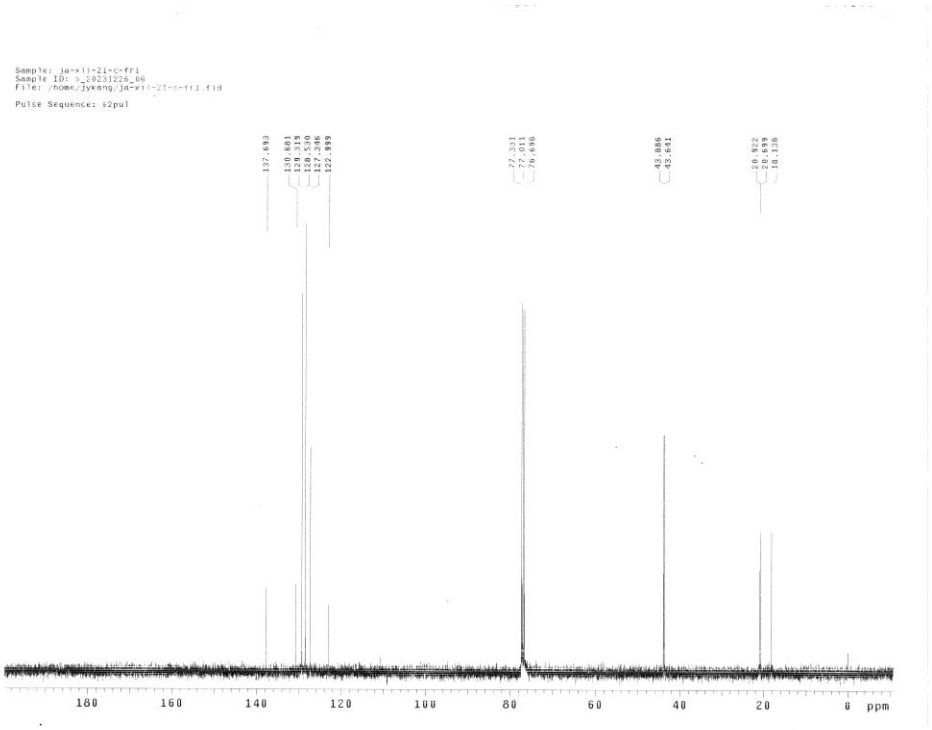

^{1}H NMR (400 MHz) in $CDCl_3$

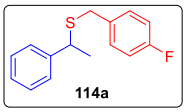

114a

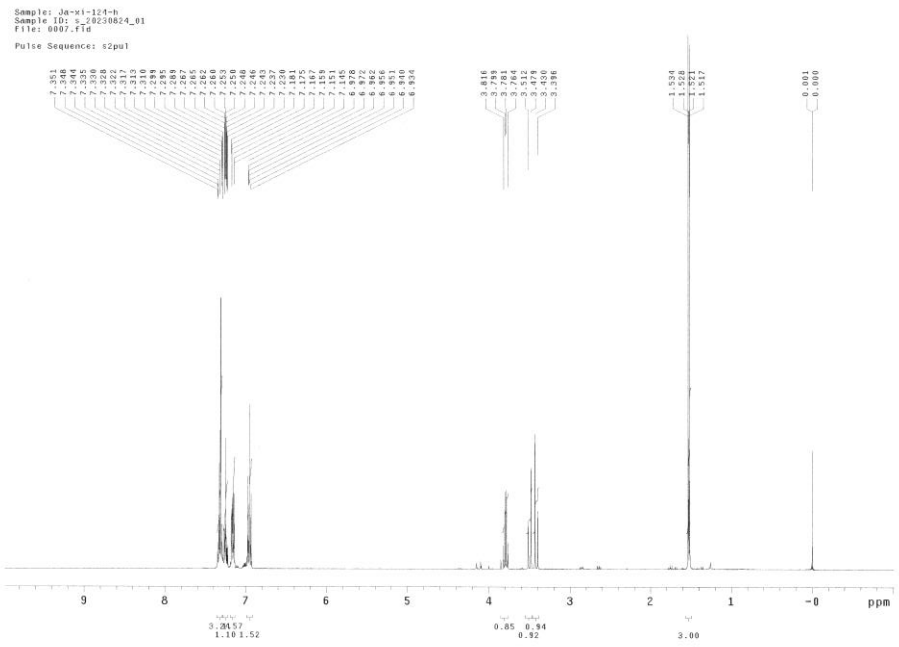

^{13}C NMR (100.5 MHz) in $CDCl_3$

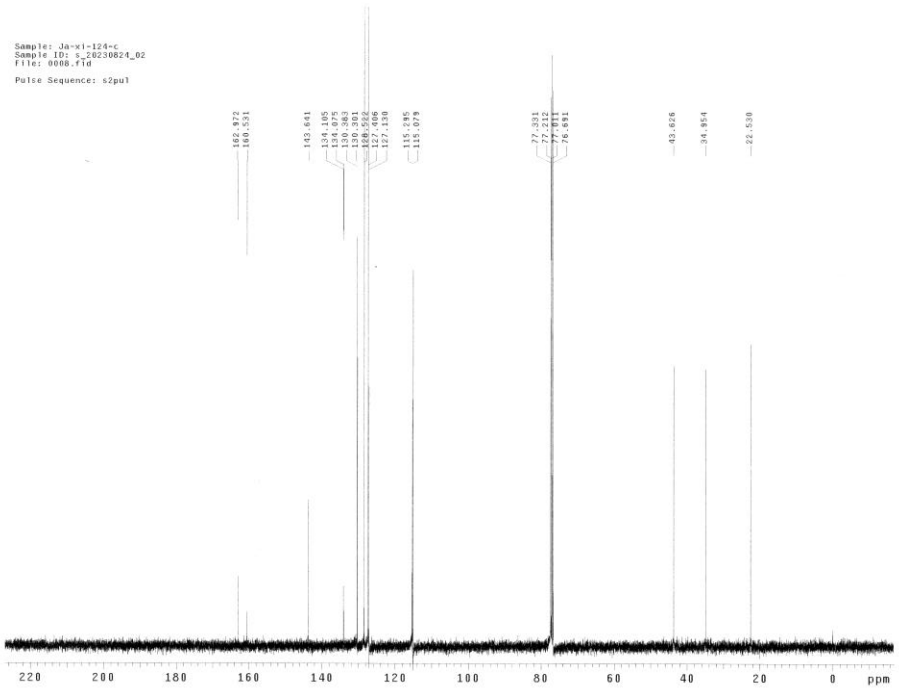

^{1}H NMR (400 MHz) in $CDCl_3$

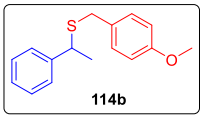

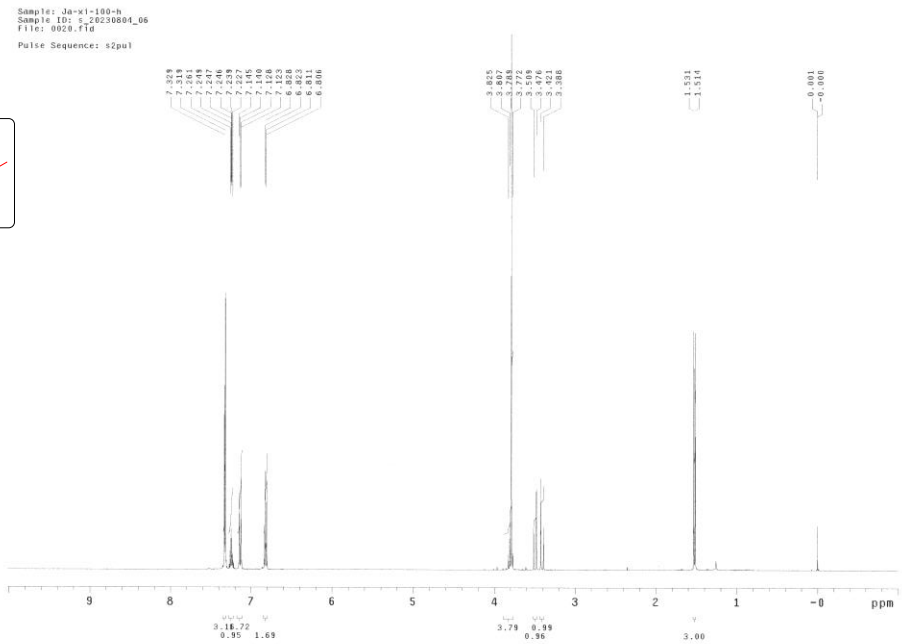

^{13}C NMR (100.5 MHz) in $CDCl_3$

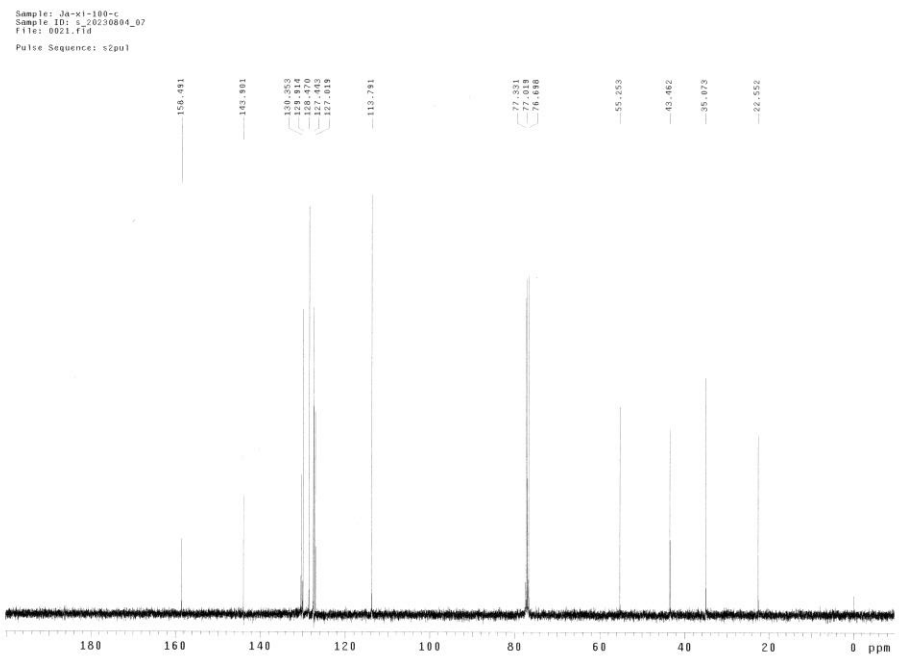

^{1}H NMR (400 MHz) in $CDCl_3$

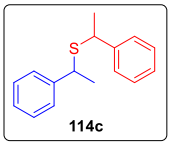

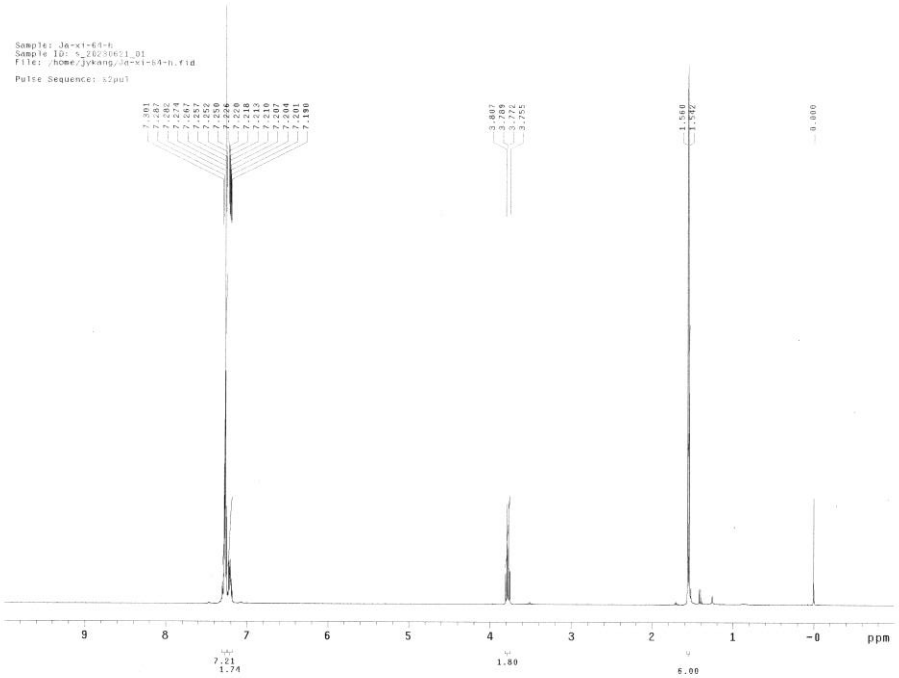

^{13}C NMR (100.5 MHz) in $CDCl_3$

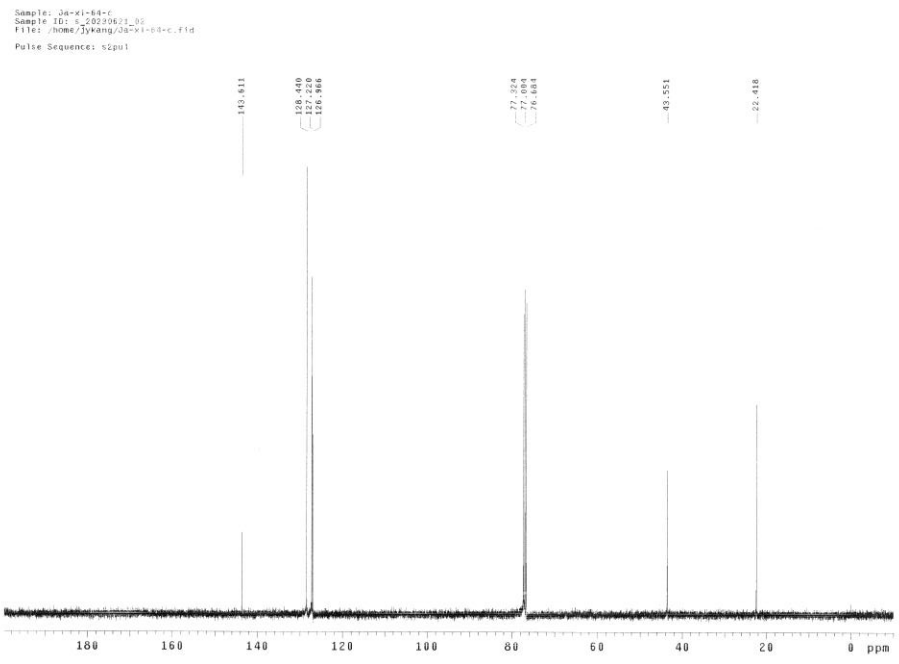

^{1}H NMR (400 MHz) in $CDCl_3$

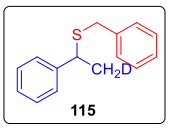

115

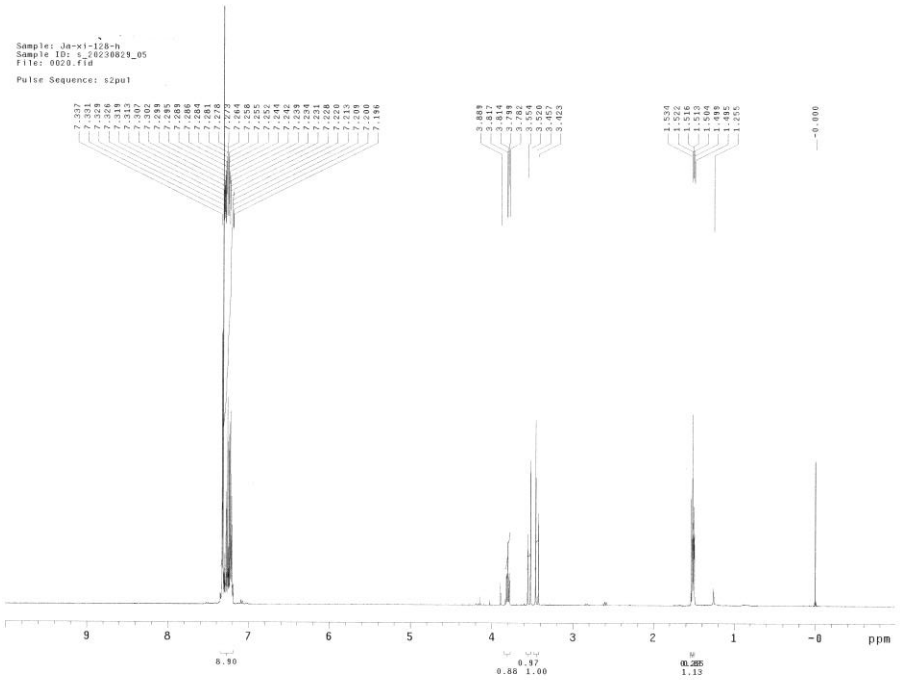

^{13}C NMR (100.5 MHz) in $CDCl_3$

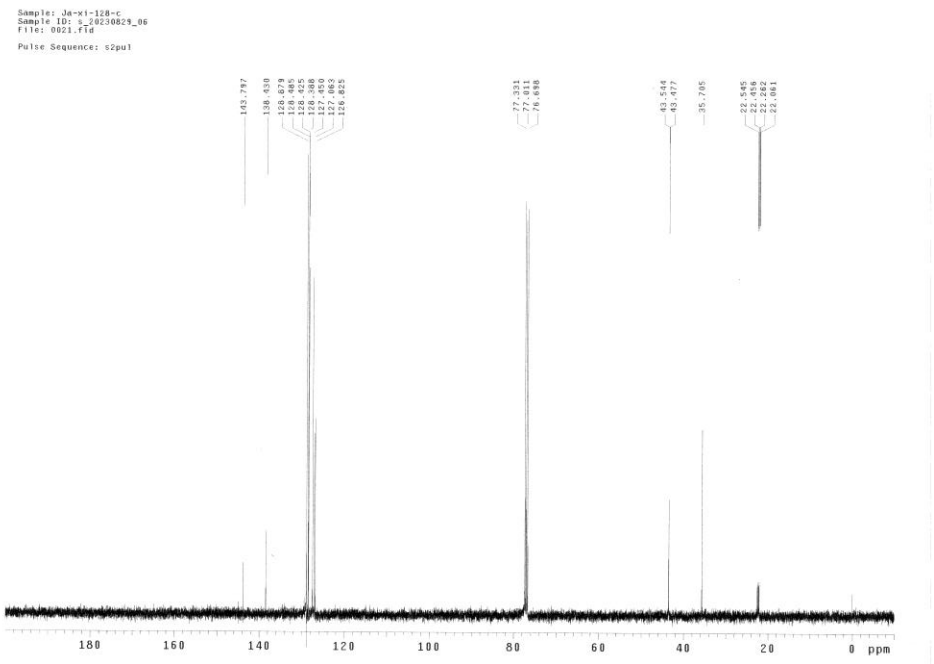

^{1}H NMR (400 MHz) in $CDCl_3$

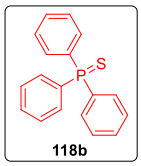

118b

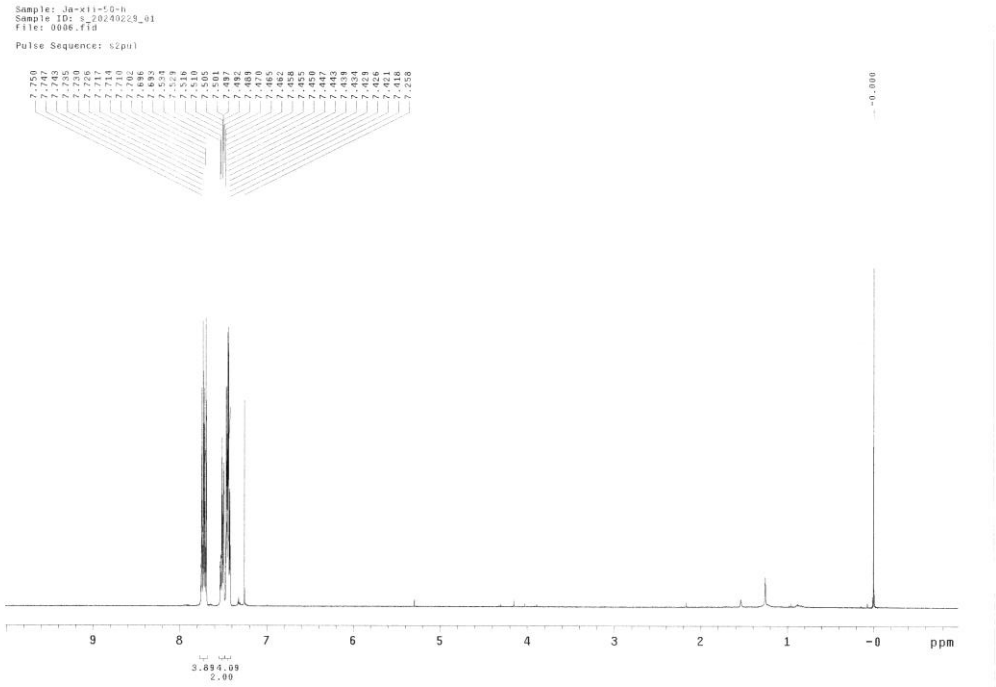

^{13}C NMR (100.5 MHz) in $CDCl_3$

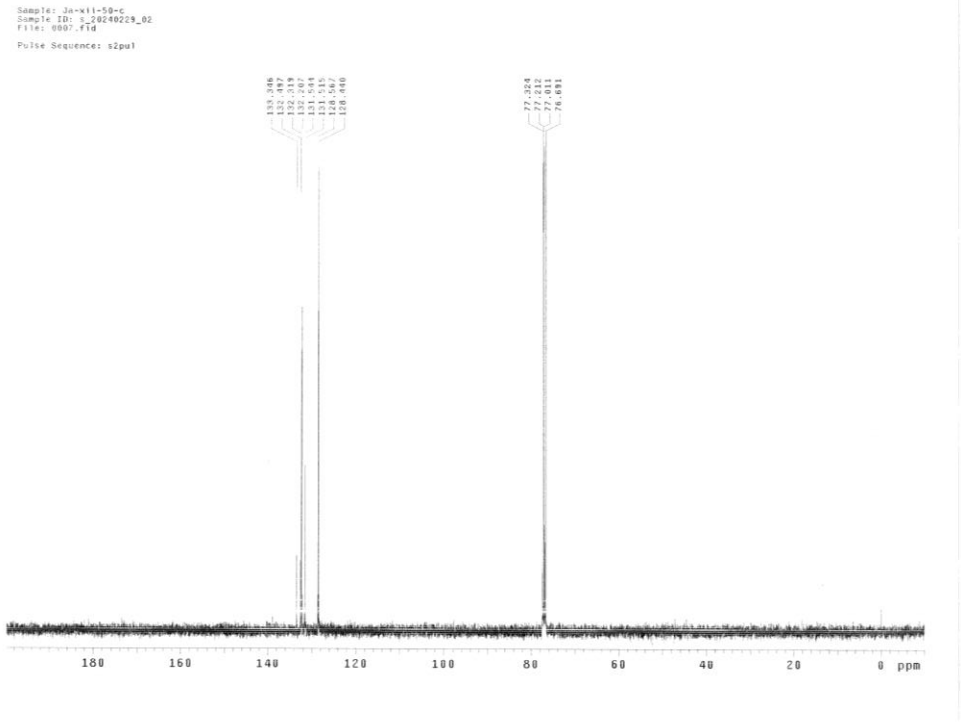

^{31}P NMR (162 MHz) in $CDCl_3$

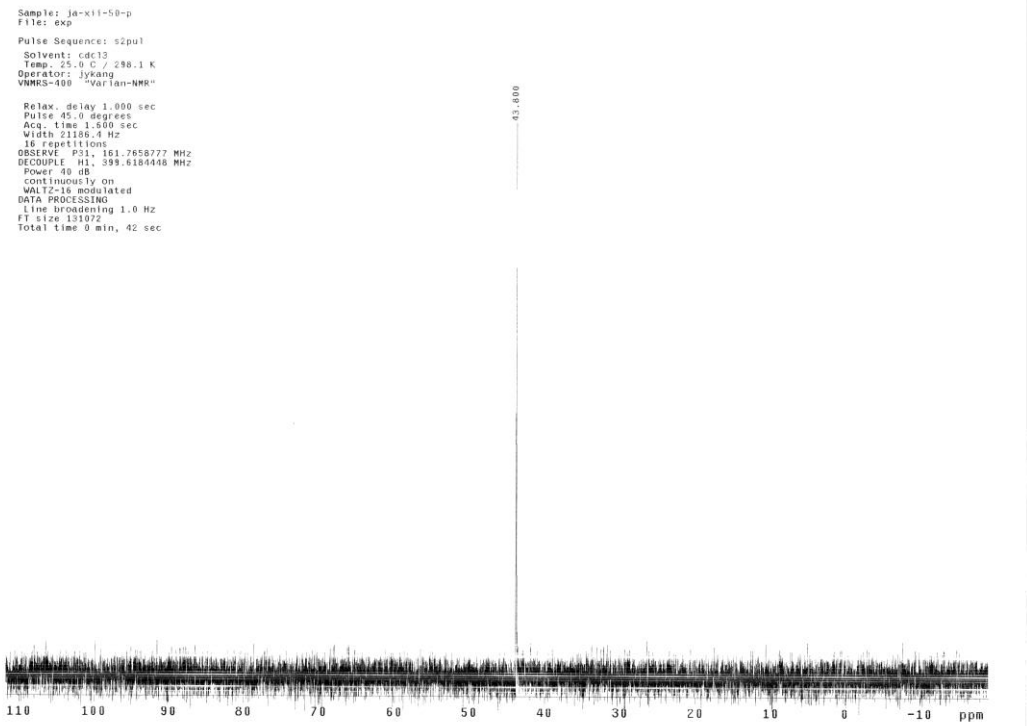

^{1}H NMR (400 MHz) in $CDCl_3$

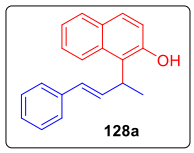

128a

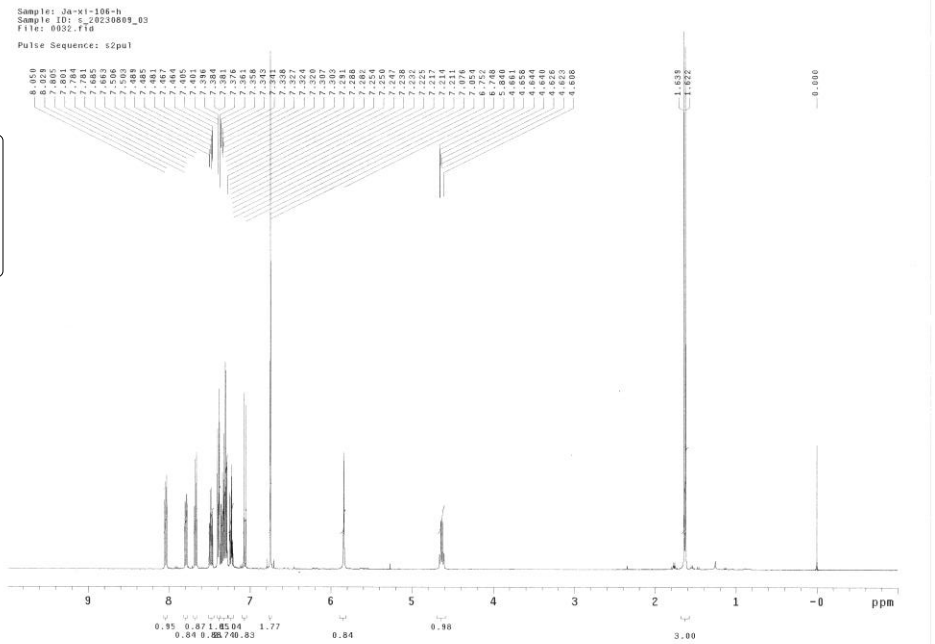

^{13}C NMR (100.5 MHz) in $CDCl_3$

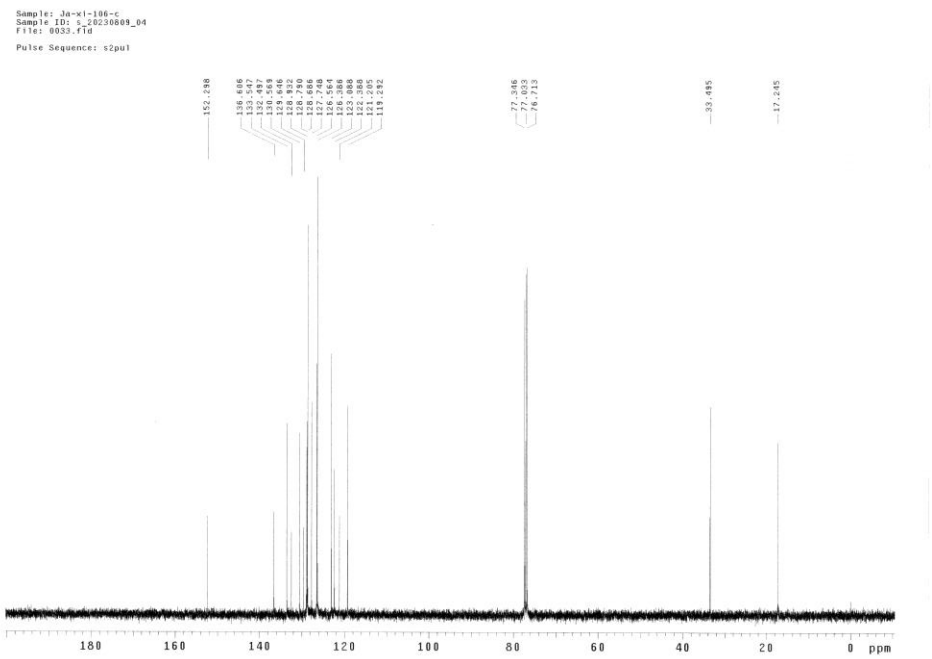

^{1}H NMR (400 MHz) in $CDCl_3$

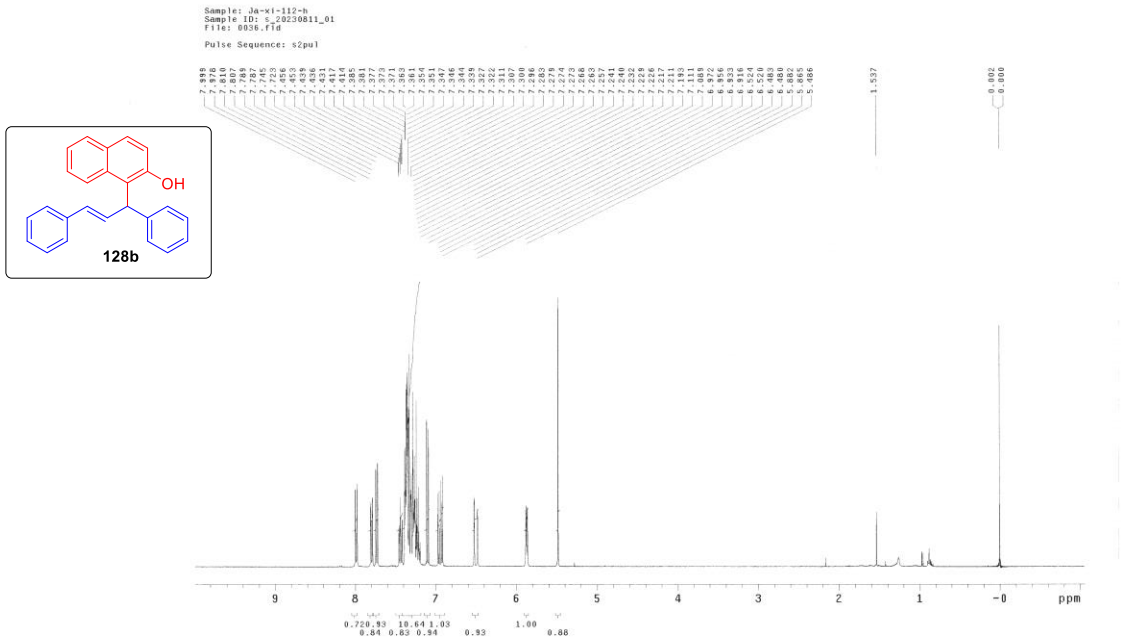

^{13}C NMR (100.5 MHz) in $CDCl_3$

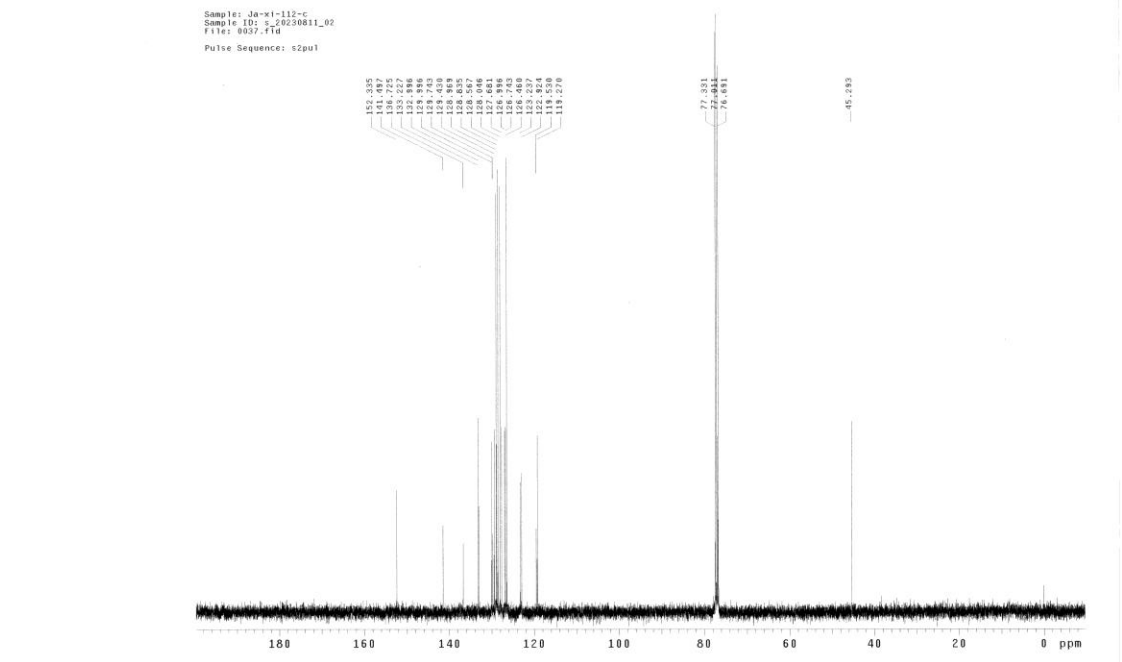

^{1}H NMR (400 MHz) in $CDCl_3$

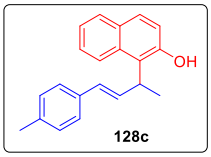

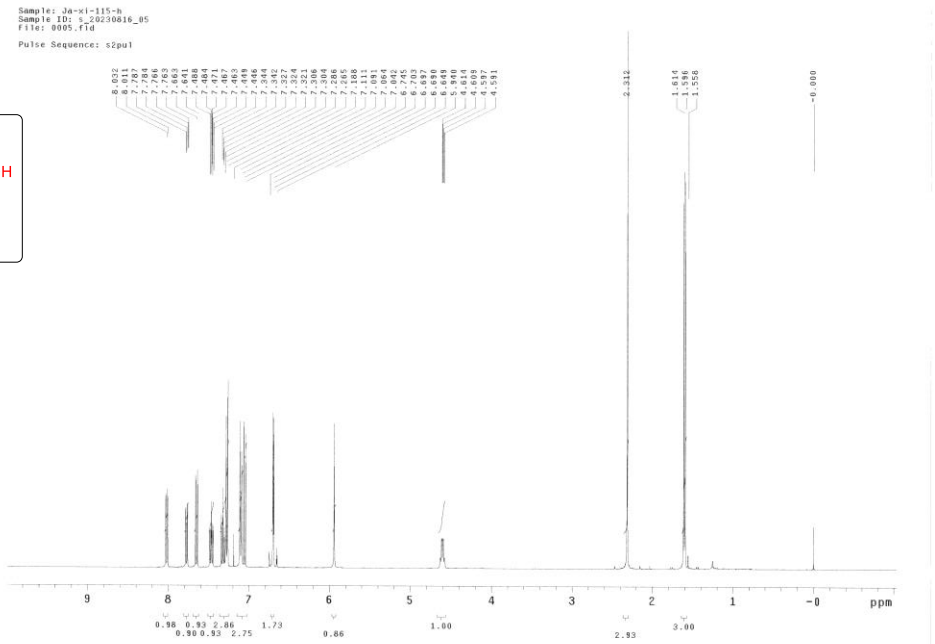

^{13}C NMR (100.5 MHz) in $CDCl_3$

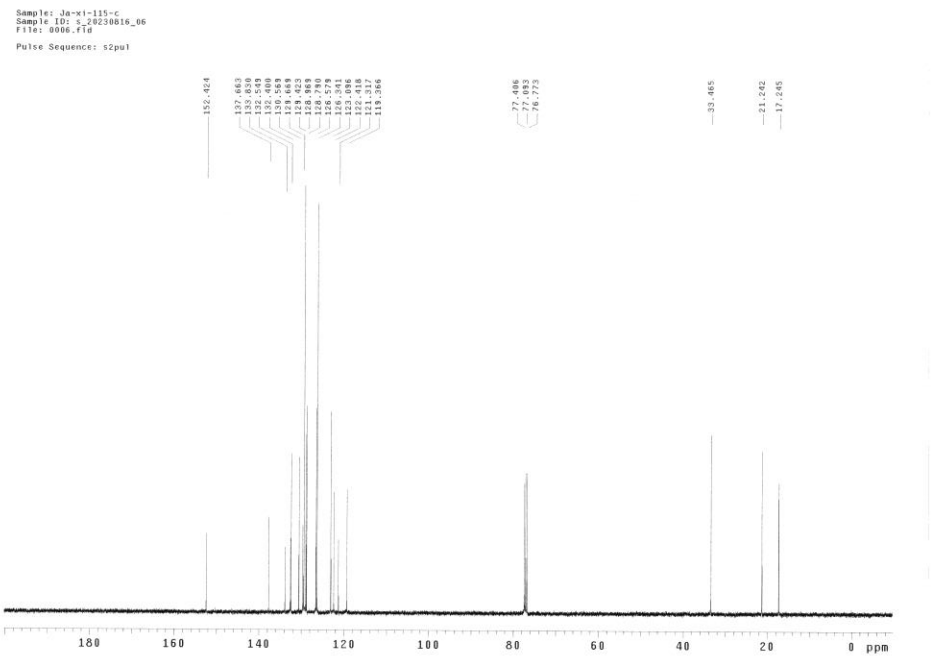

^{1}H NMR (400 MHz) in $CDCl_3$

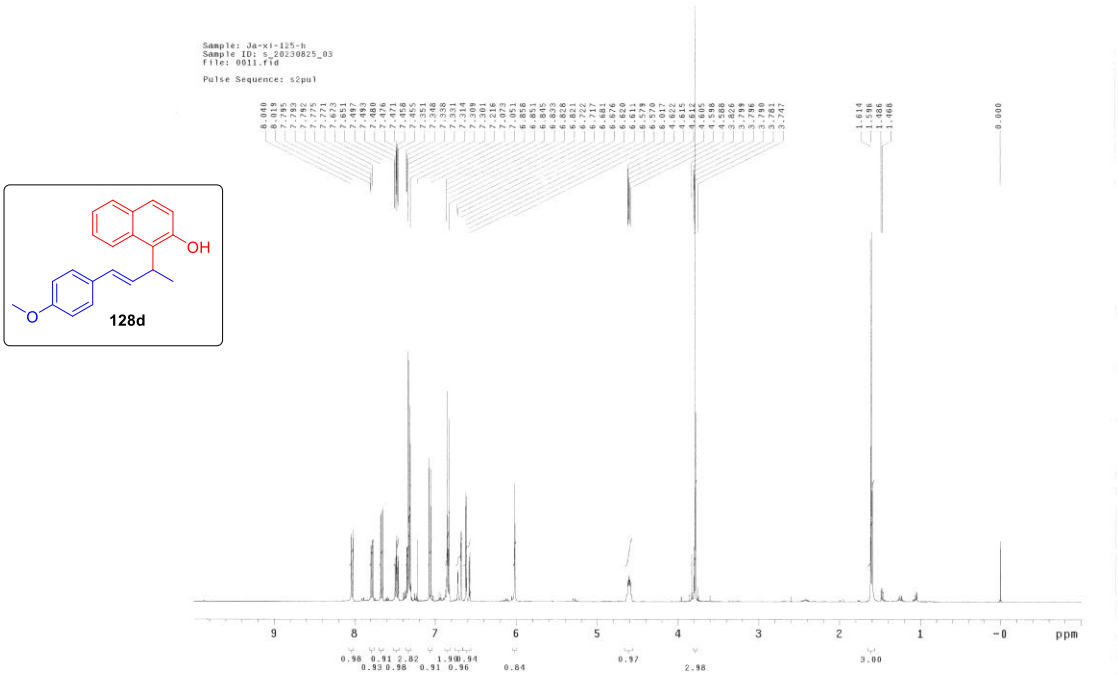

^{13}C NMR (100.5 MHz) in $CDCl_3$

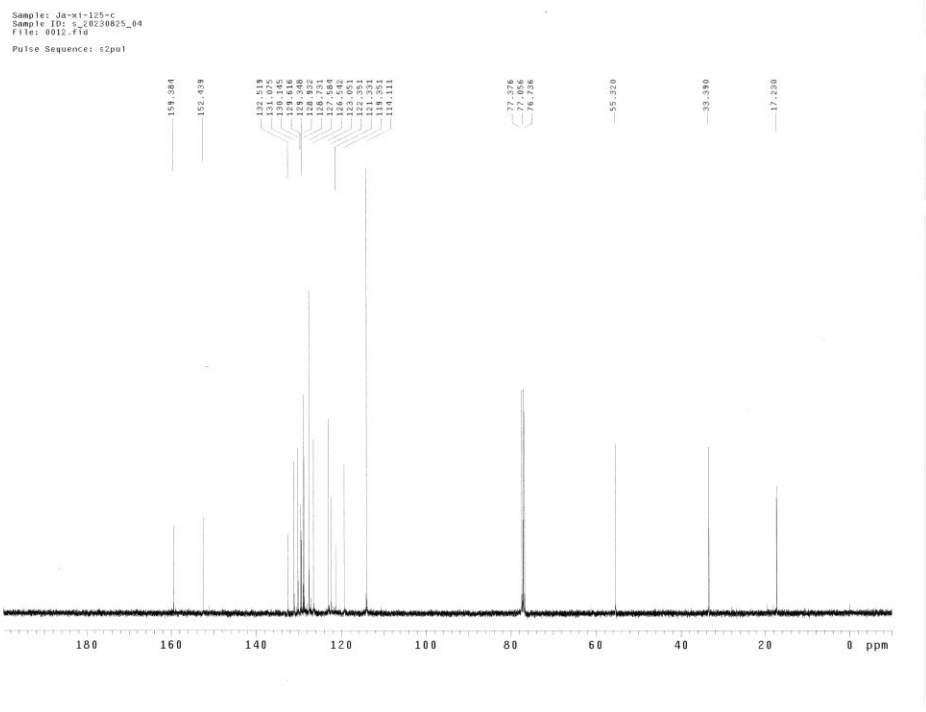

^{1}H NMR (400 MHz) in $CDCl_3$

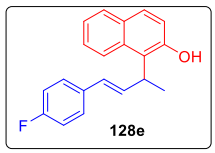

128e

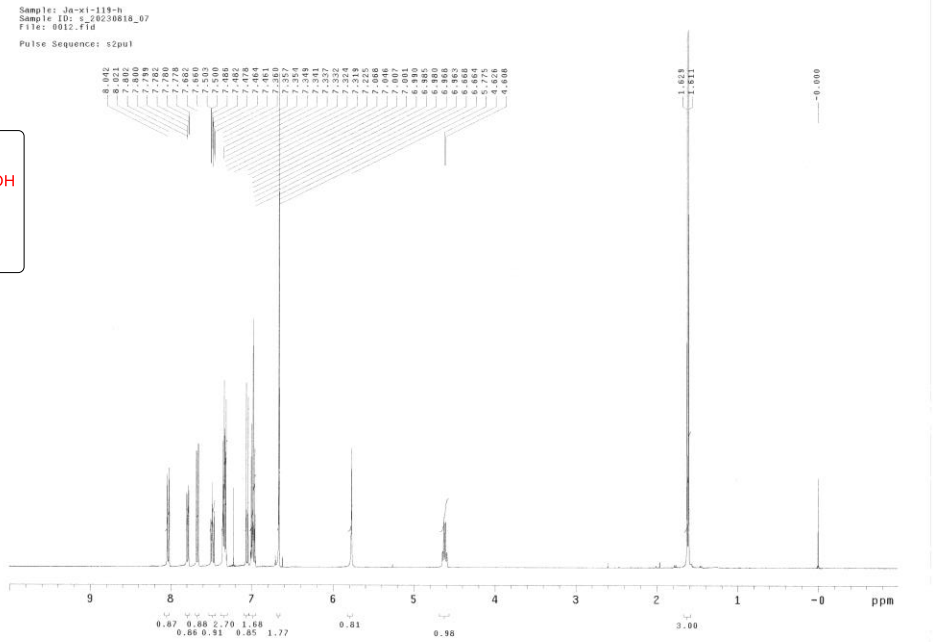

^{13}C NMR (100.5 MHz) in $CDCl_3$

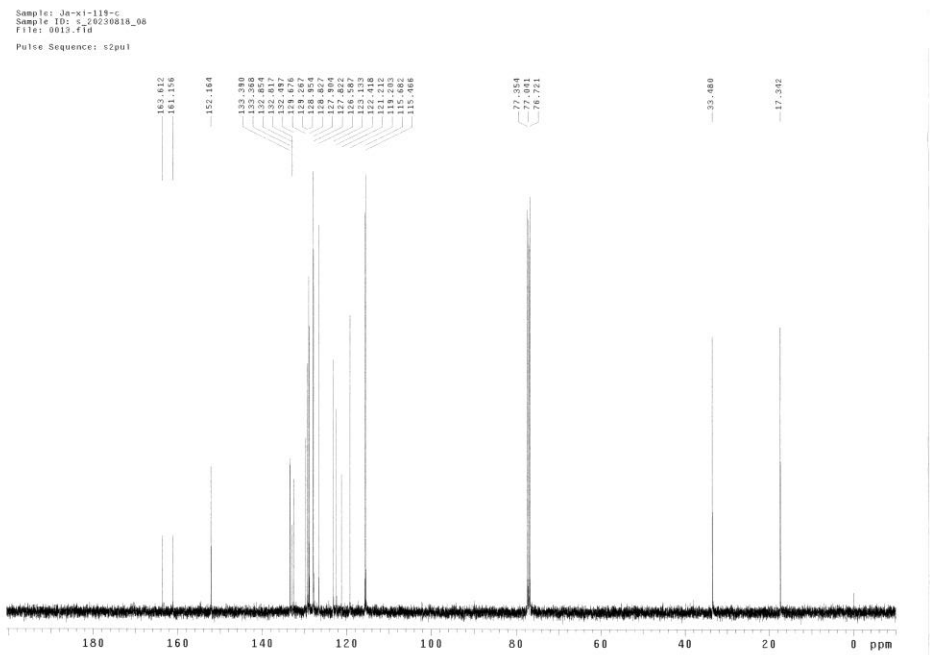

^{1}H NMR (400 MHz) in $CDCl_3$

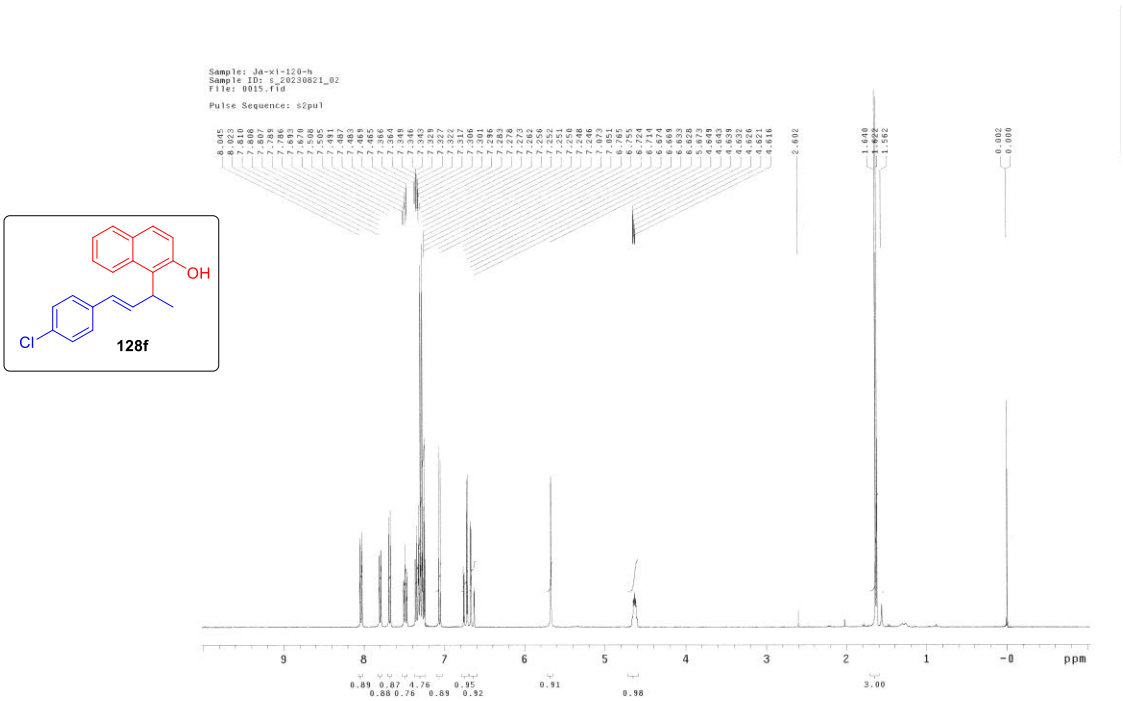

^{13}C NMR (100.5 MHz) in $CDCl_3$

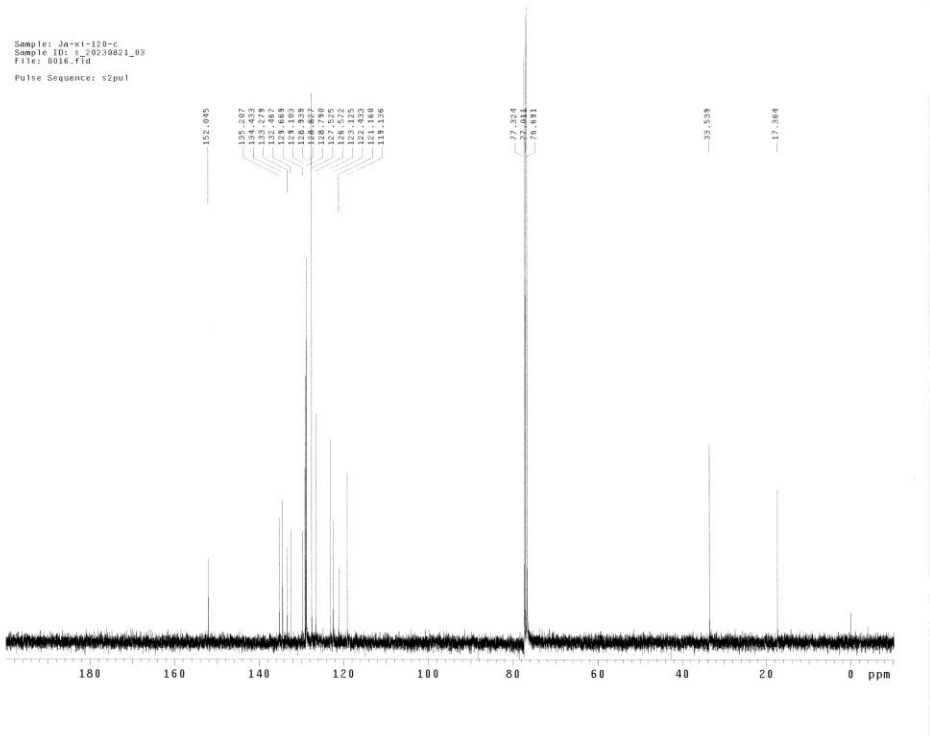

^{1}H NMR (400 MHz) in $CDCl_3$

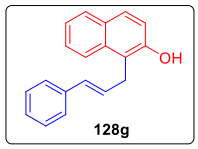

128g

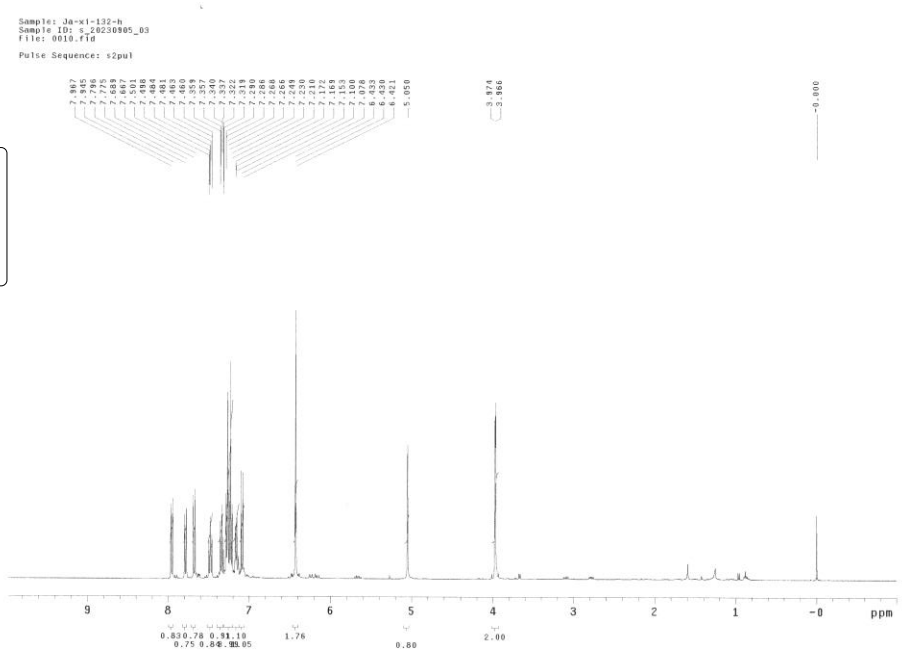

^{13}C NMR (100.5 MHz) in $CDCl_3$

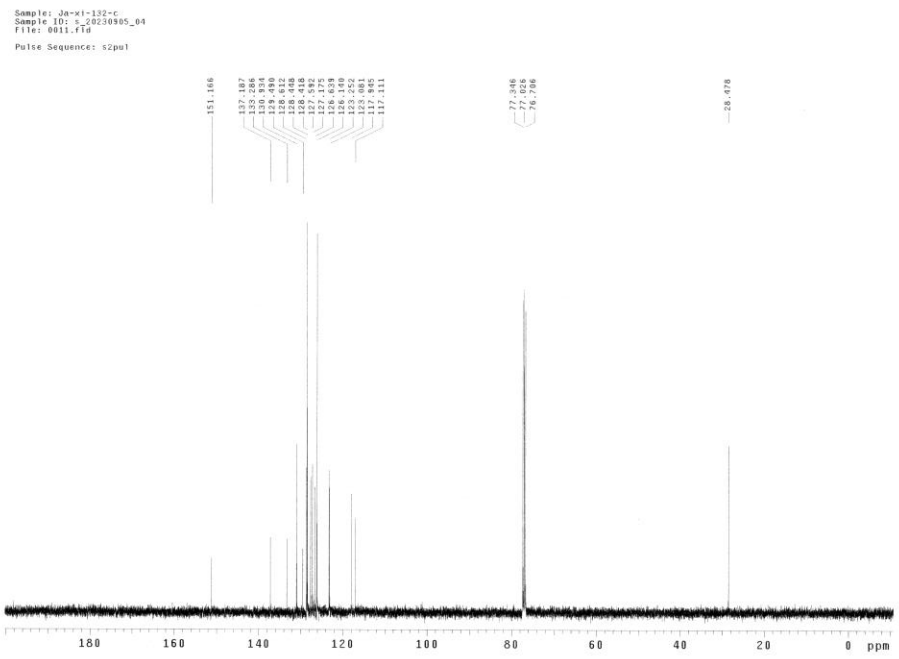

^{1}H NMR (400 MHz) in $CDCl_3$

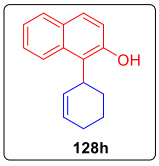

128h

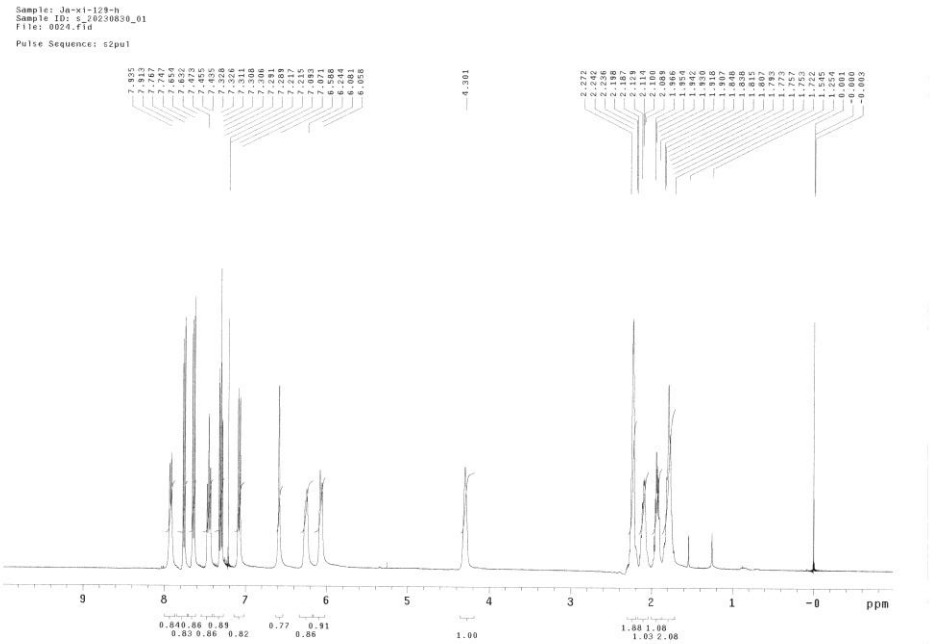

^{13}C NMR (100.5 MHz) in $CDCl_3$

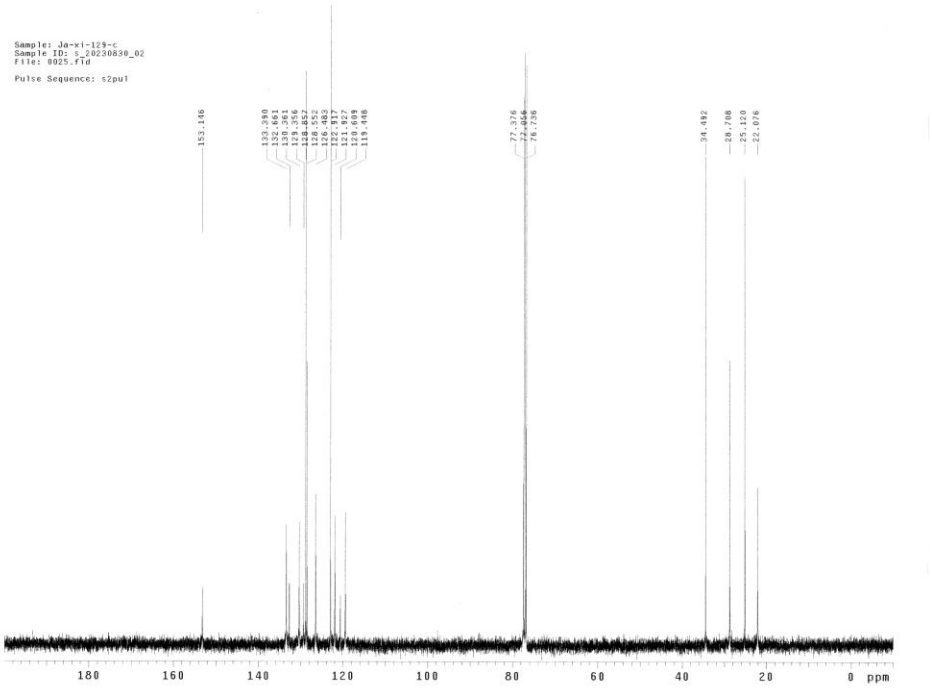

^{1}H NMR (400 MHz) in $CDCl_3$

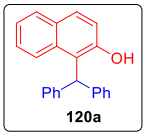

120a

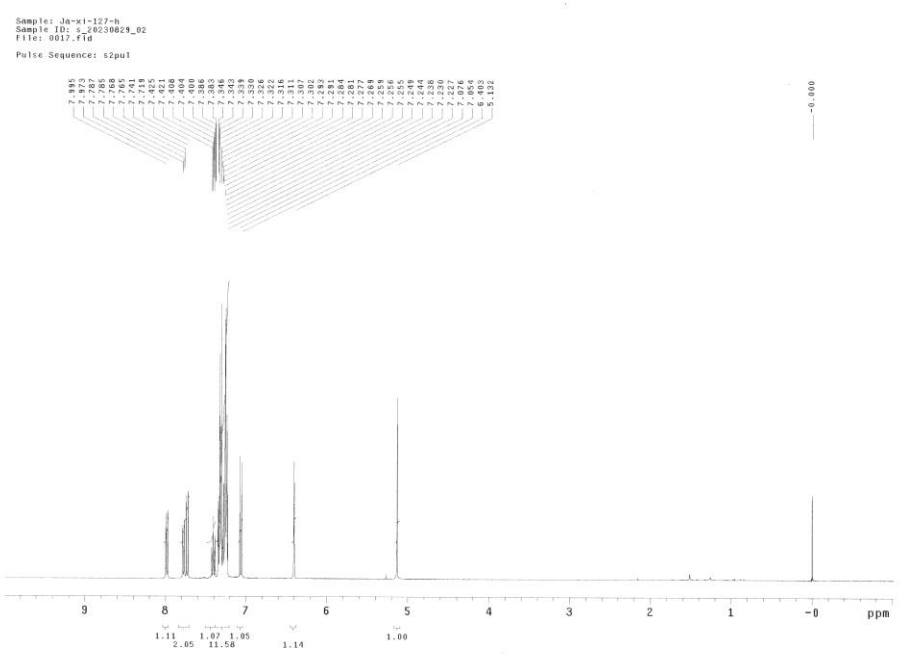

^{13}C NMR (100.5 MHz) in $CDCl_3$

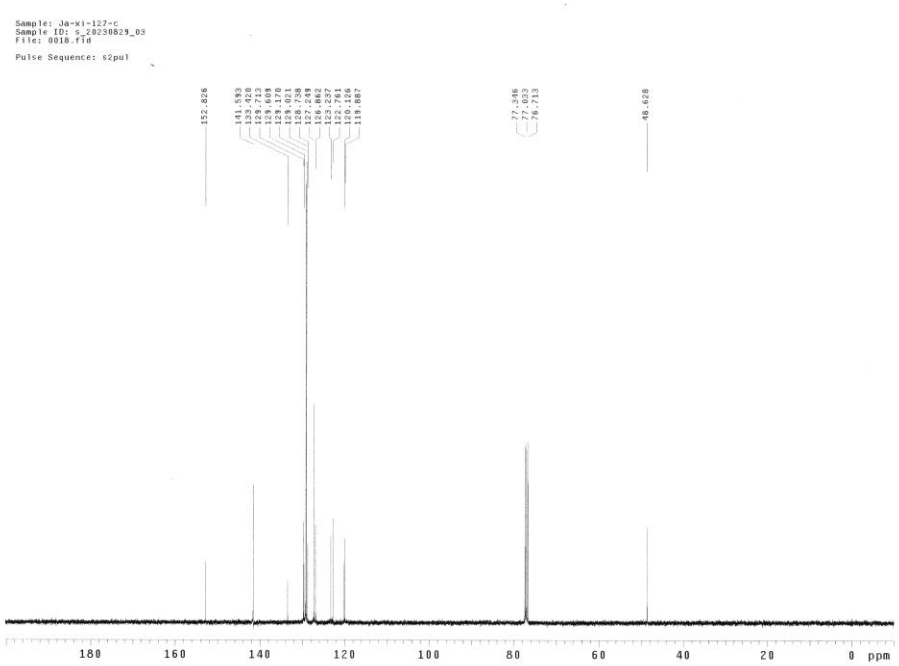

^{1}H NMR (400 MHz) in $CDCl_3$

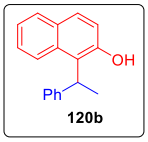

120b

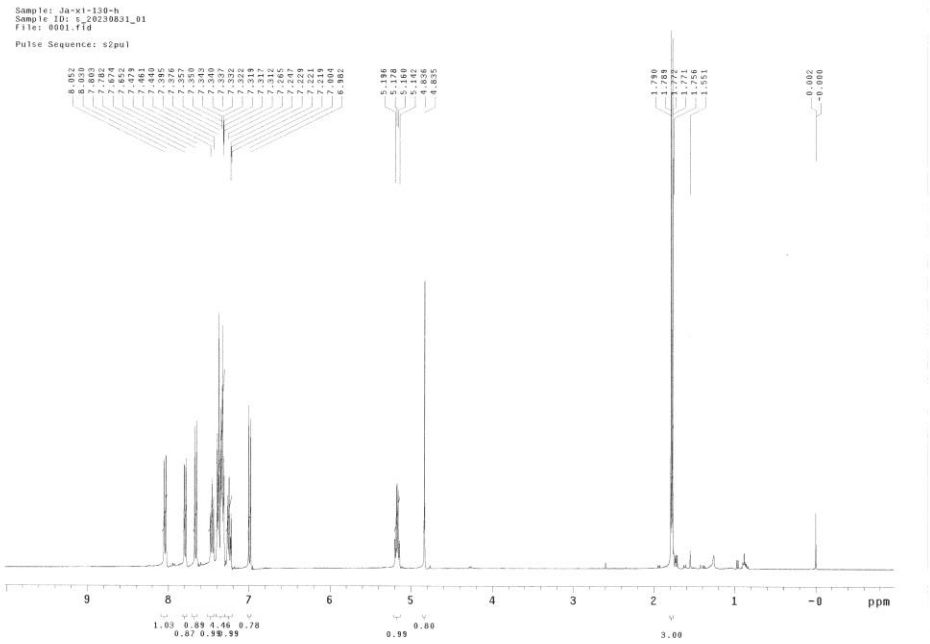

^{13}C NMR (100.5 MHz) in $CDCl_3$

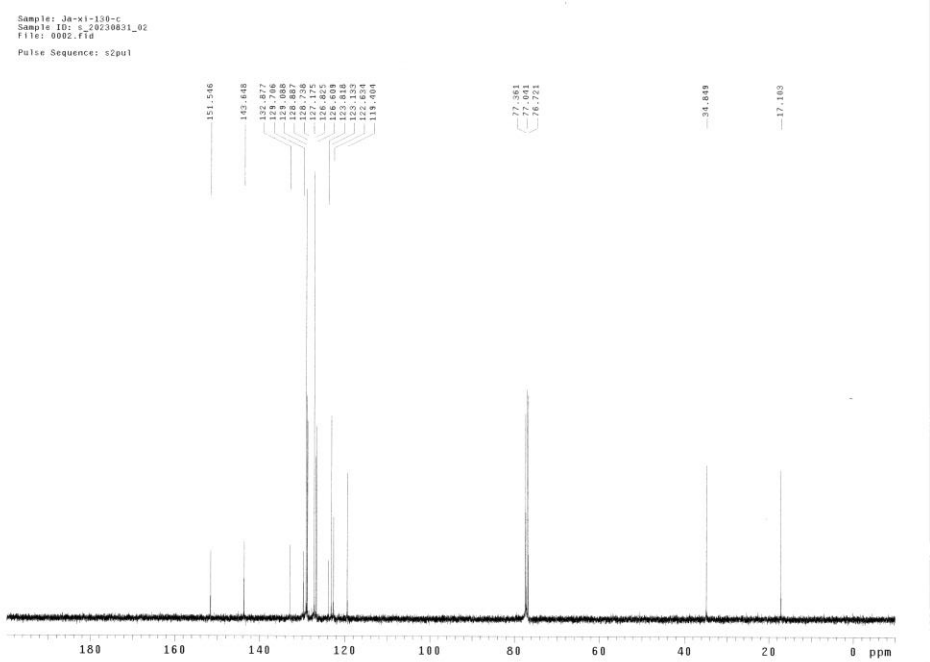

^{1}H NMR (400 MHz) in $CDCl_3$

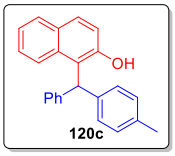

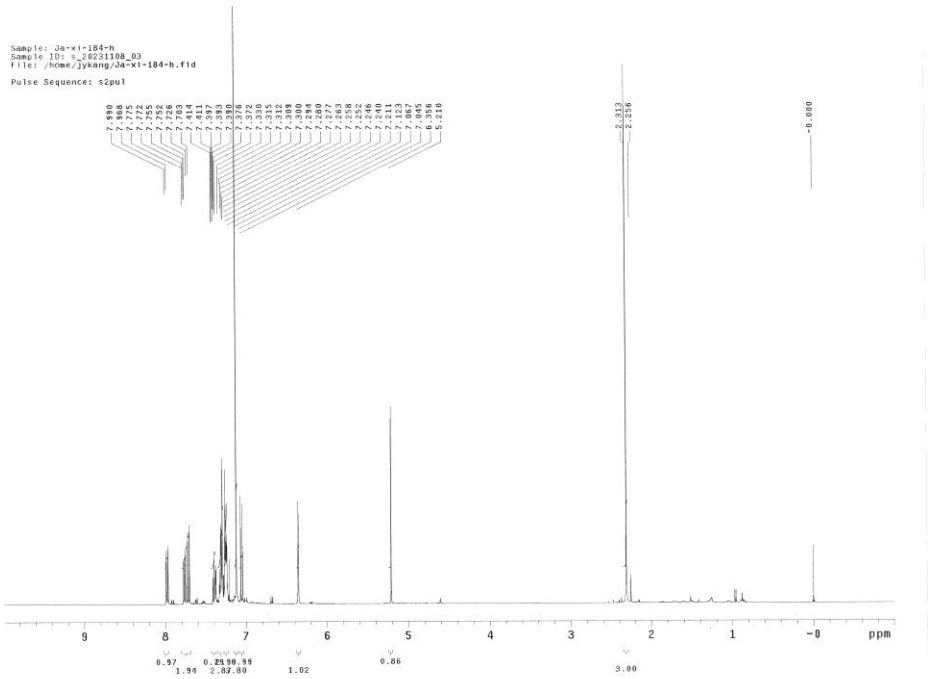

^{13}C NMR (100.5 MHz) in $CDCl_3$

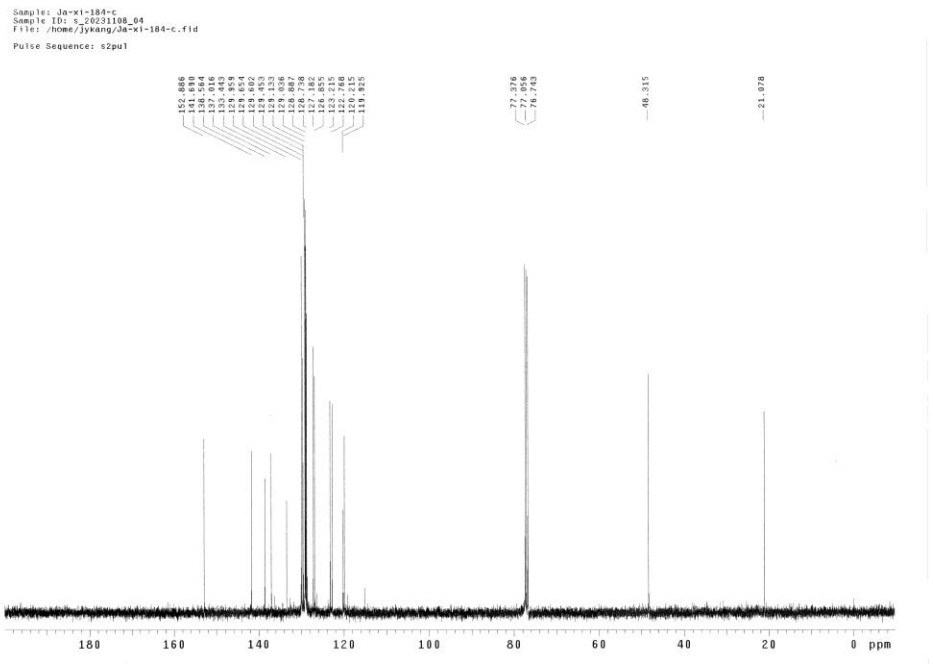

^{1}H NMR (400 MHz) in $CDCl_3$

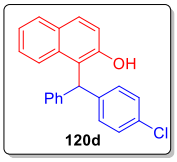

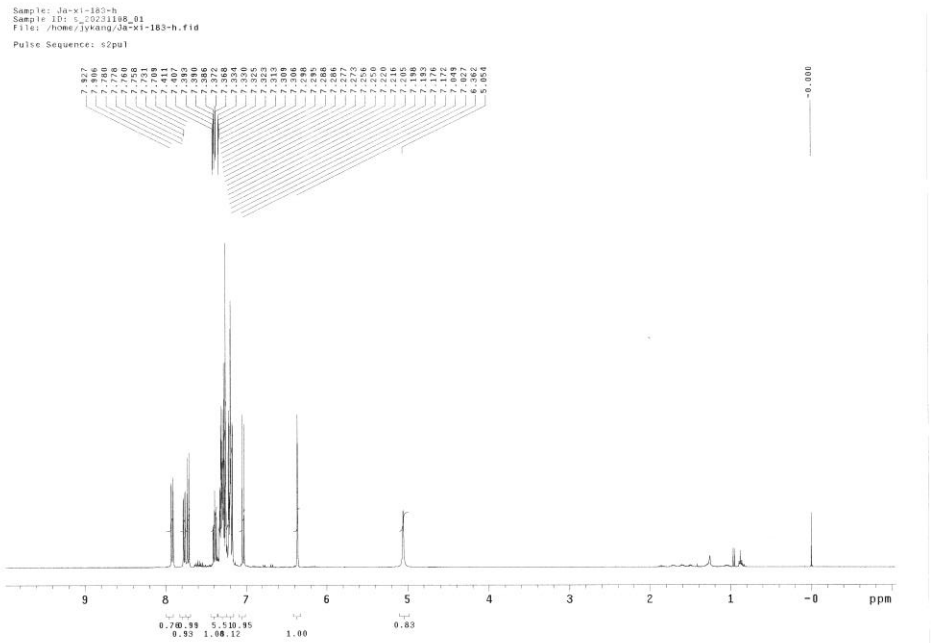

^{13}C NMR (100.5 MHz) in $CDCl_3$

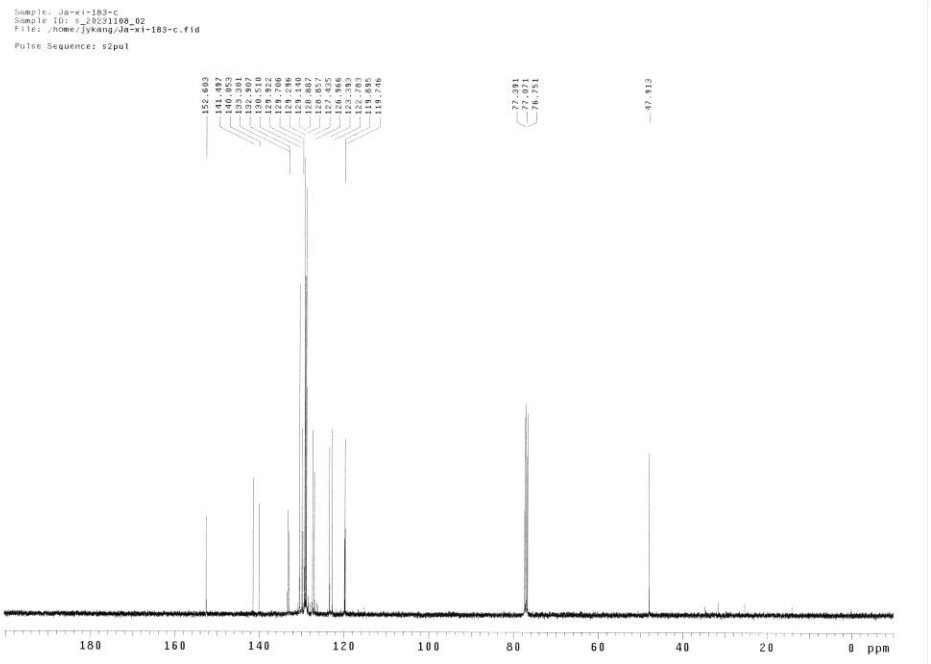

^{1}H NMR (400 MHz) in $CDCl_3$

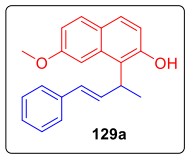

129a

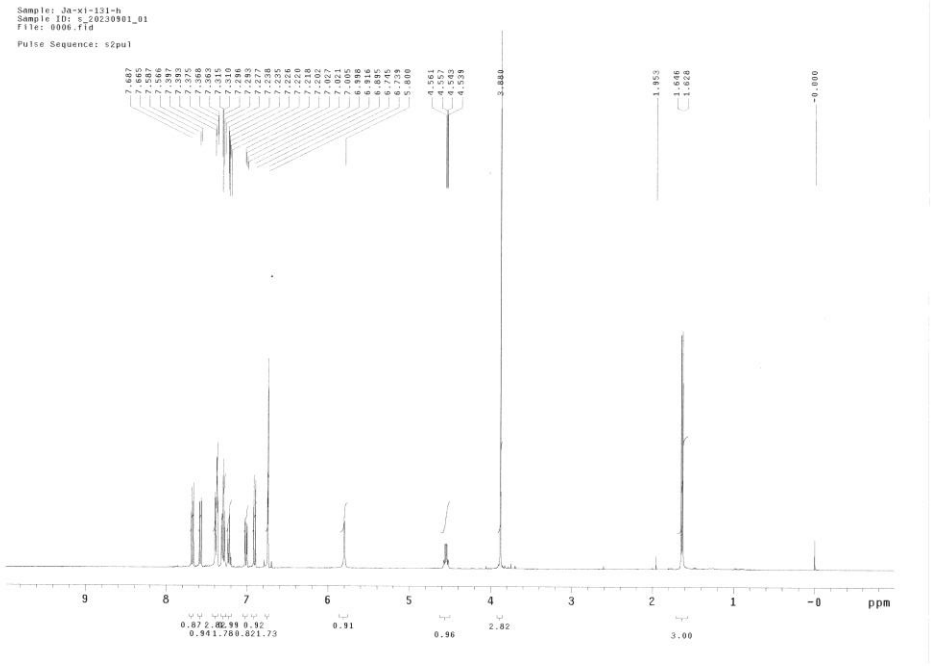

^{13}C NMR (100.5 MHz) in $CDCl_3$

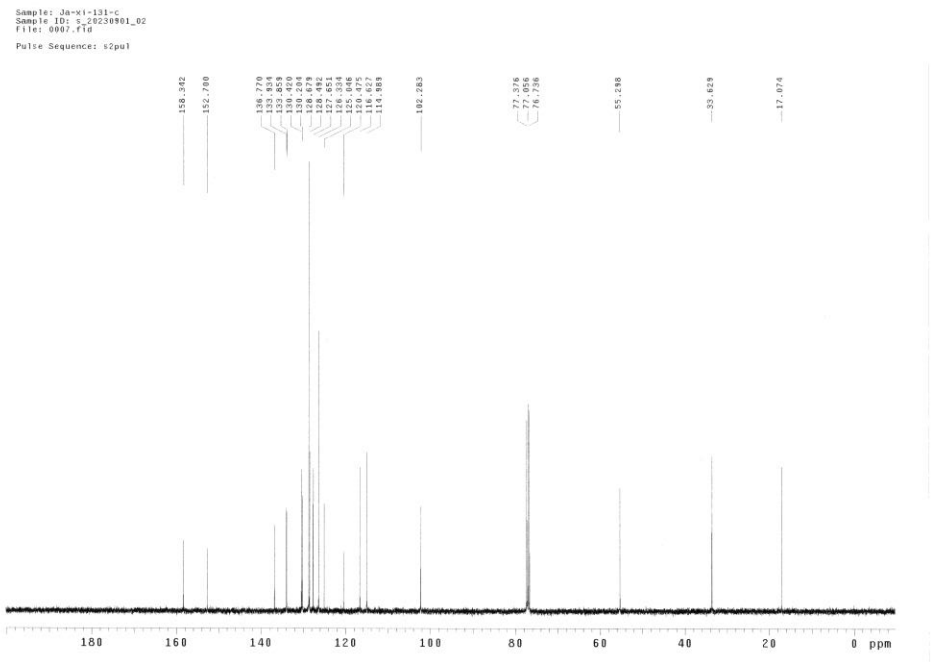

^{1}H NMR (400 MHz) in $CDCl_3$

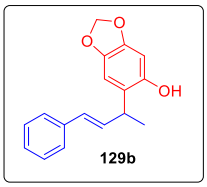

129b

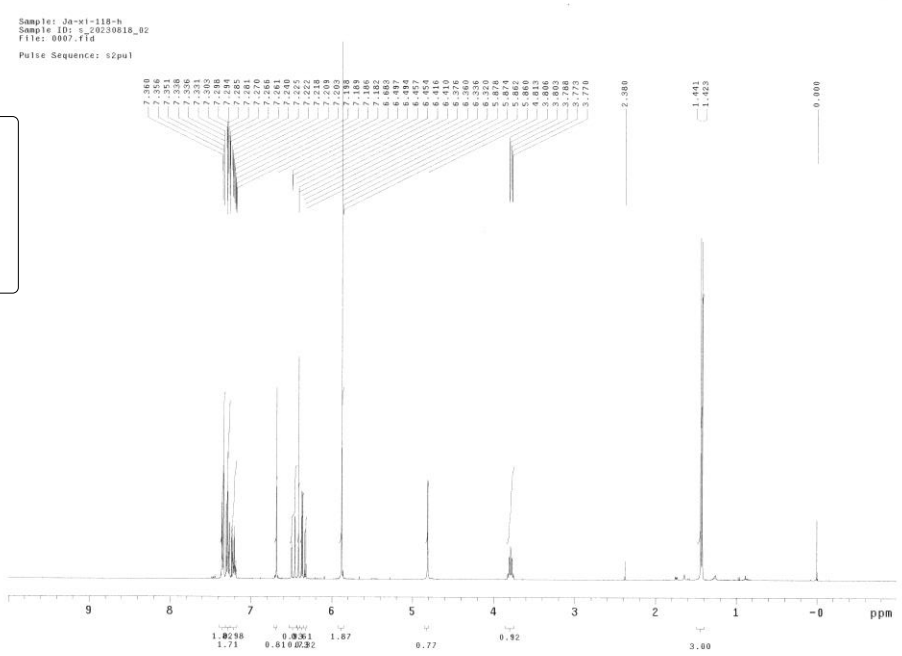

^{13}C NMR (100.5 MHz) in $CDCl_3$

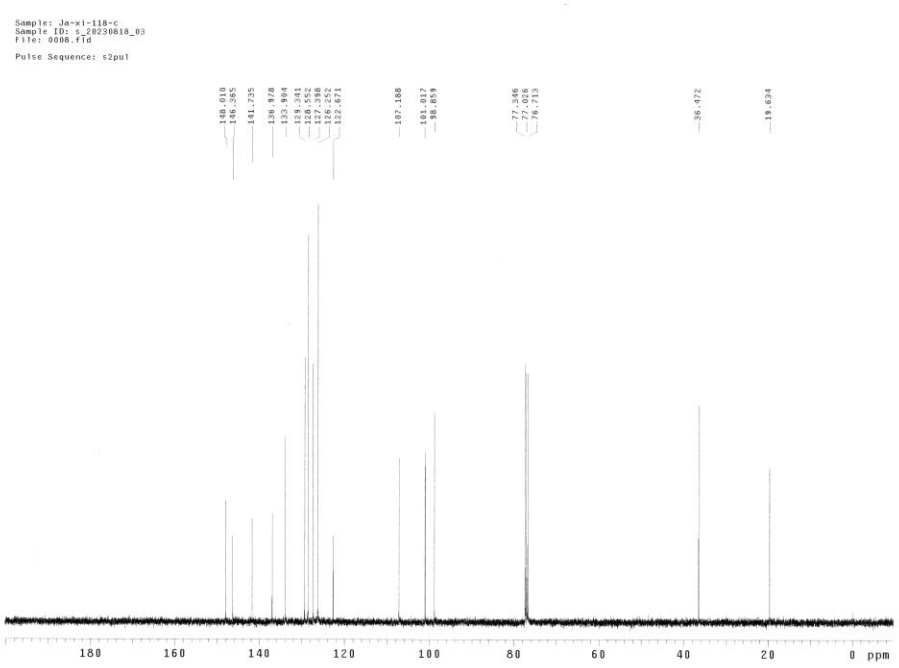

^{1}H NMR (400 MHz) in $CDCl_3$

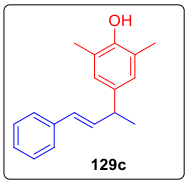

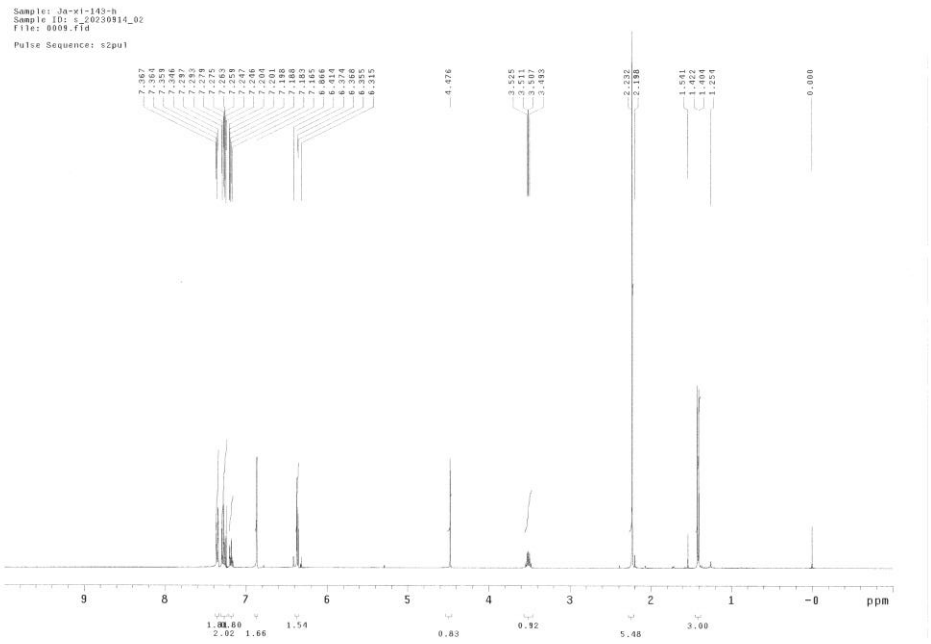

^{13}C NMR (100.5 MHz) in $CDCl_3$

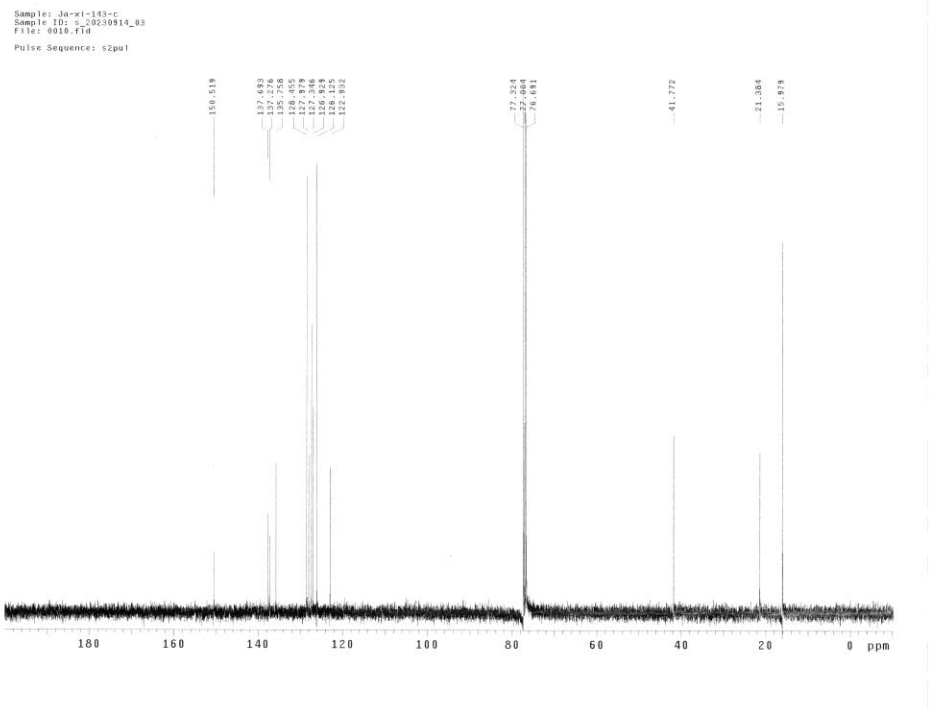

^{1}H NMR (400 MHz) in $CDCl_3$

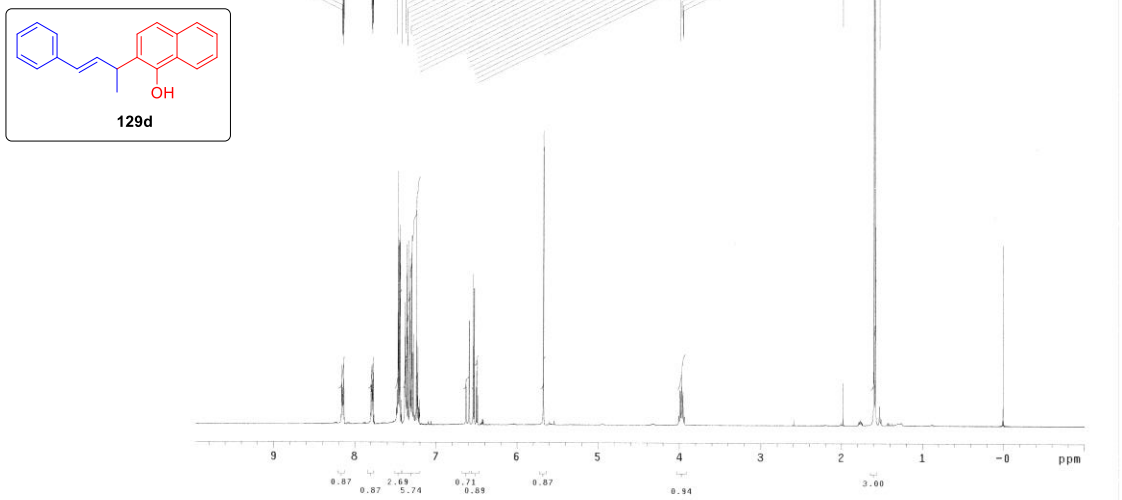

^{13}C NMR (100.5 MHz) in $CDCl_3$

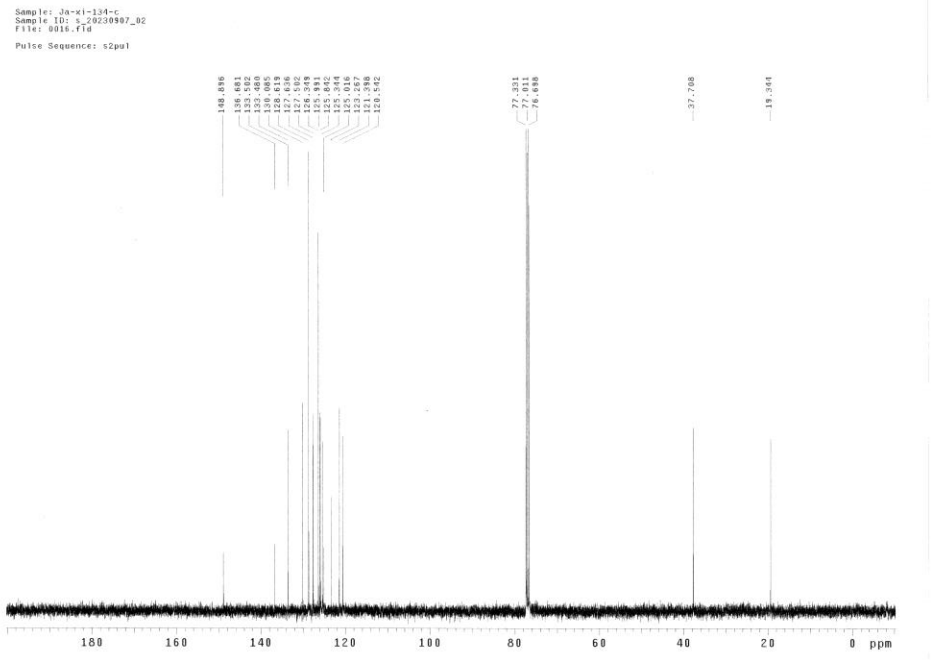

^{1}H NMR (400 MHz) in $CDCl_3$

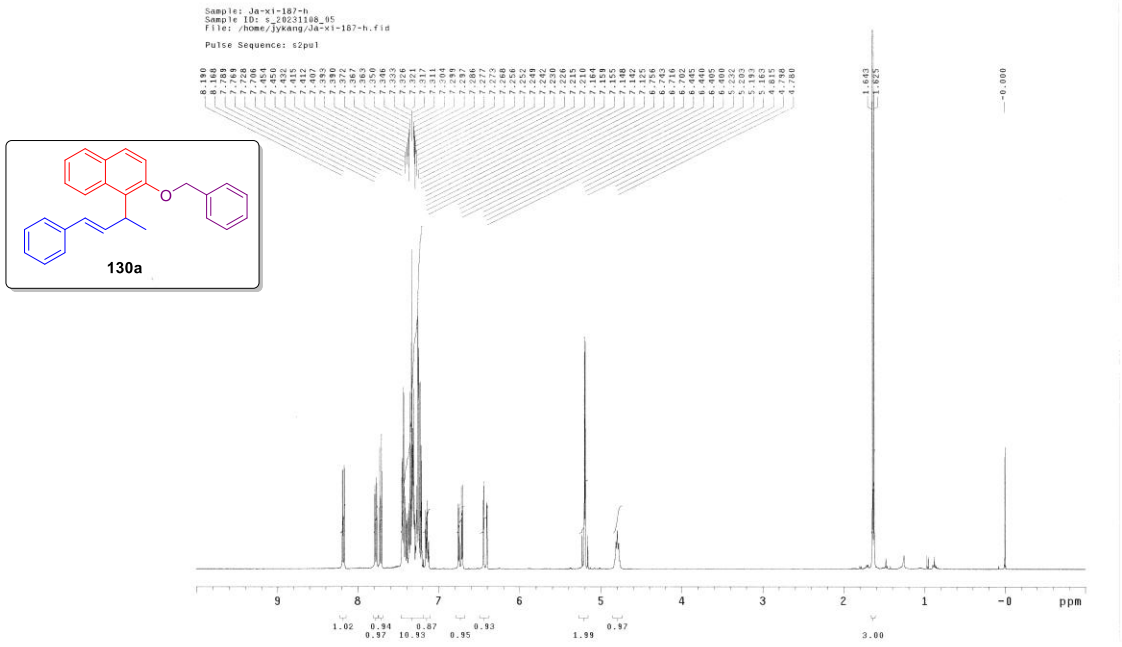

^{13}C NMR (100.5 MHz) in $CDCl_3$

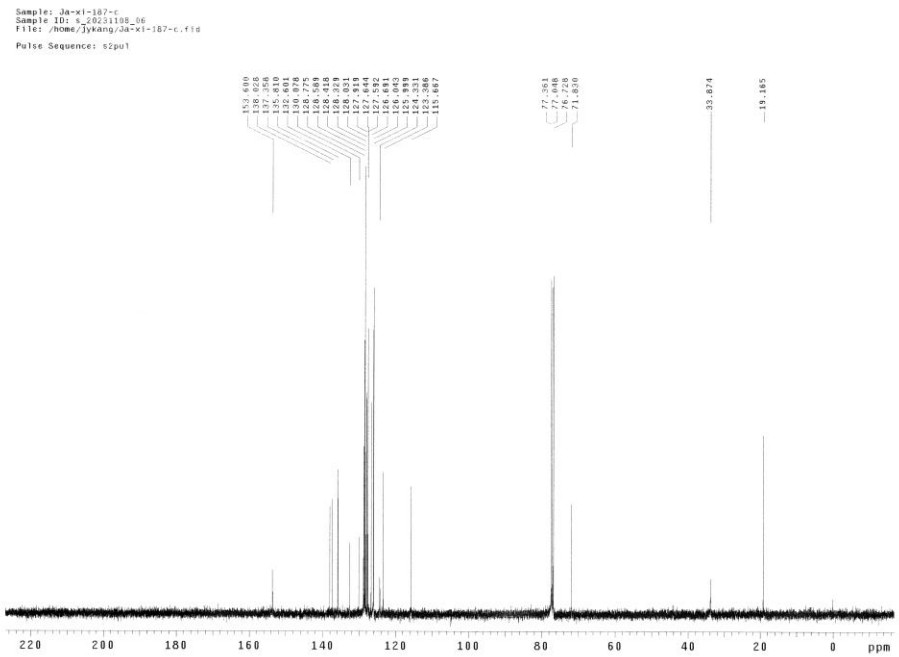

^{1}H NMR (400 MHz) in $CDCl_3$

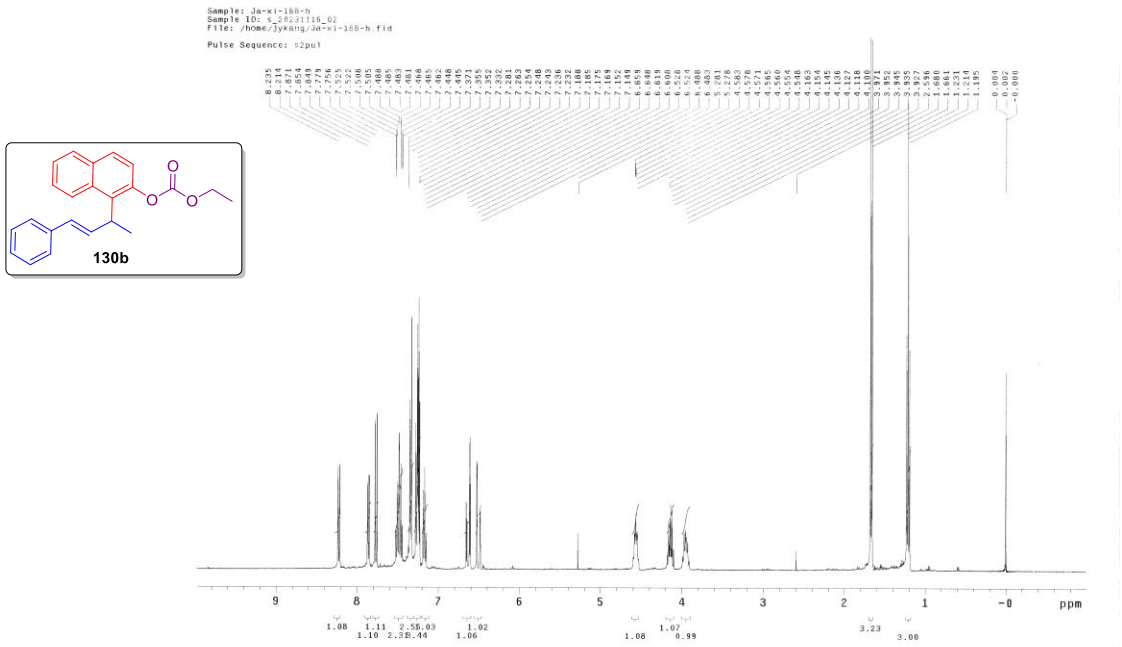

^{13}C NMR (100.5 MHz) in $CDCl_3$

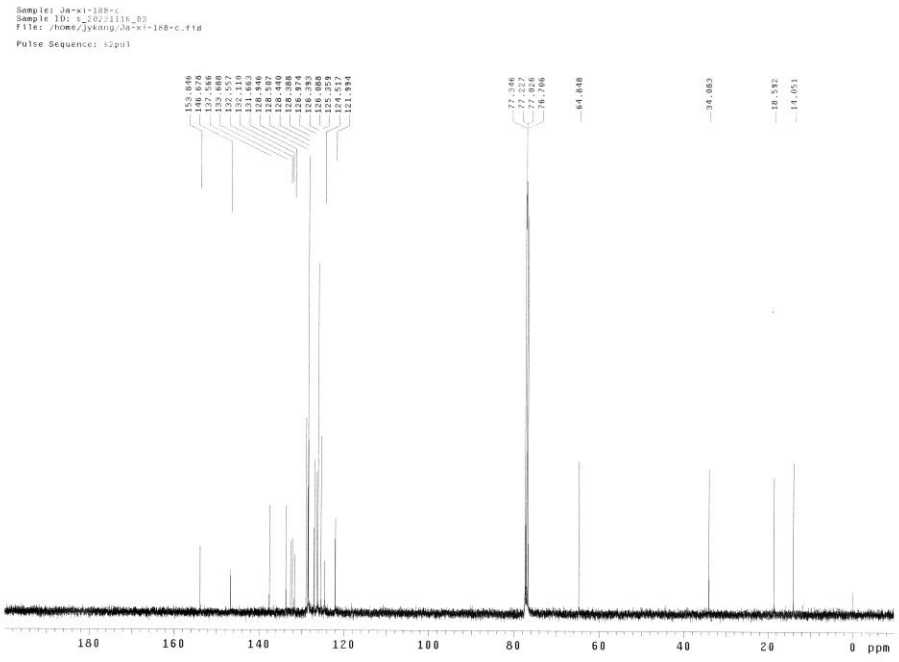

^{1}H NMR (400 MHz) in $CDCl_3$

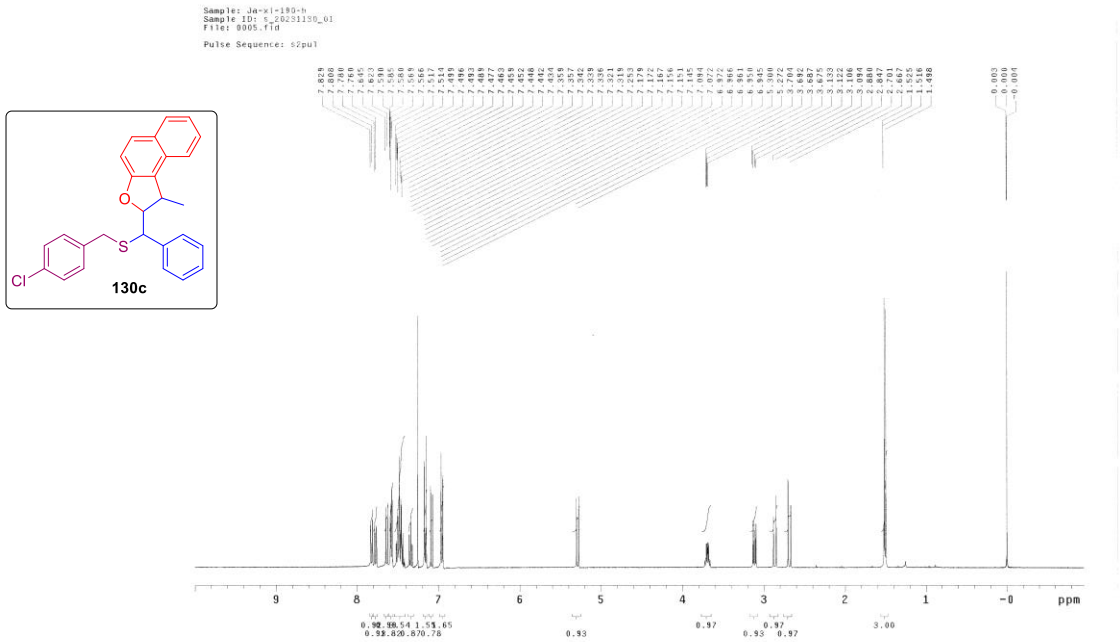

^{13}C NMR (100.5 MHz) in $CDCl_3$

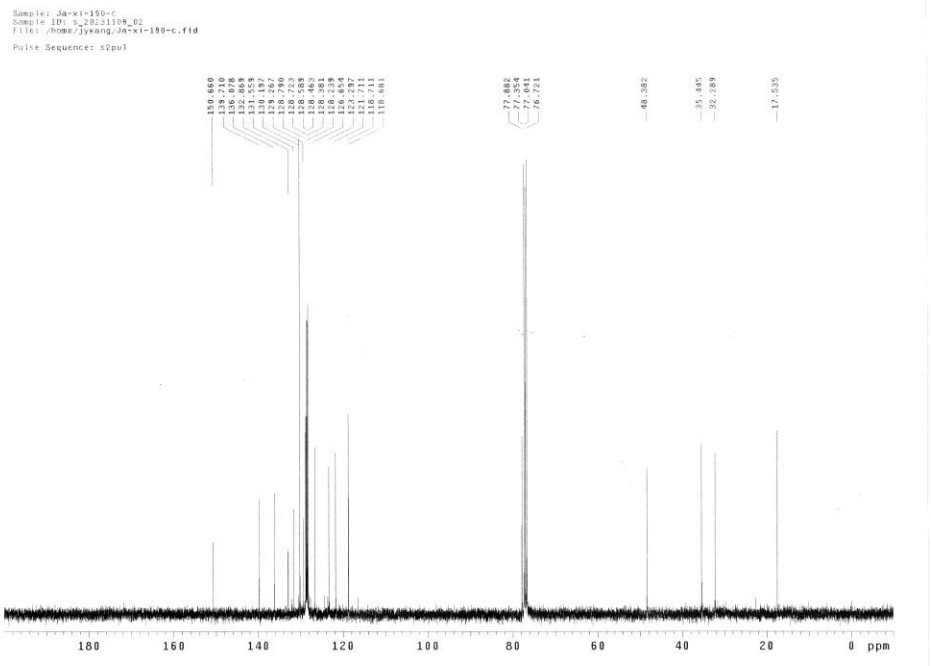

^{1}H NMR (400 MHz) in $CDCl_3$

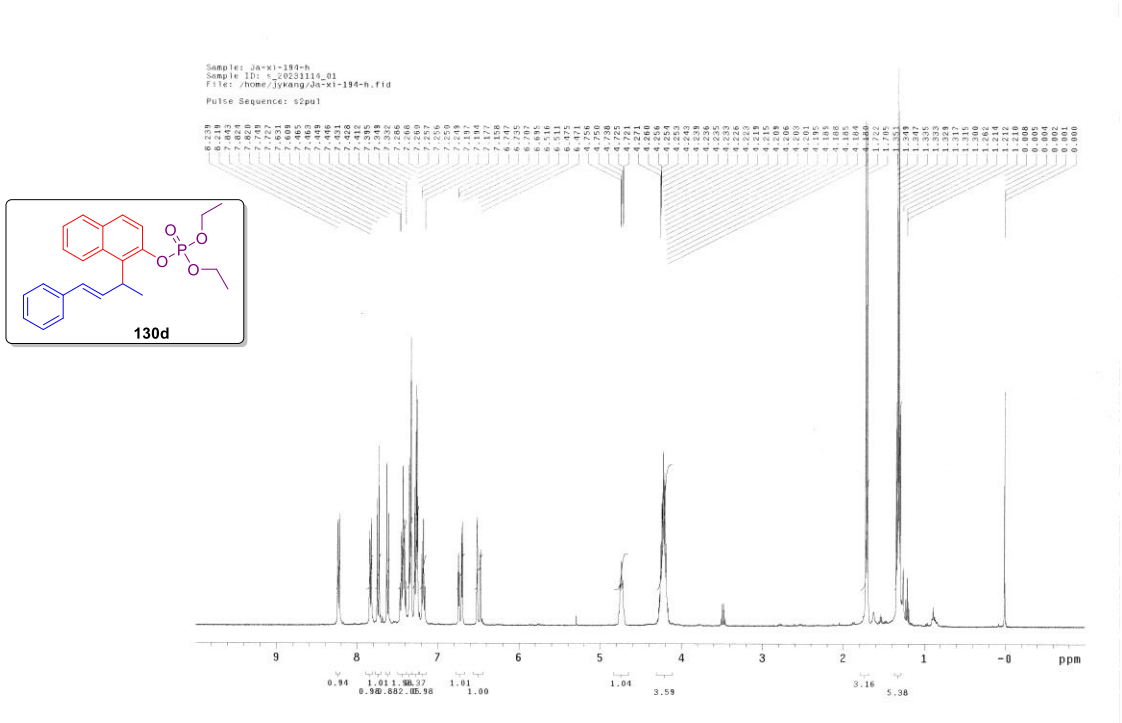

^{13}C NMR (100.5 MHz) in $CDCl_3$

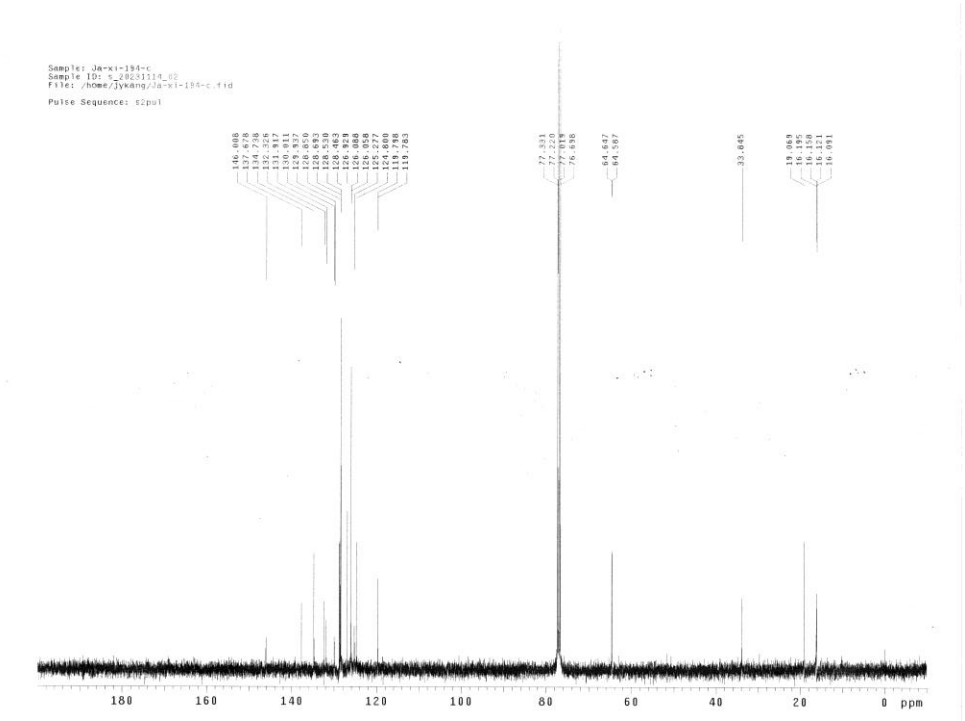

^{31}P NMR (162 MHz) in $CDCl_3$

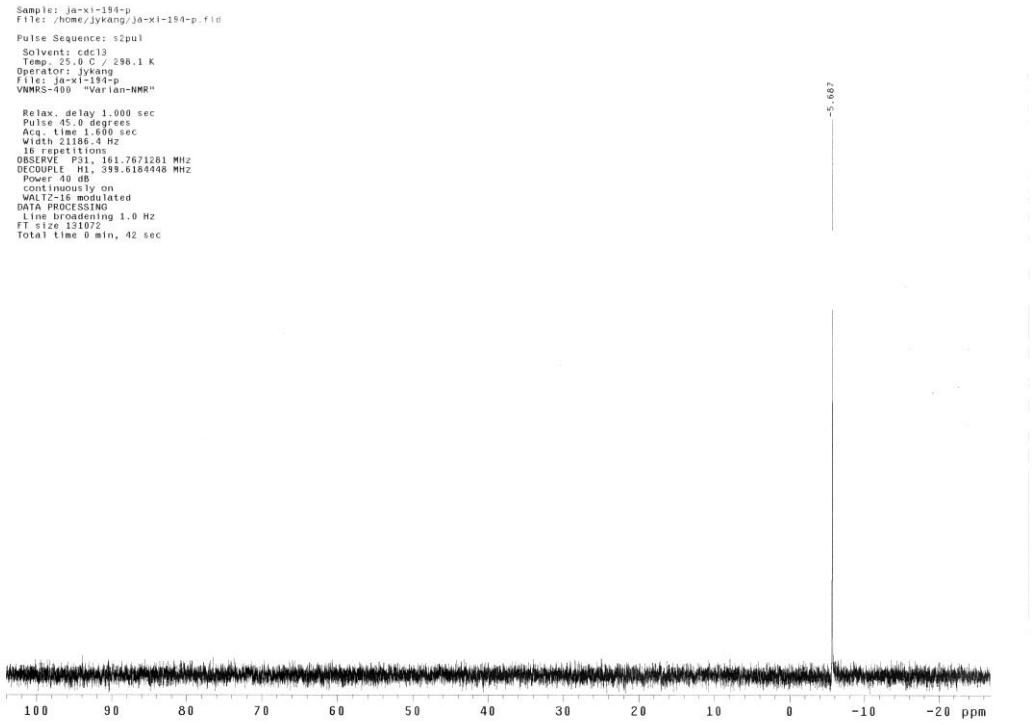

References

1. Knouse, K. W.; Flood, D. T.; Vantourout, J. C., et al. *ACS Cent. Sci.* **2021,** *7* (9), 1473-1485.

2. Columbus, I.; Ghindes-Azaria, L.; Chen, R., et al. *J. Med. Chem.* **2022,** *65* (12), 8511-8524.

3. Gamoke, B.; Neff, D.; Simons, J. *J. Phys. Chem. A* **2009,** *113* (19), 5677-5684.

4. Huang, H.; Kang, J. Y. *Synthesis* **2022,** *54* (05), 1157-1202.

5. Howell, B. A. *Polymers* **2022,** *14* (22), 4929.

6. Horsman, G. P.; Zechel, D. L. *Chem. Rev.* **2017,** *117* (8), 5704-5783.

7. Pradere, U.; Garnier-Amblard, E. C.; Coats, S. J., et al. *Chem. Rev.* **2014,** *114* (18), 9154-9218.

8. Siegel, D.; Hui, H. C.; Doerffler, E., et al. *J. Med. Chem.* **2017,** *60* (5), 1648-1661.

9. Farizatto, K. L. G.; Bahr, B. A. *Eur. Sci. J.* **2017,** *13*, 29-37.

10. Emadi, A.; Jones, R. J.; Brodsky, R. A. *Nat. Rev. Clin. Oncol* **2009,** *6* (11), 638-647.

11. Foust, B. J.; Poe, M. M.; Lentini, N. A., et al. *ACS Med. Chem. Lett.* **2017,** *8* (9), 914-918.

12. Kenny, N. P.; Rajendran, K. V.; Gilheany, D. G. *Chem. Commun.* **2015,** *51* (92), 16561-16564.

13. Mai, S.; Li, W.; Li, X., et al. *Nat. Commun* **2019,** *10* (1), 5709.

14. Li, C.; Chang, X.-Y.; Huo, L., et al. *ACS Catal.* **2021,** *11* (14), 8716-8726.

15. Atherton, F. R.; Openshaw, H. T.; Todd, A. R. *J. Chem. Soc.* **1945,** (0), 660-663.

16. Vincze, D.; Ábrányi-Balogh, P.; Bagi, P., et al. *Molecules* **2019,** *24* (21), 3859.

17. Steinberg, G. M. *J. Org. Chem.* **1950,** *15* (3), 637-647.

18. Ou, Y.; Huang, Y.; He, Z., et al. *Chem. Commun.* **2020,** *56* (9), 1357-1360.

19. Chen, Q.; Zeng, J.; Yan, X., et al. *J. Org. Chem.* **2016,** *81* (20), 10043-10048.

20. Dhineshkumar, J.; Prabhu, K. R. *Org. Lett.* **2013,** *15* (23), 6062-6065.

21. Deng, L.; Wang, Y.; Mei, H., et al. *J. Org. Chem.* **2019,** *84* (2), 949-956.

22. Quint, V.; Morlet-Savary, F.; Lohier, J.-F., et al. *J. Am. Chem. Soc.* **2016,** *138* (23), 7436-7441.

23. Hemelsoet, K.; Van Durme, F.; Van Speybroeck, V., et al. *J. Phys. Chem. A* **2010,** *114* (8), 2864-2873.

24. Tsubaki, K.; Shimooka, H.; Kitamura, M., et al. *Org. Lett.* **2019,** *21* (23), 9779-9783.

25. Fañanás-Mastral, M.; Feringa, B. L. *J. Am. Chem. Soc.* **2014,** *136* (28), 9894-9897.

26. Huang, H.; Denne, J.; Yang, C.-H., et al. *Angew. Chem. Int. Ed.* **2018,** *57* (22), 6624-6628.

27. Ash, J.; Huang, H.; Kang, J. Y. *Org. Biomol. Chem.* **2019,** *17*.

28. Huang, H.; Ash, J.; Kang, J. Y. *Org. Lett.* **2018,** *20* (16), 4938-4941.

29. Demkowicz, S.; Rachon, J.; Daśko, M., et al. *RSC Adv.* **2016,** *6* (9), 7101-7112.

30. Hyde, E. G.; Carmichael, W. W. *J. Biochem. Toxicol.* **1991,** *6* (3), 195-201.

31. Schwartz, D.; Berger, S.; Heinzelmann, E., et al. *Appl. Environ. Microbiol.* **2004,** *70* (12), 7093-7102.

32. Stowell, M. H. B.; Witte, J. F.; McClard, R. W. *Tetrahedron Lett.* **1989,** *30* (4), 411-414.

33. Parmar, D.; Sugiono, E.; Raja, S., et al. *Chem. Rev.* **2014,** *114* (18), 9047-9153.

34. Zamfir, A.; Schenker, S.; Freund, M., et al. *Org. Biomol. Chem.* **2010,** *8* (23), 5262-5276.

35. Breshears, A. T.; Brown, M. A.; Bloom, I., et al. *Inorg. Chim. Acta* **2018,** *473*, 102-111.

36. Zhang, Y.; Zhang, X.; Zhao, J., et al. *Org. Biomol. Chem.* **2021,** *19* (26), 5772-5776.

37. Gobec, S.; Plantan, I.; Mravljak, J., et al. *Bioorg. Med. Chem. Lett.* **2004,** *14* (13), 3559-3562.

38. Flynn, R. M.; Burton, D. J. *J. Fluorine Chem.* **2011,** *132* (10), 815-828.

39. Li, C.; Saga, Y.; Onozawa, S.-y., et al. *J. Org. Chem.* **2020,** *85*, 14411-14419.

40. Secco, E. A. *J. phys. Chem. Solids* **1963,** *24* (3), 469-473.

41. Ash, J.; Huang, H.; Cordero, P., et al. *Org. Biomol. Chem.* **2021,** *19* (27), 6007-6014.

42. Hudson, R. F.; Harper, D. C. *J. Chem. Soc.* **1958,** (0), 1356-1360.

43. Gobec, S.; Plantan, I.; Mravljak, J., et al. *Eur. J. Med. Chem.* **2007,** *42* (1), 54-63.

44. Babouri, R.; Traore, L.; Bekro, Y.-A., et al. *Org. Lett.* **2019,** *21* (1), 45-49.

45. Saunders, B. C.; Stacey, G. J. *J. Chem. Soc.* **1948,** (0), 695-699.

46. Sporn, M. B.; Berkowitz, D. M.; Glinski, R. P., et al. *Science* **1969,** *164* (3886), 1408-1410.

47. Duprat, M.; Bonnel, A.; Dabosi, F., et al. *J. Appl. Electrochem.* **1983,** *13* (3), 317-323.

48. Liu, Y.; Patricelli, M. P.; Cravatt, B. F. *Proc. Natl. Acad. Sci.* **1999,** *96* (26), 14694.

49. Abu-Qare, A. W.; Abou-Donia, M. B. *Food Chem. Toxicol.* **2002,** *40* (10), 1327-1333.

50. Hoover, H. S.; Blankman, J. L.; Niessen, S., et al. *Bioorganic & Medicinal Chemistry Letters* **2008,** *18* (22), 5838-5841.

51. Gupta, A. K.; Acharya, J.; Pardasani, D., et al. *Tetrahedron Lett.* **2008,** *49* (14), 2232-2235.

52. Purohit, A. K.; Pardasani, D.; Kumar, A., et al. *Tetrahedron Lett.* **2015,** *56* (31), 4593-4595.

53. Bornemann, D.; Brüning, F.; Bartalucci, N., et al. *Helv. Chim. Acta* **2021,** *104* (2), e2000218.

54. Aldersley, M. F.; Joshi, P. C.; Schwartz, H. M., et al. *Tetrahedron Lett.* **2014,** *55* (8), 1464-1466.

55. Liu, N.; Mao, L.-L.; Yang, B., et al. *Chem. Commun.* **2014,** *50* (74), 10879-10882.

56. Dąbkowski, W.; Cramer, F.; Michalski, J. *J. Chem. Soc., Perkin Trans. 1* **1992,** (11), 1447-1452.

57. Konieczko, W. T.; Łopusiński, A.; Michalski, J. *Phosphorus Sulfur Silicon Relat. Elem.* **1989,** *42* (1-2), 103-104.

58. L. N. MARKOVSKIJ* , V. E. P., A. V. KIRSANOV *Synthesis* **1973,** *12*, 787-789.

59. Lermontov, S. A.; Popov, A. V.; Zavorin, S. I., et al. *J. Fluorine Chem.* **1994,** *66* (3), 233-235.

60. Zhao, S.; Guo, Y.; Su, Z., et al. *Chin. J. Chem.* **2021,** *39* (5), 1225-1232.

61. *Justus Liebigs Ann. Chem.* **1848,** *64* (3), 339-341.

62. W. H. Sharkey, C. M. L. *Org. Synth.* **1961,** *41* (24).

63. Simons, J. H.; Harland, W. J. *J. Electrochem. Soc.* **1949,** *95* (2), 55.

64. Glüge, J.; Scheringer, M.; Cousins, I. T., et al. *Environ. Sci.: Process. Impacts* **2020,** *22* (12), 2345-2373.

65. Baizer, M. M. *J. Electrochem. Soc.* **1964,** *111* (2), 215.

66. Betke, T.; Maier, M.; Gruber-Wölfler, H., et al. *Nat Commun* **2018,** *9* (1), 5112.

67. Jones, A. M.; Banks, C. E. *Beilstein J. Org. Chem.* **2014,** *10*, 3056-3072.

68. Shono, T.; Hamaguchi, H.; Matsumura, Y. *J. Am. Chem. Soc.* **1975,** *97* (15), 4264-4268.

69. Wang, Y.; Qian, P.; Su, J.-H., et al. *Green Chem.* **2017,** *19* (20), 4769-4773.

70. Huang, M.; Dai, J.; Cheng, X., et al. *Org. Lett.* **2019,** *21* (19), 7759-7762.

71. Li, C.-Y.; Liu, Y.-C.; Li, Y.-X., et al. *Org. Lett.* **2019,** *21* (19), 7833-7836.

72. Li, Q.-Y.; Swaroop, T. R.; Hou, C., et al. *Adv. Synth. Catal.* **2019,** *361* (8), 1761-1765.

73. Wang, S.; Yang, C.; Sun, S., et al. *Chem. Commun.* **2019,** *55* (93), 14035-14038.

74. Amri, N.; Wirth, T. *Synlett* **2020,** *31* (19), 1894-1898.

75. Dong, X.; Wang, R.; Jin, W., et al. *Org. Lett.* **2020,** *22* (8), 3062-3066.

76. Xu, Z.; Li, Y.; Mo, G., et al. *Org. Lett.* **2020,** *22* (10), 4016-4020.

77. Li, C.-Y.; Liu, Y.-C.; Li, Y.-X., et al. *Org. Lett.* **2019,** *21* (19), 7833-7836.

78. Wynn, D. A.; Roth, M. M.; Pollard, B. D. *Talanta* **1984,** *31* (11), 1036-1040.

79. Bickelhaupt, F. M.; Solà, M.; Guerra, C. F. *J. Comput. Chem.* **2007,** *28* (1), 238-250.

80. Evans, F. W.; Litt, M. H.; Weidler-Kubanek, A. M., et al. *J. Org. Chem.* **1968,** *33* (5), 1837-1839.

81. Fuchigami, T.; Inagi, S. *Acc. Chem. Res.* **2020,** *53* (2), 322-334.

82. Kang, L.-S.; Luo, M.-H.; Lam, C. M., et al. *Green Chem.* **2016,** *18* (13), 3767-3774.

83. Allen J. Bard, L. R. F., *Electrochemical Methods: Fundamentals and Applications*. Wiley: Hoboken, New Jersey, 2000.

84. Liu, N.; Mao, L.-L.; Yang, B., et al. *Chem. Commun.* **2014,** *50* (74), 10879-10882.

85. Li, Q.-W.; Zhang, X.-Y.; Lu, L., et al. *Adv. Synth. Catal.* **2022,** *364* (5), 938-946.

86. Huang, Y.; Tang, J.; Zhao, X., et al. *Green Chem.* **2023,** *25* (11), 4528-4535.

87. Gabelt, B. A. T.; Hennes, E. A.; Seeman, J. L., et al. *Invest. Ophthalmol. Visual Sci.* **2004,** *45* (8), 2732-2736.

88. Kouvaris, J. R.; Kouloulias, V. E.; Vlahos, L. J. *The Oncologist* **2007,** *12* (6), 738-747.

89. Song, S.; Zhang, Y.; Yeerlan, A., et al. *Angew. Chem. Int. Ed.* **2017,** *56* (9), 2487-2491.

90. Kraus, C. L.; Trivedi, R. H.; Wilson, M. E. *J. AAPOS* **2015,** *19* (2), 116-118.e1.

91. Mitra, S.; Mukherjee, S.; Sen, S. K., et al. *Bioorg. Med. Chem. Lett.* **2014,** *24* (9), 2198-2201.

92. Fan, Y.; Lai, K.; Rasco, B. A., et al. *Food Control* **2014,** *37*, 153-157.

93. Wang, C.; Zhang, L.; Mou, Z., et al. *Org. Lett.* **2021,** *23* (11), 4261-4266.

94. Bi, X.; Li, J.; Meng, F., et al. *Tetrahedron* **2016,** *72* (5), 706-711.

95. Chen, X.-Y.; Pu, M.; Cheng, H.-G., et al. *Angew. Chem. Int. Ed.* **2019,** *58* (33), 11395-11399.

96. Huang, H.; Ash, J.; Kang, J. Y. *Org. Biomol. Chem.* **2018,** *16* (23), 4236-4242.

97. Kaboudin, B.; Abedi, Y.; Kato, J.-y., et al. *Synthesis* **2013,** *45* (16), 2323-2327.

98. Liu, T.; Zhang, Y.; Yu, R., et al. *Synthesis* **2020,** *52* (02), 253-262.

99. Liu, Y.-C.; Lee, C.-F. *Green Chem.* **2014,** *16* (1), 357-364.

100. Wen, C.; Chen, Q.; Huang, Y., et al. *RSC Adv.* **2017,** *7* (72), 45416-45419.

101. Xu, J.; Zhang, L.; Li, X., et al. *Org. Lett.* **2016,** *18* (6), 1266-1269.

102. Xue, J.-W.; Zeng, M.; Zhang, S., et al. *J. Org. Chem.* **2019,** *84* (7), 4179-4190.

103. Zhang, L.; Zhang, P.; Li, X., et al. *J. Org. Chem.* **2016,** *81* (13), 5588-5594.

104. Zhang, P.; Yu, G.; Li, W., et al. *Org. Lett.* **2021,** *23* (15), 5848-5852.

105. Zhang, X.; Wang, D.; An, D., et al. *J. Org. Chem.* **2018,** *83* (3), 1532-1537.

106. Zhu, Y.; Chen, T.; Li, S., et al. *J. Am. Chem. Soc.* **2016,** *138* (18), 5825-5828.

107. Choudhary, R.; Singh, P.; Bai, R., et al. *Org. Biomol. Chem.* **2019,** *17* (45), 9757-9765.

108. Gong, X.; Chen, J.; Liu, J., et al. *Org. Chem. Front.* **2017,** *4* (11), 2221-2225.

109. Guo, Y.; Luo, Y.; Mu, S., et al. *Org. Lett.* **2021**.

110. Desforges, E.; Grysan, A.; Oget, N., et al. *Tetrahedron Lett.* **2003,** *44* (33), 6273-6276.

111. Han, X.; Wu, J. *Org. Lett.* **2010,** *12* (24), 5780-5782.

112. Zhang, Y.; Du, S.; Yang, T., et al. *Org. Chem. Front.* **2022,** *9* (12), 3156-3162.

113. Song, X.-R.; Yang, T.; Ding, H., et al. *Synthesis* **2020,** *52* (02), 208-218.

114. Bai, W.-J.; David, J. G.; Feng, Z.-G., et al. *Acc. Chem. Res.* **2014,** *47* (12), 3655-3664.

115. Jones, R. M.; Van De Water, R. W.; Lindsey, C. C., et al. *J. Org. Chem.* **2001,** *66* (10), 3435-3441.

116. Van De Water, R. W.; Pettus, T. R. R. *Tetrahedron* **2002,** *58* (27), 5367-5405.

117. Singh, M. S.; Nagaraju, A.; Anand, N., et al. *RSC Adv.* **2014,** *4* (99), 55924-55959.

118. Liao, D.; Li, H.; Lei, X. *Org. Lett.* **2012,** *14* (1), 18-21.

119. Batsomboon, P.; Phakhodee, W.; Ruchirawat, S., et al. *J. Org. Chem.* **2009,** *74* (10), 4009-4012.

120. Nachtsheim, B. J. *Nat. Chem.* **2020,** *12* (4), 326-328.

121. Sugimoto, H.; Nakamura, S.; Ohwada, T. *Adv. Synth. Catal.* **2007,** *349* (4-5), 669-679.

122. Chen, Z.; Shi, Q.; Wang, G., et al. *Molecules* **2018,** *23* (6), 1240.

123. Zhang, B.; Liu, L.; Mao, S., et al. *Chem. Eur. J.* **2019,** *2019* (24), 3898-3907.

124. Yuan, H.; Kowah, J. A. H.; Jiang, J. *Tetrahedron Lett.* **2020,** *61* (15), 151748.

125. Aher, Y. N.; Pawar, A. B. *Org. Biomol. Chem.* **2019,** *17* (32), 7536-7546.

126. Arde, P.; Vijaya Anand, R. *Org. Biomol. Chem.* **2016,** *14* (24), 5550-5554.

127. Xiong, B.; Wang, G.; Zhou, C., et al. *Eur. J. Org. Chem.* **2019,** *2019* (20), 3273-3282.

128. Yang, B.; Yao, W.; Xia, X.-F., et al. *Org. Biomol. Chem.* **2018,** *16* (24), 4547-4557.

129. Huang, H.; Kang, J. Y. *Org. Lett.* **2017,** *19* (21), 5988-5991.

130. Lee, M. H.; Yang, Z.; Lim, C. W., et al. *Chem. Rev.* **2013,** *113* (7), 5071-5109.

131. Stephenson, T.; Li, Z.; Olsen, B., et al. *Energy Environ. Sci.* **2014,** *7* (1), 209-231.

132. Betz, S. F. *Protein Sci.* **1993,** *2* (10), 1551-1558.

133. Wright, C.; Moore, R. D. *Am. J. Med.* **1990,** *88* (6), 647-655.

134. Vogt, A.; Tamura, K.; Watson, S., et al. *J. Pharmacol. Exp. Ther.* **2000,** *294* (3), 1070.

135. Wang, J.-G.; Xiao, Y.-J.; Li, Y.-H., et al. *Bioorg. Med. Chem.* **2007,** *15* (1), 374-380.

136. Wang, L.; Bao, B.-B.; Song, G.-Q., et al. *Eur. J. Med. Chem.* **2017,** *137*, 450-461.

137. Block, E.; Ahmad, S.; Catalfamo, J. L., et al. *J. Am. Chem. Soc.* **1986,** *108* (22), 7045-7055.

138. Kaewsakul, W.; Sahakaro, K.; Dierkes, W. K., et al. *Polym Eng Sci.* **2015,** *55* (4), 836-842.

139. Iranpoor, N.; Zeynizadeh, B. *Synthesis* **1999,** *1999* (01), 49-50.

140. Chauhan, S. M. S.; Kumar, A.; Srinivas, K. A. *Chem. Commun.* **2003,** (18), 2348-2349.

141. Huang, H.; Ash, J.; Kang, J. Y. *Organic & Biomolecular Chemistry* **2018,** *16* (23), 4236-4242.

142. Korn, T. J.; Knochel, P. *Synlett* **2005,** *2005* (07), 1185-1187.

143. Karimi, B.; Hazarkhani, H.; Zareyee, D. *Synthesis* **2002,** *2002* (17), 2513-2516.

144. Priefer, R.; Lee, Y. J.; Barrios, F., et al. *J. Am. Chem. Soc.* **2002,** *124* (20), 5626-5627.

145. *Antioxid. Redox Signal.* **2013,** *18* (13), 1623-1641.

146. Wallace, T. J.; Schriesheim, A.; Bartok, W. *J. Org. Chem.* **1963,** *28* (5), 1311-1314.

147. Huang, P.; Wang, P.; Tang, S., et al. *Angew. Chem. Int. Ed.* **2018,** *57* (27), 8115-8119.

148. Arisawa, M.; Yamaguchi, M. *J. Am. Chem. Soc.* **2003,** *125* (22), 6624-6625.

149. Guo, J.; Zha, J.; Zhang, T., et al. *Org. Lett.* **2021,** *23* (8), 3167-3172.

150. Song, M.; Hu, Q.; Li, Z.-Y., et al. *Chin. Chem. Lett.* **2022,** *33* (9), 4269-4272.

151. N. Harpp, D.; G. Back, T. *Tetrahedron Lett.* **1972,** *13* (15), 1481-1484.

152. Barton, D. H. R.; Chen, C.; Michael Wall, G. *Tetrahedron* **1991,** *47* (32), 6127-6138.

153. Brzezinska, E.; Ternay, A. L., Jr. *J. Org. Chem.* **1994,** *59* (26), 8239-8244.

154. Hiver, P.; Dicko, A.; Paquer, D. *Tetrahedron Lett.* **1994,** *35* (51), 9569-9572.

155. Uragami, M.; Miyake, Y.; Tokutake, N., et al. *Langmuir* **2000,** *16* (21), 8010-8015.

156. Hunter, R.; Caira, M.; Stellenboom, N. *J. Org. Chem.* **2006,** *71* (21), 8268-8271.

157. Antoniow, S.; Witt, D. *Synthesis* **2007,** *2007* (03), 363-366.

158. Delarue Bizzini, L.; Zwick, P.; Mayor, M. *Eur. J. Org. Chem.* **2019,** *2019* (41), 6956-6960.

159. Bao, M.; Shimizu, M. *Tetrahedron* **2003,** *59* (48), 9655-9659.

160. Xiao, X.; Feng, M.; Jiang, X. *Angew. Chem. Int. Ed.* **2016,** *55* (45), 14121-14125.

161. Dai, Z.; Xiao, X.; Jiang, X. *Tetrahedron* **2017,** *73* (26), 3702-3706.

162. Xiao, X.; Xue, J.; Jiang, X. *Nat. Commun.* **2018,** *9* (1), 2191.

163. Xue, J.; Jiang, X. *Nat. Commun.* **2020,** *11* (1), 4170.

164. Chen, S.; Cao, S.; Liu, C., et al. *Org. Lett.* **2021,** *23* (19), 7428-7433.

165. Wu, S.; Hu, D.; Wan, X., et al. *J. Org. Chem.* **2022,** *87* (24), 16297-16306.

166. Yang, F.; Wang, W.; Li, K., et al. *Tetrahedron Lett.* **2017,** *58* (3), 218-222.

167. Dong, B.; Chen, Y.; Xie, S., et al. *Org. Biomol. Chem.* **2023,** *21* (5), 930-934.

168. Yang, F.; Wang, W.; Li, K., et al. *Tetrahedron Letters* **2017,** *58* (3), 218-222.

169. Zhang, Z.; Lao, T.; Deng, L., et al. *Org. Lett.* **2022,** *24* (39), 7222-7226.

170. Ash, J.; Kang, J. Y. *Org. Biomol. Chem.* **2023,** *21* (11), 2370-2374.

171. González-Pelayo, S.; López, L. A. *Eur. J. Org. Chem.* **2017,** *2017* (40), 6003-6007.

172. Toteva, M. M.; Richard, J. P., The generation and reactions of quinone methides. In *Adv. Phys. Org. Chem.* , Richard, J. P., Ed. Academic Press: 2011; Vol. 45, pp 39-91.

173. Mayer, R. J.; Breugst, M.; Hampel, N., et al. *J. Org. Chem.* **2019,** *84* (14), 8837-8858.

174. Jüstel, P. M.; Pignot, C. D.; Ofial, A. R. *J. Org. Chem.* **2021,** *86* (8), 5965-5972.

175. Lin, Y.; Tanaka, S. *Appl. Microbiol. Biotechnol.* **2006,** *69* (6), 627-642.

176. Anastas, P.; Eghbali, N. *Chem. Soc. Rev.* **2010,** *39* (1), 301-312.

177. Ida, T.; Sawa, T.; Ihara, H., et al. *Proc. Natl. Acad. Sci.* **2014,** *111* (21), 7606-7611.

178. *Antioxid. Redox Signal.* **2014,** *20* (5), 783-793.

179. Barr, L. A.; Calvert, J. W. *Circulation* **2014,** *78* (9), 2111-2118.

180. Kolluru, G. K.; Shen, X.; Bir, S. C., et al. *Nitric Oxide* **2013,** *35*, 5-20.

181. Sawa, T.; Motohashi, H.; Ihara, H., et al. *Biomolecules* **2020,** *10* (9), 1245.

182. Zivanovic, J.; Kouroussis, E.; Kohl, J. B., et al. *Cell Metab.* **2020,** *31* (1), 207.

183. Cuevasanta, E.; Möller, M. N.; Alvarez, B. *Arch. Biochem. Biophys.* **2017,** *617*, 9-25.

184. Chauvin, J.-P. R.; Griesser, M.; Pratt, D. A. *J. Am. Chem. Soc.* **2017,** *139* (18), 6484-6493.

185. Cuevasanta, E.; Lange, M.; Bonanata, J., et al. *J. Biol. Chem.* **2015,** *290* (45), 26866-26880.

186. Hansen, T.; Vermeeren, P.; Bickelhaupt, F. M., et al. *Angew. Chem. Int. Ed.* **2021,** *60* (38), 20840-20848.

187. Kawamura, S.; Otsuji, Y.; Nakabayashi, T., et al. *J. Org. Chem.* **1965,** *30* (8), 2711-2714.

188. Tsurugi, J.; Nakabayashi, T.; Ishihara, T. *J. Org. Chem.* **1965,** *30* (8), 2707-2710.

189. Nakabayashi, T.; Tsurugi, J. *J. Org. Chem.* **1963,** *28* (3), 813-816.

190. Bailey, T. S.; Zakharov, L. N.; Pluth, M. D. *J. Am. Chem. Soc.* **2014,** *136* (30), 10573-10576.

191. Bailey, T. S.; Pluth, M. D. *Free Radic. Biol. Med.* **2015,** *89*, 662-667.

192. Wood, J. L., Sulfane sulfur. In *Methods in Enzymology*, Academic Press: 1987; Vol. 143, pp 25-29.

193. Chatterji, T.; Keerthi, K.; Gates, K. S. *Bioorg. Med. Chem. Lett.* **2005,** *15* (17), 3921-3924.

194. Bailey, T. S.; Pluth, M. D. *Free Radic. Biol. Med.* **2015,** *89*, 662-667.

195. Sen, N.; Paul, Bindu D.; Gadalla, Moataz M., et al. *Mol. Cell.* **2012,** *45* (1), 13-24.

196. Yamamoto, A. *J. Atheroscler. Thromb.* **2008,** *15* (6), 304-305.

197. Knutsen, L. J. S.; Lau, J.; Petersen, H., et al. *J. Med. Chem.* **1999,** *42* (18), 3463-3477.

198. Somogyi, A.; Gugler, R. *Clin. Pharmacokinet.* **1983,** *8* (6), 463-495.

199. Levine, R. L.; Moskovitz, J.; Stadtman, E. R. *IUBMB Life* **2000,** *50* (4-5), 301-307.

200. van der Vlies, A. J.; Xu, J.; Ghasemi, M., et al. *Biomacromolecules* **2022,** *23* (1), 77-88.

201. De Clercq, P. J. *Chem. Rev.* **1997,** *97* (6), 1755-1792.

202. Wei, Y.-F.; Gao, W.-C.; Chang, H.-H., et al. *Org. Chem. Front.* **2022,** *9* (23), 6684-6707.

203. Chen, H.; Jiang, W.; Zeng, Q. *Chem. Rec.* **2020,** *20* (11), 1269-1296.

204. Clayden, J.; MacLellan, P. *Beilstein J. Org. Chem.* **2011,** *7*, 582-595.

205. Jüstel, P. M.; Pignot, C. D.; Ofial, A. R. *J. Org. Chem.* **2021,** *86* (8), 5965-5972.

206. Brotzel, F.; Mayr, H. *Org. Biomol. Chem.* **2007,** *5* (23), 3814-3820.

207. Emori, E.; Iida, T.; Shibasaki, M. *J. Org. Chem.* **1999,** *64* (14), 5318-5320.

208. Lu, H.-H.; Zhang, F.-G.; Meng, X.-G., et al. *Org. Lett.* **2009,** *11* (17), 3946-3949.

209. Wang, H.-Y.; Zhang, J.-X.; Cao, D.-D., et al. *ACS Catal.* **2013,** *3* (10), 2218-2221.

210. Rana, N. K.; Selvakumar, S.; Singh, V. K. *J. Org. Chem.* **2010,** *75* (6), 2089-2091.

211. Weaver, J. D.; Morris, D. K.; Tunge, J. A. *Synlett* **2010,** *2010* (03), 470-474.

212. Oyo, M.; Masaaki, Y. *Bull. Chem. Soc. Jpn.* **1967,** *40* (10), 2380-2382.

213. Mondal, J.; Modak, A.; Dutta, A., et al. *Chem. Commun.* **2012,** *48* (64), 8000-8002.

214. Li, X.; Liu, C.; Xue, X.-S., et al. *Org. Lett.* **2012,** *14* (17), 4374-4377.

215. Sobhani, S.; Fielenbach, D.; Marigo, M., et al. *Chem. Eur. J.* **2005,** *11* (19), 5689-5694.

216. Wang, J.-J.; Yang, H.; Gou, B.-B., et al. *J. Org. Chem.* **2018,** *83* (8), 4730-4738.

217. Nagao, Y.; Miyamoto, S.; Miyamoto, M., et al. *J. Am. Chem. Soc.* **2006,** *128* (30), 9722-9729.

218. MacLellan, P.; Clayden, J. *Chem. Commun.* **2011,** *47* (12), 3395-3397.

219. Subramanian, H.; Moorthy, R.; Sibi, M. P. *Angew. Chem. Int. Ed.* **2014,** *53* (50), 13660-13662.

220. Bolton, S. G.; Cerda, M. M.; Gilbert, A. K., et al. *Free Radic. Biol. Med.* **2019,** *131*, 393-398.

221. Li, L.; Wang, H.; Huang, D., et al. *Tetrahedron* **2012,** *68* (47), 9853-9859.

222. Gant Kanegusuku, A. L.; Roizen, J. L. *Angew. Chem. Int. Ed.* **2021,** *60* (39), 21116-21149.

223. Micallef, A. S.; Bottle, S. E. *Tetrahedron Lett.* **1997,** *38* (13), 2303-2306.

224. Frederix, P. W. J. M.; Yang, C.-H.; Groenenboom, G. C., et al. *The Journal of Physical Chemistry A* **2009,** *113* (52), 14995-15005.

225. Kim, J.; Kang, B.; Hong, S. H. *ACS Catal.* **2020,** *10* (11), 6013-6022.

226. Tang, Q.; Li, F.; Chen, H., et al. *Asian J. Org. Chem.* **2021,** *10* (7), 1687-1690.

227. Hayashi, M.; Matsuura, T.; Tanaka, I., et al. *Organic Letters* **2013,** *15* (3), 628-631.

228. C. Friedel, J.-M. C. *Compt. Rend.* **1877,** *84*, 1392-1395.

229. Tsuchimoto, T.; Tobita, K.; Hiyama, T., et al. *J. Org. Chem.* **1997,** *62* (20), 6997-7005.

230. March, J., *Advanced organic chemistry: reactions, mechanisms, and structure*. McGraw-Hill New York, 1977.

231. Heravi, M. M.; Zadsirjan, V.; Saedi, P., et al. *RSC Adv.* **2018,** *8* (70), 40061-40163.

232. Yang, M.; Koga, M.; Katoh, T., et al. *Arch. Environ. Contam. Toxicol.* **1999,** *36* (1), 99-108.

233. Zhai, Y.-Q.; Zhang, S.-Z.; Xie, J.-W., et al. *Anal. Chim. Acta* **2003,** *494* (1), 71-80.

234. Angiolillo, D. J.; Weisman, S. M. *Am. J. Cardiovasc. Drugs.* **2017,** *17* (2), 97-107.

235. Kikuchi, T.; Gontani, S.; Miyanaga, K., et al. *Acta Cryst. E.* **2019,** *75* (2), 242-245.

236. Terada, M. *Chem. Commun.* **2008,** (35), 4097-4112.

237. Rueping, M.; Uria, U.; Lin, M.-Y., et al. *J. Am. Chem. Soc.* **2011,** *133* (11), 3732-3735.

238. Brunel, J. M. *Chem. Rev.* **2005,** *105* (3), 857-898.

239. Ma, Q.; Zhang, X.; Ji, L., et al. *Polym. Chem.* **2019,** *10* (48), 6662-6668.

240. Zhu, M.; Wang, D.-C.; Xie, M.-S., et al. *Chem. Eur. J.* **2018,** *24* (58), 15512-15516.

241. Kaya, U.; Chauhan, P.; Mahajan, S., et al. *Angew. Chem. Int. Ed.* **2017,** *56* (48), 15358-15362.

242. An, J.; Lombardi, L.; Grilli, S., et al. *Org. Lett.* **2018,** *20* (23), 7380-7383.

243. Jin, M.; Ren, W.; Qian, D.-W., et al. *Org. Lett.* **2018,** *20* (22), 7015-7019.

244. Das, B. G.; Shah, S.; Das, A., et al. *Org. Lett.* **2021,** *23* (16), 6262-6266.

245. Tang, S.-B.; Tu, H.-F.; Zhang, X., et al. *Org. Lett.* **2019,** *21* (15), 6130-6134.

246. Fu, Z.; Zhu, J.; Guo, S., et al. *Chem. Commun.* **2021,** *57* (10), 1262-1265.

247. Wang, D.-C.; Cheng, P.-P.; Yang, T.-T., et al. *Org. Lett.* **2021,** *23* (20), 7865-7872.

248. Ding, L.; Wu, W.-T.; Zhang, L., et al. *Org. Lett.* **2020,** *22* (15), 5861-5865.

249. Wu, S.; Dong, J.; Zhou, D., et al. *J. Org. Chem.* **2020,** *85* (22), 14307-14314.

250. Li, G.-T.; Gu, Q.; You, S.-L. *Chem. Sci.* **2015,** *6* (7), 4273-4278.

251. Li, Z.; Peng, J.; He, C., et al. *Org. Lett.* **2020,** *22* (15), 5768-5772.

252. Liu, L.; Ji, X.; Dong, J., et al. *Org. Lett.* **2016,** *18* (13), 3138-3141.

253. Jacob, A.; Roy, T.; Kaicharla, T., et al. *J. Org. Chem.* **2017,** *82* (20), 11269-11274.

254. Kaicharla, T.; Jacob, A.; Gonnade, R. G., et al. *Chem. Commun.* **2017,** *53* (58), 8219-8222.

255. Zhang, Y.; Li, S.; Zhu, Y., et al. *J. Org. Chem.* **2020,** *85* (10), 6261-6270.

256. He, Z.; Pulis, A. P.; Procter, D. J. *Angew. Chem. Int. Ed.* **2019,** *58* (23), 7813-7817.

257. Qi, L.-W.; Li, S.; Xiang, S.-H., et al. *Nat. Catal.* **2019,** *2* (4), 314-323.

258. Coombs, G.; Sak, M. H.; Miller, S. J. *Angew. Chem. Int. Ed.* **2020,** *59* (7), 2875-2880.

259. Moliterno, M.; Cari, R.; Puglisi, A., et al. *Angew. Chem. Int. Ed.* **2016,** *55* (22), 6525-6529.

260. Narute, S.; Parnes, R.; Toste, F. D., et al. *J. Am. Chem. Soc.* **2016,** *138* (50), 16553-16560.

261. Tian, J.-M.; Wang, A.-F.; Yang, J.-S., et al. *Angew. Chem. Int. Ed.* **2019,** *58* (32), 11023-11027.

262. Paradisi, E.; Righi, P.; Mazzanti, A., et al. *Chem. Commun.* **2012,** *48* (91), 11178-11180.

263. Zhao, Y.-L.; Lou, Q.-X.; Wang, L.-S., et al. *Angew. Chem. Int. Ed.* **2017,** *56* (1), 338-342.

264. Li, C.-Y.; Xiang, M.; Zhang, J., et al. *Org. Biomol. Chem.* **2021,** *19* (35), 7690-7694.

265. Dada, R.; Singh, G.; Pareek, A., et al. *Tetrahedron Lett.* **2016,** *57* (33), 3739-3742.

266. Le Bras, J.; Muzart, J. *Tetrahedron* **2007,** *63* (33), 7942-7948.

267. Sanz, R.; Martínez, A.; Miguel, D., et al. *Adv. Synth. Catal.* **2006,** *348* (14), 1841-1845.

268. Suzuki, N.; Tsuchihashi, S.; Nakata, K. *Tetrahedron Lett.* **2016,** *57* (13), 1456-1459.

269. Yang, G.-P.; Dilixiati, D.; Yang, T., et al. *Appl. Organomet. Chem.* **2018,** *32* (9), e4450.

270. Pradhan, S.; Mishra, M.; De, P. B., et al. *Org. Lett.* **2020,** *22* (5), 1720-1725.

271. Barbero, M.; Cadamuro, S.; Dughera, S. *Synthesis* **2006,** *2006* (20), 3443-3452.

272. Pan, C.; Huang, G.; Shan, Y., et al. *Org. Biomol. Chem.* **2020,** *18* (16), 3038-3042.

273. Suzuki, Y.; Sun, B.; Sakata, K., et al. *Angew. Chem. Int. Ed.* **2015,** *54* (34), 9944-9947.

274. Suzuki, N.; Nakata, K. *Eur. J. Org. Chem.* **2017,** *2017* (47), 7075-7086.

275. Tsuji, J.; Takahashi, H.; Morikawa, M. *Tetrahedron Lett.* **1965,** *6* (49), 4387-4388.

276. Ohmiya, H.; Makida, Y.; Li, D., et al. *J. Am. Chem. Soc.* **2010,** *132* (2), 879-889.

277. Zhang, Y.; Yin, S.-C.; Lu, J.-M. *Tetrahedron* **2015,** *71* (4), 544-549.

278. Tsukamoto, H.; Sato, M.; Kondo, Y. *Chem. Commun.* **2004,** (10), 1200-1201.

279. Wu, K.-Q.; Li, H.; Zhou, A., et al. *J. Org. Chem.* **2023,** *88* (4), 2599-2604.

280. Cullen, A.; Muller, A. J.; Williams, D. B. G. *RSC Adv.* **2017,** *7* (67), 42168-42171.

281. Rao, W.; Chan, P. W. H. *Org. Biomol. Chem.* **2008,** *6* (13), 2426-2433.

282. Sánchez, Y.; Castillo, C.; Fuentealba, J., et al. *ACS Chem. Neurosci.* **2023,** *14* (15), 2590-2602.

283. Estopiñá-Durán, S.; Taylor, J. E. *Chem. Eur. J.* **2021,** *27* (1), 106-120.

284. Yamabe, S.; Yamazaki, S. *J. Phys. Org. Chem.* **2009,** *22* (11), 1094-1103.

285. Wheland, G. W. *J. Am. Chem. Soc.* **1942,** *64* (4), 900-908.

286. Olah, G. A. *Accounts of Chemical Research* **1971,** *4* (7), 240-248.

287. Dada, R.; Singh, G.; Pareek, A., et al. *Tetrahedron Lett.* **2016,** *57* (33), 3739-3742.

288. Yang, G.-P.; Dilixiati, D.; Yang, T., et al. *Appl. Organomet. Chem.* **2018,** *32* (9), e4450.

Curriculum Vitae

Name Jeffrey Ash II

Education B.S., Biochemistry, University of Nevada, Las Vegas, 2019

Ph.D., Chemistry, University of Nevada, Las Vegas, 2024

Contact Jeffrey Ash II

Department of Chemistry, University of Nevada, Las Vegas

4505 S. Maryland Pkwy. Las Vegas, NV, 89154

Jra9001@gmail.com